CASINO GAS FIELD DEVELOPMENT

PRELIMINARY
FIELD DEVELOPMENT PLAN
5738041-FDP-001-0

APPROVAL

TITLE	NAME	SIGNATURE	DATE
Casino Sub-Surface Manager	Ian Pedler		
Chief Production Engineer	Stuart Carnell		
Manager - Development Portfolio	Wilf Lammerink		
Drilling and Completions Group Executive	Frank Jones		
Casino Project Manager	David Emslie		
VP – Development Projects and Technical Services	Paul Moore		

DATE	REV	REASON FOR ISSUE	AUTHOR	CHECKED	APPROVED
16/7/04	A	To obtain review comments prior to formal production licence application.	Various	DWU	DAE
1/9/04	0	Internal and JV Review and Approval	Various	IGP	DAE
13/9/04	1	DPIE Submission	Various	IGP	DAE

DISTRIBUTION OF CONTROLLED COPIES

COPY	NAME	POSITION	COMPANY
1	P. Moore	Vice President – DPATS	Santos
2	D. Emslie	Project Manager	Santos
3	P. van Riel	Offshore Engineering Manager	Santos
4	S. Carnell	Drilling & Completions Manager	Santos
5	M. Bartnik	HDD Manager	Santos
6	D. Young	Onshore Project Engineer	Santos
7	Y Uchida	Director & General Manager	Mittwell
8	R Frith	Engineering / Production Manager	AWE
9			
10			

Contents

Figures

Tables

Enclosures

Enclosure 3.3.3 a	Top Waarre C Low Impedance Depth Map
Enclosure 3.3.3 b	Top Waarre C Main Pay Depth Map
Enclosure 3.3.3 c	Base Waarre Ca2 Depth Map
Enclosure 3.3.3 d	Top Lower Waarre A Depth Map
Enclosure 3.3.3 e	Base Waarre A Depth Map
Enclosure 3.6.4 a	Casino-1 Petrophysical Analysis
Enclosure 3.6.4 b	Casino-2 Petrophysical Analysis
Enclosure 3.6.4 c	Casino-3 Petrophysical Analysis
Enclosure 3.12.3 a	Casino Petrel Static Model Summary GRV, NPV and OGIP Data
Enclosure 4.2.7 a	Dynamic Simulation Sensitivity Scenarios
Enclosure 4.3.2 a	Ultimate Recovery Scenario Tree - P50
Enclosure 4.3.2 b	Ultimate Recovery Scenario Tree - P90
Enclosure 4.3.2 c	Ultimate Recovery Scenario Tree - P10
Enclosure 8.1.2 a	Santos Quality Asset Development Process
Enclosure 8.1.4 a	Casino Project Schedule

1 Summary of Proposed Development

1.1.1 Background

Santos Ltd (Santos) as Operator on behalf of the VIC/P44 Joint Venture proposes to develop the Casino gas field approximately 30 km offshore from Port Campbell on Victoria's southwest coast. The Casino gas field development comprises subsea installations and a pipeline that will carry gas from offshore wells to the existing TXU Iona gas plant near Port Campbell.

This preliminary Field Development Plan (FDP) is submitted as part of the process to ultimately obtain a production licence for the Casino gas field ("Field") located in exploration permit VIC/P44. The application to the Joint Authority relates to granting of a Production Licence over blocks 2432, 2433 and 2434 of Hamilton Map Sheet SJ54. Permit VIC/P44 is located in the southeast part of the offshore Otway Basin. The Casino field itself lies in water depths of 65-70m and is approximately 30km southwest of Port Campbell and 250km southwest of Melbourne.

The location of the field is shown in Figure 1.1.1-a below.

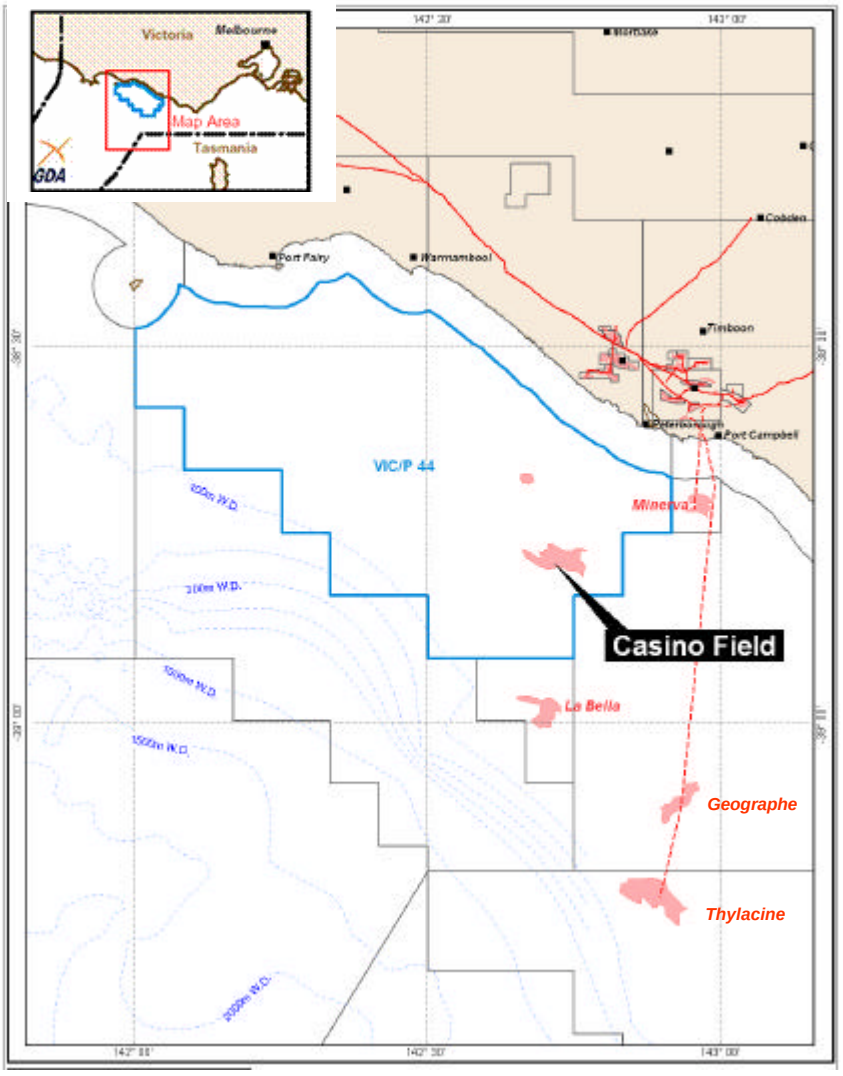

Figure 1.1.1-a: Location of Casino Field

1.1.2 Permit History

Strike Oil was awarded VIC/P44 in 1999, with a work commitment of technical studies and seismic reprocessing in Years 1 and 2 and a small (108km^2) 3D survey in Year 3. Drilling commitments were in Years 4 and 5, part of the secondary, 3 year, discretionary term. The end of Permit Year 5 is approaching and due to the activity associated with Casino there are no outstanding work commitments for the permit.

Santos signed a farmin agreement in late August 2001, taking a 50% equity and operatorship of the acreage in return for funding the bulk of the 3D acquisition and the first exploration well. In late 2001 540km^2 of 3D data and 69km of 2D seismic data was acquired over the eastern portion of the block.

On 15th July, 2003, Australian Worldwide Exploration Ltd announced that its 100% owned subsidiary Peedamullah Petroleum Pty Ltd acquired into Strike's remaining 50% interest. AWE subsequently farmed out half of this interest to Mittwell Energy Resources Pty Ltd, a wholly owned subsidiary of Mitsui & Co Ltd of Japan.

Current equities for VIC/P44 and Casino project proponents are as follows;

Santos Limited	50% (Operator)
Peedamullah Petroleum Pty Ltd	25%
Mittwell Energy Resources Pty Ltd	25%.

1.1.3 Field History

The Casino field was discovered by the exploration well Casino-1, drilled during August and September, 2002, by the semi submersible MODU Ocean Bounty. The well reached total depth of 2118 mRT (-2093mSS) in Albian aged sediments of the Eumeralla Formation, part of the Otway Group. The top of a 48m thick gas column was encountered at -1740mRT (-1715mSS) in Waarre A sands, lower part the Waarre Sandstone, Sherbrook Group, with a GDT of 1788mRT (-1763mSS).

Casino-2, drilled immediately after the first well, is approximately 4km to the east-southeast of Casino-1. Casino-2 drilled through the Waarre A GWC (-1838mSS) and MDT pressure data revealed that the Waarre A gas accumulation was approximately 200psi over pressured. The well also penetrated a younger, gas bearing sand (Waarre C) that was absent at Casino-1 and that has a gas-down-to (GDT) of 1786mRT (-1761mSS). Casino-2 reached a total depth of 2112mRT (-2087mSS) and was plugged and abandoned as a gas discovery.

The Waarre C Gas Water Contact (GWC) was not encountered by Casino-2 (GDT -1761mSS) and no pressure data was available from the Waarre C water leg. The lack of a water gradient from the Waarre C was a major technical uncertainty. If the Waarre C was over-pressured to the same degree as the Waarre A only a short gas column could exist (GWC -1850mSS). If however the Waarre C was normally pressured the Casino-2 Waarre C gas gradient intersects the regional aquifer gradient at a depth of -2007mSS, suggesting a >300m gas column.

The data from the two wells was only sufficient to declare the field a non-commercial discovery. Significant subsurface uncertainties remained, the most important being whether or not the Waarre C reservoir was over-pressured. If a similar pressure regime existed in the younger sand the field would keep its non-commercial status.

Just over a year separated the drilling of Casino-2 and Casino-3 and in that time a detailed technical review was carried out to integrate all the key learnings from Casino-1 & 2. Full integration of Casino-1 & -2 into the seismic interpretation, seismic inversion, core based sedimentology, petrology, palynology and the building a 3D static reservoir model were the main components of the sub-surface technical work carried out during Q1-Q3 2003. Seismic amplitudes provided encouragement for normally pressured Waarre C i.e. amplitudes indicated the presence of a GWC at a depth not dissimilar from the intersection of extrapolated Casino-2 pressure data with the regional aquifer. However seismic amplitude data, without supporting pressure data, is not sufficient to prove the Waarre C is normally pressured.

In addition to the technical work, commercial negotiations had been taking place between the VIC/P44 JV and TXU Australia. An innovative deal arose from these talks, whereby Casino gas was already contracted should Casino-3 prove up sufficient reserves. This effectively removed both the risk of finding a market for the gas and the time needed to find a buyer: major hurdles that are usually addressed after a field has been appraised.

The net result of subsurface and commercial work was the recommendation for an appraisal well to be drilled, with the knowledge that a successful appraisal would guarantee the development of the field.

Casino-3 was drilled with the following objectives:

- Determine the Waarre C FWL or establish new lowest known gas (LKG),
- Establish the pressure regime of the Waarre C,
- Conduct production test of the Waarre C,
- Acquire full hole core from the Waarre C,
- Establish reservoir characteristics of the Waarre A in the water leg.

Casino-3, 3.3km northeast of Casino-1 and 2.4km northwest of Casino-2, was spudded on 14th Oct 2003 by the Ocean Epoch. Waarre C sands were encountered close to prognosis and 27m of core was cut (91.5% recovered). The sands are of a similar thickness to those at Casino-2 and most importantly are gas bearing, thus demonstrating that the Waarre C was not significantly over-pressured. The well reached a driller's depth of 2135mRT within the Waarre A. Casino-3 confirmed the following:

- Waarre C is in a separate pressure regime to Waarre A,
- 37m gross (23.5m net) gas column, proving a 304m gas column for the Waarre C,
- GWC -1999mSS,
- Excellent Waarre C reservoir properties. A DST (2004 to 2013 mRT) was conducted and flowed at a maximum choke (1 inch) constrained rate of 44 mmscfd,
- The relationship between seismic amplitudes and gas bearing sands in the Casino structure,

A schematic cross section of the Casino field, following the drilling of Casino-3 is shown in Figure 1.1.3-a

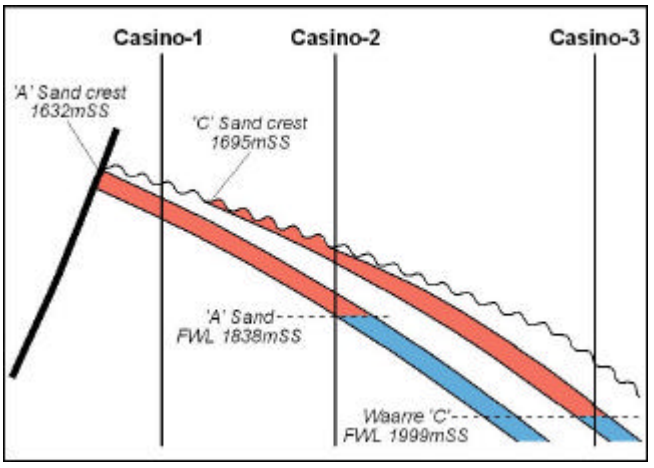

Figure 1.1.3-a: Casino Field Schematic

1.1.4 Proposed Casino Production Licence

An application for declaration of location over the Casino field was submitted in March 2004 and the Location declared in August 2004 over blocks 2432, 2433 and 2434 of Hamilton Map Sheet SJ54 as shown in Figure 1.1.4-a.

It is proposed that these same 3 blocks will form the Casino production licence covering the mapped extent of the Casino gas field. The extent of the gas pools which make up the Casino accumulation relative to the graticular block boundaries is shown in detail in Figure 1.1.4-b. Note that the gas bearing Waarre C reservoir is contained within blocks 2433 and 2434 while the gas bearing Waarre A reservoir extends into block 2432. This is shown in Figure 1.1.4-c which is a strike line from an impedance volume showing the top and base picks for the main Waarre A gas reservoir extending westward into block 2432.

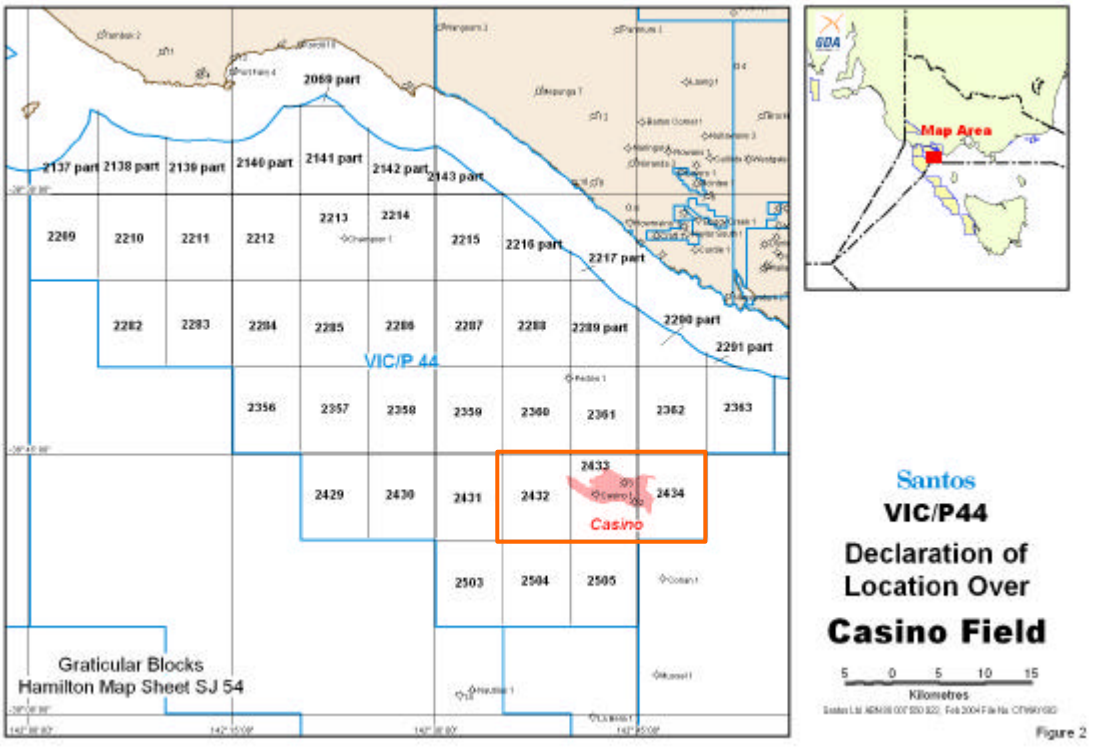

Figure 1.1.4-a: Casino Field Declared Location

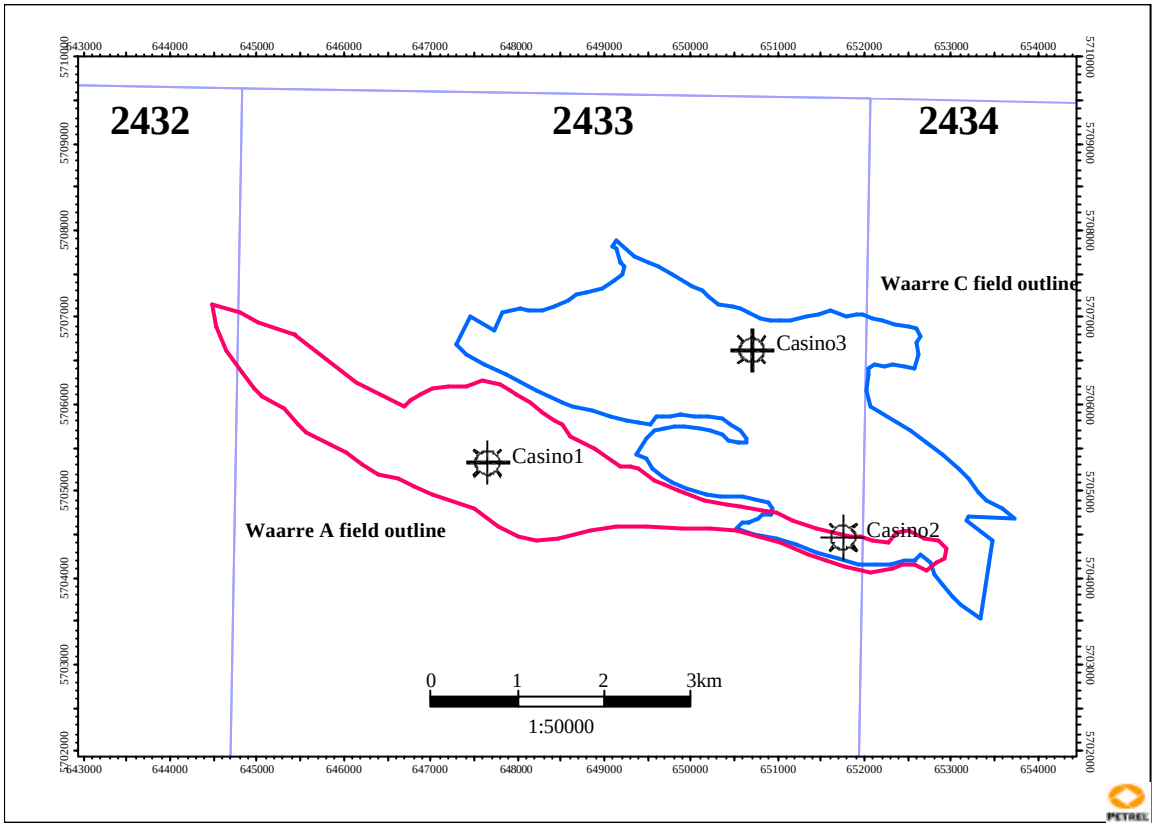

Figure 1.1.4-b: Casino Field Gas Bearing Pool Areas and Block Boundaries

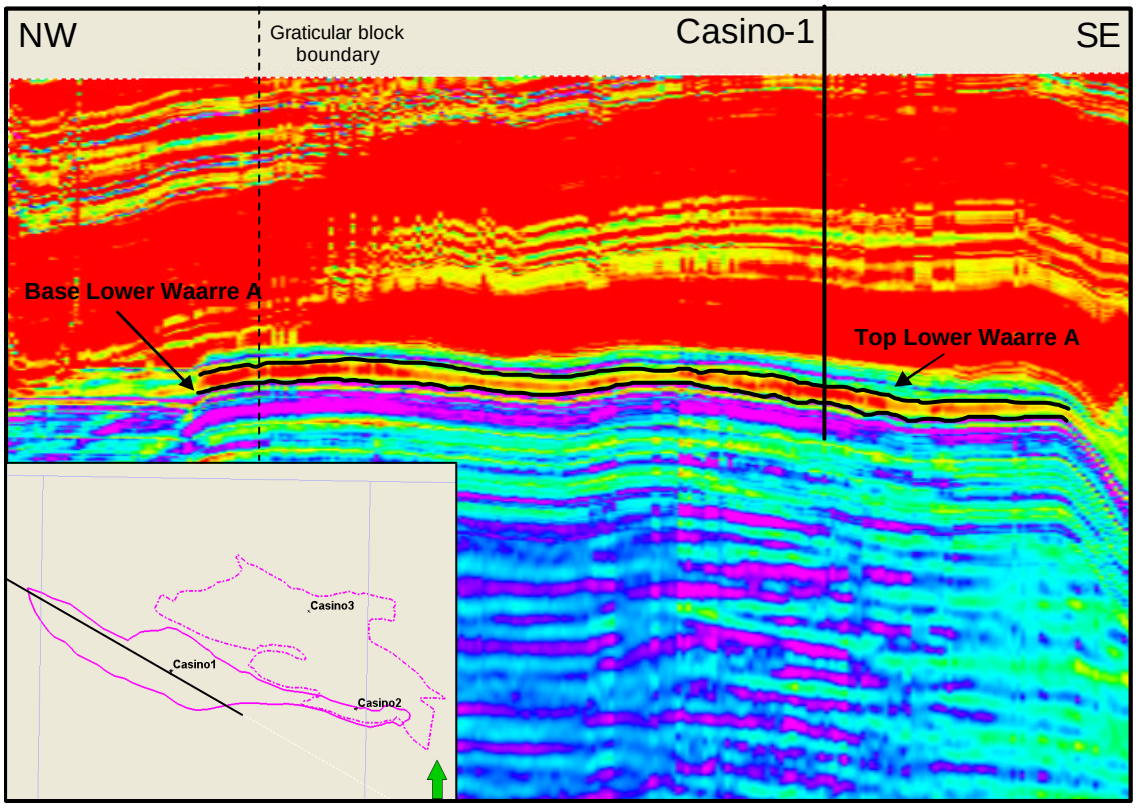

Figure 1.1.4-c: Casino Field Seismic Line showing Block Boundaries and Waarre A Reservoir Picks

1.1.5 Reserves Description

Detailed geological and reservoir studies have been completed to determine the Casino field reserves which underpins the project development. The results of this work show the Casino field Proved and Probable gas reserves are estimated to be 270 Bcf. The full distributions for Casino field gas in place and reserves are summarised in Table 1.1.5-a below.

	P90	P50	P10	Mean
OGIP (Bcf)				
Waarre C	247	312	372	310
Waarre A	74	106	140	104
Field	**332**	**420**	**496**	**414**
Reserves (Bcf)				
Waarre C	168	201	271	208
Waarre A	34	74	107	69
Field	**214**	**270**	**350**	**277**
Field Reserves (PJ)	**220**	**277**	**359**	**284**

Table 1.1.5-a: Casino Field Reserves Summary

Casino gas can be characterised as a sweet, dry gas with a gravity of 0.6 (relative to air). Inerts levels are low (2-3%) together with low levels of associated hydrocarbon liquids. A condensate/gas ratio of 1.1 bbl/MMscf was measured at the separator during the Casino-3 production test. Casino gas composition as measured during the Casino-3 production test are summarised in Table 1.1.5-b below.

Well		Casino-3
Formation		Waarre C
Composition		
N_2	mol%	2.1
CO_2	mol%	0.9
C_1	mol%	94.1
C_2	mol%	1.9
C_3	mol%	0.5
C_4	mol%	0.2
C_5+	mol%	0.3

Table 1.1.5-b: Casino Fluid Composition

1.1.6 Development

The proposed development for the Casino gas field comprises the offshore production of gas and its transportation to shore in a dedicated pipeline to the existing TXU Iona gas plant near Port Campbell for processing. Specifically, the development comprises:

- Drilling two offshore development wells, one in each of the Casino reservoirs.
- Installation of wellheads on the seafloor. No structures will be visible from shore.
- Installation of a subsea pipeline and control umbilical (each approximately 36.7 km long) on the sea floor to transfer gas from the wells to shore.
- Horizontal directional drilling (HDD) of the shore crossing from farmland outside the Port Campbell National Park.
- Construction of a buried onshore pipeline (11.5 km in length) from the shore crossing to the TXU Iona Gas Plant facility. A mainline valve site will be located in farmland near the coast.
- Processing of the gas by TXU at the Iona Gas Plant prior to distribution to Victorian and interstate customers through the existing pipeline network.

The project is shown diagrammatically in Figure 1.1.6-a.

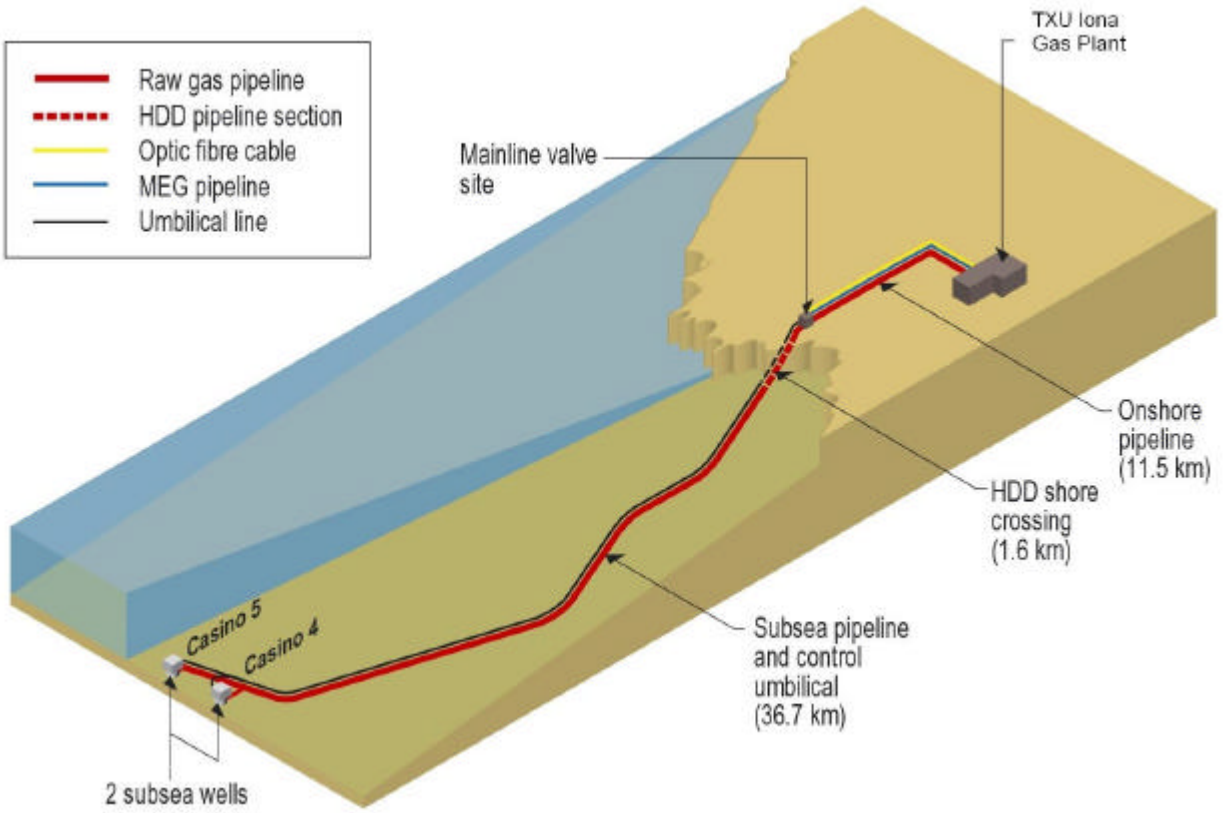

Figure 1.1.6-a: Casino Field Development Layout

1.1.7 Schedule

A summary project schedule is shown below in Figure 1.1.7-a. Key points include:

- Scheduling construction activities around favourable seasonal weather conditions,
- Building schedule space between offshore drilling and offshore pipelay activities, and HDD shore crossing construction and offshore pipelay activities.
- All regulatory and licenses to be obtained by year-end 2004,
- All orders and contracts in place by end third quarter 2004,

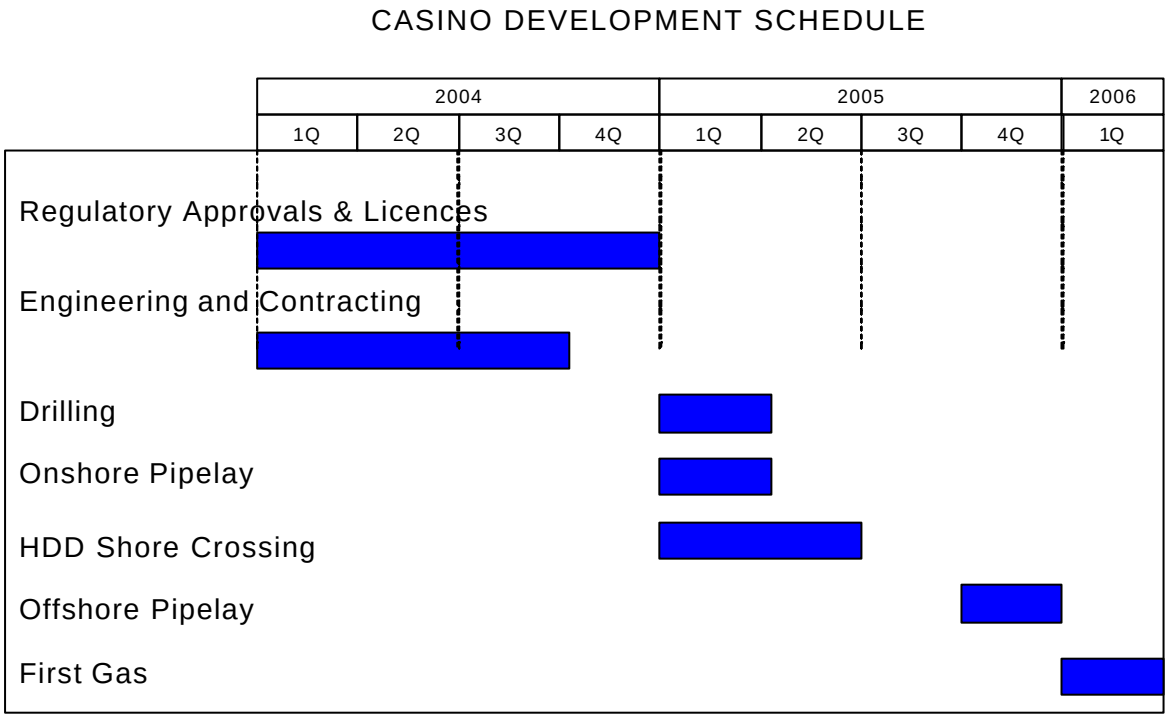

Figure 1.1.7-a: Casino Development Schedule

1.1.8 Future Potential

Additional exploration potential has been identified in the VIC/P44 area (see Section 3.14) and the facilities proposed for the Casino development will have the ability to tie-in additional gas field discoveries which may be made in future. While an initial 2 well development is planned for the Casino field, pre-investment is being made in umbilical capacity to allow for simultaneous gas production from up to 6 wells which may ultimately be tied into the Casino export pipeline.

Further, while the plateau production rate proposed for the Casino field is for 35 PJ/a of gas production, studies have shown that the 12" pipeline being installed as part of the development is capable of throughput rates of up to 50 PJ/a should this be required in future.

2 Production Overview

2.1 General

2.1.1 Overview of Annual Production

This section summarises information presented later in this document in more detail. Based on the current commercial arrangements, the field P90, P50 and P10 production profiles are summarised in Figure 2.1.1-a below. A summary of annual quantities is also presented in Table 2.1.1-a, based on an assumed first gas date of 01 February 2006.

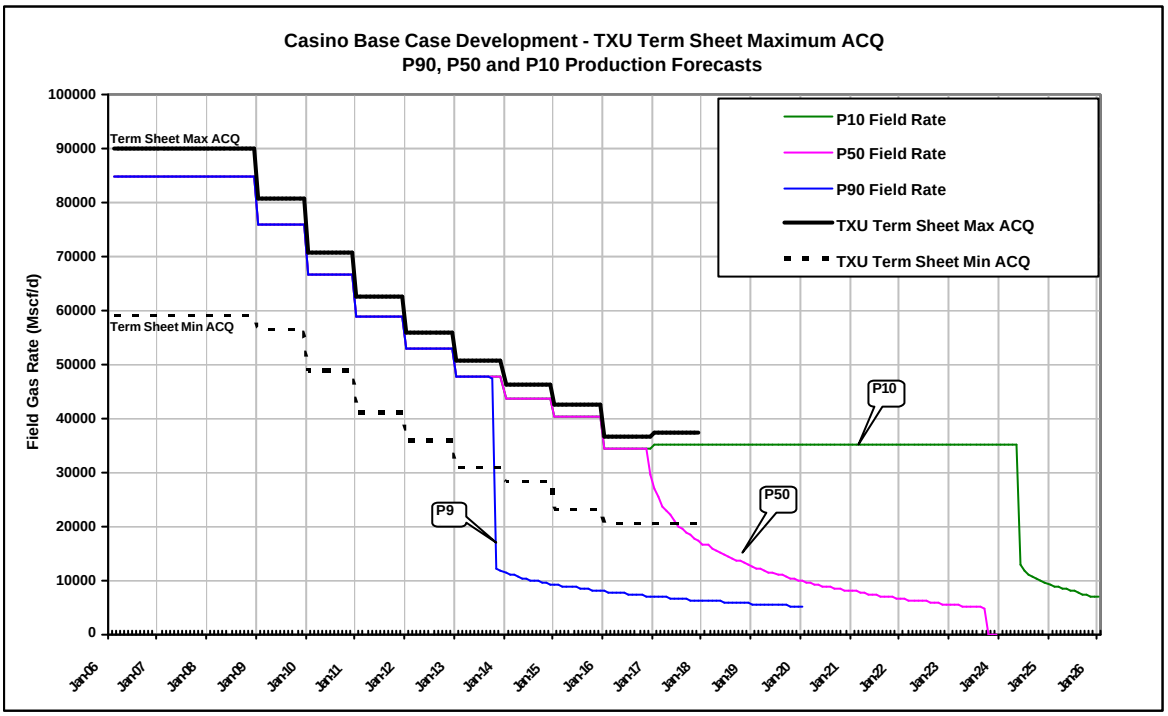

Figure 2.1.1-a: Casino Base Development Annual Production Forecast

	FIELD P90					FIELD P50					FIELD P10				
	Annual Raw Gas		Annual Fuel Gas	Annual Sales Gas	Annual Cond	Annual Raw Gas		Annual Fuel Gas	Annual Sales Gas	Annual Cond	Annual Raw Gas		Annual Fuel Gas	Annual Sales Gas	Annual Cond
	Bcf	PJ	PJ	PJ	kstb	Bcf	PJ	PJ	PJ	kstb	Bcf	PJ	PJ	PJ	kstb
Dec-06	28.5	30.3	1.2	29.1	29.1	28.5	30.3	1.2	29.1	29.1	28.5	30.3	1.2	29.1	29.1
Dec-07	31.0	33.0	1.3	31.7	31.7	31.0	33.0	1.3	31.7	31.7	31.0	33.0	1.3	31.7	31.7
Dec-08	31.1	33.1	1.3	31.7	31.7	31.1	33.1	1.3	31.7	31.7	31.1	33.1	1.3	31.7	31.7
Dec-09	27.8	29.6	1.2	28.4	28.4	27.8	29.6	1.2	28.4	28.4	27.8	29.6	1.2	28.4	28.4
Dec-10	24.4	25.9	1.0	24.9	24.9	24.4	25.9	1.0	24.9	24.9	24.4	25.9	1.0	24.9	24.9
Dec-11	21.5	22.9	0.9	22.0	22.0	21.5	22.9	0.9	22.0	22.0	21.5	22.9	0.9	22.0	22.0
Dec-12	19.4	20.6	0.8	19.8	19.8	19.4	20.6	0.8	19.8	19.8	19.4	20.6	0.8	19.8	19.8
Dec-13	14.5	15.5	0.6	14.8	14.8	17.5	18.6	0.7	17.8	17.8	17.5	18.6	0.7	17.8	17.8
Dec-14	3.7	4.0	0.2	3.8	3.8	15.9	16.9	0.7	16.2	16.2	15.9	17.0	0.7	16.3	16.3
Dec-15	3.1	3.3	0.1	3.2	3.2	14.7	15.6	0.6	15.0	15.0	14.7	15.6	0.6	15.0	15.0
Dec-16	2.8	2.9	0.1	2.8	2.8	12.9	13.7	0.5	13.2	13.2	12.6	13.4	0.5	12.9	12.9
Dec-17	2.4	2.6	0.1	2.5	2.5	7.4	7.9	0.3	7.6	7.6	12.8	13.7	0.5	13.1	13.1
Dec-18	2.2	2.3	0.1	2.2	2.2	5.3	5.6	0.2	5.4	5.4	12.8	13.7	0.5	13.1	13.1
Dec-19	2.0	2.1	0.1	2.0	2.0	4.0	4.3	0.2	4.1	4.1	12.8	13.7	0.5	13.1	13.1
Dec-20	0.0	0.0	0.0	0.0	0.0	3.3	3.5	0.1	3.3	3.3	12.9	13.7	0.5	13.2	13.2
Dec-21	0.0	0.0	0.0	0.0	0.0	2.7	2.8	0.1	2.7	2.7	12.8	13.7	0.5	13.1	13.1
Dec-22	0.0	0.0	0.0	0.0	0.0	2.2	2.4	0.1	2.3	2.3	12.8	13.7	0.5	13.1	13.1
Dec-23	0.0	0.0	0.0	0.0	0.0	1.3	1.4	0.1	1.3	1.3	12.8	13.7	0.5	13.1	13.1
Dec-24	0.0	0.0	0.0	0.0	0.0	0.0	0.0	0.0	0.0	0.0	7.0	7.4	0.3	7.1	7.1
Dec-25	0.0	0.0	0.0	0.0	0.0	0.0	0.0	0.0	0.0	0.0	2.9	3.1	0.1	3.0	3.0
Total	214.4	228.1	9.1	219.0	219.0	270.7	287.9	11.5	276.4	276.4	344.2	366.1	14.6	351.5	351.5

Table 2.1.1-a: Casino Field Production Profiles (1 Feb 2006 First Gas)

Commercial arrangements for disposal of gas from the Casino field are presently being finalised. It is envisaged these will provide significant flexibility in gas offtake rates and will allow for the field plateau rate to be extended thus accelerating production from the field. Production profiles under these arrangements are summarised in Figure 2.1.1-b and Table 2.1.1-b.

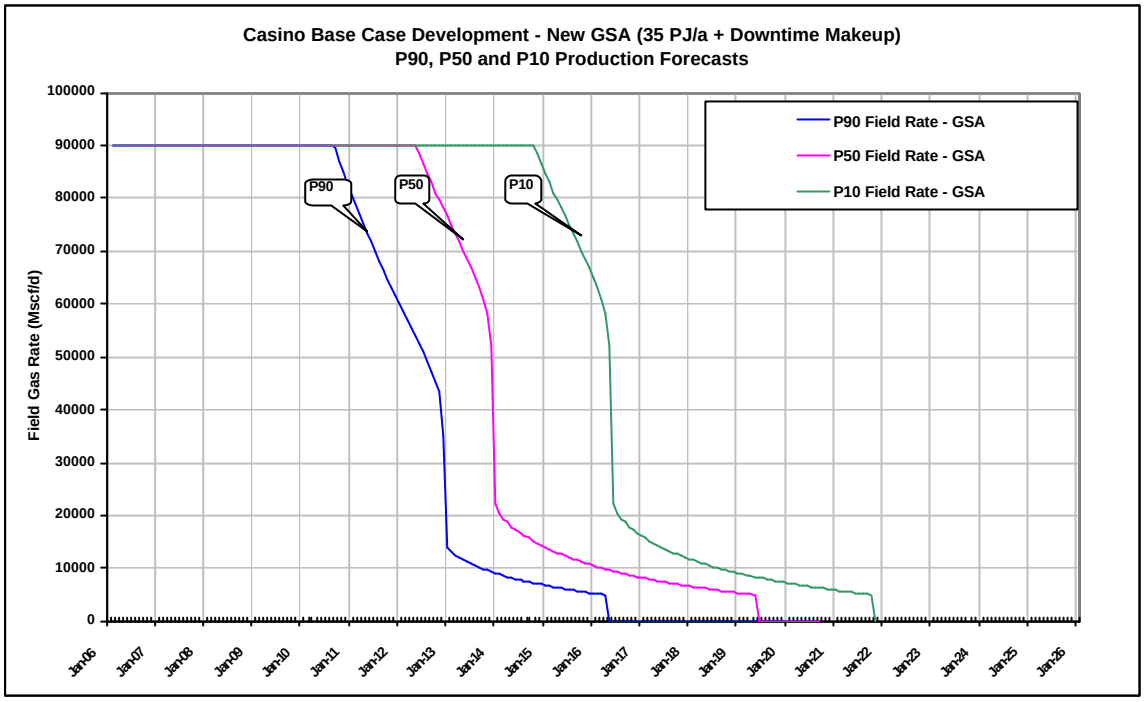

Figure 2.1.1-b: Casino Field Production Forecasts – Extended Plateau

	FIELD P90					FIELD P50					FIELD P10				
	Annual Raw Gas		Annual Fuel Gas	Annual Sales Gas	Annual Cond	Annual Raw Gas		Annual Fuel Gas	Annual Sales Gas	Annual Cond	Annual Raw Gas		Annual Fuel Gas	Annual Sales Gas	Annual Cond
	Bcf	PJ	PJ	PJ	kstb	Bcf	PJ	PJ	PJ	kstb	Bcf	PJ	PJ	PJ	kstb
Dec-06	30.1	32.0	1.3	30.7	30.7	30.1	32.0	1.3	30.7	30.7	30.2	32.1	1.3	30.8	30.8
Dec-07	33.0	35.1	1.4	33.7	33.7	33.0	35.1	1.4	33.7	33.7	32.9	35.0	1.4	33.6	33.6
Dec-08	32.9	35.0	1.4	33.6	33.6	32.9	35.0	1.4	33.6	33.6	32.9	35.0	1.4	33.6	33.6
Dec-09	32.9	35.0	1.4	33.6	33.6	32.9	35.0	1.4	33.6	33.6	33.0	35.1	1.4	33.7	33.7
Dec-10	32.3	34.3	1.4	33.0	33.0	32.9	35.0	1.4	33.6	33.6	32.9	35.0	1.4	33.6	33.6
Dec-11	25.7	27.3	1.1	26.2	26.2	33.0	35.1	1.4	33.7	33.7	32.9	35.0	1.4	33.6	33.6
Dec-12	17.7	18.8	0.8	18.1	18.1	31.2	33.2	1.3	31.9	31.9	32.9	35.0	1.4	33.6	33.6
Dec-13	4.0	4.3	0.2	4.1	4.1	23.7	25.2	1.0	24.2	24.2	33.0	35.1	1.4	33.7	33.7
Dec-14	2.9	3.1	0.1	2.9	2.9	6.2	6.6	0.3	6.3	6.3	32.7	34.7	1.4	33.4	33.4
Dec-15	2.2	2.3	0.1	2.2	2.2	4.4	4.7	0.2	4.5	4.5	27.4	29.1	1.2	27.9	27.9
Dec-16	0.5	0.5	0.0	0.5	0.5	3.4	3.6	0.1	3.5	3.5	12.5	13.3	0.5	12.8	12.8
Dec-17	0.0	0.0	0.0	0.0	0.0	2.7	2.9	0.1	2.8	2.8	5.0	5.4	0.2	5.1	5.1
Dec-18	0.0	0.0	0.0	0.0	0.0	2.2	2.3	0.1	2.2	2.2	3.8	4.0	0.2	3.9	3.9
Dec-19	0.0	0.0	0.0	0.0	0.0	0.8	0.8	0.0	0.8	0.8	3.0	3.2	0.1	3.0	3.0
Dec-20	0.0	0.0	0.0	0.0	0.0	0.0	0.0	0.0	0.0	0.0	2.4	2.5	0.1	2.4	2.4
Dec-21	0.0	0.0	0.0	0.0	0.0	0.0	0.0	0.0	0.0	0.0	1.6	1.7	0.1	1.7	1.7
Dec-22	0.0	0.0	0.0	0.0	0.0	0.0	0.0	0.0	0.0	0.0	0.0	0.0	0.0	0.0	0.0
Dec-23	0.0	0.0	0.0	0.0	0.0	0.0	0.0	0.0	0.0	0.0	0.0	0.0	0.0	0.0	0.0
Dec-24	0.0	0.0	0.0	0.0	0.0	0.0	0.0	0.0	0.0	0.0	0.0	0.0	0.0	0.0	0.0
Dec-25	0.0	0.0	0.0	0.0	0.0	0.0	0.0	0.0	0.0	0.0	0.0	0.0	0.0	0.0	0.0
Total	214.1	227.8	9.1	218.7	218.7	269.4	286.5	11.5	275.1	275.1	349.0	371.3	14.9	356.5	356.5

Table 2.1.1-b: Casino Field Production Profiles - Extended Plateau (1 Feb 2006 First Gas)

2.1.2 Flare or Venting

Flaring or venting offshore will not be possible as there will not be any facilities to allow this. Flaring or venting will only be possible at the onshore TXU Iona plant which will be managed in accordance with current operating and maintenance practices.

Sequestering of CO_2 will not be required due to the low CO_2 content in the gas.

2.1.3 Estimated Field Life

Depending on the field offtake rate and reserves outcome the Casino field life is expected to be in the range 10 – 20 years.

3 Reservoir Description

3.1 Overview

3.1.1 Overview and Workflow

The workflow employed in the conduct of the Casino Subsurface Development Planning is summarised in Figures 3.1.1-a, b and c.

Figure 3.1.1-a summarises the initial phase of work conducted from December 2003 to April 2004 and includes;

- Initial band limited inversion and initial seismic mapping
- Subsequent model based inversion of the 3D seismic volume and the refined seismic interpretation
- Basic geological studies and petrophysical analysis and construction of a first pass Petrel model using the initial mapped surfaces
- Use of several inversion volumes and acoustic impedance versus porosity relationships to build several acoustic impedance based static models in Petrel
- Use of the final mapped surfaces to build a Base Case Layered Petrel model
- Generation of SCAL based saturation versus height functions to allow OGIP to be determined from the Petrel static models
- A fast track, preliminary reservoir simulation (Phase 2) study to give an initial range of estimates for gas recovery factor for input into an initial probabilistic OGIP and reserves estimation.

Figure 3.1.1-b summarises the work conducted in May 2004 and includes;

- Generation of multiple Petrel static realisations of the Casino field to investigate the range of field OGIP
- Incorporation of the Petrel static realisations and other OGIP uncertainty parameters to develop a field OGIP distribution
- Review of the permeability uncertainty associated with the Waarre A sands
- Identification of a range of possible aquifer scenarios, and incorporation of special core analysis results to conduct the Phase 3 reservoir simulation study with the aim of identifying the major dynamic uncertainties associated with ultimate gas recovery
- Generation of second pass probabilistic OGIP and reserves estimates.

Figure 3.1.1-c summarises the work conducted from June 2004 and includes;

- Selection of candidate development well locations
- Generation of the final field reserves estimates using 3 static realisations (P90, P50 and P10) and scenario tree approach to incorporate the effect of the key dynamic uncertainties
- From this work several deterministic realisations were selected to conduct the final development planning and optimisation work.

This work is discussed in detail in Sections 3 and 4 of this Development Plan.

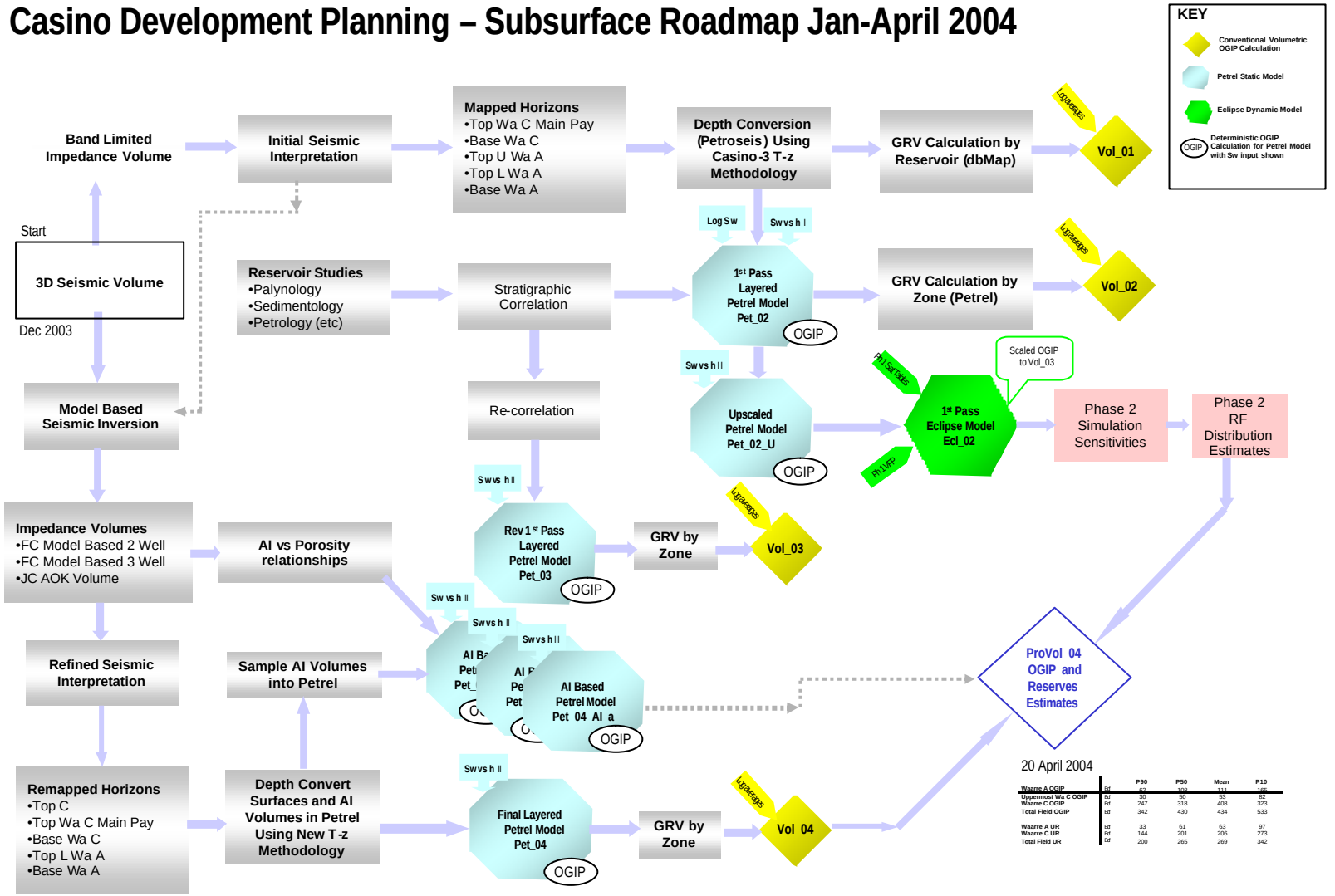

Figure 3.1.1-a: Subsurface Development Planning Roadmap : Dec 2003 – April 2004

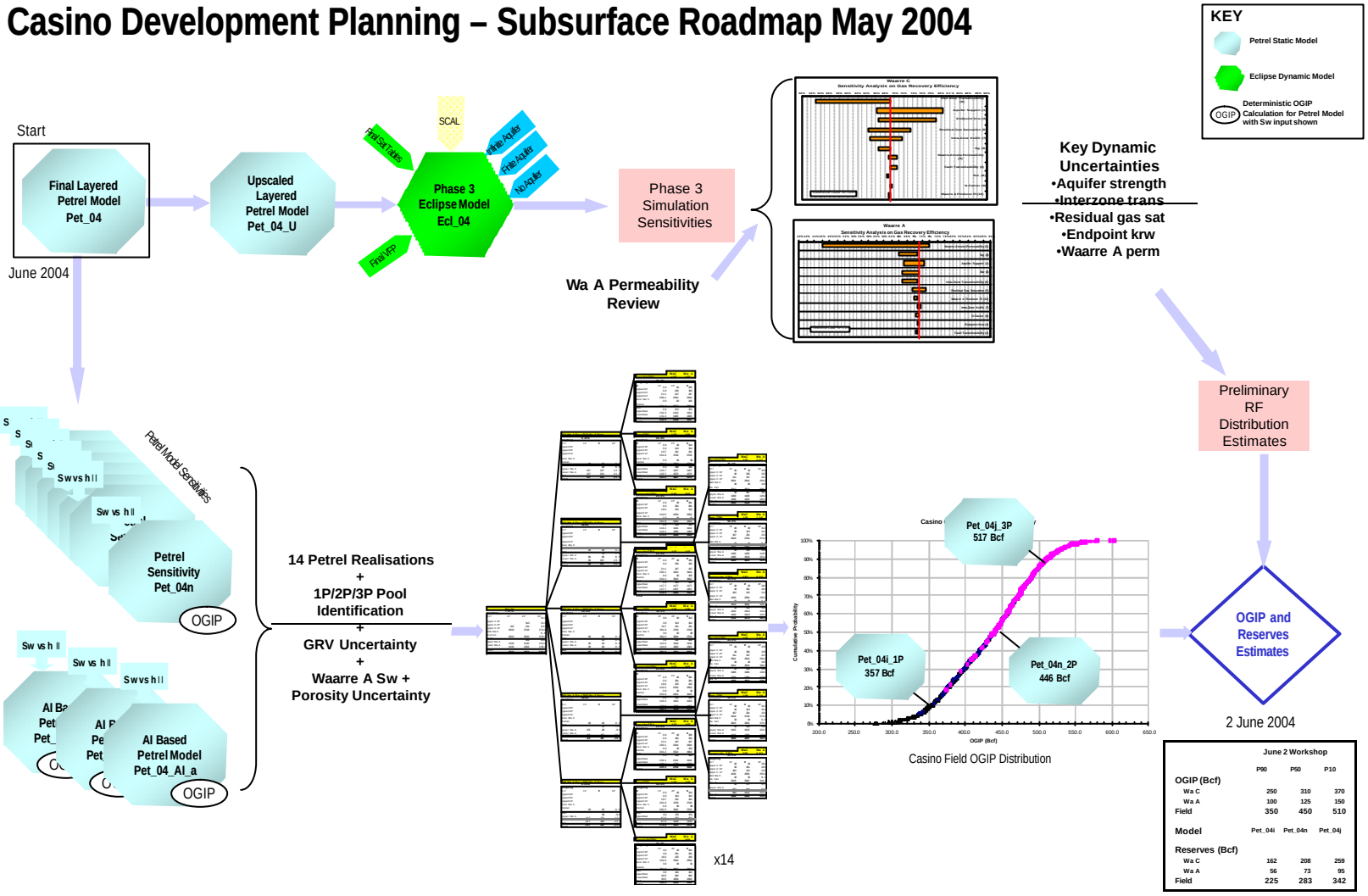

Figure 3.1.1-b: Subsurface Development Planning Roadmap : May 2004

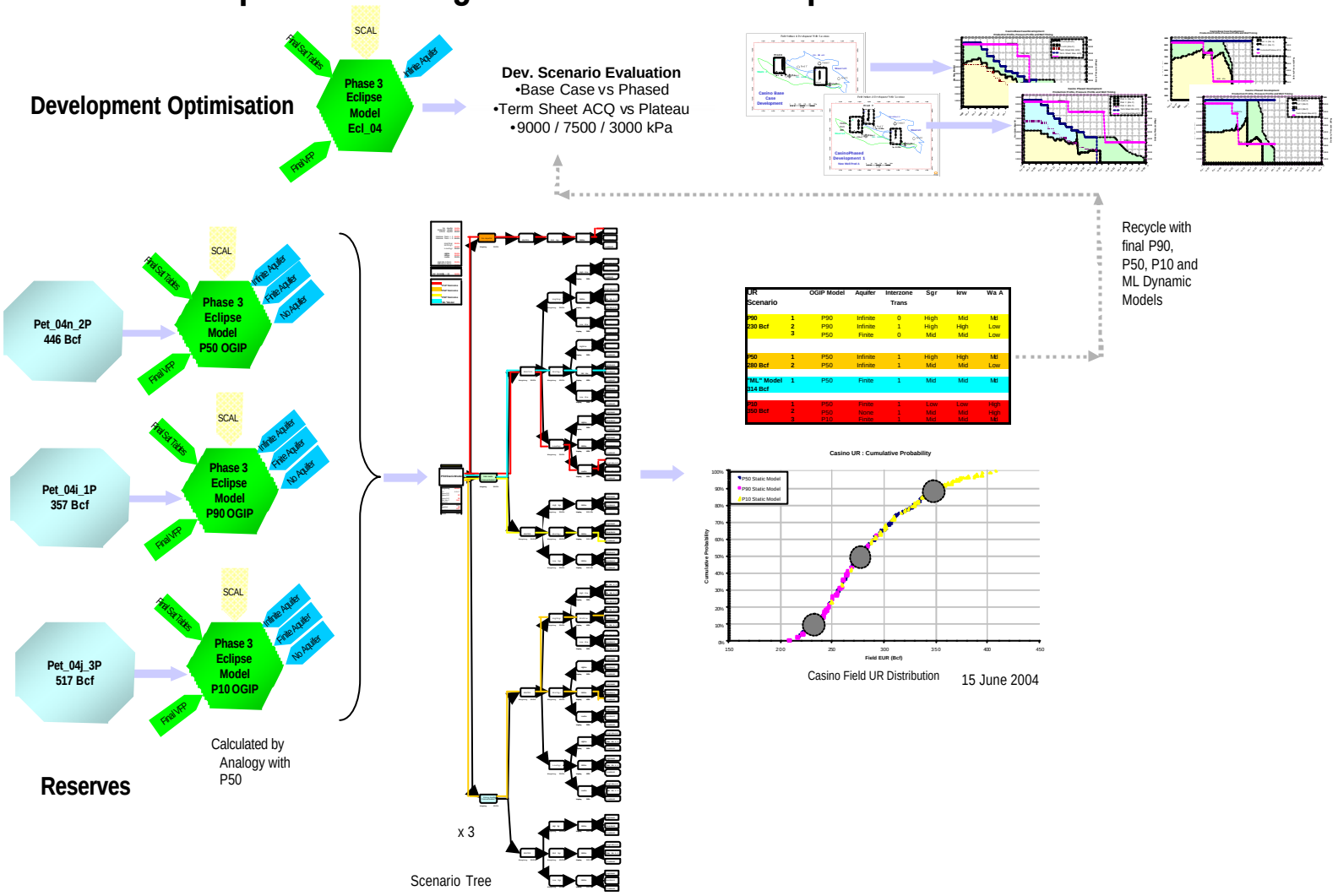

Figure 3.1.1-c: Subsurface Development Planning Roadmap : June 2004

3.2 Geological Setting

3.2.1 Introduction

A series of tectonic, climatic and geomorphologic events combined to control the facies and patterns of sedimentation on the "Casino" fault block during deposition of the Late Cretaceous Waarre Sandstone. The Otway Basin at the time lay at the eastern end of a long, narrow seaway that extended from the southwestern corner of Western Australia along the southern coast of Australia to Cape Otway in Victoria. Although Antarctica had begun to break from Australia, the rate of separation during the Cretaceous was very slow and the two continents were still joined across a wrench fault that extended from near Cape Otway southeastwards along the western side of Tasmania (Figure 3.2.1-a).

Figure 3.2.1-a: Late Cretaceous basin geometry *(refer to end of section for this figure)*

The seaway was in high latitudes as Australia had not yet begun its rapid drift northwards to its present position. This infers that there was probably a very long fetch for waves driven eastwards by circum-polar winds. High wave energy would have impacted along the southern coast of Australia, especially where the coast was oriented NW-SE, as it was along the Otway coast.

The northern side of the seaway (i.e. the southern margin of the Mussel Platform in the Casino area) was broken by a myriad of normal faults initiated during the Late Cretaceous rifting of the continents. These faults were sub-parallel to the southern coastline and most stepped down to the basin in the south, tilting the top of each block to the north (Figure 3.2.1-a). Near the eastern end of the seaway, the Shipwreck Trough provided a ~N-S re-entrant that focussed the flux of sediment into that part of the seaway (Figure 3.2.1-b). The Mussel Platform guarded the western edge of the trough from the most severe wave activity. The western edge of the Shipwreck Trough was controlled by a NNE-trending monocline rather than a distinct fault, causing the fault blocks on the Mussel Platform adjacent to the trough to plunge to the east (Figure 3.2.1-b). The well correlation shown in Figure 3.2.1-c highlights the change in thickness of the Waarre Sandstone between the Mussel Platform and the Shipwreck Trough. Figure 3.2.1-d, a seismic line tying Pecten-1A with Minerva, shows the thickening of the sedimentary sequences into the Shipwreck Trough.

Figure 3.2.1-b: Structural elements *(refer to end of section for this figure)*

Figure 3.2.1-c: Pecten – Casino –Conan – Minerva Correlation *(refer to end of section for this figure)*

Figure 3.2.1-d: Pecten –– Minerva seismic correlation *(refer to end of section for this figure)*

The onset of rift reactivation during the late Cenomanian resulted in a regional unconformity, perhaps resulting in loss of almost all of the Cenomanian in the onshore sections (Partridge, 2001). This is the first (K75) of several major unconformities which affect the distribution of Waarre reservoir sequences across the Mussel Platform. There is a resultant change in depositional setting and style from an initial non marine fluvial phase to settings with progressively greater marine influence.

Buffin (1989) describes the basal Unit A of the Waarre Sandstone from the Port Campbell Embayment as being composed of interbedded fine-grained lithic sandstones, carbonaceous mudstones and thin coals or carbonaceous stringers. In these onshore wells, Partridge (1999) has commented on the consistency of microplankton in the first samples above the unconformity with the Eumeralla Formation.

In the Casino Field there is a distinct flooding shale within the Waarre A that records the first influx of marine microplankton within the Waarre. Unlike the onshore wells where marine influenced sediments overlie the K75, this shale occurs approximately half way through the Waarre A sequence, with a fluvial dominated, sand rich lower Unit A overlying the unconformity with the Eumeralla Formation. It is proposed that this unit progressively onlaps the Mussel Platform to the north until it is either absent or very thin in Pecten 1A and the onshore wells. The Casino Field Unit A sands are very similar to those described by Buffin (1989).

Medium grained, poor to moderately well sorted, feldspathic litharenites and carbonate cemented sublitharenites predominate. Throughout Unit A sediment was dominantly derived from both a metamorphic and igneous terrane (Phillips, 2003). The presence of glaucony and framboidal pyrite supports the deposition of the sands in a marginal marine setting.

A rise in relative sea level pushed the Waarre A depositional systems northwards and the widespread, but relatively thin, Waarre B shale was deposited. The microfossils derived from cuttings indicate that the Waarre B was deposited under marginal to shallow marine rather than a fully marine setting. Unit B of Buffin (1989) is a predominantly grey to black, carbonaceous siltstones and claystones. It contains minor glauconite and contains palynological assemblages ranging from marginal to very shallow marine environments.

The upper Waarre B and the lower part of the Ca record the greatest sustained marine influence in the Waarre Sandstone. Cored sequences in Casino-2 and -3 record low to moderate proportions of microplankton and a regressive package with environments of deposition ranging from shelfal marine at the base to shallow water and shoreline facies (Lemon, 2003). Tidal channels, tidal flats, barrier bars and offshore bars were interpreted in the cored intervals. Reservoir properties are excellent. Depositionally the Ca is not dissimilar to the underlying upper Waarre A i.e. a sand dominated, lower delta plain setting. Mineralogically, a significant change in sediment provenance and depositional environments is apparent in Ca sands compared to Waarre A. Volcanic lithics are absent in Ca and there is a decline in feldspar and total lithics content. This was interpreted as the result of the cut-off of the volcanic derived source region whilst continuing sediment supply from a metamorphic/igneous terrane (Phillips, 2004).

The Waarre Ca represents a return to a sand prone depositional system with shallow marine through to fluvial facies being present. The Mussel Platform west of Pecten-1A appears to be a non depositional high with the area between Pecten-1A and Casino acting as a terrace to the Shipwreck Trough. Preserved thicknesses of Ca on the terrace range from 13m at Conan-1 to 45m at Casino-2 and 53m at Mussel-1. These thicknesses compare to 114m at Minerva-1, >100m at Geographe-1 and 166m at Thylacine-1 within the Shipwreck depocentre. It is considered that the subsequent erosion event at basal Cb (K77) may have had as much effect as the differing depositional rates for shaping this variance in Waarre Ca representation. There is evidence for truncation of the Ca sequence by the K77 across the Casino Field.

There is a distinctive change in dominant facies within the Unit C from a lower, finer grained, marine influenced to a dominantly medium to coarse grained fluvial dominated system. The subdivision is noted in stratigraphic tables by Partridge (2001) as Units Ca and Cb and is adopted in this study as it is important in delineating a major sequence boundary as well as trends in both reservoir quality and distribution.

The change to a fluvial dominated sequence of the upper Waarre Cb is recorded throughout wells in the Port Campbell Embayment, Mussel Platform and the Shipwreck Trough and the associated erosion at the base of the fluvial system (K77) greatly influences the distribution of the underlying Waarre units in some wells. The sands in Waarre Cb are mostly medium to coarse grained quartzarenites with good to excellent reservoir qualities. The fluvial sands of the Waarre Cb in Casino-2 and -3 represent a period of subsidence along the western flank of the Shipwreck Trough coincident with the progradation of fluvial systems into the area. The basal part of the Cb is fluvial dominated with greater marine influence upwards. This trend is seen in other wells in the area.

Transgression and inundation of the Waarre Cb resulted in the deposition of the marginal marine and shallow marine Flaxman Formation throughout the area. The unit consists predominantly of finer grained sediments with shale and siltstone intervals characterised by glauconite and siderite. The Flaxman Formation was described as Waarre Unit D in the Buffin (1989) study although the unit had already been described as a separate formation by Bock & Glenie (1965).

The Flaxman Formation is absent in Casino-1 and -2 having been eroded by the K85 Unconformity – see below for further details.

The relatively stable eastern flank of the Mussel Platform could, in a gross sense, be regarded as a sediment bypass zone. The bulk of the sediment has been transported across the Platform and deposited in the accommodation space provided by the Shipwreck Trough. The Waarre C penetrations in the Shipwreck Trough all contain sediments deposited in settings ranging from fluvial through to shallow marine, indicating several small scale transgressive-regressive cycles.

The Casino wells were the first wells to drill the central southeastern part of the Mussel Platform and, in addition to discovering gas, have allowed a significant improvement in the understanding of the regional geology to be made.

The biostratigraphic data from the Casino wells has modified the pre Casino-1 (Figure 3.2.1-e) understanding of the stratigraphy of the eastern part of the Mussel Platform. The correlation between Pecten, Casino and Minerva (Figure 3.2.1-c) clearly shows that the Waarre C in the centre of the Shipwreck Trough e.g. Minerva-2A (232m), is considerably thicker than that encountered on the Mussel Platform e.g. Casino-3 (53m).

Figure 3.2.1-e: Pre-Casino-1 stratigraphic chart *(refer to end of section for this figure)*

The equivalent to the upper part of the Waarre Ca in Minerva-2A, ~70m, is missing at Casino. In addition there is a considerably greater thickness of Waarre Cb at Minerva compared to Casino, 152m at Minerva-1 versus 28m at Casino-3. The Waarre Cb in Casino probably represents the upper part of the Cb equivalent in Minerva, but the biostratigraphic control is insufficient to prove this. However the biostratigraphy work does demonstrate that the boundary between the Ca and Cb in Casino represents a significant period of non-deposition. The chronostratigraphic column for the offshore Otway area incorporating the three Casino wells is shown in Figure 3.2.1-f.

Figure 3.2.1-f: Post-Casino-3 stratigraphic chart *(refer to end of section for this figure)*

The significant thickness changes can be explained in a regional sense by the effect of the K77 event at the Ca/Cb boundary and the differential subsidence between the Shipwreck Trough and the Mussel Platform. The monoclinal, eastern flank of the Mussel Platform controlled the distribution of sediment in the Casino area. West of the monocline i.e. Casino and the Mussel Platform, the Waarre is considerably thinner and contains at least one significant unconformity e.g. K77 Event. The K77 is thought to coincide with the initiation of the first phase of rifting along the Sorell fault system The WNW-ESE trending embayment, within which Casino lies, is probably one of several along the eastern flank of the Mussel Platform providing sediment to the more rapidly subsiding Shipwreck Trough.

A major time break is preserved in the well sections across the Mussel Platform. A major erosive event during the Mid Santonian (K85 Unconformity – also documented previously as the Shipwreck Unconformity) has resulted in a regional angular unconformity. This event coincides with the initiation of sea floor spreading along the eastern Australian margin and the rifting associated with the beginning of trans-tension along the Sorell fault system. In the Casino region, the effect of the K85 is well documented with the maximum erosion in Casino-1 (Waarre B to Belfast Mudstone section missing). The overlying mid Santonian section (Skull Creek Mudstone) forms the effective seal for the preserved Waarre A subcrop in Casino-1 and the Waarre Cb subcrop in Casino-2. There is more preserved Turonian section in Casino-3 where the Waarre Cb and Flaxman Formation were intersected and this is also the case in the nearby La Bella well. In the Shipwreck Trough, approximately 200 metres of additional preserved Belfast Mudstone section is intersected in the Minerva wells.

This page intentionally left blank

3.3 Structural Mapping

3.3.1 Seismic Database

The Casino field is covered by a 3D survey acquired in October/November 2001. Altogether, a total of 25,430.4 sail line km of CMP data were gathered. This provides a full-fold coverage of some 575 sq km comprising of 997 in-lines at 12.5 metres spacing. The PSTM processing of the data was completed in June 2003.

The overall quality of the data varies from good at shallow time from sea-bed down to ca. 1.6 seconds TWT when the seismic reflections start to become more incoherent and discontinuous in nature. The Casino field reservoirs are confined in an interval of fairly good reflection quality and reasonable signal to noise level.

The present post-Casino-3 seismic review is concerned primarily with a more detailed delineation and mapping of the Waarre C and Waarre A reservoirs. The near stack PSTM data are more suitable for this purpose as their ray paths are closer to normal incident and therefore give more accurate structural and clearer lithological imaging i.e. imaging the tops and bases of different lithological units. Fluid response behaviours are more commonly observed on far angle data. The near stack data are therefore used in the post-Casino-3 seismic review and inversion work.

Figure 3.3.1-a: Extent of Casino 3D seismic survey and well locations
(refer to end of section for this figure).

3.3.2 Time Interpretation – Final Field Mapping

The Casino-3 well provides an important calibration point in the full field delineation and modelling of the main Waarre C and Waarre A reservoirs. The well effectively delineates the northern extent of the Waarre C accumulation by confirming the GWC. The main objective of the geophysical work was to update the pre-Casino-3 interpretation, extend it to include two to three fault blocks of the aquifer to the north and re-run the seismic inversion. The geophysical part of this work called for a fresh and more meticulous seismic interpretation of the Casino field. The workflow behind the seismic inversion is discussed in more detail in Section 3.4.

The horizons interpreted are given in the table below.

Horizon	Lithological	Horizon Colour	Seismic Event	Interpretability	Exploration – Structural Significance
FC_Top_Waarre Cb	Top Waarre Cb	Black	Top Low Impedance	Fair	Represents uppermost limit to Waarre sands
FC_Top_Waarre C Low_Impedance	Top Waarre C Main pay	Red	Top Low Impedance	Good	Top of Main Waarre C pay
FC_Base_Waarre_C	Base Waarre C	Dark red	Base Low Impedance	Good	Base of Main Waarre C pay
FC_Top_Lower_ Waarre_A	Top Lower Waarre A	Blue	Top Low Impedance	Good	Top of Lower Waarre A pay
FC_Base_Waarre_A	Base Waarre A	Green	Base Low Impedance	Good	Base of Lower Waarre A pay

Table 3.3.2-a: Table of seismic horizons interpreted.

The nature of the inversion workflow essentially resulted in two time interpretations being made.

The initial interpretation was a based on the *band limited* seismic volume. This dataset allowed a more accurate picking of the tops and bases of the reservoir intervals to be made and reduced the number of misties within the interpretation. Reducing the misties is essential before the model based inversion is carried out.

The resulting interpretation was then used as the framework for a high resolution model based inversion. The second phase of interpretation used the *model based* impedance volume to further refine the picks.

3.3.3 Depth Conversion and Mapping

Time to Depth Conversion in Petrel

Depth conversion of the entire 3D model took place in Petrel using a mixture of velocity grids and average velocities.

The datum was provided by a Mepunga horizon time and depth grid pair. An interval velocity grid was then used to derive the top of the Upper Waarre Cb horizon / top reservoir horizon, and a second interval velocity grid was used to reflect the average interval velocity of the Waarre reservoir unit (combined Waarre C, B and A units).

All resultant surfaces were tied to the well data using the minimum curvature method. The time to depth conversion details are provided in Table 3.3.3-a.

The two way time grid of the Top Waarre C horizon is displayed in Figure 3.3.3-a, together with a section of 3D seismic data.

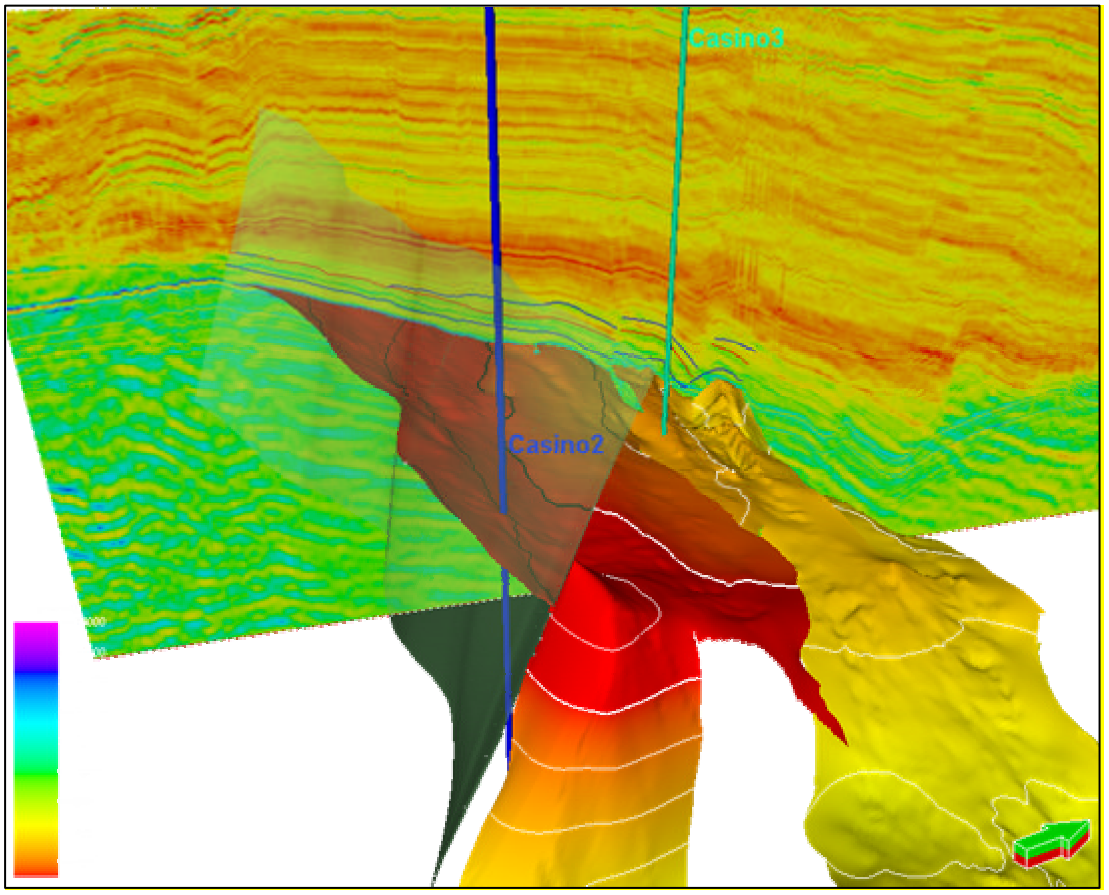

Figure 3.3.3-a: Top Waarre C TWT model with 3D seismic backdrop.

The residual values given in Table 3.3.3-a are negative when the time to depth conversion method creates a surface that is too shallow at the well locations. As mentioned, the minimum curvature method was used to flex the surfaces to match the picks at the well locations. The poorest tie is generally observed at the Casino-2 location.

Different time to depth conversion techniques were tried, prior to landing on the one described here.

Horizon	Velocity grid / method	Well Top Pick	Casino 1 residual (m)	Casino 2 residual (m)	Casino 3 residual (m)
Datum	Mepu_time_250304 combined with Mepu_welltied_dep_250304				
Top Upper Cb	Mepu_top_waarC_int_vel_260304 From datum	Top Waarre Cb	-	19.0	-3.3
Top C main pay	WaarCb_A_int_vel_290304 From Top Upper Cb	Waarre Cb main pay	-	17.6	-4.0
Base C reservoir	WaarCb_A_int_vel_290304 From Top Upper Cb	Waarre Ca1	-1.4	23.4	-1.7
Top Lower A	WaarCb_A_int_vel_290304 From Top Upper Cb	Top Lower Waarre A2	18.7	17.6	-6.4
Base A	WaarCb_A_int_vel_290304 From Top Upper Cb	Base Lower Waarre A	11.8	19.0	-3.2

Table 3.3.3-a: Time to depth conversion details.

The resultant "Top Upper Cb" depth horizon was exported as a 2D grid, and compared with the surface created following the same methodology, but using Petrosys. The difference is minimal, centring around the faults where the 3D model attempts to model "more realistic" fault cuts. The difference grid is given in Figure 3.3.3-b. Yellow and green values indicate very little difference (close to zero); dark blue and red values indicate the biggest differences, which are centred on the fault cuts. Interestingly though, there is still a mistie in the Casino-2 area, which appears linked to the high residual in this area, and the subsequent need to adjust the surface here to match the well data.

Depth maps for each of the horizons are shown in Figures 3.3.3-c, -d, -e, -f & -g and contained in Enclosures 3.3.3-a, -b, -c, -d &-e.

Figure 3.3.3-c : Top Waarre C low impedance depth map *(refer to end of section for this figure)*

Figure 3.3.3-d : Top Waarre C Main Pay depth map *(refer to end of section for this figure)*

Figure 3.3.3-e : Base Waarre C Pay depth map *(refer to end of section for this figure)*

Figure 3.3.3-f : Top Lower Waarre A depth map *(refer to end of section for this figure)*

Figure 3.3.3-g : Base Waarre A depth map *(refer to end of section for this figure)*

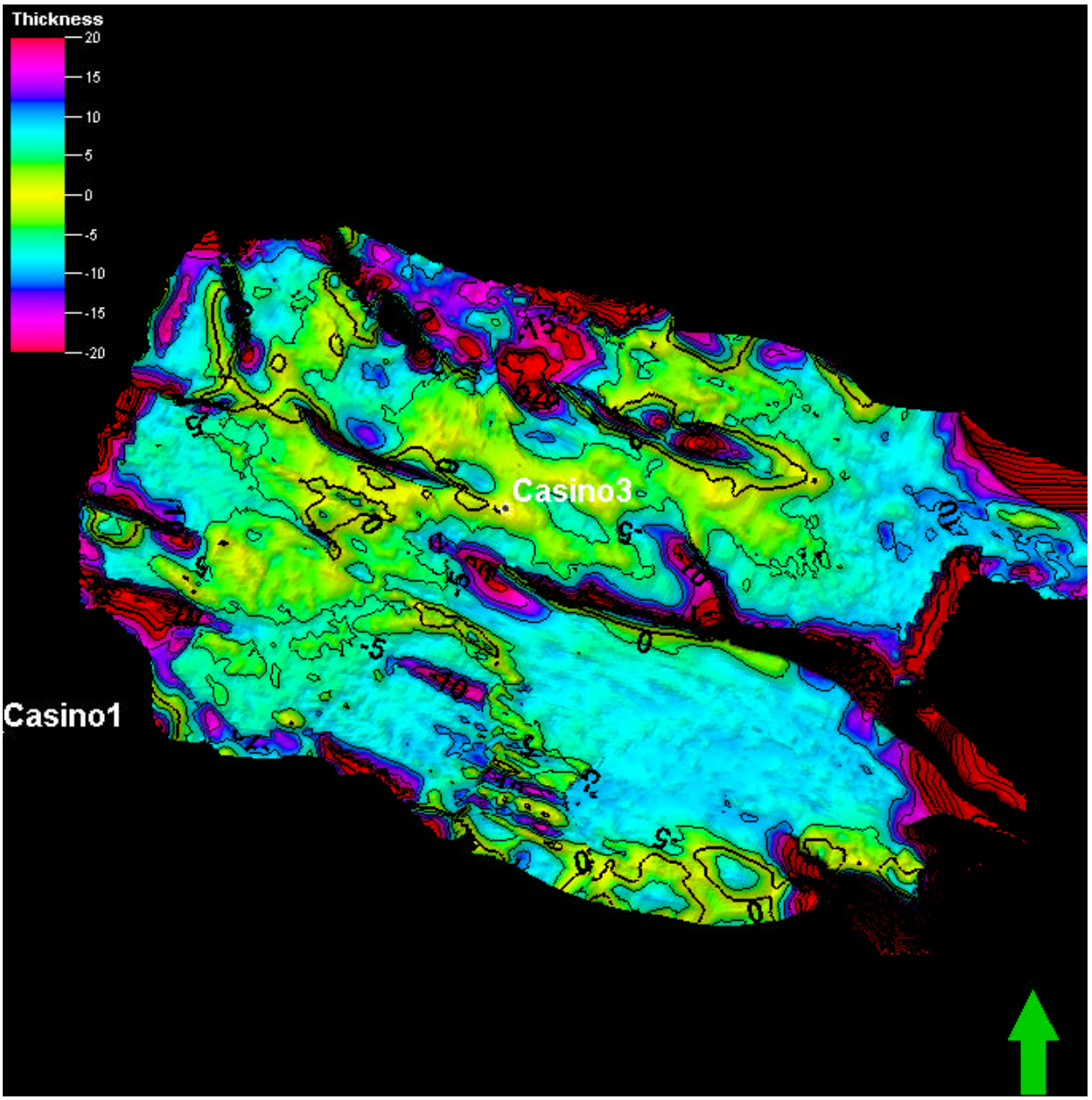

Figure 3.3.3-b: Difference map: Top Waarre Upper Cb Petrel vs Petrosys

Final Depth Maps and Trap Description

The essential shape of the Casino structure has not changed. Casino is a well defined tilted fault block, controlled to the south by a ~WNW-ESE trending fault and dip closed in the other directions.

There are some differences between the new depth maps and the pre Casino-3 maps. The bulk of these can be attributed to the re-picking using the higher resolution impedance datasets. The gross rock volumes (GRVs) derived from the two sets of maps are summarised in Section 3.12.

3.3.4 Depth Mapping Uncertainties

Two Way Time Uncertainty

Although the impedance datasets have allowed a fine tuning of the tops and bases of the gas bearing intervals the TWT interpretation is fairly straightforward. A comparison between Santos' TWT interpretation

and that of JV partner Peedamullah Petroleum Pty Ltd (Australian Worldwide Exploration) showed them to be very similar. There is little ambiguity in picking the Waarre sands over the bulk of the field.

Velocity Uncertainty

Casino-3 well provided an important velocity control point on the northern flank of the Casino structure. With two crestal wells and one on the flank good velocity control was available over the field.

Depth Maps - Sensitivities

Some work was undertaken using Petrosys to investigate the sensitivity of GRV to different gridding algorithms. Petrosys has eleven algorithms for the gridding process inherent to the well tie process. The procedure was to mimic the depth conversion of the Petrel 'base case,' carried out using the 'minimum curvature' gridding algorithm, and then extend it by using all of the gridding algorithms available in Petrosys.

To conserve time, the depth conversion procedure was carried out for all 11 gridding algorithms down to the Upper Waarre Cb horizon. Each of these grids was then subtracted from the base case to observe which gridding algorithms were most anomalous. The three most anomalous gridding algorithms were found to be 'distance weighted average', 'projected slope' and 'least squares plane'. These were then used to well tie the deeper Base C horizon to complete the container for volumetric calculations.

The volumetric calculations were carried out in Petrosys using the top and base grid volume calculation tool. The calculations were forced to honour the Waarre C gas water contact (~1999m) with the shallowest level set to this depth in the calculations. The results of the volumetric calculations are summarised in Table 3.3.4-a.

Flex method	**Volume (Mm^3)**
Petrel base case (Min Curvature)	499
Projected slope	579
Least squares plane	537
Distance weighted average	528
Indepth Depth Conversion (V_{stack})	501

Table 3.3.4-a: GRV estimates using different gridding algorithms.

A separate depth conversion using stacking velocities was carried out using the InDepth software package to provide another sensitivity to the Petrel 'base case'. This required the input of the TWT grids for the Upper Waarre Cb and Base C horizons. InDepth then calculated an average velocity grid from the surface to the Upper Waarre Cb horizon using the stacking velocity cube. This grid was subsequently used to depth convert the TWT grid and the depth deviation scaling option was used to well-tie the grid. The same procedure was followed to determine an interval velocity grid between the Upper Waarre Cb and Base Waarre C horizons and consequently depth convert the Base Waarre C TWT grid. These depth grids were then exported to Petrosys to make a GRV calculation, the result of which can be seen in Table 3.3.4-a.

The greatest variation in GRV estimate associated with gridding algorithms is approximately 16% and was produced using the projected slope algorithm. The help option on Petrosys gridding methods suggests that each algorithm should be used on a fit for purpose basis and perhaps the datasets used in this case were not suited to the projected slope algorithm. The variance of the other two algorithms from the base case was less than 8%. Finally the variation between base case GRV and the one derived from stacking velocities was marginal and provides support for the accuracy of the depth conversion methodology used.

For details on the GRV range used in the GIP sensitivities see Section 3.12.

3.3.5 Fault Interpretation

The dominant fault trend in the Casino field is ~WNW-ESE (Fig 3.3.5-a). There are several subordinate faults around the field's NW and SE margins and more to the north in the water leg, but no single fault that subdivides the field.

One significant difference from the pre Casino-3 interpretation is the absence of NE-SW trending faults. The dip closure immediately southeast of Casino-2 is the only place where this difference in interpretation could have a major impact. The post Casino-3 interpretation has a very steep dip closure to the southeast of the field, where previously there was a fault interpreted. The lack of a fault implies direct communication with the aquifer. The location for the Waarre C development well is immediately west of Casino-2. Early water breakthrough due to water sourced from the southeast was recognised as a risk and assessed in the dynamic modelling (Section 4.2).

Figure 3.3.5-a: Petrel fault map *(refer to end of section for this figure)*

Figure 3.3.5-b: Petrel 3D fault map and Top Waarre C Main Pay depth structure *(refer to end of section for this figure)*

3.4 Seismic Inversion

3.4.1 Band-Limited Impedence (Coloured Inversion)

Generally, acoustic impedance data give a layer orientated image of the sub-surface whilst the standard reflectivity data give an interface orientated image. It is easier to relate an impedance section to stratigraphy. Often, it is also possible to infer reservoir parameters such as porosity, net-to-gross and permeability from impedance data. This, of course, cannot be achieved to perfection since these profiles contain detail, which is far beyond the seismic resolution. However, reasonable detail can still be obtained from thicker, individual sand bodies or gross sand intervals if the individual sands are below seismic resolution.

The algorithm used in generating the band-limited volume is the Coloured Inversion algorithm introduced by Hampson Russell in 2003. It is quick and produces robust results even in the presence of noise. The computation is performed in the frequency domain and does not require the derivation of a wavelet, which is often a crucial process in other inversion algorithms. The algorithm models an unconstrained sparse-spike inversion using a convolution process by finding an operator that matches the amplitude spectra of the seismic and acoustic impedance traces. It begins by finding a relationship between the amplitude of the acoustic impedance logs and the logarithm of the frequency. Next, it derives the amplitude spectrum of the inversion operator from the amplitude spectrum of the seismic data. The operator is then convolved with the seismic data to produce the impedance trace. Figure 3.4.1-a shows the frequency response of a seismic trace (top left diagram) and the corresponding derived operator both in frequency and time domains (top right and bottom right diagrams respectively). The transform function for deriving the operator is plotted in the lower left diagram for a broad range of frequencies in logarithmic scale. The function is computed from impedance logs and is theoretically assumed to span an infinite frequency range.

Figure 3.4.1-a: Plots of the frequency spectrum of a seismic trace, the transformed function and the derived band-limited coloured inversion impedence operator in frequency and time domains *(refer to end of section for this figure).*

Figures 3.4.1-b and 3.4.1-c show a section of the near stack PSTM data volume and the coloured inversion impedance volume through the Casino-1, Casino-3 and Casino-2 wells, traversing from west to east. The GR curve of each well has been inserted for easier identification of the main Waarre A and Waarre C reservoir units. Overall, the coloured inversion impedance section gives a crisper and cleaner imaging. The Waarre A and Waarre C sands show out clearly as low impedance units.

Figure 3.4.1-b: Near stack PSTM seismic line through Casino-1, 3 and 2 wells, GR curves are inserted to show the Waarre A and Waarre C reservoir units *(refer to end of section for this figure)*.

Figure 3.4.1-c: Coloured inversion impedance line through Casino-1, 3 and 2 wells. GR curves are inserted to show the Waarre A and Waarre C reservoir units. Note the good well tie of the main reservoir units *(refer to end of section for this figure).*

Interpretation of the Coloured Inversion Impedance Volume

The coloured inversion impedance volume is an improved dataset. It had greatly facilitated the picking and correlation of the tops and bases of the Waarre A and Waarre C sands. Faults were also easier to pick. The interpretation was carried out on every in-line and cross-line in order to achieve greater consistency and minimize mis-ties.

Events that were picked during the seismic interpretation are listed in Table 3.4.1-a below:

Event	GeoFrame Name	Colour	Pick Convention
Top Waarre C Main Pay	FC-Top-Waarre C main pay	Green	Top low impedance unit
Base Waarre Ca2	FC_Base_Waarre_C	Light Green	Base low Impedance
Top Upper Waarre A	FC_Top_Upper_Waarre_A	Red	+/- crossing on pstm
Top Lower Waarre A	FC_Top_Lower_Waarre_A	Purple	Top low impedance unit
Base Waarre A	FC_Base_Waarre_A	Blue	Base low impedance

Table 3.4.1-a: Events picked from the coloured inversion impedance volume.

Figures. 3.4.1-d, 3.4.1-e and 3.4.1-f show the picked events listed above at Casino-1, Casino-2 and Casino-3 well locations. Of the five picks, the Top Upper Waarre A was the only horizon that was not picked on the impedance data as it does not correlate with the top of a low impedance unit. The top of the sand unit however correlates rather closely with the +/- crossing on the PSTM seismic data (Figure 3.4.1-g). The Top Upper Waarre A horizon was therefore picked on the PSTM data set where it is more accurately depicted on the data set. All the five picks were interpreted on every in-line and checked on every cross-line over the mapped area at each level shown in Figures. 3.4.1-h, 3.4.1-i, 3.4.1-j, 3.4.1-k and 3.4.1-l. The Top Waarre C Main Pay marker tracks the top of the Waarre C sand which becomes eroded over the southwestern part of the field towards Casino-1. The coloured inversion impedance volume imaged the Waarre C sand quite clearly. Figures. 3.4.1-m, 3.4.1-n and 3.4.1-o are examples of some in-line impedance sections showing the extent of the Waarre C sand.

Figure 3.4.1-d: Casino-1 well to band limited impedance tie. Negative impedance is displayed in blue and positive impedance in red *(refer to end of section for this figure)*.

Figure 3.4.1-e: Casino-2 well to band limited impedance tie. Negative impedance is displayed in blue and positive impedance in red *(refer to end of section for this figure).*

Figure 3.4.1-f: Casino-3 well to band limited impedance tie. Negative impedance is displayed in blue and positive impedance in red *(refer to end of section for this figure).*

Figure 3.4.1-g: PSTM section through Casino-1 and 3 wells with GR and sonic curves inserted. Top Upper Waarre is picked at +/- crossing (yellow horizon). Negative reflectivity is displayed in blue and positive reflectivity in red *(refer to end of section for this figure).*

Figure 3.4.1-h: Top Waarre C main pay TWT contour map (dotted dark blue horizon) *(refer to end of section for this figure)*.

Figure 3.4.1-i: Base Waarre C TWT contour map (black horizon) *(refer to end of section for this figure).*

Figure 3.4.1-j: Top Upper Waarre A TWT contour map (purple horizon) *(refer to end of section for this figure)*.

Figure 3.4.1-k: Top Lower Waarre A TWT contour map (dotted light blue horizon) *(refer to end of section for this figure)*.

Figure 3.4.1-l: Base Waarre A TWT contour map (dark green horizon) *(refer to end of section for this figure).*

Figure 3.4.1-m: In-line 6152 showing extent of younger sand. Negative impedance is displayed in blue and positive impedance in red *(refer to end of*

section for this figure).

Figure 3.4.1-n: In-line 6194 showing extent of younger sand. Negative impedance is displayed in blue and positive impedance in red *(refer to end of section for this figure).*

Figure 3.4.1-o: In-line 6166 showing extent of younger sand. Negative impedance is displayed in blue and positive impedance in red *(refer to end of section for this figure).*

For porous reservoirs, map displays of average RMS impedance extracted from within the reservoir intervals can often clearly depict the extent of the gas in the reservoirs. Figure 3.4.1-p gives the map display of the average RMS impedance extracted between the Top Waarre C and Base Waarre C horizons. A strong impedance amplitude response conformable with the GWC TWT contour at ca. 1500 ms can be clearly observed. Figure 3.4.1-q shows the average RMS impedance display for the Waarre A sand. A strong impedance amplitude response can also be observed, but this does not extend all the way up-dip to the main south bounding fault. Figure 3.4.1-r is an impedance section (Line 2798) through the amplitude response. This probably indicates that there might be a deterioration of reservoir properties in the Waarre A sand up-dip from the strong amplitude response area.

Figure 3.4.1-p: Average RMS CI impedance between Top Waarre C and Base Waarre C interval (refer to end of section for this figure).

Figure 3.4.1-q: Average RMS CI impedance between Top Lower Waarre A and Base Waarre A interval (refer to end of section for this figure).

Figure 3.4.1-r: Cross-line 2798 showing extent of low impedance anomaly in Waarre A sand (refer to end of section for this figure).

3.4.2 Small Scale Faults and Ramp Closure Southeast of Casino-2

Dip maps were also computed for the Base Waarre C and the Top Lower Waarre A horizons in an attempt to detect the presence of any small scale faults that might truncate the Waarre C and Waarre A reservoirs. Figures 3.4.2-a and 3.4.2-b show the dip maps of the Base Waarre C and Top Lower Waarre A respectively. Several small lineaments or dip features could be observed in the main field area, but these were revealed to be the result of minor flexures (Figures 3.4.2-c and 3.4.2-d). They were deemed not to have partitioned or adversely truncated the Waarre C and Waarre A sands.

Figure 3.4.2-a: Base Waarre C dip map showing minor dip features *(refer to end of section for this figure).*

Figure 3.4.2-b: Top Lower Waarre A dip map showing minor dip features *(refer to end of section for this figure).*

Figure 3.4.2-c: Cross-line 2386 through dip feature at Base Waarre C northeast of Casino-2 well *(refer to end of section for this figure).*

Figure 3.4.2-d: Cross-line 2788 through dip features at Top Lower Waarre A west northeast of Casino-1 well *(refer to end of section for this figure).*

A notable difference between the pre-Casino-3 maps and those of the present seismic review is the presence of a ramp, as opposed to a fault, to the east of the Casino-2 well. The ramp is a concern as it may act as a conduit for influx of water especially during the production of gas from the Waarre C reservoir. The ramp has been mapped in some detail. Figure 3.4.2-e shows a traverse line of the near stack PSTM seismic data through the ramp. The Waarre C and to a lesser degree the Waarre A sands appear to extend quite a considerable distance down-dip. Some thickening of the sands down the ramp is also indicated. The

existence of some aquifer support up the ramp for the Waarre C and Waarre A sands should therefore not be precluded.

Figure 3.4.2-e: Traverse line of near stack PSTM seismic data through the SE ramp indicating possible aquifer support up the ramp for Waarre C and Waarre A sands *(refer to end of section for this figure).*

3.4.3 Model Based (MB) Impedance Inversion

Because of the thin nature of the Waarre C and Waarre A reservoirs, the preferred approach for inverting the Casino-3D seismic data is the model based technique. In this approach, the generalised linear inversion algorithm attempts to modify an initial starting model until the resulting derived synthetic matches the seismic trace within some acceptable bounds. For the approach to yield meaningful results, it is important to provide the algorithm with an accurate structural framework. The horizons interpreted from the coloured impedance volume provide such a framework for the model based inversion. The framework was then populated with acoustic impedance traces generated by the triangulation and linear extrapolation of the log derived impedance traces of Casino-1, Casino-2 and Casino-3 wells to produce the starting impedance model.

When correctly applied, model based inversion is a very powerful sub-surface modelling tool. Depending on the objectives, it can be deployed for extracting information on lithologies, fluids or both from seismic. This is normally accomplished by a careful choice of input data and proper design of the starting impedance model. In the case of the present study, lithologies and reservoir properties were the primary objectives. The Casino near-stack PSTM 3D seismic volume was used because the data were less affected by the hydrocarbon effects than the far-stack data. The starting impedance model was designed using all the three Casino wells. Away from the wells to the north and to the east, the impedance profiles of Casino-3 and Casino-2 wells were assumed to persist and extrapolated linearly.

The inversion algorithm also required a wavelet to be supplied for the deconvolution of the seismic reflectivity data to impedance which was then used to correct the starting model. To achieve this end, numerous wavelets were extracted, both statistically and deterministically, at Casino-1, -2 and -3 well locations using all the available options (Figures 3.4.3-a and 3.4.3-b). The wavelet that yields the best synthetic to seismic match is a 200 ms wavelength constant phase wavelet extracted at Casino-3 location (Figure 3.4.3-c). A match of more than 79% correlation was achieved with the wavelet and it was selected for the final inversion. At Casino-1, -2 and -3 well locations the wavelet would yield inverted impedance to log impedance match of 92%, 91% and 97% respectively (Figure 3.4.3-d).

Figure 3.4.3-a: Extracted wavelets at Casino-1, Casino-2 and Casino-3 wells (200 ms constant phase wavelet) *(refer to end of section for this figure).*

Figure 3.4.3-b: Frequency spectrum of wavelets at Casino-1, Casino-2 and Casino-3 wells *(refer to end of section for this figure).*

Figure 3.4.3-c: Casino-3 seismic to synthetic match *(refer to end of section for this figure).*

Figure 3.4.3-d: Inversion using Casino-3 wavelet (MB Stochastic 40% model 60% seismic) *(refer to end of section for this figure).*

The algorithm then solved for the amount of corrections to be applied to the starting model from the seismic derived impedance. The corrections were applied iteratively until a good match was obtained between the input seismic trace and its corresponding synthetic trace. The computation option selected for the inversion was the stochastic approach with 60% weight on seismic and 40% weight on starting model. This option yielded the maximum correlation between well impedance and the inverted impedance after a series of trial inversion runs using different inversion algorithms and various combinations of parameters.

Figures. 3.4.3-e and 3.4.3-f show on map view the average starting impedance for the Top/Base Waarre C and Top Lower/Base Waarre A interval respectively. Figures. 3.4.3-g and 3.4.3-h show the model based results at the end of the inversion. The maps depict higher impedance trend and probably imply poorer

Waarre C sand development in areas to the north and northwest of Casino-3 although the starting impedance model used a low impedance profile extrapolated from that of Casino-3. This probably indicates that the inversion algorithm was doing a good job in correcting the impedance model in line with the observed seismic trend. Towards the east of the Casino field, the inversion yielded low impedance intervals. The low impedance implies better sand development in the easterly direction. This is very much in agreement with the trend observed in the Shipwreck Trough immediately to the east where the Waarre sands are considerably thicker than at Casino.

Figure 3.4.3-e: Average initial starting model impedance between Top Waarre C and Base Waarre C *(refer to end of section for this figure).*

Figure 3.4.3-f: Average initial starting model impedance between Top Lower Waarre A and Base Waarre A *(refer to end of section for this figure).*

Figure 3.4.3-g: Average MB inversion derived impedance between Top Waarre C and Base Waarre C *(refer to end of section for this figure).*

Figure 3.4.3-h: Average MB inversion derived impedance between Top Lower Waarre A and Base Waarre A *(refer to end of section for this figure).*

Figures. 3.4.3-i and 3.4.3-j show sections of the model-based inversion impedance data through the Casino-3 and Casino-1 wells respectively. The inversion impedance shows a good match to the log impedance. Overall, it has a higher resolution. The Upper Waarre Cb sand, which was otherwise difficult to resolve on both the PSTM seismic and the coloured inversion data, now stands out quite clearly.

Figure 3.4.3-i: Matching MB impedance to well at Casino-3 *(refer to end of section for this figure).*

Figure 3.4.3-j: Matching MB impedance to well at Casino-1 *(refer to end of section for this figure).*

Interpretation of the Model Based Impedance Volume

The model based impedance volume gives a more detailed imaging of lithologies. It allows the Upper Waarre Cb sand unit to be mapped in some detail. The volume also allowed the top of the main Waarre C sand to be further defined. The volume is also used for characterising the properties of the reservoirs of Casino field. Figures 3.4.3-k, 3.4.3-i and 3.4.3-m show the refined reservoir picks on the model based impedance volume. The GR, density, p-velocity, computed log impedance and porosity curves sampled in time are also displayed to indicate the position of the picks. The GR, computed log impedance and porosity curves tracks the MB inversion impedance curves quite closely.

Figure 3.4.3-k: Reservoir picks on MB impedance at Casino-3 well *(refer to end of section for this figure).*

Figure 3.4.3-l: Reservoir picks on MB impedance at Casino-1 well *(refer to end of section for this figure).*

Figure 3.4.3-m: Reservoir picks on MB inversion impedance at Casino-2 well *(refer to end of section for this figure).*

An average impedance extraction has also been carried out for the Top Waarre Cb plus 4 ms TWT interval, to capture the Upper Waarre Cb sand seen at Casino-3. The low impedance feature immediately east of the Casino-3 well indicates an area where the sand is thicker than at Casino-3 i.e. >3.5m (Figure 3.4.3-n). It has an area extent of ca. 0.73 sq km.

Figure 3.4.3-n: Map of average impedance extraction in Top Waarre Cb plus 4ms interval showing probable extent of Waarre Cb sand *(refer to end of section for this figure).*

Accuracy of model based inversion impedance

There have been some concerns regarding the accuracy of the initial impedance model, especially its prediction of the low impedance interval to the east of the Casino-3 well, within the water leg. This prediction might be too low and could give rise to the lower impedance result in the eastern area i.e. the extrapolation from the Casino-3 control point may have resulted in a model predicting too low impedance for the thickened interval to the east. There was also concern regarding the use of too many wells in the model which might result in an overly constrained model. Both these concerns were addressed by running two further model based inversions on contrastingly different starting models. The starting models are as follows:

(1) A starting model constructed using only Casino-1 and Casino-2 wells.
(2) A starting model derived from AOK velocity without wells (refer Appendix A for details).

Altogether three impedance volumes were used in the geological modelling to assess the impact of the initial starting impedance model on reservoir properties and gas in place. They are the MB inversion impedance volume using initial model derived from Casino-1, -2 and -3 wells; the MB inversion impedance volume using initial model derived from Casino-1 and -2 wells and the MB inversion impedance volume using initial model derived from AOK velocity. Figures 3.4.3-o, 3.4.3-p and 3.4.3-q show sections comparing the impedance results from the 3-well case (B) and the AOK velocity(C) to the coloured inversion volume (A). The average impedance map of the AOK velocity derived impedance volume (Figure 3.4.3-r) shows a low impedance feature very similar to that extracted from the coloured impedance (Figure 3.4.1-p). The AOK velocity derived impedance was probably modelling the fluid effects rather than the lithologies. The volume was included in the geological modelling exercise as one of the three probable outcomes to capture the range of possible uncertainties. The 2-well impedance volume was included as an intermediate outcome to address the concern of using an overly constrained 3-well model.

Figure 3.4.3-o: Sections through Casino-3 comparing (A) coloured impedance (B) 3 well MB impedance and (C) AOK velocity derived MB impedance *(refer to end of section for this figure).*

Figure 3.4.3-p: Sections through Casino-2 comparing (A) coloured impedance (B) 3 well MB impedance and (C) AOK velocity derived MB *(refer to end of section for this figure).*

Figure 3.4.3-q: Sections along IL6196 comparing (A) coloured impedance (B) 3 well MB impedance and (C) AOK velocity derived MB impedance *(refer to end of section for this figure).*

Figure 3.4.3-r: Average AOK velocity derived impedance between Top Lower Waarre C and Base Waarre C showing low impedance feature similar to that seen in the coloured impedance volume *(refer to end of section for this figure).*

3.5 Reservoir Geology

3.5.1 Depositional Environment and Controls on Sedimentation

Section 3.2 described the regional geological setting for the Casino area during the deposition of the Waarre Formation.

The sands making up the Waarre A and C reservoirs were deposited in a variety of settings, ranging between fluvial and shallow shelfal marine, along the south-eastern margin of the Mussel Platform (Figure 3.5.1-a). Analyses of the data from the 3 wells, including two cores from the Waarre C, have enabled a more detailed understanding of the depositional environments to be developed for the Casino area. The core based interpretation has driven the generation of the depositional models for the Waarre C, with additional information from petrological and biostratigraphic studies helping refine the models for both intervals.

Figure 3.5.1-a: Structural elements in the Casino area *(refer to end of section for this figure).*

Controls on sedimentation during deposition of the Waarre A

The Waarre A sands are associated with shorelines influenced by underlying fault controlled structures of the Mussel Platform. An apron of sands was deposited under shallow marine to brackish settings in a WNW-ESE oriented embayment (Figure 3.5.1-b) in an overall transgressive setting. The embayment itself fed into the Shipwreck Trough area immediately to the east where the regional depositional setting for the Waarre A is a tidally influenced delta. Younger sands were deposited progressively closer to the hinterland. A condensed section of Waarre A is present at Pecten-1A, 13km NW of Casino, and this well is probably close to the depositional limit of the Waarre A in this part of the Mussel Platform. The uppermost Waarre A appears to have been subjected to a limited amount of erosion and a phase of reworking, prior to the deposition of the Waarre B (Figure 3.5.1-c).

Figure 3.5.1-b: Underlying structures controlling the distribution of the Waarre A *(refer to end of section for this figure).*

Figure 3.5.1-c: Upper Waarre A correlation highlighting the missing section in Casino 1 *(refer to end of section for this figure).*

Controls on sedimentation during deposition of the Waarre Ca and Cb

The marine interlude represented by the Waarre B was followed by a fall in relative sea level that led to the deposition of the shallow marine/littoral Waarre Ca. The WNW-ESE oriented embayment, controlled by the underlying faulted highs, was still influencing sedimentation. Figures 3.5.1-d & -e show a potential depositional setting for the lower and upper Waarre Ca respectively, based on the regional setting and core data. The limited amount of data makes these reconstructions rather speculative, but they do serve to give an idea of the depositional settings for the reservoir sequences.

Figure 3.5.1-d: Casino Embayment depositional environments – Lower Waarre Ca *(refer to end of section for this figure).*

Figure 3.5.1-e: Casino Embayment depositional environments – Upper Waarre Ca *(refer to end of section for this figure).*

The specific controls on the sedimentation of the Waarre Ca are as follows:-

- During the period when the basal part of the Waarre Ca was deposited, shallow marine shelf sediments covered at least the eastern part of the Mussel Platform. Large, low relief offshore bars were established over the slight breaks in slope associated with the larger, underlying faults in the area.
- The northward tilt of the underlying fault blocks combined with their easterly plunge created one or more triangular embayments that opened into the Shipwreck Trough.
- An approximately E-W oriented coastline was established along the line of one of the main faults south of Casino. This coastline marked the south-western limit of the Mussel Platform. The position of the exposed coast was influenced by the earlier bars.
- The depositional strike of the tilted, plunging fault block(s) was WNW-ESE on the southern side of the embayment, but nearer E-W on the north side of the embayment beyond the Casino wells (Figures 3.5.1-d & -e).
- During initial sedimentation of the Waarre Ca in the embayment, the shoreline was in its most westerly position (Figure 3.5.1-d). The sand influx from around the headland created a NW-SE barrier complex within the embayment along with an associated back barrier area around Casino-1 and -2. As the embayment filled, its southern shoreline migrated to the NE and by upper Ca times the barrier complex had moved to the eastern end of the fault block and an isolated tidal embayment was located in the north side of the block (Figure 3.5.1-e).
- Fluvial input to the embayment was minimal and the limited amount of associated mud was restricted to the western end of the embayment around a bayhead delta.
- The wave action along the southern coast, together with re-working of the exposed offshore bars, created a supply of clean sand that moved eastwards along the coast under the combined wave action and longshore drift. This may have supplied some sands to the Casino area (Figure 3.5.1-f), but the bulk of the Casino sediments came from the N/NW.

Figure 3.5.1-f: Sand transport around the margins of the Mussel Platform
(refer to end of section for this figure).

Waarre Cb

A sharp depositional break (K77) separates the Ca from the Cb in both Casino-2 and -3. This break has been confirmed by biostratigraphic work (Section 3.2) with the equivalent of the upper Waarre Ca in Minerva being absent in the Casino area.

The fluvial Cb identified in the Casino wells and also at Minerva and Thylacine in the Shipwreck Trough, indicates the palaeo-shoreline was at times a considerable distance from the Casino area. The large thickness differences between the Waarre Cb of Casino, Minerva and Thylacine reflect the greater accommodation space available in the Shipwreck Trough and highlight the fact that at times the Casino area was most probably an area of sediment bypass. The thickening of the Cb is seen on the seismic data and occurs to the northeast of Casino-2 and east of Casino-3 (Figure 3.5.1-g). When combined with the regional structural elements a ~WNW-ESE oriented fluvial system feeding onto the Shipwreck Trough is envisaged (Figure 3.5.1-h). This apparent thickening in the northeast of the study area is probably a combination of depositional thickening into the Shipwreck Trough and post depositional erosion.

Figure 3.5.1-g: Top Cb Main Pay to Top Ca1 isopach *(refer to end of section for this figure).*

Figure 3.5.1-h: Schematic Waarre Cb palaeogeography for Casino area
(refer to end of section for this figure).

The model based acoustic impedance seismic volume provides greater resolution over the reservoir interval. For example, in Casino-3 the ~3.5m sand at the very top of the Waarre C is now resolvable. The impedance data indicates this sand becomes thicker away from the well, but remains a separate sand above the main

Waarre C interval (Figure 3.5.1-i). The Waarre C encountered by Casino-3 is equivalent to the lower part of the thicker interval east of the well. The sketch on Figure 3.5.1-i also highlights the potential for a phase of erosion following the deposition of the Cb Main Pay, but prior to the deposition of the uppermost Cb sand seen at Casino-3.

Figure 3.5.1-i: Flattened seismic line through Casino 3 and annotated sketch *(refer to end of section for this figure).*

The specific controls on the sedimentation of the Waarre Cb are as follows:-

- The underlying structural control influencing the deposition of the Ca persisted through the deposition of the Cb,
- The contact between the Ca and the Cb represents the K77 Unconformity and the upper Ca present in the Shipwreck Trough was either eroded or never deposited in the Casino area,
- An increased thickness of Cb appears to coincide with the WNW-ESE orientation of the fault controlled embayment's axis,
- The drop in relative sea level resulted in the easterly advance of the fluvial system over the shoreline deposits of the Ca,
- There appears to have been some intra Waarre Cb erosion that removed a significant volume of Cb, prior to the uppermost Waarre sand in Casino-3 being deposited.

Although it is recognised that there are alternative interpretations, the above honours the available data and represents Santos' current working model for the Waarre A and C. It is important to note that the orientation of the various facies in shallow marine settings is difficult to constrain with the limited well data. See Section 4.10 (Static Modelling) for further details.

3.5.2 Intra Waarre Correlation

The internal subdivision of the Waarre in the Casino area is constrained by the stratigraphic framework provided by the palynological studies. The internal subdivision has been primarily based on the gamma log motif, using the core data where appropriate. Figure 3.5.2-a shows the correlation of the Waarre A for the three Casino wells and Figure 3.5.2-b shows the same for the Waarre C.

Some points to note regarding the correlation:

- Good biostratigraphic agreement with seismic picks,
- Erosion due to the K85 unconformity important,
- Waarre A – Further subdivision of the Upper Waarre A is difficult. The thickest section is in Casino-3, the thinnest in Casino-1, which suggests there has been erosion and the equivalent to uppermost Waarre A in Casino-3 is not present in Casino-1,
- The gas bearing Waarre Ca can be subdivided into 3 zones. Layer Ca4 present in Casino-2 is almost completely eroded in Casino-3 due to the K77 Unconformity,
- The fluvial Waarre Cb in Casino-3 thickens at the expense of the underlying Waarre Ca4,
- There appears to have been a post Waarre C Main Pay phase of erosion producing some depositional relief into which the latest Waarre Cb and the Flaxman Fm were deposited.

Figure 3.5.2-a: Waarre A correlation *(refer to end of section for this figure).*

Figure 3.5.2-b: Waarre C correlation *(refer to end of section for this figure).*

The main point to note about the internal correlation of the Waarre, and especially the Waarre C, is that it assumes lateral continuity of the units across the field. The gamma logs over the Waarre C allow a straightforward correlation and the core data supports the subdivision. Building a 3D facies model by extrapolating core constrained facies away from well control was not deemed appropriate with such a limited dataset.

3.5.3 Reservoir Facies

Waarre A

The sands of the Waarre A are interpreted to have been deposited during an overall rise in relative sea level and were deposited in shallow marine though to brackish settings. Phillips' (2004) study of sidewall cores (e.g. MSCT 4) recognised bioturbation indicating a marine influence and the palynological work confirmed this.

Waarre Ca & Cb

The Ca is dominated by back barrier through to open marine, muddy shelf environments. Barriers, tidal channels, washover fans and flood tidal delta facies have all been recognised from the cores. Figure 4.5.3-a shows the facies interpretation and correlation between cored intervals of Casino-2 & 3 and summarises the depositional facies that can be expected.

The Waarre Cb is dominated by fluvial sands, especially in the lower part of the interval, and these represent the best reservoirs of the field. The upper part of the Cb is less sandy and is thought to be more representative of a lower energy estuarine setting, but with very limited marine influence (G. Wood pers comm.).

In the static modelling context the most important properties of each facies are its reservoir properties and where possible facies with the same properties have been grouped together. See Section 3.10.2 for details on the subdivision of the reservoir into flow units.

Figure 3.5.3-a: Casino 2 & 3 core facies interpretation, correlation and schematic cross section *(refer to end of section for this figure)*.

3.5.4 Reservoir Thickness

The Lower Waarre A ranges from 41m in Casino-1 to 32m in Casino-2 and 27m in Casino-3. The interval has not been affected by immediate post depositional erosion or the later K85 event. The gas bearing Lower Waarre A1 & A2 subdivisions in Casino-1 & 2 are virtually identical in thickness, 30.9m and 30.3m respectively, although isopachs generated in the Petrel static model show greater heterogeneity than the wells suggest (Figure 3.5.4-a & -b). The total Lower Waarre A isopach, including the Calcite Cemented Zone, is shown in Figure 3.5.4-c.

Figure 3.5.4-a: Lower Waarre A1 isopach *(refer to end of section for this figure)*.

Figure 3.5.4-b: Lower Waarre A2 isopach *(refer to end of section for this figure)*.

Figure 3.5.4-c: Total Lower Waarre isopach *(refer to end of section for this figure)*.

The Upper Waarre A is thicker in the north and northeast of the Casino area and this is reflected in the well data. Casino-3 has a gross thickness of 28m compared to 19m and 24m at Casino-1 & 2 respectively. A minor phase of post depositional erosion and the major K85 unconformity are responsible for the distribution of the preserved Upper Waarre A in the Casino area (Figure 3.5.4-d).

Figure 3.5.4-d: Upper Waarre A isopach *(refer to end of section for this figure)*.

The K85 erodes into progressively older section towards the southwest and has stripped off the Waarre B and C in the Casino-1 area. A zero thickness line for the Waarre C extends in a WNW-ESE direction northeast of Casino-1, highlighting the stratigraphic element to the Waarre C trap.

Between Casino-2 and -3 the gas bearing Waarre C has a similar gross thickness (Figure 3.5.4-e). However the isopachs of the Ca4 (Figure 3.5.4-f) and the Waarre Cb Lower Main Pay (Figure 3.5.4-g) show that the latter thickens at the expense of the former at Casino-3. The K77 Unconformity separates the two intervals.

Figure 3.5.4-e: Top Waarre Cb Main Pay to Top Waarre Ca1 isopach *(refer to end of section for this figure).*

Figure 3.5.4-f: Waarre Ca4 isopach *(refer to end of section for this figure).*

Figure 3.5.4-g: Waarre Cb Lower Main Pay isopach *(refer to end of section for this figure).*

As discussed in 3.5.1, there is a marked increase in the thickness of the Waarre Cb in the northeastern part of the field and in the water leg east of Casino-3 (Figure 3.5.4-h).

Figure 3.5.4-h: Upper Waarre Cb isopach *(refer to end of section for this figure).*

This page intentionally left blank.

3.6 Petrophysics

3.6.1 Petrophysical Database

The following wells were used in the petrophysical review:

WELL	CORE NO	CUT (Drillers Depth)	RECOVERED
Casino-1			
Casino-2	1	(1762.9 – 1784 m) 21.1 m	19.3 m
Casino-3	1	(2004- 2031 m) 27.0 m	24.7 m

Wireline Logging

WIRELINE LOGS			
SUITE/RUN NO	**TOOL STRING**	**INTERVAL (MRT)**	**BHT (DEGC)**
Casino-1			
1/1	PEX-DSI	(PEX run in high resolution mode to 1650m)	80 (10.33 hrs since circ)
	GR	TD - 95	
	SGR (Spectral GR)	TD - 1650	
	Resistivity (HALS)	TD - 742	
	SP	TD – 742	
	DT (Upper Dipole)	TD – 1650	
	DT (Waveforms – Monopole)	TD – 500	
	NPHI/TNPH	TD – 742	
	RHOB	TD - 742	
1/2	MDT-GR	1524-2016	N/A
	29 points (8 good, 10 valid tight, 5 lost seals, 2 bad data, 5 curtailed & 3 samples collected)		
1/3	CST-GR	1520-2030	N/A
	(30 of 30 shots recovered)		
Casino-2			
1/1	PEX-DSI		79.5 (9.0 hrs since circ)
	GR	TD – 93	
	SGR (Spectral GR)	TD – 1650	
	Resistivity (HALS)	TD – 690	
	SP	TD – 690	
	HCAL	TD – 690	
	DT (Upper dipole)	TD – 1650	
	DT (Waveforms – Monopole)	TD – 93	

WIRELINE LOGS			
SUITE/RUN NO	**TOOL STRING**	**INTERVAL (MRT)**	**BHT (DEGC)**
	NPHI/TNPH	TD – 690	
	RHOB	TD - 690	
1/2	MDT-GR	1753.7-1944.5	
	(32 points, 13 good, 14 Curtailed/Tight, 3 lost seals, 2 unstable, 3 samples collected)		
1/3	CST-GR	1016 - 2076	
	(26 of 30 shots recovered)		
Casino-3			
1/1	PEX-DSI		83 (15.3 hrs since circ)
	GR	TD – Surface	
	Resistivity (HALS)	TD – 635.8	
	SP	TD – 635.8	
	HCAL	TD – 635.8	
	DT (Upper dipole)	TD – 635.8	
	DT (Waveforms – Monopole)	TD – 635.8	
1/2	MDT-GR	1611.2 -2063	85.5 (33.3 hrs since circ)
	(24 points - 15 normal, 2 lost seals, 7 curtailed, 5 samples collected)		
1/3	PEX-CMR-HGNS		83 (40.0 hrs since circ)
	SGR (Spectral GR)	TD – 635.8	
	CMR	TD – 1930	
	NPHI/TNPH	TD – 635.8	
	RHOB	TD – 635.8	
1/4	MCST	Run aborted	
1/4A	MCST	2102.5 – 1970.5	
	(13 MCST cores attempted, 13 recovered)		
1/5	CST-GR	Run aborted	
1/6	CST-GR	2077.7-1162.7	

WIRELINE LOGS			
SUITE/RUN NO	**TOOL STRING**	**INTERVAL (MRT)**	**BHT (DEGC)**
	(30 cores attempted, 20 purchased, 1 lost, 2 empty, 7 misfired)		

BOREHOLE FLUIDS			
WELL	**Casino-1**	**Casino-2**	**Casino-3**
Suite Number	1/1	1/1	1/1
Mud Type	KCL/Polymer	KCL/Polymer	KCL/Polymer
Mud Weight (Lb/G)	*10.2*	*10.3*	*9.95*
KCl	*8%*	*6%*	*2%*
Rmfohmm)	*0.138 @ 24 DEGC*	*0.153 @ 20 DEGC*	*0.123 @ 30 DEGC*
Rmc (ohmm)	*0.114 @ 24 DEGC*	*0.124 @ 20 DEGC*	*0.109 @ 30 DEGC*
Rm (ohmm)	*0.397 @ 24 DEGC*	*0.199 @ 19 DEGC*	*0.394 @ 30 DEGC*
MRT (DEGC)	*80 (10.33 hrs sinc circ)*	*79.5 (9.0 hrs sinc circ)*	*83 (15.3 hrs sinc circ)*

3.6.2 Evaluation Methodology

Data Preparation and Environmental Corrections

Wireline logs were quality controlled to ensure a consistent data standard was achieved across three wells including de-spiking and depth shifting. Casino-3 wireline logs were depth shifted -2.3m to tie wireline logger's casing shoe depth to the driller's casing shoe depth before any wireline cable stretch corrections were applied. As the main data suite for all three wells was acquired using the Platform Express Tool, the majority of the logs are supplied with full environmental corrections from the logging contractor.

Interpretation Technique

Wireline logs were analysed over the Waarre Sandstone using the Multimin software package in Geolog. Multimin is a probabilistic petrophysical technique that models the reservoir based on an initial model which honours the geology and is solved via a series of simultaneous equations, the product of individual mineral responses and fluid parameters.

Casino-3 was used to define the initial reservoir parameters for the model to be used in Multimin as it contained the most comprehensive wireline suite, a full hole core with Routine Core analysis (RCAL) and Special Core Analysis (SCAL), and a full XRD/SEM petrology report over the full hole core and side wall cores.

The core derived overburden corrected porosity and permeability results were used to calibrate the petrophysical model. While it is possible to use these parameters as input variables in Multimin this reduces the overall accuracy of the model outside the cored interval. By honouring the core data the model not only replicates the core results, but provides a consistent interpretation where no core exists. The SCAL results for the Formation Resistivity Factor (FRF or m) have been used directly in the model.

The basic model can be defined as follows:

Framework	***Clays***	***Fluids***
Quartz	Kaolinite	Formation brine
Orthoclase	Illite	Gas
Siderite		Barite

Subtle variations of the models were applied to Casino-1 and -2 due to variations in log quality. For example, Casino-1 PEF log was severely affected by barite and the model had to be simplified by removing one of the minerals to enable a successful solution to be calculated. It is noted that with KCL concentrations above 3%, the potassium concentration log is effectively swamped by potassium in the borehole and contractor corrections are not entirely appropriate. As a result, the potassium log was not used in the analysis.

Figure 3.6.2-a and Figure 3.6.2-b show two cross-plots used to define the initial models in the Waarre Sandstone.

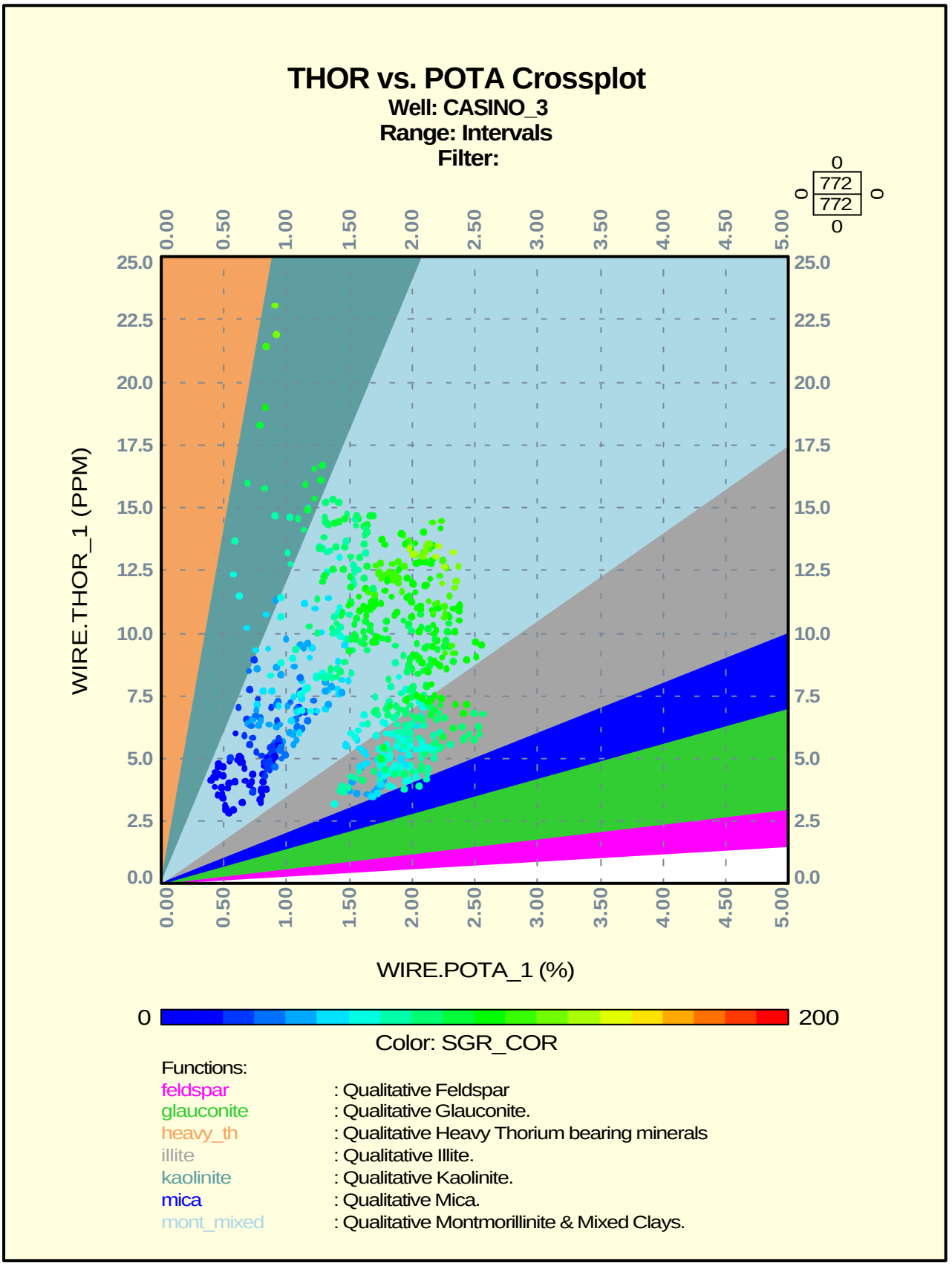

Figure 3.6.2-a: Spectral Gamma Ray Cross Plot.

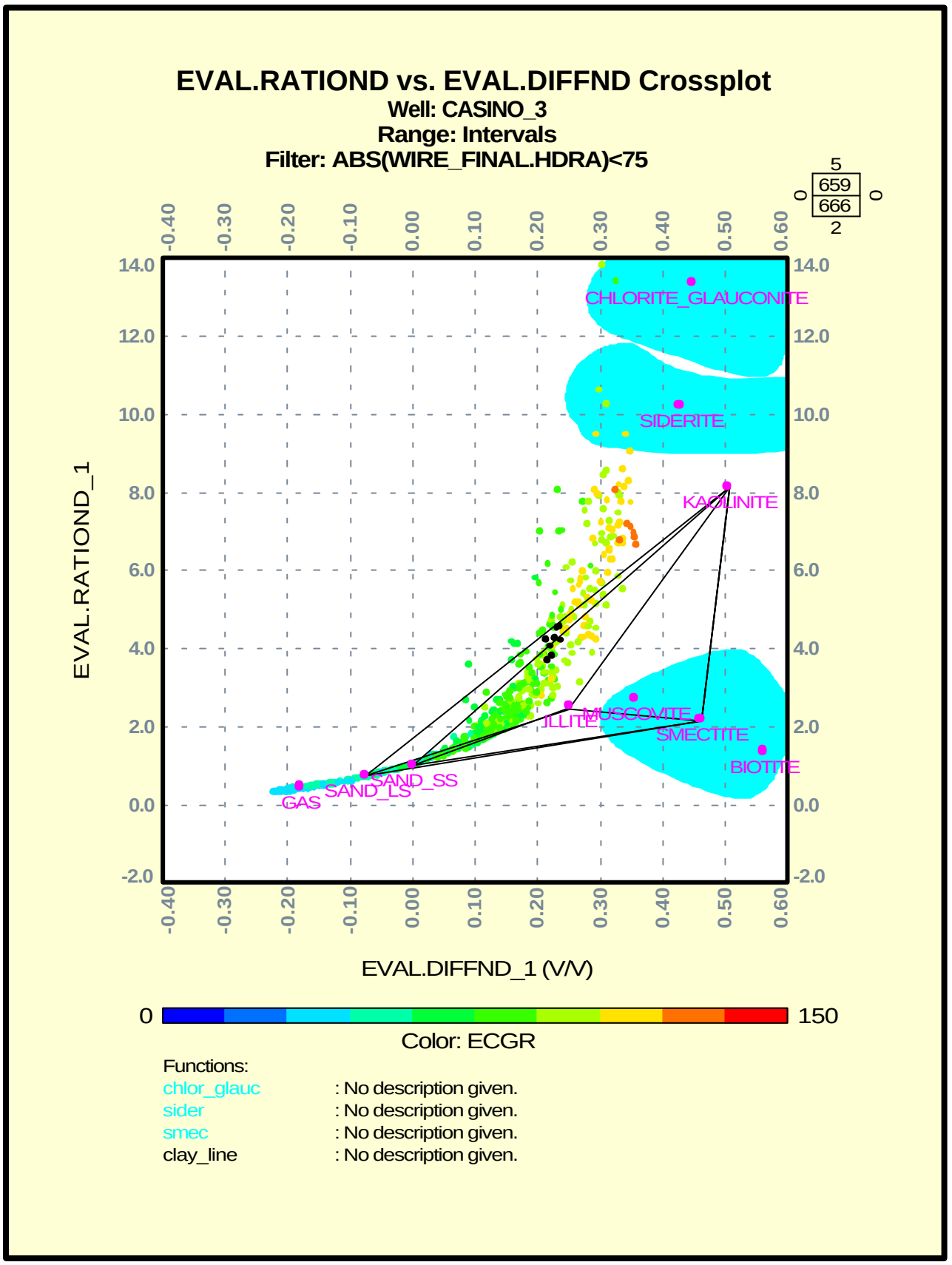

Figure 3.6.2-b: Ratio plot used to define the dominant clay minerals in the reservoir. The black points represent data points with ECGR higher than 150 API.

Using the various crossplots for each well and cross checking the validity of the modeled mineralogy using the core reports on Casino-1, -2 and -3 from Phillips (1993) it was possible to define the optimal suite of minerals for each of the wells.

The calculated volumes of minerals from Multimin were spot checked with the petrology reports.

Table 3.6.2-a (refer to the end of this section) summarises the model parameters.

Porosity Determination

Helium injection, ambient core plug porosity measurements have been corrected to Klinkenburg Overburden conditions. The net overburden conditions for determining the correction factor to be applied to ambient core porosity can be defined using the following equation:

$$S_t \cong S_v - P_i$$

Where S_t = Total Stress at reservoir depth, or Net Overburden Pressures, NOP (psi).
S_v = maximum vertical stress exerted by the weight of the overlying rock and sea water (psi).
P_i = initial reservoir pressure (psi).

Initial reservoir pressures are determined from MDT pressure measurements on the virgin reservoir. For Casino-3, two pressure regimes have been identified at 2820 psi for the Waarre Cb/Ca gas saturated reservoirs and 3100 psi for the water bearing Cb interval. The NOP also needs to be converted from an isostatic pressure measurement in the reservoir to one that is uniaxial, or the pressure applied to the core plug in the laboratory. Generally this has been accepted using a conversion factor of 0.62* NOP.

Using this conversion, the core plug values at 2200 psi are representative of the in-situ porosity. This has been cross-plotted versus the ambient core porosity, which in Casino-3 was recorded at 800 psi to remove any ambiguous expansion of the plug and subsequent regression to be calculated so as to apply a further conversion to those plugs which have not been selected for overburden corrections and is defined using the following equation and shown in Figure 4.6.2-c.

$$\Phi ob = 0.997 \Phi amb$$

Where,
Fob = Klinkenburg Overburden corrected porosity (v/v)
Famb = Ambient total core porosity (v/v)

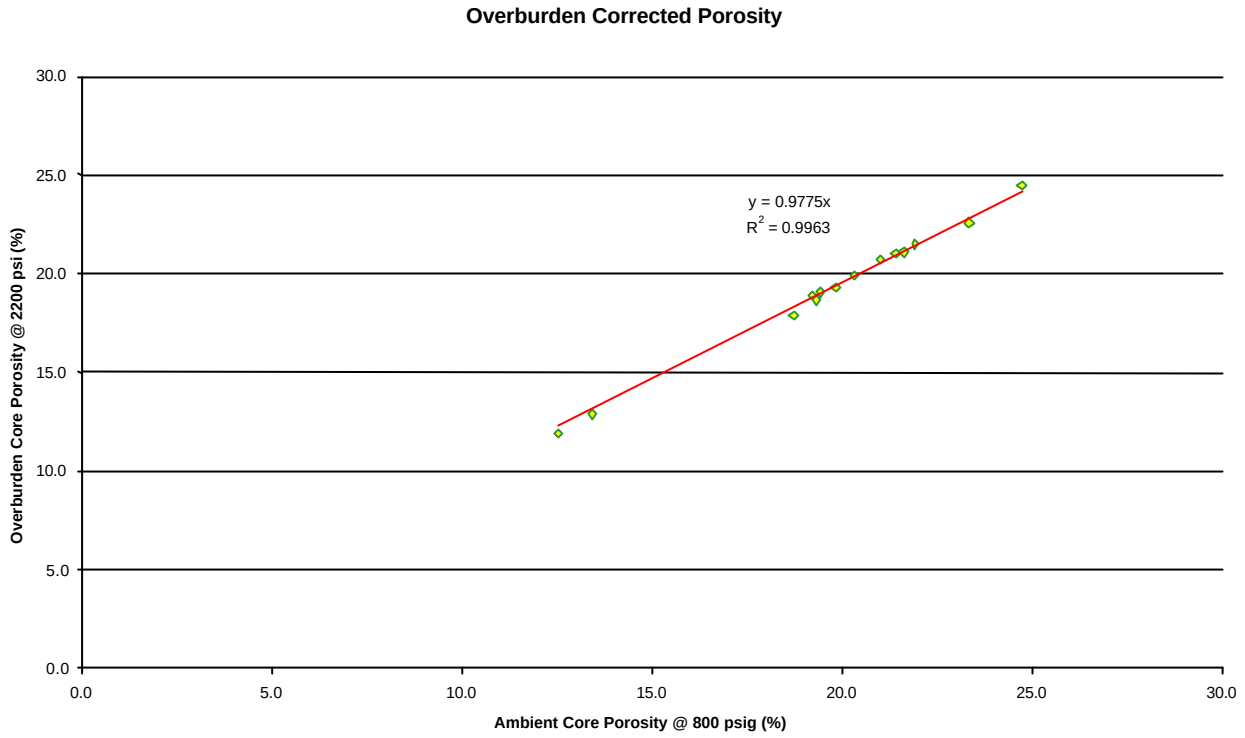

Figure 3.6.2-c: Porosity correction for Klinkenburg Overburden.

Overburden corrected core porosity was used as a calibration for the Multimin modeling. Total porosity calculated in the probabilistic approach is derived from a combination of the individual fluid components, which in the unflushed, or virgin reservoir zone is defined as follows:

$$Ft = Vol_{free\ water} + Vol_{hc} + Vol_{bound\ water}$$

Where;
$Vol_{free\ water}$ = Volume of free water in the system
Vol_{hc} = Volume of hydrocarbon (gas) in the system
$Vol_{bound\ water}$ = Volume of bound water (attributed to the clays) in the system.

The calculated porosity from Multimin was checked with the overburden corrected core porosity and an acceptable fit was observed through the cored interval, therefore it was assumed that outside of this range the model would be acceptable in defining the porosity.

Permeability

Core permeability was also corrected to overburden conditions using a similar approach. This is defined using the following equation and shown in Figure 3.6.2-d.

$$kob = 0.805kam$$

where;

kob = Klinkenburg Overburden Corrected permeability (mD)
Kam = Ambient core permeability (mD)

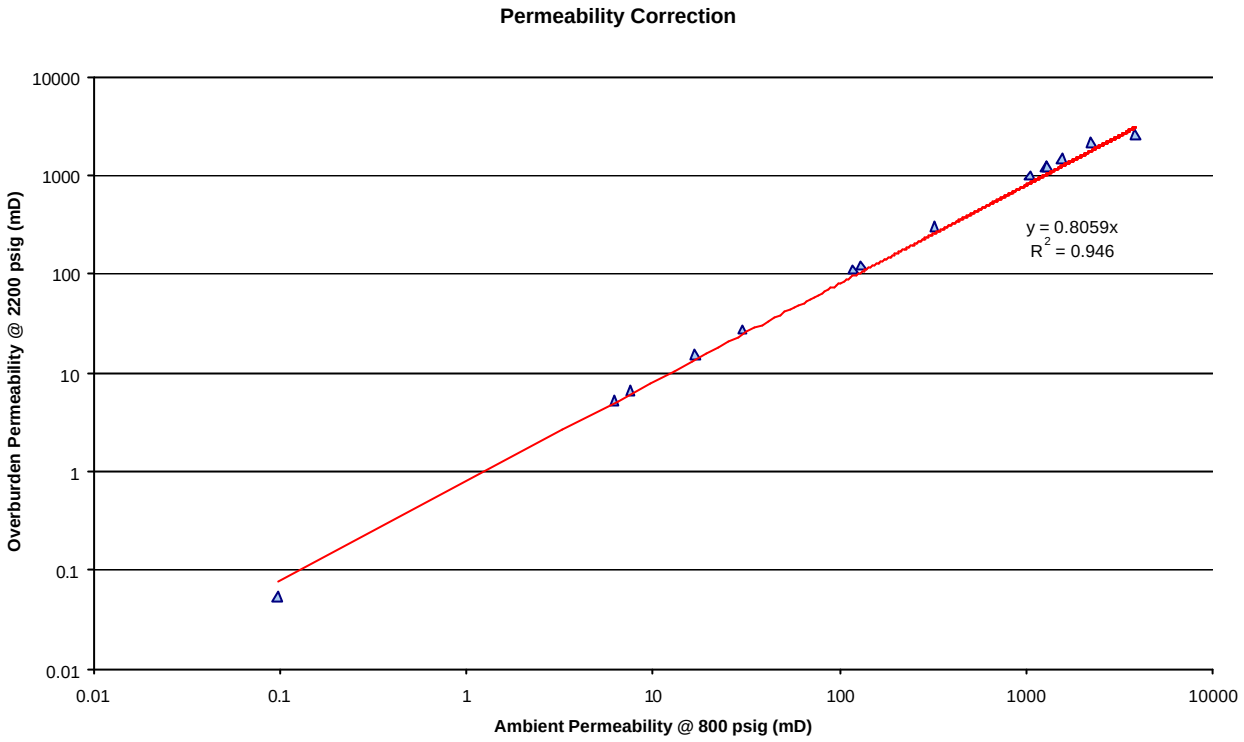

Figure 3.6.2-d: Core permeability corrected to overburden conditions

Log derived permeability was calculated by using a modified Coates Free-Fluid model. The modified model calculates intrinsic permeability based on the calibrated Coates FFI equation. The FFI permeability is defined by the following equation:

Kint = C_KFFI *PHIE*PHIE*(PHIT-BVWFFIHC)/BVWFFIHC) ** X_KFFI

Where ;
C_KFFI = constant multiplier defined calibrated to corrected core permeability
PHIE = Effective porosity (v/v)

BVWFFIHC = Hydrocarbon corrected bound fluid volume.
X_KFFI = Exponent multiplier for Free Fluid calibrated to core.

The resultant log derived permeability was compared to the core results and a reasonable fit was observed. This is shown in Figure 3.6.4-b and discussed in later in the text.

Water Saturation Modelling

The saturation model for Casino used the Dual-Water model, which requires the estimation of the clay bound water volume using the CEC (Cation Exchange Capacity) of individual minerals. SCAL analysis usually uses a bulk property on the crushed sample, therefore CEC values calculated by SCAL are not used directly in the analysis but as a check that the model is correct.

The Dual Water model assumes that the water in a formation consist of two components – a free water, often termed as formation water, and a clay bound water of different salinity and increased conductivity. The Dual-Water equation is expressed as follows;

$$Ct = \Phi_t^{mo} S_{wt}^{no} \left\{ Cfw = \frac{a v_q^h Qv}{S_w^t} (Cbw - Cfw) \right.$$

Where;
Ct = total conductivity (mmho)
Cbw = Clay bound water conductivity (mmho)
Cfw = Free water conductivity (mmho)
m_o= dual water cementation exponent
n_o = dual water saturation exponent
Qv = concentration of cations (meq/cm^3)
Vq^h = colume of clay bound water (cm^3/meq)
S_{wt} = water saturation of total porosity (v/v)
? = expansion factor for diffuse layer
F_t = total porosity (v/v)

Pickett Plot analysis in the wet Waarre C sandstone in Casino-3 suggests the formation water salinity is 15,000 ppm, which corresponds to an R_w of 0.4 OHMM @ 25 DEGC. Due to the high clay content of the Waarre A formations in the three wells, Pickett Plot analysis does not give an accurate apparent water resistivity as the clay conductivity contributes significantly to the resistivity profile, therefore adds to the uncertainty of the Rw in the Waarre A. It has been assumed that the Rw of the Waarre A is identical to the Waarre C sections and this may not be strictly correct.

Electrical properties defined by SCAL were used were available. As mentioned earlier, most of the SCAL data was used to check the validity of the model and not used directly as an input parameter. The exception is the cementation exponent, *m*. Analysis of SCAL data suggest the *m* for the Waarre Cb is 1.79. The input model used 1.8. A fixed value for the saturation exponent, *n* was set at 2.

Porosity and hydrocarbon saturation is an output of the Probabilistic approach. Accuracy of the probabilistic model is improved by calibrating the porosity and mineralogy to core.

INPUT PARAMETERS USED IN MODEL OF CASINO										
WELL	**MINERAL**	r_B	f_N	**DT**	**U**	**GR**	**THORIUM**	**POTASSIUM**	**URANIUM**	**CEC**
Casino-1	Quartz	*2.645*	*-0.05*	*50.4*	*4.78*	*12*	*1*			
	Orthoclase	*2.541*	*-0.05*	*53.49*	*7.29*	*280*	*5*			
	Siderite	*3.911*	*0.129*	*43.8*	*56.22*	*5*	*0*			
	Illite	*2.776*	*0.3*	*85.34*	*11.73*	*265*	*22*			*0.25*
	Kaolinite	*2.636*	*0.451*	*85.34*	*4.5*	*110*	*25*			*0.1*
WELL	**MINERAL**	r_B	f_N	**DT**	**U**	**GR**	**THORIUM**	**POTASSIUM**	**URANIUM**	**CEC**
Casino-2	Quartz	*2.645*	*-0.05*	*50.4*	*4.78*	*12*	*1*			
	Glauconite	*2.541*	*-0.05*	*53.49*	*7.29*	*280*	*5*			
	Smectite	*3.911*	*0.129*	*43.8*	*56.22*	*5*	*0*			
	Illite	*2.776*	*0.3*	*85.34*	*11.73*	*265*	*22*			*0.25*
	Kaolinite	*2.636*	*0.451*	*85.34*	*4.5*	*110*	*25*			*0.1*
WELL	**MINERAL**	r_B	f_N	**DT**	**U**	**GR**	**THORIUM**	**POTASSIUM**	**URANIUM**	**CEC**
Casino-3	Quartz	*2.645*	*-0.05*	*50.4*	*4.78*	*12*	*1*			
	Pyrite	*2.541*	*-0.05*	*53.49*	*7.29*	*280*	*5*			
	Calcite	*3.911*	*0.129*	*43.8*	*56.22*	*5*	*0*			
	Illite	*2.776*	*0.3*	*85.34*	*11.73*	*265*	*22*			*0.25*
	Kaolinite	*2.636*	*0.451*	*85.34*	*4.5*	*110*	*25*			*0.1*
WELL	**MINERAL**	r_B	f_N	**DT**	**U**	**GR**	**THORIUM**	**POTASSIUM**	**URANIUM**	**CEC**

Table 3.6.2-a: Summary of Input Parameters used in Model of Casino

3.6.3 Reservoir Quality

The Waarre Cb and Ca sandstone is a good quality reservoir: this is supported by the reasonably clean response on the log and the high porosity and permeability profiles. This is in turn supported by the DST in Casino-3 that flowed at a rig constrained rate of ~45 mmcfd. The petrophysical analysis suggests the sand to be quartz rich with a significant contribution of orthoclase. Based on petrology reports there is a significant contribution from the lithic fragments with a large amount of alteration from K-feldspar to Na-feldspar. The impact on petrophysics is to increase the difficulty in differentiating K-feldspar and Na-feldspar due to the diagenetic alteration. Thus the feldspars appear different in thin section but are not easily separated by logs as the alteration is not often complete and therefore will lead to a smeared response from the tools. For this reason, one feldspar was modelled and this was believed to be the final alteration product, orthoclase.

Clay concentrations in the reservoir vary depending on the depositional environment. A fair amount of the kaolin present in the lower Cb reservoir is the replacement and alteration of feldspar and mica. The pore-filling kaolin cementation is of a loosely packed nature, which in the gas reservoir acts as a storage site with slow release.

The Waarre A sandstone is the most problematic reservoir due to the lack of calibration data (cores). In Casino-1 and -3 the Waarre A sandstone has a typically shaly profile. It is difficult to determine whether the A sand is finely laminated or dispersed in nature. Core plug data is relatively inconclusive, but it is acknowledged there is evidence that the A sandstone has a predominantly laminar nature based on the few SWC core samples available. The resolution of the wireline logs does not resolve this issue and further techniques have been attempted to define this. For example, a pseudo image log was attempted from the MCFL processing, or SHARP (Schlumberger) but due to the tool not being setup optimally for this function the technique was aborted as any interpretation would have been speculative.

3.6.4 Results

A comparison between log derived porosity and Klinkenburg Overburden shows that whilst a reasonable comparison can be made there are regions where log derived porosity over predicts porosity compared to core data. This is evident in Casino-2 where there is a larger spread of data compared to Casino-3. This is partly due to the different facies present in the cores cut in Casino-2. The different facies represent a range of depositional environments from beach-barriers, lagoonal, tidal channel or fluvial environments. Figure 3.6.4-a shows the data trend in porosity with log derived porosity compared to overburden corrected core porosity. Notice that for a bulk of the data the log porosity is acceptable with a 1:1 correlation, however there are some data regions where the log derived porosity is higher than the cored porosity and is related to differences in facies encountered with the two wells.

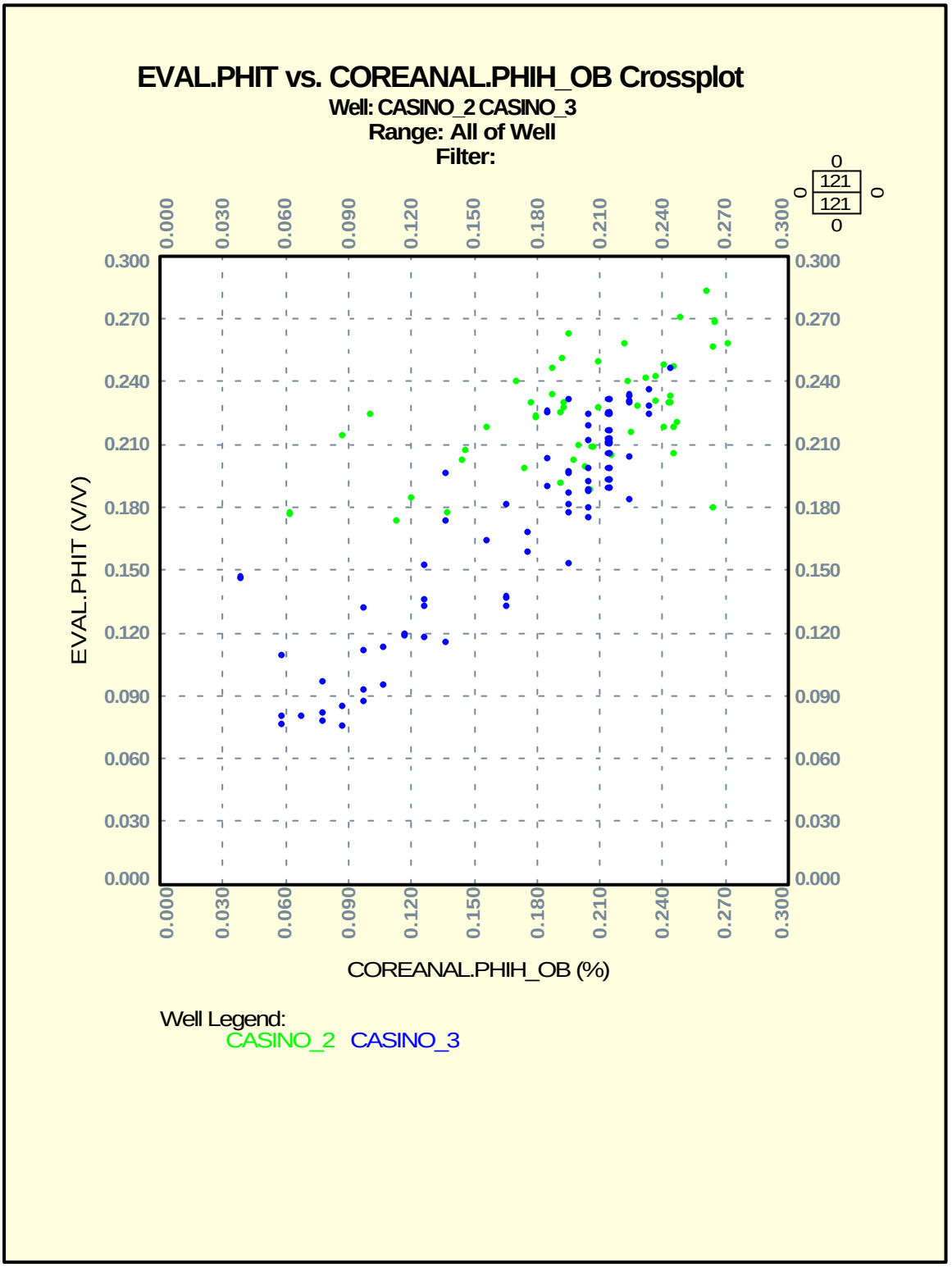

Figure 3.6.4-a: Log derived total porosity compared with overburden corrected core porosity.

Permeability

In a similar way that porosity was influenced by the different depositional environments, permeability is also influenced. Figure 3.6.4-b shows that there is an over prediction in log derived permeability compared with core, and this may be up to an order of magnitude higher than recorded from core. This relates to Waarre Cb sections where the sand is predominantly coarse grained and therefore the pore throats more easily accessible giving rise to higher permeability.

Water Saturation

Water saturation in the Waarre C reservoir is believed to be fairly accurate due to the low clay content of the formation. Increased clay content contributes to errors in Rt and CEC which impact on saturation.

Due to the variable nature of the Waarre A sand and a lack of core, the calculated saturation profile has an increased uncertainty due to estimations in clay volume, CEC and Rt. This will be discussed in an uncertainty separate report.

Core analysis has reduced the uncertainty in the ranges of *m* and *n* for the Waarre C reservoir, but due to the lack of core in the Waarre A, it was assumed that the values of 2 (for *m* and *n*) were valid. It is agreed that there is an increased risk that these numbers may not truly reflect the nature of the reservoir, but without a calibration point it was decided that 2 would an appropriate value for the sands. The range on uncertainty on *m* is discussed in a report by Keith Boyle (Santos' Chief Petrophysicist).

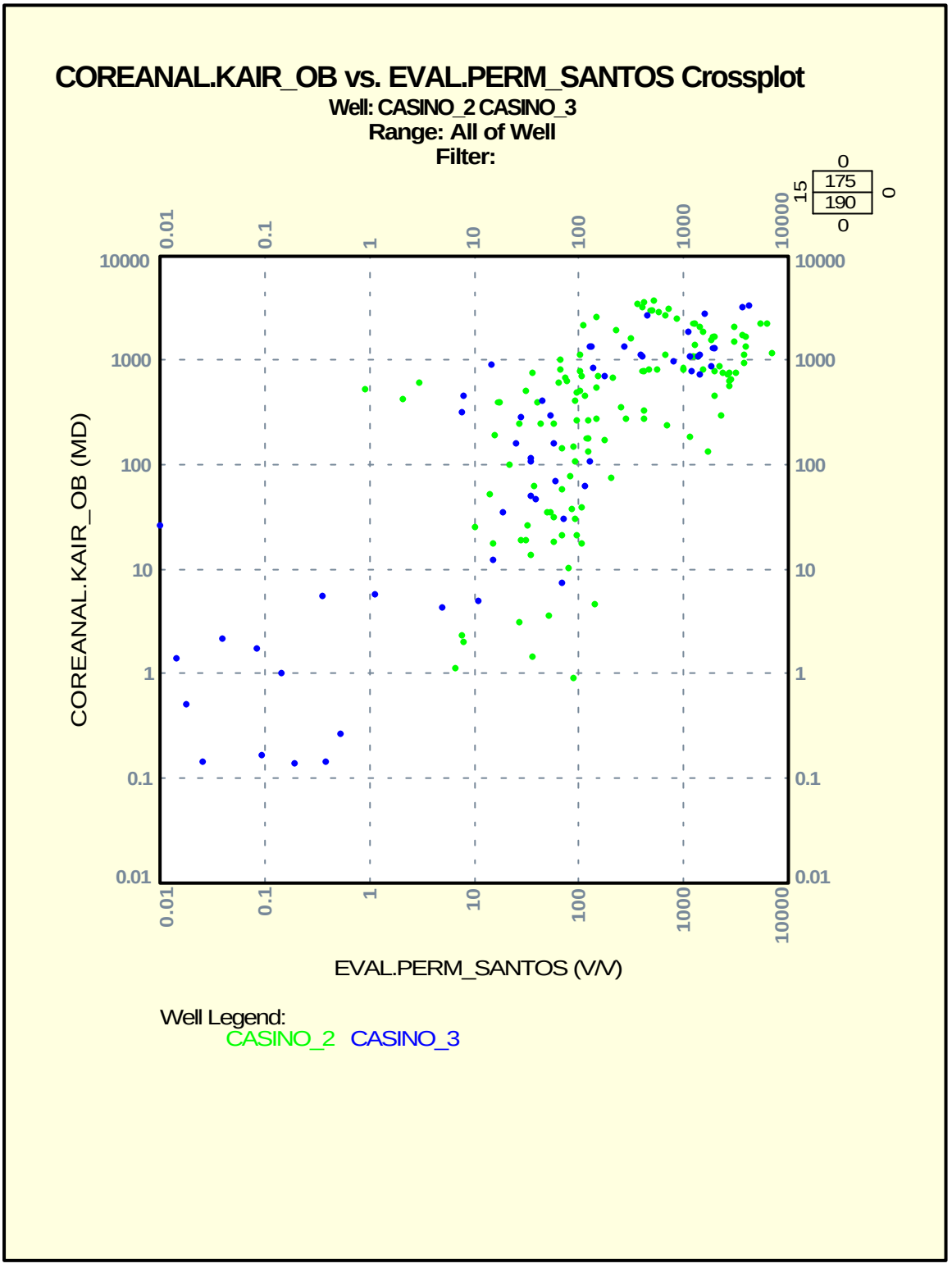

Figure 3.6.4-b: Comparison of corrected Core permeability and log derived permeability, the straight line shows perfect correlation. Points lying above the line represent log derived permeability over predicting which is partially influenced by the differences in facies..

Pay Summaries and Conclusion

Net pay has been determined calculated based on a cut-off of PHIE>10%, Vsh < 45% and Swt< 70%. Pay summaries for the wells are tabulated in Table 3.6.4-a.

Conventional gas pay has been identified in the Waarre Cb, Ca and A reservoirs. The Waarre Cb and Ca sands have a higher reservoir quality and higher permeability than the lower quality Waarre A reservoir.

Plots showing the complete petrophysical analysis for each of the Casino wells can be found in Enclosures 3.6.4-a (Casino-1), 3.6.4-b (Casino-2) and 3.6.4-c (Casino-3). Figure 3.6.4-c shows the Casino-1 log petrophysical analysis over the gas bearing Waarre A reservoir while Figures 3.6.4-d and 3.6.4-e shows the gas bearing intervals intersected in the Waarre C reservoir for the Casino-2 and Casino-3 wells.

Figure 3.6.4-c: Casino-1 Log Analysis*(refer to end of section for this figure)*

Figure 3.6.4-d: Casino-2 Log Analysis*(refer to end of section for this figure)*

Figure 3.6.4-e: Casino-3 Log Analysis*(refer to end of section for this figure)*

Santos Analysis Using Santos Cutoffs

Cut Offs
Santos Petrophysics **PHIE > 10%**
Matt Dubsky **Vclay < 45%**
Feb-04 **Swt < 70%**

Sorted By Well

	PACKAGE SUMMARY					GROSS INTERVAL SUMMARY				SAND SUMMARY					PAY SUMMARY						PERMEABILITY SUMMARY		
Well	Package Description	Top Horizon	Base Horizon	Top m MD	Base m MD	Gross Thickness m	PHIT of Gross Int v/v	PHIE of Gross Int v/v	Swt of Gross Int v/v	Net Sand m	Net Sand / Gross Thk m/m	PHIT of Net Sand v/v	PHIE of Net Sand v/v	Swt of Net Sand v/v	Net Pay m	Net Pay / Gross Thk m/m	Net Pay / Net Sand m/m	PHIT of Net Pay v/v	PHIE of Net Pay v/v	Swt of Net Pay v/v	Perm_av Arith mD	Perm_av Harm mD	Perm_av Geo mD
CASINO-1																							
Casino-1	Upper Waarre A	Upper Waarre A8	Lower Waarre A2	1739.5	1758.4	18.9	0.158	0.084	0.731	3.20	0.169	0.221	0.164	0.549	3.20	0.169	1.000	0.221	0.164	0.549			
Casino-1	Lower Waarre A2	Lower Waarre A2	Lower Waarre A1	1758.4	1770.5	12.1	0.189	0.127	0.533	6.86	0.568	0.200	0.143	0.518	6.86	0.568	1.000	0.200	0.143	0.518			
Casino-1	Lower Waarre A1	Lower Waarre A1	Basal Waarre A Calcite cmt	1770.5	1789.3	18.8	0.198	0.146	0.462	16.15	0.860	0.206	0.155	0.446	16.00	0.852	0.991	0.206	0.155	0.446			
CASINO-2																							
Casino-2	Uppermost Cb sand	Top Waarre Cb	Upper Waarre Cb Non Pay																				
Casino-2	Upper Waarre Cb Non Pay	Upper Waarre Cb Non Pay	Waarre Cb Main Pay	1748.0	1757.4	9.4	0.139	0.079	0.763	1.07	0.113	0.180	0.136	0.431	1.07	0.113	1.000	0.180	0.136	0.431			
Casino-2	Upper Cb main pay	Waarre Cb Main Pay	Intra Cb Silt	1757.4	1760.43	3.0	0.236	0.193	0.225	3.00	1.000	0.236	0.193	0.225	3.00	1.000	1.000	0.236	0.193	0.225			
Casino-2	Cb silt	Intra Cb Silt	Base Intra Cb Silt	1760.43	1761.58	1.1	0.174	0.117	0.347	0.22	0.189	0.188	0.137	0.274	0.22	0.189	1.000	0.188	0.137	0.274			
Casino-2	Lower Cb main pay	Base Intra Cb Silt	Waarre Ca4	1761.58	1766.6	5.0	0.242	0.224	0.099	4.98	1.000	0.242	0.224	0.099	4.98	1.000	1.000	0.242	0.224	0.099			
Casino-2	Ca4	Waarre Ca4	Waarre Ca3	1766.6	1773.0	6.4	0.211	0.157	0.292	5.79	0.905	0.211	0.158	0.292	5.79	0.905	1.000	0.211	0.158	0.292			
Casino-2	Ca3	Waarre Ca3	Waarre Ca2	1773.0	1778.1	5.1	0.244	0.211	0.166	5.12	1.000	0.244	0.211	0.166	5.12	1.000	1.000	0.244	0.211	0.166			
Casino-2	Ca2	Waarre Ca2	Waarre Ca1	1778.1	1786.6	8.6	0.220	0.166	0.303	7.06	0.825	0.228	0.179	0.261	7.06	0.825	1.000	0.228	0.179	0.261			
Casino-2	Ca1	Waarre Ca1	Base Waarre Ca1	1786.6	1795.0	8.4	0.124	0.023	0.926	0.00	0.000	0.227	0.181	0.244	0.00	0.000							
Casino-2	Upper Waarre A	Upper Waarre A8	Lower Waarre A2	1831.0	1854.7	23.8	0.173	0.095	0.753	5.33	0.225	0.203	0.132	0.641	3.51	0.148	0.657	0.218	0.140	0.530			
Casino-2	Lower Waarre A2	Lower Waarre A2	Lower Waarre A1	1854.7	1865.0	10.3	0.217	0.147	0.723	8.38	0.812	0.218	0.152	0.723	3.66	0.354	0.436	0.228	0.153	0.619			
Casino-2	Lower Waarre A1	Lower Waarre A1	Basal Waarre A Calcite cmt	1865.0	1885.0	19.9	0.191	0.140	0.996	17.02	0.854	0.203	0.154	0.995	0.00	0.000	0.000						
CASINO-3																							
Casino-3	Uppermost Cb sand	Top Waarre Cb	Upper Waarre Cb Non Pay	1982.0	1985.7	3.7	0.206	0.177	0.204	3.67	0.990	0.206	0.177	0.204	3.67	0.990	1.000	0.206	0.177	0.204			
Casino-3	Upper Waarre Cb Non Pay	Upper Waarre Cb Non Pay	Waarre Cb Main Pay	1985.7	1998.47	12.8	0.123	0.067	0.556	1.68	0.131	0.178	0.126	0.341	1.68	0.131	1.000	0.178	0.126	0.341			
Casino-3	Upper Cb main pay	Waarre Cb Main Pay	Intra Cb Silt	1998.47	2001.47	3.0	0.201	0.162	0.207	2.59	0.864	0.207	0.169	0.194	2.59	0.864	1.000	0.207	0.169	0.194			
Casino-3	Cb silt	Intra Cb Silt	Base Intra Cb Silt	2001.47	2002.29	0.8	0.124	0.830	0.336	0.15	0.177	0.140	0.104	0.258	0.15	0.177	1.000	0.140	0.104	0.258			
Casino-3	Lower Cb main pay	Base Intra Cb Silt	Waarre Ca4	2002.29	2010.6	8.3	0.226	0.211	0.120	8.10	0.971	0.229	0.215	0.110	8.10	0.971	1.000	0.229	0.215	0.110			
Casino-3	Ca4	Waarre Ca4	Waarre Ca3	2010.6	2011.0	0.4	0.112	0.059	0.504	0.00	0.000	0.218	0.195	0.153	0.00	0.000							
Casino-3	Ca3	Waarre Ca3	Waarre Ca2	2011.0	2018.6	7.6	0.211	0.182	0.296	7.63	1.000	0.211	0.182	0.296	7.63	1.000	1.000	0.211	0.182	0.296			
Casino-3	Ca2	Waarre Ca2	Waarre Ca1	2018.6	2025.8	7.1	0.139	0.084	0.925	3.49	0.488	0.183	0.147	0.903	0.29	0.040	0.083	0.174	0.124	0.600			
Casino-3	Ca1	Waarre Ca1	Base Waarre Ca1	2025.8	2034.9	9.2	0.127	0.065	0.898	1.37	0.150	0.173	0.138	0.820		0.000	0.000						
Casino-3	Upper Waarre A	Upper Waarre A8	Lower Waarre A2	2051.5	2079.1	27.6	0.117	0.058	0.989	5.33	0.193	0.168	0.133	0.981	0.00	0.000	0.000						
Casino-3	Lower Waarre A2	Lower Waarre A2	Lower Waarre A1	2079.1	2086.5	7.4	0.146	0.101	0.984	4.65	0.628	0.159	0.118	0.984	0.00	0.000	0.000						
Casino-3	Lower Waarre A1	Lower Waarre A1	Basal Waarre A Calcite cmt	2086.5	2100.1	13.6	0.139	0.094	0.955	5.41	0.398	0.160	0.122	0.961	0.00	0.000	0.000						

Table 3.6.4-a: Petrophysical Pay Summary of the Casino Wells

This page intentionally left blank.

3.7 Saturation Height Function

3.7.1 Background

Saturation versus height functions relates reservoir fluid saturations to reservoir properties (porosity, permeability) and height above free water level.

A rigorous study was undertaken with the aim of developing a saturation height function which populates the Petrel and Eclipse models with initial reservoir fluid saturations. Several methodologies were reviewed. The gas saturations calculated from these functions were benchmarked against log derived saturations from Casino-1, -2 and -3. A first pass function was created using limited Capillary Pressure data (at ambient conditions) from the Waarre C in Casino-2. This function was used to calculate OGIP for the Waarre A and C in the initial Petrel model (Pet_02). As part of Casino-3 SCAL programme, Capillary Pressure tests were performed on core plugs from the Waarre A and C (at ambient and net-overburden conditions). The functions derived from the Casino-3 dataset, supersedes the previous work.

Two methods have been reviewed;

1. Regression of Thomeer variables and,
2. Leverett J Function

The Regression of Thomeer variables method fits a continuous function to air-brine capillary pressure data using the Thomeer relation;

- $S_h = A*EXP\{-B/LOG(Pc/C)\}$

Where;

A, governs Swirr
B, governs function curvature
C, governs displacement pressure

Figure 3.7.1-a illustrates the fitted function for one of the Pc tests on a Casino-3 coreplug.

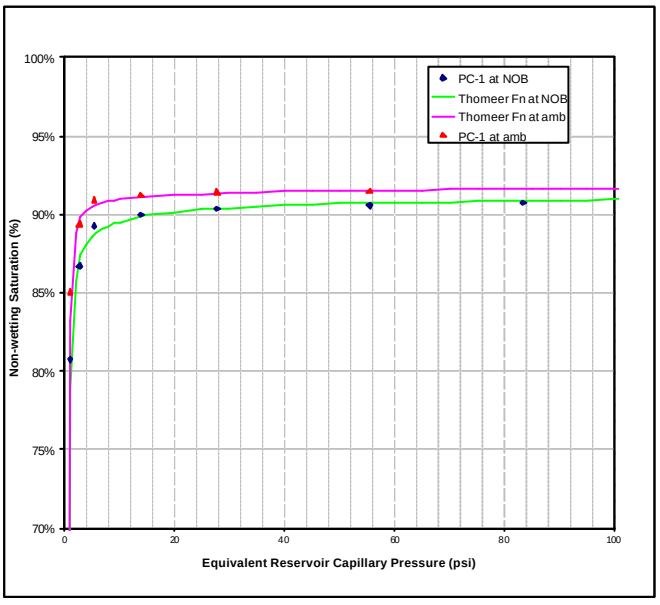

Figure 3.7.1-a: Thomeer relation fitted to Pc test data (at ambient and NOB conditions) for Casino-3 core plug No 1.

A function is then fitted to the Thomeer variables (for each Capillary Pressure curve), with in situ permeability as the independent variable. Refer to Figure 3.7.1-b. The result is a function that calculates gas saturation based on height above free water level and in situ permeability. Refer to Figure 3.7.1-c

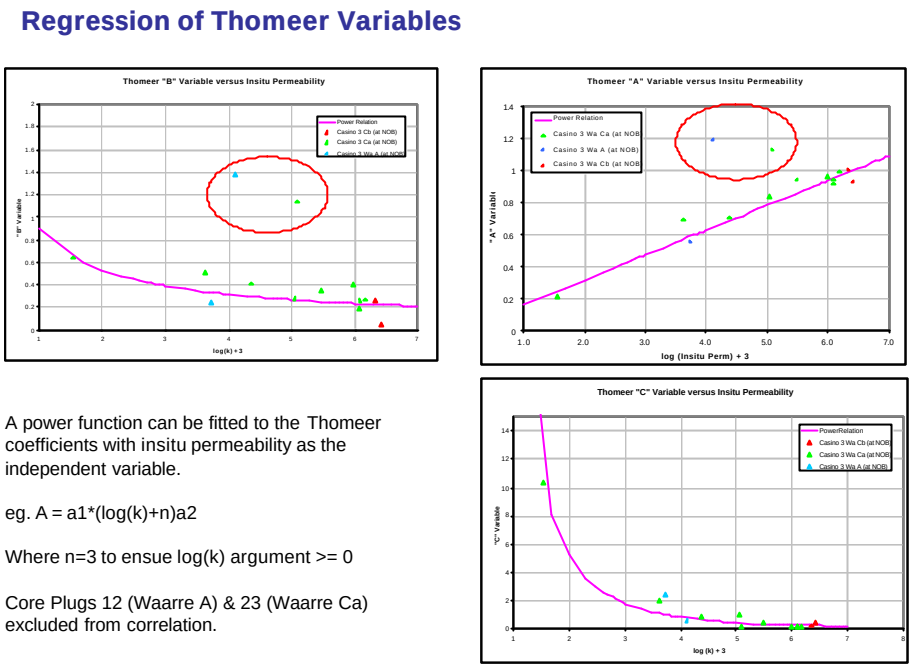

Figure 3.7.1-b: Power function fitted to the Thomeer coefficients with in situ permeability as the independent variable.

$$P_c = Equivalent\_Reservoir\_Capillary\_Pressure\_(psi)$$
$$k = Insitu\_Permeability(mD)$$
$$h = Height\_above\_FWL(m)$$
$$\nabla_{aquifer} = 1.388(psi/m)$$
$$\nabla_{gasleg} = 0.176(psi/m)$$

$$P_c = h*(\nabla_{aquifer} - \nabla_{gasleg})$$

$$Sw(\%) = 100 - Sg(\%)$$
$$IF(P_c \le C)$$
$$THEN(Sg = 0), ELSE$$
$$Sg = MAX(A*EXP^{\frac{b}{\ln(P_c - C)}} + D, 0)$$
$$A = a_1*[Log(k)+3]^{a_2}$$
$$B = b_1*[Log(k)+3]^{b_2}$$
$$C = c_1*[Log(k)+3]^{c_2}$$
$$D = MIN\{[(d_1*EXP(d_2*k)) - 1], 0.15]\}$$

$$a_1 = 1.4166, a_2 = -0.2445$$
$$b_1 = 9.8367, b_2 = -1.9991$$
$$c_1 = 6.8922, c_2 = -1.5442$$
$$d_1 = 0.954, d_2 = 3e-05$$

Step 1: Calculate Pc

Step 3: Calculate Sg

Step 2: Calculate Thomeer variables based on insitu perm

Figure 3.7.1-c: Workflow to determine Sg based on Regression of Thomeer Variable method.

The popular J-function method is based on the work of Leverett (1940) and uses the following relation;

$$J = (0.217 * Pc/g) * (k/f)^{1/2}$$

Where;

$Pc = reservoir\_capillary\_pressure\_(psia)$

$k = permeability(mD)$

$q = porosity(v/v)$

$g = Interfacial\_Tension\_of\_reservoir\_fluids\_(40dy/cm\_for\_gas-water)$

A function is then fitted to the calculated J values with Sw as the dependent variable. This function is typically created for each of the identified reservoir "facies".

3.7.2 Results

The Regression of Thomeer Variables method was found to be a good predictor of log derived saturations in the Waarre C. Figure 3.7.2-a illustrates the log derived gas saturations for Casino-2, overlayed with gas saturation calculated using the Regression of Thomeer Variables method.

The J-function method was not found to be good predictor of water saturation for the Waarre C despite attempts to create separate J functions for each reservoir sub unit.

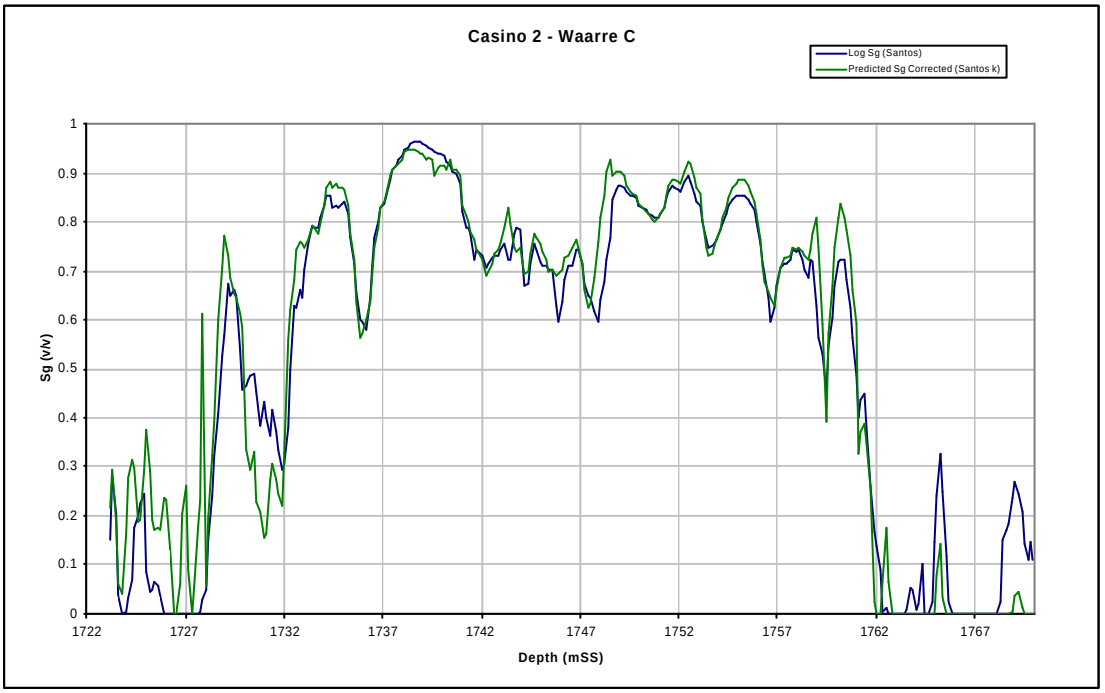

Figure 3.7.2-a: Gas saturations profiles for the Waarre C in Casino-2. Gas saturations are calculated from Santos log analysis and the "Thomeer Variable Regression" Saturation-Height Function.

For the Waarre A, the two Saturation-Height function methodologies provide differing results. The J-function method is in good agreement with the gas saturations predicted by the AWE petrophysical analysis. Note

that the gas saturations from the AWE analysis is higher than the Santos log analysis (by 10-20 su). The Thomeer Variable Regression method calculates gas saturations in general, between the Santos and AWE log analyses (See Figures 3.7.2-b and -c).

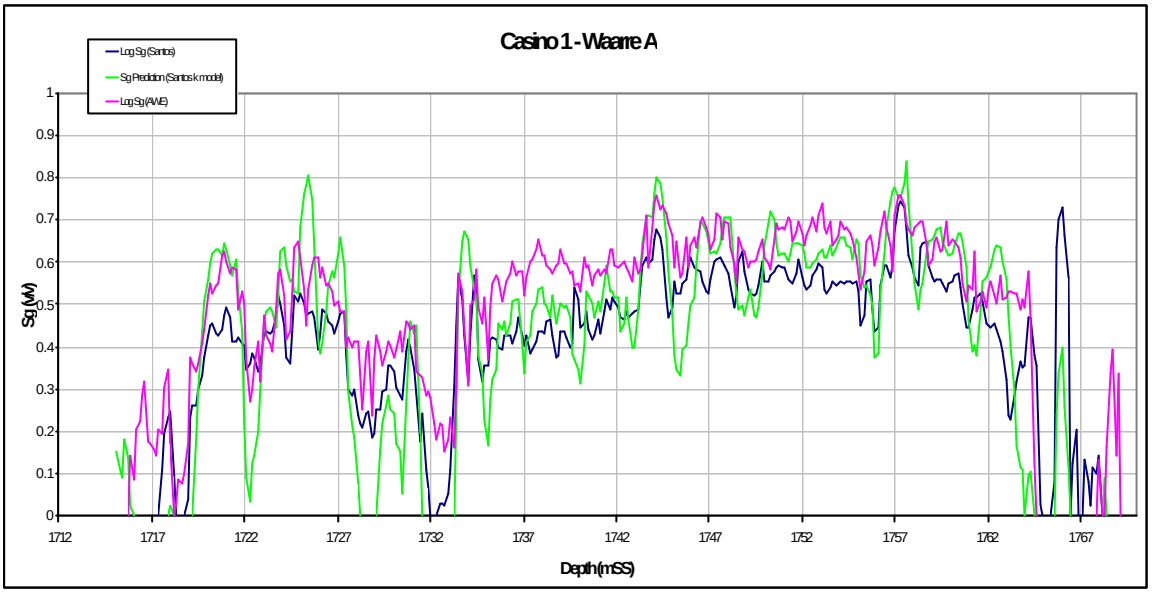

Figure 3.7.2-b: Gas saturation profiles for the Waarre A in Casino-1. Gas saturations are calculated from AWE and Santos log analysis and the "Thomeer Variable Regression" Saturation-Height function.

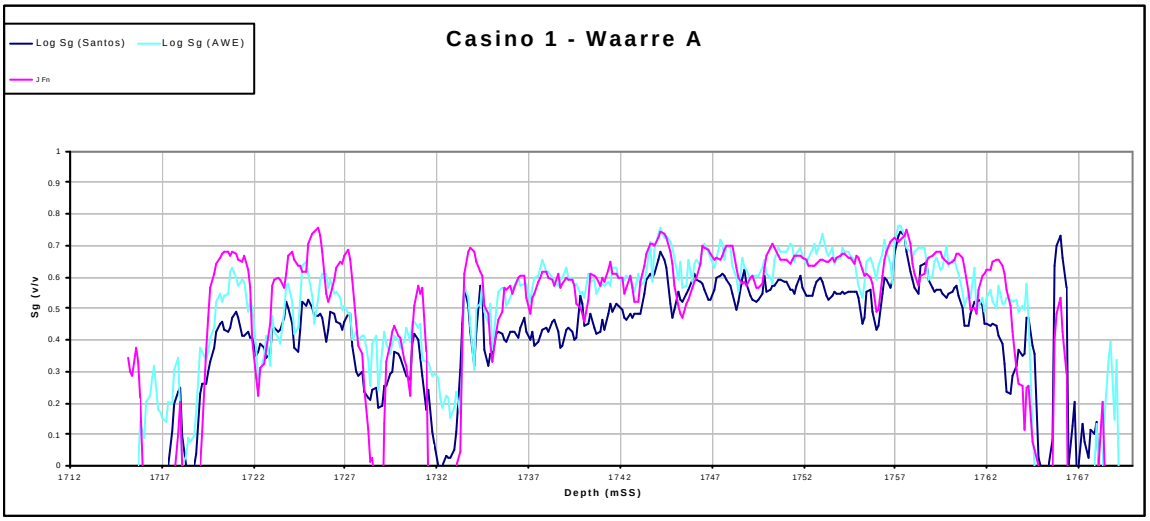

Figure 3.7.2-c: Gas saturation profiles for the Waarre A in Casino-1. Gas saturations are calculated from AWE and Santos log analysis and the "J-Function" Saturation-Height function.

Estimates of water saturation from the various analysis techniques are summarised in Table 3.7.2-a below for a common set of petrophysical cutoffs for the Waarre A in Casino-1;

	Santos Log Derived Sw	AWE Log Derived Sw	Thomeer Sw vs h function	J Function derived Sw
Upper Waarre A	0.549	0.454	0.364	0.325

Lower Waarre A2	0.518	0.392	0.438	0.382
Lower Waarre A1	0.442	0.356	0.383	0.355

Table 3.7.2-a: Comparison of average water saturations for the Waarre A in Casino-1 from log analysis and Saturation-Height function.

For calculation of OGIP for future Petrel static models it was decided to use the Thomeer Variable Regression method to represent water saturation for the Waarre C reservoir. Significant uncertainty remains regarding Waarre A water saturation and both methods have been used for this reservoir. This is described in detail in Section 3.12.

This page intentionally left blank.

3.8 Fluid Contacts

3.8.1 Summary

A summary of the Free Water Levels (FWLs) based on interpretation of the available pressure data for the Casino Field is presented in Table 3.8.1-a. Wireline pressure data indicates that the gas accumulations of the Waarre C and Waarre A reservoirs are isolated with separate FWLs. Review of regional pressure data indicates that the aquifers of both the Waarre A and Waarre C are overpressured compared to the regional aquifer of the Waarre C.

The range in FWL for each reservoir reflects the uncertainty in measurement, gauge accuracy and pre-test pressure validity.

Reservoir	Most Likely FWL (TVD mSS)	Maximum FWL (TVD mSS)	Minimum FWL (TVD mSS)
Waarre C	1999	2000	1994
Waarre A	1839	1840	1836

Table 3.8.1-a: Summary of interpreted FWLs for the Waarre C and Waarre A, Casino Field.

3.8.2 Pressure Interpretation Methodology

The most commonly used wireline pressure interpretation technique, and the one adopted for this study, is the pressure-depth diagram. This technique involves plotting stabilised formation pressure against true vertical depth. The intersection of hydrocarbon and water pressure gradient provides a free water level for the reservoir. Several authors have proposed an alternative technique, referred to as the 'Excess Pressure Plot' (Brown, 2003). This technique enhances the measurement of fluid densities and resolves small density changes and pressure barriers that are not likely to be recognised by standard analysis. Given the significant density contrast between the reservoir and aquifer fluids in Casino Field, the traditional technique of pressure versus true vertical depth was considered appropriate for this study.

3.8.3 Data Quality Control

Wireline Pressure data was acquired in Casino-1, -2 and -3 with Schlumberger's Modular Dynamic Tester (MDT) tool. The tool was run in openhole and pressures were measured with a Compensated Quartz Gauge (CQG). Overall data quality was excellent, enabling fluid limits to be determined for each reservoir. However, several data quality issues were observed. Gauge accuracy, supercharging and depth measurement issues resulted in uncertainty in FWL interpretations. This uncertainty is reflected in the range in FWL interpretations for the Waarre C & A reservoirs.

Pressure Stability

Only MDT pre-tests that achieved a stable build-up pressure were included in the interpretation. The temperature compensated quartz gauge (CQG) used in the MDT tool has a reported resolution of 0.001 psi (Economides et al, 1994). A pre-test build up was generally considered to have stabilised when the change in gauge pressure was less than 0.01 psi. For a number of pre-tests the pressure build-up was very slow due to low permeability rock. In order to save rig time and prevent tool sticking several of these tests were terminated prematurely. The final pressures from these tests had not stabilised and therefore are not representative of formation pressure. These pre-tests were excluded from the interpretation.

Another cause of unrepresentative formation pressures was tool plugging or unseating of the probe packer during the pre-test. These tests are usually characterised by a major difference in expected formation pressure and typically aborted. These tests were also excluded from the interpretation.

Supercharging

Supercharging results from leakage of mud filtrate through the filter cake, which increases sandface pressure above formation pressure. The MDT probe measures pressure near the borehole wall, thus supercharged tests have high pressures unrepresentative of the formation pressure. Where supercharging is tens to hundreds of psi in excess of formation pressure, supercharging can be identifiable solely on the basis of high pressure. Those pre-test pressures that were identified as supercharged were excluded from the interpretation. Figures 3.8.3-a and 3.8.3-b are an illustration of pre-tests for the Waarre C and A. All pressures included in the plot are interpreted to have stabilised (as discussed in the section above). Those pressures in excess of the expected formation pressure are readily identifiable and excluded from the fluid limit interpretation. An exception to this, is the pre-test of the Waarre C aquifer in Casino-3, which is discussed in the Fluid Limit Interpretation section.

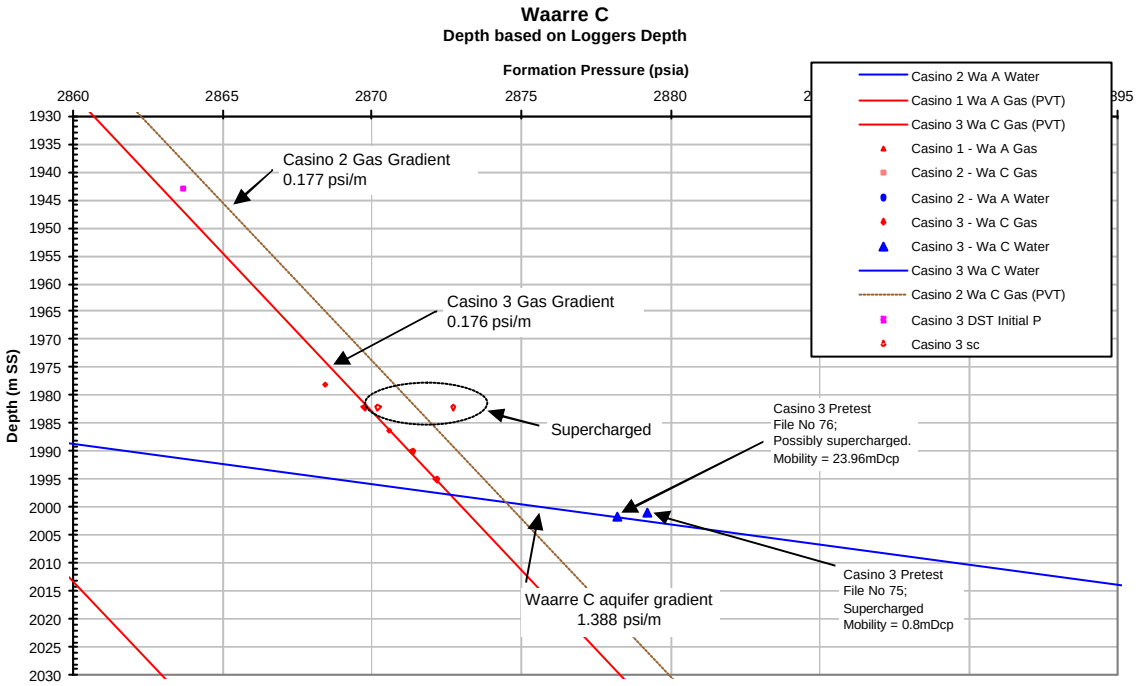

Figure 3.8.3-a: Waarre C MDT data including super charged pre-tests.

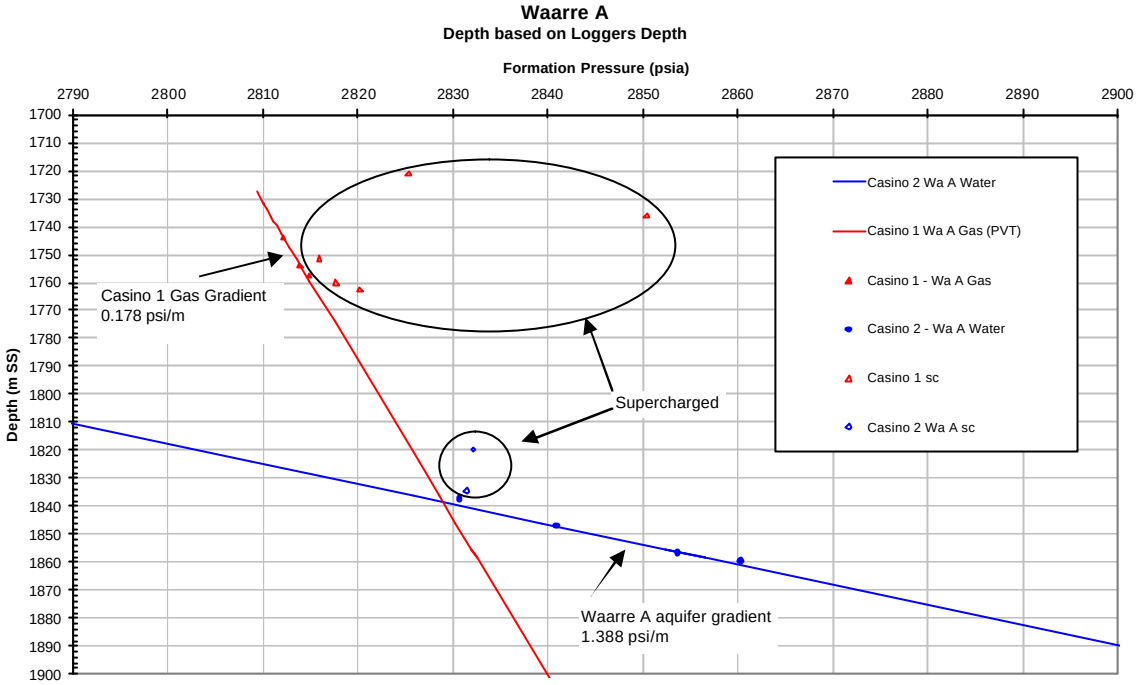

Figure 3.8.3-b: Waarre A MDT data including super charged pre-tests.

Depth Control

MDT pre-test depths are based on wireline depth measurement. In all three wells a gamma ray (GR) was run with the MDT tool. The GR was used as a correlation log to the first GR run in the hole. In all wells, Measurement While Drilling (MWD) was acquired. The MWD suite comprised a directional survey, gamma ray and resistivity. A comparison of MWD depth (equivalent to Driller's depth) against Logger's depth indicates that there is a depth discrepancy at the top of the Waarre Sandstone. Wireline logging measures depth via measuring cable length as it passes through a wheel. This measurement corrects for cable stretch to provide a true depth. However, the accuracy of the measurement is dependent on the cable stretch correction which varies based on cable type and history, therefore is prone to inaccuracy. Provided that the pipe tally is correct, Driller's depth (and MWD) should be an accurate measurement of true depth. A comparison of Driller's and Logger's depth at top Waarre Sandstone is presented in Table 3.8.3-a. Except in very shallow wells, wireline depths are usually deeper than Driller's depth by approximately 1m for every 1000m. This is the case for Casino-1 and -2, however there is an significant depth discrepancy in Casino-3. This is evident when the pre-test pressures from the Waarre C gas reservoir in Casino-2 and Casino-3 are compared. There is a significant offset in gas pressure gradient between Casino-2 and -3 when formation pressure is plotted against Logger's depth (Figure 3.8.3-c). When pressure is plotted against Driller's Depth (TVD SS) this offset is reduced (Figure 3.8.3-d).

	Driller's Depth (mRT)	Logger's Depth (mRT)	Difference
Casino-1	1761	1763	2
Casino-2	1758	1760	2
Casino-3	2002	2005.7	3.7

Table 3.8.3-a: Difference between Logger's and Driller's depth at Top Waarre C.

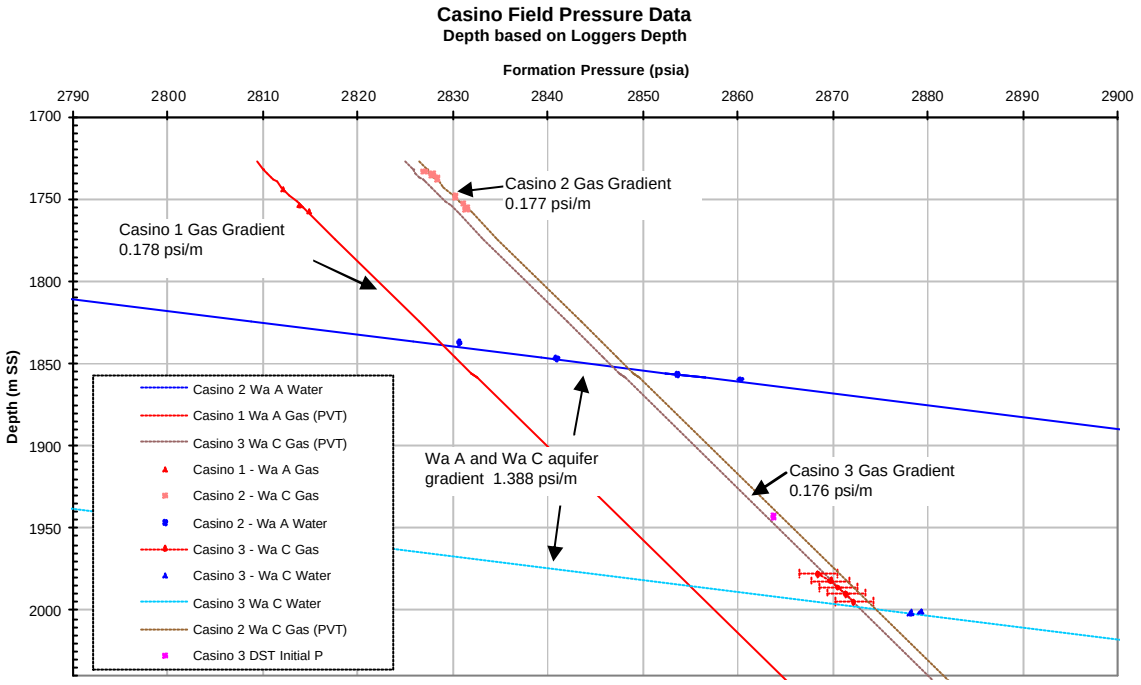

Figure 3.8.3-c: Waarre C pre-test data illustrating gas gradient offset. Depth is based on Logger's measurement.

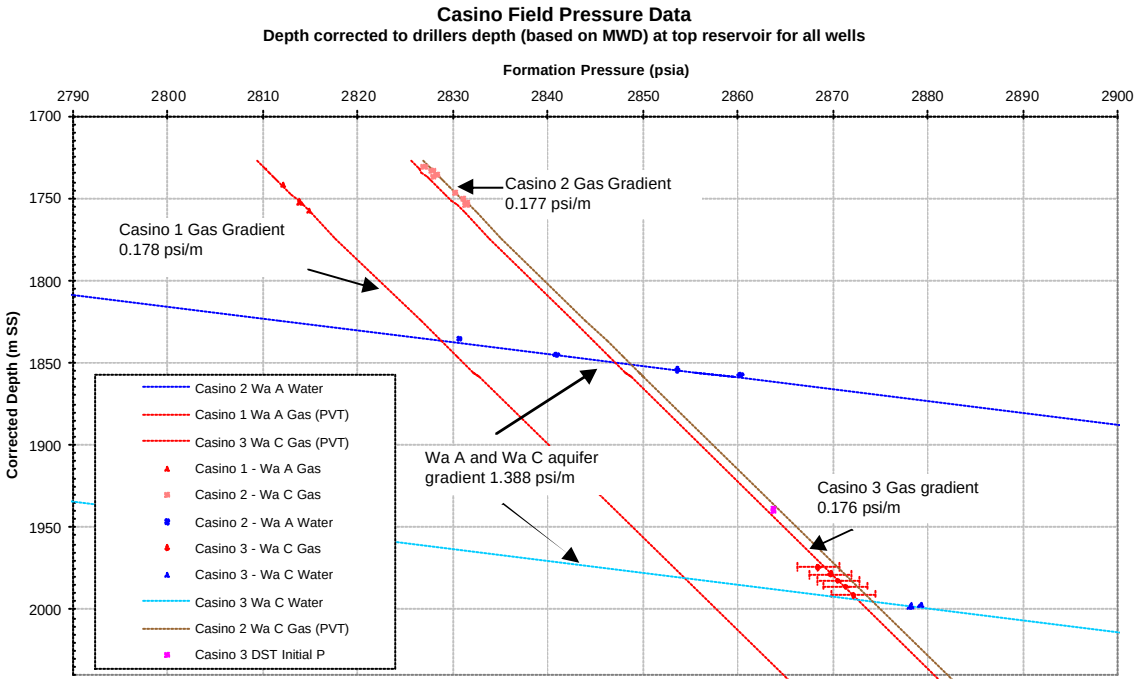

Figure 3.8.3-d: Waarre C pre-test data illustrating gas gradient offset. Depth is based on Driller's measurement.

Gauge Accuracy

Absolute-gauge and depth accuracy limits the interpretation of data from multiple wells, even where the tool type and service company are the same. Accuracy for the CQG is reported as +/- 0.01% of reading + 2 psi (Economides et al, 1994). This equates to a gauge accuracy of +/- 2.287 psi for the Casino wells. The observed offset in gas gradient in Figure 3.8.3-d may also be explained by gauge inaccuracy.

3.8.4 Fluid Limit Interpretation

Figure 3.8.4-a is a plot of pressure versus true vertical depth (sub sea above MSL) for Casino-1, -2 and -3. Pressures were obtained from both the gas reservoir and aquifer for the Waarre C and Waarre A sandstones. Consequently, a well defined FWL was evident for each reservoir.

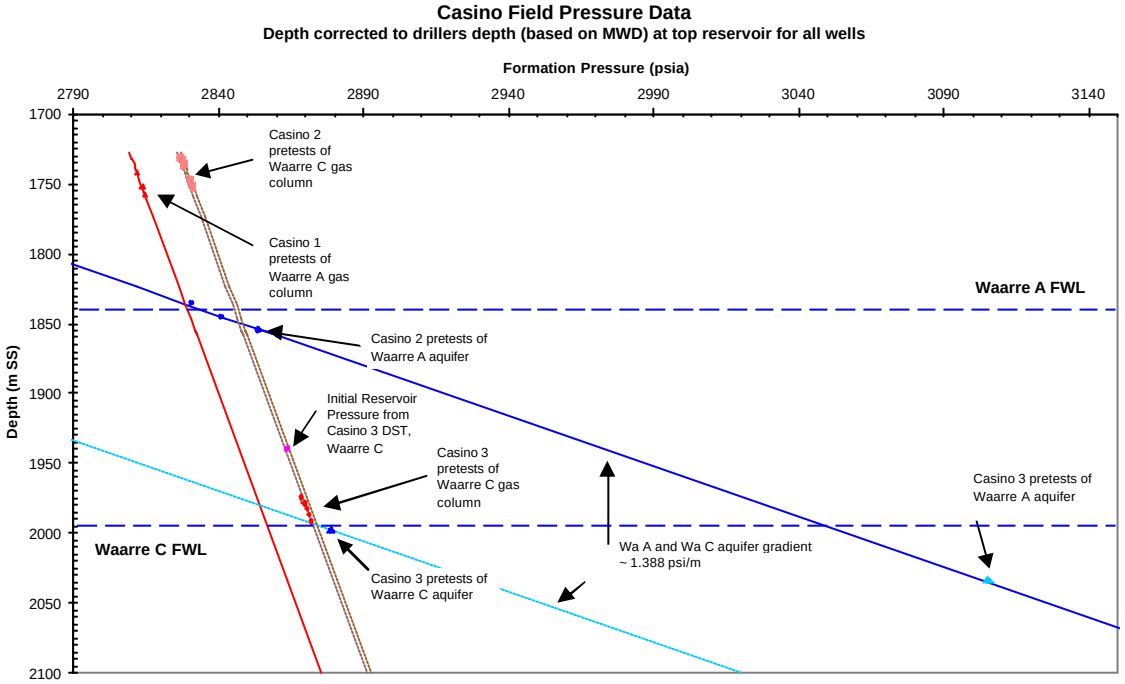

Figure 3.8.4-a: FWL interpretation for the Waarre C and A reservoirs.

The Waarre C and A gas reservoirs are isolated with separate FWLs. The Waarre A aquifer is significantly overpressured with respect to the regional aquifer for the Waarre while the Waarre C aquifer may be slightly overpressured. The following is a discussion of the interpretation of fluid limits for each reservoir.

Waarre A

A gas column for the Waarre A was intersected in Casino-1 and pressures from MDT pre-tests from this well define the gas gradient for the Waarre A. Gas samples were also acquired from Casino-1 with the MDT tool. Compositional analysis of the gas indicates that the reservoir fluid has a Specific Gravity of 0.6 (air=1), which is consistent with the gas pressure gradient of 0.17753 psi/m (0.05411 psi/ft).

The water gradient for the Waarre A reservoir in Casino was determined from valid pre-tests in Casino-2 and -3. Apparent formation water salinity calculations (based on Pickett Plots) indicate that the aquifer of the Waarre A comprises a brine salinity of 15,000 ppm (Total Dissolved Solids of 1.5%). This salinity is equivalent to a brine density of 63 lb/ft (at standard conditions) which is consistent with the water gradient from pre-tests of 1.388 psi/m (0.423 psi/ft).

As discussed under Data Quality Control, there is a difference between depth measured by drillers and the logging contractor. This discrepancy raises uncertainty about the true measured depth and therefore FWL

interpretation. The 'Minimum' and 'Most Likely' FWL interpretations for the Waarre A reflect this uncertainty. The 'Minimum' FWL is based on Driller's depth (Figure 3.8.4-c) and 'Most Likely' based on Logger's depth (Figure 3.8.4-b). As mentioned previously, Driller's depth is considered the more accurate measurement of depth. However, the major horizons within the subsurface static model are tied to Logger's depth at each of the wells. Therefore, for consistency, the 'Most Likely' FWL interpretation is considered to be based on Logger's Depth.

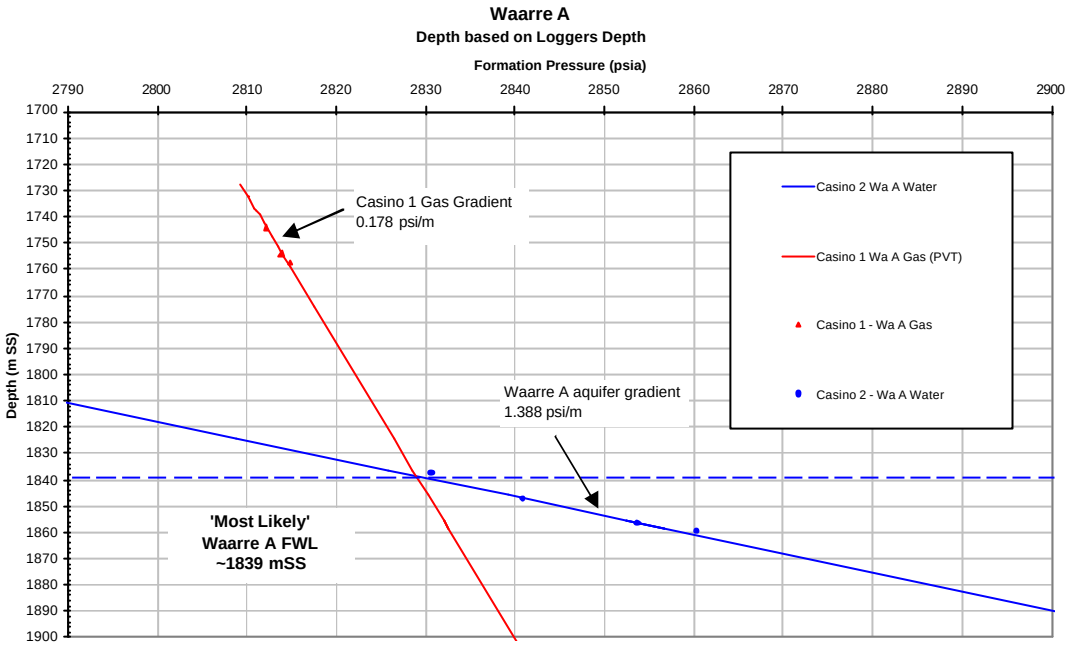

Figure 3.8.4-b: Most likely FWL interpretation for the Waarre A.

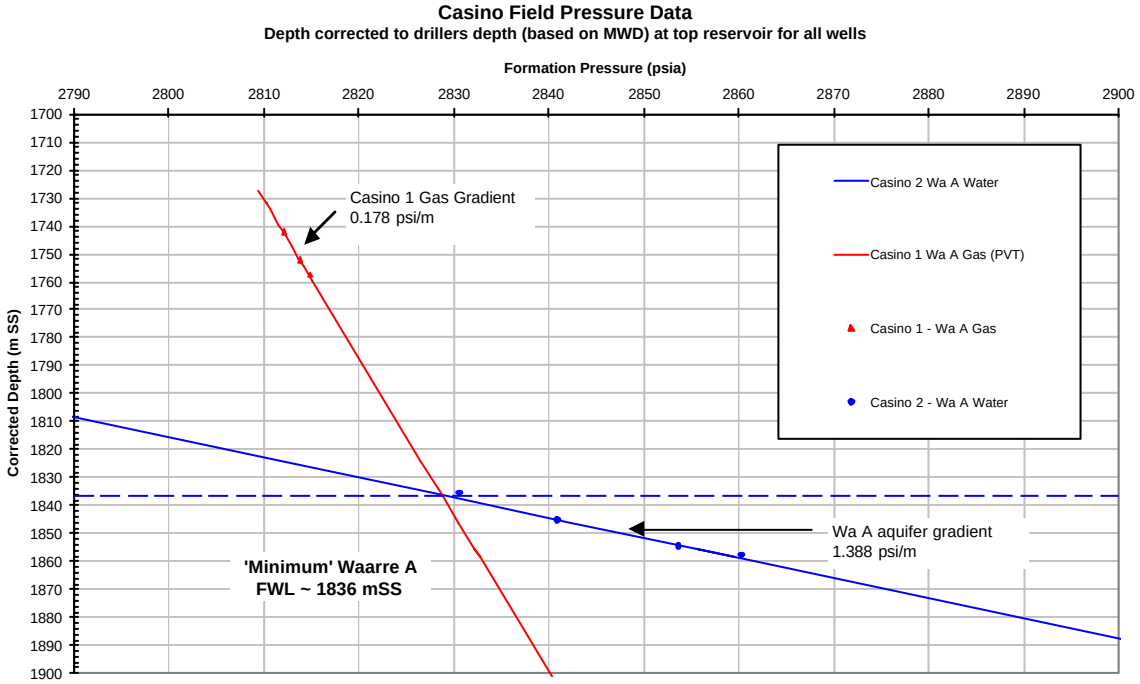

Figure 3.8.4-c: Minimum FWL interpretation for the Waarre A.

The 'Maximum' FWL interpretation for the Waarre A incorporates gauge inaccuracy. If the Casino-1 pre-tests are shifted +2 psi (the maximum gauge inaccuracy) the FWL interpretation is 1840 mSS.

Waarre C

The Waarre C gas reservoir was encountered in Casino-2 and 3. Valid pre-test formation pressures from these wells define the gas gradient for the Waarre C. Gas samples were also acquired from Casino-2 and 3 with the MDT tool. Compositional analysis of the gas indicates that the reservoir fluid has a Specific Gravity (air =1) of 0.59, which is equivalent to a gas pressure gradient of 0.177 psi/m (0.054 psi/ft).

As discussed in the section above (Data Quality Control), Figure 3.8.4-d illustrates two gas pressure gradients for the Waarre C. These gas gradients represent the range of uncertainty of the position of the gas gradient for the Waarre C. The intersection of these gradients and the water gradient represents the 'Minimum' and 'Most Likely' FWL interpretations.

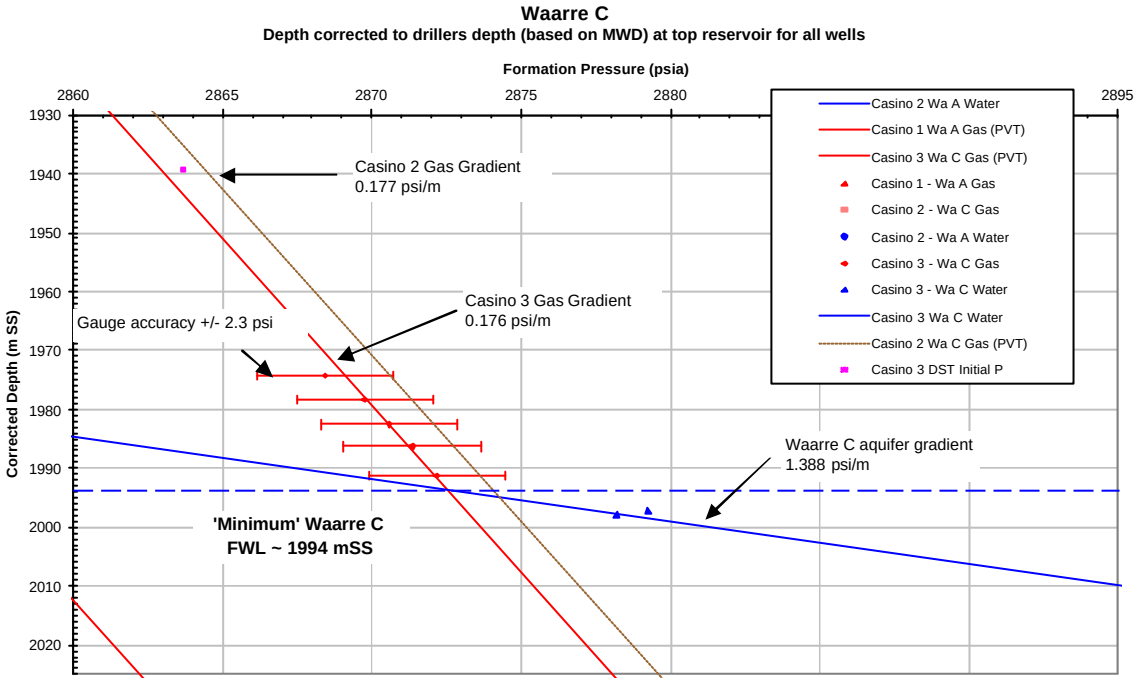

Figure 3.8.4-d: Minimum FWL interpretation for the Waarre C.

The minimum gas line is based on gas gradient from Casino-3 PVT fitted to the Casino-3 pre-tests of the Waarre C, plotted against Driller's depth (Figure 3.8.4-d) The 'Most Likely' gas line is based on the gas gradient from Casino-2 PVT, fitted to the Casino-2 pre-tests of the Waarre C, plotted against Logger's depth (Figure 3.8.4-e).

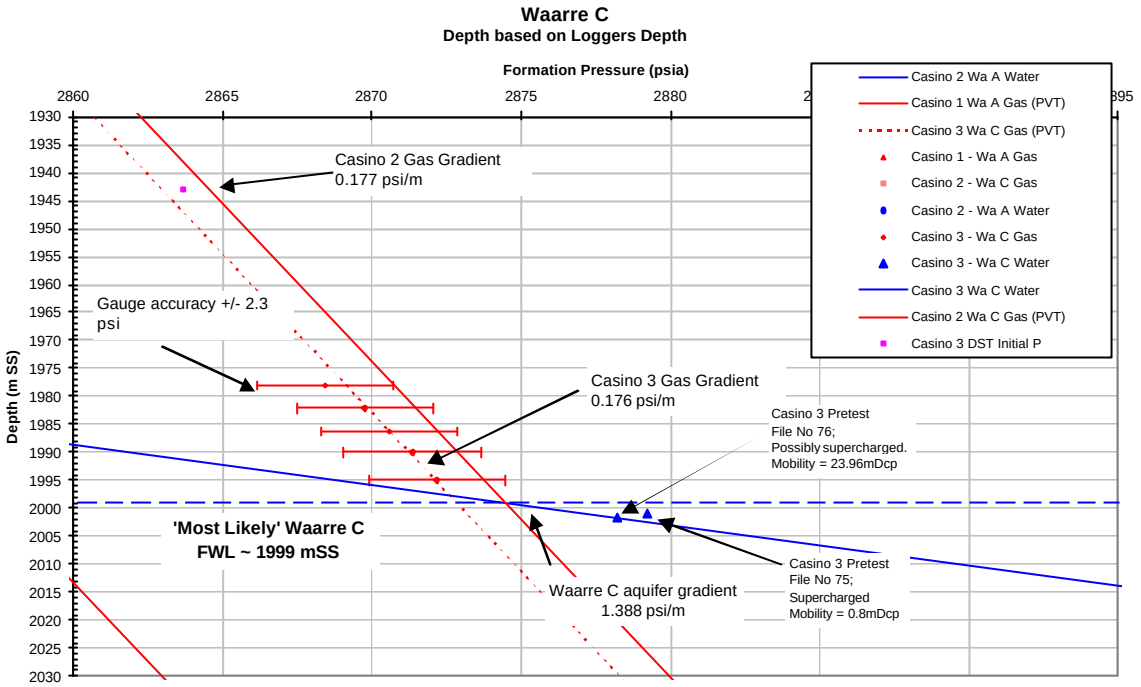

Figure 3.8.4-e: Most likely FWL interpretation for the Waarre C.

The 'Minimum' and 'Most Likely' FWL interpretations are based on the respective gas gradients intersecting a water gradient. The water gradient is the same as the Waarre A (1.388 psi/m) fitted to the only valid pre-test of the Waarre C aquifer (at 2001.5 mSS). However, it cannot be certain if this pre-test is not supercharged. Consequently the maximum FWL interpretation is based on the interpreted 'Water Up To' based on wireline log interpretation of Casino-3 i.e. 2000 m TVDSS.

Regional Interpretation

Casino pressure data was also reviewed in a regional context. Presented in Figure 3.8.4-f is pressure data for the Waarre Sandstone of the Otway Basin. A well defined regional pressure gradient is evident for the Waarre C aquifer. The aquifer is normally pressured. Slight deviations from the regional gradient are interpreted to be a result of variation in formation water salinity, gauge inaccuracies, possible supercharging and depth control uncertainties. Highlighted in Figure 3.8.4-f is the aquifer pressure data of the Waarre C in the Minerva Field which falls on the regional aquifer gradient. Illustrated in Figure 3.8.4-g is the Casino & Minerva pressure data. The aquifer gradient for Minerva defines the regional pressure gradient for the Waarre aquifer. Evident from the plot are the overpressured aquifers of the Waarre C and A in the Casino Field. The Waarre A aquifer is significantly overpressured by approximately 190 psi while the Waarre C appears to be slightly overpressured by 14 psi.

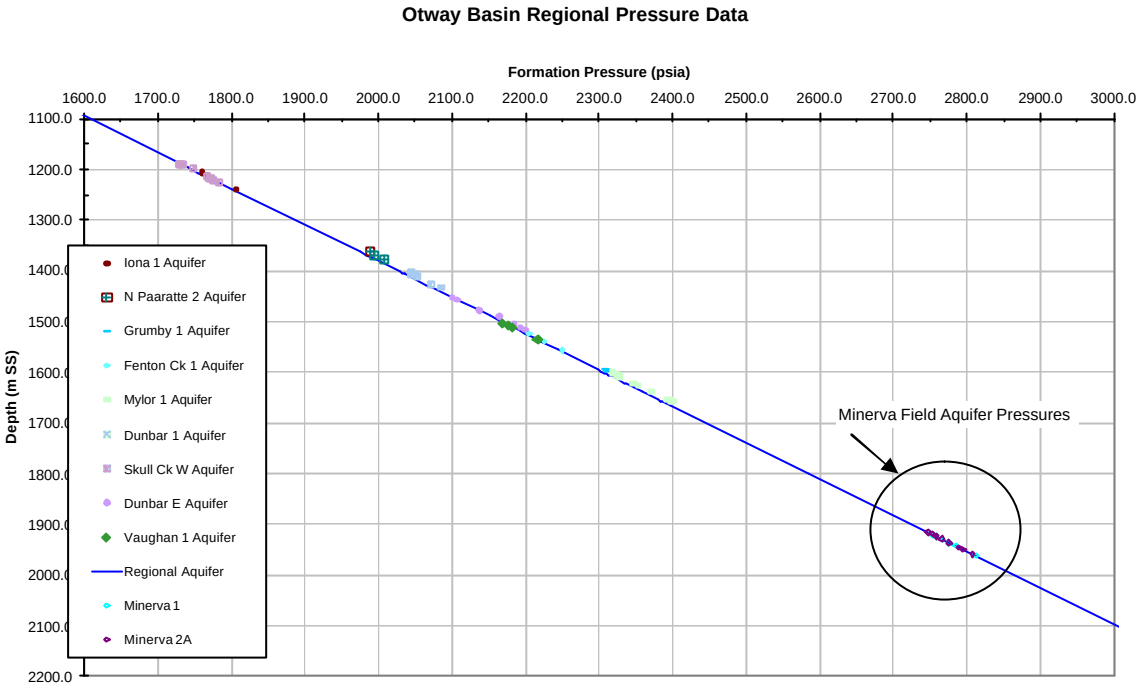

Figure 3.8.4-f: Regional aquifer gradient for the Waarre Sandstone.

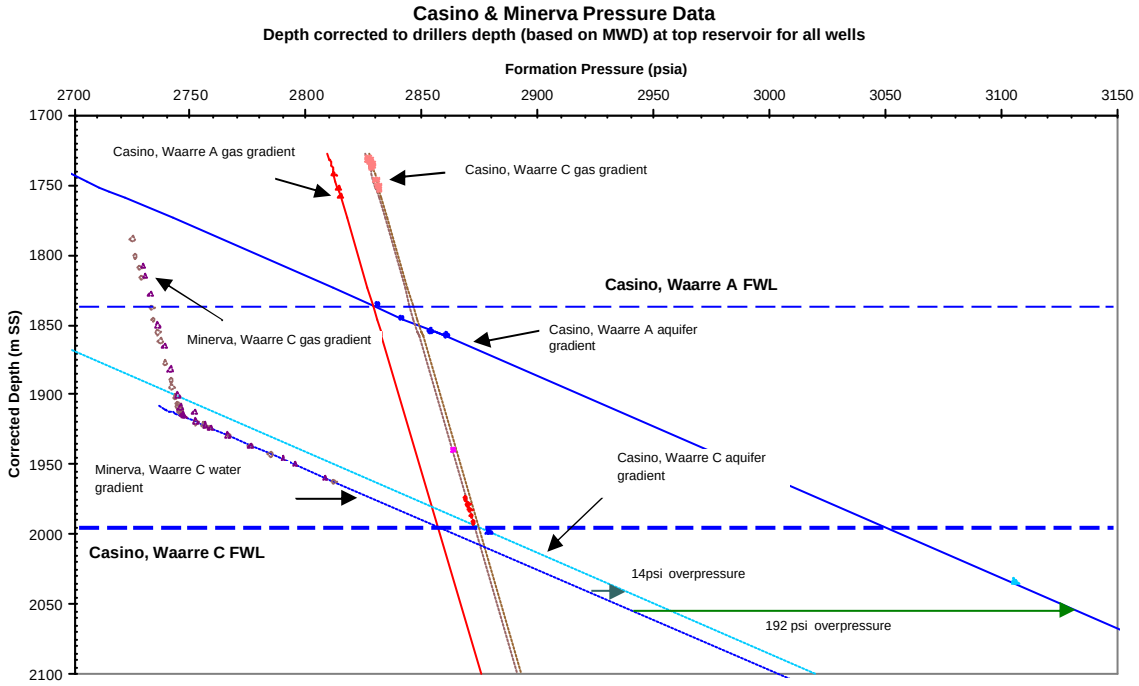

Figure 3.8.4-g: Casino and Minerva pressure data, illustrating overpressured aquifers of the Waarre C and A.

This page intentionally left blank.

3.9 Fluid Properties

3.9.1 Fluid Description

Reservoir fluid samples have been collected from all Casino wells. Fluid samples were collected from the Waarre A reservoir using the Schlumberger wireline formation tester (MDT) on Casino-1. Samples were also collected from the Waarre C reservoir using the MDT on Casino-2 and Casino-3.

In addition, separator gas and liquid samples were collected for recombination during the Production Test conducted on the Waarre C reservoir on Casino-3. A summary of the results of compositional analysis of these samples can be found in Table 3.9.1-a below. This shows the Casino fluid can be characterised as a sweet, dry gas. Inerts levels are low (2-3%) together with low levels of associated hydrocarbon liquids. A condensate/gas ratio of 1.1 bbl/MMscf was measured at the separator during the Casino-3 production test.

Well		Casino-1	Casino-2	Casino-3	Casino-3
Formation		Waarre A	Waarre C	Waarre C	Waarre C
Sample Type		MDT	MDT	MDT	DST
Sample Depth	m KB	1782.5	1764.0	1982.9, 2004.5	2004 - 2013
Sample ID		2 Sample Average	2 Sample Average	3 Sample Average	3 Sample Average
H2S	mol%	0.00	0.00	0.00	0.00
N2	mol%	3.19	2.03	2.11	2.12
CO2	mol%	0.67	0.97	0.74	0.88
C1	mol%	93.60	94.54	94.50	94.15
C2	mol%	1.51	1.67	1.77	1.93
C3	mol%	0.45	0.41	0.45	0.45
iC4	mol%	0.14	0.12	0.09	0.09
nC4	mol%	0.13	0.10	0.09	0.10
iC5	mol%	0.05	0.02	0.03	0.03
nC5	mol%	0.04	0.02	0.02	0.02
nC6	mol%	0.05	0.05	0.03	0.04
C7	mol%	0.09	0.06	0.07	0.07
C8	mol%	0.04	0.02	0.04	0.06
C9	mol%	0.04	0.02	0.02	0.03
C10	mol%	0.02	0.01	0.02	0.01
C11	mol%	0.03	0.00	0.01	0.01
C12+	mol%	0.01	0.00	0.02	0.02
Inerts	mol%	3.85	2.99	2.85	3.00
LPG's	mol%	0.71	0.63	0.63	0.64
C5+	mol%	0.34	0.18	0.25	0.27
C8+	mol%	0.12	0.04	0.10	0.13
LPG Content	bbl/MMscf	4.92	4.31	4.28	4.38
C5+ Content	bbl/MMscf	3.52	1.71	2.71	2.97
MW		17.37	17.13	17.17	17.27
SG (air=1)		0.60	0.59	0.59	0.60
Sep GLR	bbl/MMscf	n.a.	n.a.	n.a.	1.10

Table 3.9.1-a: Casino Field Compositional Summary.

3.9.2 Trace Element Analysis

In addition to the conventional sample analysis reported above, specific sampling for trace element analysis was conducted during the Casino-3 Production Test. This included analysis for H_2S, Carbonyl Sulphide (COS), mercaptans and mercury.

The results of this analysis are summarised in Table 3.9.2-a below and show minimal levels of trace element contaminants.

Test Period	H_2S by Tube v ppm	CO_2 by Tube mol%	Mercaptan by UOP v ppm	H_2S by UOP v ppm	COS by UOP v ppm	Hg ng/m^3
Main Flow 1	<0.2	0.25	<0.1	<0.1	<0.1	11.3
Main Flow 2	<0.2	0.30	<0.1	<0.1	<0.1	15.3
Main Flow 3	<0.2	0.60	<0.1	<0.1	<0.1	14.4

Table 3.9.2-a: Casino-3 Production Test Trace Element Analysis

3.9.3 Gas PVT Analysis

A constant mass study was conducted on the Casino-1 reservoir fluid sample. No dew point was encountered at reservoir temperature indicating the reservoir fluid is a dry gas.

For reservoir simulation, dry gas PVT tables were generated using the Petroleum Experts PROSPER modelling software package. Black oil correlations for viscosity, formation volume factor and compressibility factor were matched to the constant mass experimental data. The matched correlations were used to generate PVT tables for the expected range in reservoir pressure. The results are summarised in Table 3.9.3-a below.

Pressure Psia	Bg rb/Mscf	Visc cP
514.7	5.9955	0.0140
606.5	5.0590	0.0141
698.4	4.3698	0.0142
790.2	3.8419	0.0144
882.0	3.4249	0.0145
973.9	3.0875	0.0147
1065.7	2.8091	0.0148
1157.6	2.5756	0.0150
1249.4	2.3773	0.0152
1341.2	2.2069	0.0153
1433.1	2.0591	0.0155
1524.9	1.9298	0.0157
1616.7	1.8158	0.0159
1708.6	1.7148	0.0161
1800.4	1.6246	0.0163
1892.3	1.5438	0.0166
1984.1	1.4710	0.0168
2075.9	1.4052	0.0170
2167.8	1.3455	0.0173
2259.6	1.2910	0.0175
2351.4	1.2413	0.0177
2443.3	1.1958	0.0180
2535.1	1.1539	0.0182
2626.9	1.1153	0.0185
2718.8	1.0797	0.0188
2810.6	1.0468	0.0190
2902.5	1.0162	0.0193
2994.3	0.9878	0.0196
3086.1	0.9613	0.0198
3178.0	0.9366	0.0201
3269.8	0.9136	0.0204
3361.6	0.8920	0.0206
3453.5	0.8717	0.0209
3545.3	0.8527	0.0212
3637.2	0.8348	0.0215
3729.0	0.8180	0.0217
3820.8	0.8021	0.0220
3912.7	0.7871	0.0223
4004.5	0.7729	0.0226
4096.3	0.7594	0.0229
4188.2	0.7467	0.0231
4280.0	0.7346	0.0234
4371.8	0.7231	0.0237
4463.7	0.7122	0.0240
4555.5	0.7017	0.0242
4647.4	0.6918	0.0245
4739.2	0.6823	0.0248
4831.0	0.6733	0.0250
4922.9	0.6647	0.0253
5014.7	0.6564	0.0256

Table 3.9.3-a: Casino Dry Gas PVT Data.

3.9.4 Formation Water Properties

No reliable formation water samples have been obtained from the Casino field. Water PVT properties have been generated using the apparent water salinity from the Petrophysical analysis.

The data used for reservoir simulation are summarised in Table 3.9.4 below;

Pressure (psia)	Bw (rb/stb)	Compressibility (psi^{-1})	Viscosity (cP)
2811	1.0236	3.06×10^{-6}	0.405622

Table 3.9.4-a: Water PVT properties.

3.10 Static Model - Geological

3.10.1 Static Modelling - Overview

The Petrel static model was constructed using the five depth converted surfaces and associated faults. See Section 3.3.3 for details of the depth conversion methodology.

A number of 3D static models were constructed in order to evaluate the hydrocarbon-in-place distribution and associated sensitivities. The static models also provided the input for the dynamic simulation modelling – Section 4.2.

Two sets of static models were built using the same structural framework. The first incorporated a detailed 'layered cake' sub-division of the reservoirs (Section 3.5.2), whilst the second set of models incorporated the model based impedance volumes generated from the 3D seismic. The impedance based models were constructed in order to derive a relationship between impedance and porosity therefore allowing the use of the seismic dataset to generate a 3D model of reservoir distribution in Casino. The results of the latter are described in Section 3.11. All Petrel models are stored on the shared directory j:/emu/project/sbu/Otway/Permits/VIC_P44/E_and_E_Technical/Geoscience/Geology/Petrel/Casino_Def_Phase.

The following text summarises the workflow of the of the 'layer cake' model – regarded as the Base Case Model.

3.10.2 Structural Modelling

Fault Modelling

The faults in the Petrel model were generated by creating Key Pillars. These are lines that define the slope and shape of the faults, using the imported fault sticks in this case. Each fault is defined by a series of Key Pillars, which can be adjusted to match the shape of the fault to the input data. Figure 3.10.1-a shows a plan view of the faults used in the Petrel model. The fault sticks were imported in the time domain and after the fault modelling was completed they were depth converted.

Figure 3.10.2-a: 2D view of fault model *(refer to end of section for this figure).*

There are 18 faults within the model, the bulk of which are oriented in a NW-SE direction. There are no N-S or NE-SW faults mapped and the Casino field is essentially dip closed to the west, north and east. Pressure data from Casino-3 has confirmed pressure communication between it and Casino-2. Compartmentalisation appears not to be an issue in the Casino field.

Once the fault model had been constructed the 3D framework was generated, using a Petrel process called Pillar Gridding. A number of vertical pillars are created that extend along the fault planes and between the faults. The spacing of the pillars determines the horizontal cell size of the 3D grid. In the Base Case model the XY values for individual grid cells is 75x75m. Another model, using the same faults, was generated with an XY spacing of 100x100m. The coarser grid model was used as the Petrel model into which the Base Case reservoir properties were upscaled, ready for exporting to Eclipse.

A number of the faults were chosen to provide the grid with a J direction and arbitrary faults were modelled as zig zags for the Pillar Gridding process to produce a clearer and smoother skeleton grid.

The Pillar Gridding process automatically oriented the 3D grid to fit the fault model. In this case the grid is oriented NW-SE, resulting in a rotation angle of -23.7 deg.

Depth Surfaces

The following depth horizons, tied to the wells, were imported into Petrel:

Top Upper Waarre Cb – equivalent to the top of the Waarre C interval in Casino area
Top Waarre C Main Pay – equivalent to the top of the main gas bearing interval of the Waarre C
Top Waarre Ca1 – equivalent to base of the Waarre C gas bearing interval
Top Lower Waarre A – top of the main gas bearing interval for the Waarre A
Base Lower Waarre A – base of the main gas bearing interval for the Waarre A

Horizon Name	Depth Grid	Nature (for horizon model construction)
Top Waarre C	Top Upper Waarre Cb	Erosional
Top Waarre C Main Pay	Top Waarre C Main Pay	Discontinuous
Top Waarre Ca1	Base Waarre Ca2-Top Ca1	Base
Top Lower Waarre A	Top Lower Waarre A	Conformable
Base Waarre A	Base Waarre A	Conformable

Table 3.10.2-a: Imported depth surfaces *(refer to end of section for this figure).*

The 5 depth surfaces essentially provide four seismically defined containers within the model:
- Top Waarre C to Top Waarre C Main Pay,
- Top Waarre C Main Pay to Top of Waarre Ca1,
- Top Waarre Ca1 to Top Lower Waarre A and
- Top Lower Waarre A to Base Waarre A.

After the 3D framework was generated and checked, the imported depth surfaces were inserted into the Petrel model and five structural horizons created. A distance of 200m was taken around each fault to ensure a proper fault cut. This allows Petrel to ignore the input data within 200m of a fault cut and avoids the pull-ups and push-downs that can be generated by 2D mapping packages.

As further sub-division based on conventional seismic data is not possible, the framework provided by the five imported depth grids was further subdivided using the well based reservoir picks and ensuring the newly created horizons conformed to the wells.

When populating the whole model with the well based, fine scale sub-division Petrel honours the tops picked in the wells and created the reservoir zones using the *base up* approach (with respect to the controlling structural horizon) in the upper three zones and the *top down* for the fourth i.e. the Lower Waarre A. The *top down* approach keeps the thickness of the Lower Waarre A1 and A2 consistent with the well thicknesses and the excess is taken up by the Calcite Cemented Zone.

Table 3.10.1-b summarises the reservoir zones used in the Base Case model and the thickness ranges for each interval.

RESERVOIR ZONATION AND THICKNESS RANGES	
Reservoir Unit	**Thickness Range (m)**
Upper Waarre Cb	0 – 3.7
Waarre Cb Non Pay	0 – 9.67
Upper Waarre Cb Lower Pay	0 – 3.86
Waarre Cb Upper Main Pay	0 - 3
Intra Cb Silt	0 – 1.15
Waarre Cb Lower Main Pay	0 – 8.34
Waarre Ca4	0 – 6.4
Waarre Ca3	0 – 7.82
Waarre Ca2	0 – 8.55
Waarre Ca1	0 – 9.16
Lowermost Ca	0 – 17.18
Waarre B	0 – 18.77
Upper Waarre A	18.91 – 27.61
Lower Waarre A2	7.41 – 12.08
Lower Waarre A1	13.58 – 19.94
Calcite cemented zone	2.07 – 10.27

Table 3.10.2-b: Casino reservoir zonation and thickness ranges.

Figure 3.10.1-b highlights the position of the seismic picks on a schematic well summary plot and Table 3.10.1-c summarises the internal breakdown of the reservoir intervals within the Petrel static model.

Figure 3.10.2-b: Seismic picks ***(refer to end of section for this figure)***

Surface	Casino1		Casino2		Casino3	
	mSS	MD	mSS	MD	mSS	MD
Top Waarre Cb Pay	-	-	-	-	-1959.6	1982
Upper Waarre Cb Non Pay	-	-	-1722.82	1748	-1963.31	1985.71
Upper Waarre Cb - Lower Pay	-	-	-1728.38	1753.57	-1972.98	1995.38
Waarre Cb Upper Main Pay	-	-	-1732.25	1757.43	-1976.07	1998.47
Intra Cb Silt	-	-	-1735.25	1760.43	-1979.07	2001.47
Waarre Cb Lower Main Pay	-	-	-1736.39	1761.58	-1979.89	2002.29
Waarre Ca4	-	-	-1741.37	1766.56	-1988.23	2010.63
Waarre Ca3	-	-	-1747.77	1772.96	-1988.6	2011
Waarre Ca2	-	-	-1752.89	1778.08	-1996.42	2018.82
Waarre Ca1	-	-	-1761.43	1786.63	-2003.38	2025.78
Lowermost Waarre Ca	-	-	-1769.83	1795.02	-	-
Waarre B	-	-	-1787	1812.2	-2012.6	2035
Top Upper Waarre A	-1713.95	1739.52	-1805.76	1830.97	-2029.09	2051.49
Lower Waarre A2	-1732.81	1758.43	-1829.5	1854.72	-2056.7	2079.1
Lower Waarre A1	-1744.87	1770.51	-1839.82	1865.04	-2064.11	2086.51
Top Waarre A Calcite Cement Zone	-1763.58	1789.3	-1859.75	1884.108	-2077.69	2100.09
Base Lower Waarre A1	-1773.8	1799.57	-1861.82	1887.05	-2083.83	2106.23

Table 3.10.2-c: Reservoir zone top for the Casino wells.

3.10.3 Gross Reservoir Architecture

Well to well correlation (Section 3.5.2 for details), incorporating all available sources of data, has allowed a fairly straightforward correlation to be made. The Base Case model is essentially made up of a series of sub-parallel reservoir zones. The presence or absence of individual zones appears to be determined by post depositional erosion rather than syn-depositional processes.

Waarre A

The Waarre A has been subdivided into two sub-units – Upper Waarre A and Lower Waarre A. Based on log correlations the latter has been further subdivided into three flow units – Lower Waarre A2, Lower Waarre A1 and the Calcite Cemented zone (Figure 3.10.3-a).

Figure 3.10.3-a: Waarre A reservoir sub-division *(refer to end of section for this figure).*

The internal subdivision of the Upper Waarre A is not as straightforward as the Lower Waarre A. The interval is thickest in Casino-3 (28m) and thins to 19m at Casino-1, where the K85 Unconformity truncates the section. A reliable correlation between the individual sands within the interval was not possible with the existing well data. After discussions, which included the JV partners, it was agreed that the Base Case model would not attempt to sub-divide the interval and no formal subdivision of the interval would be made. Figures 3.10.3 -b & -c are Petrel generated isopachs for the two Waarre A intervals.

Figure 3.10.3-b: Upper Waarre A isopach *(refer to end of section for this figure).*

Figure 3.10.3-c: Lower Waarre A isopach *(refer to end of section for this figure).*

Waarre C

Separating the Waarre Ca/Cb from the Upper Waarre Cb in Casino-2 & -3 has followed the well log correlation. The combined thickness of the Waarre C gas pay in Casino-2 and Casino-3 is similar, 41m and 43.75m respectively, and has been assumed to be internally consistent between the two wells. The subdivision into the flow units listed in Table 3.10.2-c is driven by the core based facies correlation between the two wells (Figure 3.10.3-d). Figure 3.10.3-e is a combined isopach for the Upper Waarre Cb and Waarre C Main Pay and Figures 3.10.3-f & -g are the individual isopachs. Both the Upper Waarre Cb and Waarre C Main Pay intervals thicken in a NNE direction from the Casino-2 location with the bulk of the thickening in the Waarre C Main Pay interval. East of Casino-3 the Waarre C Main Pay interval also thickens - as shown by the isopach (Figure 3.10.3-f).

Figure 3.10.3-d: Waarre C reservoir sub-division *(refer to end of section for this figure).*

Figure 3.10.3-e: Combined Upper Waarre Cb and Ca/Cb Main Pay isopach *(refer to end of section for this figure).*

Figure 3.10.3-f: Waarre Ca/Cb Main Pay isopach *(refer to end of section for this figure).*

Figure 3.10.3-g: Upper Waarre Cb Pay and Non Pay isopach *(refer to end of section for this figure).*

The fluvial Waarre Cb has incised more deeply into the underlying Ca4 in the Casino-3 area and flattening on the base of the Ca4 clearly shows the back-barrier/lagoonal interval in Casino-2 is virtually absent in Casino-3. The underlying package of barrier/tidal channel sands appear to correlate between the two wells (Figure 3.10.3-d) suggesting a layered subdivision of the Ca is not unreasonable.

Cross plotting the Waarre C poroperms was a very useful exercise, as it demonstrated a clear overlap of reservoir properties for many of the core derived depositional facies. The beach barrier, tidal channel and tidal delta facies (Waarre Ca2 & 3) all cluster together, with the back barrier/lagoonal facies (Waarre Ca4) slightly offset (Figure 3.10.3-h). The cross plotting exercise has demonstrated that different depositional facies can be grouped into the same flow unit and leads to simpler modelling.

Figure 3.10.3-h: Waarre C PHIT vs Perm – Casino-2 & 3 *(refer to end of section for this figure).*

A similar cross plotting exercise was carried out for the Waarre A, but the lack of detailed, core based, internal sub-division made these less meaningful (Figure 3.10.3-i).

Figure 3.10.3-i: Waarre A PHIT vs Perm – Casino-1, 2 & 3 *(refer to end of section for this figure).*

3.10.4 Layer Thickness & Upscaling

Once the individual zones had been created they are subdivided into layers. Deciding upon the layer thickness for upscaling the individual reservoir zones was an iterative process. A series of upscaled porosity and permeability logs were generated using different layer thicknesses and compared to the original well data. It was found that the permeability log in particular was sensitive to layer thickness e.g. upscaling using 1m layering in the Waarre C did not fully capture the whole range of permeabilities within the interval, especially the thin high permeability intervals. The chosen layering strikes a balance by capturing the variation present within the zones, but not creating a layering so fine that the number of cells within the model becomes too large. Overlaying the petrophysical property logs with their upscaled equivalents is the best way to check whether or not the layering within a particular zone is optimum. Figure 3.10.4-a shows a

plot of the various upscaled permeability logs versus Waarre C of Casino-2 and Figure 3.10.4-b the Waarre A from Casino-1. The layering used in the Base Case is summarised in Table 3.10.4-a below and represents a balance between honouring the well data and building a workable Petrel model. Nevertheless the Base Case model is still large, as Table 3.10.4-b shows.

Figure 3.10.4-a: Casino-2 Waarre C up-scaled permeability compared to original *(refer to end of section for this figure).*

Figure 3.10.4-b: Casino-1 Waarre C up-scaled permeability compared to original *(refer to end of section for this figure).*

RESERVOIR ZONATION AND INTERNAL LAYERING		
Reservoir Unit	**Internal Layering**	**Layer Number**
Upper Waarre Cb	¦ base 0.4m	1 to 20
Waarre Cb Non Pay	Proportional 1 layer	21
Upper Waarre Cb Lower Pay	¦ base 0.4m	22 to 46
Waarre Cb Upper Main Pay	¦ base 0.4m	47 to 178
Intra Cb Silt	¦ base 0.4m	179 to 186
Waarre Cb Lower Main Pay	¦ base 0.4m	187 to 227
Waarre Ca4	¦ base 0.4m	228 to 269
Waarre Ca3	¦ base 0.4m	270 to 308
Waarre Ca2	¦ base 0.4m	309 to 354
Waarre Ca1	Proportional, 4 layers	355 to 358
Lowermost Ca	Proportional 1 layer	359
Waarre B	Proportional 1 layer	360
Upper Waarre A	¦ base 0.6m	361 to 541
Lower Waarre A2	¦ base 0.6m	542 to 620
Lower Waarre A1	¦ base 0.6m	621 to 758
Calcite cemented zone	Proportional 1 layer	759

Table 3.10.4-a: Casino Base Case Reservoir Zonation and Internal Layering.

Base Case Model	
X Y increment	75 x 75m
Total number of cells	6.09 million
Total number of defined cells	1.08 million
Orientation of grid	-23.7 deg

Table 3.10.4-b: Casino Base Case Petrel Model Statistics.

3.10.5 Property Modelling

In a reservoir modelling context the most important properties of each facies are its petrophysical properties. The straightforward internal subdivision of the Waarre A and C described above has reduced the complexity in the reservoir modelling by correlating reservoirs of similar properties. The properties of these layers are populated in the Petrophysical Modelling module. The Facies Modelling module was not used.

Petrophysical Modelling

The petrophysical modelling process populates all the cells in the 3D grid with properties e.g. porosity and permeability. The modelling process requires upscaled well logs as a starting point. These were generated using the layer thickness shown in Table 3.10.4-a.

The Petrel upscaling option chosen to populate the 3D model was the Moving Average algorithm. The algorithm uses an average for interpolation. The average is weighted by the inverse of the distance. Table 3.10.4-a summarises the porosity results for each of the reservoir zones and Table 3.10.4-b the permeability.

DISTRIBUTIONS OF POROSITY FOR THE RESERVOIR ZONES MODELLED WITHIN THE WAARRE RESERVOIR UNITS								
Reservoir Zone	**Well Ø Min dec**	**Well Ø Max dec**	**Well Ø Mean dec**	**Well Ø STD**	**Model Ø Min dec**	**Model Ø Max dec**	**Model Ø Mean dec**	**Model Ø STD**
Upper Waarre Cb Pay	0.13	0.25	0.21	0.04	0.14	0.24	0.2	0.02
Upper Waarre Cb Lower Pay	0.11	0.22	0.15	0.03	0.09	0.2	0.15	0.01
Upper Waarre Cb Main Pay	0.16	0.28	0.22	0.03	0.16	0.27	0.18	0.02
Intra Cb Silt	0.1	0.2	0.15	0.03	0.12	0.2	0.16	0.01
Lower Waarre Cb Main Pay	0.12	0.27	0.23	0.02	0.15	0.26	0.23	0.02
Waarre Ca4	0.11	0.25	0.21	0.03	0.11	0.24	0.21	0.02
Waarre Ca3	0.15	0.28	0.22	0.03	0.17	0.28	0.22	0.01
Waarre Ca2	0.07	0.27	0.18	0.06	0.08	0.27	0.19	0.04
Upper Waarre A	0.08	0.26	0.15	0.05	0.08	0.25	0.13	0.03
Lower Waarre A2	0.06	0.26	0.19	0.04	0.1	0.24	0.19	0.02
Lower Waarre A1	0.05	0.26	0.18	0.04	0.08	0.24	0.17	0.02

Table 3.10.5-a: Porosity ranges for the reservoir zones – for the wells and model.

DISTRIBUTIONS OF PERMEABILITY FOR THE RESERVOIR ZONES MODELLED WITHIN THE WAARRE RESERVOIR UNITS								
Reservoir Zone	**Well k Min mD**	**Well k Max mD**	**Well k Mean mD**	**Well k STD**	**Model k Min mD**	**Model k Max mD**	**Model k Mean mD**	**Model k STD**
Upper Waarre Cb Pay	16	2995	985	850	67	2481	687	250
Upper Waarre Cb Lower Pay	0	189	18	37	0	91	3	3
Upper Waarre Cb Main Pay	9	2454	697	748	10	1972	103	207
Intra Cb Silt	0	59	11	17	2	82	11	4
Lower Waarre Cb Main Pay	0	11833	3999	2906	25	11567	2932	1626
Waarre Ca4	0	685	99	114	0	278	87	36
Waarre Ca3	8	7171	64	1501	32	4841	555	414
Waarre Ca2	0	2925	262	614	0	2604	178	229
Upper Waarre A	0	465	9	35	0	290	1	4
Lower Waarre A2	0	436	20	49	0	198	8	7
Lower Waarre A1	0	797	38	64	0	389	12	13

Table 3.10.5-b: Permeability ranges for the reservoir zones – for the wells and model.

Figure 3.10.5-a contains a selection of layers from the model showing porosity for the Waarre A and Figure 3.10.5-b shows a selection from the Waarre C. Figures 3.10.5-c, -d, -e, & -f are a series fence diagrams through the Petrel model showing the distribution of porosity and permeability for both the Waarre A and the

Waarre C. Figure 3.10.5-g contains a number of crossplots that highlight the relationship between porosity and permeability for the well data, upscaled well data, the Petrel model and the three combined.

Figure 3.10.5-a: Waarre A up-scaled porosity – Base Case model ***(refer to end of section for this figure).***

Figure 3.10.5-b: Waarre C up-scaled porosity – Base Case model ***(refer to end of section for this figure).***

Figure 3.10.5-c: Lower Waarre A visualisation of porosity distribution ***(refer to end of section for this figure).***

Figure 3.10.5-d: Waarre C visualisation of porosity distribution ***(refer to end of section for this figure).***

Figure 3.10.5-e: Lower Waarre A visualisation of permeability distribution ***(refer to end of section for this figure).***

Figure 3.10.5-f: Waarre C visualisation of permeability distribution***(refer to end of section for this figure).***

Figure 3.10.5-g: Poroperm cross plots – well only, up-scaled data, properties from model and combined datasets ***(refer to end of section for this figure).***

3.10.6 Water Saturation

Workflow for Static Model Population of Water Saturation (Sw)

Two separate methods were used to calculate Sw in the static model. A Thomeer Sg-Height relationship and a Leverett J function were generated by the reservoir engineer (see Section 3.7). Sws were calculated for the Waarre C and A using both these functions.

The Base Case saturation model uses the Thomeer Sg-Height relationship for both the Waarre C and the Waarre A.

An upside scenario uses the Leverett J function derived Sw for the Waarre A. See Section 3.7 for discussion.

Petrel's Property Calculator facility, under the model's Properties heading, was used to calculate Sw for the Waarre A and C using both the Thomeer and the J function methodologies. The resulting saturations were then combined into a Base Case Sw (Thomeer only) and an Upside Sw (Thomeer for the Waarre C and J function for the Waarre A).

Figures 3.10.6 -a & -b show the Base Case Sw against the well derived Sw for the Waarre A and C gas bearing wells respectively.

Figure 3.10.6-a: Lower Waarre A – Well derived Sw vs P50 Model's Sw ***(refer to end of section for this figure).***

Figure 3.10.6-b: Lower Waarre C – Well derived Sw vs Model's Sw ***(refer to end of section for this figure).***

3.10.7 Sensitivities

The GIP from the Base Case static model can be compared those generated from the Elastic Impedance GIP volumes. The latter represent an independent methodology for generating additional field wide porosity models and subsequently the calculation of GIP.

It is recognised that the Base Case static model is just one representation of the Casino field's reservoir geology. In considering variations to the Base Case model the following has to be borne in mind:

- Casino-1 and -2 drilled high up on the structure and the northern flank of the field was drilled by Casino-3. These control points ensure only a small variation can be expected from any sensitivities applied to the depth conversion,
- Well data has to be honoured e.g. intra seismic reservoir sub-divisions and porosity ranges associated with the various facies etc,
- The correlation between the wells and the assumption that the gross reservoir architecture is represented by sub parallel layers present throughout the field leaves little scope for invoking the presence of a large volume of an undrilled, non reservoir facies away from well control. Although the seismic impedance work does not support the presence of a large and distinct volume of non reservoir facies within the Waarre reservoirs, some variation in Net to Gross can be expected.

There is little scope for a significant GRV variation for the field and insufficient well data to create a realistic facies model for reservoir facies prediction away from control as a way of varying Net to Gross. The best method for generating a series of differing pore volumes for the field was in varying the way Petrel sub-divides the individual reservoir zones.

In the Base Case model each individual reservoir interval was subdivided into a number of sub-layers using the *Follow Base* principle – see Table 3.10.4-a. The Waarre C reservoir zones were sub-divided into layers 40cm thick. The basal 40cm layer for each reservoir zone would be parallel to the underlying structural surface – i.e. following the base. The following 40 cm layer would be above, but still parallel to the first one. This building of sub-layers from the base up continues until the upper depth surface bounding the reservoir interval is reached. In this fashion the whole of the reservoir zone would be sub-divided into a series of 40cm thick layers. Should an individual zone be 4m thick in Casino-2 and Casino-3 then 10 sub-layers would be created. However a zone 2m thick at Casino-2 and 4m at Casino-3 would have 5 sub-layers at the former well and 10 at the latter. The upper bounding surface will determine the lateral extent of the 5 shallowest sub-layers. Figure 3.10.7-a is a schematic section showing the Base Case Waarre C reservoir sub-divisions and the geometry of the internal layering. The Waarre Ca4 interval best highlights the way *Follow Base* populates the model. The sub layers are progressively truncated by the overlying base to the Waarre Cb Lower Main Pay unit.

Figure 3.10.7-a: Waarre C intra layer sub-division – Base Case *(refer to end of section for this figure).*

Within Petrel options are available to populate zones by *Follow Base*, *Follow Top* and *Proportionally*. A number of different static models were generated using a combination of the above three. One of the first scenarios modelled proportionally sub-divided all the reservoir zones, but maintained a similar number of sub-layers at the wells as the Base Case model. It was found that the resulting net pore volume and the resultant GIP volumes for the Waarre C were significantly lower.

This *Proportional* scenario is thought to be unduly pessimistic as it does not reflect the expected geometry of the reservoir intervals. However the *Follow Base* model can be considered unrealistic for some of the reservoir zones. The net result is that a number of hybrid models were produced using a combination of *Follow Base*, *Follow Top* and *Proportional* to populate the reservoir zones. Figure 3.10.7-b is one such hybrid scenario. Here the Waarre Ca2 and Ca3 has been populated proportionally and the Waarre Cb Lower Main Pay using *Follow Top*, reflecting an infilling of topography.

Figure 3.10.7-b: Waarre C intra layer sub-division – Hybrid Case *(refer to end of section for this figure).*

Table 3.10.7-a summarises the layering sensitivities carried out.

Independent of the above are the GIP volumes generated from the three impedance models. These represent a further set of scenarios that model the 3D variation in reservoir quality throughout the Casino field.

Gas In Place

The volumetric module in Petrel was used to calculate Gas in Place (GIP) for the Base Case model and all the sensitivities run on this model. The resulting GIP volumes are summarised in Section 3.12.

	Final Layered Petrel Model and Sensitivities											
Case ID	**Pet_04**	**Pet_04b**	**Pet_04c**	**Pet_04d**	**Pet_04e**	**Pet_04f**	**Pet_04g**	**Pet_04i**	**Pet_04m**	**Pet_04n**	**Pet_04j**	**Pet_04k**
Date	6-Apr-04	6-Apr-04	20-May-04	20-May-04	20-May-04	20-May-04	21-May-04	21-May-04	26-May-04	26-May-04	7-May-04	7-May-04
Petrel Sensitivity	Base	Waarre A Sw Model	Layering Sensitivity 1	Layering Sensitivity 2	Layering Sensitivity 3	Layering Sensitivity 4	Layering Sensitivity 5	Sensitivity 7 using Workflow Tool	Layering Sensitivity 8	Layering Sensitivity 9	Upper Cb Main Pay Sensitivity	Silt Sensitivity 1
Petrel Model Notes - Zone												
Waarre C	Follow Base	Follow Base	Follow Top	Follow Base Follow Base	Follow Top	Follow Top	Follow Base Follow Base	Follow Base	Follow Base	Follow Base Follow Base	Follow Base	Follow Base
Waarre A	Follow Top	Follow Top	Follow Top		Follow Top	Follow Top		Follow Top	Follow Base		Follow Top	Follow Top
Petrel Model - Interzone Layering												
Upper Cb "Impedance" 3P Pay												
Upper Cb Non Pay												
Upper Cb "Casino-3" 2P Pay	Base Up	Base Up	Base Up	Proportional	Proportional	Top Down	Top Down	Base Up	Base Up	Base Up	Base Up	Base Up
Upper Cb Non Pay	Proportional	Proportional	Proportional	Proportional	Proportional	Proportional	Proportional	Proportional	Proportional	Proportional	Proportional	Proportional
Upper Cb Lower 1P Pay (Corr. from C-3 to C-2)	Base Up	Base Up	Base Up	Proportional	Proportional	Top Down	Top Down	Base Up	Base Up	Base Up	Base Up	Base Up
Upper Cb main pay	Base Up	Base Up	Base Up	Proportional	Proportional	Top Down	Top Down	Base Up	Proportional	Base Up	Proportional	Base Up
Cb silt	Base Up	Base Up	Base Up	Proportional	Proportional	Top Down	Top Down	Proportional	Proportional	Proportional	Base Up	Base Up
Lower Cb main pay	Base Up	Base Up	Base Up	Proportional	Proportional	Top Down	Top Down	Top Down	Top Down	Top Down	Base Up	Base Up
Ca4	Base Up	Base Up	Base Up	Proportional	Proportional	Top Down	Top Down	Base Up	Base Up	Base Up	Base Up	Base Up
Ca3	Base Up	Base Up	Base Up	Proportional	Proportional	Top Down	Top Down	Proportional	Proportional	Proportional	Base Up	Base Up
Ca2	Base Up	Base Up	Base Up	Proportional	Proportional	Top Down	Top Down	Proportional	Proportional	Base Up	Base Up	Base Up
Ca1	Proportional	Proportional	Proportional	Proportional	Proportional	Proportional	Proportional	Proportional	Proportional	Proportional	Proportional	Proportional
Upper Waarre A	Base Up	Base Up	Base Up	Proportional	Proportional	Proportional	Proportional	Base Up	Base Up	Base Up	Base Up	Base Up
Lower Waarre A2	Base Up	Base Up	Base Up	Proportional	Proportional	Top Down	Top Down	Base Up	Base Up	Base Up	Base Up	Base Up
Lower Waarre A1	Base Up	Base Up	Base Up	Proportional	Proportional	Top Down	Top Down	Base Up	Base Up	Base Up	Base Up	Base Up
Waarre A Calcite cmt	Proportional	Proportional	Proportional	Proportional	Proportional	Proportional	Proportional	Proportional	Proportional	Proportional	Proportional	Proportional

Table 3.10.7-a: Summary the layering sensitivities.

3.10.8 Upscaling & Exporting to Eclipse

The Base Case Petrel static model was upscaled into an Eclipse model. The latter had a grid XY increment of 100mx100m. The layering within the reservoir zones is summarised in Table 3.10.8-a.

Reservoir Unit	Eclipse Model Internal Layering	Base Case Fine Scale Layering	Upscaled Layering
Upper Waarre Cb	¦ base 1m	1 to 20	1 to 9
Waarre Cb Non Pay	Proportional 1	21	10
Upper Waarre Cb Lower Pay	¦ base 1m	22 to 46	11 to 26
Waarre Cb Main Pay2	¦ base 1m	47 to 178	27 to 31
Intra Cb Silt	Proportional 1*	179 to 186	32
Waarre Cb Main Pay1	¦ base 1m	187 to 227	33 to 56
Waarre Ca4	¦ base 1m	228 to 269	57 to 73
Waarre Ca3	¦ base 1m	270 to 308	74 to 97
Waarre Ca2	¦ base 1m	309 to 354	98 to 129
Waarre Ca1	Proportional 4	355 to 358	130 to 133
Lowermost Ca	Proportional 1	359	134
Waarre B	Proportional 1	360	135
Upper Waarre	Proportional 15*	361 to 541	136 to 150
Lower Waarre A2	¦ base 2m	542 to 620	151 to 167
Lower Waarre A1	¦ base 2m	621 to 758	168 to 194
Calcite cemented zone	Proportional 1	759	195

** Follow base in Base Case model – changed to Proportional to reduce the number of layers within the Eclipse model*

Table 3.10.8-a: Casino Eclipse Petrel Model Reservoir Layering.

Porosity and permeability, including Kv sensitivities, were exported from Petrel in an Eclipse format. Only the PHIT grid and the associated arithmetically upscaled permeability models from the Base Case were exported for the dynamic simulation. For the Kv sensitivities the permeability property was multiplied by 0.5, 0.1 and 0.01 using the Petrel calculator. These permeabilities was used as the input for the upscaled Perm K direction in the tensor based upscaling process, with the original permeability grid being used for the Perm I and J directions. Table 3.10.8-b summarises the parameters used to export the Base Case properties.

Parameter	Description	Method	Weighting
Porosity	Phit	Arithmetic	Bulk volume
Permeability 1	Perm (Kv/Kh = 1)	Flow Based Tensor – closed boundary	NA
Permeability 2	Perm (Kv/Kh = 0.1)	Flow Based Tensor – closed boundary	NA
Permeability 3	Perm (Kv/Kh = 0.01)	Flow Based Tensor – closed boundary	NA
Permeability 4	Perm (Kv/Kh = 0.5)	Flow Based Tensor – closed boundary	NA

Table 3.10.8-b: Eclipse Upscaling Parameters.

This page intentionally left blank.

3.11 Static Reservoir Modelling – Impedance Based

3.11.1 Introduction

A series of 3D static reservoir models were constructed for the Casino field to evaluate the hydrocarbon-in-place distribution and associated sensitivities, and to provide input into the 3D dynamic simulation phase. This section covers the model that was created specifically to include the 3D seismic data volume.

The static reservoir model was build using the Petrel software application, and the final model is called: ***Casino_Imp_Mar_2004.pet.*** All Petrel models are stored on the shared directory j:/emu/project/sbu/Otway/Permits/VIC_P44/E_and_E_Technical/Geoscience/Geology/Petrel/Casino_Def_Phase.

Logs for the three exploration wells, faults, time grids and velocity grids were loaded and formed the basis for the 3D model.

Table 3.11.1-a provides a listing of well details and formation tops as encountered by the wells that formed the basis for this model. The two-way-time picks listed were derived by back-interpolation of the time grids and should resemble the original seismic picks closely.

Well Details	**Casino-1**		**Casino-2**		**Casino-3**	
DFE	25		25		22.4	
Easting (m)	647654.99		651752.73		650704	
Northing (m)	5705323.93		5704463.69		5706627	
Formations	**ms TWT**	**m ss**	**ms TWT**	**m ss**	**ms TWT**	**m ss**
Top Reservoir	1326	1714	1371	1723	1515	1960
Top Waarre C Low Impedance	1326	1714	1375	1732	1522	1973
Base Waarre C	1326	1714	1394	1761	1539	2003
Top Lower Waarre A	1351	1733	1429	1830	1565	2057
Base Lower Waarre A	1373	1773	1448	1862	1580	2084

Table 3.11.1-a: Well details for Petrel model.

3.11.2 Structural Model

Building of the structural model occurred in the time domain using the time horizons and identified fault segments from the 3D seismic dataset.

The Waarre Sandstone is a conventional clastic shallow marine deposit, and has been subdivided into number of stratigraphic units, assisted by 3D seismic data. Five seismic reflection surfaces are mapped across the field. Point files of the picks, and/or Zmap 2D grid files, were loaded into Petrel and subsequently gridded, to form the basis of the 3D time model. The details for the time structural model construction are given in Table 3.11.2-a.

A distance of 200 metres was taken around each fault, to ensure a proper “fault cut”. This allows Petrel to “ignore” data within 200 metre of a fault cut, and hence avoid the pull-ups and push-downs that tend to be generated by 2D mapping packages. No further smoothing was applied.

Horizon Name	Time Grids	Nature (for horizon model construction)
Top Upper Cb	FC_Top_Waarre_Cb_16mar_095510 (for modelling purposes, used the merged Top Waarre CB, Top Waarre C LowImp and Base C grids)	erosional
Top C Main Pay	FC_Top_WaarreC_LowImp_10mar_164203 (for modelling purposes, used the merged Top Waarre C LowImp and Base C grids)	discontinuous
Base C reservoir	FC_Base_C_10mar_163630	base
Top Lower A	FC_TLA_10mar_163934	conformable
Base A	FC_Base_A_10mar_163155	conformable

Table 3.11.2-a: - Surface TWT data used in the modelling process.

After time to depth conversion, an erosion tolerance gap of 2 metres was applied (i.e. all zones under the erosional top surface were eliminated in areas where the total thickness is less than 2 metres). This eliminates erroneous zones, introduced by input surface mis-matches.

3.11.3 Stratigraphy

These five horizons effectively create four stratigraphic units, which are briefly discussed in the following section.

Upper Cb Stratigraphic Unit

The Upper Cb was intersected only in the Casino-2 and -3 wells. The entire section down to the base of the C reservoir is eroded in the Casino-1 well. To assist the modelling, a “top reservoir” surface was created by merging the Top Cb, Top C Low Imp and Base C surfaces to provide a common “top reservoir” envelope.

The top of the unit is defined on seismic by an erosive horizon interpreted to represent a sequence boundary.

Waarre C Main Pay Stratigraphic Unit

This unit is also only present in the Casino-2 and -3 wells, and has been eroded in the Casino-1 area. It contains the bulk of the reservoir rock.

Non reservoir; Waarre Ca1, Waarre B and Upper Waarre A Stratigraphic Units

These combined units form the non-reservoir interval, separating the Waarre C reservoir from the Waarre A, in this model.

There are some thin gas bearing sands in the Upper Waarre A in both the Casino-1 and -2 wells, however, the resolution of the seismic does not allow for a clear definition of these. The top of the Waarre A is poorly resolved and difficult to trace on the seismic volume.

Lower Waarre A Stratigraphic Unit

This unit is present in all three Casino wells. It extends across the entire area. The Waarre A is sealed by the Waarre B shale, which forms part of the non-reservoir units. This unit has a different GWC from the Waarre C interval.

3.11.4 Time to Depth Conversion in Petrel

Depth conversion of the entire 3D model took place in Petrel using a mixture of velocity grids and average velocities.

See Section 3.3.3 for details.

3.11.5 Model Geometry and Layering

As the seismic grid size is approximately 25 x 25 metres, using the 75 x 75 m grid designed for the base case model of the Casino field would introduce a significant upscaling error as there is significant variation in AI in an areal sense around the well locations. A first attempt at 75x75 m indicated that significant heterogeneity is lost in a lateral sense as displayed by Figure 3.11.5-a.

To keep the model size workable, the model was refined to a 25x25 metre grid spacing, but slightly reduced in extent, the northernmost water bearing section was excluded from the model (see Figure 3.11.5-b).

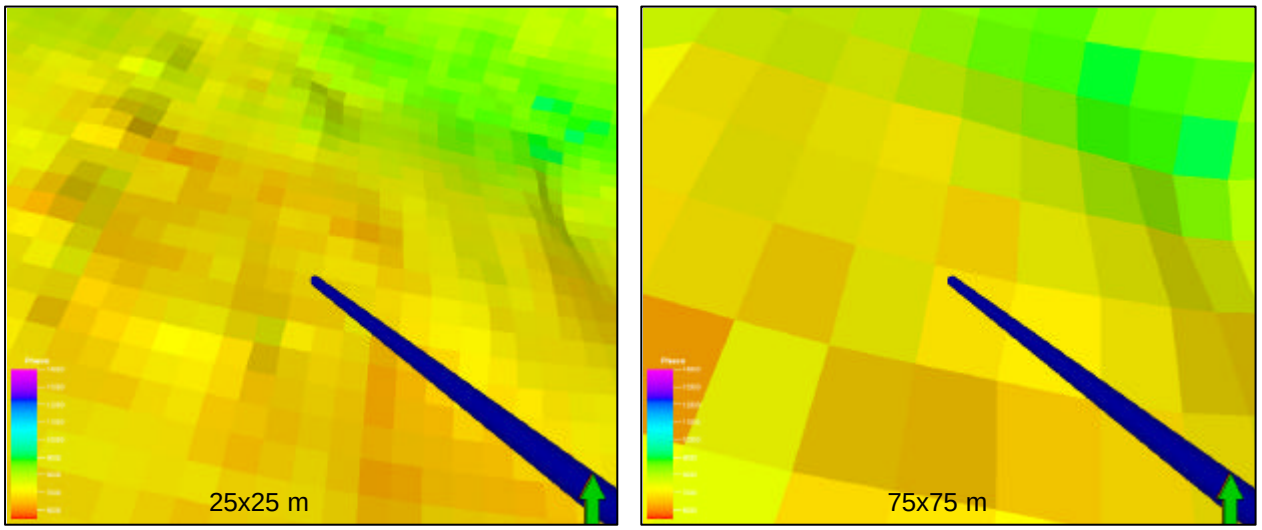

Figure 3.11.5-a: Comparing the 75x75 m grid with the 25x25 m grid at the Casino-2 well location.

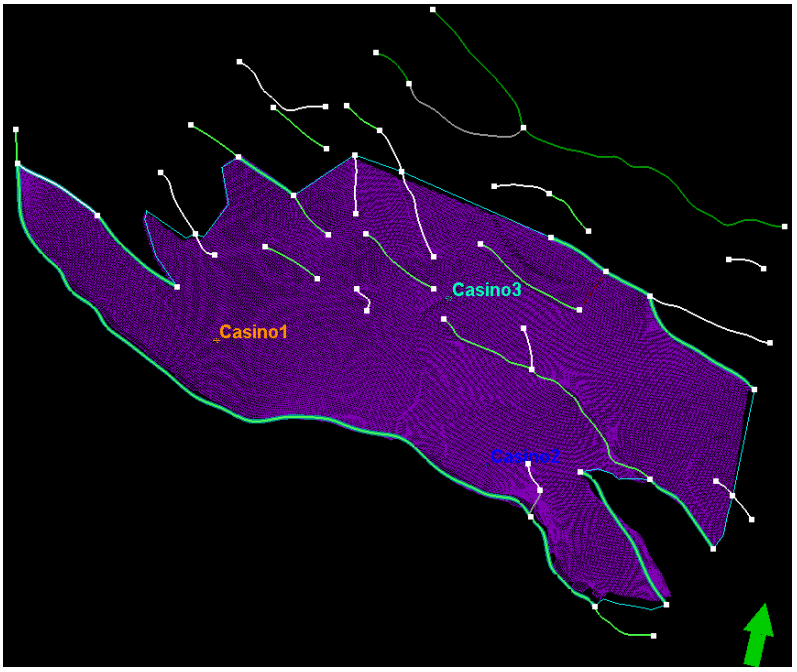

Figure 3.11.5-b: Outline of the main faults and grid boundary.

In a vertical sense, the seismic provides an approximately 2 metre resolution. Hence the layering of the reservoir units for this particular Petrel model proceeded with 2 metre thick layers, following the base of the units to resemble the erosive nature of the top of the reservoir.

The model contains in a vertical sense the section between the top of the Upper Waarre Cb Formation and the Base Waarre A seismic marker, encompassing all possible reservoir sands in the Waarre Formation. The resultant grid is 443 by 156 cells with a total of 153 layers. This brings the total number of cells to 10.4 million, of which 1.9 million have defined values (i.e. are active cells).

Units	Internal Layering	Layer Numbers
Upper Cb	|| base, 2 m	1 to 20
C reservoirs	|| base, 2 m	21 to 74
Non Reservoir	Proportional, 1 layer	75
Lower A	|| base, 2 m	76 to 156

Table 3.11.5-a: Modelled Units and Layering.

3.11.6 Seismic Volume

Three seismic acoustic impedance seismic volumes were loaded:

Inv_fc_mb1001.sgy represents the FC_Casino_MB_23feb2004_without_Cas3 volume generated in-house by the Casino team, using two wells. This data volume needs to be shifted down 1000 msec, to provide the correct depth.

JC_t104.sgy is an acoustic impedance volume that was generated by a consultant, John Cant, and updated late March. This volume is also referred to in the text as the “JC” volume.

Inv_fc_allwells represents the FC_Casino_MB_17Feb2004 volume generated in-house as an alternative volume, using 3 wells. This data volume also needs to be shifted down 1000 msec, to provide the correct interval. This volume is also referred to in this text as the "FC_3well" volume.

The seismic volumes were attached to the 3D depth model and subsequently depth converted using the same velocity model as the 3D TWT model. To get a quick impression of the seismic volume, the seismic was resampled into the 3D model as a property, using the "closest" algorithm.

To get the detailed impedance volume, the exact algorithm, combined with arithmetic averaging, was used as an overnight job.

The resultant property volumes were then clipped; values below 6000 were set to undefined on the three seismic volumes. These values occurred predominantly on the upper, lower and side edges of the model, and appear to result from averaging zero value cells into the model. The minimum cut-off value of 6000 is based on AI log values observed in the wells.

Seismic Resampling Techniques

Resampling of the seismic data makes it match the 3D grid cells. Initial resampling was done using the closest algorithm as this provides a quick quality check of the 3D volume. The Exact algorithm took between 8 – 10 hours to run.

- ***Closest:*** each property cell will be contributed to only by the closest (or most central) seismic cell. This method is very fast, but unsuitable for geological grids that have a lower resolution than the seismic volume. Well suited for resampling discrete value (e.g. facies) volumes.

- ***Exact***: all seismic cells intersecting the property cell will contribute to the average calculations, but volume correction is performed. This method will take a long time, but will produce the most accurate results in all cases.

Figure 3.11.6-a displays a slice from two of the three acoustic impedance scenarios.

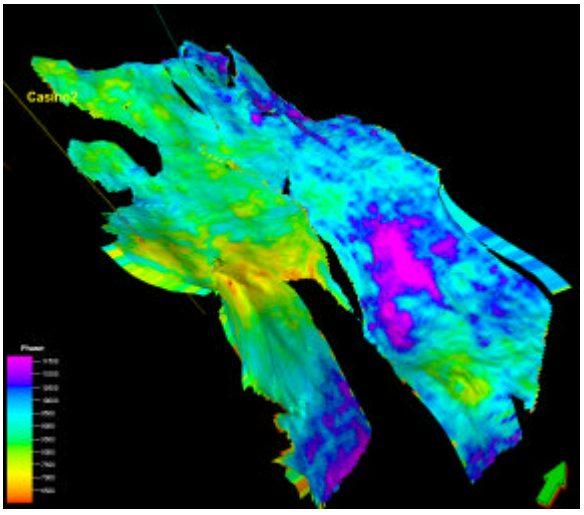

JC AI volume

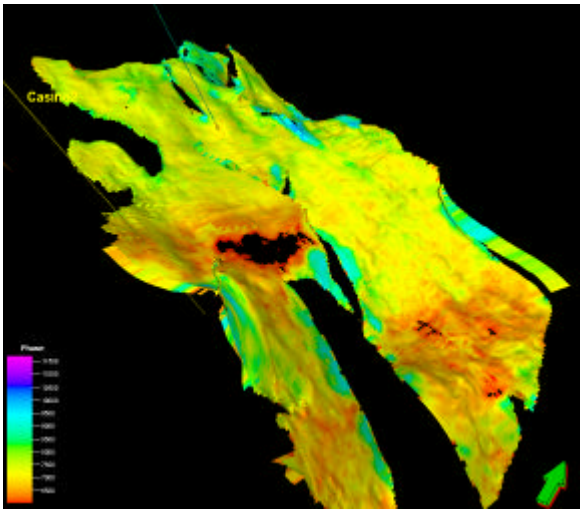

FC 3 well AI volume

Figure 3.11.6-a: Acoustic Impedance Property (exact), Layer 65 – towards Base Waarre C.

The following is a list of property files that has been created:

Properties:	
Inv_fc_allwells_closest	*FC 3well AI model, closest seismic resampling algorithm*
Inv_fc_allwells_closest clip5500	*FC 3well AI model, closest resampling, values below 5500 set to undefined*
Inv_fc_allwells_exact	*FC 3well AI model, exact seismic resampling algorithm*
Inv_fc_allwells_exact_clip6000	*FC 3well AI model, exact resampling, values below 6000 set to undefined*
Inv_fc_allwells_exact_clip6000_gascap	*FC 3well AI model, exact resampling, values below 6000 set to undefined, gascap sections only*
Inv_fc_mb1001_closest	*FC 2well AI model, closest seismic resampling algorithm*
Inv_fc_mb1001_closest cli6000	*FC 23well AI model, closest resampling, values below 5500 set to undefined*
Inv_fc_mb1001_exact	*FC 2well AI model, exact seismic resampling algorithm*
Inv_fc_mb1001_exact_clip6000	*FC 2well AI model, exact resampling, values below 6000 set to undefined*
Inv_fc_mb1001_exact_clip6000_gascap	*FC 2well AI model, exact resampling, values below 6000 set to undefined, gascap sections only*
Jc_t104_closest	*JC AI model, closest seismic resampling algorithm*
Jc_t104_closest cli6000	*JC AI model, closest resampling, values below 5500 set to undefined*
Jc_t104_exact	*JC AI model, exact seismic resampling algorithm*
Jc_t104_exact_clip6000	*JC AI model, exact resampling, values below 6000 set to undefined*
Jc_t104_exact_clip6000_gascap	*JC AI model, exact resampling, values below 6000 set to undefined, gascap sections only*

Table 3.11.6-a: List of seismic property files.

3.11.7 Petrophysical Properties

Porosity and permeability were derived from petrophysical log evaluation and used to populate the models.

Well Log Upscaling

The logs were averaged (upscaled) over the defined layers using the following techniques:

- PHIT was averaged over the model layers using arithmetic averaging
- Kint was averaged over the model layers using arithmetic averaging

The averaged (upscaled) logs were checked for their consistency with the original log (see Figure 3.11.7-a).

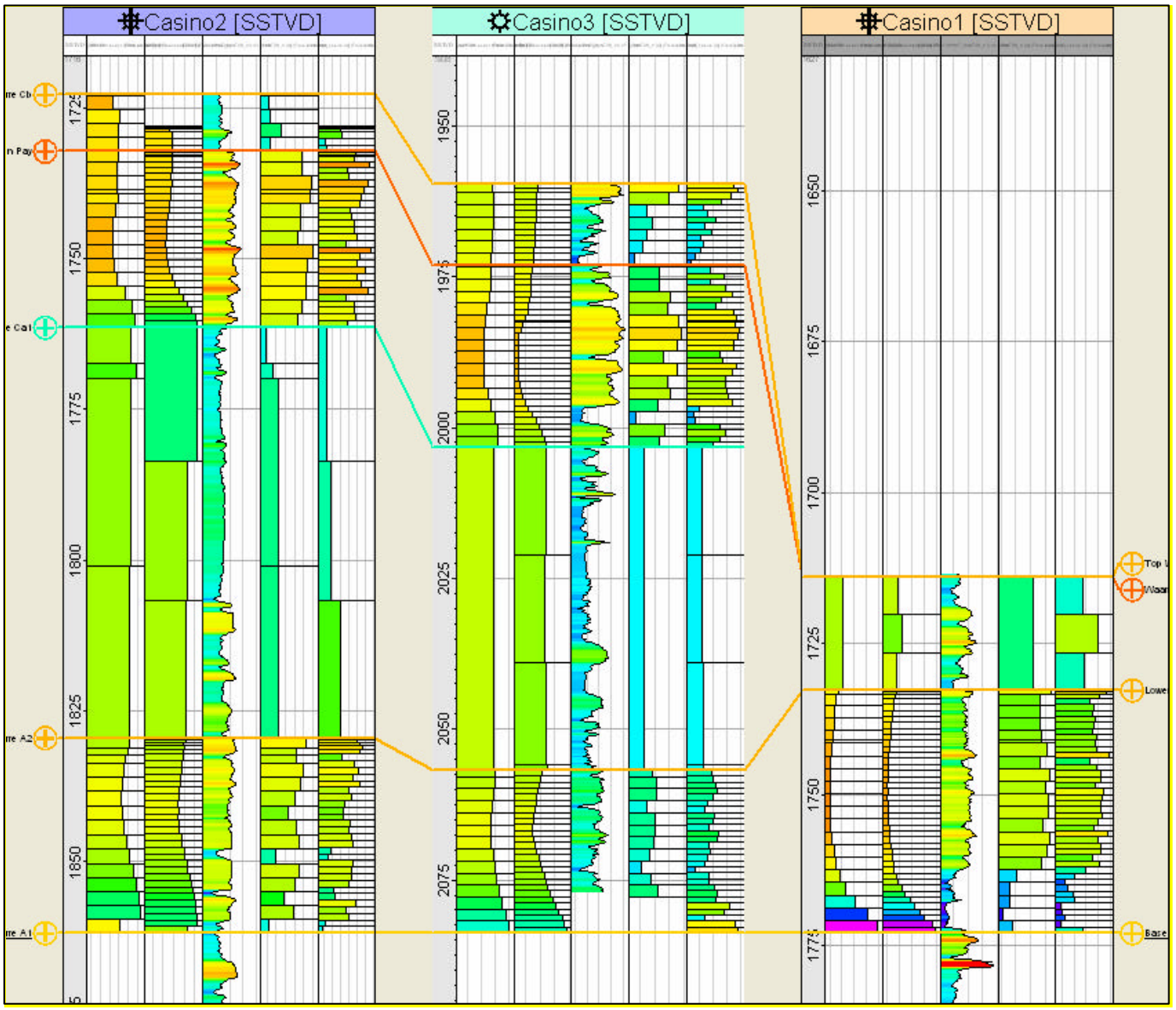

Figure 3.11.7-a: From left to right for each of the 3 wells: AI back interpolated 25x25x2m, AI back interpolated 75x75x1m, original PHIT, upscaled PHIT 2m, upscaled PHIT 1m.

3.11.8 Variograms

Variograms are used in the 3D modelling process to reflect the variation in the horizontal and vertical property distribution when using kriging or Sequential Gaussian Simulation techniques.

When another property is used as a co-kriging variable to provide a 3D trend (like in this case the Acoustic Impedance property), a high correlation coefficient gives a close match between the properties, and the lateral distribution of the property to be created is less influenced by the variogram. Where a low correlation coefficient between the trend property and the property to be modelled is derived, the variogram will play a larger role in the 3D distribution of the property.

The horizontal variogram range that was used was derived from an initial inspection of the seismic inversion volume (FC 2 wells, 75x75 m model, all reservoirs). This provides a much better handle on lateral variation over the field than the 3 wells.

The vertical range was derived from the variance plot of the PHIT log data.

Base Case Variogram	
function	spherical
sill	1
nugget	0.1
anisotropy	none
Orientation major axis	75 degrees
Major range	500 metres
Minor range	1800 metres
Vertical range	15 metres

Table 3.11.8-a: Variogram Details.

Using a variogram and Sequential Gaussian Simulation ensures that the variations observed in the logs across the defined flow zones are represented in a similar proportion in the model, both in a vertical and in a lateral sense.

Future Work

It is recommended that, when time allows, a more detailed inspection of the seismic volume is carried out, to verify the variogram for the different reservoirs, as there does appear to be some variation between the reservoirs and the different inversion volumes. Preferably, this work would concentrate on the agreed base case AI volume.

3.11.9 Porosity

The porosity was modelled over the reservoir intervals using Sequential Gaussian Simulation, and followed a two step routine:

1. Using the variogram and transformations made in the data analysis process for each of the three zones:

    a. The output range was set to the existing range of upscaled values.
    b. A well log based relationship, derived from the gas bearing section in the three wells, was applied to the data. As an alternative scenario, a 3D trend was derived between the PHIT and the AI volume, using the AI over the gascap and the upscaled log data.
    Appendix A (see Section 3.11.15) shows the upscaled well values with super-imposed the log derived PHIT – AI relationship. In grey, the upscaled relationship is displayed, with the corresponding correlation coefficient.
    c. The data was normalized.

2. Populated the 3D volume using Sequential Gaussian Simulation, using the data transformations and variogram from the data analysis phase. Collocated co-kriging with the AI volume over the gascap (or for the log relationship the entire volume), deriving an estimated correlation coefficient from the data for each of the three zones.

    a. In the case of using the relationship from the upscaled logs, the data set for the Upper Cb interval was limited, and the same relationship and correlation coefficient was used as was derived over the C interval.
    b. For the model using the log derived AI vs. PHIT relationship, the relationship derived from the gascap was applied to the entire volume (gas and water).

To create a model that fully reflects the total amount of gas-in-place; the total porosity value was used.

The three AI volumes are quite different. They have different minimum and maximum values, and a different mean. They are also different at the well locations, and hence the PHIT vs AI relationships which would be derived from the actual (upscaled) model data vs the relationships as derived from the well log data, are different for each AI volume. As a consequence, the correlation coefficient (cc) varies between the volumes

and zones, and hence the influence of the variogram (lower cc = higher influence variogram) on each of the porosity volumes.

On volumes where the derived cc is low, the effect of the variogram, and hence the seed value, is higher. A change in seed value between different realisations would generate a quite different PHIT volume.

Future Work

Note that there appears to be an area to the north of Casino-2 which has very low AI values in the Waarre C. By using the 6000 cut-off for Acoustic Impedance, the values in this area are set to indeterminate. However, the variogram used in property population still ensures a smooth interpolation across this area. The very low values indicate either an error in the AI volume, or more likely, better reservoir quality than seen in any of the wells. It is recommended that an alternative PHIT and perm model is created, preferably from the unclipped AI model, without applying the minimum – maximum output range, to get an idea of the possible reservoir quality in this area.

Table 3.11.9-a provides the range of porosities as observed in the logs, and the range represented in the model after upscaling (arithmetically averaging of the log values) over the units, and Table 3.11.9-b the PHIT vs. AI relationship.

Phit	Upper Cb		C reservoir		Lower A	
	log	upsc 2 m	log	upsc 2 m	log	upsc 2 m
min	0.06	0.08	0.07	0.08	0.04	0.06
max	0.25	0.23	0.28	0.25	0.26	0.23
mean	0.139	0.140	0.206	0.205	0.171	0.172
stdev	0.0433	0.0410	0.0440	0.0366	0.0496	0.0437
corr with Perm		0.85		0.87		0.82

Table 3.11.9-a: Porosity Details.

Phit vs Accoustic Impedance	Phit vs AI from logs phit=a*AI+b			Phit vs AI FC volume phit=a*AI+b			Phit vs AI JC volume phit=a*AI+b			Phit vs AI FC 3well volume phit=a*AI+b		
	a	b	r2	a	b	r2	a	b	r2	a	b	r2
Upper Cb to Top Main Pay gas	-0.00003	0.4395	0.45	using Cb main pay			using Cb main pay			using Cb main pay		
Cb Main Pay to top Ca1 gas	-0.00005	0.5939	0.88	-0.000026	0.38597	-0.43	-0.000025	0.421575	-0.52	-0.000034	0.456469	-0.69
Lower Waarre A gas	-0.00003	0.4622	0.89	-0.000020	0.327871	-0.41	-0.000015	0.344562	0.21	-0.000049	0.535415	-0.78

Table 3.11.9-b: Porosity vs Acoustic Impedance Relationship.

Figure 3.11.9-a is a slice from two of the porosity volumes derived from the AI datasets.

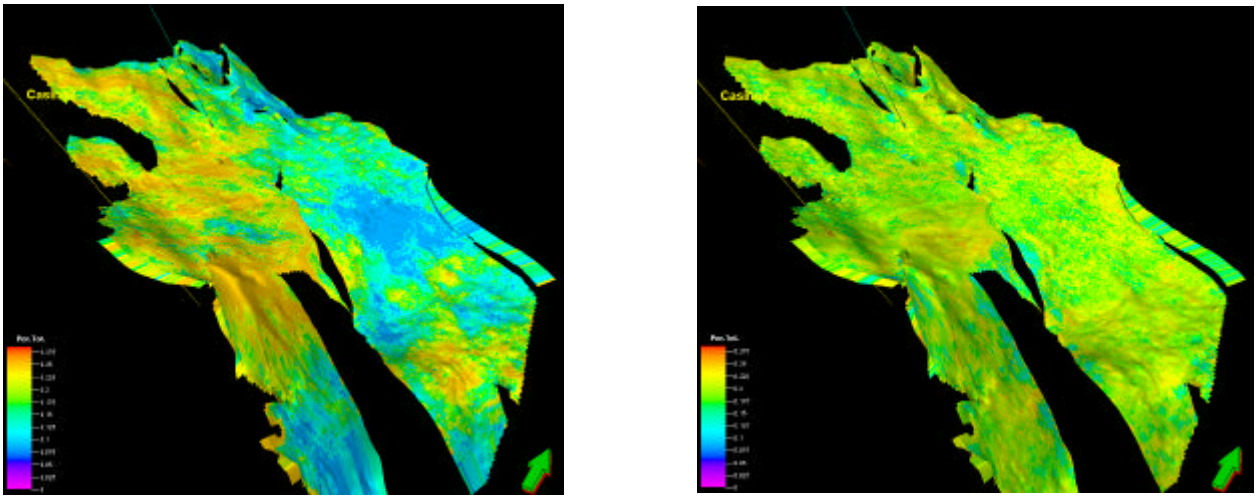

PHIT from JC AI volume | PHIT from FC 3 well AI volume

Figure 3.11.9-a: Porosity models from seismic inversion, Layer 65 – towards Base Waarre C.

The following is a list of property files that has been created:

Properties:	
PHIT_fc_inv_allwells_gascap	*FC 3well AI model, trend derived from upscaled logs, gascap only*
PHIT_fc_inv_allwells_logrelation	*FC 3well AI model, trend derived from original log*
PHIT_fc_inv_gascap	*FC 2well AI model, trend derived from upscaled logs, gascap only*
PHIT_fc_inv_logrelation	*FC 2well AI model, trend derived from original log*
PHIT_jc_inv_gascap	*JC AI model, trend derived from upscaled logs, gascap only*
PHIT_jc_inv_logrelation	*JC AI model, trend derived from original logs*

Table 3.11.9-c: List of total porosity property files.

3.11.10 Permeability

Upscaling of the permeability logs can be done using arithmetic, geometric or harmonic averaging techniques. Determining the effective permeability values is much more complex than straightforward averaging. This is because permeability is the relationship between the dynamic properties of flow rate and pressure differential. For example, in a system with a low Kv/Kh ratio, the correct upscaled permeability will depend most heavily on the fine layers in which there are completions.

The arithmetic upscaled permeability will give higher values than the geometric, which in turn is higher than the harmonic upscaled permeability. Often, in rather homogeneous reservoirs (Kv/Kh =1), geometric is a good choice. Depending on the direction of the layering versus the dominant flow direction, arithmetic or harmonic may be closer.

For Casino, it was decided by the team to use arithmetic upscaled logs as a base case. Permeability volumes were only derived from the PHIT volumes that used the log derived relationships, and consisted of merged gascap and water leg porosity volumes.

The permeability was modelled over the reservoir intervals using Sequential Gaussian Simulation, and following a process similar to the porosity modelling:

1. Using the variogram and transformations made in the data analysis process for each of the three zones:
   a. The output range was set to the existing range of upscaled values
   b. A 3D trend was derived between the perm and the PHIT volume.
   c. The data was labelled as a logarithmic property.
   d. The data was normalized.

2. Co-located co-kriging with the PHIT volume, deriving an estimated correlation coefficient for each of the three zones.

Perm	Upper Cb		C reservoir		Lower A	
	log	upsc 2 m	log	upsc 2 m	log	upsc 2 m
min	0	0.015	0	0.005	0	0
max	2995	1133	11833	5770	797	175
mean	162	178	1327	1404	28	26
stdev	494	410	2187	1860	57	32

Table 3.11.10-a: Permeability Details.

The Casino field displays a clear porosity – permeability relationship. Figure 3.11.10-a provides the PHIT vs kint trend for the Casino logs directly from the Petrel data analysis, for the reservoir units only. The original log data is displayed as blue points, the upscaled (averaged) log data as green.

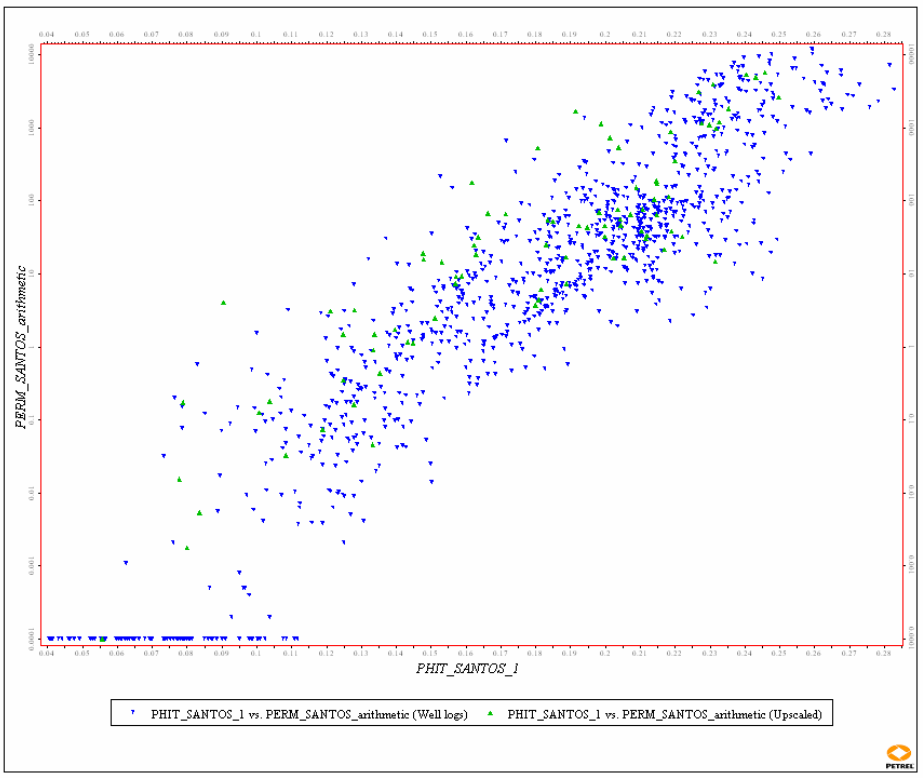

Figure 3.11.10-a: Casino Field PHIT – Permeability relationship.

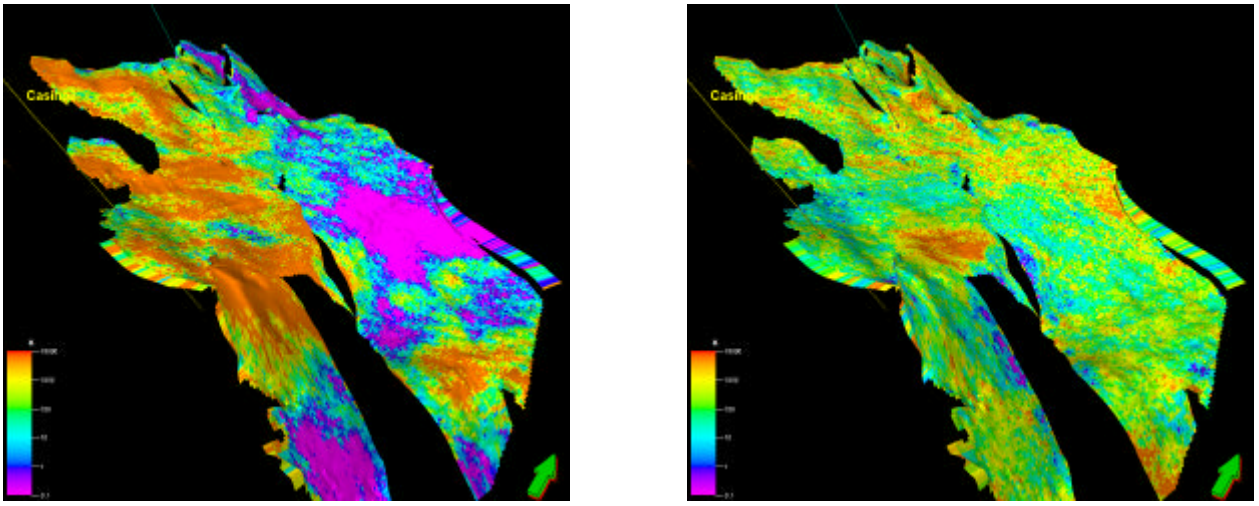

Perm from JC AI volume

Perm from FC 3 well AI volume

Figure 3.11.10-b: Permeability models from seismic inversion, Layer 65 – towards Base Waarre C.

The following is a list of property files that has been created:

Properties:	
Perm_arithmetic_fc_inv_allwells_log	*arithm upscaled perm co-kriged with PHIT_fc_inv_allwells_logrelation*
Perm_arithmetic_fc_inv_log	*arithm upscaled perm co-kriged with PHIT_ fc_inv _logrelation*
Perm_arithmetic_jc_inv_log	*arithm upscaled perm co-kriged with PHIT_ jc_inv _logrelation*

Table 3.11.10-b: List of permeability property files.

3.11.11 Fluid Contacts

The contacts used are those resulting from log and well bore pressure data. Further details about the RFT analysis are provided in the Casino FDP.

A FWL of 1999 mss was used for the Waarre C reservoirs, and 1839 mss for the Waarre A reservoirs. Table 3.11.11(a) summarises the main data used in the modelling.

Data	Value
Waarre A FWL (m ss)	-1839
Waarre C FWL (m ss)	-1999

Table 3.11.11-a: General data used for static model.

3.11.12 Volumetrics: NPV

The base case volumetrics were based on the base case structural model, and reservoir properties populated between the well locations using the “moving average” algorithm. This seismic derived property model was run to provide a sensitivity to those. Appendix B (see Section 3.11.16) provides a detail of the volumetric results, split per stratigraphic unit and flow zones.

Porosity scenarios created using the seismic inversion data

As mentioned in Section 3.11.6, three seismic volumes were loaded. This leads to at least three scenarios when deriving porosity – acoustic impedance relationship from the upscaled data. In addition, the log derived relationship was used on either volume, which provides a total of six different net pore volume (NPV) estimates, as displayed in Table 3.11.12-a.

The "NPV xyz" volumes are the volumes derived using the porosity model derived from the relationship between the upscaled AI values and the upscaled PHIT values. The "NVP xyz log rel" volumes are those that were derived using the porosity model created using the relationship based on the well log PHIT and AI values.

The largest differences occur in the Waarre A volume, especially when using the JC inversion volume. As can be seen in Appendix A (see Section 3.11.15), the relationship between AI and PHIT for the Waarre A is a close to horizontal, or possibly even reverse line (i.e. higher AI gives higher PHIT). As a result, the correlation coefficient here is very low and the cloud of data points is large.

Interval	GRV	NPV FC inv	NPV FC inv log rel.	NPV JC inv	NPV jc inv log rel	NPV FC3well	NPV FC 3 well log rel	Variation
		MM m3	MM m3	MM m3	MM m3	MM m3	MM m3	
Upper Waarre C	179	24	26	29	27	27	26	0.21
Waarre C	308	58	57	64	63	61	60	0.11
Waarre A	250	42	41	45	29	36	31	0.56
Total	736	124	124	137	118	124	118	0.16

Table 3.11.12-a: Net Pore Volume ranges derived from the scenarios.

3.11.13 Upscaling

The resultant 3D static model was upscaled into a 100x100 metre but more orthogonal grid, with verticalized and zig-zag faults for ease of handling in Eclipse.

It is recognised that a significant amount of lateral detail is lost in this exercise, and it is recommended that future work includes more detailed sector models around the proposed well locations. These can be created in Petrel, and the relevant part of the original 25x25 m grid can be upscaled in them.

Eclipse model structure

The ***Eclipse Input Model*** was created using the same depth grids as the AI model. The faults were all copied, and then changed to pure vertical faults (selecting the vertical fault pillar option for each fault in turn). The pillar gridding process used zigzag faults, and the linear grid lines option, all to optimise the grid orthogonality.

The seismic horizons were gridding using a fault distance of 200 metres, as dipping faults have now been changed in vertical faults which caused slight changes in the surfaces close to the grids.

Zones were introduced using the well picks and applying a conformable layering method (phantoming from a seismic horizon up or down, matching the well picks). All zones present in the base case Petrel model were created in the Eclipse input model. Layering proceeded using in general 1 metre thick layers, parallel to the base of the unit, to keep the model size workable in Eclipse. For the AI model, this means effectively downscaling of the properties in a vertical sense, and upscaling in a lateral sense!

Upscaling Parameters

The upscaling parameters used for the properties are given in Table 3.11.13-a. Only the PHIT models that were derived using the log relationship, and their corresponding permeability models, were upscaled for using in dynamic simulation. For the permeability, a Kv property was created by multiplying the perm by 0.1.

This Kv was then used as input to the upscaled Perm K direction in the tensor based upscaling process, where the original permeability grids were used as input to the Perm I and J directions. Satnums were created based on the resulting Perm I grids.

Parameter	Description	Method	Weighting
Porosity	PHIT	Arithmetic	Bulk volume
Permeability	Perm (Kv / Kh = 0.1)	Flow Based Tensor – closed boundary	NA

Table 3.11.13-a: Upscaling parameters.

The log relationship derived PHIT and perm properties were upscaled, and subsequently exported to provide property input files to Eclipse.

3.11.14 Suggestions for future modelling work

The following is a list for suggested future work on the Casino model. It is in no way prioritised, and is anticipated to be expanded following similar exercises from a Geophysical and Reservoir Engineering point of view:

- Note that there appears to be an area to the north of Casino-2 which has very low AI values in the Waarre C. These values are at times set to indeterminate when an AI cut-off is used. However, the variogram ensures smooth interpolation across this area. These values indicate either an error in the AI volume, or, more likely, better reservoir quality than seen in any of the other wells. It is recommended that an alternative PHIT and perm model is created, without applying the minimum – maximum output range, to get an idea of the possible reservoir quality in this area.
- It is recommended that, when time allows, a more detailed inspection of the seismic volume is carried out, to verify the variogram for the different reservoirs, as there does appear to be some variation between the reservoirs and the different inversion volumes. Preferably, this work would concentrate on the agreed base case AI volume.
- It is recognised that a significant amount of detail is lost in this exercise when looking at detailed well performance predictions, especially in the vertical sense. It is recommended that future work includes detailed sector model around the proposed well locations. These can be created in Petrel, and the relevant part of the AI data can be upscaled in them, and properties can be recreated using the relationships derived in this exercise..
- As a significant part of the modelled area is below the gas-water contact, variation in seed values used in the sequential Gaussian simulation process can result in ranges in pore volume of up to 5% (based on empirical test done on the Oyong Field).

3.11.15 Appendix A : Phit vs AI Relationships

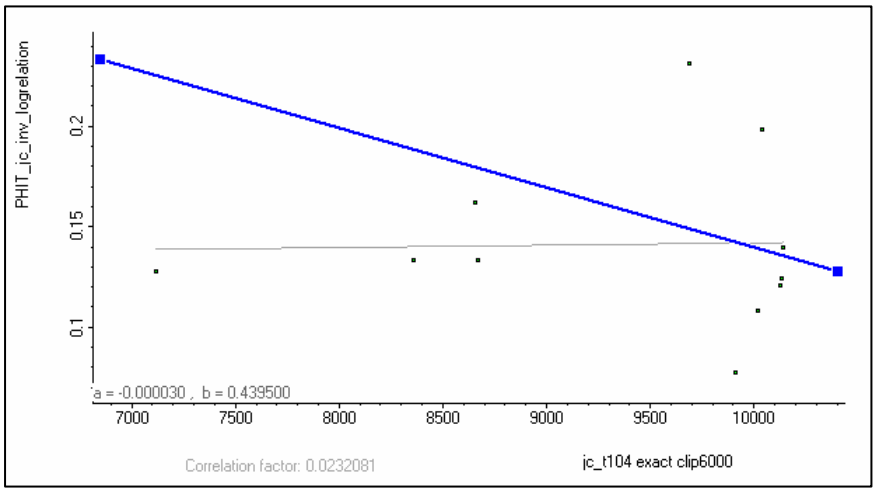

Figure 3.11.15-a: Phit vs AI log derived relationship: JC inversion, Top Cb interval.

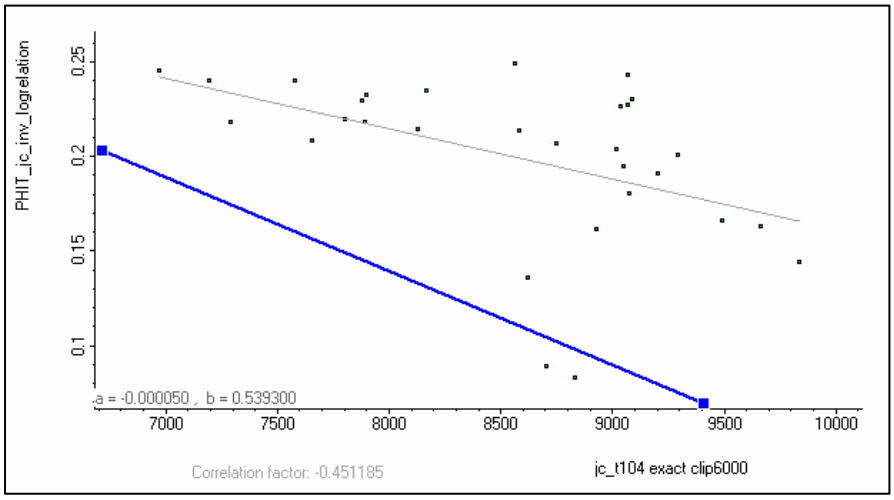

Figure 3.11.15-b: Phit vs AI log derived relationship: JC inversion, Waarre C interval.

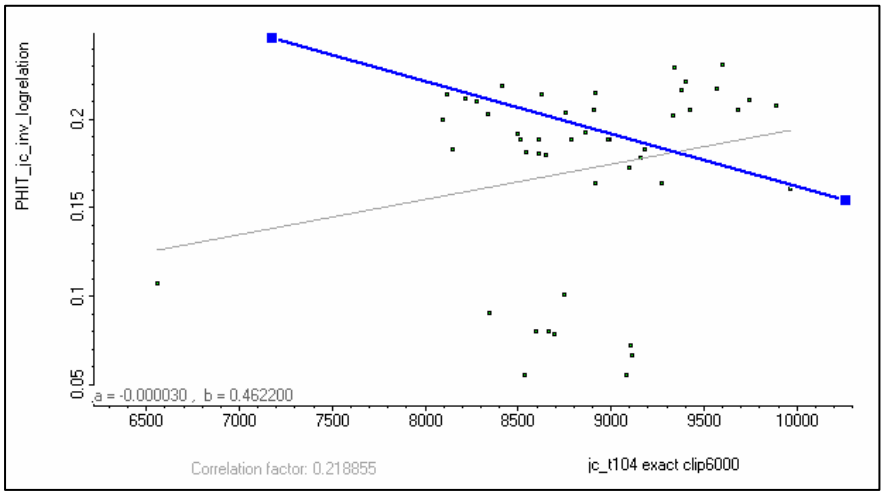

Figure 3.11.15-c: Phit vs AI log derived relationship: JC inversion, Waarre A interval.

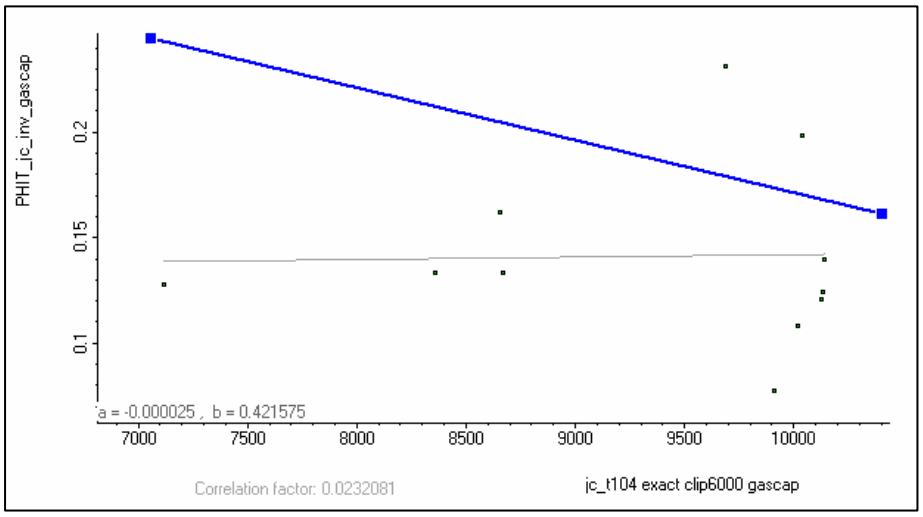

Figure 3.11.15-d: Phit vs AI upscaled data relationship: JC inversion, Top Cb interval.

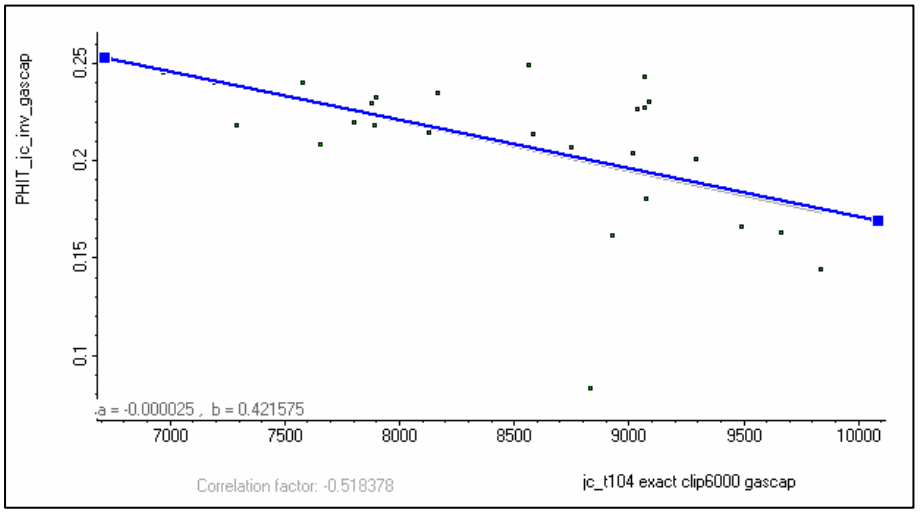

Figure 3.11.15-e: Phit vs AI upscaled data relationship: JC inversion, Waarre C interval.

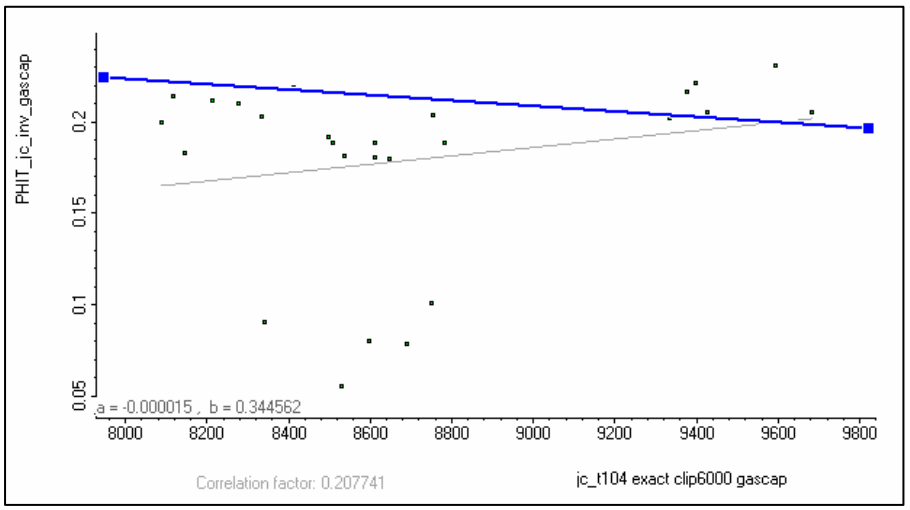

Figure 3.11.15-f: Phit vs AI upscaled data relationship: JC inversion, Waarre A interval.

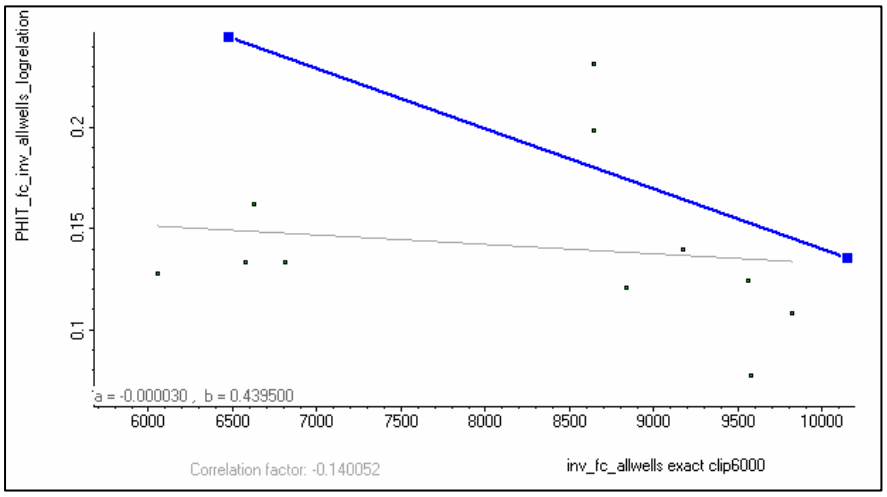

Figure 3.11.15-g: Phit vs AI log derived relationship: FC 3well inversion, Top Cb interval.

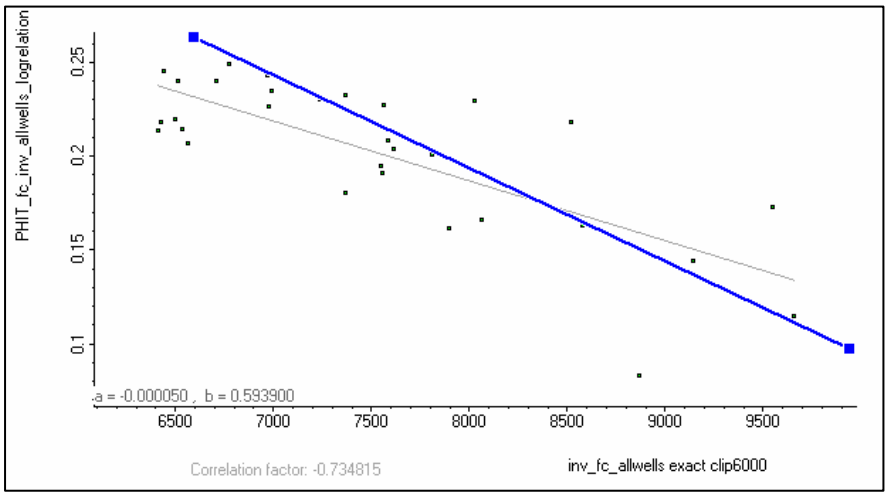

Figure 3.11.15-h: Phit vs AI log derived relationship: FC 3well inversion, Waarre C interval.

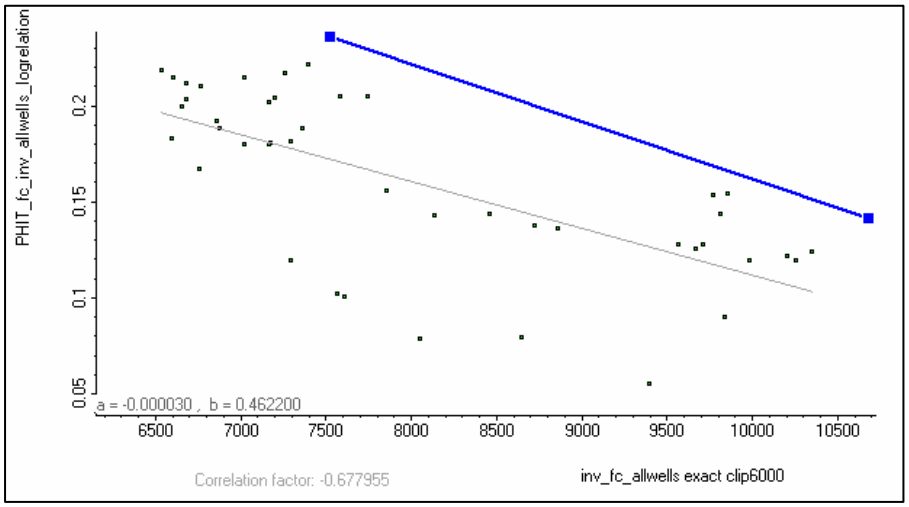

Figure 3.11.15-i: Phit vs AI log derived relationship: FC 3well inversion, Waarre A interval.

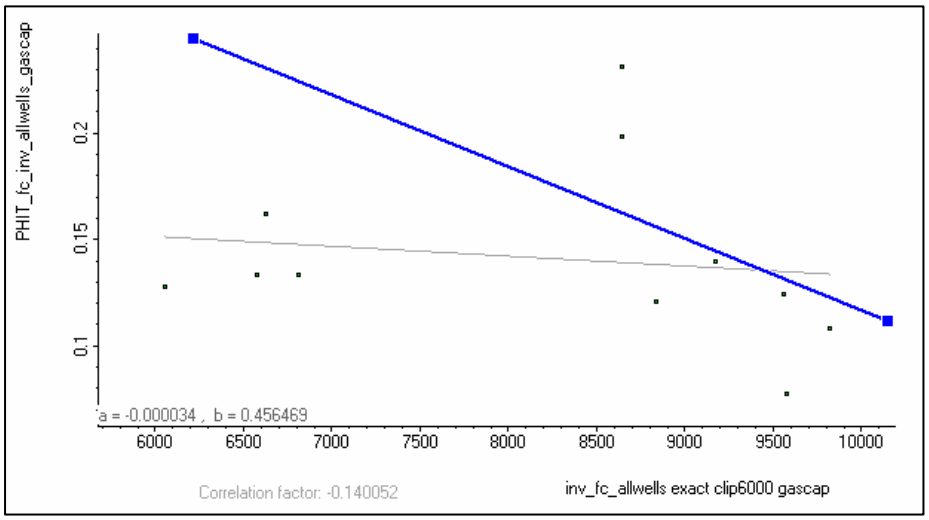

Figure 3.11.15-j: Phit vs AI upscaled data relationship: FC 3well inversion, Top Cb interval.

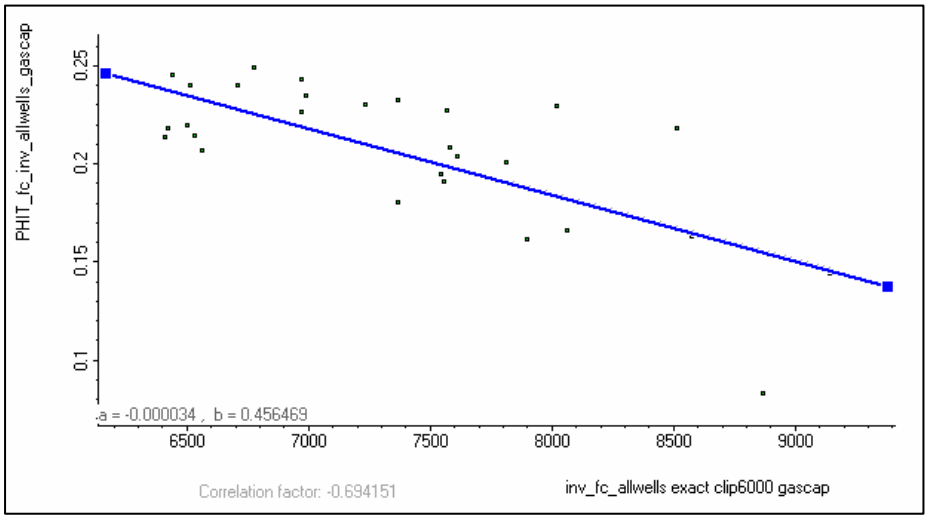

Figure 3.11.15-k: Phit vs AI upscaled data relationship: FC 3well inversion, Waarre C interval.

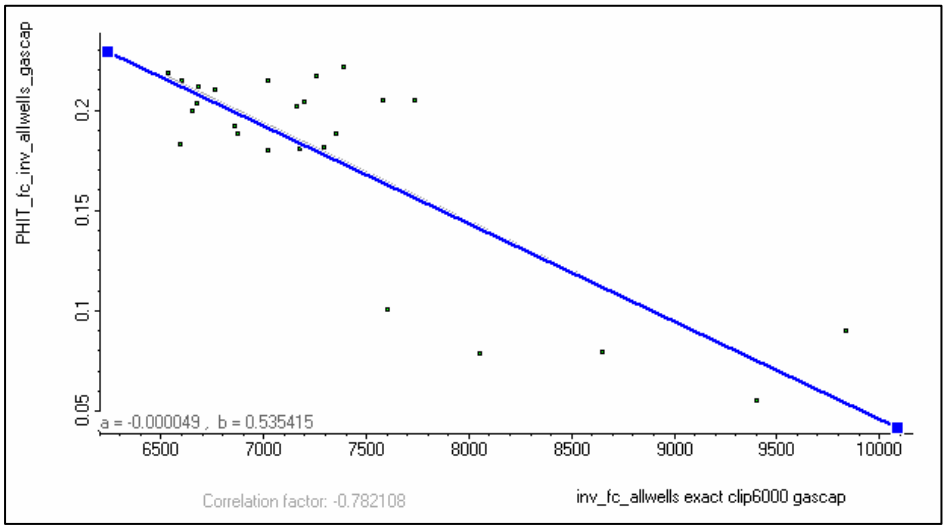

Figure 3.11.15-l: Phit vs AI upscaled data relationship: FC 3well inversion, Waarre A interval.

3.11.16 Appendix B : Static Volumetrics – AI Based Models

Petrel 2003SE	Schlumberger Information Solutions		
User name	spija		
Project	Casino Imp Mar 2004.pet		
Model	Casino AI model field only		
Grid	TWT AI model 25x25 (DC)		
Date	Thursday, April 08 2004 11:28:51		
Input XY unit	m		
Input Z unit	m		
Employed units:			
Oil:	m^3	Multiplier	10^6
Gas:	ft^3	Multiplier	10^9
Bulk, net and pore volumes:	m^3	Multiplier	10^6
##########	##########	##########	##########
Run name:	Volume Run 1		
Includes gas zone only.			
Summary of main results.			
	Bulk Volume[*10E6m^3]	Por Volume[*10E6m^3]	
Grand Total:	736.219374	124.22203	
Totals all Result Types			
	Bulk Volume[*10E6m^3]	Por Volume[*10E6m^3]	
Zones			
Top Cb	178.60827	23.537444	
C	308.088537	58.350701	
B and Upper A	0	0	
Lower A	249.522567	42.333888	
Detailed Results			
	Bulk Volume[*10E6m^3]	Por Volume[*10E6m^3]	
Top Cb	178.60827	23.537444	
	Bulk Volume[*10E6m^3]	Por Volume[*10E6m^3]	
C	308.088537	58.350701	
	Bulk Volume[*10E6m^3]	Por Volume[*10E6m^3]	
B and Upper A	0	0	
	Bulk Volume[*10E6m^3]	Por Volume[*10E6m^3]	
Lower A	249.522567	42.333888	
Lower gas contact:			
Volms			
General Properties			
Porosity:	PHIT_fc_inv_gascap		
Net gross:	Const value:	1	
Properties in the gas zone:			

FC 3 Well AI Model
Phit Upscaled Data Gascap Relationship

Petrel 2003SE	Schlumberger Information Solutions		
User name	spija		
Project	Casino Imp Mar 2004.pet		
Model	Casino AI model field only		
Grid	TWT AI model 25x25 (DC)		
Date	Thursday, April 08 2004 11:08:56		
Input XY unit	m		
Input Z unit	m		
Employed units:			
Oil:	m^3	Multiplier	10^6
Gas:	ft^3	Multiplier	10^9
Bulk, net and pore volumes:	m^3	Multiplier	10^6
##########	##########	##########	##########
Run name:	Volume Run 1		
Includes gas zone only.			
Summary of main results.			
	Bulk Volume[*10E6m^3]	Por Volume[*10E6m^3]	
Grand Total:	736.219374	124.16887	
Totals all Result Types			
	Bulk Volume[*10E6m^3]	Por Volume[*10E6m^3]	
Zones			
Top Cb	178.60827	26.155275	
C	308.088537	57.444699	
B and Upper A	0	0	
Lower A	249.522567	40.568896	
Detailed Results			
	Bulk Volume[*10E6m^3]	Por Volume[*10E6m^3]	
Top Cb	178.60827	26.155275	
	Bulk Volume[*10E6m^3]	Por Volume[*10E6m^3]	
C	308.088537	57.444699	
	Bulk Volume[*10E6m^3]	Por Volume[*10E6m^3]	
B and Upper A	0	0	
	Bulk Volume[*10E6m^3]	Por Volume[*10E6m^3]	
Lower A	249.522567	40.568896	
Lower gas contact:			
Volms			
General Properties			
Porosity:	PHIT_fc_inv_logrelation		
Net gross:	Const value:	1	
Properties in the gas zone:			

Phit Log based Relationship

Petrel 2003SE	Schlumberger Information Solutions		
User name	spija		
Project	Casino Imp Mar 2004.pet		
Model	Casino AI model field only		
Grid	TWT AI model 25x25 (DC)		
Date	Thursday, April 08 2004 11:07:58		
Input XY unit	m		
Input Z unit	m		
Employed units:			
Oil:	m^3	Multiplier	10^6
Gas:	ft^3	Multiplier	10^9
Bulk, net and pore volumes:	m^3	Multiplier	10^6
##########	##########	##########	##########
Run name:	Volume Run 1		
Includes gas zone only.			
Summary of main results.			
	Bulk Volume[*10E6m^3]	Por Volume[*10E6m^3]	
Grand Total:	736.219374	137.146271	
Totals all Result Types			
	Bulk Volume[*10E6m^3]	Por Volume[*10E6m^3]	
Zones			
Top Cb	178.60827	28.558463	
C	308.088537	63.863288	
B and Upper A	0	0	
Lower A	249.522567	44.72452	
Detailed Results			
	Bulk Volume[*10E6m^3]	Por Volume[*10E6m^3]	
Top Cb	178.60827	28.558463	
	Bulk Volume[*10E6m^3]	Por Volume[*10E6m^3]	
C	308.088537	63.863288	
	Bulk Volume[*10E6m^3]	Por Volume[*10E6m^3]	
B and Upper A	0	0	
	Bulk Volume[*10E6m^3]	Por Volume[*10E6m^3]	
Lower A	249.522567	44.72452	
Lower gas contact:			
Volms			
General Properties			
Porosity:	PHIT_ic_inv_gascap		
Net gross:	Const value:	1	
Properties in the gas zone:			

JC AI Model
Phit Upscaled Data Gascap Relationship

Petrel 2003SE	Schlumberger Information Solutions		
User name	spija		
Project	Casino Imp Mar 2004.pet		
Model	Casino AI model field only		
Grid	TWT AI model 25x25 (DC)		
Date	Thursday, April 08 2004 11:07:20		
Input XY unit	m		
Input Z unit	m		
Employed units:			
Oil:	m^3	Multiplier	10^6
Gas:	ft^3	Multiplier	10^9
Bulk, net and pore volumes:	m^3	Multiplier	10^6
##########	##########	##########	##########
Run name:	Volume Run 1		
Includes gas zone only.			
Summary of main results.			
	Bulk Volume[*10E6m^3]	Por Volume[*10E6m^3]	
Grand Total:	736.219374	118.449404	
Totals all Result Types			
	Bulk Volume[*10E6m^3]	Por Volume[*10E6m^3]	
Zones			
Top Cb	178.60827	27.208034	
C	308.088537	62.650887	
B and Upper A	0	0	
Lower A	249.522567	28.590482	
Detailed Results			
	Bulk Volume[*10E6m^3]	Por Volume[*10E6m^3]	
Top Cb	178.60827	27.208034	
	Bulk Volume[*10E6m^3]	Por Volume[*10E6m^3]	
C	308.088537	62.650887	
	Bulk Volume[*10E6m^3]	Por Volume[*10E6m^3]	
B and Upper A	0	0	
	Bulk Volume[*10E6m^3]	Por Volume[*10E6m^3]	
Lower A	249.522567	28.590482	
Lower gas contact:			
Volms			
General Properties			
Porosity:	PHIT_ic_inv_logrelation		
Net gross:	Const value:	1	
Properties in the gas zone:			

Phit Log based Relationship

Petrel 2003SE	Schlumberger Information Solutions		
User name	spija		
Project	Casino Imp Mar 2004.pet		
Model	Casino AI model field only		
Grid	TWT AI model 25x25 (DC)		
Date	Thursday, April 08 2004 11:30:44		
Input XY unit	m		
Input Z unit	m		
Employed units:			
Oil:	m^3	Multiplier	10^6
Gas:	ft^3	Multiplier	10^9
Bulk, net and pore volumes:	m^3	Multiplier	10^6
##########	##########	##########	##########
Run name:	Volume Run 1		
Includes gas zone only.			
Summary of main results.			
	Bulk Volume[*10E6m^3]	Por Volume[*10E6m^3]	
Grand Total:	736.219374	123.794501	
Totals all Result Types			
	Bulk Volume[*10E6m^3]	Por Volume[*10E6m^3]	
Zones			
Top Cb	178.60827	26.660844	
C	308.088537	61.360615	
B and Upper A	0	0	
Lower A	249.522567	35.773042	
Detailed Results			
	Bulk Volume[*10E6m^3]	Por Volume[*10E6m^3]	
Top Cb	178.60827	26.660844	
	Bulk Volume[*10E6m^3]	Por Volume[*10E6m^3]	
C	308.088537	61.360615	
	Bulk Volume[*10E6m^3]	Por Volume[*10E6m^3]	
B and Upper A	0	0	
	Bulk Volume[*10E6m^3]	Por Volume[*10E6m^3]	
Lower A	249.522567	35.773042	
Lower gas contact:			
Volms			
General Properties			
Porosity:	PHIT_fc_inv_allwells_gascap		
Net gross:	Const value:	1	
Properties in the gas zone:			

FC 2 Well AI Model
Phit Upscaled Data Gascap Relationship

Petrel 2003SE	Schlumberger Information Solutions	
User name	spija	
Project	Casino Imp Mar 2004.pet	
Model	Casino AI model field only	
Grid	TWT AI model 25x25 (DC)	
Date	Thursday, April 08 2004 11:30:06	
Input XY unit	m	
Input Z unit	m	
Employed units:		
Oil:	m^3	Multiplier
Gas:	ft^3	Multiplier
Bulk, net and pore volumes:	m^3	Multiplier
##########	##########	##########
Run name:	Volume Run 1	
Includes gas zone only.		
Summary of main results.		
	Bulk Volume[*10E6m^3]	Por Volume[*10E6m^3]
Grand Total:	736.219374	117.822394
Totals all Result Types		
	Bulk Volume[*10E6m^3]	Por Volume[*10E6m^3]
Zones		
Top Cb	178.60827	26.332426
C	308.088537	60.223174
B and Upper A	0	0
Lower A	249.522567	31.266794
Detailed Results		
	Bulk Volume[*10E6m^3]	Por Volume[*10E6m^3]
Top Cb	178.60827	26.332426
	Bulk Volume[*10E6m^3]	Por Volume[*10E6m^3]
C	308.088537	60.223174
	Bulk Volume[*10E6m^3]	Por Volume[*10E6m^3]
B and Upper A	0	0
	Bulk Volume[*10E6m^3]	Por Volume[*10E6m^3]
Lower A	249.522567	31.266794
Lower gas contact:		
Volms		
General Properties		
Porosity:	PHIT_fc_inv_allwells_logrelation	
Net gross:	Const value:	1
Properties in the gas zone:		

Phit Log based Relationship

This page intentionally left blank.

3.12 Field OGIP Distribution

3.12.1 Overview of Methodology

Early work conducted to assess the Gas-in-Place distribution for the Casino field was based on purely probabilistic approach where a range of input distributions were combined using a Crystal Ball Monte Carlo spreadsheet. This approach is shown diagrammatically in Figure 3.12.1 a below.

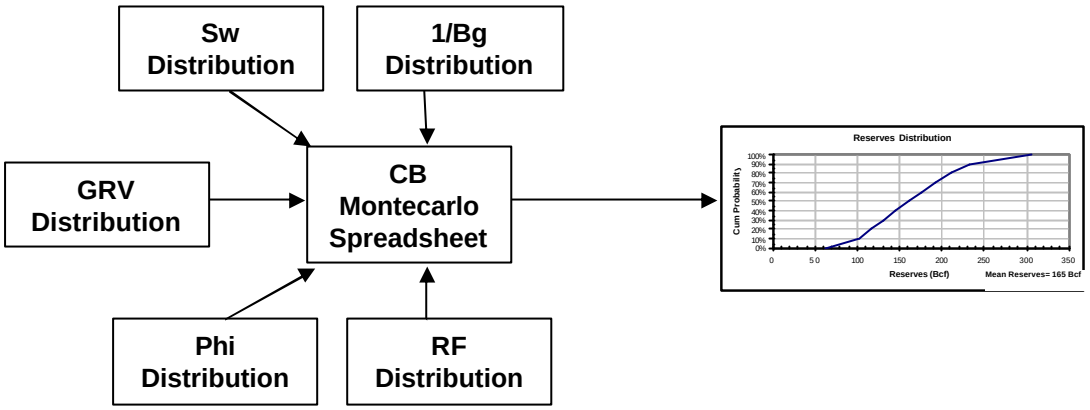

Figure 3.12.1-a : Probabilistic Methodology

As part of the ongoing Santos peer review process concerns were raised that this approach was not transparent enough. A common concern was that this approach does not allow for a deterministic realisation of the P90 Case, i.e. “Show me the P90. What does it look like?”

Another issue raised included how to combine account for gas pools deemed to contribute to Probable but not Proven reserves in an overall field Gas-in-Place distribution.

The final methodology chosen to represent the Casino field OGIP distribution has been designed to address these issues and builds the range based on a number of deterministic outcomes, rather than a “Black Box” type probabilistic approach. A four step process has been used as follows;

1. Identify gas pools deemed to contribute to Proven, Probable and Possible reserves
2. Use the multiple Petrel static model realisations to represent the range of field OGIP and track the Proven, Proven and Probable, and Proven, Probable and Possible OGIP for each model.
3. Include the effect of other uncertainties in OGIP which are not adequately addressed by the multiple Petrel static model realisations
4. Combine the OGIP realisations into a single distribution
5. Identify deterministic scenarios to represent the P90, P50 and P10 cases.

This methodology is described in detail in the following sections.

3.12.2 Characterisation of Gas Pools contributing to Proven, Probable and Possible Reserves

The objective of this section is to summarise the gas pools that have been deemed to contribute to Proven, Probable and Possible reserves. This has been considered in both an areal sense and by vertical reservoir unit.

Waarre A

The area of the Waarre A with low impedance on the band limited impedance volume above the MDT derived Free Water Level is considered to be a “Proven” pool area. This area excludes approximately 15% of the GRV in an area of higher impedance near the main bounding fault as shown in Figure 4.12.2-a. This

area has been excluded from the “Proven” area due to its distinctly different impedance character and the possibility of more complex faulting in this area.

The entire Waarre A area above the FWL is considered “Probable” pool area and is justified based on the following as Casino-1, Casino-2 and Casino-3 have confirmed reservoir continuity over the field.

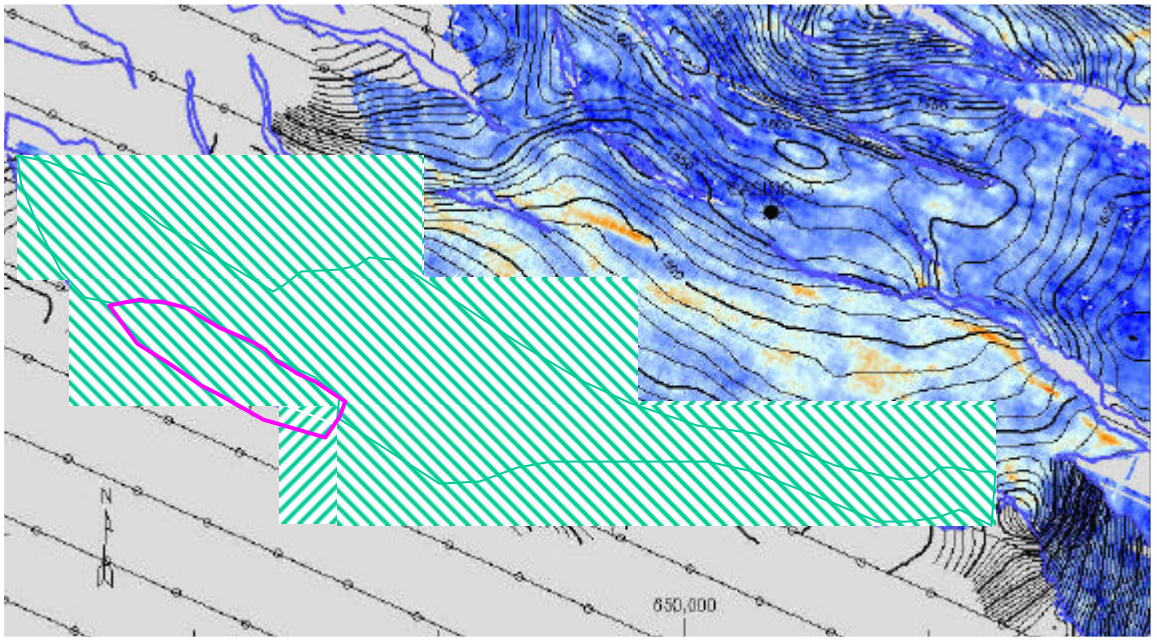

Figure 3.12.2-a : Waarre A Proven , Proven and Probable and 3P Pool Area

The treatment of the individual Waarre A reservoirs is summarised in Figure 3.12.2 b.

The Lower Waarre A reservoir is treated as contributing to Proven gas reserves. The basis for this is as follows;

- The presence of the interval being gas bearing is supported by log interpretation, formation pressures and the recovery of a gas sample from 1782.5m in Casino-1.
- The evidence for formation producibility (as described in Section 3.13 based on MDT drawdown permeabilities and a demonstrated relationship with core permeability).

The Upper Waarre A is not treated as contributing to Proven reserves, but is treated as a pool contributing to Probable reserves. While there is evidence from log interpretation of this unit being hydrocarbon bearing, no reservoir fluid sample has been recovered, nor have any valid formation pressures been measured in the gas bearing interval.

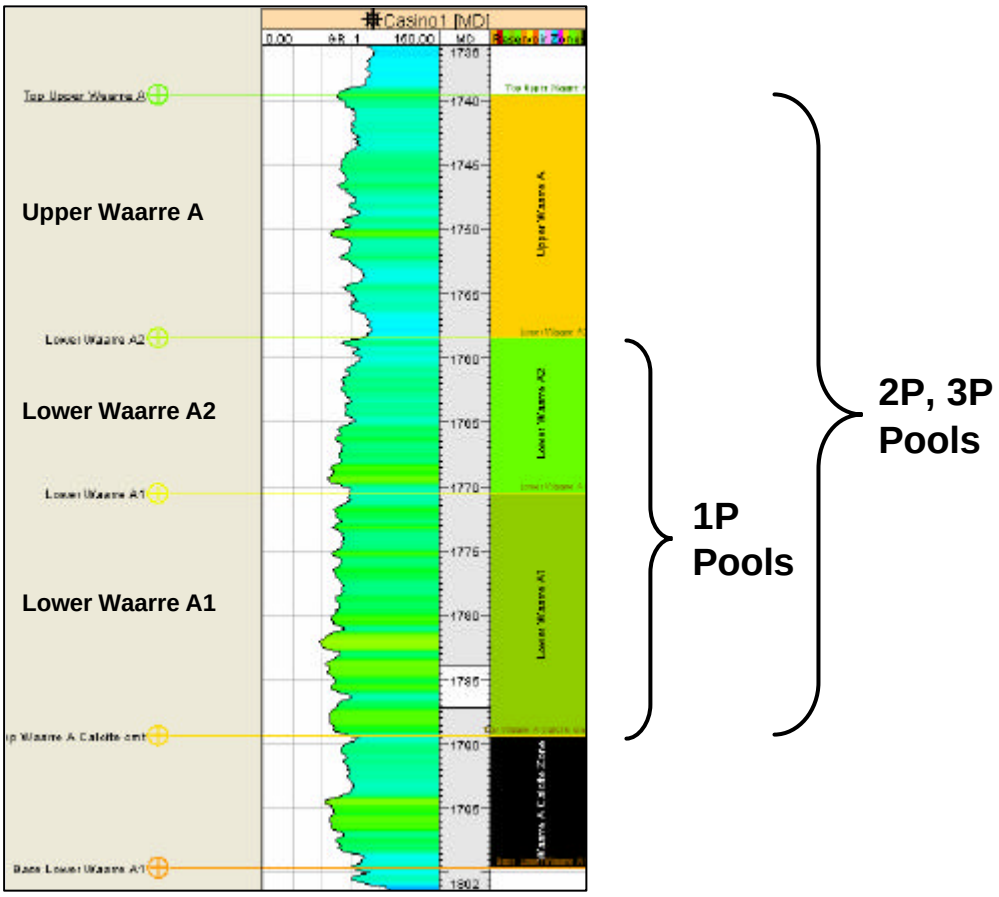

Figure 3.12.2-b : Treatment of Waarre A Reservoirs

Waarre C

The treatment of the Waarre C pool area is shown in Figure 3.12.2 c. With the exception of the mapped "outlier" adjacent to the updip truncation edge, the entire pool area down to the MDT derived Free Water Level is considered "Proven". This is based on the following;

- The results of Casino-2 and Casino-3 which prove continuity of the reservoir from the crest to the Gas-Water-Contact.
- Seismic mapping, which does not support the presence of any isolated reservoir compartments
- The pressure data interpretation, which supports the presence of a continuous gas column
- Seismic amplitudes, which are conformable to the structural closure

The area of the "outlier" shown on Figure 3.12.2-c has been excluded from the OGIP contributing to proven reserves due to concerns that is may not be connected to the producing well. These volumes are included in the Probable category.

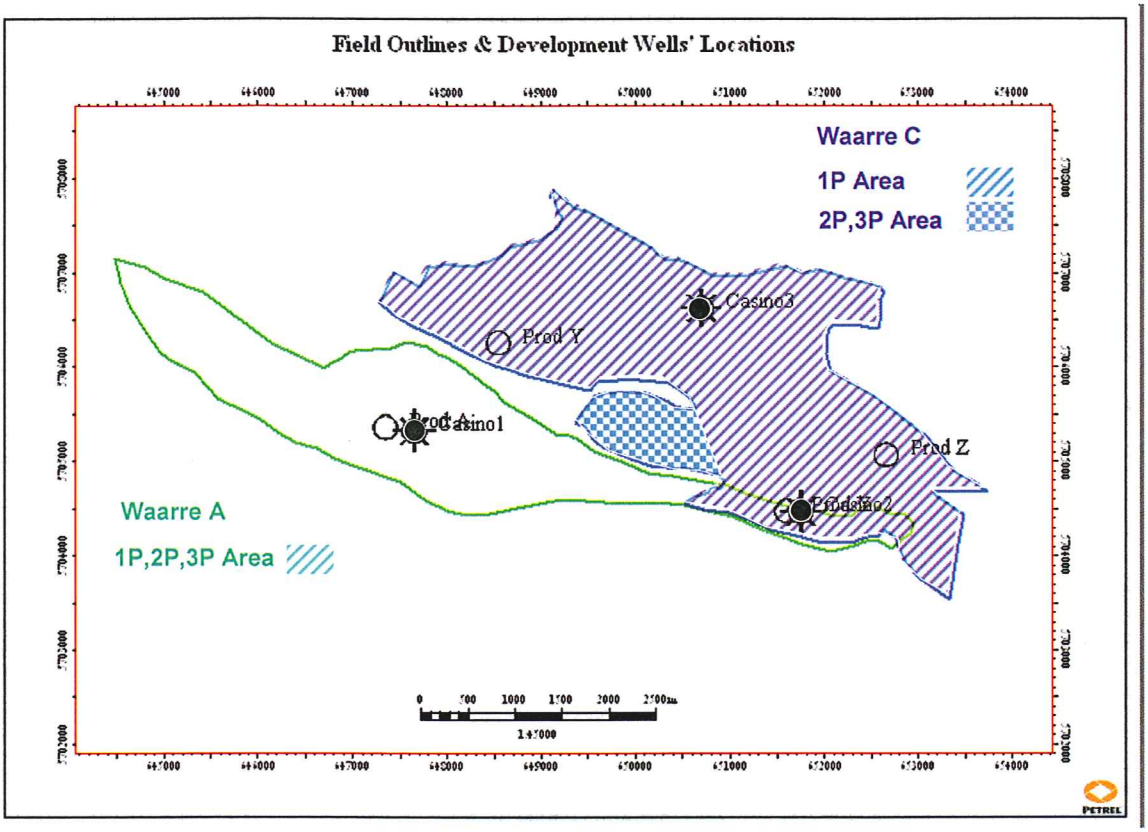

Figure 3.12.2-c : Waarre C Pool Area Categorisation

The treatment of the individual Waarre C reservoirs is shown in Figure 3.12.2-d. Based on log data, core and production test data, the main gas bearing Waarre C reservoirs which are present at Casino-2 and correlatable across the field to Casino-3 are treated as contributing to Proven Gas-in Place. This includes the following units;

- Upper Cb Lower Pay
- Upper Cb Main Pay
- Cb Silt
- Lower Cb Main Pay
- Ca4
- Ca3
- Ca2

The Upper Waarre Cb sand intersected at Casino-3 but not correlatable to Casino-2 has been attributed as contributing to Probable reserves. This is on the basis that the sand appears to merge into the main Waarre C reservoir sands updip of Casino-3. This sand is referred to as the Upper Cb Casino-3 "2P" Sand.

Two Waarre C reservoirs are also identified as contributing to Possible gas reserves. The seismic impedance volume suggests the presence of another Upper Cb sand that not been penetrated by either Casino-2 or Casino-3. This sand is referred to as the Upper Cb "Impedance" 3P Sand. At the time this Gas-in-Place distribution was prepared the volumes associated with this possible reservoir sand has not been addressed in detail. For the purposes of Possible volume attribution this sand was given the same volume of Gas-in-Place as the Upper Cb Casino-3 "2P" Sand". Subsequent more detailed modelling of this unit in Petrel has shown this to be a reasonable assumption.

A small amount of Gas-in-Place contributing to Possible reserves is also carried for the Ca1 reservoir unit. This unit is not interpreted to have any pay quality sand at the Casino-2 location. At the downdip Casino-3 location the sand is intersected below the FWL but shows slightly improved reservoir quality. A small

amount of Possible OGIP is carried on the basis that some of this better quality sand may extend updip and into the gas bearing interval.

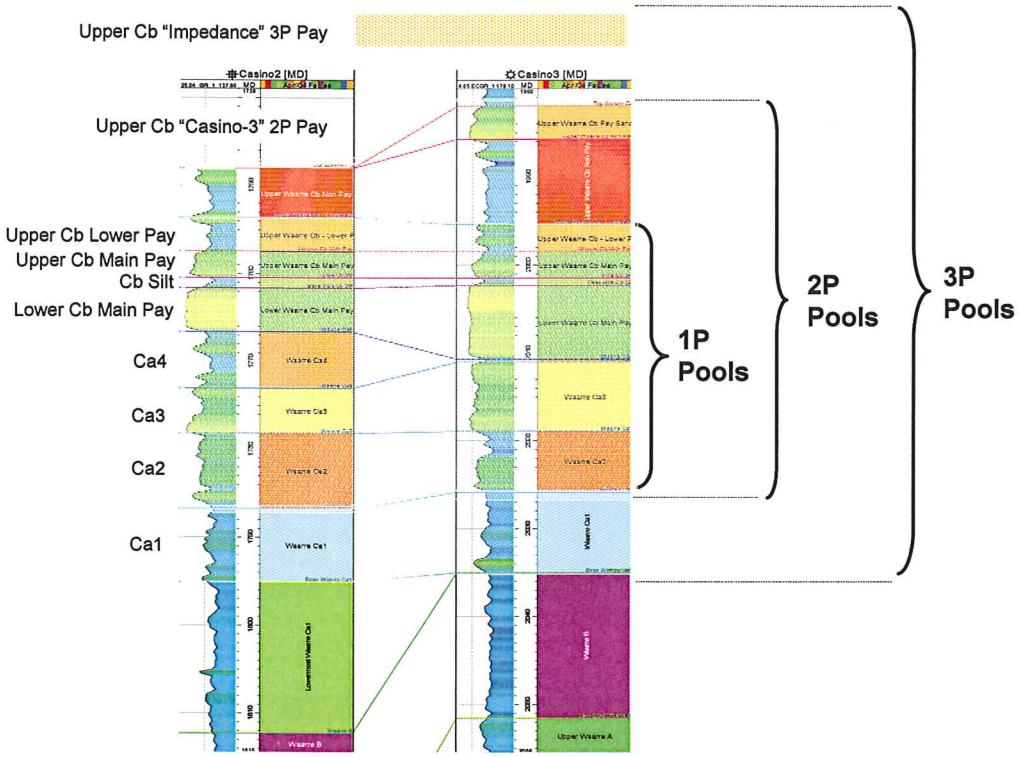

Figure 3.12.2-d : Waarre C Reservoir Categorisation

3.12.3 Petrel Model Gas-In-Place

A total of fourteen separate Petrel model realisations have been used to provide the initial distribution of field OGIP. These include eleven geological based layered Petrel models (as described in Section 3.10) and three impedance based Petrel models (as described in Section 3.11). For each of these fourteen models the Proven, Probable and Possible Gas-in-Place has been determined as described in Section 3.12.2.

A summary of the OGIP calculated for these realisations can be found in Table 3.12.3-a. Full details of these models including the calculated Gross Rick Volume, Net Pore Volume and Original Gas in Place can be found on Enclosure 3.12.3-a.

Figure 3.12.3-b shows how the breakdown of 1P, 2P and 3P OGIP has been achieved for a single Petrel realisation. The 2P (Proven and Probable) OGIP volumes are those obtained from the Petrel model. The 1P (Proven) volumes show the exclusion of any OGIP in the Upper Waarre A and a reduction in volumes in the main Waarre C reservoirs with the exclusion of volumes in the outlier. The 3P (Proven, Probable and Possible) volumes show the inclusion of additional OGIP associated with the Upper Cb "Impedance" sand and the Ca1. Note the approximation whereby the Upper Cb "Impedance" sand is given the same OGIP as the Upper Cb Casino-3 "2P" sand.

	Final Layered Petrel Model and Sensitivities												AI Based Petrel Models		
Case ID	**Pet_04**	**Pet_04c**	**Pet_04d**	**Pet_04e**	**Pet_04f**	**Pet_04g**	**Pet_04i**	**Pet_04m**	**Pet_04n**	**Pet_04j**	**Pet_04k**		**Pet_AI_04_FC3_a**	**Pet_AI_04_FC2_a**	**Pet_AI_04_JC_a**
OGIP															
Waarre C															
Upper Cb "Impedance" 3P Pay	*not modelled*	*not modelled*	*not modelled*	*not modelled*	*not modelled*	*not modelled*	*not modelled*	*not modelled*	*not modelled*	*not modelled*	*not modelled*				
Upper Cb Non Pay													*not broken out*	*not broken out*	*not broken out*
Upper Cb "Casino-3" 2P Pay	31.3	27.8	34.1	31.9	32.1	33.8	32.7	32.7	32.7	31.3	31.3				
Upper Cb Non Pay															
Upper Cb Lower 1P Pay (Corr. from C-3 to C-2)	23.1	19.4	26.0	15.8	16.0	20.8	23.2	23.2	23.2	23.1	23.1				
Subtotal Upper Waarre Cb	**54.4**	**47.2**	**60.1**	**47.7**	**48.1**	**54.6**	**55.9**	**55.9**	**55.9**	**54.4**	**54.4**		**81.0**	**85.2**	**84.0**
Upper Cb main pay	37.6	32.6	47.9	28.5	34.4	42.9	37.4	47.9	37.4	48.1	57.5				
Cb silt	5.6	5.4	5.0	4.9	5.3	4.7	5.0	5.0	5.0	5.6			*not broken out*	*not broken out*	*not broken out*
Lower Cb main pay	84.3	89.8	60.6	64.7	88.9	87.3	83.3	83.3	83.3	84.3	56.7				
Ca4	26.4	29.2	16.1	15.7	28.7	24.4	26.4	26.4	26.4	26.4	26.2				
Ca3	68.7	68.7	52.0	51.2	65.1	64.4	52.0	52.0	52.0	68.7	68.2				
Ca2	52.1	54.1	36.4	35.1	40.1	38.7	36.4	36.4	52.2	52.1	52.9				
Subtotal Waarre C Main	**274.7**	**279.8**	**217.9**	**200.0**	**262.5**	**262.4**	**240.5**	**251.0**	**256.2**	**285.2**	**261.5**		**273.8**	**251.9**	**310.3**
Ca1	9.8	8.1	9.0	8.1	8.1	9.0	10.6	9.7	9.7	9.9	9.9				
Subtotal Upper Waarre Cb	**54.4**	**47.2**	**60.1**	**47.7**	**48.1**	**54.6**	**55.9**	**55.9**	**55.9**	**54.4**	**54.4**		**81.0**	**85.2**	**84.0**
Subtotal Waarre C Main	**274.7**	**279.8**	**217.9**	**200.0**	**262.5**	**262.4**	**240.5**	**251.0**	**256.2**	**285.2**	**261.5**		**273.8**	**251.9**	**310.3**
Subtotal 1P OGIP (Upper Cb Lower Pay + Main)	**297.8**	**299.2**	**243.9**	**215.8**	**278.5**	**283.3**	**263.6**	**274.1**	**279.4**	**308.4**	**284.6**				
Subtotal Upper Waarre Cb Plus Main	**329.2**	**327.0**	**278.0**	**247.7**	**310.6**	**317.0**	**296.4**	**306.9**	**312.1**	**339.7**	**316.0**		**354.8**	**337.0**	**394.3**
Subtotal All Waarre C	**329.2**	**327.0**	**278.0**	**247.7**	**310.6**	**317.0**	**296.4**	**306.9**	**312.1**	**339.7**	**316.0**		**354.8**	**337.0**	**394.3**
Waarre A															
Upper Waarre A	14.8	13.8	20.1	19.9	19.9	20.1	14.0	13.9	14.0	14.8	14.8		*not included in model*	*not included in model*	*not included in model*
Lower Waarre A2	38.5	38.0	37.2	37.2	36.9	36.9	38.0	38.0	38.0	38.5	38.5		*not broken out*	*not broken out*	*not broken out*
Lower Waarre A1	61.5	61.7	61.1	61.1	61.2	61.3	61.5	61.5	61.5	61.5	61.5				
Subtotal Lower Waarre A	**100.0**	**99.7**	**98.3**	**98.3**	**98.1**	**98.2**	**99.5**	**99.5**	**99.5**	**100.0**	**100.0**		**65.8**	**116.3**	**65.5**
Waarre A Calcite cmt	10.6	14.4	10.5	10.5	10.5	10.5	10.5	10.5	10.5	10.6	10.6		*included in L Wa A*	*included in L Wa A*	*included in L Wa A*
Subtotal Lower Waarre A	**100.0**	**99.7**	**98.3**	**98.3**	**98.1**	**98.2**	**99.5**	**99.5**	**99.5**	**100.0**	**100.0**		**65.8**	**116.3**	**65.5**
Subtotal Lower Waarre A + Upper Waarre A	**114.8**	**113.5**	**118.4**	**118.2**	**118.0**	**118.3**	**113.5**	**113.4**	**113.5**	**114.7**	**114.8**		**65.8**	**116.3**	**65.5**
Subtotal All Waarre A	**125.3**	**127.9**	**128.9**	**128.7**	**128.5**	**128.8**	**124.0**	**123.9**	**124.0**	**125.3**	**125.3**		**65.8**	**116.3**	**65.5**
Total Field - U + Main Wa C + U + L Wa A	**443.9**	**440.6**	**396.4**	**365.9**	**428.6**	**435.3**	**409.8**	**420.3**	**425.6**	**454.4**	**430.7**				
Total Field	**454.5**	**454.9**	**406.9**	**376.5**	**439.2**	**445.9**	**420.4**	**430.8**	**436.1**	**465.0**	**441.3**		**420.6**	**453.3**	**459.8**

Table 3.12.3-a : Casino Petrel Model OGIP - Detail

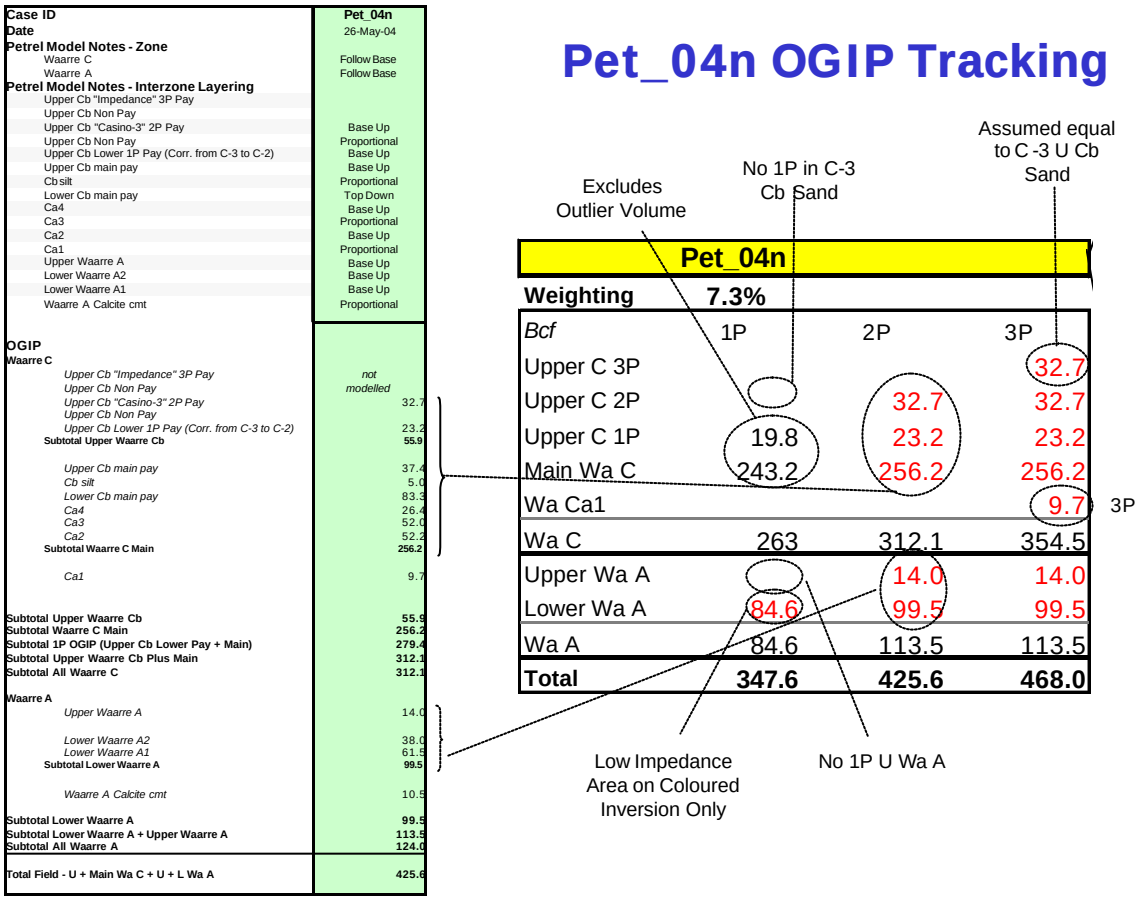

Figure 3.12.3-a : Example of Proven, Probable and Possible OGIP Breakout for Petrel Model Pet_04

The treatment of the impedance based models requires some comment. For the Waarre A, only the interval between the Top Lower Waarre A and Base Waarre A seismic picks was modelled, which excludes the Upper Waarre A. For this exercise, Upper Waarre A volumes have been added to the three impedance based models using a typical figure from the layered models.

Also, subsequent to completion of the impedance based modelling, concerns were raised that the OGIP estimates in the Waarre A based on the JC AI Volume were erroneous. Hence for the purpose of this exercise, both the Upper Waarre A and Lower Waarre A OGIP in the JC AI volume Petrel model (Pet_AI_04_JC) have been overwritten with typical figures from layered models.

It should also be noted that due to the nature of the AI models, there is no breakout of the individual Gas-in-Place by unit in the Upper Waarre Cb. The AI models report a total OGIP for the interval between the Top Waarre C and Top Waarre C main pay. In order to achieve this breakout, the layered models have been used as guide in allocating the total OGIP reported from the Impedance models into the individual reservoir units.

This is shown for the impedance based Petrel model Pet_AI_04_JC in Figure 3.12.3-c below:

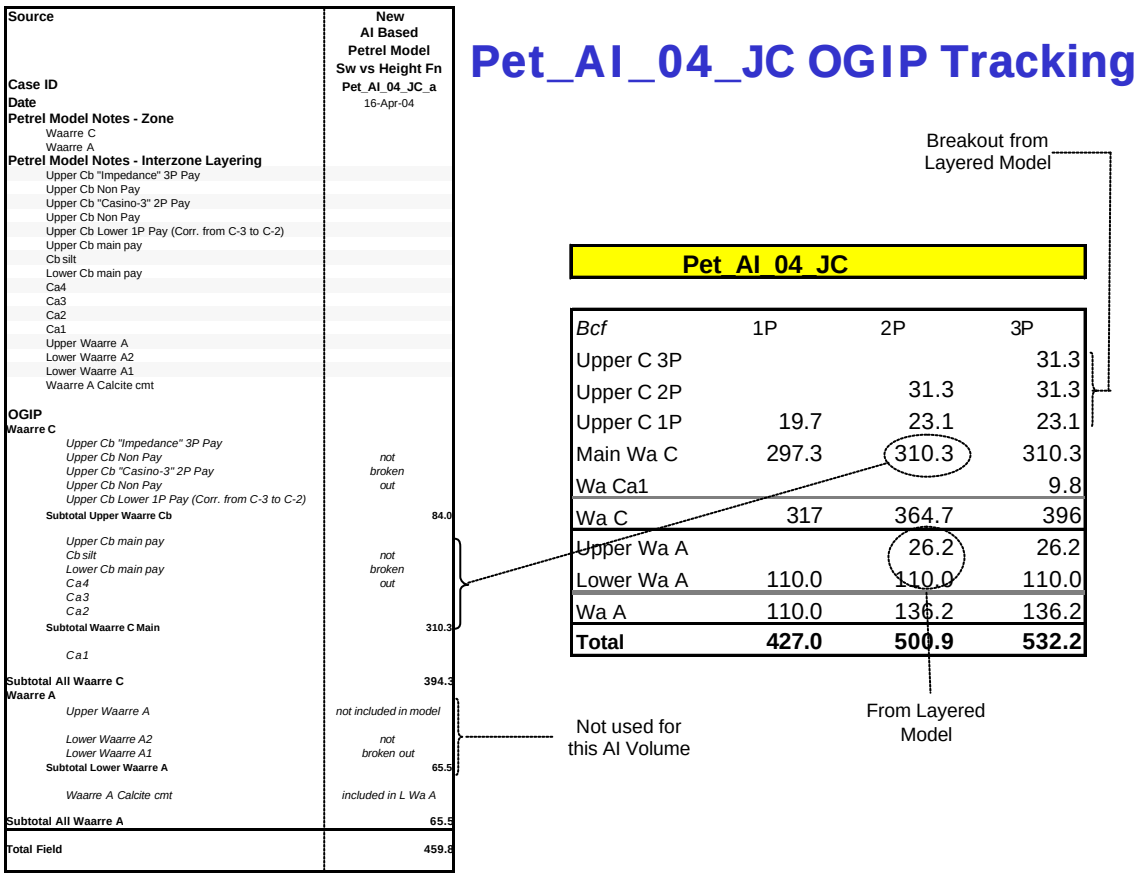

Figure 3.12.3-b : Proven, Probable and Possible OGIP Breakout for AI Based Petrel Model Pet_AI_04_JC

Table 3.12.3-b shows the 1P, 2P and 3P OGIP as determined for each of the fourteen Petrel models used in the constructing the initial OGIP distribution for the Casino field.

Pet_04			
Weighting	**7.27%**		
Bcf	1P	2P	3P
Upper C 3P			31.3
Upper C 2P		31.3	31.3
Upper C 1P	19.7	23.1	23.1
Main Wa C	261.8	274.8	274.8
Wa Ca1			9.8
Wa C	281.5	329.2	370.3
Upper Wa A		14.8	14.8
Lower Wa A	85.0	100.0	100.0
Wa A	85.0	114.8	114.8
Total	**366.5**	**444.0**	**485.1**

Pet_04c			
Weighting	**7.27%**		
Bcf	1P	2P	3P
Upper C 3P			27.8
Upper C 2P		27.8	27.8
Upper C 1P	16	19.4	19.4
Main Wa C	266.8	279.8	279.8
Wa Ca1			8.1
Wa C	282.8	327.0	362.9
Upper Wa A		13.8	13.8
Lower Wa A	84.7	99.7	99.7
Wa A	84.7	113.5	113.5
Total	**367.5**	**440.5**	**476.4**

Pet_04d			
Weighting	**7.3%**		
Bcf	1P	2P	3P
Upper C 3P			34.1
Upper C 2P		34.1	34.1
Upper C 1P	22.6	26.0	26.0
Main Wa C	204.9	217.9	217.9
Wa Ca1			8.1
Wa C	227.5	278	320.2
Upper Wa A		20.1	20.1
Lower Wa A	83.6	98.3	98.3
Wa A	83.6	118.4	118.4
Total	**311.1**	**396.4**	**438.6**

Pet_04e			
Weighting	**7.3%**		
Bcf	1P	2P	3P
Upper C 3P			31.9
Upper C 2P		31.9	31.9
Upper C 1P	12.4	15.8	15.8
Main Wa C	187	200	200
Wa Ca1			8.1
Wa C	199.4	247.7	287.7
Upper Wa A		19.9	19.9
Lower Wa A	83.6	98.3	98.3
Wa A	83.6	118.2	118.2
Total	**283.0**	**365.9**	**405.9**

Pet_04f			
Weighting	**7.3%**		
Bcf	1P	2P	3P
Upper C 3P			32.1
Upper C 2P		32.1	32.1
Upper C 1P	12.6	16	16
Main Wa C	249.5	262.5	262.5
Wa Ca1			8.1
Wa C	262.1	310.6	350.8
Upper Wa A		19.9	19.9
Lower Wa A	83.4	98.1	98.1
Wa A	83.4	118.0	118.0
Total	**345.5**	**428.6**	**468.8**

Pet_04g			
Weighting	**7.3%**		
Bcf	1P	2P	3P
Upper C 3P			33.8
Upper C 2P		33.8	33.8
Upper C 1P	17.4	20.8	20.8
Main Wa C	249.4	262.4	262.4
Wa Ca1			9
Wa C	266.8	317	359.8
Upper Wa A		20.1	20.1
Lower Wa A	83.5	98.2	98.2
Wa A	83.5	118.3	118.3
Total	**350.3**	**435.3**	**478.1**

Pet_04i			
Weighting	**7.3%**		
Bcf	1P	2P	3P
Upper C 3P			32.7
Upper C 2P		32.7	32.7
Upper C 1P	19.8	23.2	23.2
Main Wa C	227.5	240.5	240.5
Wa Ca1			10.6
Wa C	247.3	296.4	339.7
Upper Wa A		14.0	14.0
Lower Wa A	84.6	99.5	99.5
Wa A	84.6	113.5	113.5
Total	**331.9**	**409.9**	**453.2**

Pet_04j			
Weighting	**7.3%**		
Bcf	1P	2P	3P
Upper C 3P			31.3
Upper C 2P		31.3	31.3
Upper C 1P	19.8	23.2	23.2
Main Wa C	272.2	285.2	285.2
Wa Ca1			9.9
Wa C	292	339.7	380.9
Upper Wa A		14.8	14.8
Lower Wa A	85.0	100.0	100.0
Wa A	85.0	114.7	114.7
Total	**377.0**	**454.4**	**495.6**

Pet_04k			
Weighting	**7.3%**		
Bcf	1P	2P	3P
Upper C 3P			31.3
Upper C 2P		31.3	31.3
Upper C 1P	19.8	23.2	23.2
Main Wa C	248.5	261.5	261.5
Wa Ca1			10.6
Wa C	268.3	316	357.9
Upper Wa A		14.8	14.8
Lower Wa A	85.0	100.0	100.0
Wa A	85.0	114.8	114.8
Total	**353.3**	**430.8**	**472.7**

Pet_04m			
Weighting	**7.3%**		
Bcf	1P	2P	3P
Upper C 3P			32.7
Upper C 2P		32.7	32.7
Upper C 1P	19.8	23.2	23.2
Main Wa C	238	251	251
Wa Ca1			9.7
Wa C	257.8	306.9	349.3
Upper Wa A		13.9	13.9
Lower Wa A	84.6	99.5	99.5
Wa A	84.6	113.4	113.4
Total	**342.4**	**420.3**	**462.7**

Pet_04n			
Weighting	**7.3%**		
Bcf	1P	2P	3P
Upper C 3P			32.7
Upper C 2P		32.7	32.7
Upper C 1P	19.8	23.2	23.2
Main Wa C	243.2	256.2	256.2
Wa Ca1			9.7
Wa C	263	312.1	354.5
Upper Wa A		14.0	14.0
Lower Wa A	84.6	99.5	99.5
Wa A	84.6	113.5	113.5
Total	**347.6**	**425.6**	**468.0**

Pet_Al_04_FC3			
Weighting	**6.7%**		
Bcf	1P	2P	3P
Upper C 3P			31.3
Upper C 2P		31.3	31.3
Upper C 1P	19.7	23.1	23.1
Main Wa C	260.8	273.8	273.8
Wa Ca1			9.8
Wa C	280.5	328.2	369.3
Upper Wa A		14.0	14.0
Lower Wa A	55.9	65.8	65.8
Wa A	55.9	79.8	79.8
Total	**336.4**	**408.0**	**449.1**

Pet_Al_04_FC2			
Weighting	**6.7%**		
Bcf	1P	2P	3P
Upper C 3P			31.3
Upper C 2P		31.3	31.3
Upper C 1P	19.7	23.1	23.1
Main Wa C	238.9	251.9	251.9
Wa Ca1			9.8
Wa C	258.6	306.3	347.4
Upper Wa A		14.0	14.0
Lower Wa A	98.9	116.3	116.3
Wa A	98.9	130.3	130.3
Total	**357.5**	**436.6**	**477.7**

Pet_Al_04_JC			
Weighting	**6.7%**		
Bcf	1P	2P	3P
Upper C 3P			31.3
Upper C 2P		31.3	31.3
Upper C 1P	19.7	23.1	23.1
Main Wa C	297.3	310.3	310.3
Wa Ca1			9.8
Wa C	317	364.7	405.8
Upper Wa A		14.0	14.0
Lower Wa A	84.6	99.5	99.5
Wa A	84.6	113.5	113.5
Total	**401.6**	**478.2**	**519.3**

Table 3.12.3-b : Casino Petrel Model OGIP

The initial OGIP distribution arising from the analysis to this stage is shown in Figure 3.12.3-c. Note that at this stage a separate distribution of 1P, 2P and 3P OGIP is shown and that all the Petrel models have been treated as equiprobable. This has the affect of treating the AI based Petrel models with a 20% weighting and the layered Petrel models with an approximate 80% weighting.

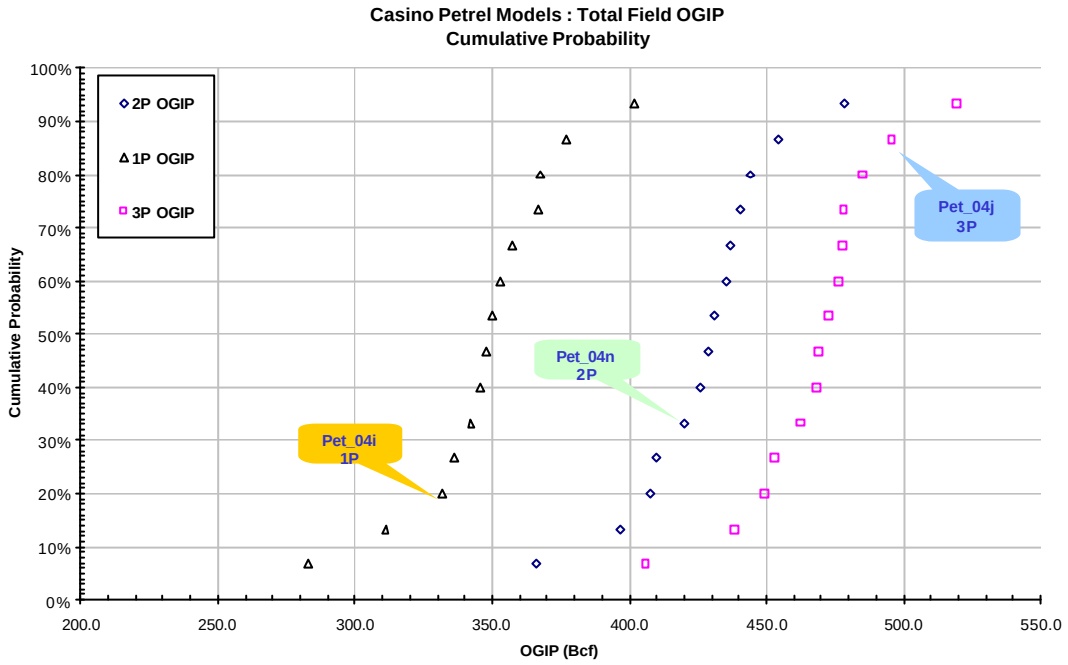

Figure 3.12.3-c : Initial Distribution of Casino OGIP from 1P, 2P and 3P Petrel Models

3.12.4 Additional OGIP Uncertainties

Background

The OGIP distribution shown at the conclusion of Section 3.12.3 is largely a distribution based on different Waarre C porosity trends arising from different methods of populating the static model. While these different methods result in a large range of OGIP outcomes in the Waarre C reservoir, the range observed in the Waarre A is quite tight. The next step in constructing the field OGIP distribution is to add in the effect of other significant uncertainties including;

- Gross Rock Volume (GRV) uncertainty
- Waarre A water saturation uncertainty
- Waarre A porosity uncertainty associated with different model population techniques

The basis for the uncertainties associated with these elements is summarised in the following sections.

3.12.5 Gross Rock Volume Uncertainty

Each of the Petrel models described in Section 3.12.3 are based on the same structural framework. Gross Rock Volume uncertainty has been recognised in the following areas;

- Seismic Pick
- Bounding fault location (Waarre A reservoir)
- Updip pinchout edge location (Waarre C reservoir only)
- Free Water Level
- Time-Depth conversion and flexing method applied during depth conversion process

These uncertainties have initially been considered separately and then combined together to give a single uncertainty range to use to represent GRV uncertainty in the Casino field.

Seismic Pick

At this stage, no attempt has been made to produce a Lowside or Highside structural interpretation and as a result the uncertainty associated with this parameter is difficult to quantify. The range chosen to represent this uncertainty has been based on GRV variations observed between the initial Waarre C Main reservoir picks based on the band limited impedance volume (~ 330 Mm^3) and the final picks using the model based impedance volume (~ 300 Mm^3). The range observed (10%) has been used to give a GRV uncertainty range as shown in Table 3.12.5-a.

Seismic Pick Uncertainty			
Maximum GRV	+10%	Minimum GRV	-10%

Table 3.12.5-a : Seismic Pick GRV Uncertainty Parameters

Main Bounding Fault Location (Waarre A)

The sensitivity to the location of the main bounding fault in the Waarre A has been examined by calculating the GRV change associated with moving the fault 50m north and south of the current location as shown in Figure 3.12.5-a.

The resulting GRV uncertainty range is shown in Table 3.12.5-b.

Waarre A Fault Location Uncertainty			
Maximum GRV	+8%	Minimum GRV	-8%

Table 3.12.5-b : Waarre A Fault Location Uncertainty Parameters

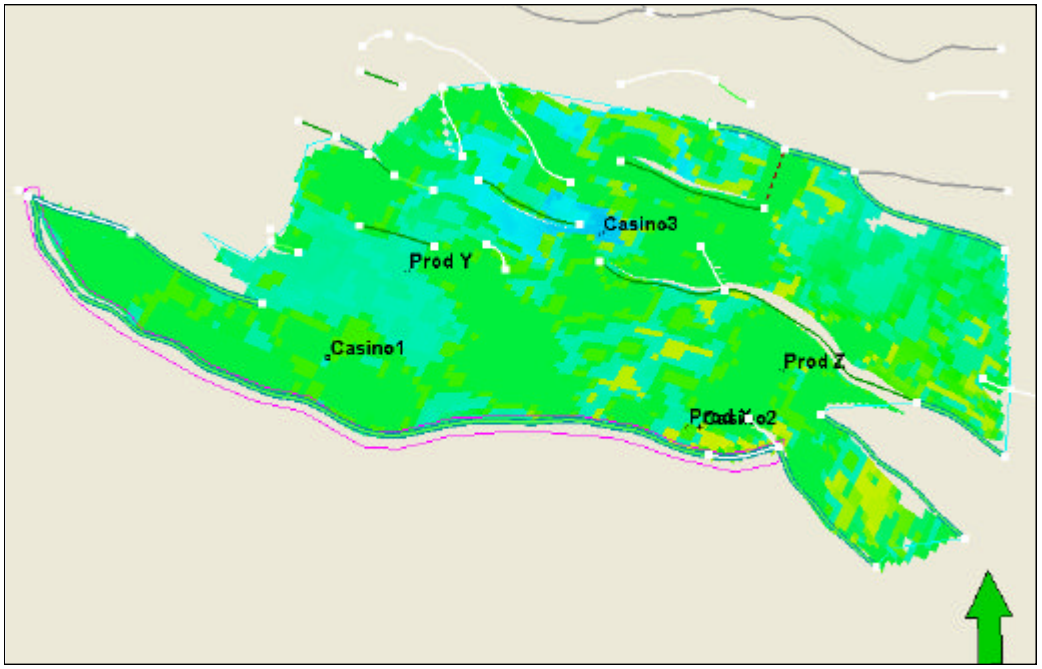

Figure 3.12.5-a : Waarre A Main Bounding Fault Location GRV Sensitivity

Pinchout Edge Location (Waarre C)

The sensitivity to the location of the pinchout edge location in the Waarre C has been examined by calculating the GRV change associated with moving the pinchout 100m north and south of the current location as shown in Figure 3.12.5-b.

The resulting GRV uncertainty range is shown in Table 3.12.5-b.

Waarre C Pinchout Edge Location Uncertainty			
Upper Cb			
Maximum GRV	+12%	Minimum GRV	-12%
Main C			
Maximum GRV	+5%	Minimum GRV	-5%

Table 3.12.5-c : Waarre C Pinchout Edge Location GRV Sensitivity

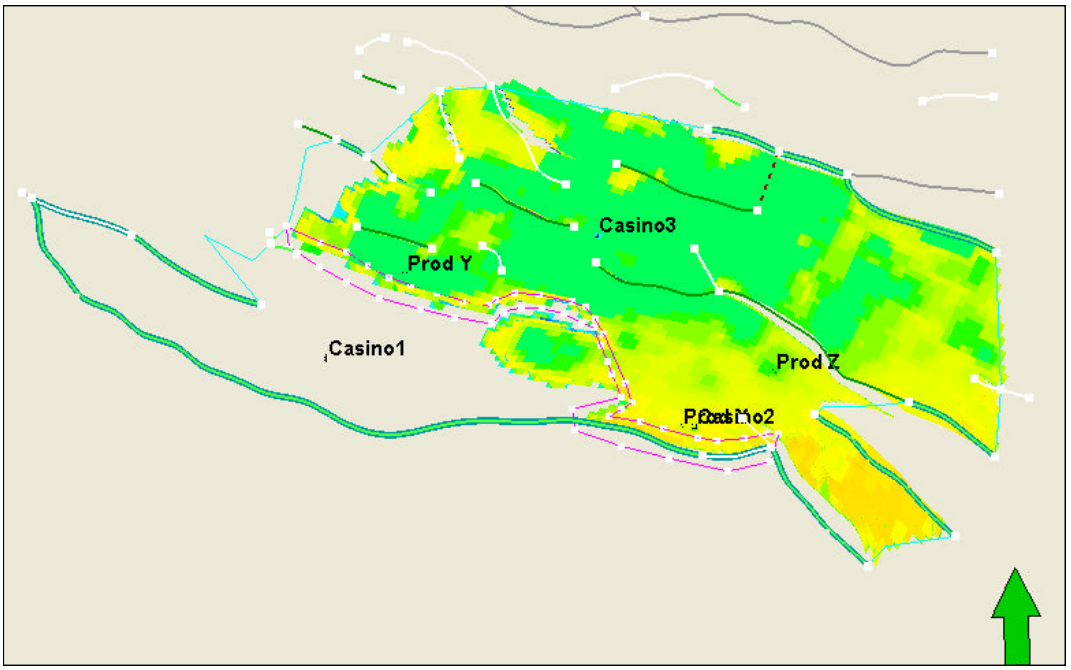

Figure 3.12.5-b : Waarre C Pinchout Edge Location GRV Sensitivity

Free Water Level Uncertainty

The range of Free Water Levels for the field is documented in Section 3.8. The GRV impact associated with the minimum and maximum FWL is summarised in Table 3.12.5-d.

Free Water Level Uncertainty			
Waarre C	Max -2000 mSS	ML -1999 mSS	Min -1994 mSS
Maximum GRV	+1%	Minimum GRV	-3%
Waarre A	Max -1840 mSS	ML -1838 mSS	Min -1836 mSS
Maximum GRV	+1%	Minimum GRV	-2%

Table 3.12.5-d : Waarre C Pinchout Edge Location GRV Sensitivity

Depth Conversion / Surface Flexing

The Base Case depth conversion methodology used for the Casino field is described in Section 3.3. The sensitivity of GRV to depth conversion methodology was checked by depth converting the same time surfaces using an alternate method based on stacking velocities. No significant variation was observed.

The sensitivity of GRV to flexing algorithms was also checked by using comparing the results using the base case Minimum Curvature algorithm to results obtained using a Distance Weighted Average algorithm. The GRV impact associated with these different methods is summarised in Table 3.12.5-e.

Flexing Algorithm Uncertainty			
Maximum GRV	+3%	Minimum GRV	-3%

Table 3.12.5-e : Flexing Algorithm GRV Uncertainty

Overall GRV Uncertainty

The GRV uncertainties described above have been combined probabilistically to give a single GRV uncertainty parameter to apply to the base OGIP estimates. In combining these parameters all the above factors have been considered to be independent.

The results of this analysis are shown in Table 3.12.5-f. Note the ranges for both reservoirs are slightly different, however for simplicity in subsequent calculations the P90 – P10 range determined for the Waarre A reservoir (0.93 – 1.07) has been used to represent the GRV uncertainty associated with both reservoirs.

Overall GRV Uncertainty Factor				
Waarre A				
Min : 0.86	P90 : 0.93	P50 : 1.00	P10 : 1.07	Max : 1.13
Waarre C				
Min : 0.88	P90 : 0.93	P50 : 0.99	P10 : 1.05	Max : 1.11

Table 3.12.5-f : Overall GRV Uncertainty Factor

3.12.6 Waarre A Water Saturation

In the absence of definitive core data, significant uncertainty remains in the Waarre A water saturation. A large range is evident from various petrophysical based estimates (Section 3.6) and SCAL based saturation vs height functions (Section 3.7).

Lower Waarre A

Figure 3.12.6-a shows three alternate petrophysical interpretations of water saturation over the Lower Waarre A interval of Casino-1. The lowest interpreted water saturation shown is from the interpretation performed by AWE. For the purposes of Waarre A Gas-in-Place estimation this is treated as a “P10” water saturation estimate. The middle curve is from the Santos log interpretation described in Section 3.6 and is treated as the “P50” water saturation estimate. The curve showing the highest water saturation has been generated as a “P90” water saturation estimate by changing the input petrophysical parameters.

For calculation of OGIP in Petrel, alternate saturation versus height functions have been used to approximate these petrophysical analyses as shown in Figure 3.12.6-a.

The “P50” saturation model was approximated using the Thomeer saturation versus height function described in Section 3.7 with the “P50” Waarre A permeability input described in Section 3.13 (log permeability model divided by 2). As can be seen in Figure 3.12.6-a, this provides an excellent match to the “P50” petrophysical interpretation.

The “P90” saturation model was also approximated using the Thomeer saturation versus height function described in Section 3.7 but using the “P90” Waarre A permeability input described in Section 3.13 (log permeability model divided by 8). This also provides an excellent match to the “P90” petrophysical interpretation.

The “P10” saturation model was approximated using the J function described in Section 3.7 which provides an excellent match to the “P10” petrophysical interpretation as shown.

The impact of these alternate water saturation outcomes on Lower Waarre A OGIP is summarised in Table 3.12.6. For simplicity, a symmetrical P10/P90 range of +/- 18.5 Bcf relative to the P50 case has been used to capture the uncertainty in OGIP associated with water saturation in the Lower Waarre A.

Basis	P50 Sw Model Thomeer Function with P50 perm model	P90 Sw Model Thomeer Function with P90 perm model	P10 Sw Model J Function with log perm model
OGIP from Petrel Model Pet_04n (Bcf)	100.0	79.6	118.5
Differential from P50 Case		(-20.4)	(+18.5)

Table 3.12.6-a : OGIP variation with Sw Uncertainty in Lower Waarre A

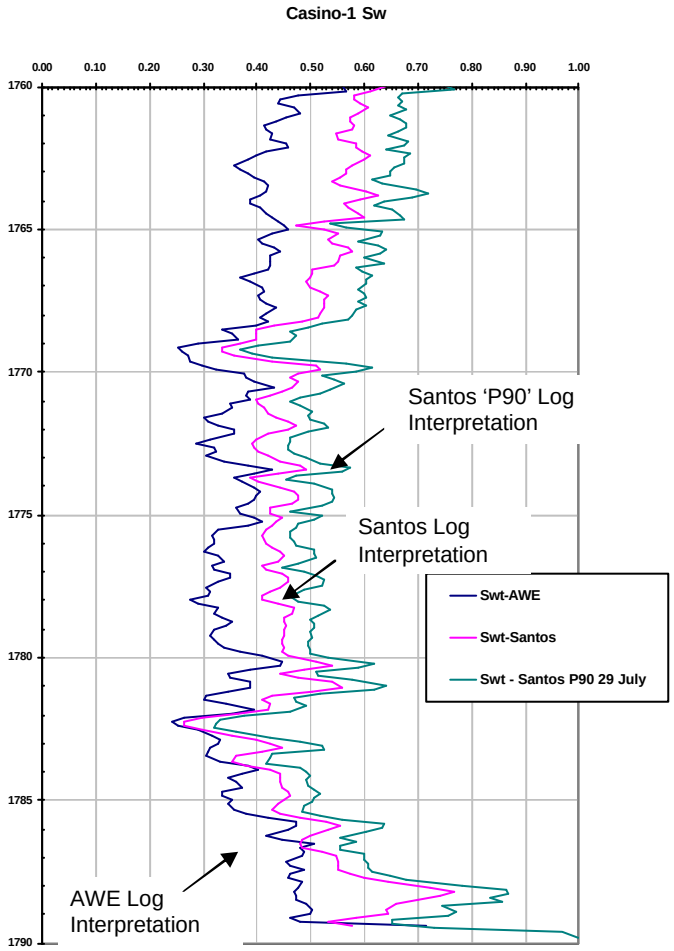

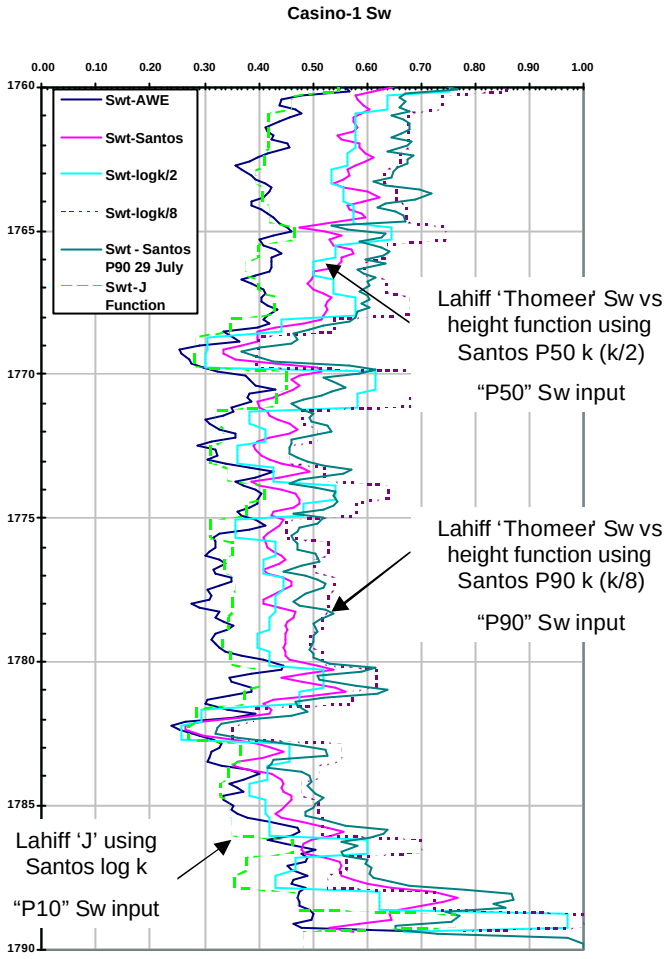

Figure 3.12.6-a : Water Saturation Models – Lower Waarre A

Upper Waarre A

As shown in Section 3.7 both of the saturation versus height functions were found to significantly under predict water saturation in the Upper Waarre A interval, compared to the petrophysical analysis. The best match to the "P50" petrophysical estimate of water saturation was obtained using the Thomeer Function and the "P90" permeability model as shown in Figure 3.12.6-b. This was used as the "P50" water saturation model when calculating Upper Waarre A OGIP in the Petrel static models.

Upside and downside impact on Upper Waarre A OGIP associated with water saturation uncertainty is summarised in Table 3.12.6 - b.

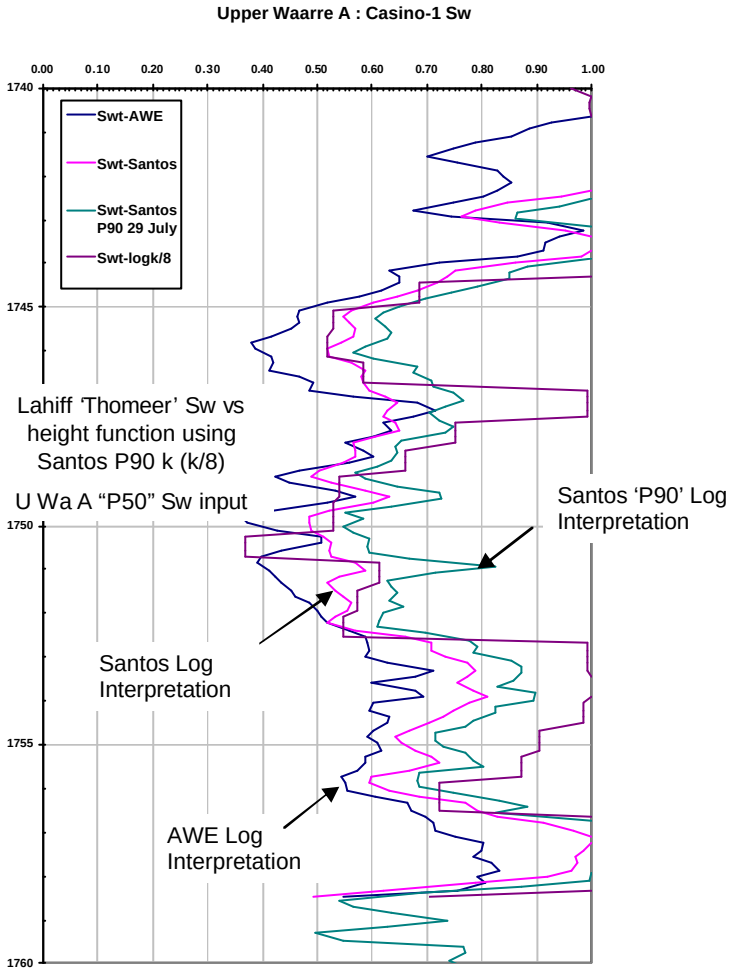

Figure 3.12.6-b : Water Saturation Models – Upper Waarre A

Basis	P50 Sw Model Thomeer Function with P90 perm model	P90 Sw Model Estimate (assumes symmetrical to P10)	10 Sw Model Thomeer Function with P50 perm model
OGIP from Petrel Model Pet_04n (Bcf)	15	7	23
Differential from P50 Case		(-8)	(+8)

Table 3.12.6-b : OGIP variation with Sw Uncertainty in Upper Waarre A

3.12.7 Waarre A Static Model Population Method

The geological based Petrel static models used as a basis for the field's Gas-in-Place distribution use a moving average of Casino-1, Casino-2 and Casino-3 porosity to populate the model. Casino-3 is located well below the Waarre A FWL and is poorer quality reservoir than Casino-1 and Casino-2.

To provide an upside or P10 result in terms of Waarre A porosity distribution a case was constructed where only the two wells in the gas zone (Casino-1 and Casino-2) were used to populate the model. The results of using this alternate approach are summarised in Table 3.12.7-a for the Lower Waarre A reservoir and show an increase of approximately 5 Bcf for the P10 Case. No separate downside case was created with the downside or P90 being assumed to be equal to the upside (minus 5 Bcf)

Basis	P50 Porosity Model Moving Average of Casino-1,2-and 3	P10 Porosity Model Moving Average of Casino-1 and 2 only	P90 Porosity Model Assumed symmetrical with P10 Case
OGIP from Petrel Model Pet_04n (Bcf)	100.0	105.0 (+5)	95 (-5)

Table 3.12.7-a : OGIP variation with Porosity Population Technique in Lower Waarre A

3.12.8 Creating the Field OGIP Distribution – Part 1 : Scenario Tree Approach

For the final OGIP distribution a "Scenario Tree" approach was used to combine the individual deterministic cases. An example of the scenario tree can be found in Figure 3.12.8-a.

The scenario tree takes as a starting point the base Gas-in-Place from each Petrel model and progressively combines uncertainties associated with Waarre A water saturation, Waarre A porosity population and Gross Rock Volume.

To keep the scenario tree to a manageable size the uncertainties associated with Waarre A water saturation and Waarre A porosity population have been combined into a single set of 5 uncertainties as follows;

Mid – Mid case : P50 Sw / P50 Porosity Distribution (50% weighting)
High – Mid case: P10 Sw / P50 Porosity Distribution (18.75% weighting)
High – High case : P10 Sw / P10 Porosity Distribution (6.75% weighting)
Low – Mid case : P90 Sw / P50 Porosity Distribution (18.75% weighting)
Low – Low case P90 Sw / P90 Porosity Distribution (6.75% weighting)

For each of these 5 cases a P90, P50 and P10 GRV scenario is created using a 25% / 50% / 25% weighting. Hence for each individual Petrel model a total of 15 separate deterministic scenarios is created as follows;

- Base Petrel Model x 5 Sw/Porosity Scenarios x 3 GRV Scenarios.

A tree such as this was constructed for each of the fourteen Petrel static models used to create a total of 210 scenarios for each of 1P, 2P and 3P Gas-in-Place.

The results of this analysis are shown in Figures 3.12.8-b, c and d. Figure 3.12.8-c shows the distribution of the field's 2P OGIP and is plotted in such a way as to show the contribution of each of the fourteen base Petrel static models. Figures 3.12.b and d show the same plot for the field's 1P OGIP and 3P OGIP respectively. Figure 3.12.8-e shows a consolidation of the 1P, 2P and 3P OGIP on a single plot.

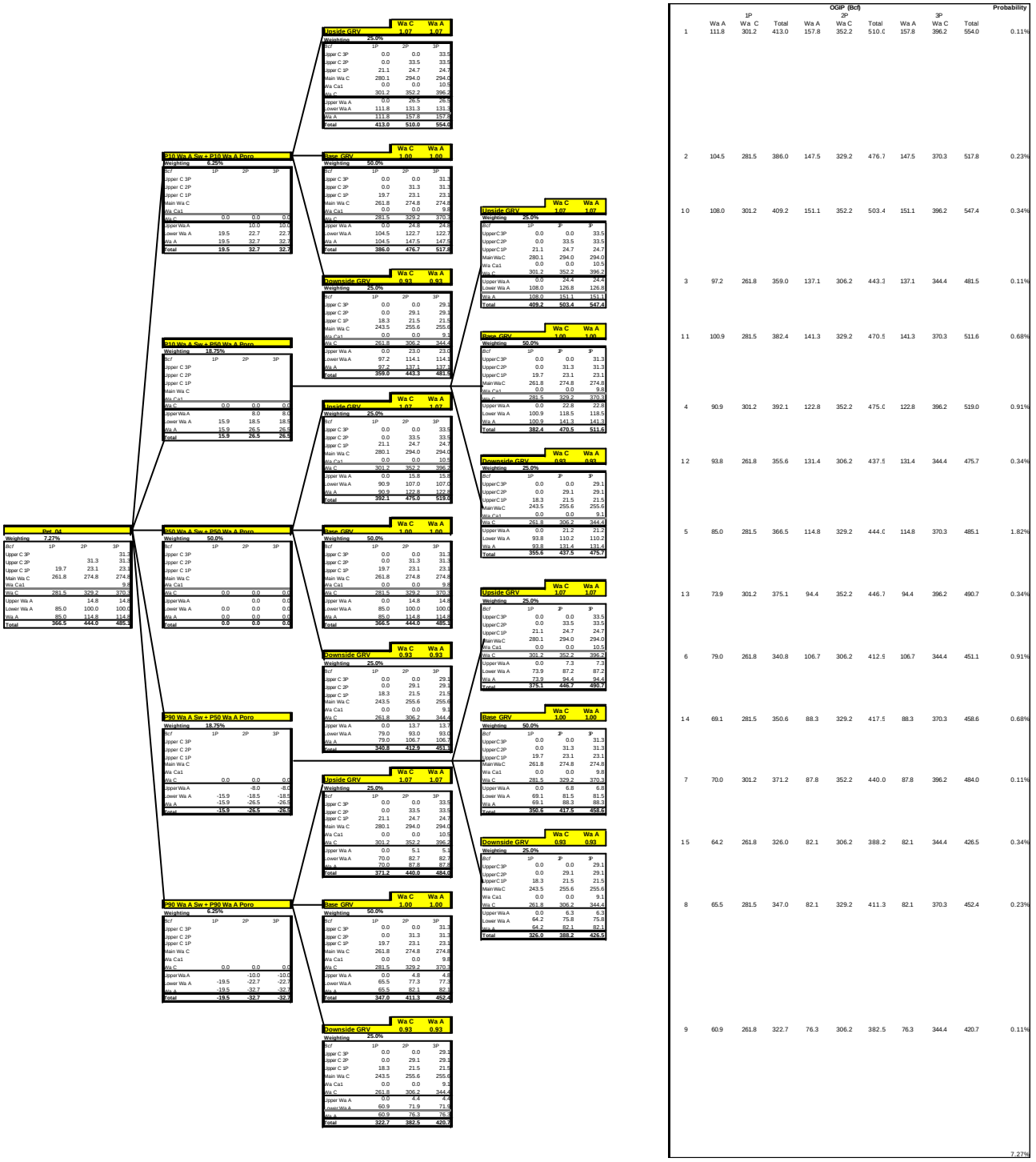

	OGIP (Bcf) 1P Wa A	1P Wa C	1P Total	2P Wa A	2P Wa C	2P Total	3P Wa A	3P Wa C	3P Total	Probability
1	111.8	301.2	413.0	157.8	352.2	510.0	157.8	396.2	554.0	0.11%
2	104.5	281.5	386.0	147.5	329.2	476.7	147.5	370.3	517.8	0.23%
10	108.0	301.2	409.2	151.1	352.2	503.4	151.1	396.2	547.4	0.34%
3	97.2	261.8	359.0	137.1	306.2	443.3	137.1	344.4	481.5	0.11%
11	100.9	281.5	382.4	141.3	329.2	470.5	141.3	370.3	511.6	0.68%
4	90.9	301.2	392.1	122.8	352.2	475.0	122.8	396.2	519.0	0.91%
12	93.8	261.8	355.6	131.4	306.2	437.5	131.4	344.4	475.7	0.34%
5	85.0	281.5	366.5	114.8	329.2	444.0	114.8	370.3	485.1	1.82%
13	73.9	301.2	375.1	94.4	352.2	446.7	94.4	396.2	490.7	0.34%
6	79.0	261.8	340.8	106.7	306.2	412.9	106.7	344.4	451.1	0.91%
14	69.1	281.5	350.6	88.3	329.2	417.5	88.3	370.3	458.6	0.68%
7	70.0	301.2	371.2	87.8	352.2	440.0	87.8	396.2	484.0	0.11%
15	64.2	261.8	326.0	82.1	306.2	388.2	82.1	344.4	426.5	0.34%
8	65.5	281.5	347.0	82.1	329.2	411.3	82.1	370.3	452.4	0.23%
9	60.9	261.8	322.7	76.3	306.2	382.5	76.3	344.4	420.7	0.11%
										7.27%

Figure 3.12.8-a : Scenario Tree Used to Compound Uncertainties for Each Petrel Static Model

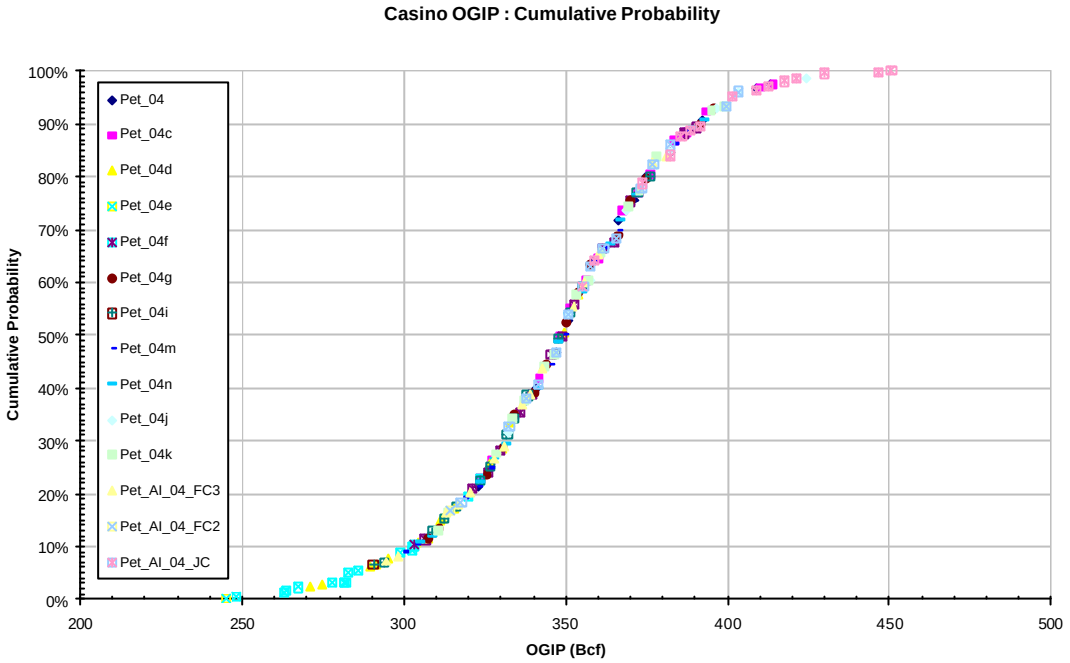

Figure 3.12.8-b : Casino Field 1P OGIP Distribution showing contribution by base Petrel model

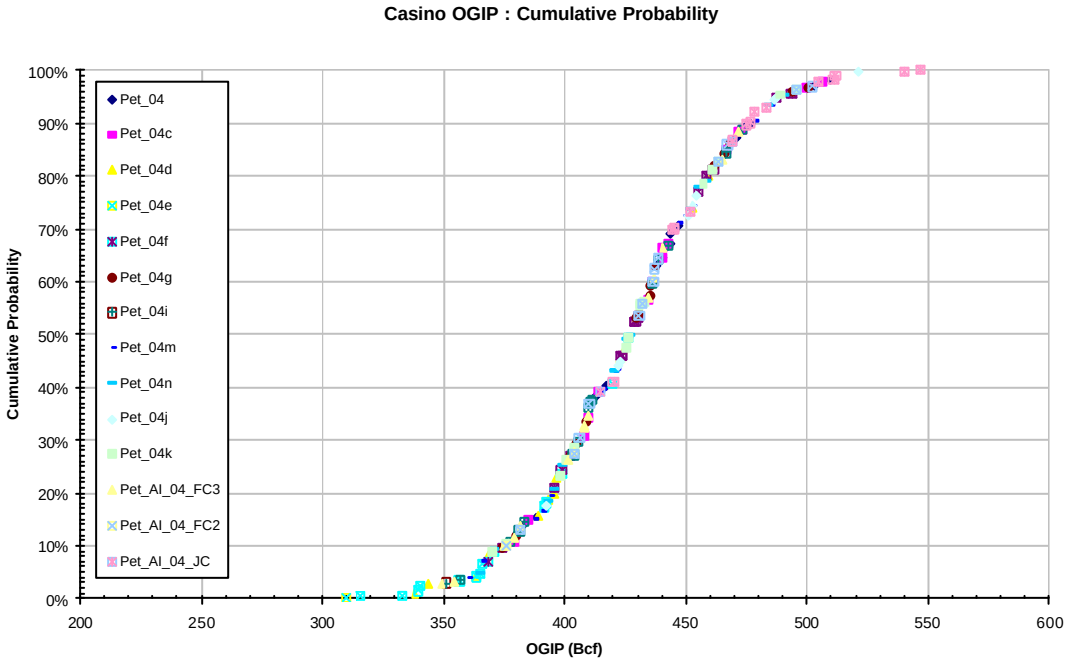

Figure 3.12.8-c : Casino Field 2P OGIP Distribution showing contribution by base Petrel model

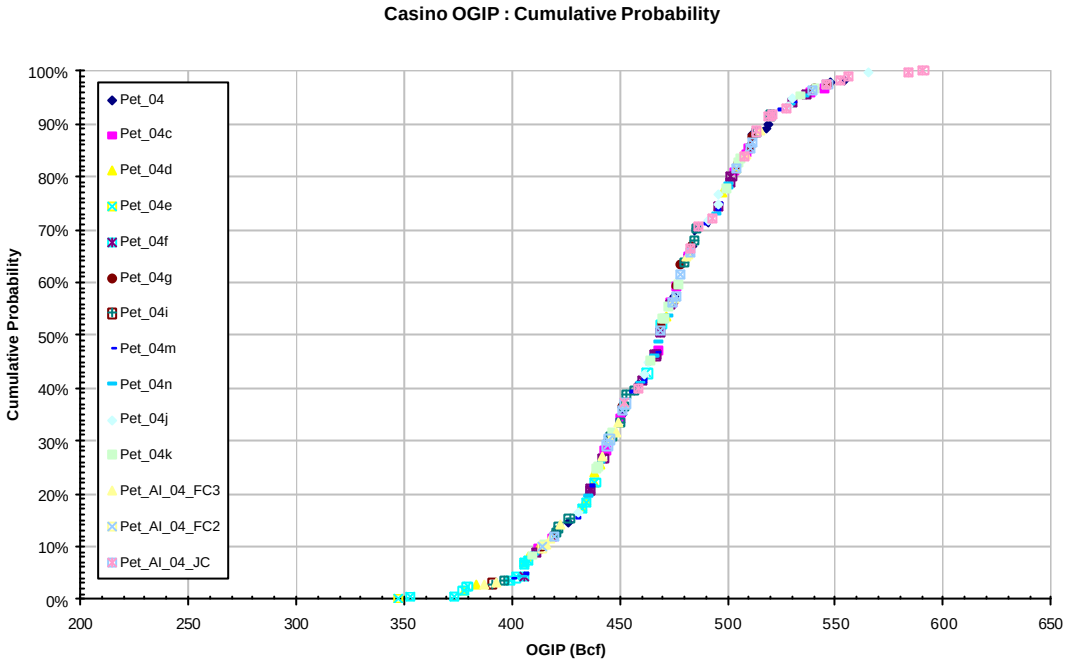

Figure 3.12.8-d : Casino 3P OGIP Distribution showing contribution by base Petrel model

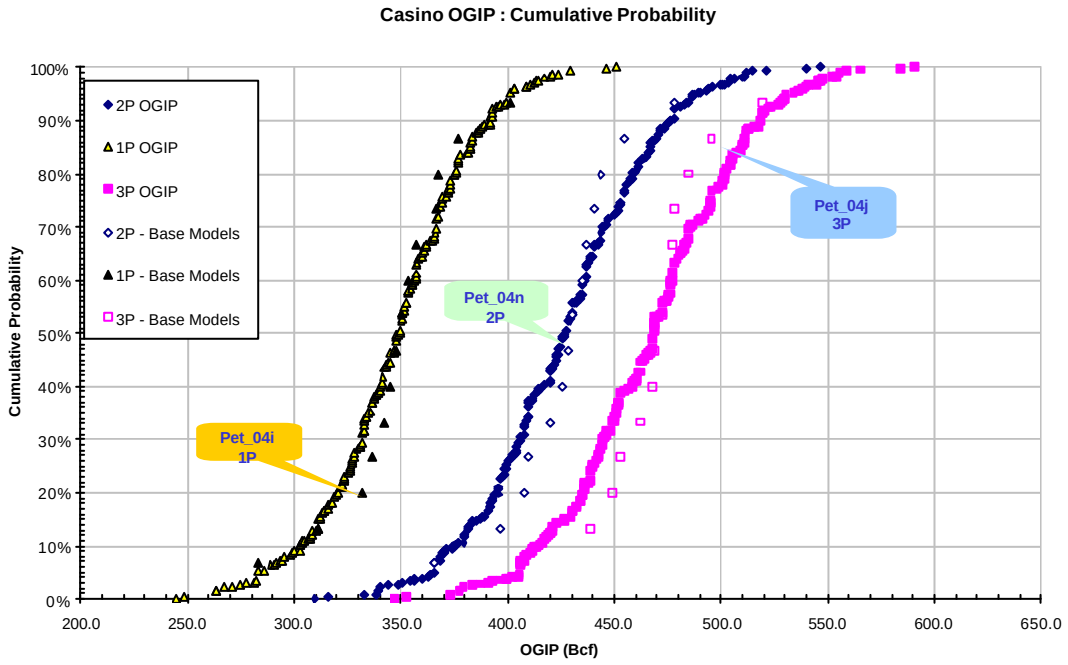

Figure 3.12.8-e : Casino Field 1P,2P and 3P OGIP Distributions

3.12.9 Creating the Field OGIP Distribution – Part 2 : Creating a Single Distribution

The previous section described the creation of separate distributions for Casino field's 1P, 2P and 3P OGIP. The final stage in creating the Casino field's OGIP distribution is to combine these into a single distribution.

This has been achieved by treating each of the 630 individual outcomes within the 1P, 2P and 3P distributions as equally likely and forming a single distribution. The process of merging the three distributions as shown in Figure 3.12.9-a with the final distribution of Casino field's OGIP shown in Figure 3.12.9-b.

Also shown in Figure 3.12.9-c and d are the final distributions for individual Waarre A and Waarre C OGIP respectively.

The final results are summarised in Table 3.12.9-a

Casino OGIP (Bcf)	P90	P50	P10
Waarre C	247	312	372
Waarre A	74	106	140
Field	**332**	**420**	**496**

Table 3.12.9-a : Final Casino Field Reserves

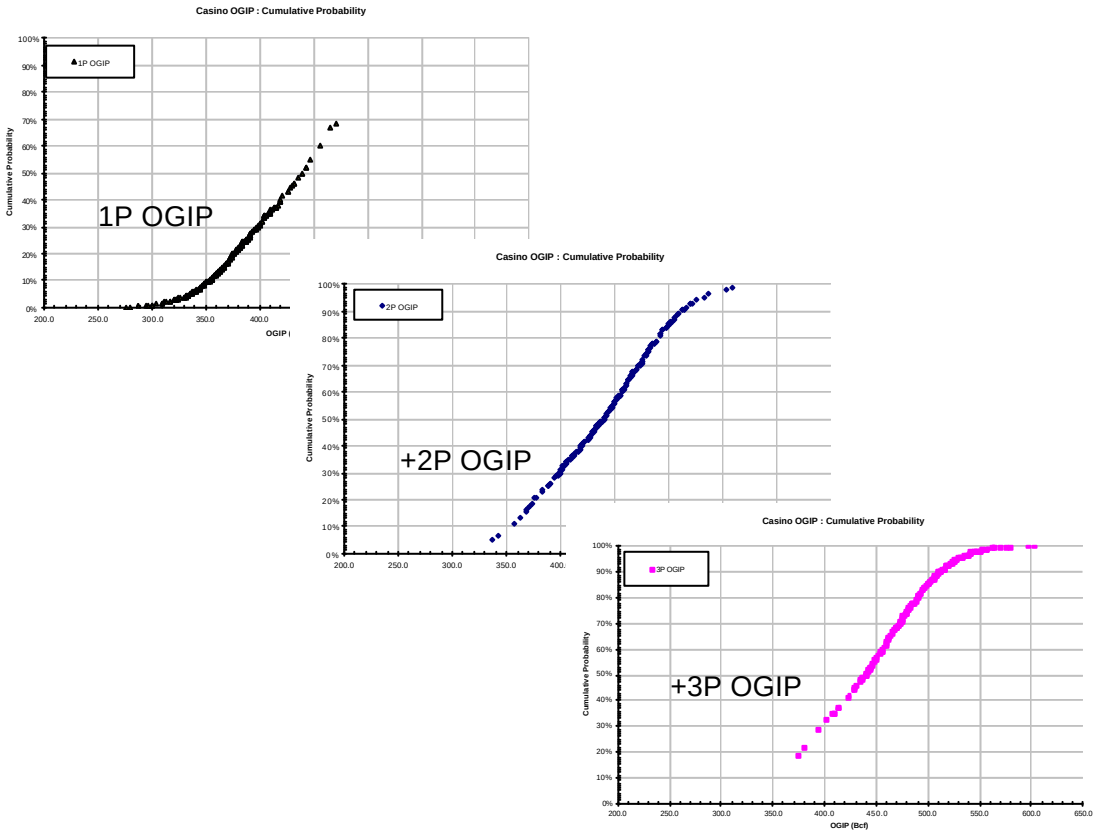

Figure 3.12.9-a : Combining the Distributions

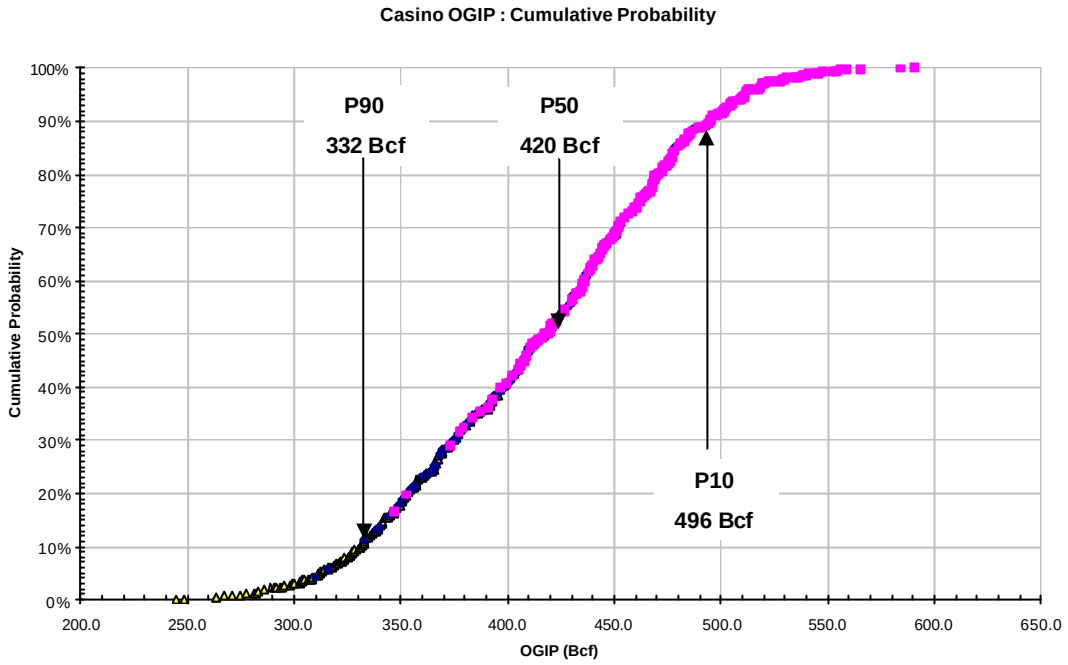

Figure 3.12.9-b : Final Casino Field OGIP Distribution

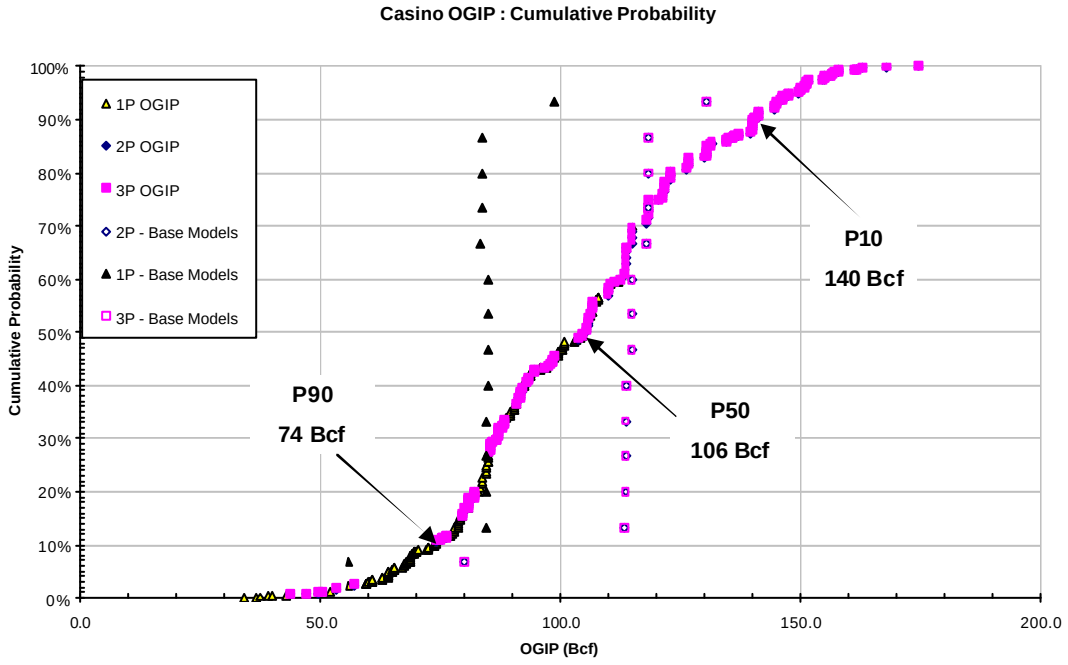

Figure 3.12.9-c : Waarre A OGIP Distribution

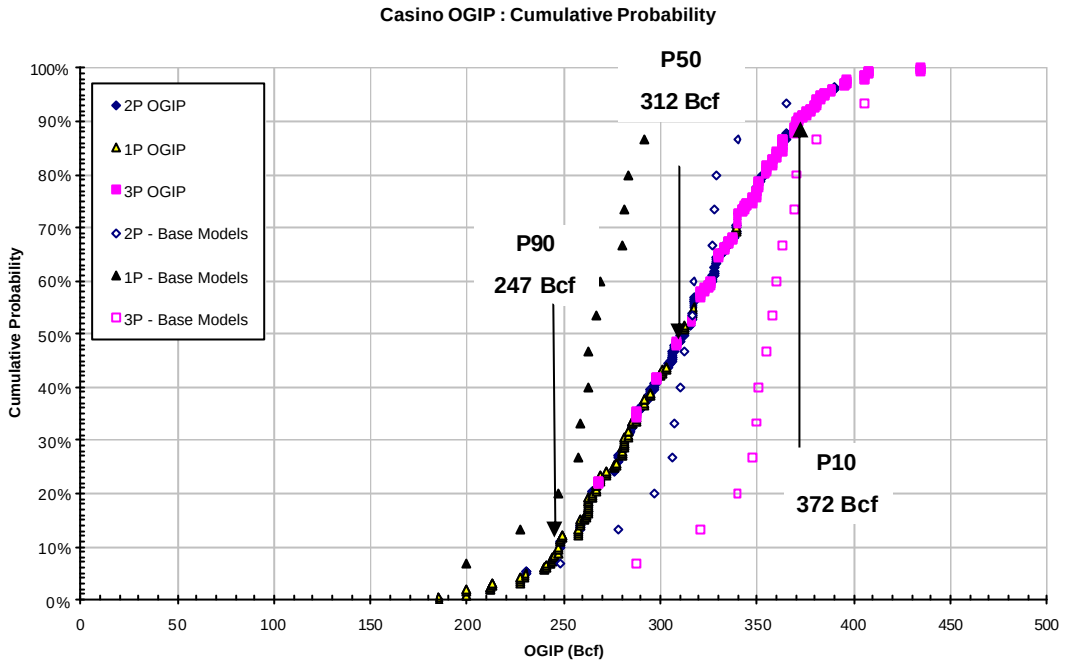

Figure 3.12.9-d : Waarre C OGIP Distribution

3.12.10 Selecting Representative P90, P50 and P10 Static Models

Following creation of the final Casino field OGIP distribution, individual Petrel models were selected to represent the field's P90, P50 and P10 OGIP with a deterministic scenario. The approach taken has been to select the closest 1P Petrel deterministic realisation to represent the P90, the closest 2P Petrel deterministic realisation to represent the P50 and the closest 3P Petrel deterministic realisation to represent the P10. The deterministic scenarios chosen are shown in Figure 3.12.10-a.

Tables 3.12.10-a, b and c show a detailed breakdown of each model chosen to represent the P90, P50 and P10 OGIP respectively.

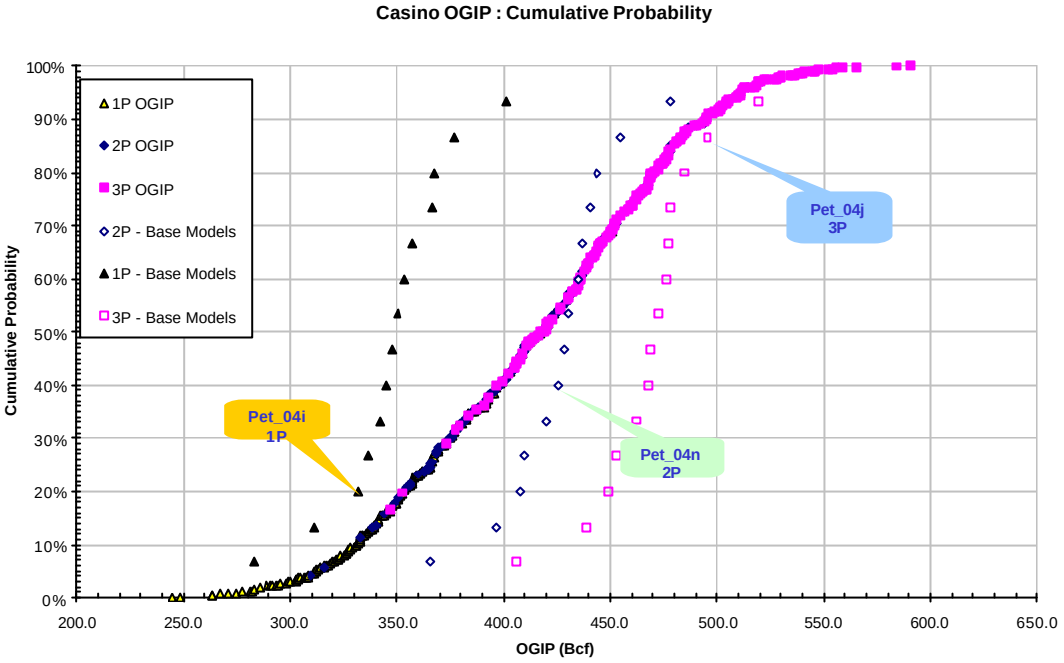

Figure 3.12.10-a : Selection of Deterministic Petrel Scenarios to Match Field P90, P50 and P10 OGIP

P50 Case

Pet_04n : 2P

	P50 OGIP	Model OGIP
Wa C	312*	312
Wa A	106*	114
Total	420	426

* Not additive, shown for information only

Pet_04n			
Weighting	**7.3%**		
Bcf	1P	2P	3P
Upper C 3P			32.7
Upper C 2P		32.7	32.7
Upper C 1P	19.8	23.2	23.2
Main Wa C	243.2	256.2	256.2
Wa Ca1			9.7
Wa C	263	312.1	354.5
Upper Wa A		14.0	14.0
Lower Wa A	84.6	99.5	99.5
Wa A	84.6	113.5	113.5
Total	**347.6**	**425.6**	**468.0**

Table 3.12.10-a : P50 Petrel Model Details

P90 Case

Pet_04i : 1P

	P90 OGIP	Model OGIP
Wa C	247*	247
Wa A	74*	85
Total	332	332

* Not additive, shown for information only

Pet_04i			
Weighting	**7.3%**		
Bcf	1P	2P	3P
Upper C 3P			32.7
Upper C 2P		32.7	32.7
Upper C 1P	19.8	23.2	23.2
Main Wa C	227.5	240.5	240.5
Wa Ca1			10.6
Wa C	247.3	296.4	339.7
Upper Wa A		14.0	14.0
Lower Wa A	84.6	99.5	99.5
Wa A	84.6	113.5	113.5
Total	**331.9**	**409.9**	**453.2**

Table 3.12.10-b : P90 Petrel Model Details

P10 Case

Pet_04j : 3P

	P10 OGIP	Model OGIP
Wa C	372*	381
Wa A	140*	115
Total	496	496

* Not additive, shown for information only

Pet_04j			
Weighting	**7.3%**		
Bcf	1P	2P	3P
Upper C 3P			31.3
Upper C 2P		31.3	31.3
Upper C 1P	19.8	23.2	23.2
Main Wa C	272.2	285.2	285.2
Wa Ca1			9.9
Wa C	292	339.7	380.9
Upper Wa A		14.8	14.8
Lower Wa A	85.0	100.0	100.0
Wa A	85.0	114.7	114.7
Total	**377.0**	**454.4**	**495.6**

Table 3.12.10-c : P10 Petrel Model Details

3.13 Waarre A Permeability Basis

3.13.1 Background

The evidence for the Waarre A being gas bearing and the extent of the column is strong and based on;

- Gas shows indicated while drilling the interval in Casino-1
- Log interpretation of Casino-1 and Casino-2
- Gas sample recovery from the MDT in Casino-1
- Gas and water gradients indicated from formation pressures measured from Casino-1, Casino-2 and Casino-3

However, in the absence of whole core and production test data from the gas bearing interval of the Waarre A reservoir, considerable uncertainty exists regarding the true in situ permeability of this formation. This section describes the basis for the permeability range finally chosen for the Waarre A reservoir and forms the justification for considering this to be a proven, producible hydrocarbon resource.

3.13.2 MDT Pre-Test Derived Formation Permeability

A total of 11 MDT pre-tests were attempted in the Waarre A formation of Casino-1. Assuming spherical flow, the drawdown mobility (M=k/μ md/cP) measured on these pre-tests can be corrected to give an estimate of true formation permeability as follows;

$$k = \frac{M*\mu}{k_v/k_h * (k_{rw})^{1/3}}$$

Where;
k= formation permeability (md)
μ = fluid viscosity (cP)
M = drawdown mobility from MDT pre-test (md/cP)
k_v/k_h =anistropy
k_{rw} = endpoint water relative permeability

These corrections have been made for the Casino-1 MDT data and are summarised in Table 3.13.2-a below;

Corrected Depth m MDKB	**MDT Drawdown Mobility** md/cP	**MDT Permeability** md
1746.0	8.0	27
1751.0	7.7	26
1761.0	2.4	8
1763.0	0.8	3
1769.0	47.8	162
1773.0	0.2	1
1776.5	10.5	36
1782.5	9.4	32
1785.0	1.2	4
1787.5	14.4	49

Table 3.13.2-a: Casino-1 Permeability from MDT pre-test drawdown

3.13.3 Log Derived Permeability Model

Petrophysical logs have been used to derived permeability estimates using the modified Coates Free Fluid model as described in Section 3.6.2. This model provides a reasonable fit to the permeability measured from MDT pre-tests as shown in Figures 3.13.3-a and 3.13.3-b below.

Figure 3.13.3-a shows the log permeability model and the log permeability model upscaled from log resolution to 1m compared to the permeability from MDT pre-tests at Casino-1.

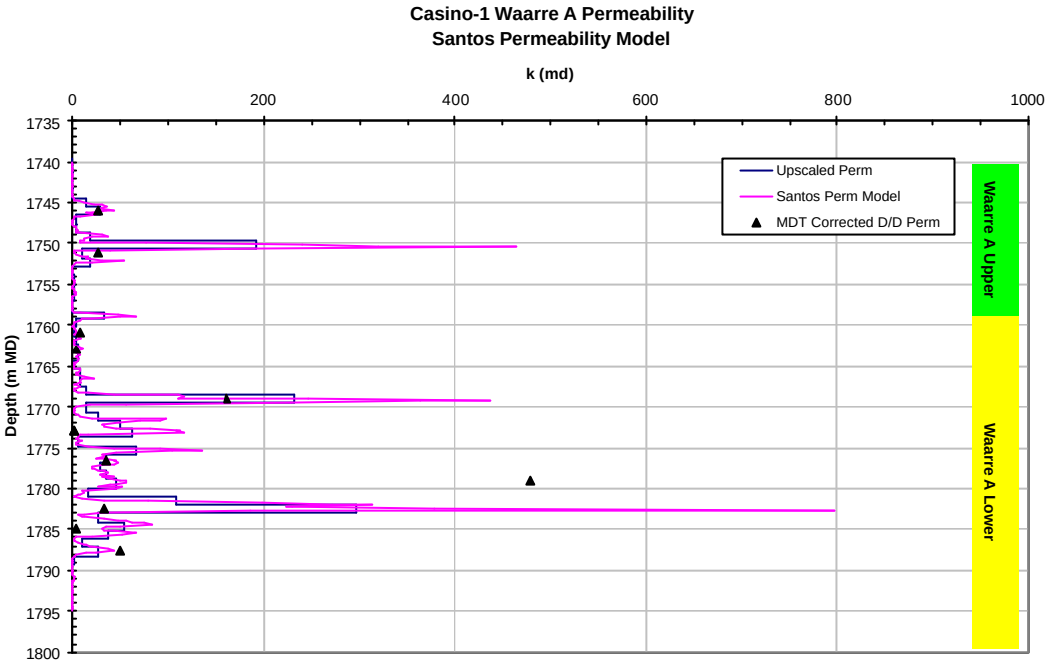

Figure 3.13.3-a: Casino-1 MDT Permeability and Log Derived Model

Figure 3.13.3-b shows the same data in cross plot and also included MDT derived permeabilities from Casino-2, derived in the manner as described in Section 3.13.2.

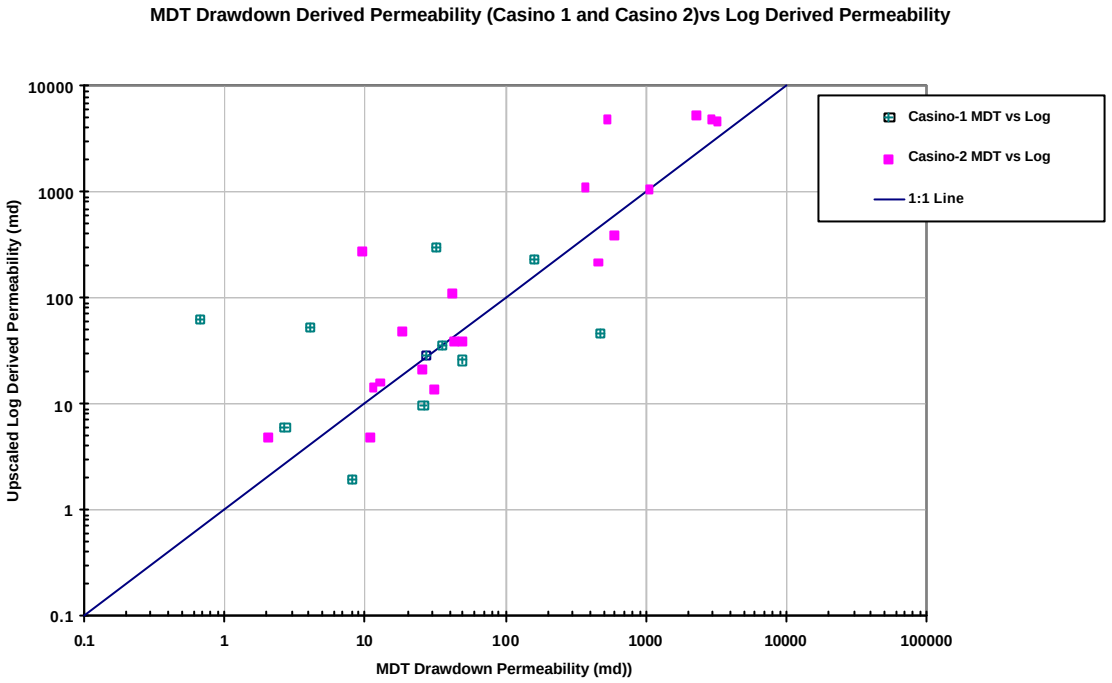

Figure 3.13.3-b: Cross Plot of Casino-1,2 MDT Permeability and Log Derived Model (1m Upscaled)

3.13.4 Casino-3 MSCT Data

Several Mechanical Sidewall Cores (MSCT's) were recovered from the water bearing Waarre A interval in the Casino-3 well. It should be noted that the Waarre A at this location is interpreted to have significantly poorer reservoir quality than the Casino-1 and Casino-2 wells (Table 3.13.4-a) but the limited MSCT data obtained does indicate the presence of permeabilities of up to 18 md in the Casino-3 well (Table 3.13.4-b).

Well	Gross Thickness m	PHIT of Gross Int v/v
UPPER WAARRE A		
Casino-1	18.9	0.158
Casino-2	23.8	0.173
Casino-3	27.6	0.117
LOWER WAARRE A2		
Casino-1	12.1	0.189
Casino-2	10.3	0.217
Casino-3	7.4	0.146
LOWER WAARRE A1		
Casino-1	18.8	0.198
Casino-2	19.9	0.191
Casino-3	13.6	0.139

Table 3.13.4-a: Comparison of Waarre A average porosity from Casino-1, 2 and 3

Formation	Depth mKB	MSCT Perm Klink / Ovb Corrected mD
WaA	2059.2	5.75
WaA	2060.2	18.67
WaA	2060.7	12.42
WaA	2068.2	1.03
WaA	2080.2	0.06
WaA	2091.2	6.58

Table 3.13.4-b: Casino-3 MSCT Data

3.13.5 Validity of MDT Pre-Test Derived Permeability as an Indicator of True Formation Permeability

Section 3.13.4 shows the log based relationship developed for the Waarre A at Casino is a reasonable fit to the MDT derived pre-test permeabilities. However further comfort was required to demonstrate that these MDT derived permeability measurements are a true reflection of intrinsic formation permeability. A literature search found a 3rd Party dataset from a nearby field including extensive core and MDT data which when coupled with similar data from the Casino field, was used to investigate this relationship.

The methodology followed was as follows;

- Overburden corrected core data was depth corrected to tie MDT depths
- All available MDT drawdown mobility data was corrected to permeability using the method described in Section 3.13.2
- A search window of +/- 0.1m was used to find MDT Permeability / Core Permeability pairs within this window.
- A second set of MDT Permeability / Core Permeability pairs was also created with the search window relaxed to +/- 0.3m.

The results of this process, combining the 3rd Party dataset and the Casino data, are shown in Figure 3.13.5-a. This shows a strong correlation between MDT derived permeability and core permeability, however in the permeability range expected for the Waarre A (0.1 – 100 md) the MDT derived permeability appears to overestimate true core derived permeability.

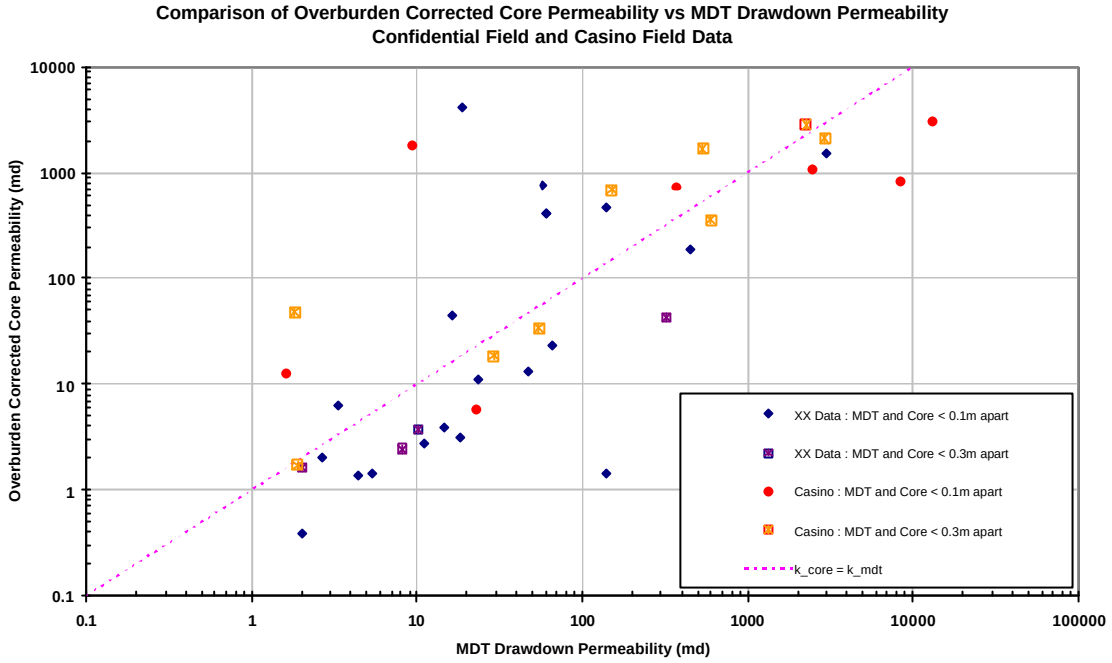

Figure 3.13.5-a: Overburden Corrected Core Permeability and MDT Drawdown Derived Permeability Cross Plot

This dataset has been further analysed by limiting the analysis to data in the range 0.1 to 100 md and removing outlying data (Figure 3.13.5-b).

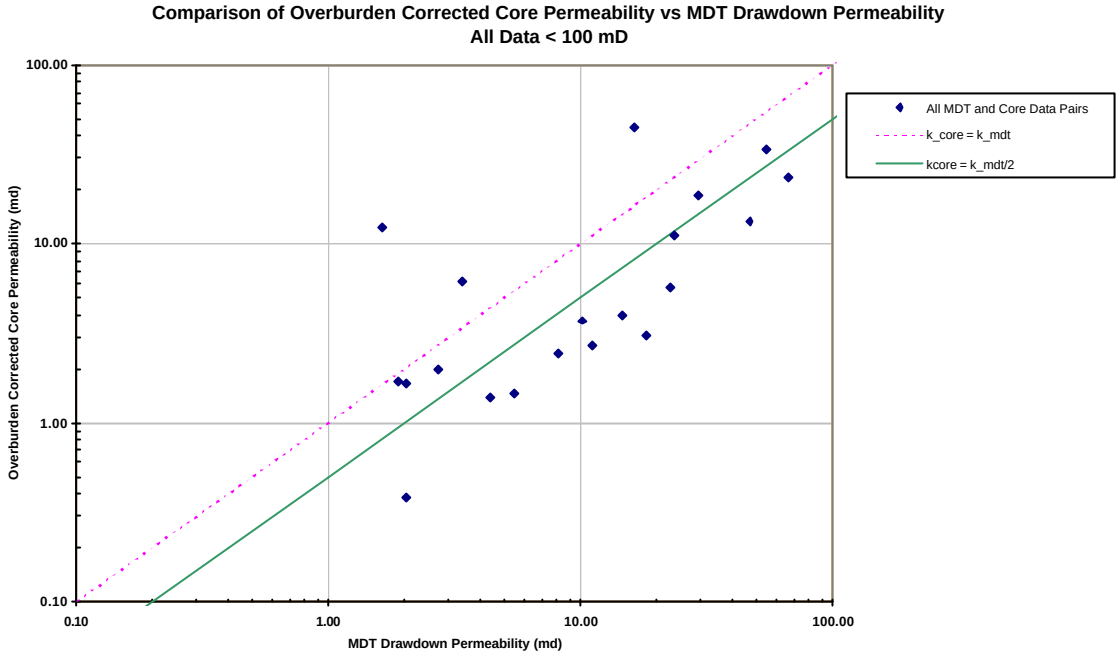

Figure 3.13.5-b: Overburden Corrected Core Permeability and MDT Drawdown Derived Permeability Cross Plot – Filtered Data

A line of best fit has been established with the relationship $k_{core} = 0.5*k_{mdt}$. This indicates that based on this dataset the true formation permeability is about 50% of the permeability indicated from the MDT. Hence, for the Waarre A of Casino the permeability derived using the log based model (which was shown in Section 3.13.3 to be an approximate fit to the MDT derived permeability) has been reduced by 50% to represent the "P50" estimate of Waarre A formation permeability i.e.

- P50 Waarre A Permeability = 0.5 * Log Permeability

3.13.6 Upside and Downside Permeability Model

Downside ("P90") Permeability Model

Significant scatter is evident in the relationship between log derived permeability and MDT permeability (Figure 3.13.3-b). The downside or "P90" permeability model chosen to represent the Waarre A permeability reflects this uncertainty.

The relationship chosen is as follows;

- P90 Waarre A Permeability = 0.125 * Log Permeability
  = 0.25 * P50 Waarre A Permeability

This was chosen as shown in Figure 3.13.6-a. Note that approximately 85% of the data points lie to the right of the line with Log Permeability = 4 times MDT permeability. When combined with the 50% reduction for the MDT perm vs Core Perm used for the "P50" Case this gives a downside permeability reduction factor of 0.125 to be applied to the log derived permeability.

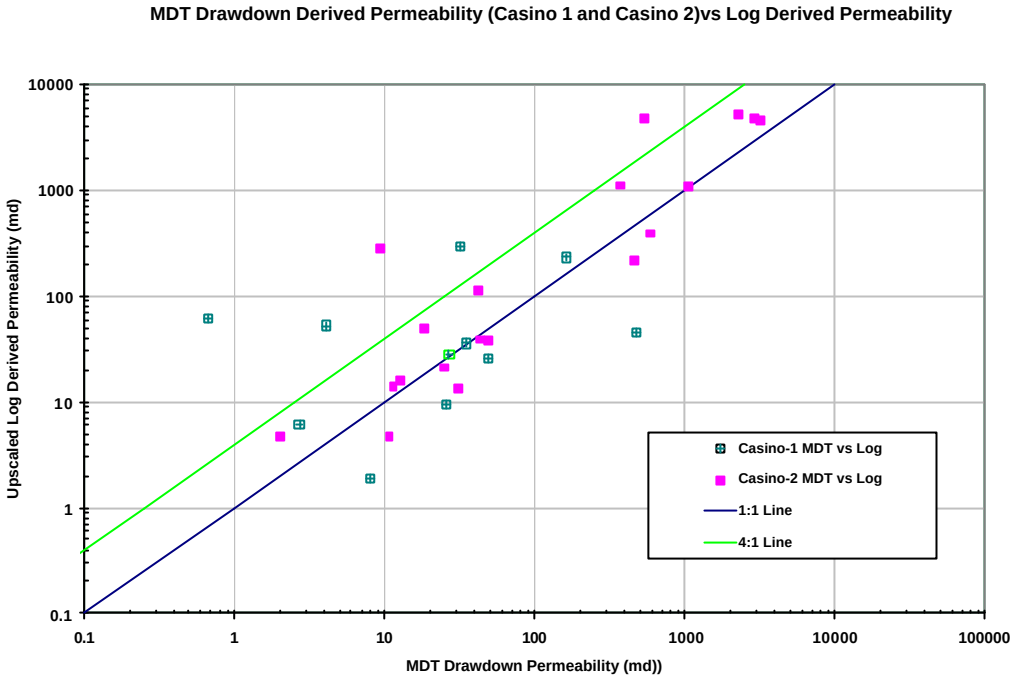

Figure 3.13.6-a: Overburden Corrected Core Permeability and MDT Drawdown Derived Permeability Cross Plot – Filtered Data

Upside ("P10") Permeability Model

The upside Waarre A permeability model has been set with a 5 times increase in permeability relative to the P50 Case;

- P50 Waarre A Permeability = 2.5 * Log Permeability
  = 5 * P50 Waarre A Permeability

This accounts for positive uncertainty in the underlying log permeability versus MDT permeability relationship.

The overall range of permeability modelled for the Waarre A formation is shown in Figure 3.13.6-b using Casino-1 as the reference. Table 3.13.6-a shows the same data expressed as average permeability over the gross reservoir interval for Casino-1.

	Casino-1 Average Permeability (md)		
	P90	**P50**	**P10**
Upper Waarre A	2	8	40
Lower Waarre A	5	21	105

Table 3.13.6-a: Casino-1 Waarre A – Average Permeability

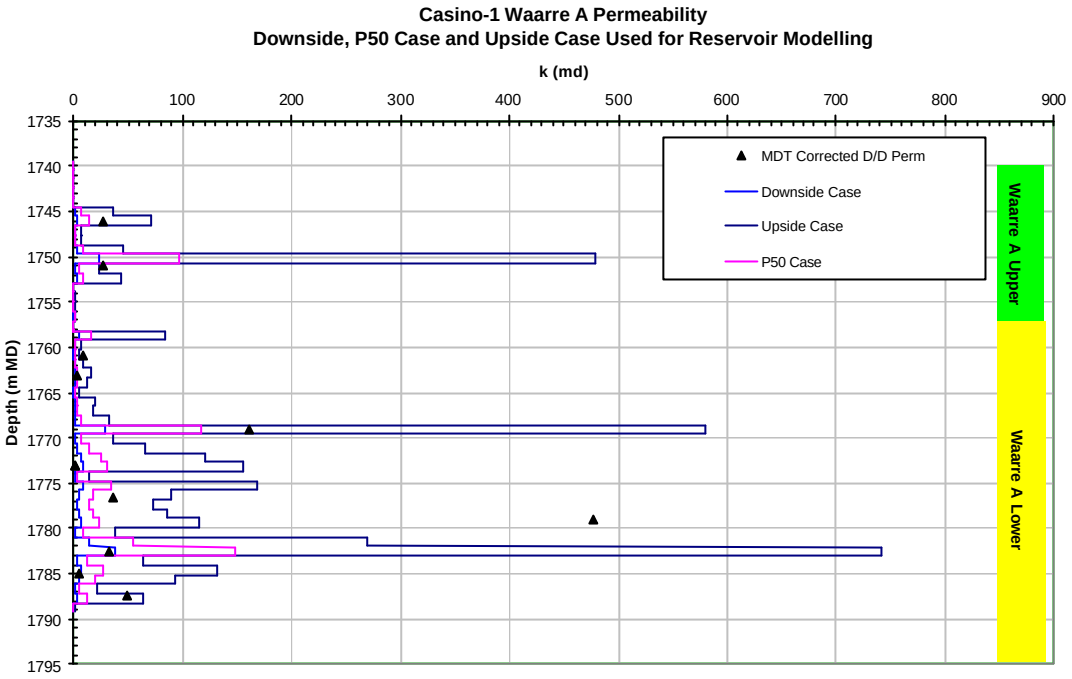

Figure 3.13.6-b: Range of Permeability Outcomes for Waarre A : Casino-1

3.14 Near Field Exploration

3.14.1 Near Field Exploration Potential

Additional exploration potential exists in the eastern part of VIC/P44 adjacent to the Casino field. As shown in Figure 3.14.1-a. most of these prospects lie within the area covered by the Casino 3D seismic survey and include both Waarre A and Waarre C targets.

These prospects are generally too small to justify a standalone development but may be economic exploration targets based on a tie-in to the Casino facilities. Based on this prospectivity, additional pre-investment is being made in the Casino production facilities to allow for up to 6 wells to be connected to the Casino pipeline and produced simultaneously. Also, while the plateau production rate from the Casino field is planned to be 35 PJ/a, the 12" pipeline to be installed as part of the development is capable of throughput rates of up to 50 PJ/a subject to available markets.

The first of these Casino near field exploration prospects to be drilled will be Martha, located approximately 18km north of Casino on the northern edge of the greater Pecten High. The well, scheduled to be drilled in the fourth quarter of 2004 will target the Waarre formation. The Martha structure is a tilted fault block with 3 way dip closure and updip fault closure and forms the highest point on the greater Pecten High.

Several prospects are mapped within the area of the proposed Casino Production License. Block 2432 includes the Children-Elanora complex and the Hercules B Prospect. These features form the southern-most part of the Greater Pecten High Trend. Seismic interpretation indicates truncation of the Waarre reservoir targets is occurring locally by the regionally important K85 Unconformity, thereby diminishing the prospectivity of both the Children-Elanora complex and Hercules B prospect despite their proximity to Casino.

The easternmost block 2434 also includes the Juliet Prospect. This has a thick and well-preserved section of Flaxman Formation through to Waarre C and A, being adjacent to the Shipwreck Trough and not subject to erosional truncation by the K85 Unconformity. The structure is, however, small in area and is on the edge of the Casino 3D seismic survey. It is a possible candidate for a future tie-back into Casino, being likely to produce at high flow rates but with a relatively small total resource.

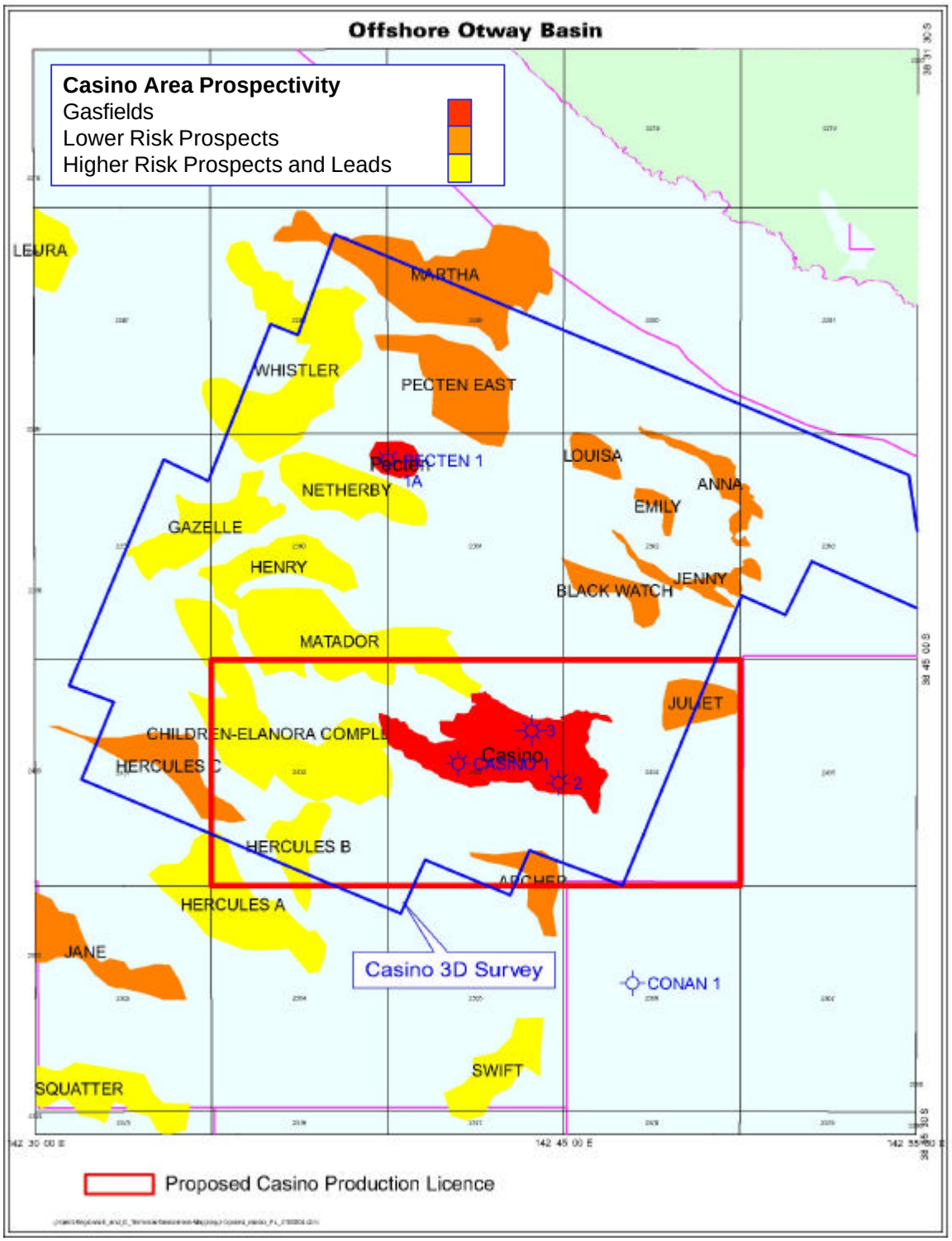

Figure 3.14.1-a: Casino Area Prospectivity

3.15 References & Enclosures

3.15.1 References

3.2 Introduction

Bock, P.E. & Glenie R.C. 1965. Late Cretaceous and Tertiary depositional cycles in south-western Victoria, Proceedings Royal Society of Victoria, 79 (1), 153-163.

Buffin, A.J. 1989. Waarre Sandstone development within the Port Campbell Embayment, The APPEA Journal, 29 (1), 299-311.

Lemon, N. 2003. Casino-3 Core Logging Report (unpublished).

Partridge, A.D. 1999. Late Cretaceous to Tertiary geological evolution of the Gippsland Basin, Victoria. Latrobe University PhD Thesis (unpublished).

Partridge, A.D. 2001. Revised stratigraphy of the Sherbrook Group, Otway Basin. PESA Eastern Australian Basins Symposium, p455-465.

Phillips S.E. 2003. Petrology Report, Casino-1 & 2, Otway Basin (VIC P/44), unpublished.

Phillips S.E. 2004. Petrology Report, Casino-3, Otway Basin (VIC P/44), unpublished.

3.6 Petrophysics

Boyle, K, Internal Santos Report

N. Lemon, 2004. Personal Communication

Nieto, J.A., Yale, D.P. and Evans, R.J. (1994). Improved Methods for Correcting Core Porosity to Reservoir Conditions. The Log Analyst, May-June, pp 21-30.

Phillips, S.E, 2003. Petrology report, Casino-3. Otway Basin (Vic/P44)

Phillips, S.E, 2003. Petrology report, Casino-1 & Casino-2. Otway Basin (Vic/P44). Nieto, J.A., Yale, D.P. and Evans, R.J. (1994). Improved Methods for Correcting Core Porosity to Reservoir Conditions. The Log Analyst, May-June, pp 21-30

3.8 Fluid Contacts

Brown, A. 2003, Improved Interpretation of Wireline Pressure Data. AAPG Bulletin, v. 87, No. 2, p. 295-311.

Economides, MJ. Daniel Hill, A & Ehlig-Economides, C. 1994, Petroleum Production Systems. Prentice Hall Petroleum Engineering Series, p. 285-288.

3.15.2 Enclosures

Enclosure 3.3.3 a	Top Waarre C Low Impedance Depth Map
Enclosure 3.3.3 b	Top Waarre C Main Pay Depth Map
Enclosure 3.3.3 c	Base Waarre Ca2 Depth Map
Enclosure 3.3.3 d	Top Lower Waarre A Depth Map
Enclosure 3.3.3 e	Base Waarre A Depth Map
Enclosure 3.6.4 a	Casino-1 Petrophysical Analysis
Enclosure 3.6.4 b	Casino-2 Petrophysical Analysis
Enclosure 3.6.4 c	Casino-3 Petrophysical Analysis
Enclosure 3.12.3 a	Casino Petrel Model Summary GRV, NPV and OGIP Data

4 Reservoir Development

4.1 Development Concept Overview

4.1.1 Concept Basis

The basic premise for the Casino development is to deliver gas to the customer in accordance with the Term Sheet executed in August 2003. A feature of the Term Sheet is that it allows for Casino gas to be delivered to and processed by the existing TXU Iona Gas Storage.

The development concept chosen for Casino is described in Section 6.

4.1.2 Subsurface Planning Basis

Required Raw Gas Production Rates

The Term Sheet executed with the customer allows for flexibility in the annual volumes delivered between a Minimum ACQ and a Maximum ACQ as set out in Table 4.1.2-a below.

Contract Year	Minimum ACQ PJ	Maximum ACQ PJ
2006	23	35
2007	23	35
2008	23	35
2009	22	31.4
2010	19	27.5
2011	16	24.3
2012	14	21.8
2013	12	19.7
2014	11	18.0
2015	9	16.6
2016	8	14.2
2017	8	14.5
Total	**188**	**293**

Table 4.1.2-a: Term Sheet Gas Sales Requirements

Figure 4.1.2-b shows a simplified flowchart used to illustrate the raw gas requirements in order to meet the Term Sheet volumes shown in Table 4.1.2-a. It should be noted that according to the Term Sheet the Contract Quantities include a requirement for 4% fuel and the actual sales volumes are net of this amount. Based on this model, 1 Bcf of raw Casino gas yields 1.02 PJ of net sales gas.

Based on this model, Table 4.1.2-b shows the annual rates required over the life of the Term Sheet to meet the Maximum ACQ. Note that these rates do not allow for any downtime. The Term Sheet allows for 21 days downtime per year for the upstream facilities and does not allow for any make up of under deliveries associated with downtime. If this is included the average daily rate over the calendar year is shown in Table 4.1.2-c.

The final approach taken to modelling reservoir production has been to set the simulation models to produce the annual volumes shown in Table 4.1.2-c (i.e. including downtime) but to ensure that on any day the field can produce the daily rates shown Table 4.1.2-b.

Figure 4.1.2-b summarises the annual average daily raw production profile used for reservoir modelling.

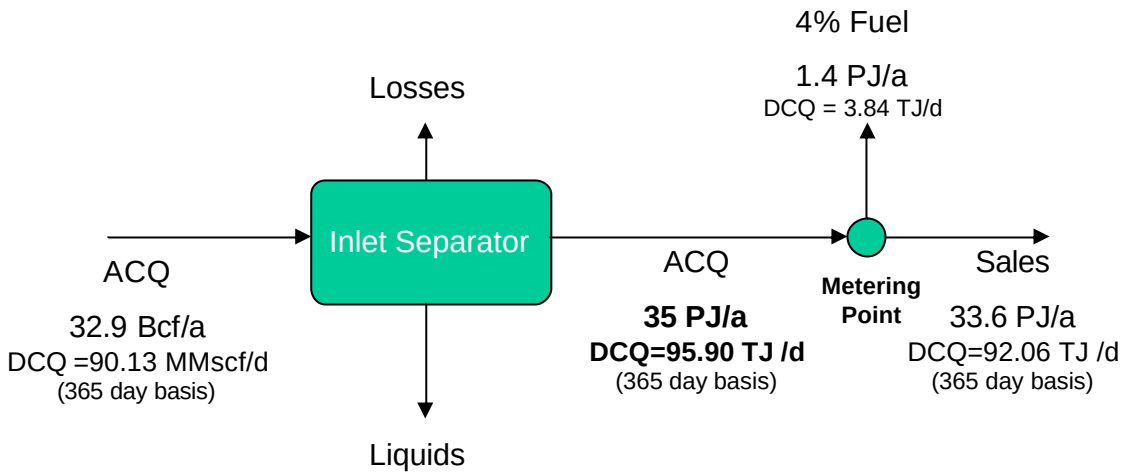

Figure 4.1.2-a: Simplified Casino Process Model

	Raw Gas	Total Gas	Fuel Gas	Sales Gas	Raw Gas	Total Gas	Fuel Gas	Sales Gas
	Bcf	PJ	PJ	PJ	MMscf/d	TJ/d	TJ/d	TJ/d
Feb 2006	32.90	35.0	1.40	33.60	90.14	95.89	3.84	92.05
Jan 2007	32.90	35.0	1.40	33.60	90.14	95.89	3.84	92.05
Jan 2008	32.90	35.0	1.40	33.60	90.14	95.89	3.84	92.05
Jan 2009	29.52	31.4	1.26	30.14	80.87	86.03	3.44	82.59
Jan 2010	25.85	27.5	1.10	26.40	70.82	75.34	3.01	72.33
Jan 2011	22.84	24.3	0.97	23.33	62.58	66.58	2.66	63.91
Jan 2012	20.49	21.8	0.87	20.93	56.14	59.73	2.39	57.34
Jan 2013	18.52	19.7	0.79	18.91	50.74	53.97	2.16	51.81
Jan 2014	16.92	18.0	0.72	17.28	46.36	49.32	1.97	47.34
Jan 2015	15.60	16.6	0.66	15.94	42.75	45.48	1.82	43.66
Jan 2016	13.35	14.2	0.57	13.63	36.57	38.90	1.56	37.35
Jan 2017	13.63	14.5	0.58	13.92	37.34	39.73	1.59	38.14

Table 4.1.2-b: Term Sheet Production Requirements and Sales Volumes – No Downtime

	Raw Gas	Total Gas	Fuel Gas	Sales Gas	Annual Average Rates			
					Raw Gas	Total Gas	Fuel Gas	Sales Gas
	Bcf	PJ	PJ	PJ	MMscf/d	TJ/d	TJ/d	TJ/d
Feb 2006	31.01	32.99	1.32	31.67	84.95	90.37	3.61	86.76
Jan 2007	31.01	32.99	1.32	31.67	84.95	90.37	3.61	86.76
Jan 2008	31.01	32.99	1.32	31.67	84.95	90.37	3.61	86.76
Jan 2009	27.82	29.59	1.18	28.41	76.22	81.08	3.24	77.83
Jan 2010	24.36	25.92	1.04	24.88	66.75	71.01	2.84	68.17
Jan 2011	21.53	22.90	0.92	21.99	58.98	62.74	2.51	60.24
Jan 2012	19.31	20.55	0.82	19.72	52.91	56.29	2.25	54.04
Jan 2013	17.45	18.57	0.74	17.82	47.82	50.87	2.03	48.83
Jan 2014	15.95	16.96	0.68	16.29	43.69	46.48	1.86	44.62
Jan 2015	14.71	15.64	0.63	15.02	40.29	42.86	1.71	41.15
Jan 2016	12.58	13.38	0.54	12.85	34.47	36.67	1.47	35.20
Jan 2017	12.85	13.67	0.55	13.12	35.19	37.44	1.50	35.94

Table 4.1.2-c: Term Sheet Production Requirements and Sales Volumes – Including 21 Days Downtime Per Year

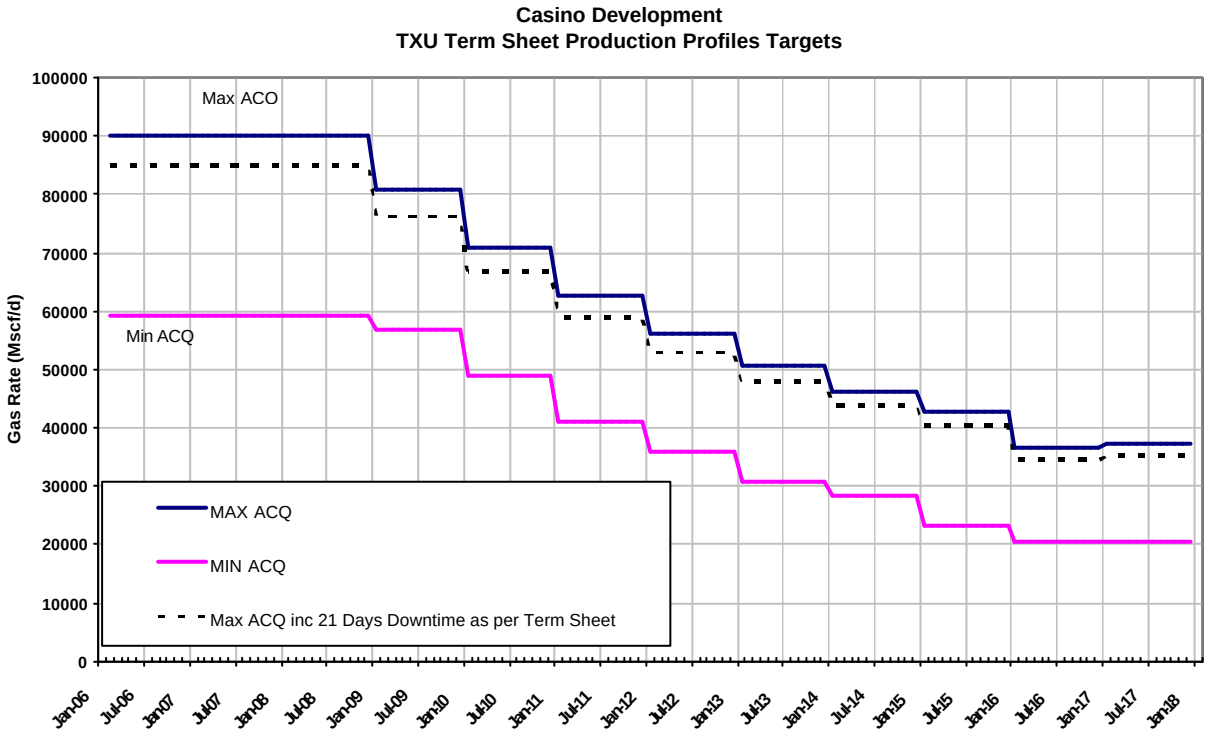

Figure 4.1.2-b: Casino Term Sheet Gas Requirements – Raw Gas Ex Field

Raw Gas Delivery Pressure

The Term Sheet gas sales arrangements for Casino sets out the required delivery pressure at the Iona plant as 9000 kPa, but also allow for the implementation of a low pressure delivery service where the customer provides for a compression service to allow the delivery pressure to be reduced to 3000 kPa.

These requirements have been honoured in dynamic simulation studies of the Casino field by the use of a production network model where the required discharge pressure is specified explicitly.

4.1.3 Development Well Location Options

This section summarises the development well location options considered as part of the Casino development planning process, the basis for the choice of these locations and the final locations selected and evaluated. Note that due to the layout of the field there is no location where the Waarre A and Waarre C reservoirs can be drained by a common surface location hence no options were considered with sequential production of the two reservoirs from a single wellbore.

Waarre C Well Locations

Three potential Waarre C well locations designated Prod X, Prod Y and Prod Z have been considered during development planning work. Based on the observed reservoir quality from the Waarre C in Casino-1 and Casino-2 a vertical completion is expected to result in sufficient productivity. Hence all these candidate wells are considered as vertical wells only.

The locations of these wells are shown on a structure map of the Top Waarre C Main Pay horizon in Figure 4.1.3-a. A larger scale map showing these well locations can be found in Enclosure 3.3.3-b. A summary of well locations and predicted formation tops can be found in Table 4.1.3-a.

The first comment which must be made regarding Waarre C well location options is that the number of realistic alternatives available are quite limited. The expected moderate to strong water drive requires a well location as near to the structural crest as possible and with this consideration the Prod X Location stands out as the prime Waarre C development well location. The well is located as high as possible on the structure and is effectively a twin well to Casino-2 (which was plugged and abandoned) so little uncertainty regarding reservoir quality is expected.

Figure 4.1.3-b shows cross sections through the Prod X location from both a layer based Petrel model and a AI based Petrel model. Note the predicted intersection of the Top Waarre C main pay horizon at -1727m SS, leaving minimal attic volume to the structural crest for the reservoir at -1695m SS. This location could be moved slightly updip but this would result in reduced reservoir thickness. At this location there is 241m of vertical relief from the base of the main Waarre C gas reservoir (i.e. Top Ca1) to the Free Water Level at -1999m SS.

All development scenarios envisaged for the Casino field include a development well at the Prod X location.

Two secondary Waarre C development well locations have also been considered. The location designated Prod Y is approximately 3.5 km northwest of Prod X and located on a small structural high in the west of the field. Figure 4.1.3-c shows two cross sections through the location. The well is approximately 90m downdip from Prod X but still has 147m of vertical relief from the base of the main Waarre C gas reservoir (i.e. Top Ca1) to the Free Water Level at -1999m SS. The rationale for this choice of location is twofold. Firstly, the location will provide initially for full redundancy of gas supply to meet the contracted gas supply in the event of a failure of the prime Waarre C development well located at the Prod X location. Because of its structural location this well will water out much earlier than Prod X, but up until this occurs it could provide significant security of supply benefits. The second rationale for this location is to mitigate against poor areal sweep of the Waarre C reservoir and potential early water breakthrough on Prod X.

This location has been used in development planning as the second Waarre C development well location, if required.

The Prod Z location, approximately 1 km to the northeast of Prod X, has also been considered as a potential Waarre C development well location. This was selected as a potential location to intersect the Upper Waarre Cb reservoir sands (absent at Prod X but intersected downdip at Casino-3 and evident from the seismic inversion volumes) and a much thicker section of the Main Waarre C pay interval. Drilling at this location would guarantee recovery from the Upper Waarre Cb reservoir and move this gas from the 2P to the 1P reserve category.

This location has not been pursued as a potential second Waarre C well location as initial screening of this location showed it to be much more susceptible to earlier water arrival than the Prod Y location. Close inspection of the impedance volume suggests that the Upper Waarre Cb sands targeted by this location merge into the main Waarre C reservoir and that that these reserves will probably be drained by the crestal well Prod X thus making this well redundant.

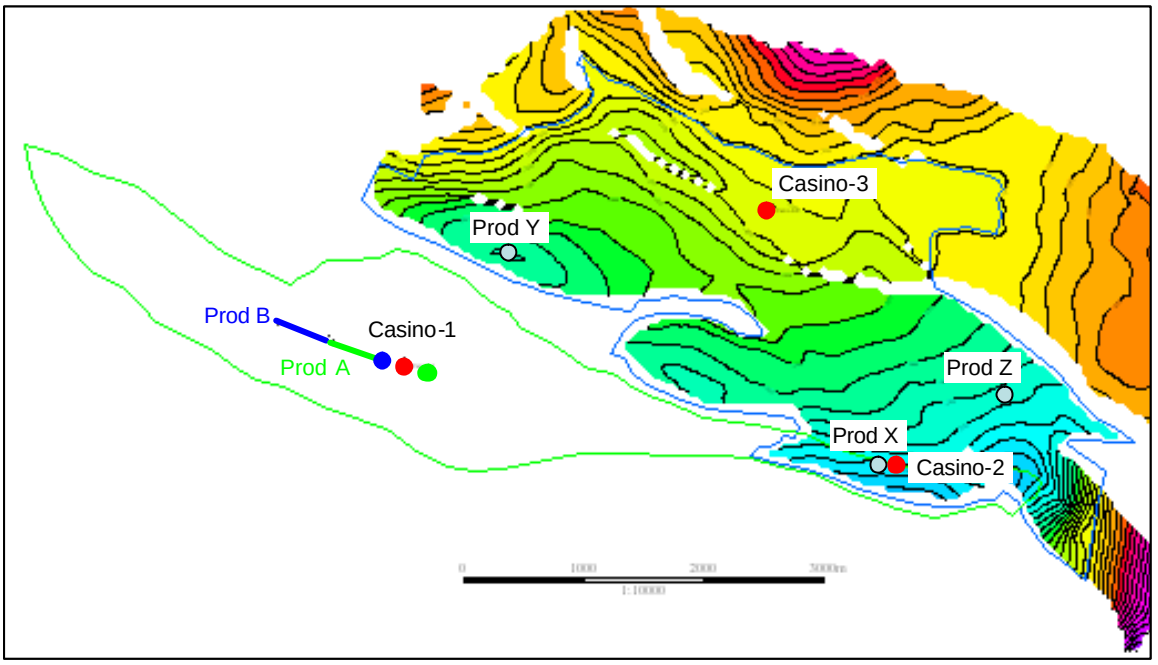

Figure 4.1.3-a: Top Waarre C Main Pay Showing Waarre C Well Locations

	X Coord	Y Coord	Top Waarre C	Top Cb Main Pay	Top Ca1
	m	m	m SS	m SS	m SS
Prod X	651603.0	5704471.0	-1722	-1727	-1758
Prod Y	648553.0	5706260.0	-1809	-1813	-1852
Prod Z	652662.0	5705065.0	-1765	-1781	-1847

Table 4.1.3-a: Waarre C Well Locations

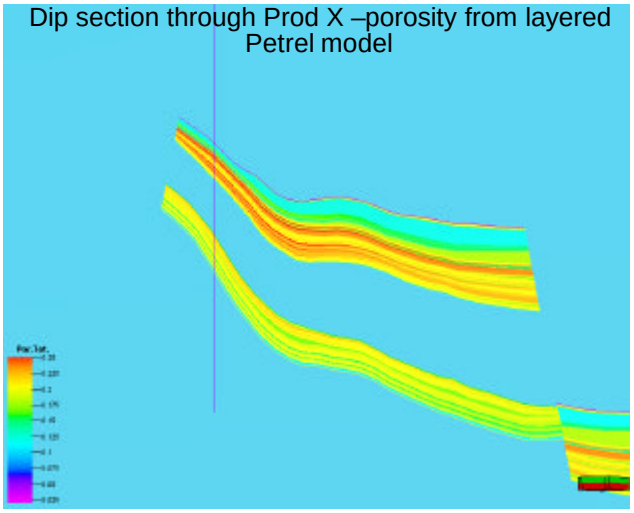

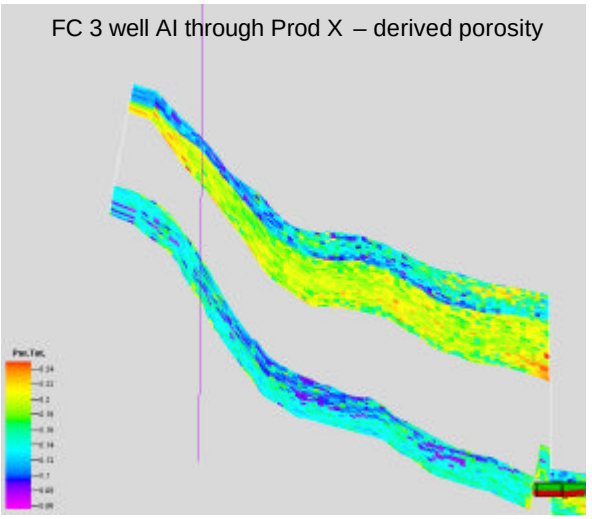

Figure 4.1.3-b: Cross Sections Through Prod X Location

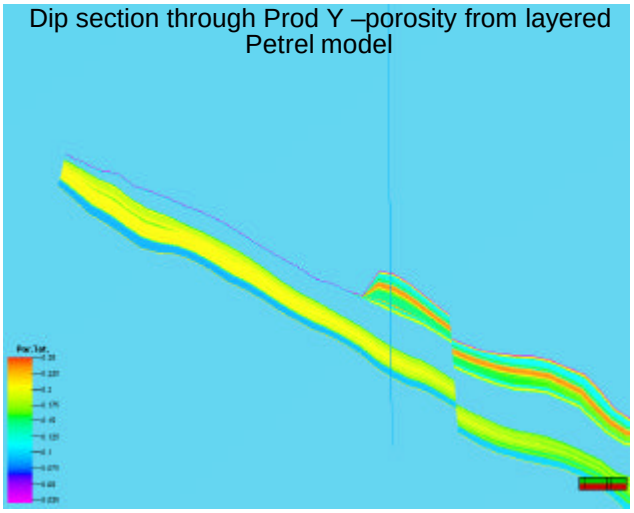

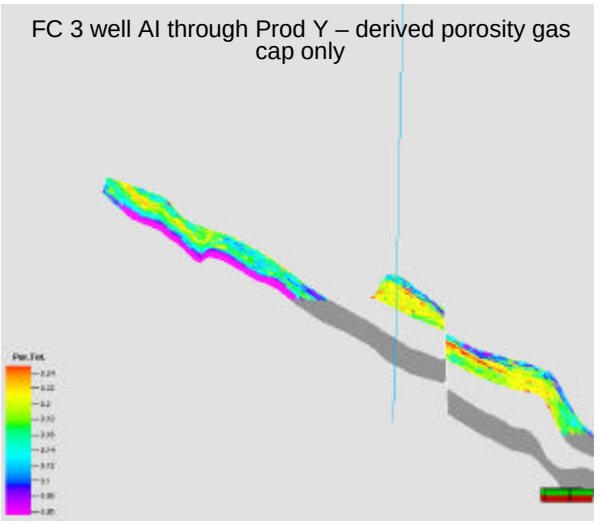

Figure 4.1.3-c: Cross Sections Through Prod Y Location

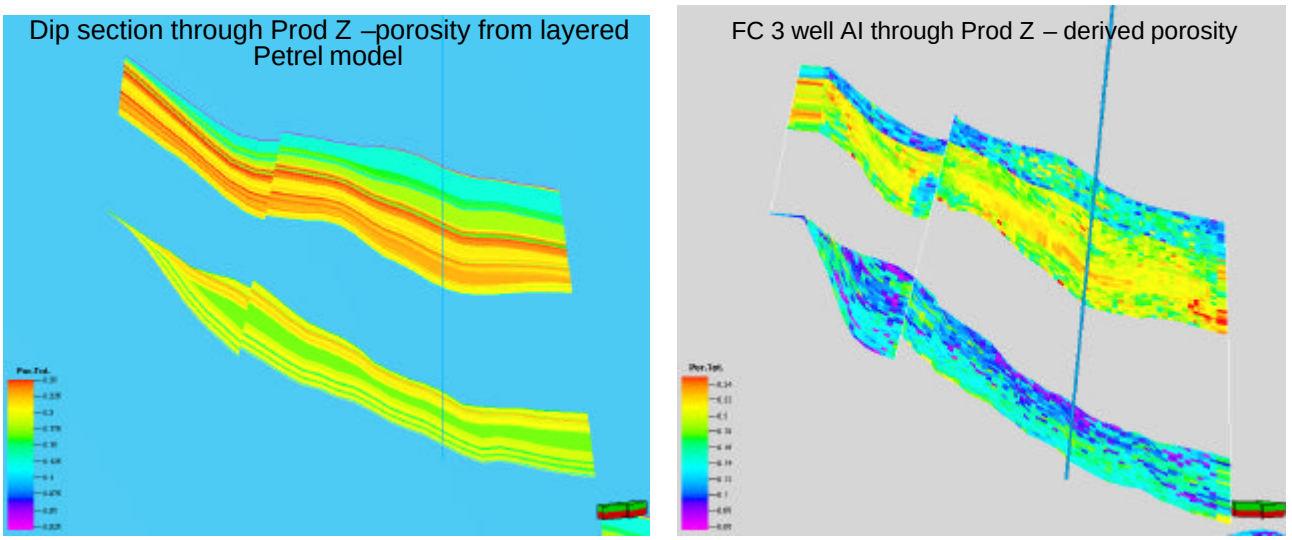

Figure 4.1.3-d: Cross Sections Through Prod Z Location

Waarre A Well Locations

Initially a single Waarre A well location designated Prod A was considered during development planning work. This was chosen as a high angle well with approximately 400m of reservoir penetration through the Waarre A formation based on a well productivity study described in Section 4.2.6. The Prod A location was chosen such that the heel of the high angle well is close to well control and less than 200m from Casino-1 with the toe located further updip. It was decided to locate the well in this orientation as the intersection of the higher permeability Lower Waarre A reservoir will be as far updip as possible.

Near the end of the development planning process, the consideration of a possible Waarre A pilot was introduced. The pilot hole would be drilled to allow a core to be cut over the Waarre A reservoir to reduce the considerable uncertainty that presently exists regarding the potential productivity of this well. This information would be used to make the final decision on whether to complete the Waarre A and to finalise the development well design. With the introduction of a pilot hole, the possibility of moving the Waarre A development well further updip and away from Casino-1 well control has been considered. The location designated Prod B shows a potential updip development well location.

The locations of these wells are shown on a structure map of the Top Lower Waarre A horizon in Figure 4.1.3-e. A larger scale map showing these well locations can be found in Enclosure 3.3.3-d. A summary of well locations and predicted formation tops can be found in Table 4.1.3-b. Figure 4.1.3-f shows a strike section through both a layer based Petrel model and a AI based Petrel model. The location of these wells is also shown in Figure 4.1.3-g on a map of the original band limited impedance volume for the Waarre A.

While the Prod A location was used for development planning purposes a final decision on the location of a possible pilot hole and development well has yet to be made.

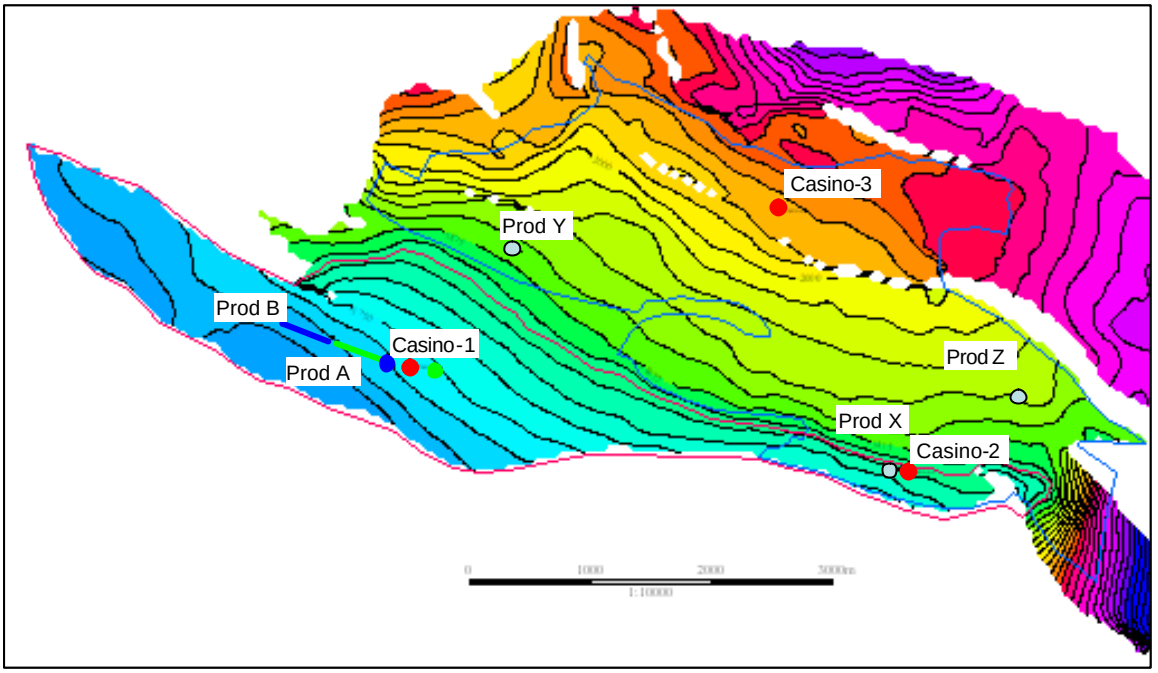

Figure 4.1.3-e: Top Lower Waarre A Showing Waarre A Well Locations

	X Coord	Y Coord	Top Upper Waarre A	Top Lower Waarre A2	Base Lower Waarre A1
	m	m	m SS	m SS	m SS
Prod A Surface Location / Pilot*	647842.0	5705235.0	-1722	-1742	-1774
Prod A Heel	647471.3	5705364.8		-1722	
Prod A Toe	647082.3	5705502.4			-1729.5
Prod B Surface Location / Pilot*	647466.2	5705375.9	-1707	-1722	-1755
Prod B Heel	647012.7	5705529.7		-1698.5	
Prod B Toe	646624.0	5705667.0			-1712

* Estimate Only based on 400m offset from heel

Table 4.1.3-b: Waarre A Well Locations

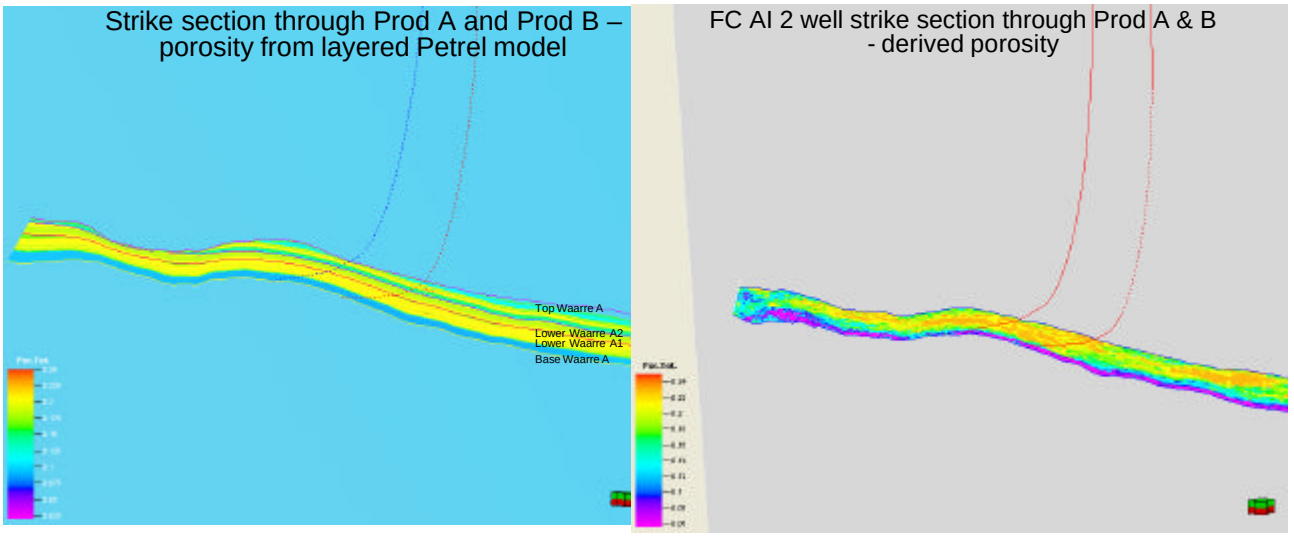

Figure 4.1.3-f: Cross Sections Through Prod A and Prod B Locations

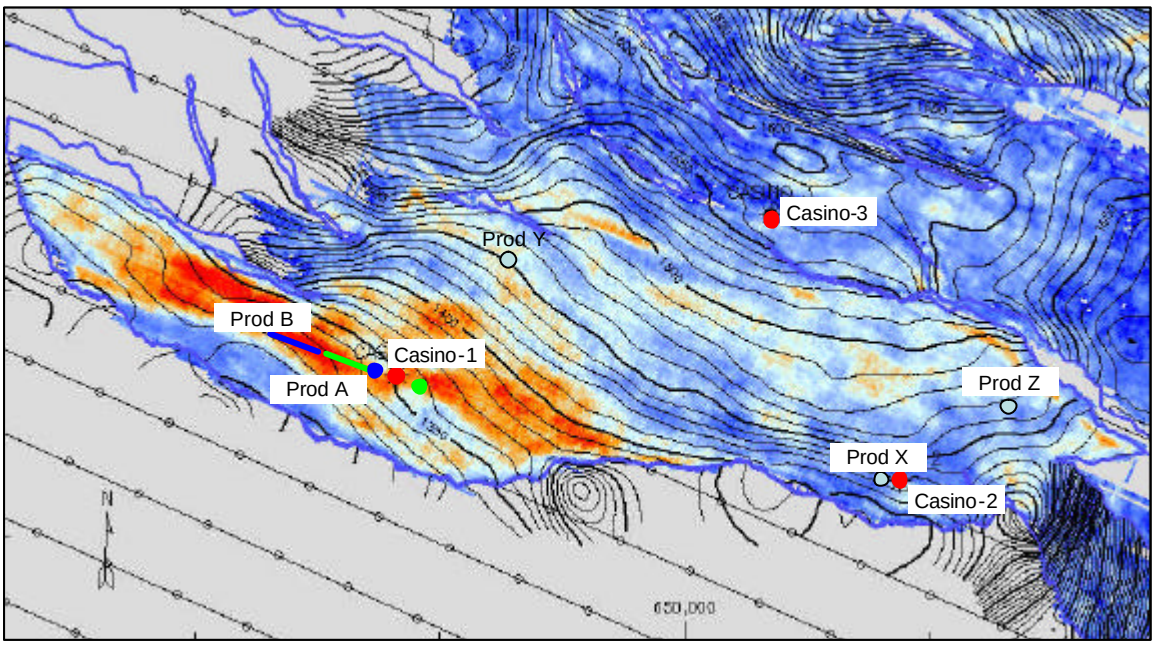

Figure 4.1.3-g: Average RMS CI impedance between Top Lower Waarre A and Base Waarre A interval. Showing Waarre A Development Well Locations

4.1.4 Development Planning Summary

For the evaluation of field reserves described in Section 4.2 and 4.3 a fixed development scenario has been chosen and used for all dynamic simulation work. This is referred to as the Base Case development (Figure 4.1.4-a) and is a 2 well development with Prod X and Prod A drilled and completed at the start of the field life. The target production profile is as per the Term Sheet maximum ACQ with 21 days per year downtime as described in Table 4.1.2-c and shown in Figure 4.1.2-b. For simplicity, field discharge pressure is set initially to the minimum delivery pressure of 3000 kPa assuming that this low pressure delivery service is assumed to be available when required to maintain offtake rate at the Maximum ACQ.

For the field development planning work described in Section 4.4 alternative development scenarios have been investigated and the following issues have been addressed;

- Timing requirements for implementation of low pressure delivery service (i.e. discharge pressure < 9000 kPa)
- Security of supply and well redundancy
- Impact of offtake at an extended plateau of 35 PJ/a

4.2 Dynamic Reservoir Modelling

4.2.1 Work Flow

The black oil simulator, ECLIPSE 100 was used for all dynamic simulation work for the definition phase of the project. The work flow of the dynamic modelling effort is captured in Section 3.1. This section discusses the simulation effort for Phase 3. The previous phases of simulation work were superseded by Phase 3 and consequently were not used for reserve estimation and development planning work that is presented in this report. The Phase 3 study can be broken down into four sequential stages;

I. Model construction; incorporated the results of the static modelling effort, Casino SCAL programme, PVT studies, aquifer modelling and production network modelling.
II. Recovery factor sensitivity stage; identified the major reservoir uncertainties which impact on Waarre C and Waarre A recovery efficiencies.
III. "Scenario Tree" stage; formed the basis of the reserve estimates for the Waarre C and Waarre A. From this work models were selected which represented the P90, P50 and P10 ultimate recovery outcomes.
IV. "Development Optimisation" stage; investigated the various development options with the P90, P50 and P10 models. Results from this stage formed the basis of the field sub-surface development plan.

The following sections discuss stage i. model construction and stage ii. recovery factor sensitivity study. The reader is referred to Sections 4.3 and 4.4 for a discussion of stages iii. and iv.

4.2.2 Dynamic Model Construction – Grid Design and Static Reservoir Properties

The reservoir simulation grid and associated static reservoir properties have been constructed in the geological modelling package, Petrel. The static properties (porosity and permeability) were populated within the grid at a 'geological' scale and upscaled for use within the simulator. The reader is referred to Sections 3.10 and 3.11 for a detailed discussion of the geological modelling effort.

The upscaled grid is an irregular cartesian grid with corner point geometry. The grid cells are approximately rectangular. The grid columns are roughly parallel (E-W) to the pinch out edge of the Waarre C and the major faults of the model. The orientation of this grid permits robust modelling of fluid flow within the vicinity of the major geological features. Cell size and layering for the simulation models is presented in Section 3.10.7.

Figure 4.2.2-a illustrates the simulation grid geometry with porosity as the displayed property.

Corner point geometry allows cells to have non-rectangular shapes, which is necessary to model pinchouts and erosional surfaces within the field. The PINCH keyword was used to generate connections across these features. In the interest of avoiding throughput-related convergence problems, cells within the simulation grid with a pore volume less than 4000 rbbls were deactivated with the MINPV keyword. These deactivated cells represented approximately 1% of the pore volume of the entire model.

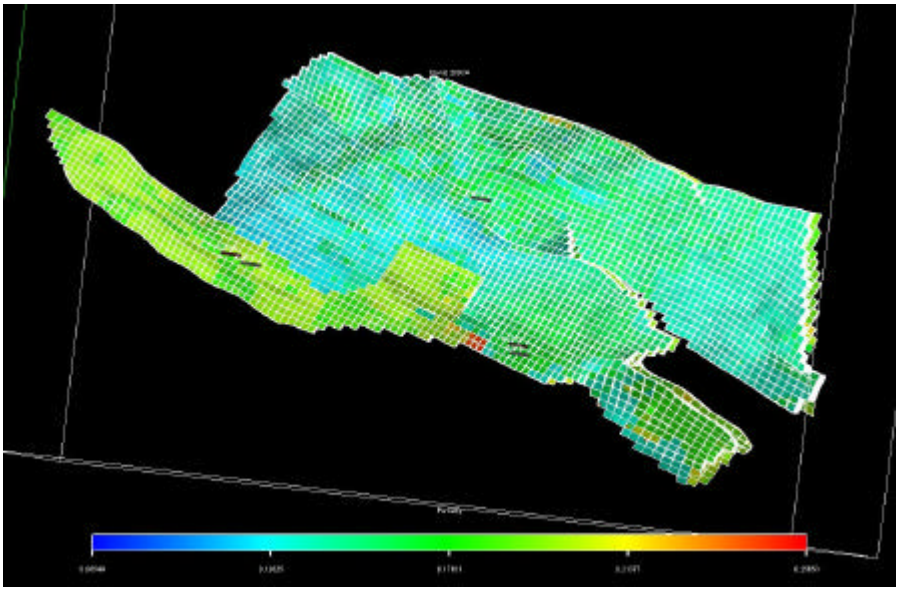

Figure 4.2.2-a: Simulation grid with porosity as the displayed property.

4.2.3 Dynamic Model Construction – Model Initialisation

Initialisation refers to defining the initial conditions of the simulation i.e. the pressures and phase saturation at the start date of the simulation. The method selected to initialise the model was equilibration. Equilibration is the procedure of defining the initial saturation of each phase and initial hydrostatic pressure gradients based on fluid contacts and pressures at a known depth. ECLIPSE assumes that the pressures and saturations are in equilibrium. For this reason, equilibration is appropriate for initialising a simulation prior to production or injection and therefore the appropriate method to model the Casino reservoirs.

The following sections describe key inputs into model initialisation and methods used to determine them.

Initial Reservoir Pressure & Fluid Limits

The reader is referred to Section 3.8 for a detailed discussion of the fluid limits and initial reservoir pressures for the Waarre C and A reservoirs within the Casino Field. As the Waarre C and Waarre A reservoirs are isolated with separate FWLs, equilibration regions were created for each reservoir. Table 4.2.3-a summarises the inputs for each equilibration region.

Reservoir	Equilibration Region	Initial Reservoir Pressure (psia)	Gas-Water Contact (ft SS)	Datum Depth (ft SS)
Waarre C	1	2873	6558.4	6558.4
Waarre A	2	2828	6033.4	6033.4

Table 4.2.3-a: Summary of inputs for each Equilibration Region.

Fluid Properties

The Waarre A and C reservoirs comprise a sweet gas with very similar composition. A constant mass study was conducted on a reservoir fluid sample collected from the Waarre A in Casino-1. No dew point was encountered at reservoir temperature indicating the reservoir fluid is a dry gas.

The numerical simulation of the Casino reservoirs is a two-phase problem (water-gas), therefore only dry gas PVT tables were generated. The tables were generated using Petroleum Experts' PROSPER modelling package. Black Oil correlations for Viscosity, Gas Formation Volume Factor (Bg) and Deviation Factor (Z) were matched to the constant mass experiment. The matched correlations were used to generate PVT tables for the expected range in reservoir pressure.

No reliable formation water samples have been obtained from the Casino field. Water PVT properties have been generated using the apparent formation water salinity which was determined from the petrophysical analysis.

The reader is referred to Section 3.9 for a detailed discussion of the fluid properties of the Casino reservoirs.

Saturation Function Tables

A saturation function is a table of relative permeability and capillary pressure versus saturation. A function was created for all phases (gas and water) within the model.

The saturation function within the simulation model has several purposes:

- To specify capillary pressures so that initial saturation of each phase (gas & water) can be calculated.
- To specify residual gas saturation (Sgr) where gas-water displacement occurs.
- To provide the relative permeability data required to calculate fluid mobility and to solve the flow equations between cells and from cell to well and vice versa.

Saturation tables were developed for 24 permeability regions within the simulation grid. Each permeability region was represented by a SATNUM region. The permeability range for each SATNUM region is summarised in Table 4.2.3-b.

Waarre C			Waarre A		
Satnum	**Perm Min**	**Perm Max**	**Satnum**	**Perm Min**	**Perm Max**
1	>=0	<=0.05	14	>=0	<=0.05
2	>0.05	<=0.1	15	>0.05	<=0.1
3	>0.1	<=0.5	16	>0.1	<=0.5
4	k>0.5	<=1	17	k>0.5	<=1
5	>1	<=5	18	>1	<=5
6	>5	<=10	19	>5	<=10
7	>10	<=50	20	>10	<=50
8	>50	<=100	21	>50	<=100
9	>100	<=500	22	>100	<=500
10	>500	<=1000	23	>500	<=1000
11	>1000	<=5000	24	>1000	<=5000
12	>5000	<=10000			
13	>10000				

Table 4.2.3-b: SATNUM regions and respective permeability range.

The following sections detail the inputs into the saturation tables; initial phase saturation, residual phase saturation and relative permeability behaviour of each phase.

Initial Phase Saturation

The initial phase saturations are taken from saturation endpoints defined within saturation function tables. In the transition zone the phase saturation is governed by capillary pressure. The definition of capillary pressure is;

$Pc = Pw - Pg$

Pc = Capillary Pressure.
Pw = Pressure of the water phase.
Pg = Pressure of the gas phase.

which can be readily calculated at any depth as the difference between the hydrostatic pressures of the phases (i.e. gas and water). ECLIPSE uses look-up tables which comprise capillary pressure curves to determine the transition zone water and gas saturations.

The initial phase saturations, including the look-up tables of Pc versus Sw and Pc versus Sg were determined from the saturation height functions. The methodology for determining the saturation-height functions is detailed in Section 3.7.

Relative Permeability and Residual Gas Saturation

Producing gas fields in the Otway Basin have demonstrated that there is a high likelihood of significant aquifer influx within the gas reservoirs of the Waarre C Sandstones. Simple pressure depletion of gas reservoirs poses little problem in determining recovery efficiencies for a gas reservoir, however ultimate recovery is more difficult to predict if there is significant aquifer ingress into the reservoir. Two parameters which have a significant impact on overall recovery factor for water drive reservoirs is the mobilisation efficiency (Em) and displacement efficiency (Ed). Mobilisation efficiency is the maximum possible gas recovery for a fraction of the initial gas-in-place and is defined as;

Em = (Sgi – Sgr) / Sgi

where Sgi (=1-Swi) is the initial gas saturation, Swi is the irreducible water saturation and Sgr is the true residual gas saturation (refer to definition below).

Displacement efficiency is the fraction of moveable gas displaced from the swept zone;

Ed = (Sgi – Sg) / (Sgi-Sgr)

where Sg is the remaining gas saturation in the swept zone (refer to definition below).

The most important factors influencing Ed and Em is true residual gas saturation, end-point relative permeabilities of each phase and the shape of the relative permeability curves. Consequently, one of the main objectives of the Casino SCAL programmes was to determine these parameters.

Published literature on residual gas saturation is somewhat confusing largely due to confusion in terminology. Consequently, it is necessary to define terms pertaining to residual gas saturation that will be used within this report. The following definitions are those presented in Stiles (1999).

True Residual Gas Saturation is the minimum gas saturation which can be achieved under the forces of viscous, capillary and gravitational forces. It is the gas saturation at which gas relative permeability approaches zero.

Remaining Gas Saturation or (Effective Gas Saturation) is the minimum gas saturation which is actually achieved at the end of field life on a microscopic basis, i.e. within those pores contacted and swept by the displacement process.

Residual Gas Saturation is the final value of gas saturation in a laboratory displacement tests.

Figure 4.2.3-a illustrates the definitions above. Note that in this figure the remaining gas saturation is only an estimate and is determined by simulation modelling.

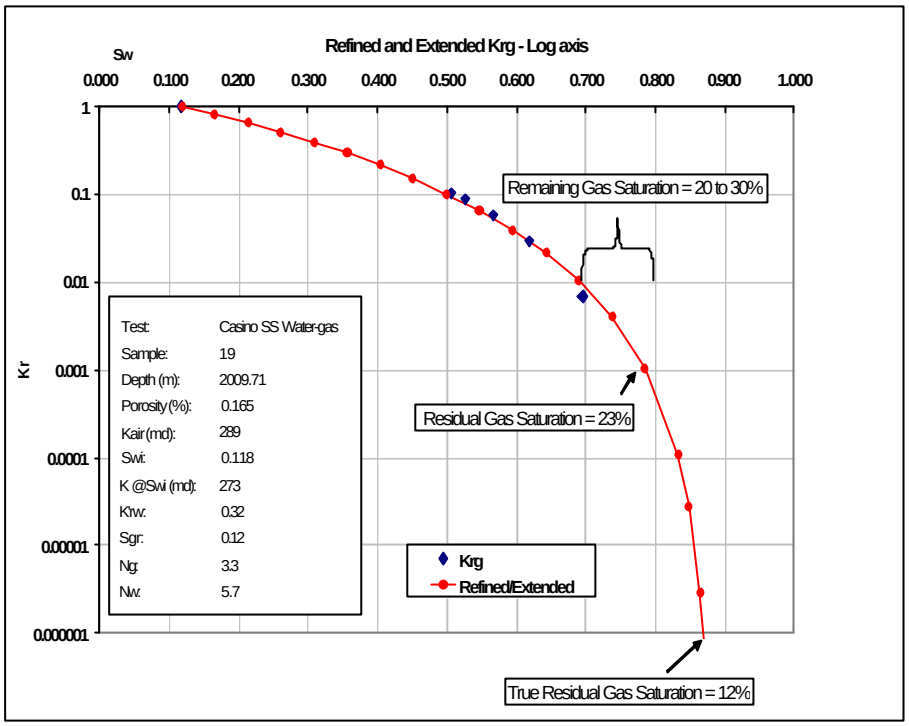

Figure 4.2.3-a: Gas Relative Permeability Curve illustrating the definitions of Residual Gas Saturation.

There are several methods to determine residual gas saturation from laboratory measurements; steady-state waterflood, unsteady-state waterflood, centrifuge displacement, co-current imbibition and counter-current imbibition. A review of several of these techniques is presented in Stiles (1999). As part of the Casino SCAL programmes, centrifuge and counter-current imbibition tests were performed on Casino-2 core plugs from the Waarre C while unsteady-state and steady state waterflood experiments were performed on Casino-3 core plugs from the Waarre C and A. Results of these SCAL programmes are presented in Corelab (2003) and Corelab (2004).

Figures 4.2.3-b and 4.2.3-c illustrate residual gas saturations from each of the core plug tests plotted against initial Sw and ambient permeability respectively. From these plots it is clearly evident that residual gas saturation measured from a laboratory tests not only depends on reservoir properties but also the type of test. The unsteady-state tests yielded the highest values of Sgr ranging from 14 to 33% pore volume (PV) while the centrifuge measurements resulted in the lowest Sgr values of 5 to 13% PV. The steady-state waterflood tests resulted in Sgr values of 14% to 25% PV. Stiles (1999) concludes that the best indication of true residual gas saturation is from centrifuge capillary pressure measurements, as performed on Casino-2 core plugs. Stiles (1999) also stated that results from waterfloods generally yield values of Sgr greater than the true residual gas saturation, due to capillary effects and/or low flooding rates.

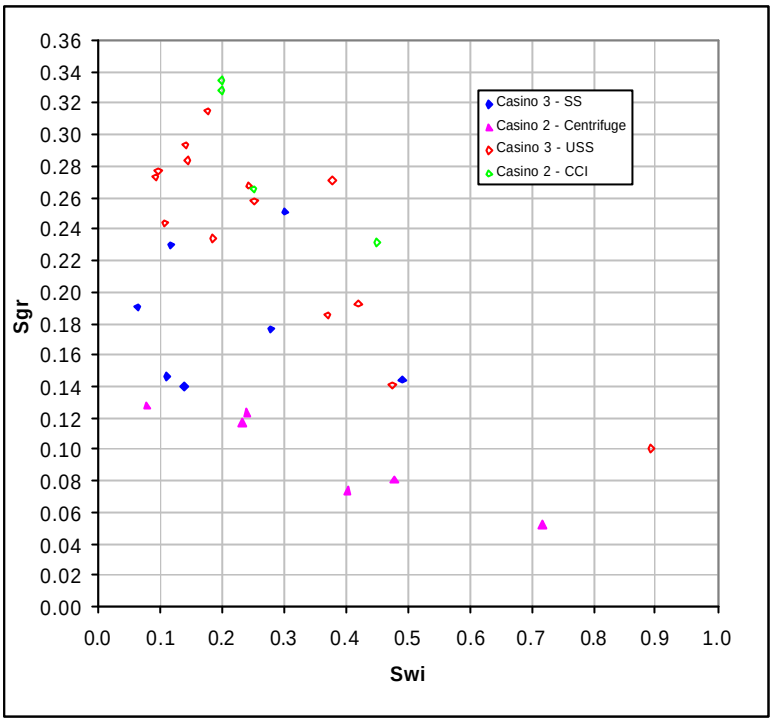

Figure 4.2.3-b: A plot of residual gas saturation versus initial Sw as measured from various lab tests of Casino-2 and 3 core plugs.

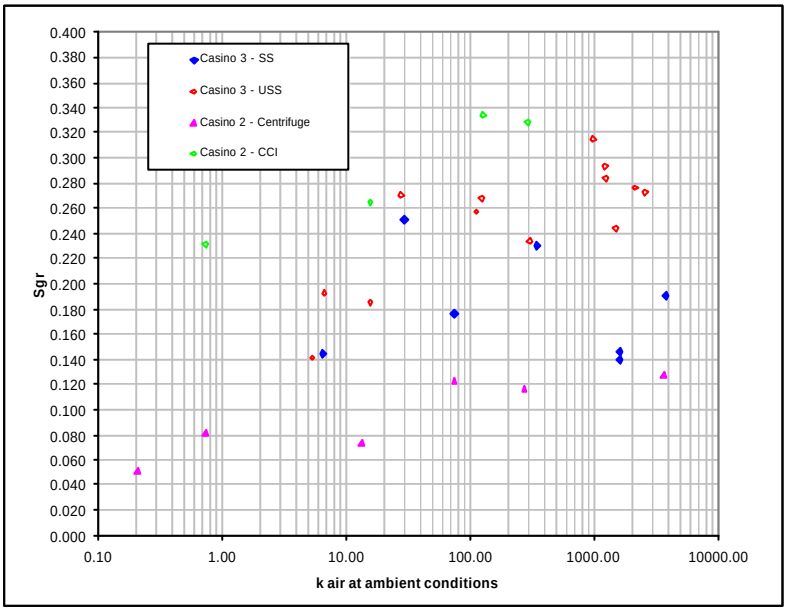

Figure 4.2.3-c: A plot of residual gas saturation versus ambient permeability as measured from various lab tests of Casino-2 and 3 core plugs.

The steady-state waterflood tests were the only lab tests that measured Krw and Krg for different water saturations on each plug. The other lab tests measured Krg and Krw at end-point conditions only. Consequently the rock curves that were developed for the simulation work were based primarily on the steady-state data. However the steady-state results did require some refinement.

The results of the steady-state tests were refined by extending the Krg & Krw curve from the lab measured Sgr to the true Sgr according to the method of Stiles (1999). The results of this analysis and refinement are

illustrated in Figure 4.2.3-d. Extending the curves results in a Sgr which is more consistent to the Sgr from the centrifuge work.

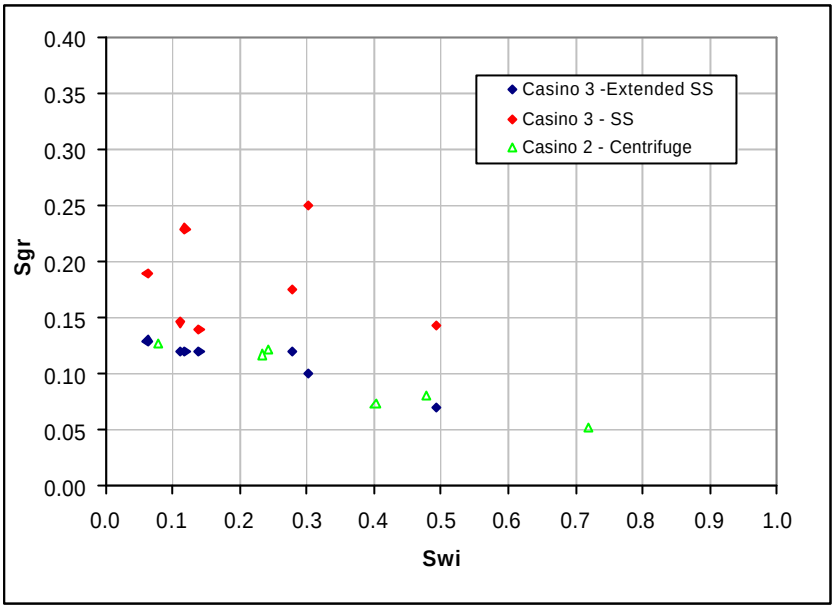

Figure 4.2.3-d: A plot of residual gas saturation versus ambient permeability as measured from various lab tests of Casino-2 and 3 core plugs.

Table 4.2.3-c is a summary of the interpretations of each steady-state test performed on Casino-3 core plugs;

Steady-State Waterflood Tests on Casino 3 Core Plugs												Extended and Refined Steady-State data as per Stiles (1999) method			
					Initial Conditions		Terminal Conditions								
Sample Number	Sample Depth, meters	Perm at amb	Specific Permeability to Air, millidarcys	Porosity, %	Water Saturation, fraction pore space	Effective Permeability to Gas, millidarcys	Gas Saturation, fraction pore space	Effective Permeability to Water, millidarcys	Relative Permeability to Water*, fraction	Gas Recovery, fraction pore space	Gas Recovery, fraction gas in place	Sgr	Krw'	Nw	Ng
2	2004.59	3780.00	3300.	22.6	0.063	2980.	**0.190**	808.	0.271	0.747	0.797	0.130	0.400	5.040	2.960
19	2009.71	346.00	289.	16.5	0.118	273.	**0.230**	35.5	0.130	0.652	0.739	0.120	0.320	5.700	3.300
29	2012.69	1600.00	1560.	21.5	0.140	1260.	**0.140**	339.	0.269	0.720	0.837	0.120	0.300	3.980	3.150
34	2014.29	1610.00	1470.	20.5	0.111	1180.	**0.146**	447.	0.379	0.743	0.836	0.120	0.500	7.340	2.960
52	2019.60	74.40	65.2	21.9	0.280	59.3	**0.176**	6.40	0.108	0.544	0.756	0.120	0.250	5.700	3.160
54	2020.27	6.58	4.56	15.6	0.492	2.34	**0.144**	0.269	0.115	0.364	0.717	0.070	0.300	4.520	2.990
8	2062.50	29.30	26.3	17.6	0.302	22.3	**0.251**	0.870	0.039	0.447	0.640	0.100	0.200	5.300	2.750
											Average	**.11**	**.3**	**5.4**	**3.0**

Table 4.2.3-c: Results and interpretations of the Steady-State waterflood tests performed on Casino-3 core plugs.

By extending the steady-state data to lower Sgr, the relative permeability to water at this gas saturation (Krw') also requires refinement. The steady-state Krw' was extended to values that were consistent with the centrifuge data. The average of the extended Krw' data was 0.3.

Corey Functions were fitted to the extended steady-state data. The average Corey exponent for Krg (Ng) is 3 and the average Corey exponent for Krw (Nw) is 5.4.

Figures 4.2.3-e and 4.2.3-f illustrate extended relative permeability curves for water and gas for Casino-3 core plug No 19.

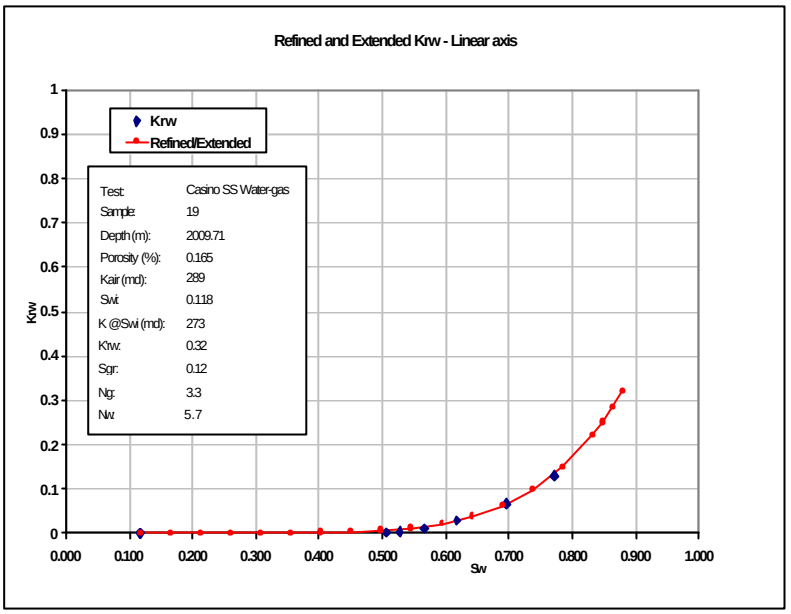

Figure 4.2.3-e: Extended steady-state water relative permeability curve for Core Plug 19

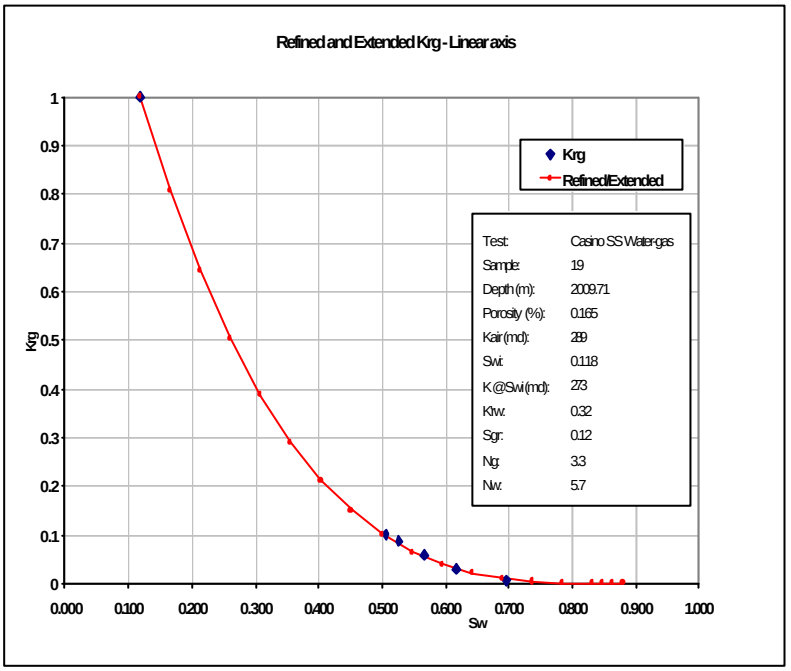

Figure 4.2.3-f: Extended steady-state gas relative permeability curve for Core Plug 19

Simulation model relative permeability curves and residual gas saturation.

Rock relative permeabilities and capillary pressures are measured on core-plugs under diffuse-flow conditions. If fluids are not homogeneously distributed within the area and across the depth spanned by a simulation gridblock i.e. due to Pc, relative permeability lab tests (or 'rock' curves) may not be applicable in a simulator.

A key parameter in determining the applicability of rock curves to a model is the width of the capillary transition zone relative to the height spanned by a particular grid block. The following dimensionless number gives a measure of this parameter;

$$N_c / r = \Delta Pc / \Delta rgh$$

$$\Delta Pc\_(Pa) = \max imum\_capillary\_pressure$$
$$h\_(m) = grid\_block\_thickness = 1m$$
$$g\_(m/s^2) = acceleration\_due\_to\_gravity = 9.8m/s^2$$
$$\Delta r\_(kg/m^3) = denisty\_difference\_between\_two\_phases = 860\,kg/m^3$$

N c/p >>1 Capillary transition zone very large compared with the gridblock thickness allowing rock curves to be used.
Nc/p << 1 Capillary transition zone very small compared with the gridblock thickness, allowing fluids to be modelled with a sharp interface.

The average permeability of the Waarre C is approximately 500mD, based on the Casino-3 welltest and average of Casino-2 log derived permeability. A Casino-3 Pc test on a rock of 990mD comprises a capillary transition zone of approximately 30 m (Lab Pc=50psi). Refer to Figure 4.2.3-g. The average grid block thickness for the Waarre C is 1m. With these inputs, Nc/p is significantly greater than 1 indicating that the Waarre C comprises a large capillary transition zone (or, more strictly speaking, a large transition zone as compared with the gridblock thickness) therefore supporting the assumption that the fluids are homogeneously distributed within the gridblocks. In this case the use of rock curves within the simulator is justified. However, in the case of the very high permeability Waarre Cb interval, where in situ permeabilities exceed 3000mD, grid block thickness becomes significant compared to capillary transition zone thickness. Under these conditions Nc/p is not significantly greater than 1 and the assumption of diffuse-flow conditions within the simulator may not hold. Instead, segregated flow conditions may dominate and the use of pseudo-relative permeability curves or smaller grid block thickness may be necessary. If rock curves are used within the simulator and segregated flow conditions do exist, the effective mobility of water may be overstated. As a recommendation for future work a 'fine scale' geological model will be taken to the simulator to assess the impact of the grid upscaling process on water ingress into the Waarre C reservoir.

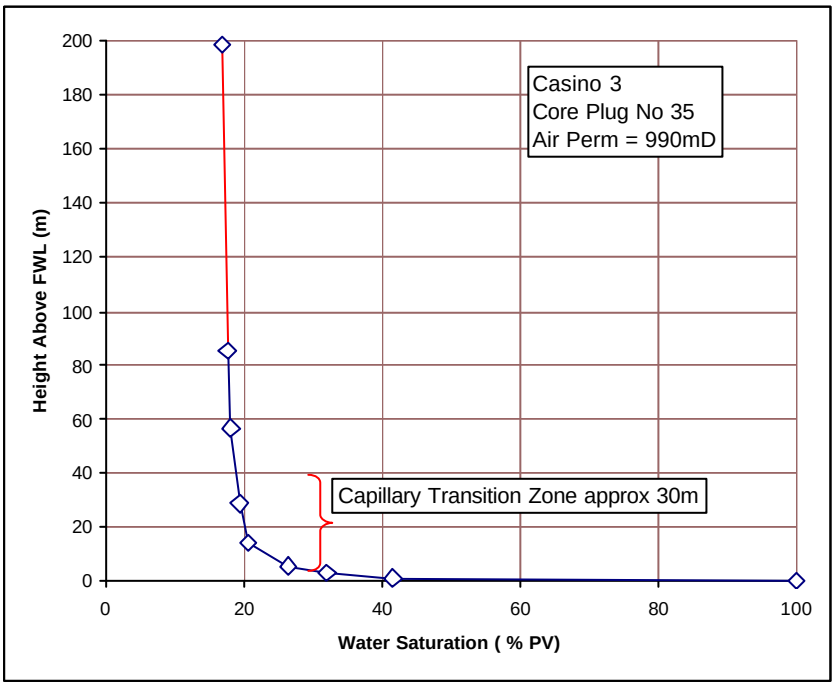

Figure 4.2.3-g: Results of the centrifuge capillary pressure test on Casino-3 Core Plug No 35.

A simulation exercise was undertaken to investigate the likely range in remaining gas saturation in the Waarre C reservoirs. Remaining gas saturation is the gas saturation remaining in a rock pore at the end of fluid displacement or at field abandonment. It is a practical rather than a theoretical result in that it is not only controlled by rock and fluid properties but also by the physical processes and forces operating in the

reservoir. Saturation tables were built with the extended steady-state relative permeability curves. True residual gas saturation values ranged from 5 to 15% PV. The range reflects the relationship between in situ permeability and Sgr that was developed from the Casino-2 centrifuge (air-brine) tests. Refer to Figure 4.2.3-h. This relationship was used to generate Sgr values for each SATNUM region. The other inputs that define the relative permeability curve (Krw', Ng and Nw) were based on the average of the extended steady-state data. These parameters were held constant for each SATNUM region.

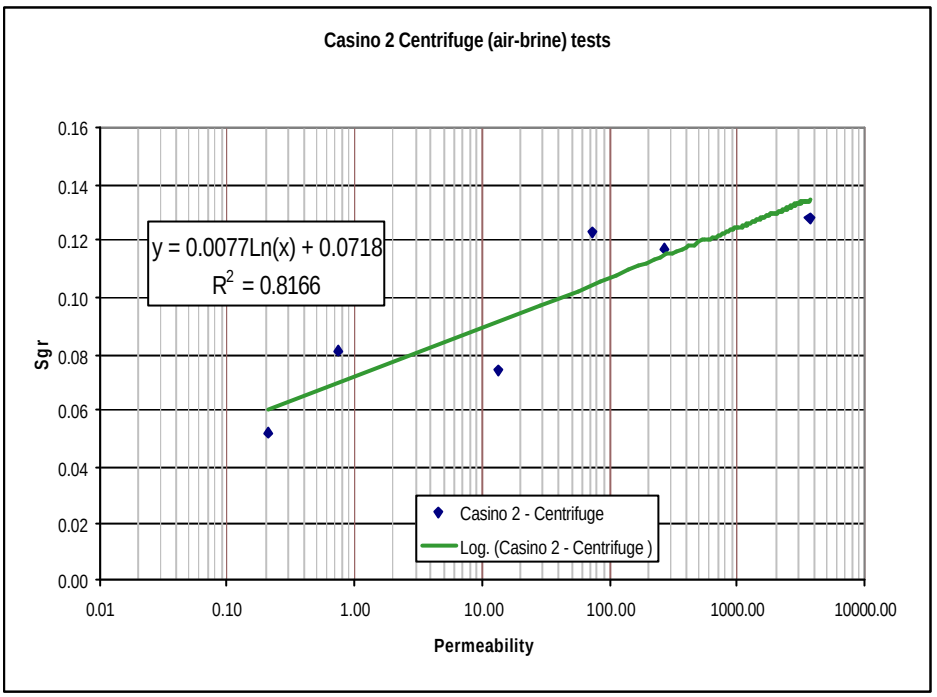

Figure 4.2.3-h: An illustration of the relationship between Sgr and permeability. Sgr results are from the centrifuge (air-brine) tests of Casino-2 core plugs. This relationship was used to generate Sgr values for each SATNUM region.

Figure 4.2.3-i is an illustration of the Waarre C simulation grid for a layer within the high permeability, Lower Cb Main Pay reservoir unit. The displayed property is water saturation. At field abandonment the remaining gas saturation is 14-17% with a true residual gas saturation of 13%. Figure 4.2.3-j is an illustration of the Waarre C simulation grid for a layer within the low permeability, Waarre Ca2 reservoir unit. The displayed property is water saturation. At field abandonment the remaining gas saturation is 7-8% with a true residual gas saturation of 6%. Based on the relative permeability curves the effective permeability to gas at the remaining gas saturation is 1.06e-04 mD. This suggests that gas is mobile within the simulation model at very low permeabilities and that the remaining gas saturation will reach true residual gas saturation in the simulation model. This is considered to be an unlikely event within the reservoir and the remaining gas saturation should be significantly higher than the true residual gas saturation. To capture the uncertainty in remaining gas, saturation tables were built with the following true residual gas saturations;

- Most Likely Sgr of 18% based on the average Sgr from the steady-state tests.
- Lowside Sgr of 12% based on the average Sgr from the centrifuge tests.
- Highside Sgr of 24% based on the average Sgr from the unsteady-state tests.

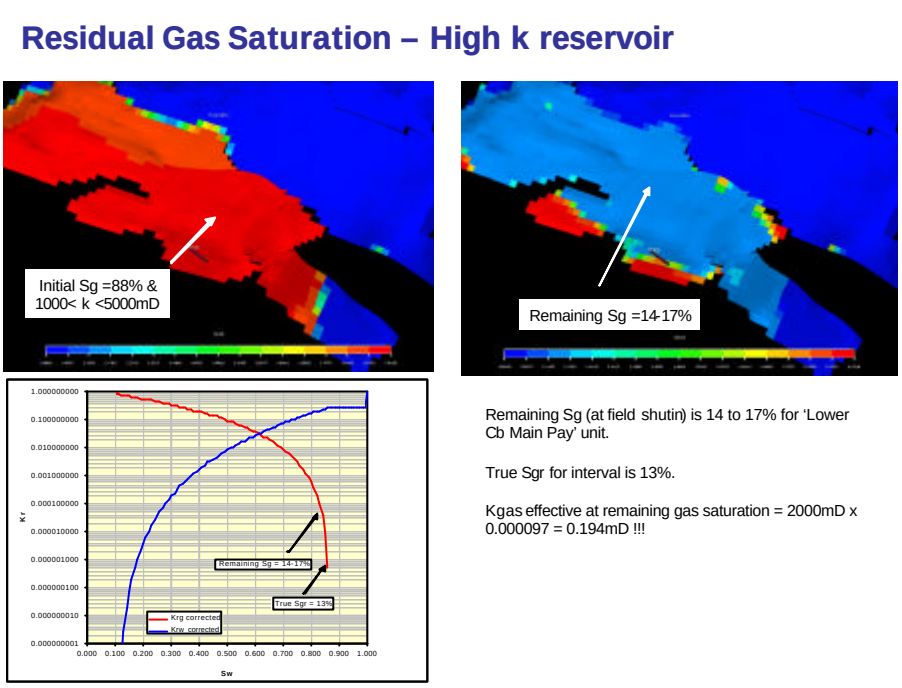

Figure 4.2.3-i: An illustration of the remaining gas saturation in the 'Lower Cb Main Pay' reservoir unit of the Waarre C.

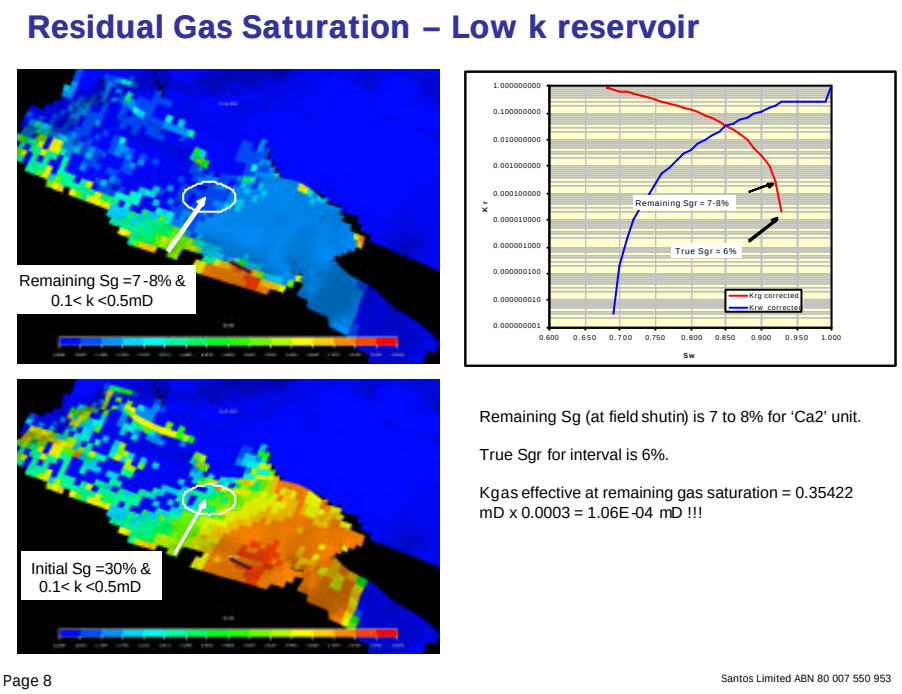

Figure 4.2.3-j: An illustration of the remaining gas saturation in the 'Waarre Ca2' reservoir unit of the Waarre C.

4.2.4 Dynamic Model Construction – Aquifer Modelling

Onshore producing analogies of the Waarre C in the Otway Basin exhibit aquifer pressure support. Consequently, a considerable effort was undertaken in order to model the possible range of outcomes for aquifer ingress into the gas reservoirs of the Casino Field. Pressure support within the ECLIPSE simulation models was provided by analytical aquifers. Two types of analytical aquifers were built during the dynamic modelling effort;

- An infinite acting aquifer represented by a Carter-Tracy aquifer.
- A finite aquifer represented by a Fetkovich aquifer.

Analytical aquifers were attached at the periphery of the model at two locations which are referred to as south-east (SE) aquifer and Main aquifer. The locations of these aquifers are illustrated in Figure 4.2.4-a.

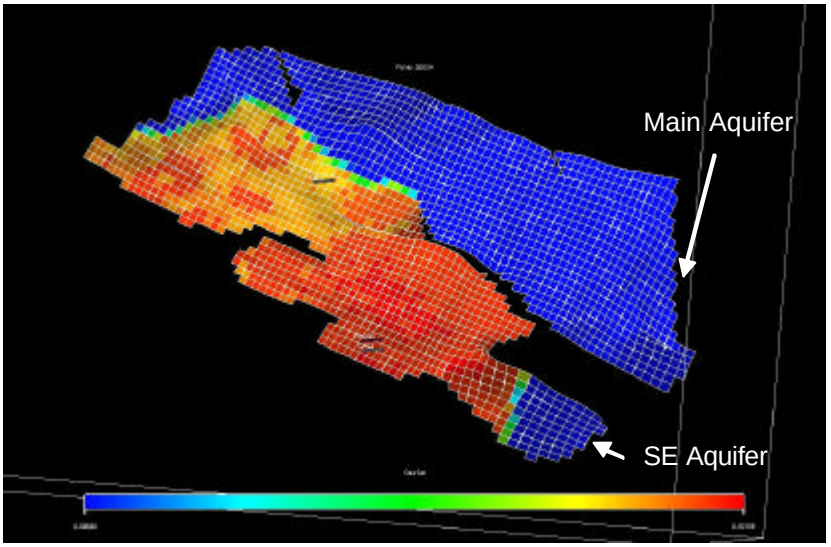

Figure 4.2.4-a: An illustration of the simulation grid for the Waarre C and points where the analytical aquifers are attached. Initial water saturation is the property displayed within the grid.

Aquifers were built for each reservoir unit within the Waarre C. Table 4.2.4-a summarises the aquifers built for the Casino model.

Main Closure Aquifer	***Note***
1 Upper Wa Cb Pay	In 'P50' Case the following zones are deactivated;
2 Upper Wa Cb Lower Pay	* Zone 2; Upper Wa Cb Non Pay
3 Upper Wa Cb Main Pay	* Zone 10; Wa Ca1
4 Intra Cb Silt	Upper Wa Cb Pay (Zone 1) is not present at SE Dip closure
5 Lower Cb Main Pay	
6 Ca4	
7 Ca3	
8 Ca2	
SE-Dip Closure Aquifer	
9 Upper Wa Cb Lower Pay	
10 Upper Wa Cb Main Pay	
11 Lower Cb Main Pay	
12 Ca4	
13 Ca3	
14 Ca2	

Table 4.2.4-a: Aquifers for the Waarre C.

The models assume a radial homogenous formation, of constant height, porosity and permeability and predict superimposed pressure drawdown as a function of distance and time from production. The Carter-Tracy model is defined by thickness, influence angle, permeability, porosity and reservoir radius. Influence angle was based on a reservoir radius of 9000' and aquifer width of 2950' and 7220' for the SE and Main aquifers respectively. Aquifer width is defined as the width of the analytical aquifer where it is attached to the simulation grid. The parameters which define the Carter-Tracy Aquifer is summarised in the table below.

Main Closure Aquifer										
Aqu ID	k mD	Phit v/v	Ct (Cw + Ct) 1/psi	net h ft	gross h	N:G v/v	ro ft	encroachment angle deg	Bw rb/stb	Uw cp
1	445	0.19	7.17E-06	30	45	0.67	9000	45	1.02	0.406
2	445	0.19	7.17E-06	53	79	0.67	9000	45	1.02	0.406
3	445	0.19	7.17E-06	16	24	0.67	9000	45	1.02	0.406
4	445	0.19	7.17E-06	3	4	0.67	9000	45	1.02	0.406
5	445	0.19	7.17E-06	79	118	0.67	9000	45	1.02	0.406
6	445	0.19	7.17E-06	52	78	0.67	9000	45	1.02	0.406
7	445	0.19	7.17E-06	79	118	0.67	9000	45	1.02	0.406
8	445	0.19	7.17E-06	105	157	0.67	9000	45	1.02	0.406
Total				**417**	**622**					
SE-Dip Closure Aquifer										
9	445	0.19	7.17E-06	53	79	0.67	9000	18	1.02	0.406
10	445	0.19	7.17E-06	16	24	0.67	9000	18	1.02	0.406
11	445	0.19	7.17E-06	78	116	0.67	9000	18	1.02	0.406
12	445	0.19	7.17E-06	52	78	0.67	9000	18	1.02	0.406
13	445	0.19	7.17E-06	79	118	0.67	9000	18	1.02	0.406
14	445	0.19	7.17E-06	104	155	0.67	9000	18	1.02	0.406
Total				**382**	**570**					

Table 4.2.4-b: Parameters which define the infinite Carter-Tracy analytical aquifer for each reservoir unit of the Waarre C

Aquifer porosity was determined from the average porosity of the Waarre C in the Casino field. Aquifer thickness is based on interval thickness of the Waarre C units at the periphery of the model where the analytical aquifers are attached. Aquifer permeability is based on the permeability interpreted from the Casino-3 welltest.

A regional structural element map of the Waarre is illustrated in Figure 4.2.4-b. This map indicates that the Waarre C may not be infinite in size as compared to the gas reservoirs of the Casino field. No-flow or interference boundaries may be present in the form of offset producing fields and faulting. Minerva field to the north-east of Casino is scheduled for start up in late-2004 at a DCQ of approximately 150 TJ/day from the Waarre C. An interference boundary is interpreted to be between Casino and Minerva. To the south the Thylacine field is schedule for start up in mid-2006. This field will develop the Flaxmans and Waarre Formations with an initial DCQ of 200 TJ/day. An interference boundary is interpreted between Casino and Thylacine. To the east, the Shipwreck Fault is interpreted to be a no-flow boundary and the eastern limit of the Casino Waarre C aquifer. Based on these limits and the assumed aquifer properties in the table below an aquifer volume of 42000 mmstb was calculated for the finite aquifer case.

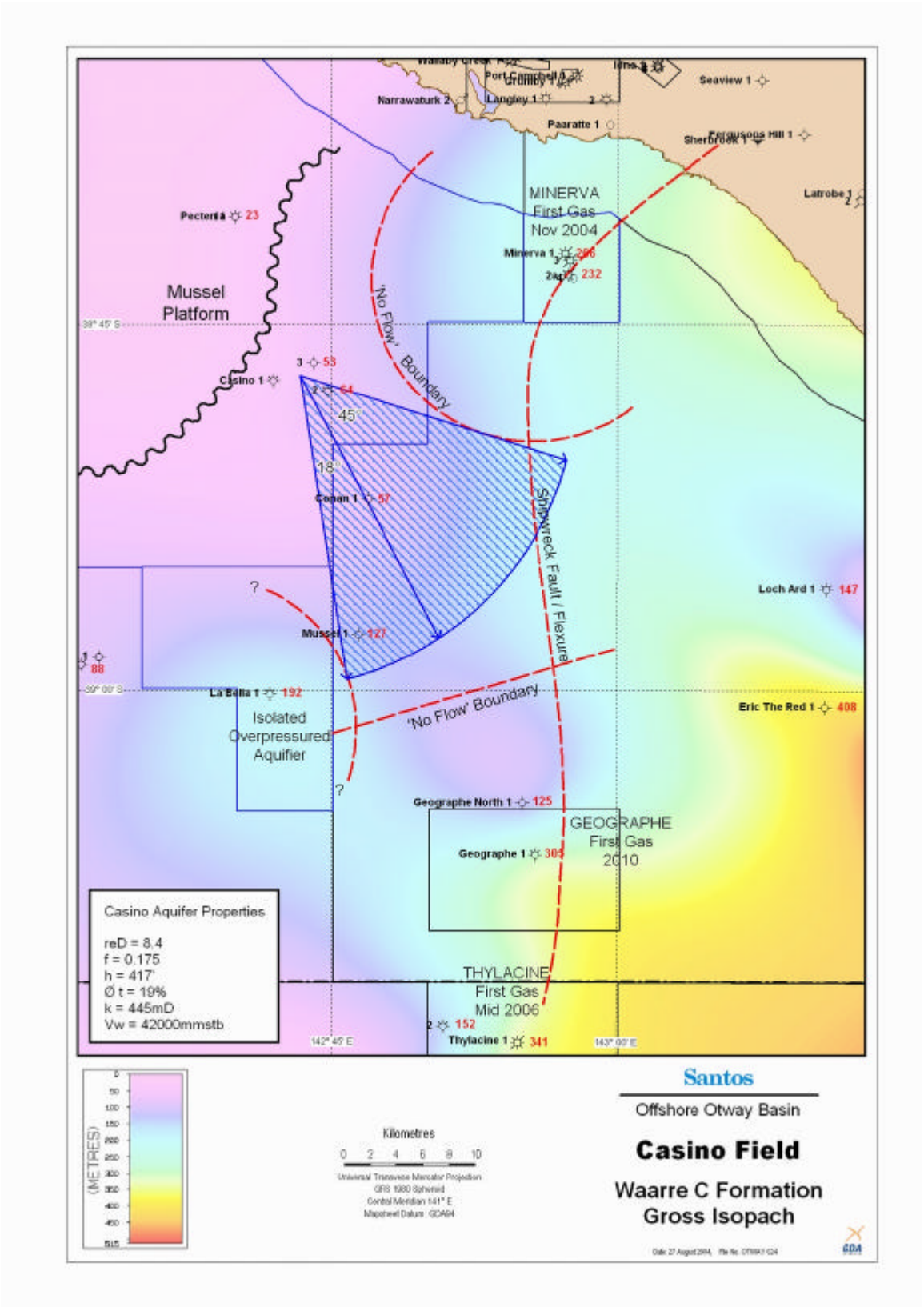

Figure 4.2.4-b: Regional structural element map illustrating the extent of the finite aquifer

To model a finite aquifer within the Casino simulation model, a Fetkovich analytical aquifer was built. The Fetkovich aquifer uses a simplified approach based on a pseudosteady-state productivity index and a material balance relationship between the aquifer pressure and cumulative influx. This model assumes that the pressure response in felt uniformly throughout the entire aquifer.

Water influx from the analytical aquifer to the simulation grid was determined from aquifer productivity index. As detailed in Dake (1978) pp. 328-329, aquifer productivity index (J) is defined as;

$$J = Semi - Steady\ \_State\ \_Aquifer\ \_PI\ \_(stb/day/psi)$$

$$J = \frac{2pfkh(7.08 * 10^{-3})}{(m(\ln r_e / r_o) - 0.75)}$$

$$re = outer\ \_radius\ \_of\ \_aquifer$$

$$ro = inner\ \_radius\ \_of\ \_aquifer$$

$$u = water\ \_vis\ \cos ity$$

$$k = aquifer\ \_permeabili\ ty$$

$$h = aquifer\ \_net\ \_thickness$$

$$f = encroachme\ nt\ \_angle\ / 360^{0}$$

Aquifer permeability, porosity, thickness and influence angle for the Fetkovich model is based on those parameters determined for the Carter-Tracy analytical aquifer model. Table 4.2.4 summarises the parameters used in the Fetkovich analytical aquifer.

Main Closure Aquifer															
Aqu ID	k mD	Phit v/v	Ct (Cw + Ct) 1/psi	net h ft	gross h	N:G v/v	ro ft	re ft	reD	f	Aquifer Area ft2	Bw rb/stb	Uw cp	Vw stb	J (Semi Steady State) stb/day/psi
1	445	0.19	7.17E-06	30	45	0.67	9000	75459	8.4	0.125	2.20E+09	1.02	0.406	2.19E+09	133
2	445	0.19	7.17E-06	53	79	0.67	9000	75459	8.4	0.125	2.20E+09	1.02	0.406	3.87E+09	235
3	445	0.19	7.17E-06	16	24	0.67	9000	75459	8.4	0.125	2.20E+09	1.02	0.406	1.17E+09	71
4	445	0.19	7.17E-06	3	4	0.67	9000	75459	8.4	0.125	2.20E+09	1.02	0.406	2.19E+08	13
5	445	0.19	7.17E-06	79	118	0.67	9000	75459	8.4	0.125	2.20E+09	1.02	0.406	5.78E+09	350
6	445	0.19	7.17E-06	52	78	0.67	9000	75459	8.4	0.125	2.20E+09	1.02	0.406	3.80E+09	230
7	445	0.19	7.17E-06	79	118	0.67	9000	75459	8.4	0.125	2.20E+09	1.02	0.406	5.78E+09	350
8	445	0.19	7.17E-06	105	157	0.67	9000	75459	8.4	0.125	2.20E+09	1.02	0.406	7.68E+09	465
Total				**417**	**622**									**3.05E+10**	
SE-Dip Closure Aquifer															
9	445	0.19	7.17E-06	53	79	0.67	9000	75459	8.4	0.05	8.82E+08	1.02	0.406	1.55E+09	94
10	445	0.19	7.17E-06	16	24	0.67	9000	75459	8.4	0.05	8.82E+08	1.02	0.406	4.68E+08	28
11	445	0.19	7.17E-06	78	116	0.67	9000	75459	8.4	0.05	8.82E+08	1.02	0.406	2.28E+09	138
12	445	0.19	7.17E-06	52	78	0.67	9000	75459	8.4	0.05	8.82E+08	1.02	0.406	1.52E+09	92
13	445	0.19	7.17E-06	79	118	0.67	9000	75459	8.4	0.05	8.82E+08	1.02	0.406	2.31E+09	140
14	445	0.19	7.17E-06	104	155	0.67	9000	75459	8.4	0.05	8.82E+08	1.02	0.406	3.04E+09	184
Total				**382**	**570**									**1.12E+10**	

Table 4.2.4-c: Parameters which define the Fetkovich finite analytical aquifer for each reservoir unit of the Waarre C

4.2.5 Dynamic Model Construction – Production Network Modelling and Vertical Lift Performance.

The ECLIPSE "Network" option was employed to model the flow from the wellhead to the inlet at the gas processing facility. The Network option is designed to provide variable tubing head pressure (THP) limits to groups of wells, which depend on the groups' flow rates according to a set of pipeline pressure loss relationships. The option calculates the well THP limits dynamically by balancing the flow rates and pressure losses in the network.

A schematic of the production network for Casino is presented in Figure 4.2.5-a

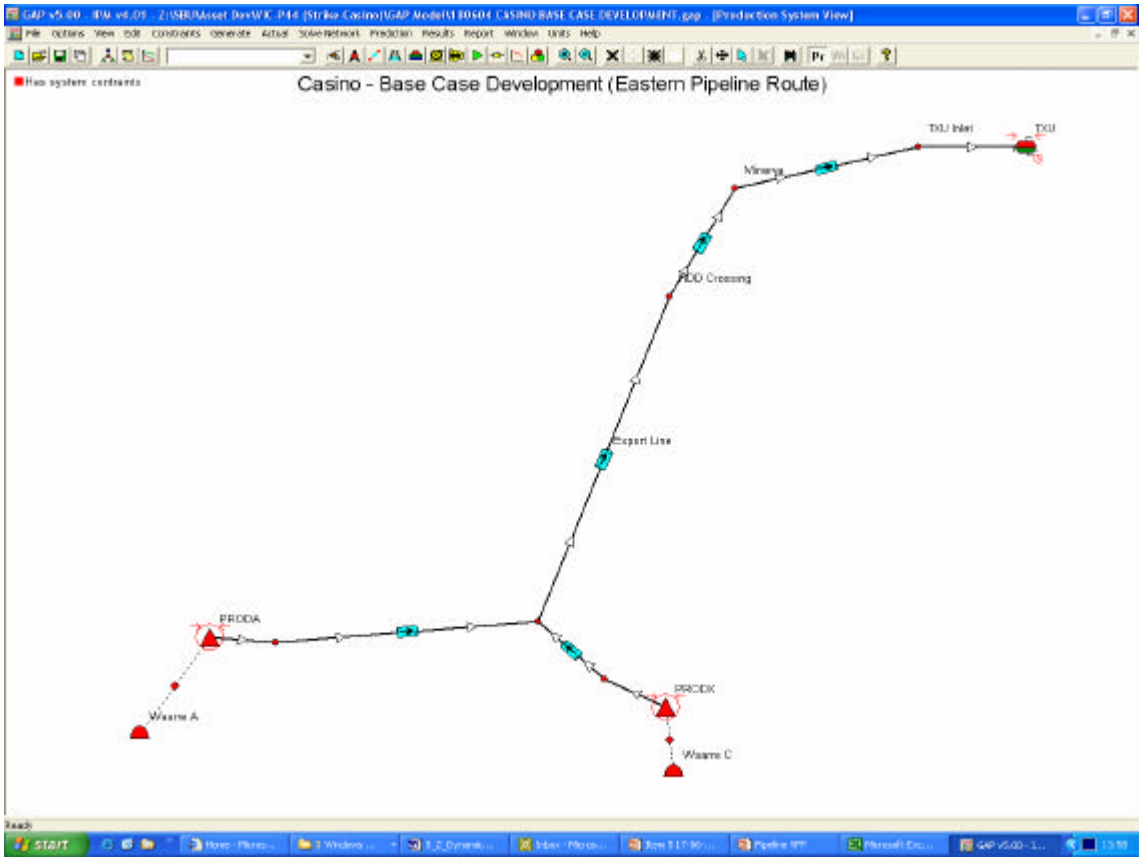

Figure 4.2.5-a: Schematic of the Casino production network.

A 12" multiphase pipeline exports gas from the Casino field to the inlet of the Iona gas plant. Figure 4.2.5-b illustrates the onshore and offshore pipeline lengths and elevations of this route. Hydraulic flow tables were generated using Petroleum Experts software, PROSPER. The Beggs & Brill correlation was used to model horizontal flow along the export pipeline.

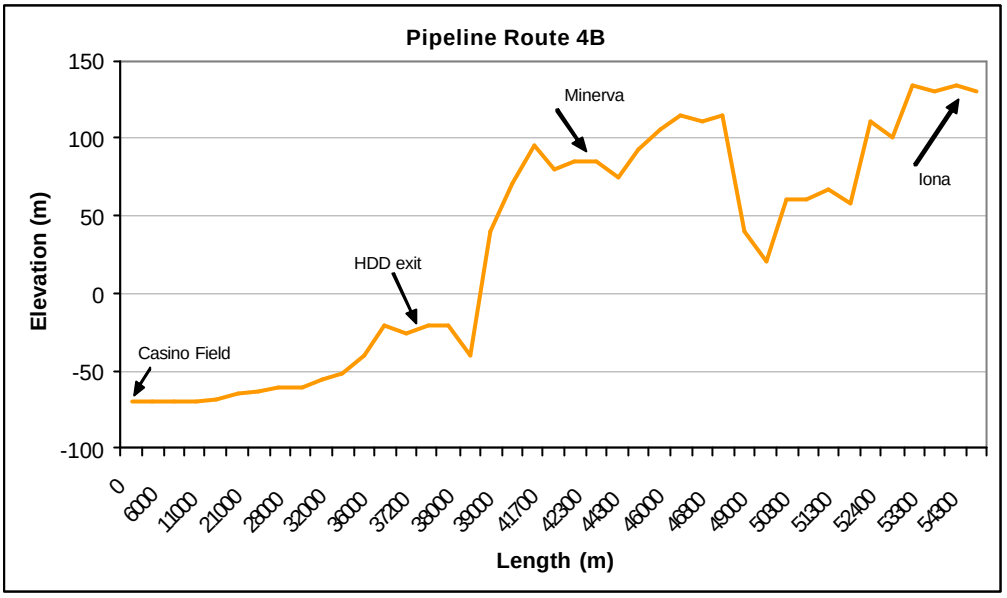

Figure 4.2.5-b: Offshore and Onshore pipeline route elevations and lengths.

Well production rates are controlled within the model by fixed plant capacity at a constant inlet pressure. Vertical Lift Tables for each producer were generated within PROSPER. Petroleum Experts correlation was used to model pressure losses through the production tubing.

4.2.6 Dynamic Model Construction – Well locations and Productivity.

Development well locations within the simulation model are illustrated in Figure 4.2.6-a. The proposed producers comprise one sub-horizontal well, PRODA, which will develop the Waarre A and potentially two vertical wells which will develop the Waarre C, PRODX and PRODY.

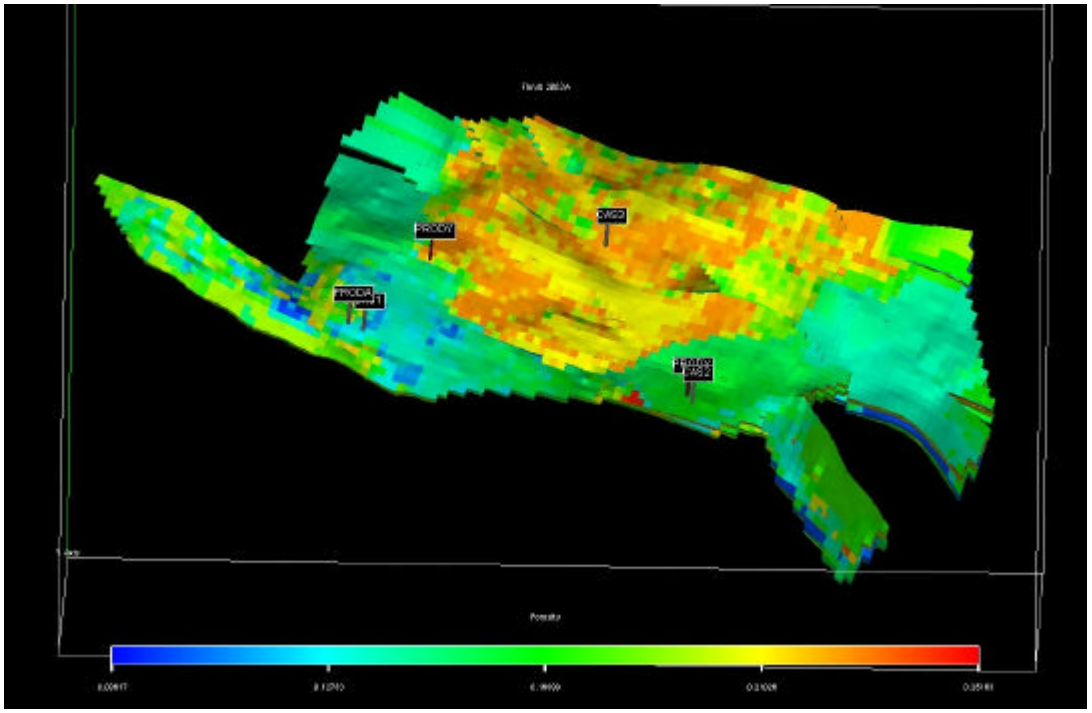

Figure 4.2.6-a: Simulation grid illustrating the location of the development wells. The property displayed within the grid is porosity.

Waarre C Producers – Well Productivity

The productivity of the Waarre C producers (PRODX and PRODY) has been investigated within the Casino full field simulation model.

A DST performed at Casino-3 was a test of the Waarre C. An interpretation of the final build-up period indicated that the test interval comprised a kh of 41000 mD-ft (effective permeability to gas). The reader is referred to Steyn (2004) for a detailed discussion of the well test and interpretation thereof.

A comparison of the kh interpreted from the well test and the kh of the Casino-3 well in the simulation model indicated that the kh of the well in the simulation model is too high. Refer to Table 4.2.6-a. A multiplier of 0.63 was required to match the kh of Casino-3 in the model to the interpreted welltest. This productivity multiplier was enabled within ECLIPSE using the WPIMULT keyword. The same productivity multiplier was also applied to the Waarre C production wells, PRODX and PRODY within the model. The kh of the development wells are also summarised in Table 4.2.6-a below.

Well	Completed Interval (m)	WPIMULT	Well kh (md-ft)	Well kh (md-m)
Casino-3	102	1	74281	22641
PRODX	34	1	110127	33567
PRODY	36	1	53177	16208
Casino-3	102	0.63	46797	14264
PRODX	34	0.63	69380	21147
PRODY	36	0.63	74281	22641

Table 4.2.6-a: Summary of well kh

Waarre C & A Producers – Well Skin

Skin, S, is a dimensionless number which represents the additional pressure drop at the near well bore region. Skin comprises two components (i) mechanical or Darcy Skin and (ii) non-Darcy flow factor, D. Both of these parameters are required to define the productivity of a well within the simulator.

For all wells within the simulation models, the mechanical skin is 2. This skin was based on the mechanical skin interpreted from the Casino-3 DST. Casino-3 was an appraisal well which was plugged and abandoned. Consequently, little consideration was given to selecting drilling practises which would minimise formation damage and hence skin. For the development wells, a drilling fluid will be selected which will minimise spurt fluid loss and hence minimise formation damage. Arguably there may be justification to reduce the mechanical skin of the development wells within the simulation model, however as Figure 4.2.6-b illustrates the impact of skin on well productivity index is minimal, and as such it was not considered necessary to re-work the skin values.

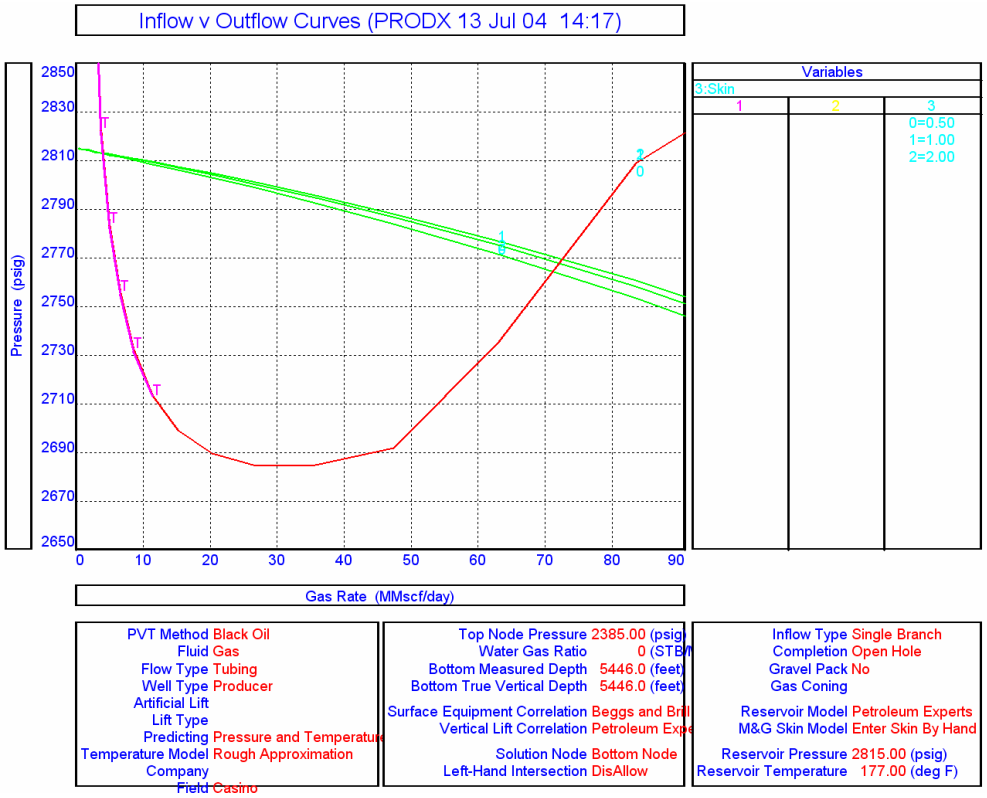

Figure 4.2.6-b: Sensitivity of PRODX inflow performance to Mechanical Skin. Skin values of 0.5, 1 and 2.

The non-Darcy flow factor can be derived empirically or from transient multi-rate testing. Table 4.2.6-b is a summary of the non-Darcy Flow Factors derived for Casino-3 and the development wells within the simulation model (PRODX and PRODA).

The D factor of 4.7 e-4 1/mscfd was obtained from the interpretation of a multi-rate test. The reader is referred to Steyn (2004) for an interpretation of this welltest. Several empirical methods were investigated with the objective to find a method which replicates the D-factor from the welltest and then apply this method to the development wells within the simulation model, PRODX, PRODY and PRODA. The empirical methods trialled are outlined in Dake (1978) pp 255-260 and Barker and Vincent (1998). A D-factor was also derived from Petroleum Experts Inflow-Performance Modelling software PROSPER.

The methods detailed by Dake (1978) and Barker and Vincent (1998) require a term referred to as the Beta-Factor. This factor can be routinely measured from core analysis.

Several plugs were selected from the Casino-2 and 3 core plug suite and the B-Factor measured at net overburden conditions. The results of these tests are presented in Figure 4.2.6-c.

The Dake (1978) method was calculated with a B-Factor from the Casino core measurements and a correlation developed by Dake (1978) based on a non-referenced lab data set. The Barker & Vincent (1988) D-factor was calculated based on a B-Factor correlation developed by Behrenbruch and Kozma (1984). This correlation is based on test data from the North Rankin field and modified by Barker & Vincent (1988) for the effect of perforation damage.

Replicating the conditions of the Casino-3 welltest, the Barker & Vincent (1988) method provides a D-factor that is closest to the well test derived D-factor from Casino-3. This match was refined by modifying the Kdp term in the Barker & Vincent (1988) equation. This term is the effective permeability of the crushed zone around the perforations. Well test data for the North Rankin area show that in general Kdp may be 0.33 to 0.1 of the true formation permeability for 800 psi underbalance perforations (Barker & Vincent 1988). In order to get a good match to the D-factor from the Casino-3 well test a ratio of 0.1150 was used.

The Barker & Vincent (1988) method was then used to determine D-factors for the proposed development wells with the 'Base Case' completion design. For PRODA the completion design is a deviated well (85deg) with a 400m open-hole section and wire wrapped stand alone sandscreens. For PRODX and PRODY the completion design is a vertical well with 30m of open-hole section and expandable sand screens.

There is a significant degree of heterogeneity within both the Waarre C and Waarre A reservoirs. Consequently it is unlikely that the entire open-hole section will be contributing to inflow at any one time. D-Factor is inversely proportional to the area of inflow into the well, as a result the effective inflow length (or height) h has a significant impact on the magnitude of the non-Darcy skin factor. In order to capture this uncertainty a range of D-factors have been determined for each of the wells in the simulation model and are presented in Table 4.2.6-c.

non-Darcy Skin (D) Values

		PRODA Dev Well (85 deg) 400 m OH, Stand Alone Screen	PRODX & PRODY Vert Well 35m OH, ESS	Casino 3 (DST)	
Porosity=		0.139	0.22	0.22	Avg from log analysis
Swi =		0.4	0.15	0.15	
Gas Grav=		0.6	0.6	0.6	PVT props
k=	md	50	440	445	Welltest interp
h=	ft	1312.0	92.2	92.2	Log analysis
Lp (perf length)=	ft	2.0000	2.0000	1.5553	API tables (3 3/8" HSD - Slb Powerjet TCP)
Rp (perf radius)=	ft	0.0250	0.0250	0.0144	API tables (3 3/8" HSD - Slb Powerjet TCP)
visc=	cp	0.0183	0.0183	0.0183	PVT props
spf=	per ft	6	6	6	
Hp (perf interval) =	ft	1312.0	92.2	29	9m perfs
dam ratio=		0.2000	0.2000	0.1150	Welltest from Nth Rankin range 0.33 to 0.1
Rw (well radius)=	ft	0.3542	0.5000	0.5000	
Beta Factor					
Dake (1978) =	/ft	3.63E+08	3.28E+07	3.24E+07	
Behrenbruch & Kozma (1984)=	/ft	8.60E+08	9.84E+07	1.69E+08	
Casino Core=	/ft	1.60E+08	1.96E+07	1.94E+07	
non-Darcy Skin					
Petroleum Experts IPR=	/mcfd	1.04905E-05	4.35072E-05	4.33845E-05	
Dake (1978)=	/mcfd	2.8451E-06	2.2848E-05	2.3067E-04	
Barker & Vincent (1988)=	/mcfd	6.6418E-07	9.5152E-06	4.7939E-04	
Dake (1978) with Casino Core Beta	/mcfd	1.2571E-06	1.3661E-05	1.3814E-04	

Table 4.2.6-b: Calculated D Factors for Casino-3 and the Waarre C and A development wells within the simulation model.

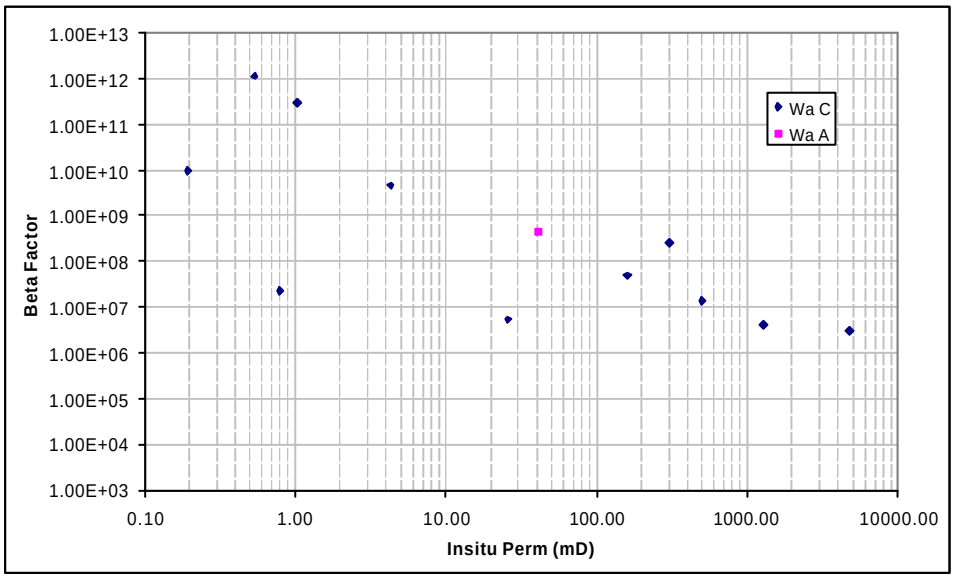

Figure 4.2.6-c: Beta Factors measured at net overburden conditions from Casino-2 and Casino-3 core plugs.

D-Factor Barker & Vincent (1988) method	**PRODA** Dev Well (85 deg) 400 m OH. Stand Alone Screen	**PRODX & PRODY** Vert Well 35m OH. ESS
Lowside (100% effective h)	6.6418E-07	9.5152E-06
Highside (25% effective h)	1.0627E-05	1.5224E-04
Most Likely (50% effective h)	**2.6567E-06**	**3.8061E-05**

Table 4.2.6-c: Calculated D Factors for Casino-3 and the Waarre C and A development wells within the simulation model.

Waarre A Well Productivity: Phase 1 Study.

The productivity of a Waarre A completion has been investigated using a 50 layer sector model based on the Waarre A reservoir properties as seen at Casino-1. The initial phase of this work was conducted to evaluate the expected initial productivity of various well designs ranging from vertical to near horizontal (85 degrees) as shown in Figure 4.2.6-d below.

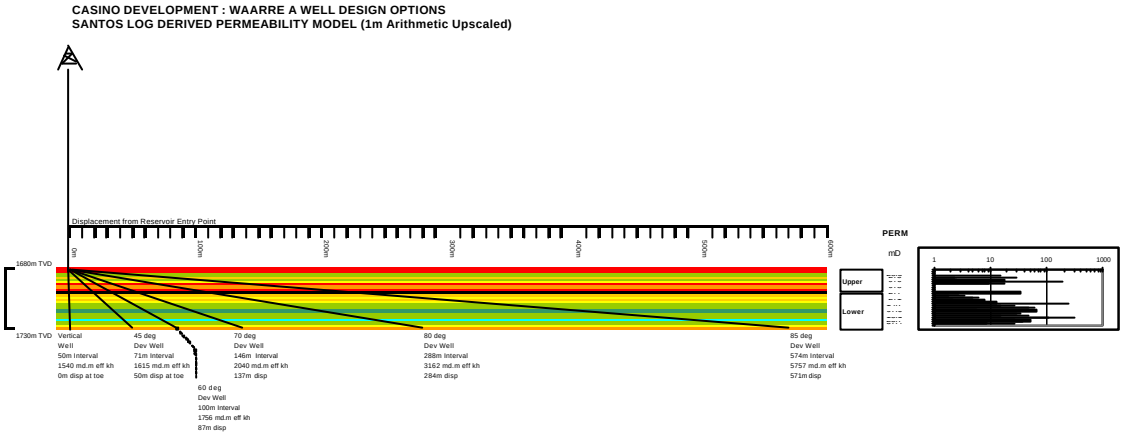

Figure 4.2.6-d: Waarre A Well Design Options Evaluated.

Further details of the well design alternatives shown in Figure 4.2.6-d including well deviation, reservoir penetration and well offset at TD can be found in Table 4.2.6-d.

	Dev Angle	**Pay Penet-ration**	**Well Offset**
	deg	m	m
Vertical Well	0	50	0
45 Degree Well	45	71	50
60 Degree Well	60	100	87
70 Degree Well	70	146	137
80 Degree Well	80	288	284
85 Degree Well	85	574	571

Table 4.2.6-d: Waarre A Well Parameters.

For this initial work the initial "uncalibrated" Santos log permeability model was used to provide the layer permeability. This was previously shown in Figure 3.13.3-a in Section 3.13. Table 4.2.6-e shows the resulting transmissibility (kh) estimates for the Casino-1 well based on the log scale data and the data upscaled to 1m layer thickness as used in the sector model. Also shown is the split between the kh contribution from the Upper and Lower Waarre A reservoirs. Note that based on the "uncalibrated" log permeability model the Casino-1 well is predicted to have a total kh of approximately 1500 md.m (5000 md.ft) split 20% / 80%.

	Base Santos Perm Model kv/kh=0.1 kh		
	md.ft	md.m	
Casino-1 Log Scale Data			
Upper Waarre A	984	300	Casino-1
Lower Waarre A (Main Pay)	4238	1292	Data
Total	**5221**	**1592**	
Casino-1 Log Data Upscaled to 1m			
Upper Waarre A	981	299	Casino-1
Lower Waarre A (Main Pay)	4240	1293	Data
Total	**5221**	**1592**	

Table 4.2.6-e: Casino-1 kh Estimates.

The Geoquest Eclipse "Schedule" software was used to evaluate the expected kh of the range of development well designs shown in Figure 4.2.6-d for several permeability models. This included the following;

- Base "uncalibrated" Santos log derived permeability model
- Base "uncalibrated" Santos log derived permeability model with downside k_v/k_h (0.01)
- Alternate permeability model from AWE commissioned log analysis. (Note that this predicts considerably higher permeability than the Santos model and was used to represent an upside outcome at the time)
- Base "uncalibrated" Santos log derived permeability model divided by 3. This was used at the time to represent a downside permeability outcome

The results of this analysis are shown in Table 4.2.6-f and Figure 4.2.6-e. Table 4.2.6-f shows the predicted kh for various well types for each permeability model while Figure 4.2.6-e shows the nominal initial well potential for each case based on an initial Tubing Head Pressure of 500 psi. Figure 4.2.6-f shows the relative productivity of the various well options compared to a vertical well as a function of hole deviation.

Sector Model Well k*h	Santos Downside Perm Model (=k/3) kv/kh=0.1 kh		Santos Perm Model, D'side kv/kh kv/kh=0.01 kh		Base Santos Perm Model kv/kh=0.1 kh		Base AWE Perm Model kv/kh=0.1 kh	
	md.ft	md.m	md.ft	md.m	md.ft	md.m	md.ft	md.m
Vertical Well	1684	513	5052	1540	5052	1540	7805	2379
45 Degree Well	1766	538	5077	1547	5299	1615	8186	2495
60 Degree Well	1920	585	5127	1563	5760	1756	8900	2713
70 Degree Well	2231	680	5239	1597	6692	2040	10340	3152
80 Degree Well	3458	1054	5808	1770	10374	3162	16027	4885
85 Degree Well	6297	1919	7658	2334	18889	5757	29185	8896

Table 4.2.6-f: Predicted kh for Various Well Designs and Permeability Models.

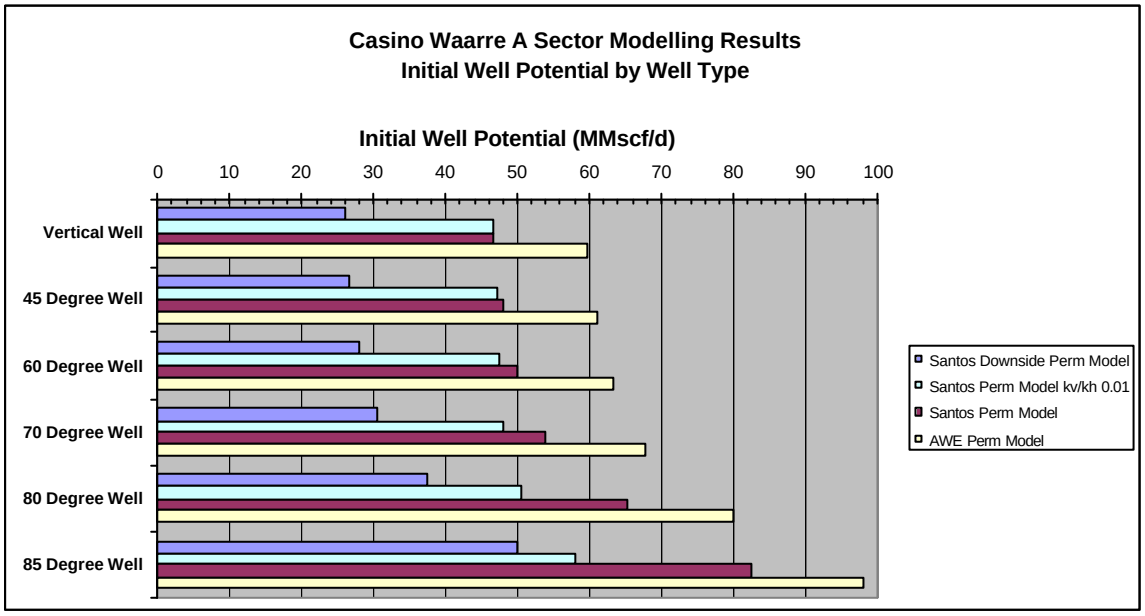

Figure 4.2.6-e: Initial Well Potential for Various. Well Designs and Permeability Models

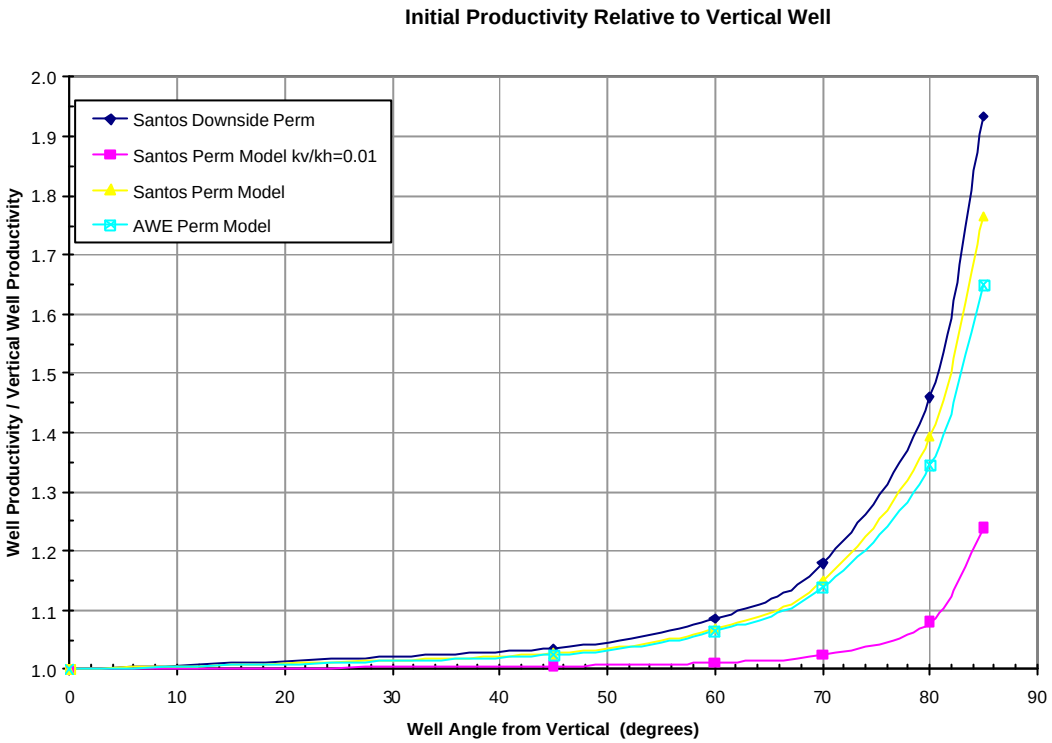

Figure 4.2.6-f: Relative Productivity Compared to a Vertical Well

Based on the results of this work and the considerable uncertainty in actual Waarre A permeability all further development planning for the Casino development has considered only a high angle /subhorizontal well (>80 degrees deviation Waarre A. This mitigates against the possibility of a downside permeability outcome.

Waarre A Well Productivity : Final Well PI for Reserves and Development Planning.

The basis for the final range of Waarre A permeability outcomes to be modelled for field reserves estimation and development planning has previously been described in Section 3.13. The final "P90", "P50" and "P10" models are summarised in Figure 4.2.6-g, based on the Casino-1 well.

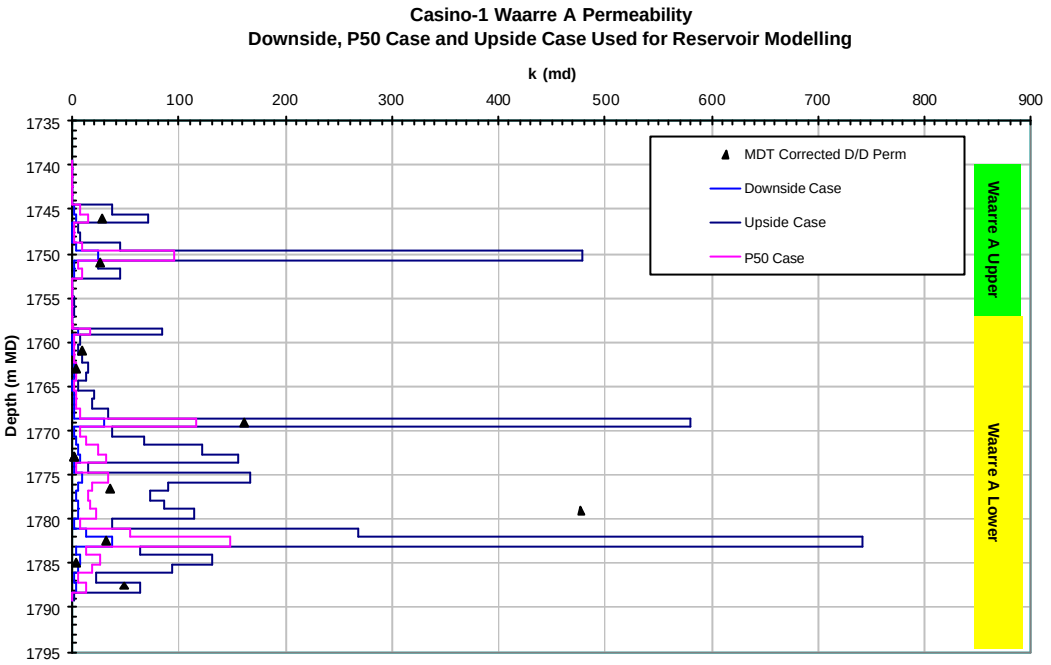

Figure 4.2.6-g: Waarre A Permeability Range

The same sector model approach described above was used to determine the expected kh for the Waarre A development well under the final range of permeability models. The results of this work are summarised in Table 4.2.6-g. Also shown in this table are the values for well kh actually input to the full field reservoir model. Note that an intermediate value between the 80 degree and 85 degree well was used to represent an approximate 400m penetration of the Waarre A reservoir contributing to well productivity.

The table includes estimates of well kh calculated using the assumed vertical:horizontal permeability ratio (k_v/k_h) of 0.1 and also shows a downside scenario where k_v/k_h is reduced by an order of magnitude to 0.01. Note that low k_v/k_h significantly reduces the well productivity benefit associated with a high angle production well.

This impact is shown in Figure 4.2.6-h which shows the range of well productivity outcomes expected for the Waarre A development well derived from a simple sector model as a function of cumulative gas production. This works shows that at the high end of the range of permeability outcomes ("P10" model) the Waarre A producer will have an initial potential gas production rate in excess of the 90 MMscf/d Daily Contract Quantity. If the Waarre A permeability outcome is at the P90 level gas production potential is predicted to be in the range 10 – 50 MMscf/d.

Well Type	Formation Penetration	P90 Permeability Model Log Perm / 8		P50 Permeability Model Log Perm / 2		P10 Permeability Model Log Perm * 2.5	
		k_v/k_h=0.1	k_v/k_h=0.01	**k_v/k_h=0.1**	k_v/k_h=0.01	**k_v/k_h=0.1**	k_v/k_h=0.01
	m	md.ft		md.ft		md.ft	
Vertical Well	50	**650**		**2600**		**13000**	
80 degree subhorizontal well	288	**1300**	750	**5200**	3000	**26000**	15000
85 degree subhorizontal well	574	**2400**	1000	**9500**	4000	**47000**	20000
As input to reservoir model	~400	**1875**		**7500**		**37500**	

Table 4.2.6-g: Waarre A kh Inputs for Reservoir Modelling

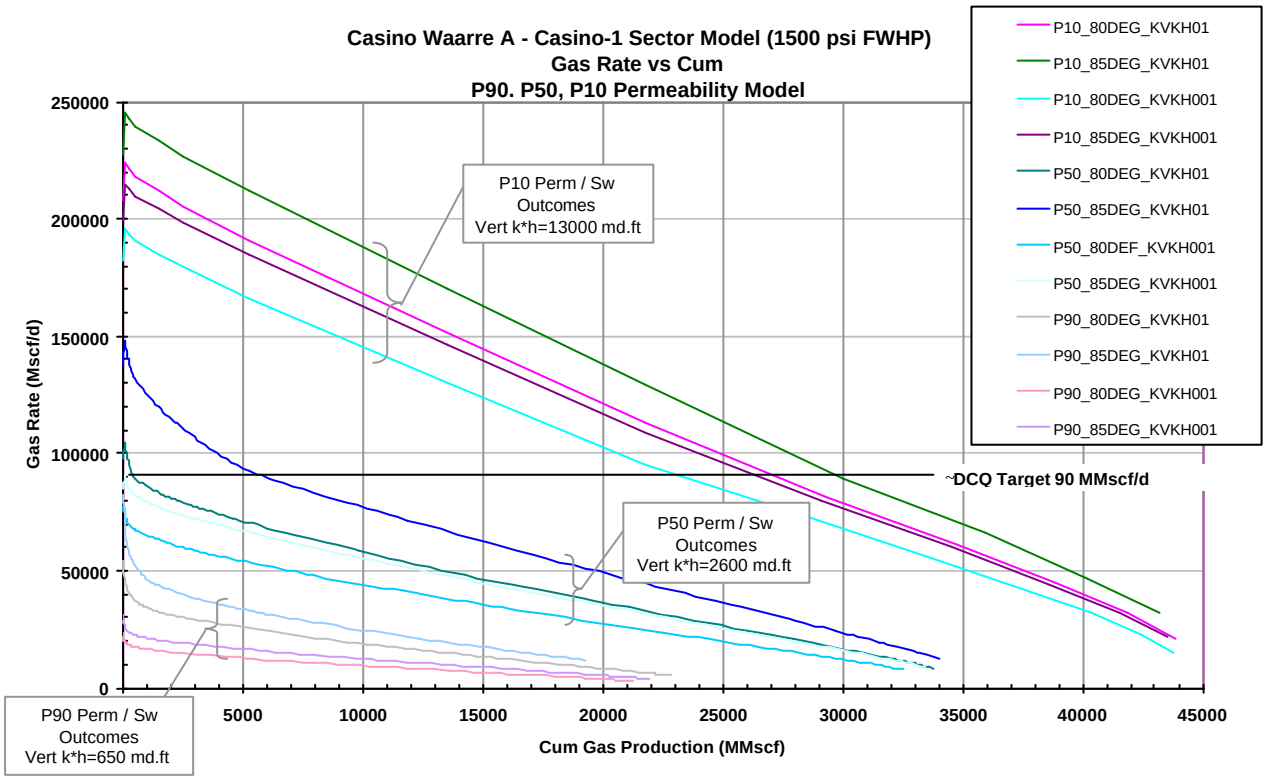

Figure 4.2.6-h: Final Sector Model results for Waarre A Development Well

Well Production Constraints

Production constraints were enabled within ECLIPSE at the well level. No water handling facilities exist at the Iona Gas Facility (apart from water of condensation) and as such the producing wells will be shut-in once free water production occurs. This case was simulated within ECLIPSE by setting a water-gas-ratio constraint of 20 bbls/mmscf. Once this constraint is exceeded the well is shut-in. If free water production does not occur throughout the life of the well, the well will reach abandonment conditions once it cannot deliver against line pressure at a rate of 2 mmscf/d.

An additional constraint was set at the field level. Once field deliverability could not meet 5 mmscf/d all remaining producing wells were shut-in. The constraint of 5 mmscf/d equates to an annual sales volumes of approximately 2 PJ. This is the minimum economic rate in order to payback annual field operating costs.

4.2.7 Recovery Factor Sensitivity Analysis.

In order to understand the main reservoir uncertainties which will impact upon recovery efficiency for the Waarre C and Waarre A reservoirs a simulation study was undertaken once model construction had taken place. Reservoir uncertainties are those parameters which we have no control over and need to address by ensuring that the possible "states of nature" are adequately modelled within the simulator. Elements that comprise the development plan eg. well number, location and type were not considered in this phase of the study as they are considered to be elements which are controllable.

All the sensitivities that were performed in this phase of the study were based on the 'base case' development scenario viz. one vertical well in the Waarre C (PRODX) and one sub-horizontal well in the Waarre A (PRODA). All producers are completed with 7" OD production tubing. The field was produced at the maximum ACQ from the TXU Term Sheet at a constant delivery pressure of 3000 kPa from RFSU. Gas is delivered to shore via a 12" multiphase pipeline.

A 'Reference Case' simulation model was constructed with what was perceived as the 'most likely' reservoir parameters at the time of the study. Refer to Enclosure 4.2.7-a for these parameters.

Enclosure 4.2.7-a summarizes the reservoir uncertainties that were addressed and the range associated with these uncertainties. From these cases a 'tornado diagram' was constructed which highlight those parameters which have a significant impact on recovery factor (RF). Refer to Figures 4.2.7-a and 4.2.7-b.

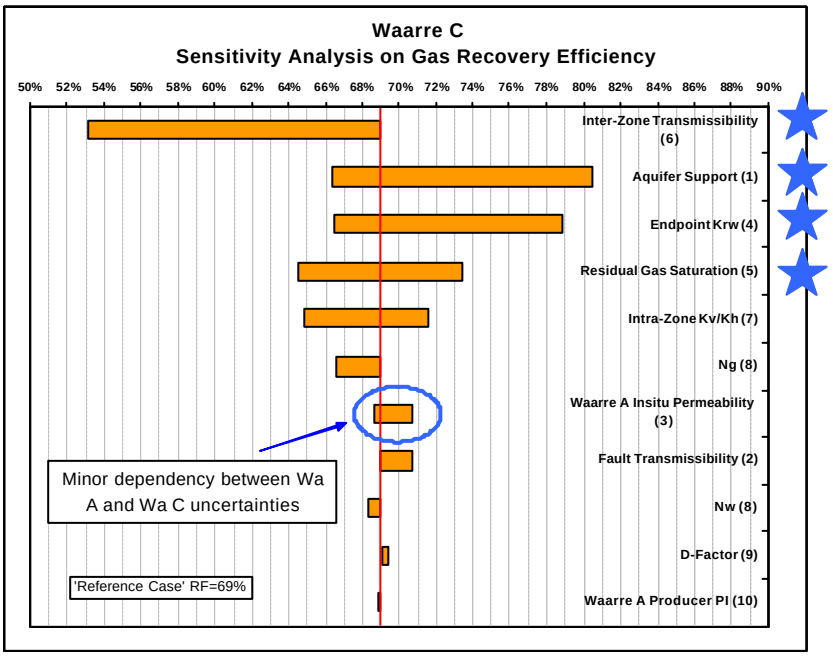

Figure 4.2.7-a: Recovery Factor "Tornado Diagram" for the Waarre C

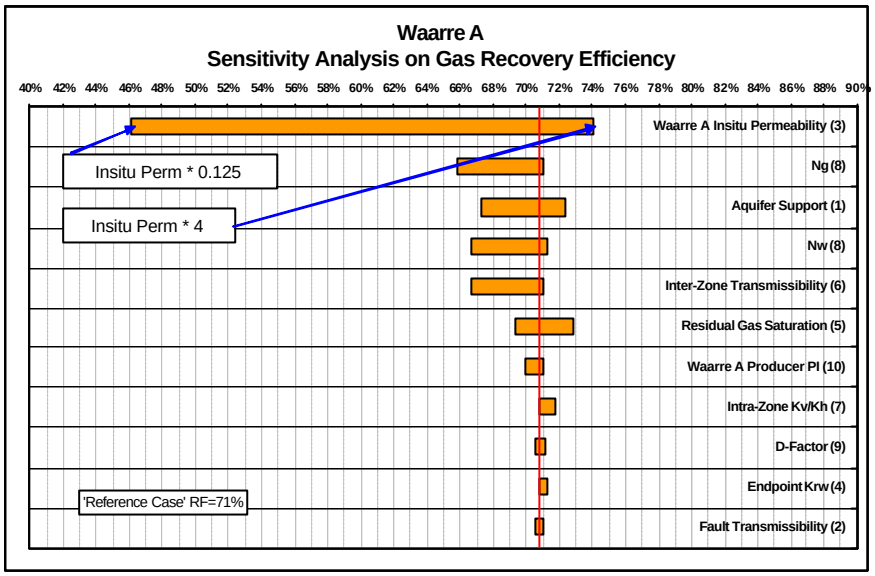

Figure 4.2.7-b: Recovery Factor "Tornado Diagram" for the Waarre A

Those parameters that were considered to have a significant impact on Waarre C RF were; "Inter-Zone" Transmissibility, aquifer pressure support, endpoint relative permeability of water (Krw') and residual gas saturation (Sgr). Of the sensitivities run, in situ permeability had the most significant impact on Waarre A RF. As illustrated in Figure 4.2.7-a there is some interdependency between the Waarre A and Waarre C RF however this is considered minor compared to the impact of uncertainty associated with the above mentioned reservoir parameters. The following is a discussion of those uncertainties that had a significant impact on Waarre C and Waarre A RFs.

"Inter-Zone' Transmissibility Barrier.

As outlined in Section 3.10, 11 reservoirs units were identified for the Waarre C and 4 units for the Waarre A. In the 'Inter-Zone' transmissibility case a non-flow or transmissibility barrier was invoked between these units within the simulator. This was implemented with the MULTZ and MULTZ- keywords. The transmissibility barrier prevented the flow of fluid in a vertical direction (both up and down). Geologically this case would most likely take the form of a laterally continuous impermeable lithology such as a shale or hardstreak. The impact of this case on RF is summarised in Table 4.2.7-a. Evident from these results is that an 'Inter-Zone' transmissibility barrier has a minor impact on Waarre A RF but has a significant impact on Waarre C RF. The impact on Waarre C RF is associated with displacement efficiency or the fraction of moveable gas displaced from the swept zone. Figure 4.2.7-c is an illustration of a cross-section through the simulation model with water saturation as the displayed property. The cross-section is a north-south slice through the layers that comprise the Waarre C. The well located at the southern end of the cross-section is the crestally located producer PRODX. This figure illustrates aquifer ingress into the Waarre C reservoir over the course of production. It is clear from this figure that the displacement front is non-uniform with water-breakthrough occurring at the PRODX well via the high permeability Lower Cb Main Pay reservoir unit. With transmissibility barriers within the Waarre C, vertical equilibrium no longer dominates the displacement process. In this instance viscous dominated flow occurs resulting in the scenario of water 'over-riding' gas. The phenomena results in poor Displacement Efficiency and hence low RF for the Waarre C. Figure 4.2.7-d is an illustration of the same cross-section presented in Figure 4.2.7-c but with the transmissibility barriers removed. In this case, vertical equilibrium dominates flow resulting in a uniform displacement front and high recovery efficiencies for the Waarre C.

An additional simulation case was run where a workover (W/O) of the well was performed once water ingress occurred. The W/O isolated the water producing interval thus permitting the well to be re-opened. The W/O improves recovery efficiency for the Waarre C from 53% to 59%.

	Reference (No 'Inter-Zone' Trans Barrier)	Inter-Zone' Trans Barrier	Inter-Zone' Trans Barrier with W/O
Waarre A Recovery Efficiency	67%	67%	67%
Waarre C Recovery Efficiency	69%	53%	59%
First Water Production at PRODX	Oct-21	Sep-16	Sep-16
PRODX Shut-In	Oct-21	Sep-16	Dec-18

Table 4.2.7-a: Summary of RF results for 'Inter-Zone' transmissibility cases.

'Inter-Zone' Transmissibility Barrier – Waarre C

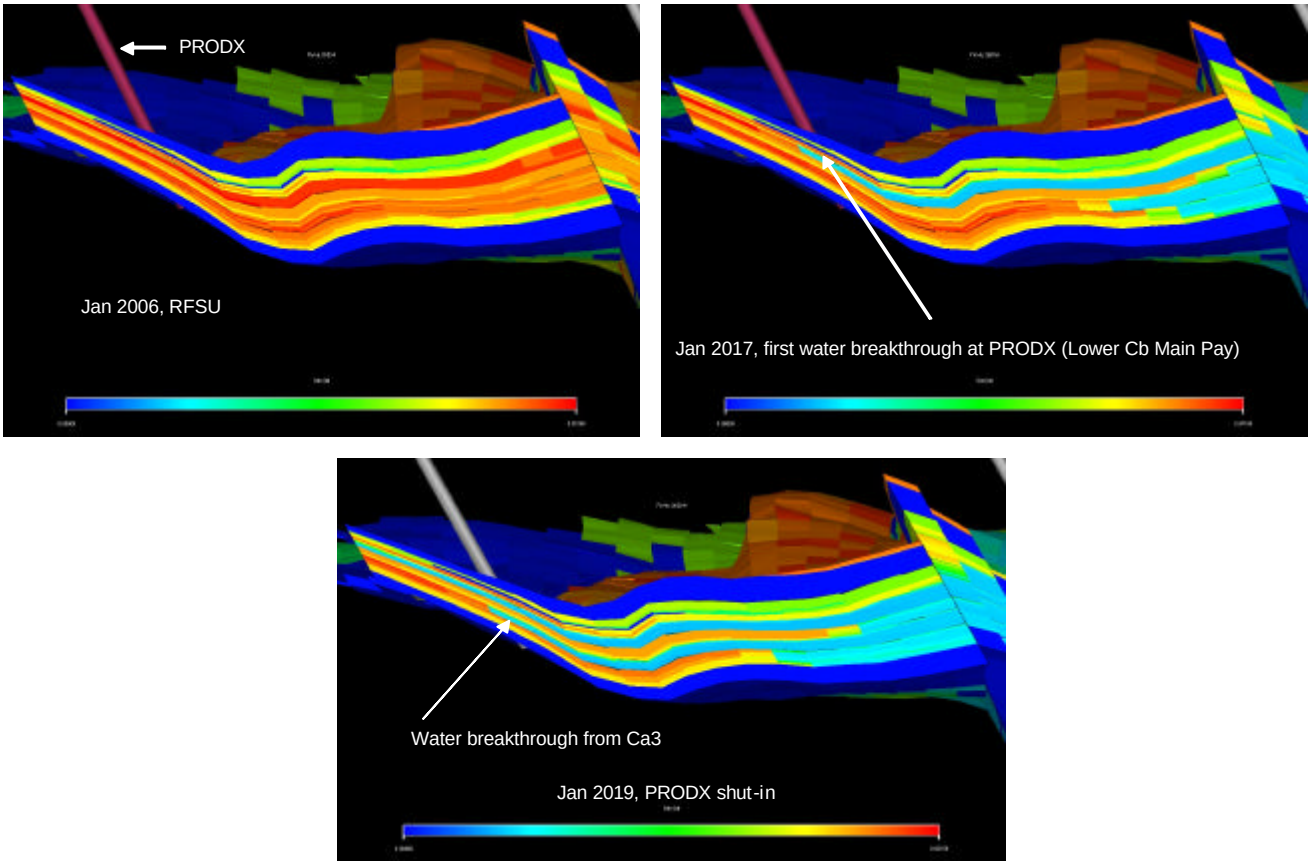

Page 8

Santos Limited ABN 80 007 550 953

Figure 4.2.7-c: Cross-section through the simulation model illustrating water ingress into the Waarre C gas reservoir over the course of production. 'Inter-Zone' Transmissibility barriers are present within the Waarre C.

No 'Inter-Zone' Transmissibility Barrier – Waarre C

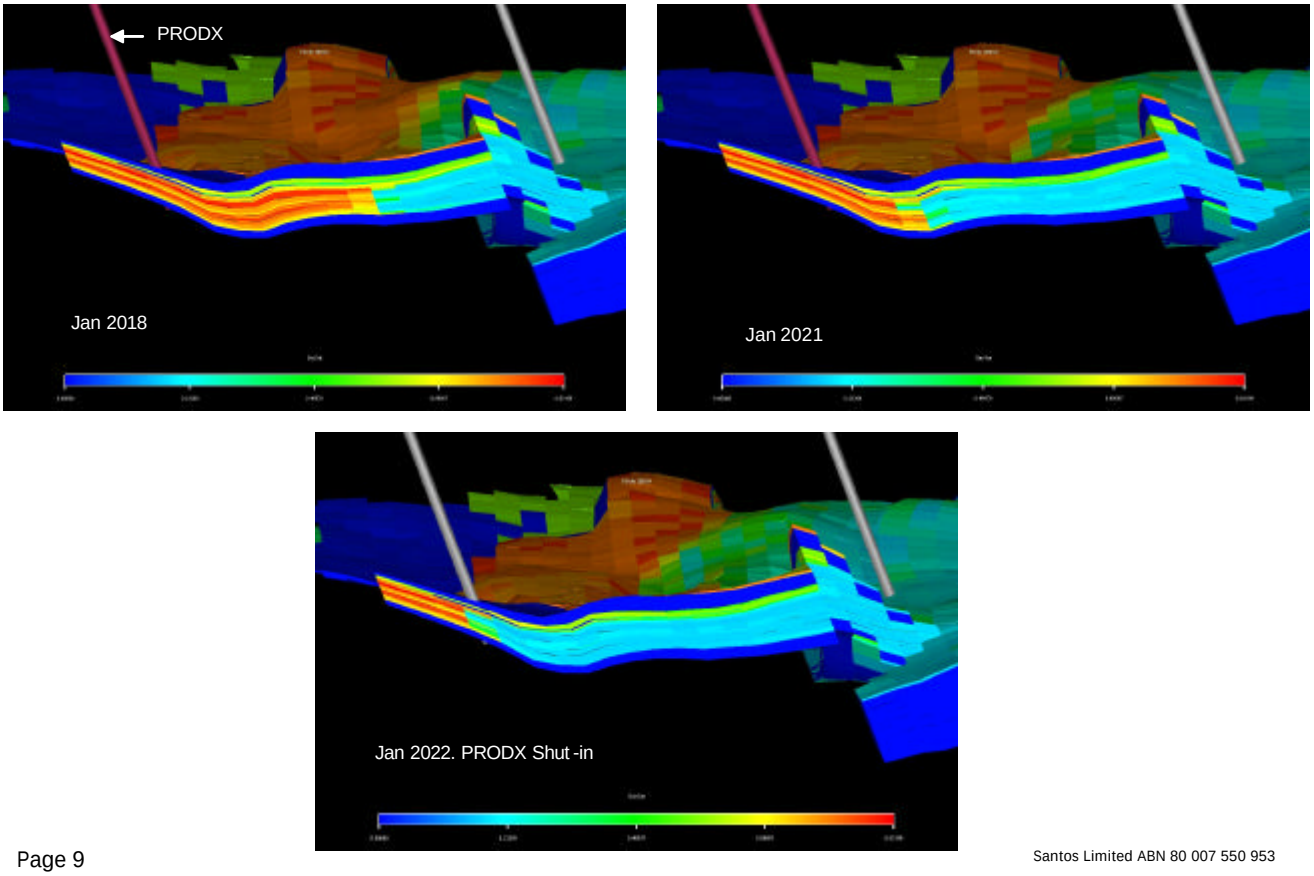

Figure 4.2.7-d: Cross-section through the simulation model illustrating water ingress into the Waarre C gas reservoir over the course of production. 'Inter-Zone' transmissibility barriers are not present within the Waarre C.

Aquifer Model

Onshore producing analogies of the Waarre sandstones in the Otway Basin exhibit aquifer pressure support. Consequently a considerable effort was undertaken in order to model the possible range of outcomes for aquifer ingress into the gas reservoir of the Casino field. Pressure support within the ECLIPSE simulation models was provided by analytical aquifers. Sensitivities were performed which assessed the impact of;

- including and excluding an analytical aquifer for the Waarre C and Waarre A reservoirs
- the type of analytical aquifer (infinite and finite) and,
- the parameters that define the analytical aquifers (thickness, permeability and influence angle).

Table 4.2.7-b summarises the results of these cases with respect to impact on Waarre C and A RFs.

	Waarre C						Waarre A	
	Reference	Case A	Case B	Case C	Case E	FAQ*	Reference	Case D
Recovery Efficiency	69%	80%	66%	69%	74%	71%	71%	71%
Analytical Aquifer	Carter-Tracy	None	Carter-Tracy	Carter-Tracy	Carter-Tracy	Fetkovich	None	Carter-Tracy
Aquifer Attached to	Attached to Main & SE Dip Closures	No analytical aquifer	Attached to Main & SE Dip Closures	Attached to Main Closure Only	Attached to Main & SE Dip Closures	Attached to Main & SE Dip Closures	No analytical aquifer	Attached to SE & Main Closures
Aquifer Volume (mmstb)	Infinite	n/a	Infinite	n/a	Infinite	42 000	n/a	Infinite
Total h (ft)	473 / 382	n/a	473 / 382	473	**215 / 145**	**417/382**	n/a	270 / 270
k (mD)	445	n/a	**890**	445	445	445	n/a	20
Radius (ft)	9000	n/a	9000	9000	9000	9000	n/a	9000
Influence Angle (deg)	45 + 18	n/a	45 + 18	**45**	45 + 18	45 + 18	n/a	45 + 18

*** Fetkovich aquifer case run on 'P50' static model. All other cases run on 'ML' static model. 'Reference Case' Aquifer run on 'P50' Model resulted in RF of 68%**

Table 4.2.7-b: Summary of analytical aquifer sensitivity cases and impact on Waarre C and Waarre A RF.

Of the Waarre C cases, the absence of an analytical aquifer results in the highest RF of 80%, compared to the analytical aquifer cases which resulted in RFs of 66% to 74%.

As described in 4.2.4 an infinite (Carter-Tracy) and finite (Fetkovich) analytical aquifers were constructed for the Waarre C. A sensitivity was run for both cases where the parameters that define the aquifers (permeability, influence angle, thickness) were not changed, but the volume of aquifer between cases was altered. In the Carter-Tracy case the volume of analytical aquifer was infinite as compared to the Fetkovich case which comprised an aquifer of 42,000 mmstb. The RF for these cases was 68% and 71% respectively. Figure 4.2.7-e and 4.2.7-f illustrate why the Fetkovich aquifer case results in an improvement in RF. Figure 4.2.7-e is a plot of rate and cumulative water influx from the analytical aquifer into the simulation grid. Within the first 2 years after production commences rate and cumulative influx for both cases is the same. However as the pressure within the finite Fetkovich aquifer declines so to does the aquifer productivity index and therefore rate and cumulative influx. Figure 4.2.7-f is an illustration of average reservoir pressure for the Lower Waarre Cb main pay. As the rate of water influx into the simulation grid for is less for the Fetkovich aquifer the degree of aquifer pressure support is also reduced compared to the infinite aquifer case. This results in lower abandonment pressures for the Waarre C and hence higher RF.

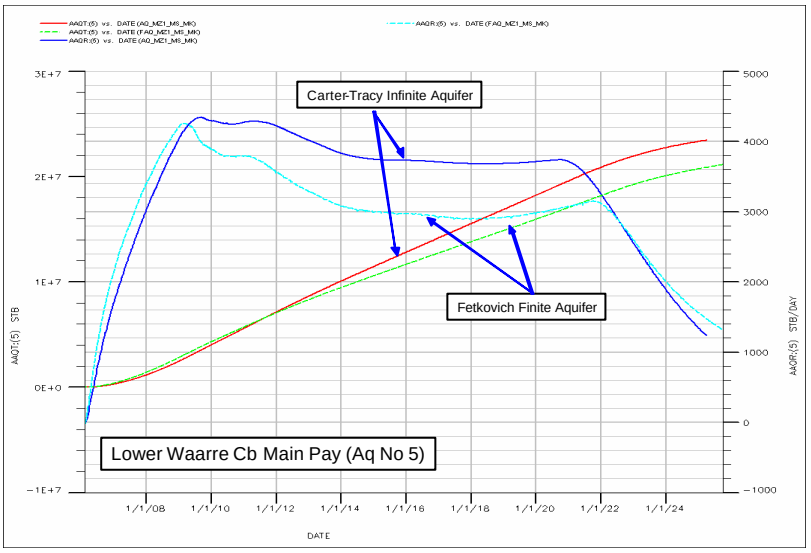

Figure 4.2.7-e: Cumulative aquifer influx and rate for the Fetkovich and Carter-Tracy analytical aquifers.

Analytical Aquifer Modelling Results

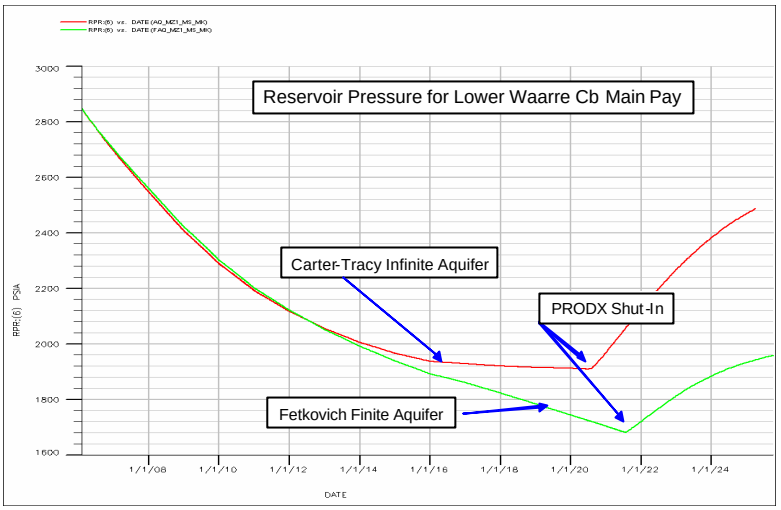

Figure 4.2.7-f: Average reservoir pressure for the Lower Waarre Cb Main Pay for the Fetkovich and Carter-Tracy analytical aquifer cases.

Waarre A RF was insensitive to the presence or absence of an analytical aquifer. In both cases volumetric depletion was the dominate drive mechanism resulting in a RF of 71%. Attaching an analytical aquifer to the Waarre A is interpreted to have an insignificant affect on RF due to the low permeability nature of the reservoir. As outlined in Section 3.13 the Waarre A comprises rock with in situ permeabilities generally within the range of 0.1 to 100 mD (with an average of approximately 20 mD). At these permeabilities water is relatively immobile resulting in minor water ingress into the Waarre A reservoir.

Relative Permeability to Water Endpoint (Krw')

Relative Permeability to water at residual gas saturation does have a significant impact for the Waarre C RF. However, as there is insignificant water movement within the Waarre A gas reservoirs, Krw' does not have an impact on Waarre A RF. Table 4.2.7-c summarises the results of the Krw' sensitivity cases with respect to Waarre A and C RF.

	Lowside Krw '(0.1)	Most Likely Krw' (0.3)	Highside Krw' (0.45)
Waarre C RF	79%	69%	66%
Waarre A RF	71%	71%	71%

Table 4.2.7-c: Summary of Krw' sensitivity bases and the impact on Waarre C and Waarre A RF.

As described in Section 4.2.3, Krw' was determined from the Casino-2 and 3 SCAL programme. The most likely Krw' value of 0.3 is based on the average of the centrifuge (air-brine) displacement tests. However as Figure 4.2.7-g illustrates there is a significant range in Krw' values measured on the core plugs depending on both rock properties and the type of test. For the purposes of this sensitivity a highside Krw' of 0.45 and lowside Krw' 0.1 was selected. The highside Krw' case results in water becoming more mobile and hence arriving early at the producer while the lowside Krw' case results in water becoming relative immobile and volumetric depletion becoming the dominate drive mechanism. The lowside Krw' scenario results in a high RF as low abandonment pressures are achieved.

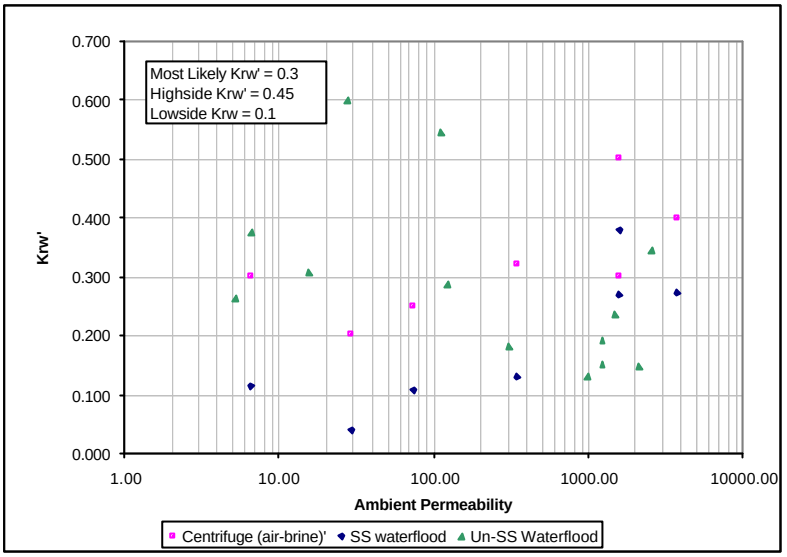

Figure 4.2.7-g: Krw' versus ambient permeability for the Casino-2 and 3 lab tests.

Residual Gas Saturation (Sgr)

As described in Section 4.2.3, there is uncertainty in remaining gas saturation. Consequently a range in Sgr was determined for the simulation modelling. The range is as follows;

- Most Likely Sgr of 18% based on the average Sgr from the steady-state tests.
- Lowside Sgr of 12% based on the average Sgr from the centrifuge tests.
- Highside Sgr of 24% based on the average Sgr from the unsteady-state tests.

Table 4.2.7-d summarises the impact that the Sgr range has on Waarre C RF. As there is no significant water ingress into the Waarre A gas reservoir, the Waarre A RF is insensitive to Sgr.

	Lowside Sgr (=12%)	Most Likely Sgr (=18%)	Highside Sgr (=24%)
Waarre C RF	73%	69%	65%
Waarre A RF	73%	71%	69%

Table 4.2.7-d: Summary of Sgr sensitivity bases and the impact on Waarre C and Waarre A RF.

Waarre A in situ Permeability

As described in Section 3.11 one of the greatest uncertainties in developing the Waarre A is the in situ permeability of the reservoir. To test the impact this uncertainty has on Waarre A RF a permeability multiplier was enabled to enhance or degrade the permeability within the grid. Table 4.2.7-e summarises the results of these cases.

	Reference	Case 3A	Case 3B	Case 3C	Case 3D	Case 3E
Description	k x 1	k x 4	k / 4	k / 2	k / 8	k / 6
Field Plateau Length	Oc-21	Sep-22	Nov-19	Dec-20	Oct-18	Mar-19
Field Abandonment	Apr-24	Oct-22	Jan-26	Jan-26	Jan-26	Jan-26
Recovery Efficiency	**71%**	**74%**	**58%**	**67%**	**46%**	**51%**

*** Note; PRODA Shutin for Case 3A as it exceeds WGR constraint**
+Design Life of Facilities is Jan-26

Table 4.2.7-e: Summary of Waarre A in situ permeability cases and there impact on Waarre A RF.

4.3 Field Reserves

4.3.1 Background

This section describes the workflow employed to reach the final estimates for the Casino field reserves. The work incorporates the results of the final field OGIP distribution described in section 3.12 and the dynamic sensitivity analysis described in Section 4.2.

The approach taken can be summarised as follows;

- Using the identified P90, P50 and P10 realisations (see Section 3.12), populate a dynamic uncertainty scenario tree for each case
- Determine the parameter weightings to be applied to each dynamic uncertainty parameter
- Combine the weighted ultimate recovery outcomes from each scenario tree into a single ultimate recovery distribution and determine the P90, P50 and P10 ultimate recovery
- Identify individual simulation cases from the respective scenario trees to provide representative deterministic cases for the P90, P50 and P10 ultimate recovery.

4.3.2 Dynamic Scenario Tree

Overview

A Scenario Tree approach has been used to combine the key dynamic uncertainties identified in Section 4.2. The scenario tree combines uncertainties in the following parameters;

- Waarre C Aquifer strength - 3 alternative case
    - No aquifer
    - Finite regional aquifer
    - Infinite aquifer
- Waarre C Interzone transmissibility – 2 alternative cases
    - Flow allowed between Waarre C zones (Interzone transmissibility = 1)
    - No Flow allowed between Waarre C zones (Interzone transmissibility = 0)
- Residual gas saturation – 3 alternative cases
    - "High" Sg_r
    - "Mid" Sg_r
    - "Low" Sg_r
- Endpoint water relative permeability at residual gas saturation – 3 alternative cases
    - "High" k_{rw}
    - "Mid" k_{rw}
    - "Low" k_{rw}
- Waarre A permeability – 3 alternative cases
    - P10 permeability model
    - P50 permeability model
    - P90 permeability model

A simple factorial combination of these uncertainties would require 162 individual cases to be run for each of the P90, P50 and P10 static models or 486 total cases! The actual number of cases run was been considerably reduced following consideration the appropriateness of various combinations of uncertainty parameters. For example, in the no aquifer case, additional uncertainty associated with parameters such as Sg_r and k_{rw} was deemed to have only minor significance so only a single "no aquifer" case was run with mid range estimates fo these parameters. Similarly, with Interzone Transmissibility set to zero, uncertainty associated with Sg_r was investigated but uncertainty associated with k_{rw} was deemed to be second order.

A further significant simplification was made possible by treating the Waarre A recovery variation associated with the uncertainty in formation permeability as independent to Waarre C recovery. While not strictly true, the degree of dependence is minor and these various simplifications allowed a reduction in the number of cases run for the P50 scenario tree from 162 down to less than 30. By using this approach, it was necessary

to run only two Waarre A sensitivity cases (a P10 permeability model case and a P90 permeability mode case) and apply incremental or decremental Waarre A gas recovery to all other Waarre C sensitivity cases.

Waarre A Sw – Permeability Dependency
It should be noted that in constructing the Scenario Trees full dependency was assumed between Waarre A water saturation uncertainty (which impacts OGIP) and Waarre A formation permeability (which impacts recovery factor). This is shown in Figure 4.3.2 – a and results in high Waarre A recovery factors being directly correlated with high Waarre A OGIP

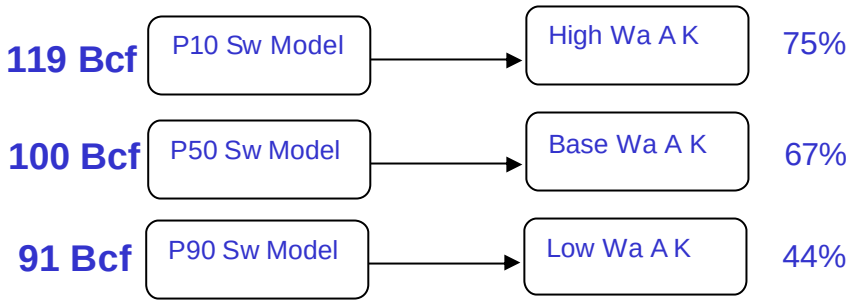

Figure 4.3.2-a: Waarre A Sw – Recovery Factor dependency

Scenario Tree

An example of the "P50" scenario tree showing how these parameters are combined can be found in Figure 4.3.2-a. Each scenario tree has a total of 75 individual cases created from a combination of the various uncertainty parameters.

The full set of scenario trees can be found in a more readable form in Enclosures 4.3.2-a, -b & -c.

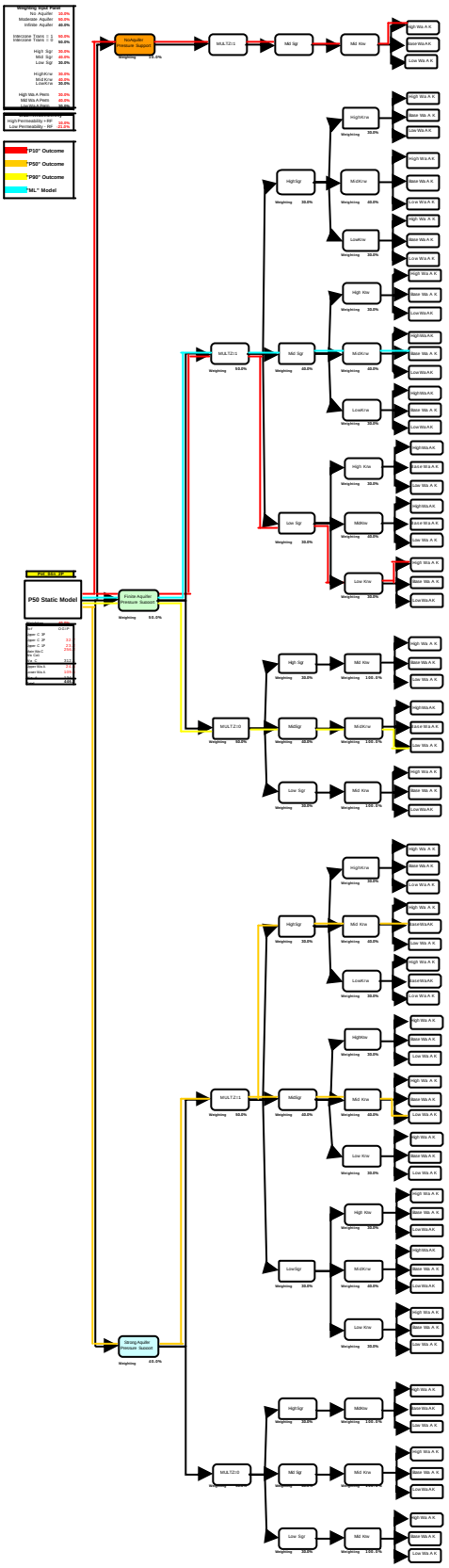

Figure 4.3.2-b: Casino P50 Scenario Tree

A further significant simplification was made with the P90 Scenario Tree by not running any cases with the finite regional aquifer and populating these results with the results from the infinite aquifer case. This is somewhat conservative as ultimate recoveries from the infinite aquifer case are slightly lower. This was considered appropriate for the P90 Case.

In the interests of time, a completely different approach was taken for the P10 Scenario Tree. For the P10 case the recovery factors for each branch of the tree were populated with the figures from the P50 scenario tree and the P10 OGIP used to back calculate ultimate recovery for each branch of the tree.

4.3.3 Parameter Weightings

This section describes the parameter weightings using to combine the 75 individual cases on each scenario tree and the 3 scenario trees into a single distribution. Careful consideration of the appropriate weightings is important as it can not be assumed all outcomes are equiprobable.

Aquifer Strength

Aquifer weighting parameters are summarised on Table 4.3.3-a. based on regional experience the "No Aquifer" case is considered unlikely and assigned a commensurately low weighting of 10%. The "Finite Regional Aquifer" provides marginally less pressure support than the "Infinite Aquifer" case and based on regional experience and a regional view of the Waarre C is considered the most likely outcome with a 50% weighting. The "Infinite Aquifer" has been given a 40% weighting and can also be considered to represent a Finite Aquifer with improved connectivity to the reservoir.

As described in Section 4.3.2 for the P90 Case, "Infinite Aquifer" has effectively been weighted at 90%.

Aquifer Strength	Weighting
No aquifer	10%
Finite regional aquifer	50%
Infinite aquifer	40%

Table 4.3.3-a: Aquifer Strength Weighting Parameters

Residual Gas Saturation, Endpoint Gas Relative Permeability and Waarre A Formation Permeability

The weighting parameters used for residual gas saturation, endpoint gas relative permeability and Waarre A formation permeability are summarised in Table 4.3.3-b. These sensitivity parameters have been combined using a 30% weighting for the downside (or P90) case, a 40% weighting for the mid (or P50) case and a 30% weighting for the upside (or P10) case.

Residual Gas Saturation	Weighting
High Sgr	30%
Mid Sgr	40%
Low Sgr	30%
Endpoint Gas Relative Permeability	
High krw	30%
Mid krw	40%
Low krw	30%
Waarre A Permeability	
P90 Permeability Model	30%
P50 Permeability Model	40%
P10 Permeability Model	30%

Table 4.3.3-b: Weighting Parameters for Sgr, Endpoint Gas Relative Permeability and Waarre A Formation Permeability

Interzone Transmissibility

The Interzone Transmissibility=0 case, while considered an unlikely outcome has been given a proportionally higher weighting (50%) than could be expected (Table 4.3.3-c). This is because this case has been used a proxy for outcomes with reduced sweep efficiency which may not be captured in the reservoir modelling conducted to date.

Interzone Transmissibility	Weighting
Interzone Transmissibility = 0	50%
Interzone Transmissibility = 1	50%

Table 4.3.3-c: Interzone Transmissibility Weighting Parameters

Static Model Realisation

The outcomes from the P90, P50 and P10 Scenario Trees have also been combined using a 30% weighting for the P90 case, a 40% weighting for P50 case and a 30% weighting for the P10 case as shown in Figure 4.3.3-d

Static Realisation	Weighting
P90 Model	30%
P50 Model	40%
P10 Model	30%

Table 4.3.3-d: Static Model Weighting Parameters

4.3.4 Field Ultimate Recovery Distribution

A purpose built spreadsheet was used to create the final field ultimate recovery distribution. Figure 4.3.4-a shows the how the outcomes from the P90, P50 and P10 scenario trees combine to give the final combined distribution shown in Figure 4.3.4-b. The individual distributions for Waarre C and Waarre A ultimate recovery can be found in Figure 4.3.4-c and 4.3.4-d. Results are summarised in Table 4.3.4-a

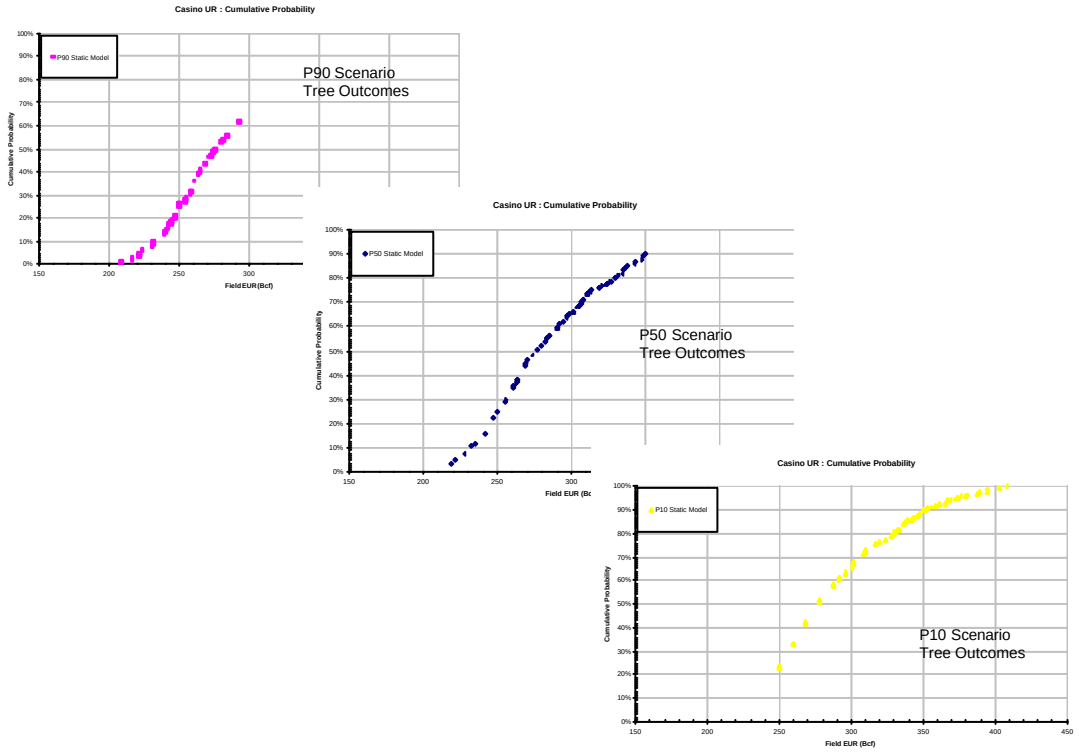

Figure 4.3.4-a: Combination of Outcomes From P90, P50 and P10 Scenario Trees

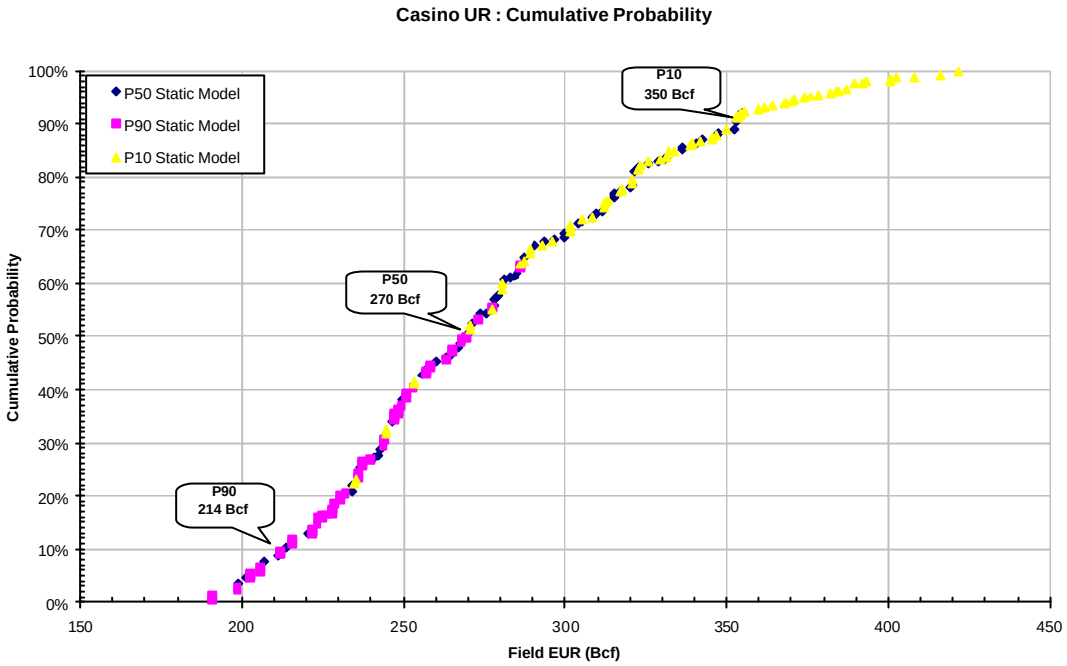

Figure 4.3.4-b: Final Casino Field Ultimate Recovery Distribution

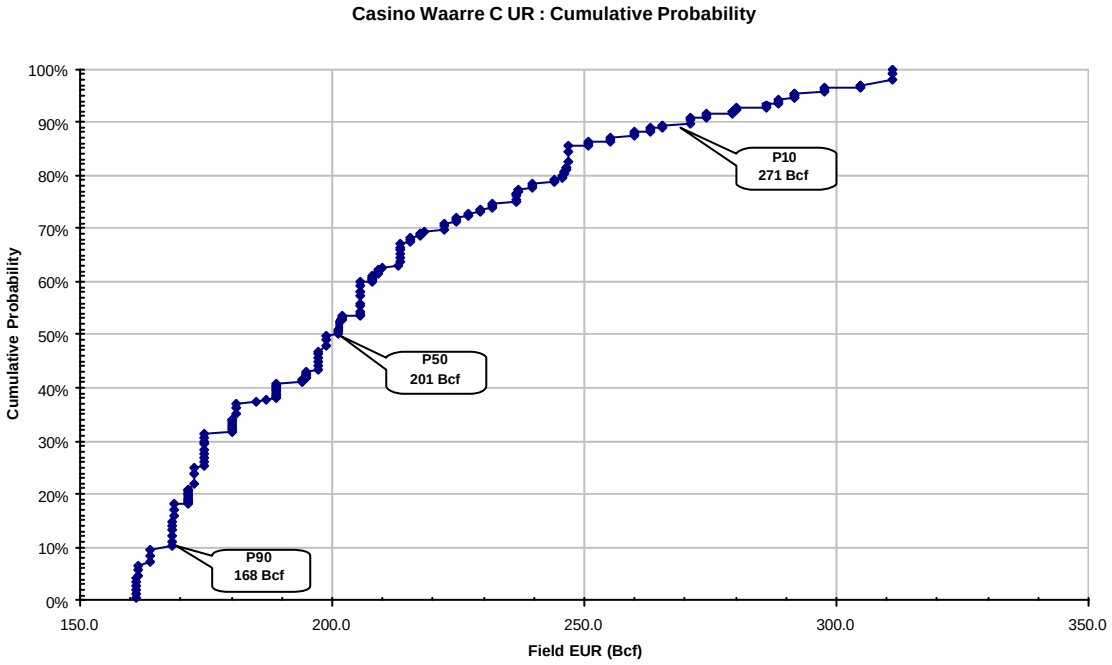

Figure 4.3.4-c: Final Casino Field Waarre C Ultimate Recovery Distribution

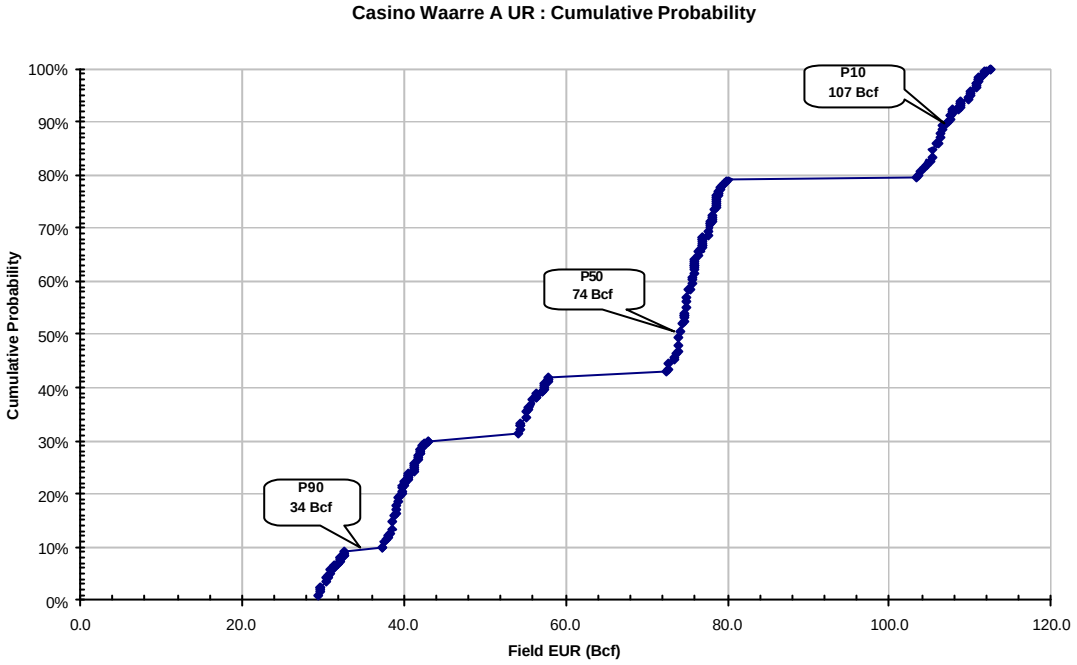

Figure 4.3.4-d: Final Casino Field Waarre A Ultimate Recovery Distribution

	P90	P50	P10	Mean
OGIP (Bcf)				
Waarre C	247	312	372	310
Waarre A	74	106	140	104
Field	**332**	**420**	**496**	**414**
Reserves (Bcf)				
Waarre C	168	201	271	208
Waarre A	34	74	107	69
Field	**214**	**270**	**350**	**277**
Field Reserves (PJ)	**220**	**277**	**359**	**284**

Table 4.3.4-a: Casino Field Reserves Summary

4.3.5 Selection of Representative P90, P50 and P10 Cases

The final stage of the reserves process was to select individual deterministic cases to represent the field P90, P50 and P10 reserve outcomes shown in Table 4.3.4-a. The selection of these particular cases is shown by the coloured bands on the respect scenario trees (Enclosures 4.3.2-a, -b & -c). Note that different combinations of reserves uncertainty parameters can give a similar reserves outcome. For example, a P90 type reserves outcome can be obtained with the P50 OGIP model but an unfavourable combination of other parameters. Similarly, a P10 type reserves outcome can also be obtained with the P50 OGIP model but with no aquifer support in the Waarre C.

Three individual cases were initially chosen to represent the P90 case, two were chosen for the P50 and three were chosen to represent the P10. The details of these cases are summarised in Table 4.3.5-a.

	Case	ECLIPSE Model	OGIP Model	Aquifer	Interzone Trans	Sgr	Krw	Waarre A Perm	Recovery Efficiency			Ultimate Recovery		
									Wa C	Wa A	Field	Wa C	Wa A	Field
P90 UR	1	AQ_MZ0_HS_MK	P90	Infinite	0	High	Mid	Mid	65	64	64	**161**	**70**	**232**
230 Bcf	2	AQ_MZ1_MS_HK_LLPERM	P90	Infinite	1	Mid	High	Low	75	47	66	**186**	**51**	**237**
	3	FAQ_MZ0_MS_MK_LLPERM	P50	Finite	0	Mid	Mid	Low	57	44	53	**179**	**60**	**239**
P50 UR	1	AQ_MZ1_HS_HK	P50	Infinite	1	High	High	Mid	62	66	63	**194**	**90**	**284**
280 Bcf	2	AQ_MZ1_MS_MK_LLPERM	P50	Infinite	1	Mid	Mid	Low	70	47	63	**218**	**65**	**283**
ML UR	1	FAQ_MZ1_MS_MK	P50	Finite	1	Mid	Mid	Mid	71	67	70	**223**	**92**	**315**
314 Bcf														
P10 UR	1	FAQ_MZ1_LS_LK_HPERM	P50	Finite	1	Low	Low	High	77	80	78	**241**	**110**	**351**
350 Bcf	2	NOAQ_MZ1_MS_MK_HPERM	P50	None	1	Mid	Mid	High	79	78	79	**247**	**107**	**354**
	3	FAQ_MZ1_MS_MK	P10	Finite	1	Mid	Mid	Mid	68	65	68	**255**	**89**	**344**

Table 4.3.5-a: Deterministic Cases Investigated to Represent P90, P50 and P10 Outcomes

The production profiles from the 3 different P90 cases investigated (Figure 4.3.5-a) show that despite the different ways the cases are created the production outcomes are very similar.

Examples of P50 and P10 production profiles can be found in Figures 4.3.5-b and 4.3.5-c.

The final cases chosen to provide representative deterministic cases for development planning work were as follows;

- P90 P90 Case 1 (P90M1)
- P50 P50 Case 1 (P50M1)
- P10 P10 Case 3. (P10M3)

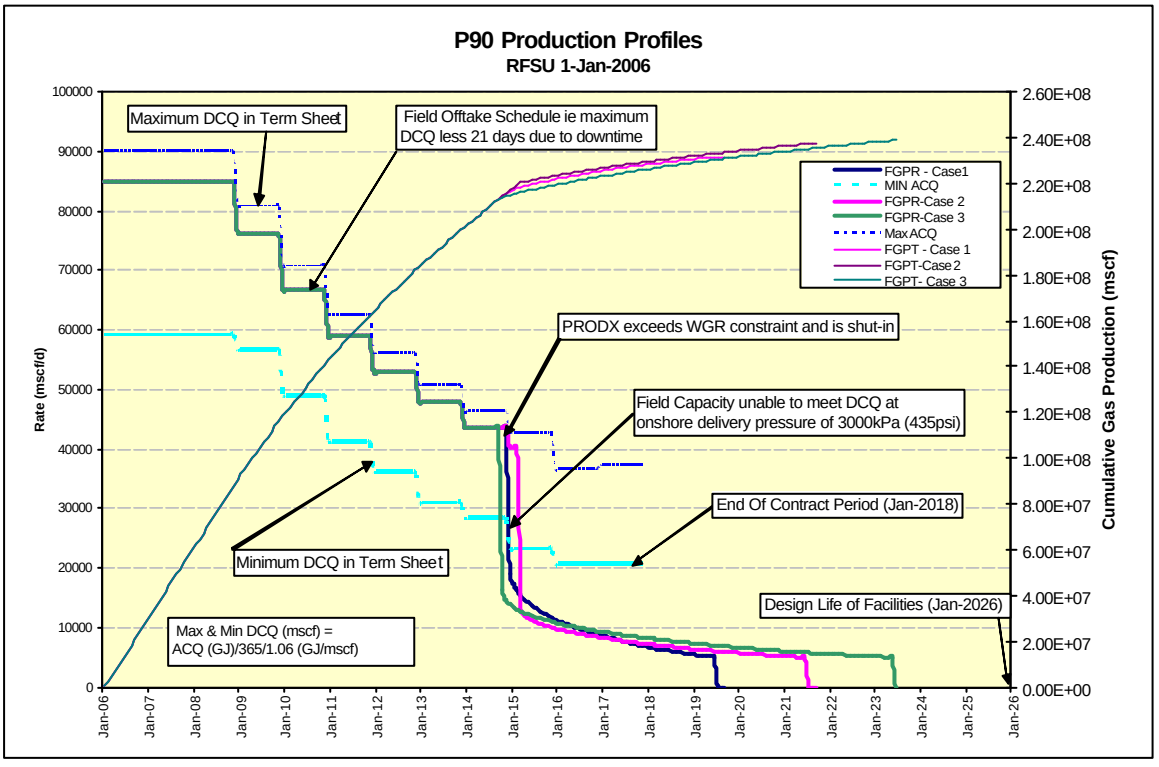

Figure 4.3.5-a: Alternate P90 Realisations

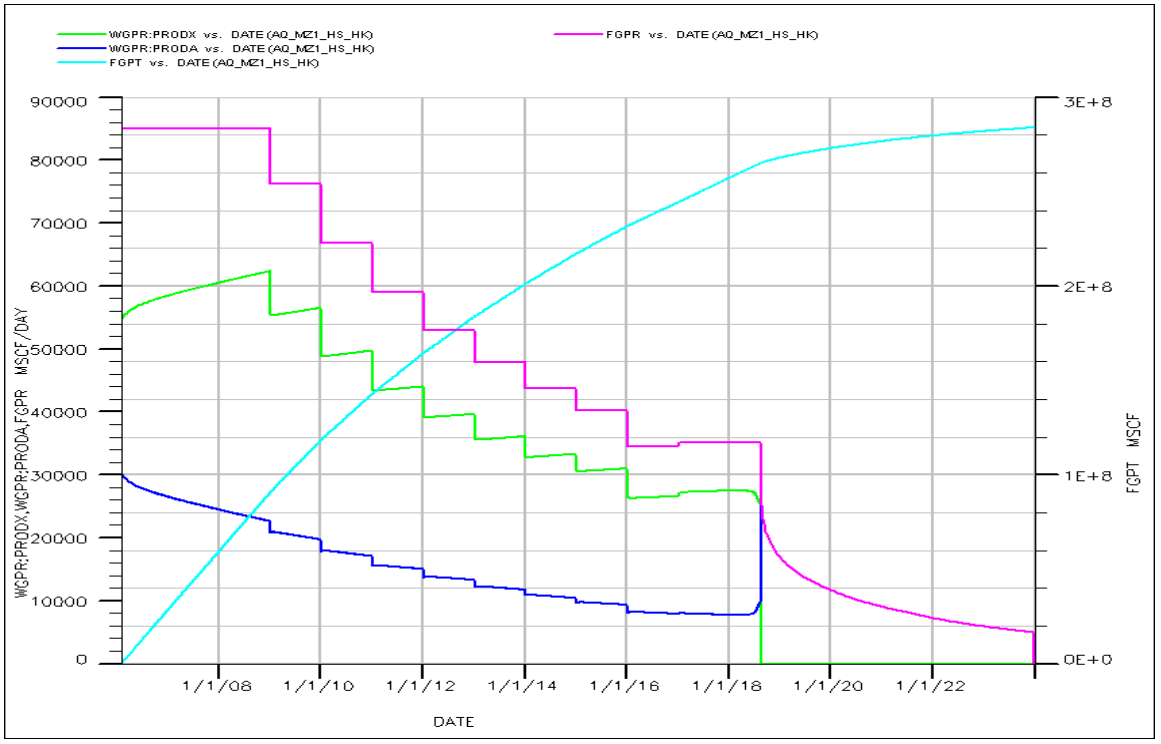

Figure 4.3.5-b: P50 Production Forecast (P50 Case 1)

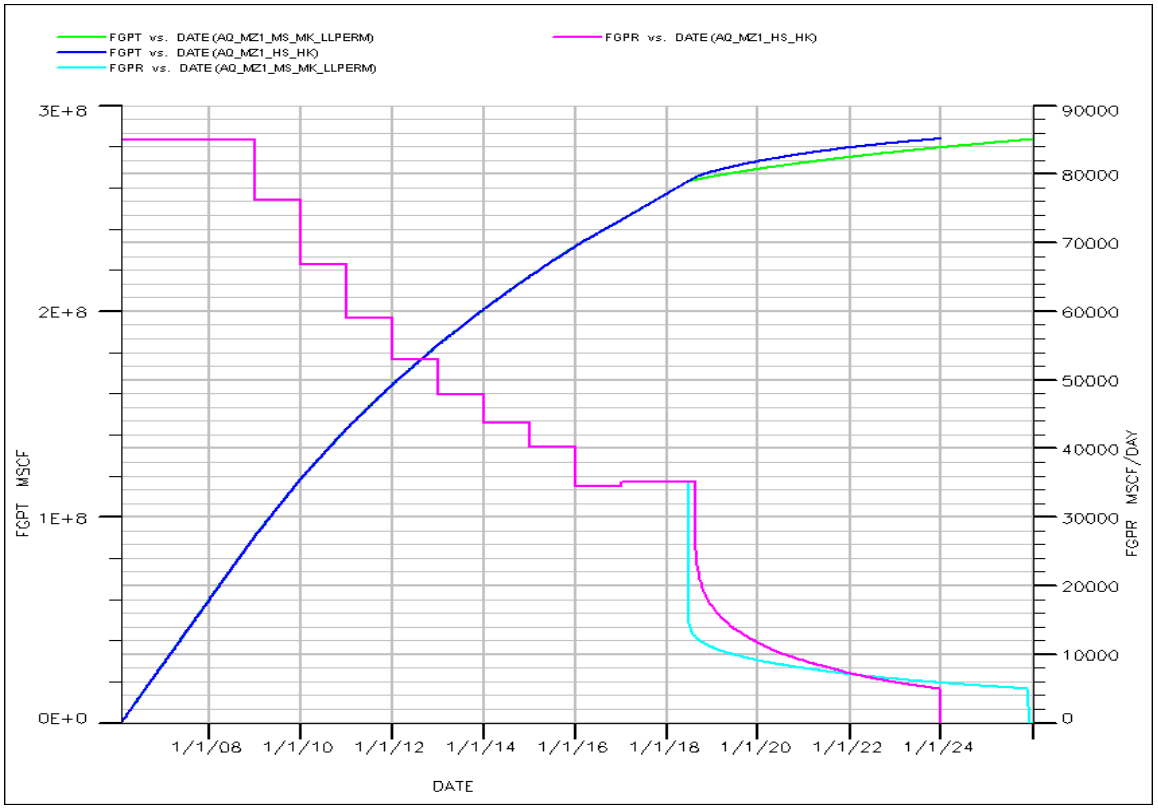

Figure 4.3.5-c: Alternate P50 Realisations

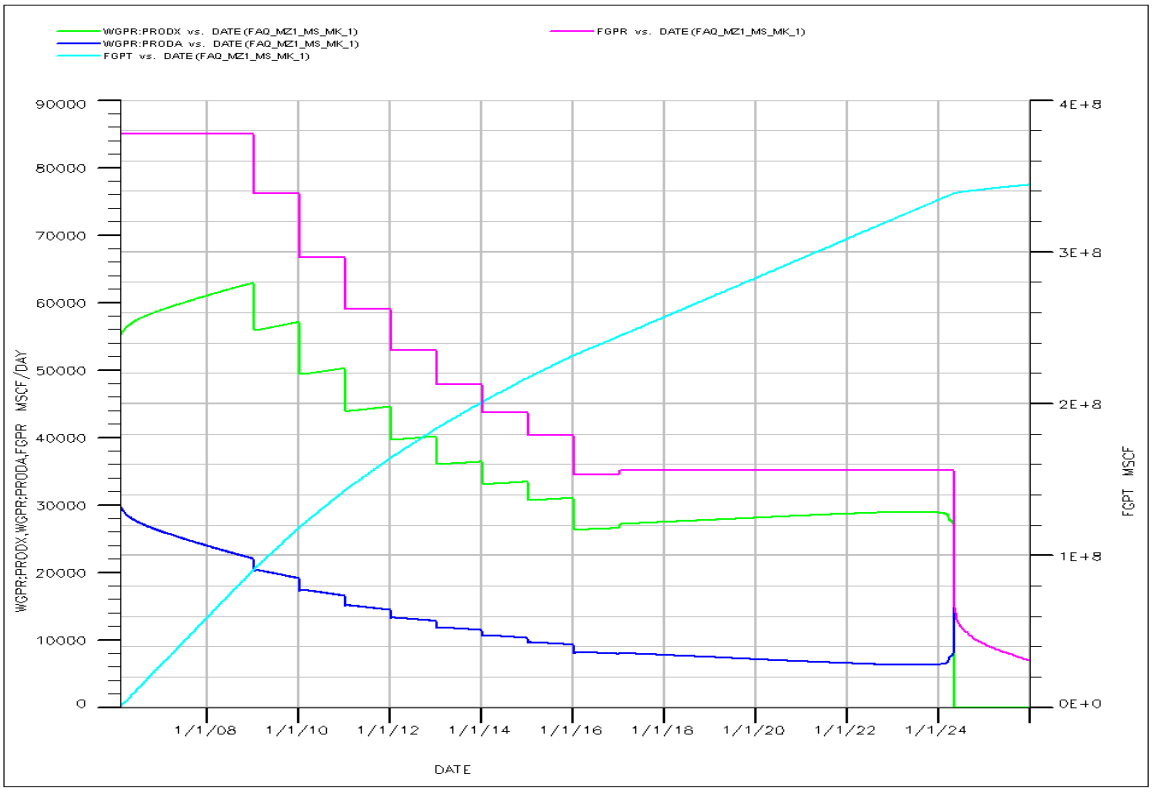

Figure 4.3.5-d: P10 Production Forecast (P10 Case 3)

4.3.6 Final Production Profile Summary

The field P90, P50 and P10 profiles for production under the Term Sheet are summarised in Figure 4.3.6-a below. A summary of annual quantities can be found in Table 4.3.6-a. It should be noted that all these profiles are based on a first gas date of 1 February, 2006.

Negotiations currently in progress may result in a final commercial outcome where as much Casino gas as possible is sold on an extended plateau. Production profiles under this scenario can be found in Figure 4.3.6-b and Table 4.3.6-b.

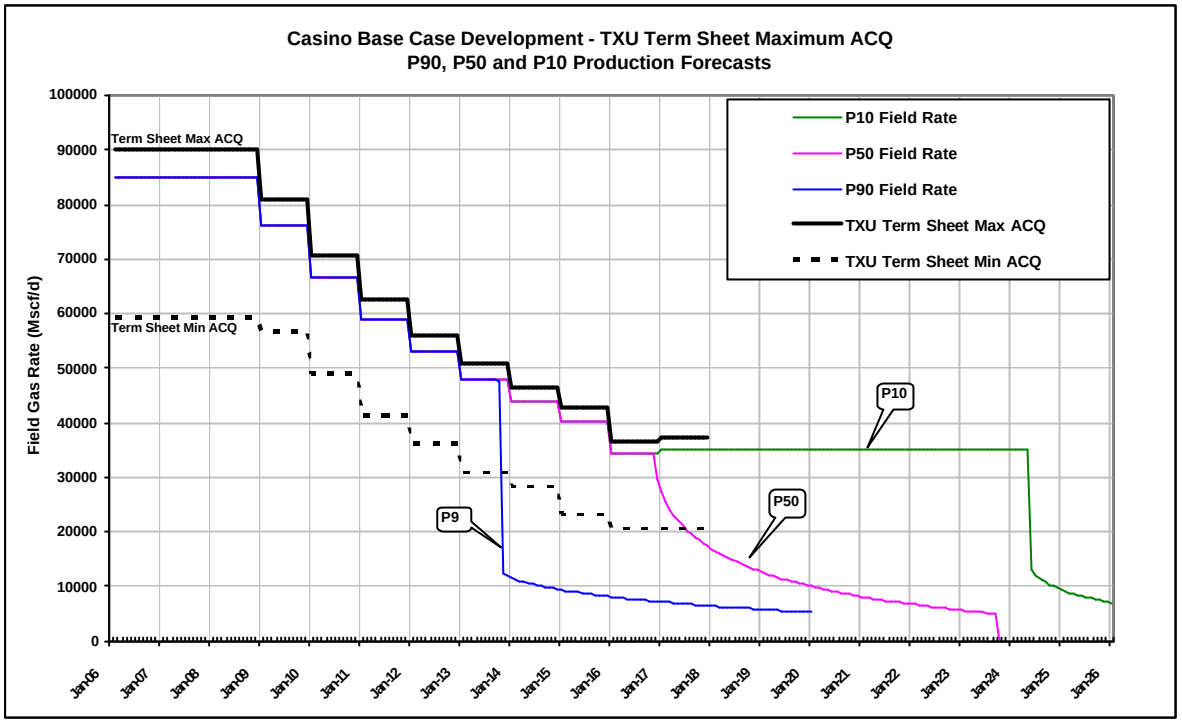

Figure 4.3.6-a: Casino Field Production Forecasts – Term Sheet

	FIELD P90					FIELD P50					FIELD P10				
	Annual Raw Gas		Annual Fuel Gas	Annual Sales Gas	Annual Cond	Annual Raw Gas		Annual Fuel Gas	Annual Sales Gas	Annual Cond	Annual Raw Gas		Annual Fuel Gas	Annual Sales Gas	Annual Cond
	Bcf	PJ	PJ	PJ	kstb	Bcf	PJ	PJ	PJ	kstb	Bcf	PJ	PJ	PJ	kstb
Dec-06	28.5	30.3	1.2	29.1	29.1	28.5	30.3	1.2	29.1	29.1	28.5	30.3	1.2	29.1	29.1
Dec-07	31.0	33.0	1.3	31.7	31.7	31.0	33.0	1.3	31.7	31.7	31.0	33.0	1.3	31.7	31.7
Dec-08	31.1	33.1	1.3	31.7	31.7	31.1	33.1	1.3	31.7	31.7	31.1	33.1	1.3	31.7	31.7
Dec-09	27.8	29.6	1.2	28.4	28.4	27.8	29.6	1.2	28.4	28.4	27.8	29.6	1.2	28.4	28.4
Dec-10	24.4	25.9	1.0	24.9	24.9	24.4	25.9	1.0	24.9	24.9	24.4	25.9	1.0	24.9	24.9
Dec-11	21.5	22.9	0.9	22.0	22.0	21.5	22.9	0.9	22.0	22.0	21.5	22.9	0.9	22.0	22.0
Dec-12	19.4	20.6	0.8	19.8	19.8	19.4	20.6	0.8	19.8	19.8	19.4	20.6	0.8	19.8	19.8
Dec-13	14.5	15.5	0.6	14.8	14.8	17.5	18.6	0.7	17.8	17.8	17.5	18.6	0.7	17.8	17.8
Dec-14	3.7	4.0	0.2	3.8	3.8	15.9	16.9	0.7	16.2	16.2	15.9	17.0	0.7	16.3	16.3
Dec-15	3.1	3.3	0.1	3.2	3.2	14.7	15.6	0.6	15.0	15.0	14.7	15.6	0.6	15.0	15.0
Dec-16	2.8	2.9	0.1	2.8	2.8	12.9	13.7	0.5	13.2	13.2	12.6	13.4	0.5	12.9	12.9
Dec-17	2.4	2.6	0.1	2.5	2.5	7.4	7.9	0.3	7.6	7.6	12.8	13.7	0.5	13.1	13.1
Dec-18	2.2	2.3	0.1	2.2	2.2	5.3	5.6	0.2	5.4	5.4	12.8	13.7	0.5	13.1	13.1
Dec-19	2.0	2.1	0.1	2.0	2.0	4.0	4.3	0.2	4.1	4.1	12.8	13.7	0.5	13.1	13.1
Dec-20	0.0	0.0	0.0	0.0	0.0	3.3	3.5	0.1	3.3	3.3	12.9	13.7	0.5	13.2	13.2
Dec-21	0.0	0.0	0.0	0.0	0.0	2.7	2.8	0.1	2.7	2.7	12.8	13.7	0.5	13.1	13.1
Dec-22	0.0	0.0	0.0	0.0	0.0	2.2	2.4	0.1	2.3	2.3	12.8	13.7	0.5	13.1	13.1
Dec-23	0.0	0.0	0.0	0.0	0.0	1.3	1.4	0.1	1.3	1.3	12.8	13.7	0.5	13.1	13.1
Dec-24	0.0	0.0	0.0	0.0	0.0	0.0	0.0	0.0	0.0	0.0	7.0	7.4	0.3	7.1	7.1
Dec-25	0.0	0.0	0.0	0.0	0.0	0.0	0.0	0.0	0.0	0.0	2.9	3.1	0.1	3.0	3.0
Total	**214.4**	**228.1**	**9.1**	**219.0**	**219.0**	**270.7**	**287.9**	**11.5**	**276.4**	**276.4**	**344.2**	**366.1**	**14.6**	**351.5**	**351.5**

Table 4.3.6-a: Casino Field Production Profiles (1 Feb 2006 First Gas)

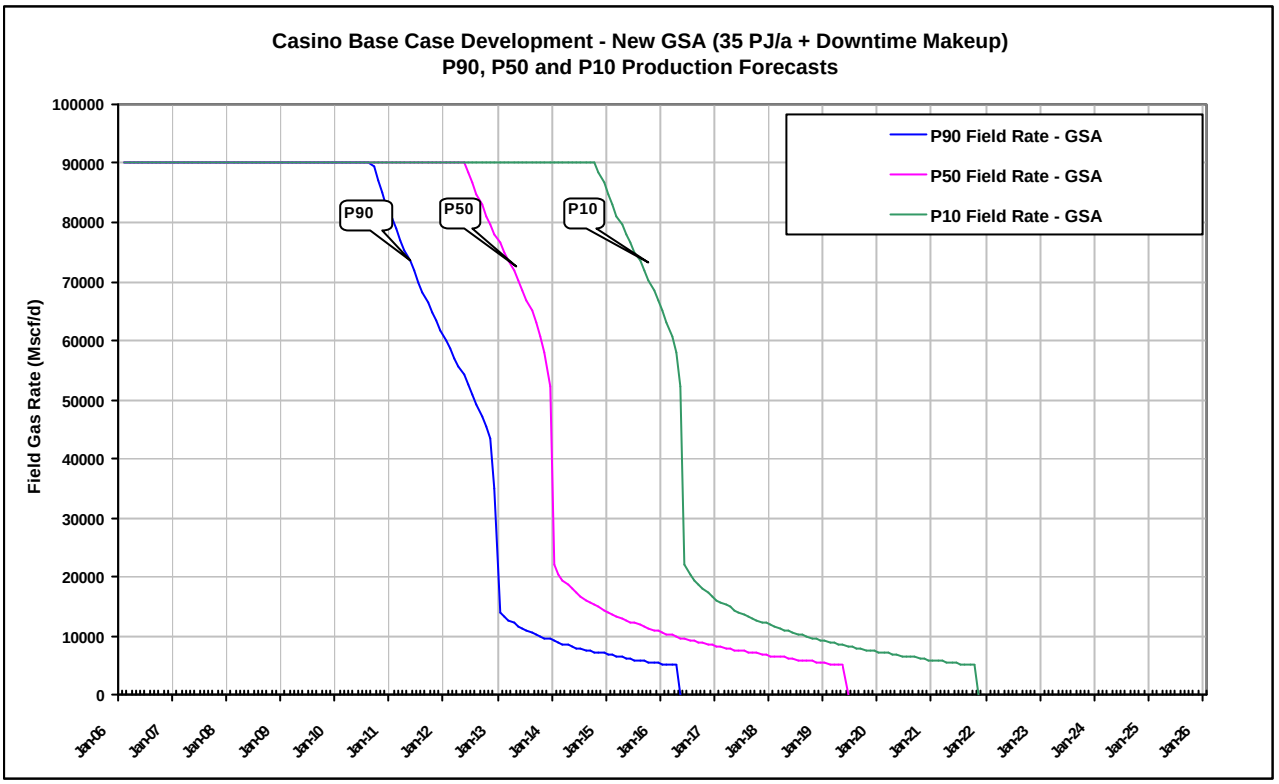

Figure 4.3.6-b: Casino Field Production Forecasts – Extended Plateau

	FIELD P90					FIELD P50					FIELD P10				
	Annual Raw Gas		Annual Fuel Gas	Annual Sales Gas	Annual Cond	Annual Raw Gas		Annual Fuel Gas	Annual Sales Gas	Annual Cond	Annual Raw Gas		Annual Fuel Gas	Annual Sales Gas	Annual Cond
	Bcf	PJ	PJ	PJ	kstb	Bcf	PJ	PJ	PJ	kstb	Bcf	PJ	PJ	PJ	kstb
Dec-06	30.1	32.0	1.3	30.7	30.7	30.1	32.0	1.3	30.7	30.7	30.2	32.1	1.3	30.8	30.8
Dec-07	33.0	35.1	1.4	33.7	33.7	33.0	35.1	1.4	33.7	33.7	32.9	35.0	1.4	33.6	33.6
Dec-08	32.9	35.0	1.4	33.6	33.6	32.9	35.0	1.4	33.6	33.6	32.9	35.0	1.4	33.6	33.6
Dec-09	32.9	35.0	1.4	33.6	33.6	32.9	35.0	1.4	33.6	33.6	33.0	35.1	1.4	33.7	33.7
Dec-10	32.3	34.3	1.4	33.0	33.0	32.9	35.0	1.4	33.6	33.6	32.9	35.0	1.4	33.6	33.6
Dec-11	25.7	27.3	1.1	26.2	26.2	33.0	35.1	1.4	33.7	33.7	32.9	35.0	1.4	33.6	33.6
Dec-12	17.7	18.8	0.8	18.1	18.1	31.2	33.2	1.3	31.9	31.9	32.9	35.0	1.4	33.6	33.6
Dec-13	4.0	4.3	0.2	4.1	4.1	23.7	25.2	1.0	24.2	24.2	33.0	35.1	1.4	33.7	33.7
Dec-14	2.9	3.1	0.1	2.9	2.9	6.2	6.6	0.3	6.3	6.3	32.7	34.7	1.4	33.4	33.4
Dec-15	2.2	2.3	0.1	2.2	2.2	4.4	4.7	0.2	4.5	4.5	27.4	29.1	1.2	27.9	27.9
Dec-16	0.5	0.5	0.0	0.5	0.5	3.4	3.6	0.1	3.5	3.5	12.5	13.3	0.5	12.8	12.8
Dec-17	0.0	0.0	0.0	0.0	0.0	2.7	2.9	0.1	2.8	2.8	5.0	5.4	0.2	5.1	5.1
Dec-18	0.0	0.0	0.0	0.0	0.0	2.2	2.3	0.1	2.2	2.2	3.8	4.0	0.2	3.9	3.9
Dec-19	0.0	0.0	0.0	0.0	0.0	0.8	0.8	0.0	0.8	0.8	3.0	3.2	0.1	3.0	3.0
Dec-20	0.0	0.0	0.0	0.0	0.0	0.0	0.0	0.0	0.0	0.0	2.4	2.5	0.1	2.4	2.4
Dec-21	0.0	0.0	0.0	0.0	0.0	0.0	0.0	0.0	0.0	0.0	1.6	1.7	0.1	1.7	1.7
Dec-22	0.0	0.0	0.0	0.0	0.0	0.0	0.0	0.0	0.0	0.0	0.0	0.0	0.0	0.0	0.0
Dec-23	0.0	0.0	0.0	0.0	0.0	0.0	0.0	0.0	0.0	0.0	0.0	0.0	0.0	0.0	0.0
Dec-24	0.0	0.0	0.0	0.0	0.0	0.0	0.0	0.0	0.0	0.0	0.0	0.0	0.0	0.0	0.0
Dec-25	0.0	0.0	0.0	0.0	0.0	0.0	0.0	0.0	0.0	0.0	0.0	0.0	0.0	0.0	0.0
Total	214.1	227.8	9.1	218.7	218.7	269.4	286.5	11.5	275.1	275.1	349.0	371.3	14.9	356.5	356.5

Table 4.3.6-b: Casino Field Production Profiles - Extended Plateau (1 Feb 2006 First Gas)

4.4 Development Planning

4.4.1 Export Pipeline Sizing Discussion

A nodal analysis study was performed to determine the optimal pipeline size for the export line from the Casino field to the inlet at the Iona Gas Facility. The pipeline route and elevation is illustrated in Figure 4.4.1-a. Vertical Lift Tables were built for the 12" and 14" pipelines and integrated within the ECLIPSE Network option. Refer to Chapter 4.2 for a description of the construction of the production network model within ECLIPSE. The field offtake rate in the forecasts was at a nominal plateau rate of 50PJ/a, which is considered to be the initial market capacity. The initial delivery pressure at the Iona Gas Facility is 9000 kPa which falls to 3000 kPa once field deliverability cannot meet DCQ. Figure 4.4.1-b is an illustration of field rate and delivery pressure for the 12" and 14" pipeline cases. Evident from the figure is the minor extension of plateau length for the 14" case compared to the 12" case. Similarly the requirement for boost compression is deferred by several months for the 14" case.

Figure 4.4.1-c illustrates the inflow performance of the respective pipelines. These inflow performance plots were generated within the nodal analysis package PROSPER. The pressure loss along the pipelines is similar for the 12" and 14" pipeline OD cases expect in very high offtake rates (i.e. > 140 mmscf/d). This observation supports the results from the ECLIPSE modelling effort i.e. the 14" onshore/offshore pipeline does not add any significant plateau length to field rate nor defer the requirement for boost compression.

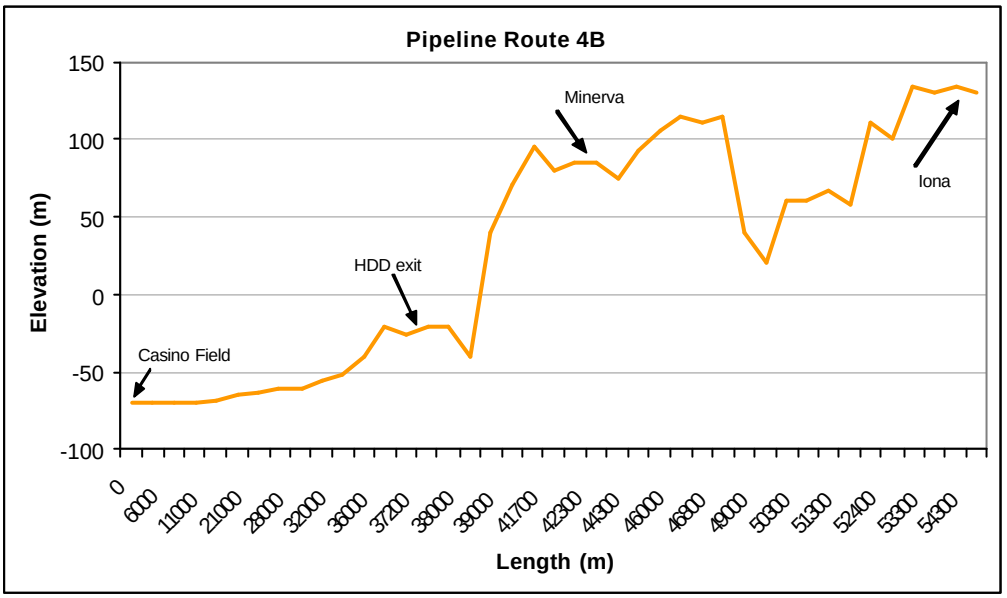

Figure 4.4.1-a: Offshore and Onshore Pipeline elevations and lengths

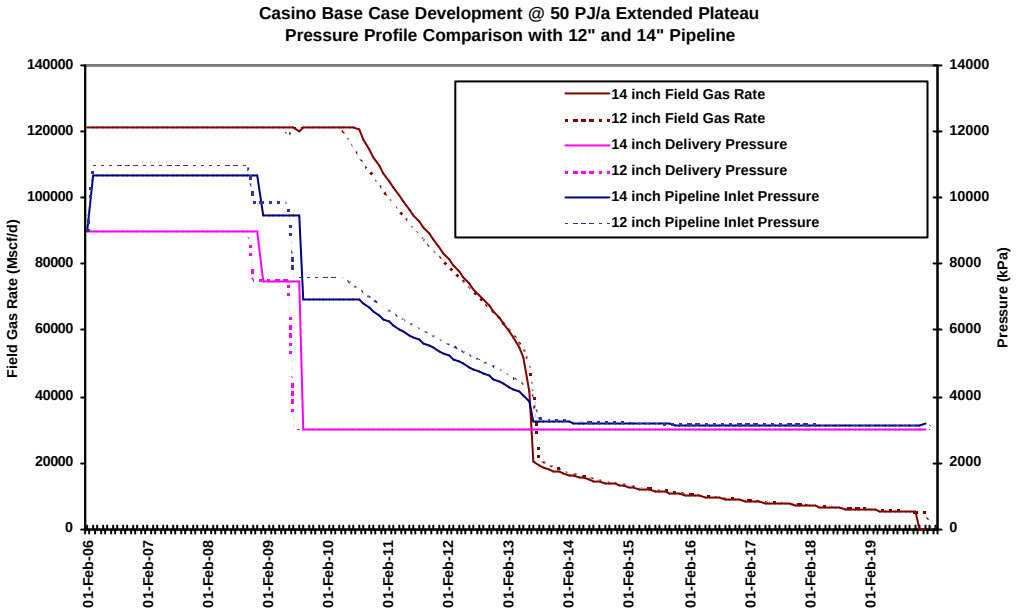

Figure 4.4.1-b: Eclipse forecast for 'Base Case' Development at 50 PJ/a. Sensitivity to pipeline size, 12" and 14" OD.

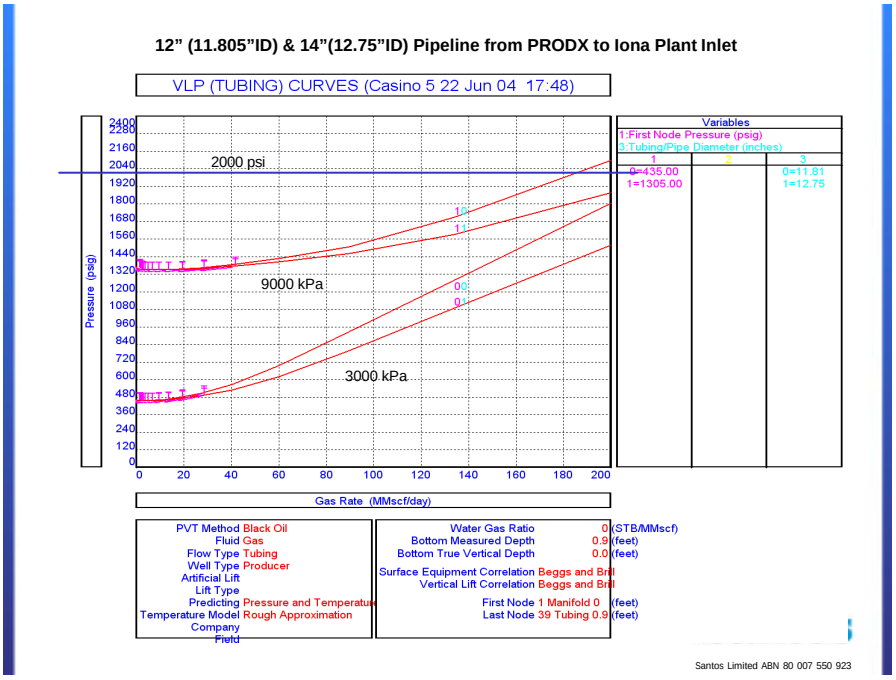

Figure 4.4.1-c: Inflow performance of 12" and 14" export pipelines at a delivery pressure of 3000 kPa and 9000 kPa. Maximum Allowable Operating Pressure (MAP) is 2000 psia.

4.4.2 Tubing Size Selection Discussion

Tubing size selection was based on a well performance modelling study. The results of the study indicated that the productivity of the development wells will benefit from a large tubing size. This increase in well productivity extends the plateau length of field rate and may also defer the requirement for boost compression. A tubing OD of 7" (6.18" ID) was selected for the proposed completion design for both the Waarre A and Waarre C development wells.

Well inflow and vertical flow performance was modelled using Petroleum Expert's nodal analysis package, PROSPER. The proposed development wells included in the study were the Waarre C producers, PRODX and PRODY, and the Waarre A producer, PRODA. The conceptual well design for the Waarre C producers comprised vertical wells with a 30m openhole section completed with Expandable Sand Screens (ESS). The Waarre A producer, PRODA, is a sub-horizontal well with 400-500m of openhole section completed with wire-wrapped sand screens. Refer to Section 5 for a further discussion of completion design for the proposed Casino Development wells.

The IRP model selected for the Waarre C producers was the Petroleum Experts model. The Petroleum Experts inflow option uses a multi-phase pseudo pressure function to allow for changing gas and condensate saturations around the wellbore. It assumes that no condensate banking occurs and that all the condensate that drops out is produced. Transient effects on P.I. are accounted for.

The inputs into the inflow performance model for PRODX and PRODA are summarised in Table 4.4.2-a below.

	PRODX and PRODY
IPR Model	Petroleum Experts
Reservoir Permeability (mD)	465
Reservoir thickness (ft)	100
Production Interval (ft)	100
Wellbore Radius (ft)	0.354
Dietz Shape Factor	0.304481
Drainage Area (acres)	1000
Reservoir Porosity (v/v)	0.2
Connate Water Saturation (v/v)	0.2
Non-Darcy Flow Factor, D (mscf/day-1)	3.81E-05
Mechanical Skin	2

Table 4.4.2-a: Inputs into the IPR model for PRODX and PRODY.

Reservoir permeability for the Waarre C producers, PRODX and PRODY are based on the interpretation of the Casino 3 DST. Refer to Steyn (2003) for a discussion of the test interpretation.

The derivation of the Skin values (Mechanical and Non-Darcy) for the development wells is discussed in Chapter 4.2

The completion strategy for the Waarre C wells is to perforate the entire reservoir interval intersected by the well ie. 100'. Edge water drive is expected to be the dominate drive mechanism from the Waarre C, consequently it is considered appropriate to perforate the entire reservoir interval in the well. To partially perforate the reservoir in the PRODX and PRODY wells will reduce well productivity (due to partial penetration skin) without necessarily increasing standoff from the GWC.

The deviated or sub-horizontal PRODA well will be completed over a 400 to 500m openhole section with a wire wrapped sand screen. A 400 to 500m section equates to a 80 to 85 deg well through the Upper and Lower Waarre A reservoirs. To model horizontal well inflow, the Kuchuk and Goode model was selected. The model couples the reservoir inflow with the horizontal section of wellbore from the heel to the toe. The inputs in the model are summarised in Table 4.4.2-b below.

	PRODA
IPR Model	Horizontal Well - dp friction loss in wellbore (Kuchuk & Goode)
Reservoir Permeability (mD)	12
Reservoir thickness (ft)	151
Horiz Anisotropy	1
Vert Anisotropy	0.1
Well Length (ft)	1640
Reservoir Length (ft)	9850
Reservoir Width (ft)	4900
Length Distance to Reservoir Edge (ft)	6000
Width Distance to Reservoir Edge (ft)	2450
Bottom of Reservoir to Well Centre (ft)	75
Porosity (v/v)	0.18
Connate Water Saturation (v/v)	0.45
Mechanical Skin	2
Non-Darcy Skin	2.66E-06
Wellbore Radius (ft)	0.354
Zone Roughness	0.0006

Table 4.4.2-b: Inputs into the IPR model for PRODA.

Vertical Flow Performance was based on the Petroleum Experts correlation. This correlation was selected as it provided the best match to the flowing conditions of the Casino-3 DST. Refer to Steyn (2004) for a detailed discussion of the test interpretation. Petroleum Experts correlation combines the best features of existing correlations. The correlation uses the Gould et al flow map and the Hagedorn Brown correlation in slug flow, and Duns and Ros for mist flow. In the transition regime, a combination of slug and mist results are used.

Figures 4.4.2-a and 4.4.2-b are downhole diagrams of the development wells constructed within PROSPER. The vertical flow performance of the wells was based on these well designs.

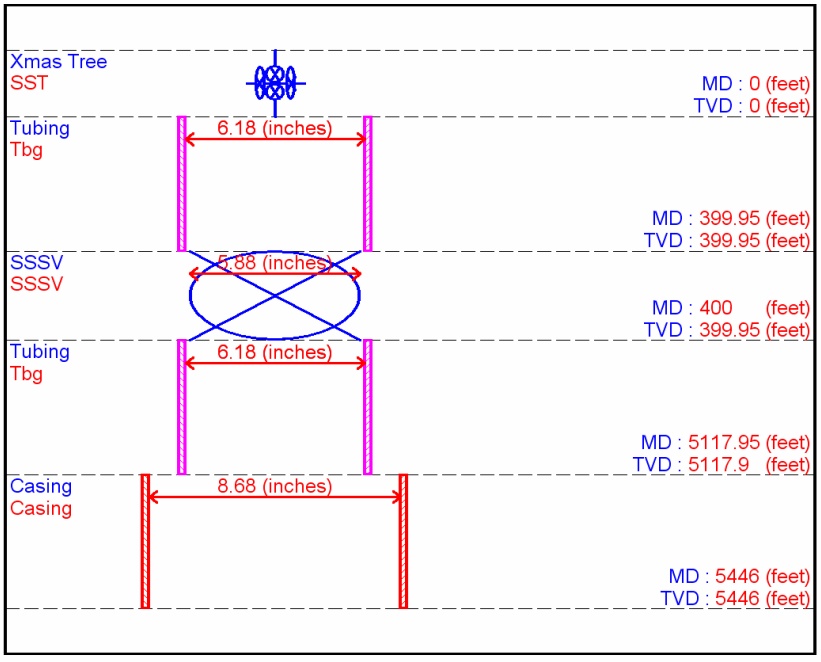

Figure 4.4.2-a: Downhole diagram for PRODX and PRODY

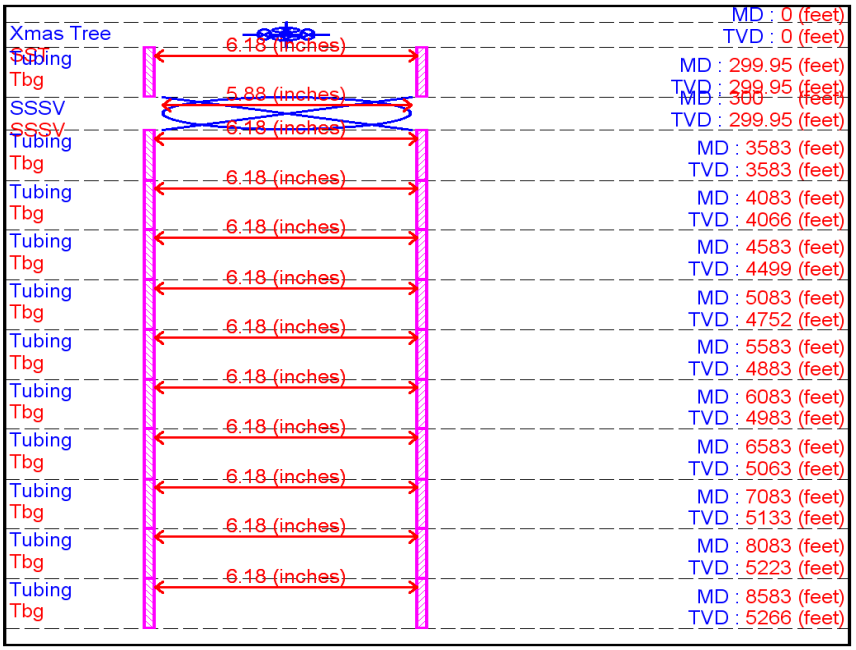

Figure 4.4.2-b: Downhole diagram for PRODA

Figure 4.4.2-c is an illustration of a sensitivity of well productivity to tubing size for the Waarre C producers, PRODX and PRODY. This sensitivity was performed at two tubing sizes (7" OD and 5 ½" OD). The nodal analysis was performed at initial reservoir pressure with the well flowing against a THP of 2300 psia (15862 kPa). Evident from this figure is significant improvement in well productivity with the larger tubing size. The majority of the pressure loss from sandface to wellhead is associated with friction. A large tubing ID results in a larger cross-section to flow and hence a lower gas velocity. This lower gas velocity results in a lower friction pressure loss through the tubing. The same conclusions may also be drawn from are also Figure 4.4.2-d, a nodal analysis plot of the PRODA well at initial reservoir conditions. The impact of the larger tubing size on well deliverability is less due to the poorer productivity of the Waarre A reservoir. The lower productivity results in lower offtake rates and hence lower friction pressure loss in the tubing.

The TXU Iona gas plant, which will processes the Casino gas, only has the capability to handle small volumes of water associated with condensation, therefore the producing wells will be shut-in once free water production occurs. Due to this restriction, it was not considered necessary to size the completion tubing based on the ability to lift free water late in field life.

ECLIPSE simulation runs were performed with 5 ½" and 7" tubing size for the producing wells in the model. This sensitivity was performed on the 'Base Case' development scenario at a field rate plateau of 35PJ/a. The 'Base Case' scenario comprises two producers, PRODX and PRODA with an initial delivery pressure of 9000 kPa (1305 psia) at the Iona Plant. This delivery pressure falls to 3000 kPa (435 psia) once field deliverability cannot meet DCQ. As illustrated in Figure 4.4.2-e, plateau length is extended with 7" tubing in the development wells compared to 5 ½" tubing. Similarly the requirement for boost compression (to a plant inlet pressure of 3000 kPa) is deferred by approximately 18 months in the 7" tubing case. The incremental field ultimate recovery (~4 Bcf) is insignificant for the 7" tubing case compared to the 5 ½" tubing case.

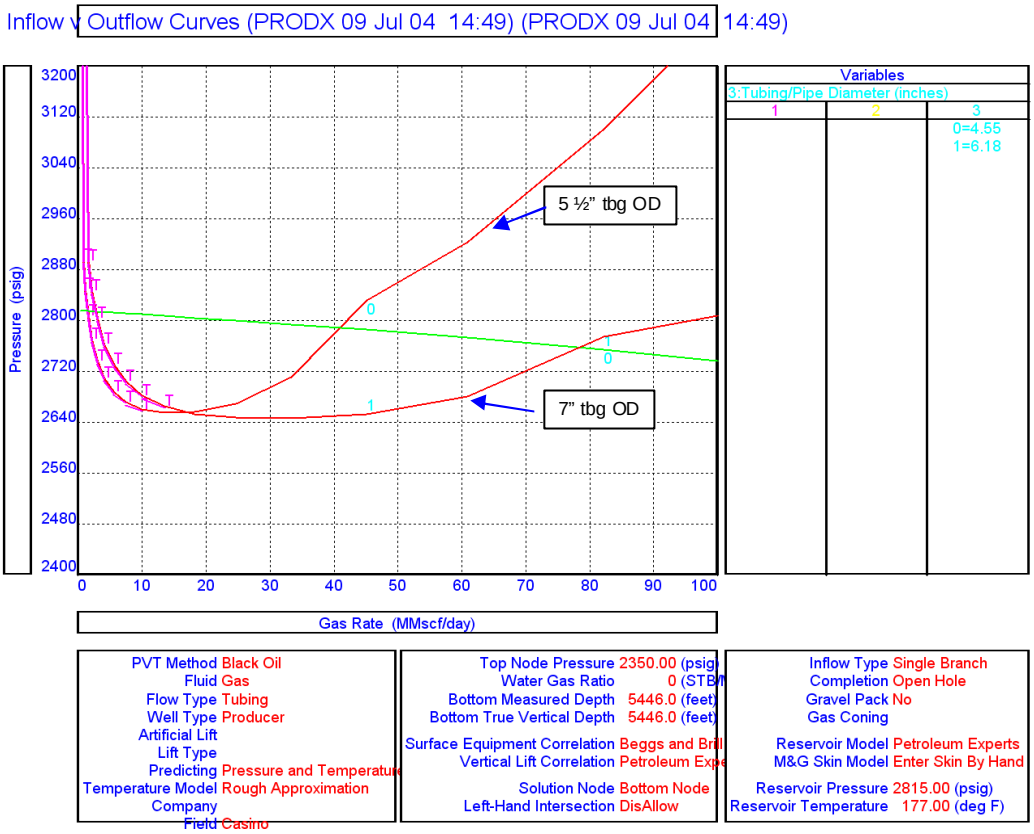

Figure 4.4.2-c: Inflow/Outflow well performance for PRODX and PRODY. Sensitivity to tubing size.

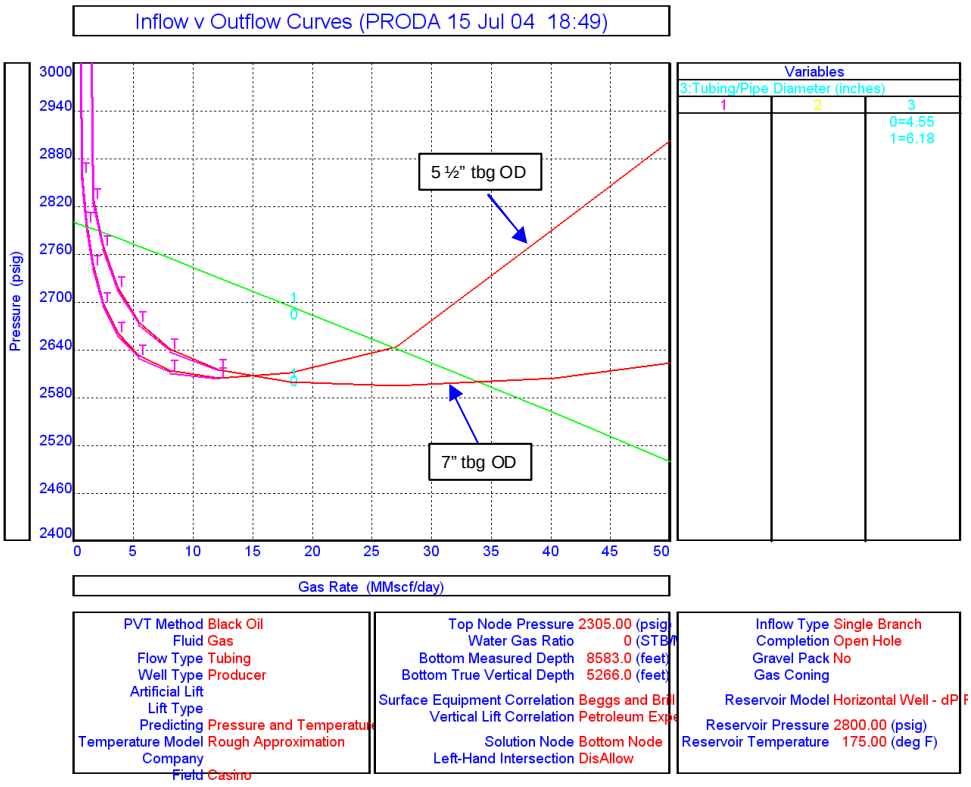

Figure 4.4.2-d: Inflow/Outflow well performance for PRODA. Sensitivity to tubing size.

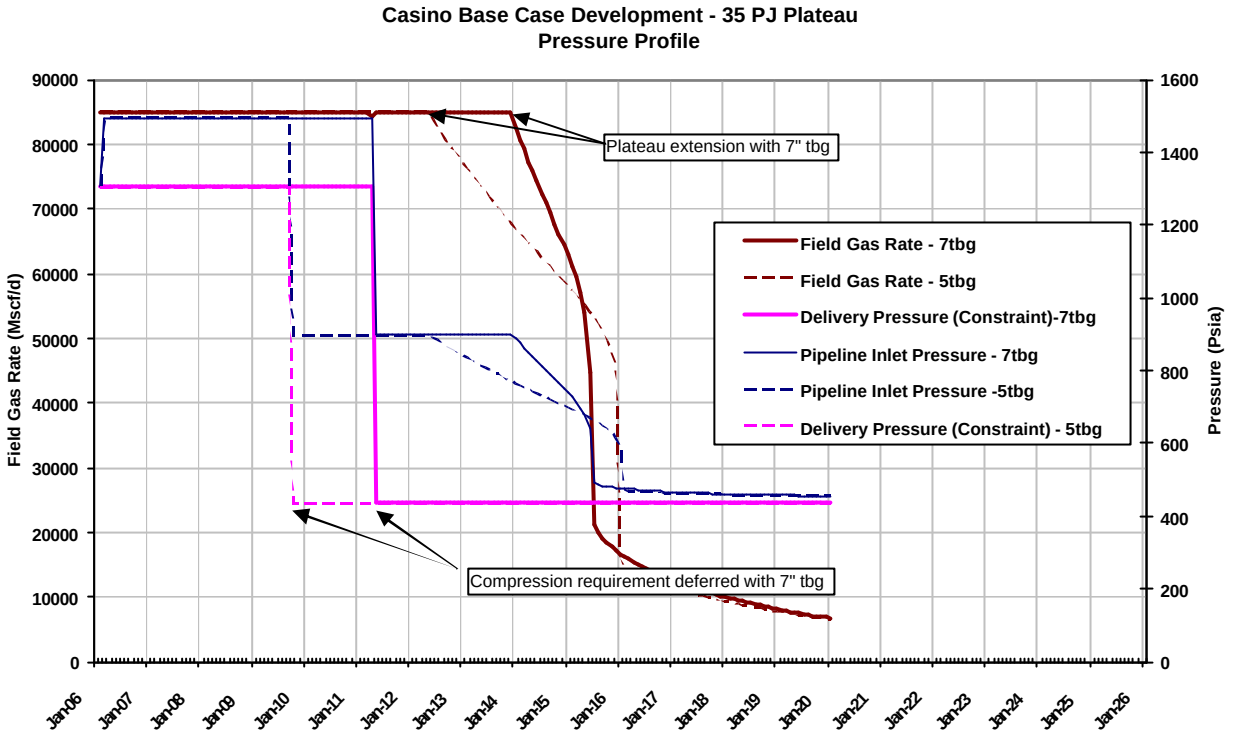

Figure 4.4.2-e: ECLIPSE forecasts for 'Base Case' development at 35PJ/a. Sensitivity to 7" and 5 ½" tubing OD.

4.4.3 Development Scenarios

Two alternate subsurface development scenarios have been evaluated for Casino. The Base Case development is shown in Figure 4.4.3-a. and allows for an initial two well development of the field using the Prod X and Prod A wells. There is no firm second phase of development, however in the event of early water breakthrough at the Prod X well, a second Waarre C development well at Prod Y is allowed as a contingency to improve the areal sweep for this reservoir. Figure 4.4.3-b shows the sequence of field development operations for this scenario. Note that the possibility of a subcommercial Waarre A development well is shown on this flowchart. While this is considered extremely unlikely this possibility cannot be completely ruled out until the development well is drilled.

The Base Case development is economically attractive as it offers the lowest capex outcome whereby Casino reserves can be exploited. The major risk associated with this scenario relate to the uncertainty of Waarre A well productivity (which may be quite low) and the consequent risk to gas supply should the Prod X well fail for any period due to a mechanical or reservoir failure.

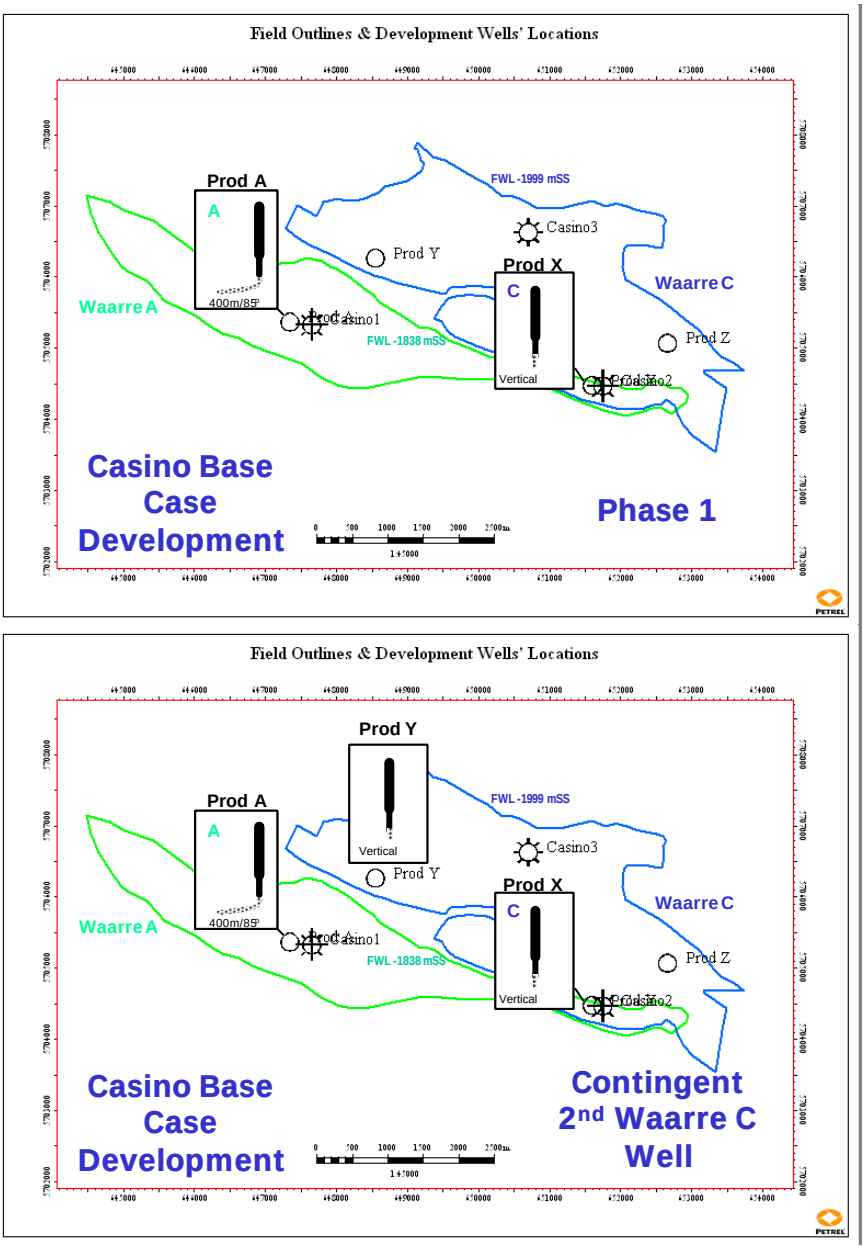

Figure 4.4.3-a: Casino Base Case Development

BASE CASE DEVELOPMENT

NO WAARRE A PILOT HOLE

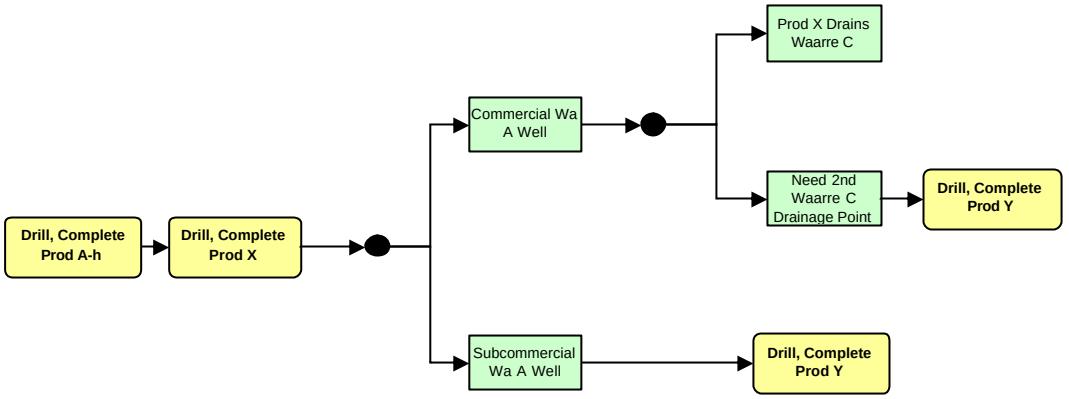

Figure 4.4.3-b: Casino Base Case Development – Sequence of Operations

The alternate development scenario considered for Casino is a Phased Development whereby development of the Waarre A reservoir is delayed to a second phase and the initial development is targeted on larger reserves base in the Waarre C reservoir only. This development is shown schematically in Figures 4.4.3-c and 4.4.3-d. In this case two wells Prod X and Prod Y are drilled in the first development phase in the Waarre C reservoir. The gas contract is met from these wells until the down dip Prod Y waters out and at this time the Waarre A well Prod A is brought on-line.

The Phased Development scenario is potentially less economically attractive than the Base Case development due to the firm requirement for 3 development wells. However, this development scenario has two significant advantages. The major advantage relates to security of gas supply. While the two Waarre C wells are on-line, either well could meet the gas contract in the event of a mechanical failure in the other. This scenario was also thought to potentially increase the recovery from the Waarre C reservoir due to improved areal sweep.

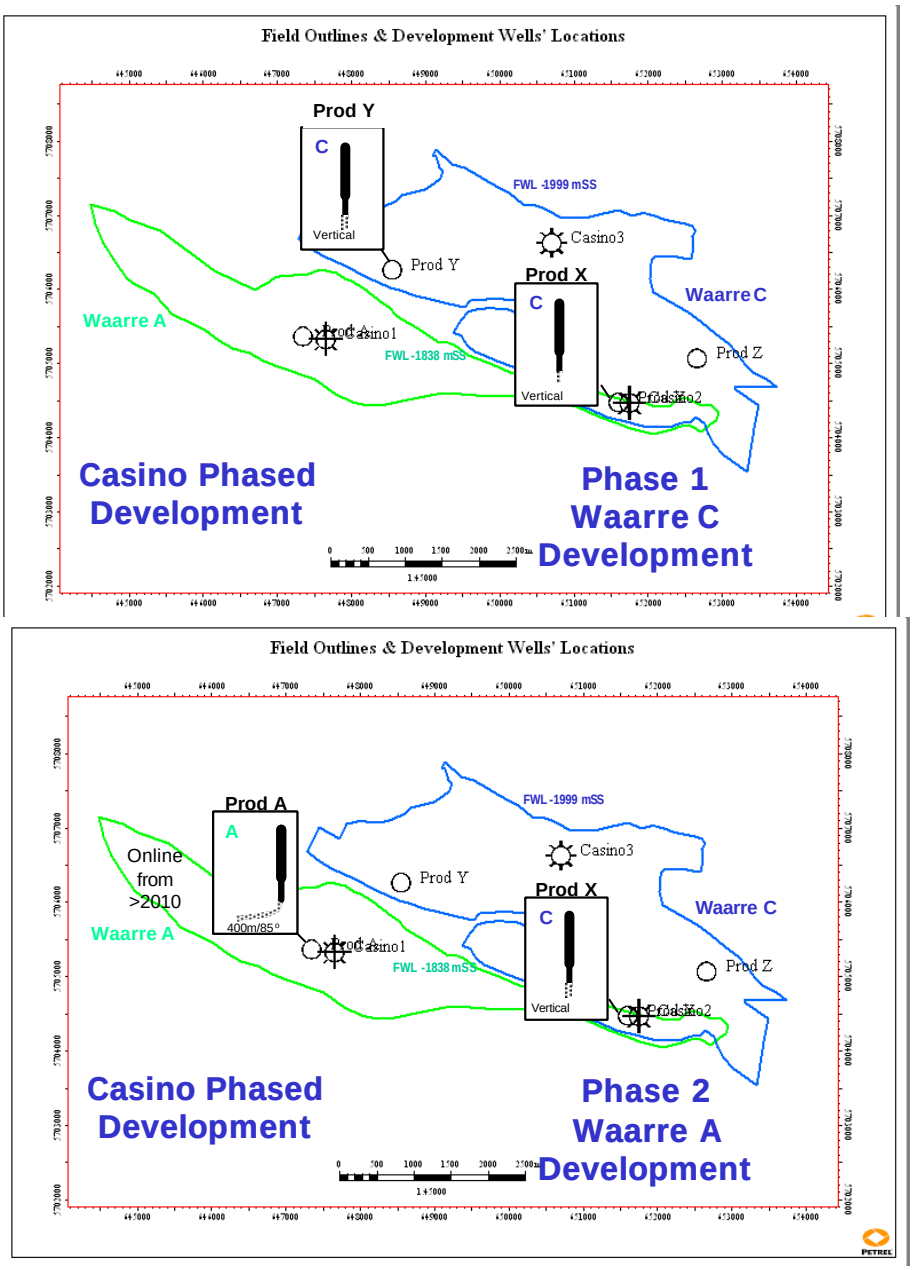

Figure 4.4.3-c: Casino Phased Development

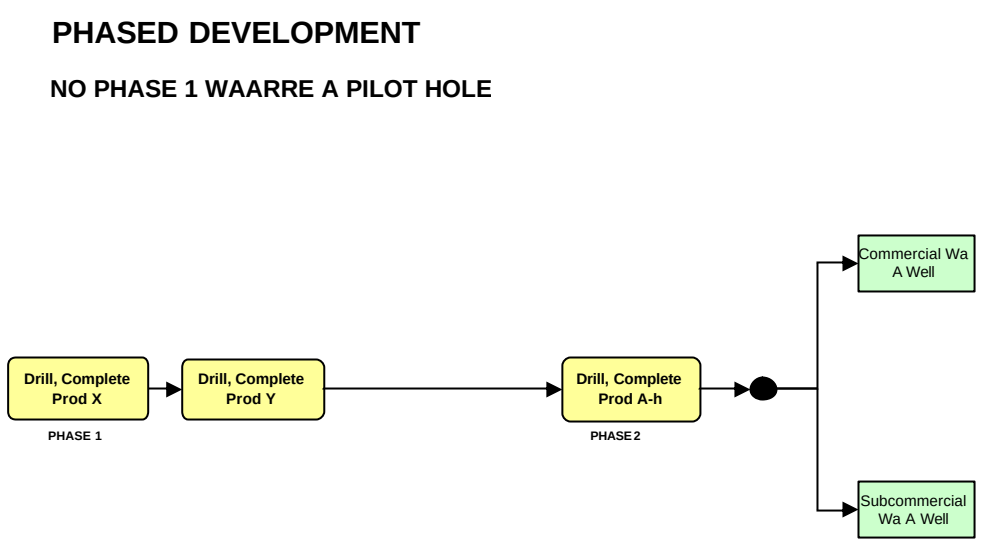

Figure 4.4.3-d: Casino Phased Development – Sequence of Operations

The production performance of these two development scenarios were evaluated using the initial P90, P50 and P10 reservoir models identified as described in Section 4.3. As this work was done in parallel with the final field reserves assessment, some minor changes were made to the final field P90, P50 and P10 reservoir models after the completion of the development scenario evaluation, however the conclusions reached during this phase of work remain valid.

Note that all these representative models chosen achieve their respective outcome using the most likely (P50) Waarre A permeability model. As an additional sensitivity the P50 and P90 reservoir models were also used with both the upside (P10) Waarre A permeability model and the downside (P90) Waarre A permeability model. This results in some additional outcomes either side of the P50 and P90 reserves cases. For example, the P90 Model with the P90 Waarre A permeability gives a reserves outcome around the P96 level while the P90 model with the P10 Waarre A permeability gives a reserves outcome around the P85 level.

These additional cases were included to ensure the effect of Waarre A permeability uncertainty on field deliverability modelling is correctly captured and reflected in the expected timing of compression requirements and redundancy.

Cases were investigated with production at the rates described under the Term Sheet for gas sales and also at an extended 35 PJ/a plateau. Other sensitivity cases were run with no aquifer pressure support in the Waarre C and with the Waarre A reservoir de-activated to investigate the expected production profiles in the highly unlikely event of not successfully completing a Waarre A development well.

4.4.4 Results

For reference a complete set of summary results from these development planning cases can be found in Table 4.4.4 –a.

The implications of these results are discussed in more detail in the following sections.

Case ID No	Eclipse Model ID	Base Model	Waarre A Perm Model	Development Scenario	Market	Comp Required	Prod Y Waters Out	Prod X Waters Out	Recovery to 2017 (Bcf) Wa C	Wa A	Total	Field Life Recovery (Bcf) Wa C	Wa A	Total	Notes
	P90 Reserves											**168.0**	**57.0**	**230.0**	
	P50 Reserves											**200.0**	**86.0**	**280.0**	
	P10 Reserves											**264.0**	**102.0**	**350.0**	
101	P90M1_MPERM_BASE_MAXTERM	P90	P50	Base	Max ACQ	Aug-10	n.a	Aug-14	161.0	66.7	227.7	161.0	70.0	231.0	P90 Model - Base Case
102	P90M1_LLPERM_BASE_MAXTERM	P90	P90	Base	Max ACQ	Sep-09	n.a	Sep-13	169.0	41.5	210.5	169.0	46.6	215.6	P90 Model with low Wa Perm
103	P90M1_HPERM_BASE_MAXTERM	P90	P10	Base	Max ACQ	Jun-11	n.a	Jul-15	156.0	82.8	238.8	156.0	83.1	239.1	P90 Model with high Wa Perm
104	P90M1_MPERM_PHASED_MAXTERM	P90	P50	Phased	Max ACQ	May-09	Feb-10	Nov-13	165.6	60.7	226.3	165.6	69.7	235.3	P90 Model - Phased
105	P90M1_MPERM_BASE_35PLAT	P90	P50	Base	35 PJ/a ext	Dec-09	n.a	Dec-13	175.0	67.8	242.8	175.0	70.0	245.0	P90 Model 35 PJ/a - Base Case
106	P90M1_LLPERM_BASE_35PLAT	P90	P90	Base	35 PJ/a ext	May-09	n.a	May-13	177.0	42.5	219.5	177.0	46.5	223.5	P90 Model 35 PJ/a with low Wa Perm
107	P90M1_HPERM_BASE_35PLAT	P90	P10	Base	35 PJ/a ext	Mar-10	n.a	Jul-14	174.0	83.0	257.0	174.0	83.0	257.0	P90 Model 35 PJ/a with high Wa Perm
108	P90M1_MPERM_PHASED_35PLAT	P90	P50	Phased	35 PJ/a ext	Mar-09	Jan-10	Apr-13	176.1	63.8	239.9	176.1	69.6	245.7	P90 Model 35 PJ/a - Phased
109	P90M1_MPERM_BASE_MINTERM	P90	P50	Base	Max/Min ACQ	n.a.	n.a	Jan-18	138.0	54.7	192.7	138.0	70.9	208.9	P90 Model Step down to Min ACQ
110	P90M1_PRODX_PRODY_MINTERM	P90	excluded	Phased	Max/Min ACQ	Jul-09	Jul-10	Jul-14	163.5	0.0	163.5	163.5	0.0	163.5	P90 No Waarre A, Step down to Min ACQ
111	P90_NOAQ_BASE_MAXTERM	P90	P50	Base	Max ACQ	May-10	n.a	well dies	191.0	66.9	257.9	204.0	72.9	276.9	P90 Model - No Aquifer Support
112	P50M1_MPERM_BASE_MAXTERM	P50	P50	Base	Max ACQ	Sep-14	n.a	Jan-18	195.9	61.9	257.8	195.9	89.4	285.3	P50 Model - Base Case
113	P50M1_LLPERM_BASE_MAXTERM	P50	P90	Base	Max ACQ	Aug-12	n.a	Jun-16	201.3	43.1	244.4	201.3	63.2	264.5	P50 Model with low Wa Perm
114	P50M1_HPERM_BASE_MAXTERM	P50	P10	Base	Max ACQ	Aug-16	n.a	Jan-19	187.0	69.4	256.4	194.8	102.3	297.1	P50 Model with high Wa Perm
115	P50M1_MPERM_PHASED_MAXTERM	P50	P50	Phased	Max ACQ	Mar-12	May-12	Jan-17	210.8	47.2	258.0	210.8	87.5	298.3	P50 Model - Phased
116	P50M1_MPERM_BASE_35PLAT	P50	P50	Base	35 PJ/a ext	May-11	n.a	Jul-15	215.6	79.1	294.7	215.6	88.9	304.5	P50 Model 35 PJ/a - Base Case
117	P50M1_LLPERM_BASE_35PLAT	P50	P90	Base	35 PJ/a ext	Aug-10	n.a	Oct-14	217.7	48.8	266.5	217.7	62.8	280.5	P50 Model 35 PJ/a with low Wa Perm
118	P50M1_HPERM_BASE_35PLAT	P50	P10	Base	35 PJ/a ext	Apr-11	n.a	Apr-16	214.5	100.5	315.0	214.5	102.6	317.1	P50 Model 35 PJ/a with high Wa Perm
119	P50M1_MPERM_PHASED_35PLAT	P50	P50	Phased	35 PJ/a ext	Oct-10	Nov-11	Feb-15	228.1	70.0	298.1	228.1	88.4	316.5	P50 Model 35 PJ/a - Phased
120	P50M1_MPERM_BASE_MAXTERM_RM	P50	P50	Base	Max ACQ	Feb-13	n.a	Jan-17	194.9	62.4	257.3	194.9	88.9	283.8	P50 Produce Waarre alone for 1st 3 years
121	P50M1_MPERM_BASE_MAXTERM_RM2	P50	P50	Base	Max ACQ	Jan-11	n.a	Sep-14	211.0	46.4	257.4	211.0	87.0	298.0	P50 Produce Waarre C alone to depletion
122	P50M1_PRODX_PRODY_MINTERM	P50	excluded	Phased	Max/Min ACQ	Jan-14	Jul-13	May-19	192.8	0.0	192.8	202.7	0.0	202.7	P50 No Waarre A, Step down to Min ACQ
123	P50M1_PRODX_PRODY_MAXTERM	P50	excluded	Phased	Max ACQ	Jan-11	Apr-12	Aug-15	224.2	0.0	224.2	224.2	0.0	224.2	P50 No Waarre A, Maintain Max ACQ
124	P10M3_MPERM_BASE_MAXTERM	P10	P50	Base	Max ACQ	n.a.	n.a	Jul-24	190.0	67.6	257.6	255.0	89.1	344.1	P10 Model - Base Case
125	P10M3_MPERM_PHASED_MAXTERM	P10	P50	Phased	Max ACQ	n.a.	Oct-14	Dec-22	236.0	21.9	257.9	270.0	74.3	344.3	P10 Model - Phased Case

Table 4.4.4-a: Development Planning Simulation Cases

4.4.5 Term Sheet ACQ : Base Case and Phased Development

Results

The results of sets of cases examining the impact of individual parameters are discussed below. Examples of production and pressure plots for Case 112 and Case 115 (the respective P50 Base Case and Phased Development simulation runs) can be found in Figure 4.4.5-a – d.

Recovery – Base Case vs Phased Development

The results of a set of cases run to evaluate the Base Case versus the Phased Development can be found in Table 4.4.5-a below;

Case ID No	Base Model	Waarre A Perm Model	Dev Scenario	Comp Required	Prod Y Waters Out	Prod X Waters Out	Recovery to 2017 (Bcf) Wa C	Wa A	Total	Field Life Recovery (Bcf) Wa C	Wa A	Total	Notes
"P90" Model Cases													
101	P90	P50	Base	Aug-10	n.a	Aug-14	161.0	66.7	227.7	161.0	70.0	231.0	P90 Model - Base Case
104	P90	P50	Phased	May-09	Feb-10	Nov-13	165.6	60.7	226.3	165.6	69.7	235.3	P90 Model - Phased
"P50" Model Cases													
112	P50	P50	Base	Sep-14	n.a	Jan-18	195.9	61.9	257.8	195.9	89.4	285.3	P50 Model - Base Case
115	P50	P50	Phased	Mar-12	May-12	Jan-17	210.8	47.2	258.0	210.8	87.5	298.3	P50 Model - Phased

Table 4.4.5-a: Production at Term Sheet ACQ, P90, P50 and P10, Base Case and Phased Development

The Phased Development, and the associated second firm Waarre C well (Prod Y) does not result in any substantial increase in reserves as shown by a comparison of like for like cases. Using the P90 model (Cases 101 and 104) the second Waarre C well adds only 4 Bcf of recovery while at the P50 level (Cases 112 and 115 the increase is approximately 13 Bcf. In the absence of any reservoir compartmentalisation and with the good areal sweep as predicted by the simulation model, the second Waarre C well is effectively providing for redundancy in gas supply and allowing for accelerating Waarre C gas production.

Compression Timing

The results of a set of cases run to evaluate the expected timing requirement for compression can be found in Table 4.4.5-b below;

Case ID No	Base Model	Waarre A Perm Model	Dev Scenario	Market	Comp Required	Prod Y Waters Out	Prod X Waters Out	Recovery to 2017 (Bcf) Wa C	Wa A	Total	Field Life Recovery (Bcf) Wa C	Wa A	Total	Notes
"P90" Model Cases														
101	P90	P50	Base	Max ACQ	Aug-10	n.a	Aug-14	161.0	66.7	227.7	161.0	70.0	231.0	P90 Model - Base Case
102	P90	P90	Base	Max ACQ	Sep-09	n.a	Sep-13	169.0	41.5	210.5	169.0	46.6	215.6	P90 Model with low Wa Perm
103	P90	P10	Base	Max ACQ	Jun-11	n.a	Jul-15	156.0	82.8	238.8	156.0	83.1	239.1	P90 Model with high Wa Perm
104	P90	P50	Phased	Max ACQ	May-09	Feb-10	Nov-13	165.6	60.7	226.3	165.6	69.7	235.3	P90 Model - Phased
"P90" Model with No Aquifer														
111	P90	P50	Base	Max ACQ	May-10	n.a	well dies	191.0	66.9	257.9	204.0	72.9	276.9	P90 Model - No Aquifer Support
"P50" Model Cases														
112	P50	P50	Base	Max ACQ	Sep-14	n.a	Jan-18	195.9	61.9	257.8	195.9	89.4	285.3	P50 Model - Base Case
113	P50	P90	Base	Max ACQ	Aug-12	n.a	Jun-16	201.3	43.1	244.4	201.3	63.2	264.5	P50 Model with low Wa Perm
114	P50	P10	Base	Max ACQ	Aug-16	n.a	Jan-19	187.0	69.4	256.4	194.8	102.3	297.1	P50 Model with high Wa Perm
115	P50	P50	Phased	Max ACQ	Mar-12	May-12	Jan-17	210.8	47.2	258.0	210.8	87.5	298.3	P50 Model - Phased

Table 4.4.5-b: Production at Term Sheet ACQ, Compression Timing

For the Base Case scenario, compression is required;

- as early as September, 2009 (Case 102, P90 model, P90 Waarre A permeability), i.e. late in the 4th year of production or,
- as late as August 2016 (Case 114, P50 model, P10 Waarre A permeability). Note that compression timing has not been rigorously investigated using the P10 reservoir model.

For the Phased Development, compression is required slightly earlier as shown in Case 102 (P90 Model, Phased Development) where compression is required in May 2009. The downdip Waarre C well, Prod Y is predicted to water out from February 2010 to October 2014.

The tubing head pressure profiles for the development wells are illustrated in Figure 4.4.5-b (Case 112, Base Case, P50 model, P50 Waarre A permeability model) and Figure 4.4.5-d (Case 115, Phased Development, P50 model, P50 Waarre A permeability model). Note that even given the forecast strong aquifer support in the Waarre C the reservoir is subject to significant pressure decline as gas offtake rates outstrip the ability of the edge waterdrive to supply water to the reservoir. The decline in average reservoir pressure in one of the major Waarre Cb reservoir units for Case 112 is shown in Figure 4.4.5-e. Note the recharge in Waarre C reservoir pressure after production ceases from the well.

A further case has been run to investigate the impact of aquifer strength on the compression timing requirement by removing the analytical aquifer support from the P90 simulation model (Case 111). Results show that removing the analytical aquifer support accelerates the compression requirement by only 3 months.

Waarre C Water Breakthrough

The crestal Waarre C producer, Prod X, is forecast to water out as early as September, 2013 (Case 102, P90 model, P90 Waarre A permeability). Note that a poor Waarre A permeability outcome results in a marginal increase in Waarre C production prior to water breakthrough and illustrates the rate dependency of recovery from the waterdrive Waarre C reservoir as a poor Waarre A producer results in increased demand on the Waarre C well.

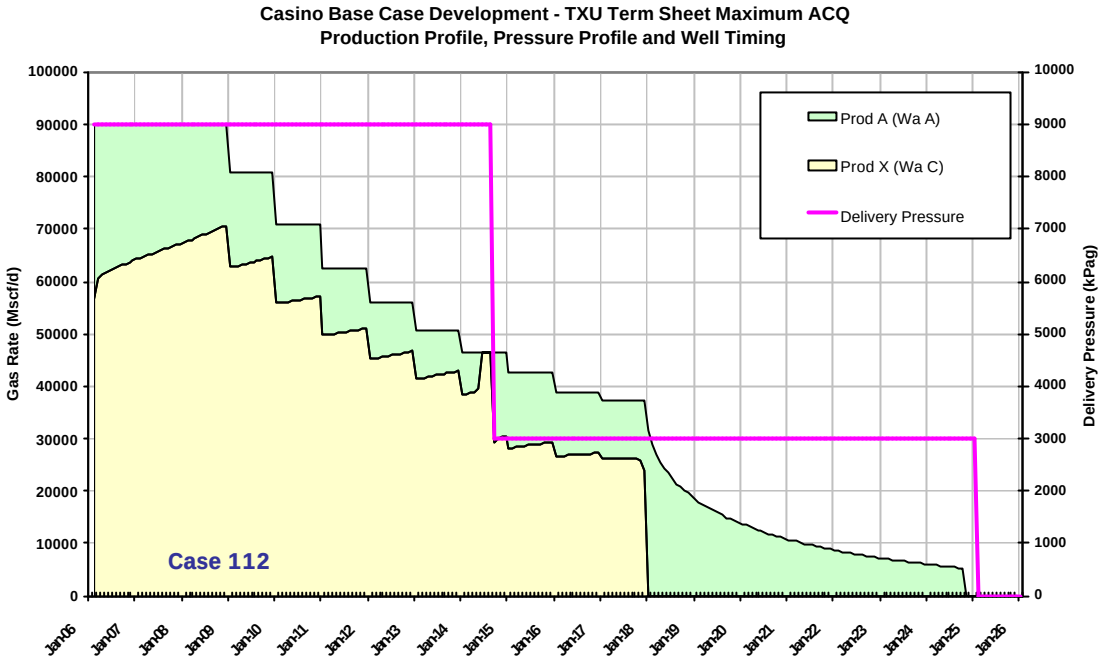

Figure 4.4.5-a: Casino Base Case Development – P50 Production Profile (Case 112)

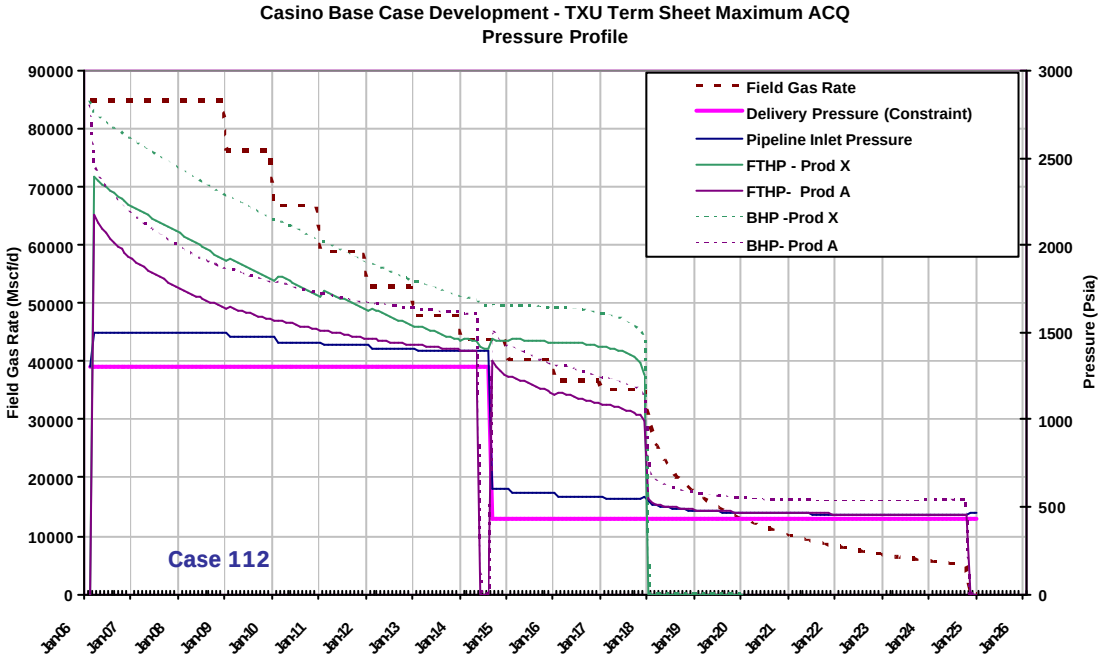

Figure 4.4.5-b: Casino Base Case Development – P50 Production and Pressure Profile

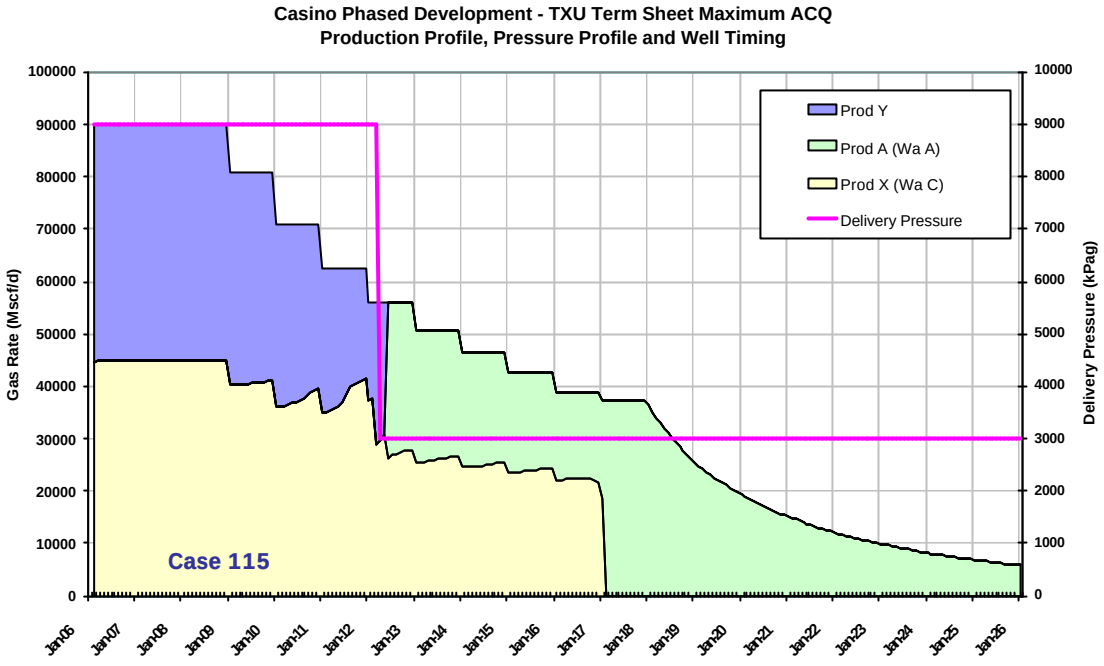

Figure 4.4.5-c: Casino Phased Case Development – P50 Production Profile

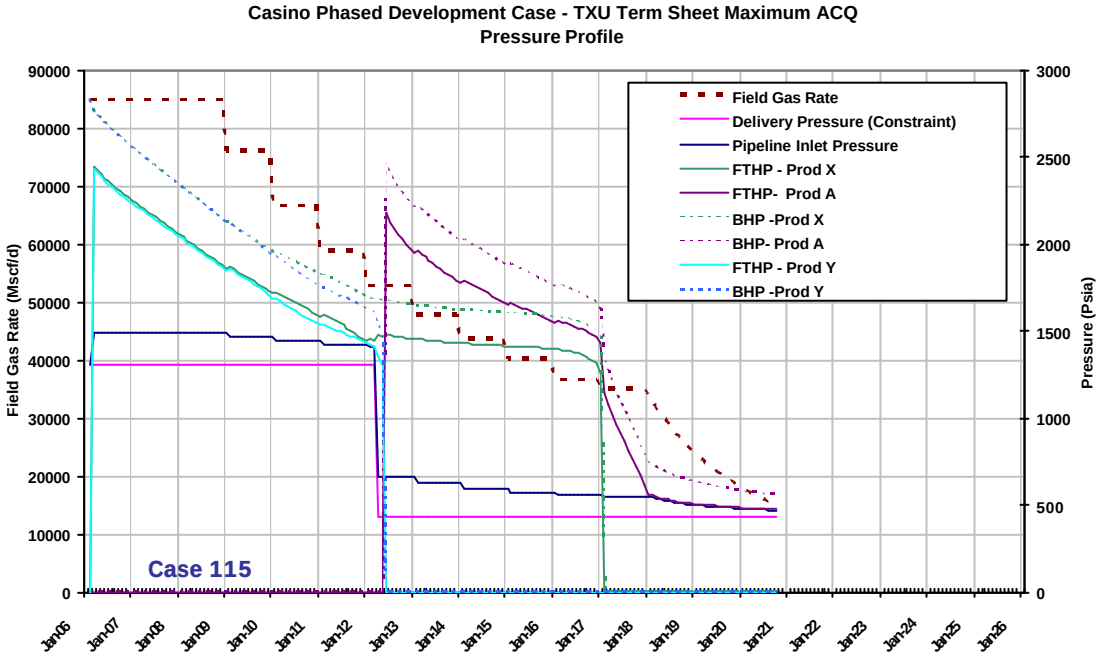

Figure 4.4.5-d: Casino Phased Development – P50 Production and Pressure Profile

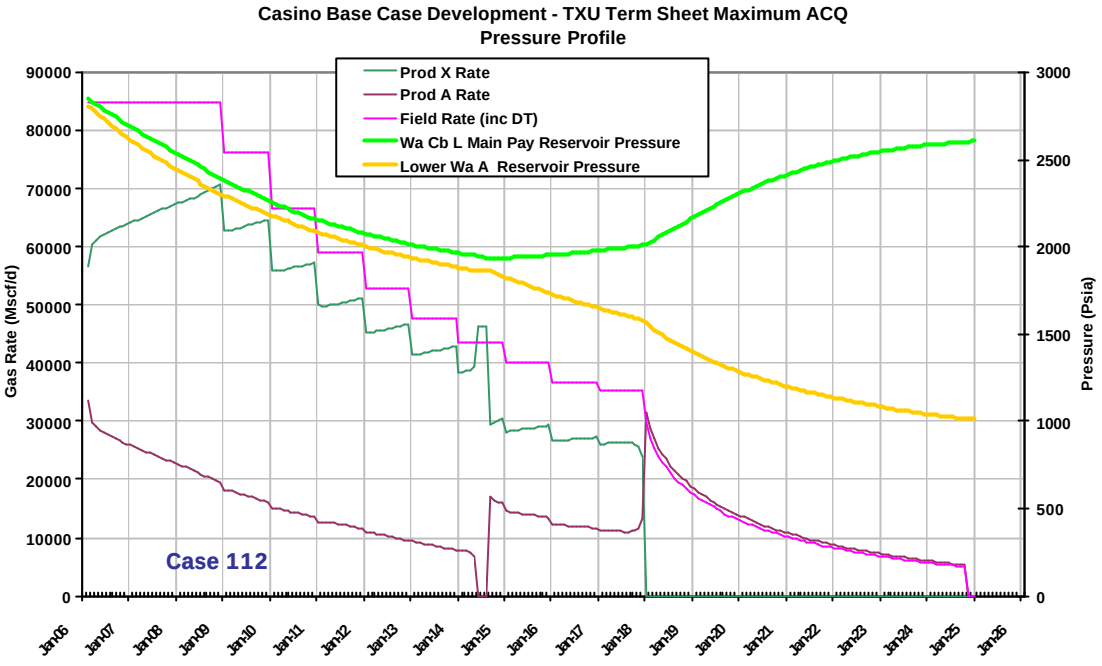

Figure 4.4.5-e: Casino Phased Development – P50 Production and Pressure Profile

Well Redundancy – Security of Supply Analysis

This is a key issue of differentiation between the Base Case and Phased Development. The provision of a redundant well has not been considered as a basic requirement for Casino development planning work. Depending on the Waarre A permeability encountered the Base Case development leaves significant exposure to production shortfall in the event of a failure of the Prod X well for either mechanical or reservoir related reasons. The impact of a Prod X well failure has been examined simplistically by assuming such an event occurs on 1 January 2009 and the well is not returned to production for approximately six months. While this duration may seem large it is consistent with experience in the region where for example no semi submersible MODU of opportunity is likely to be available in the area for a well intervention and a mobilisation from the North West Shelf or from out of country may be necessary.

The resulting production shortfall for the Base Case, for the range of expected Waarre A permeability outcomes is shown in Figure 4.4.5-f. Note that for the Phased Development, the second Waarre C producing well (Prod Y) provides for complete redundancy and no production shortfall eventuates.

For the Base Case development with the P50 – P90 Waarre A permeability outcome the potential exposure is substantial with 8 – 11 Bcf of potential production shortfall. In the event of an upside Waarre A permeability outcome the shortfall is less significant and through preferential production of the Waarre C early in the field life the shortfall can be completely eliminated as shown in Figure 4.4.5-g.

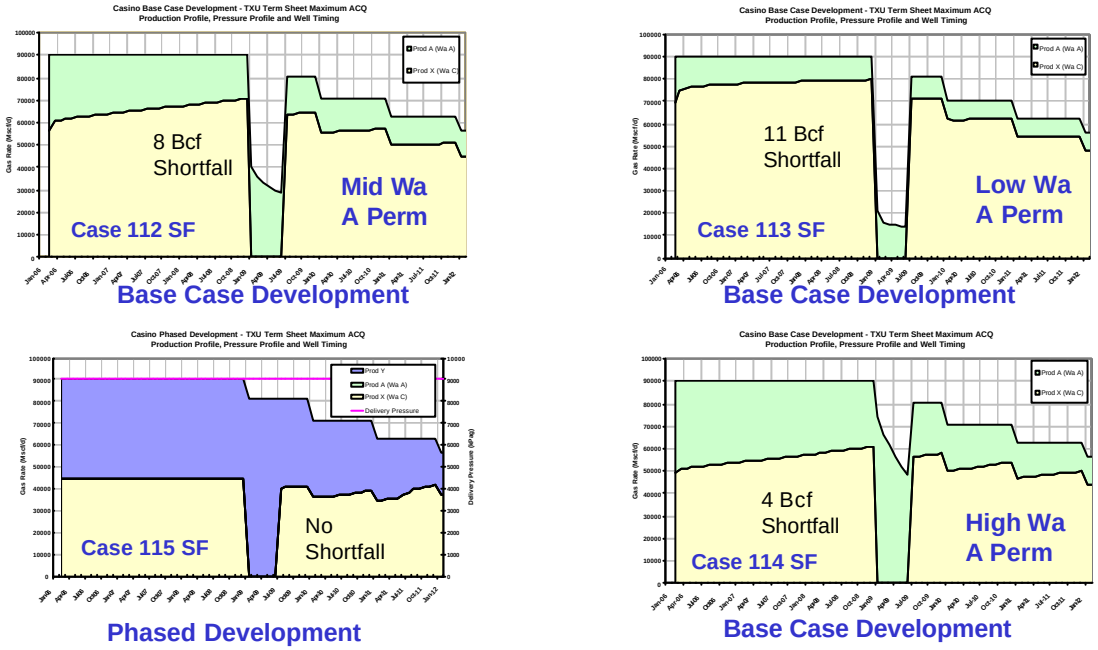

Figure 4.4.5-f: Shortfall Evaluation : Base Case and Phased Development

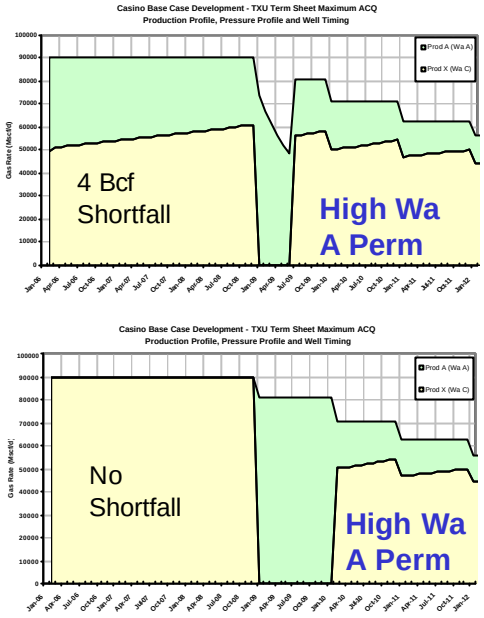

Figure 4.4.5-g: Shortfall Evaluation : Base Case, High Waarre A Permeability

Reservoir Management Strategy

Following on from this dscussion, two full life Base Case development scenarios were investigated where initial production was preferentially supplied from the Waarre C producer Prod X. The aim of these cases was to ensure this reservoir management strategy was not prejudicing total field recovery. Scenarios were run where Prod X meets total demand for the first 3 years of the field life before Prod A is brought on-line (Case 120) and where Prod X was produced alone to meet contract Max ACQ until no longer able to do so (Case 121). For reference, these results can be compared to Case 112 which uses the same P50 Model but with both wells brought on-line from first gas and produced in proportion to their respect well productivities. These results are summarised in Table 4.4.5-c.

This work further shows the positive impact on Waarre C gas recovery through acceleration. Figure 4.4.5-h (Case 121) shows the case where Prod X is produced to depletion, prior to commencing production from the Waarre A with increased gas recovery. This increase is due to the modelled moderate to strong waterdrive on the Waarre C reservoir. Increasing the offtake rate on this reservoir has the effect of reducing the pressure at which gas is trapped by the advancing waterflood resulting in increased gas recovery.

Case ID No	Base Model	Waarre A Perm Model	Dev Scenario	Market	Comp Required	Prod Y Waters Out	Prod X Waters Out	Recovery to 2017 (Bcf) Wa C	Wa A	Total	Field Life Recovery (Bcf) Wa C	Wa A	Total	Notes
"P50" Model Cases														
112	P50	P50	Base	Max ACQ	Sep-14	n.a	Jan-18	195.9	61.9	257.8	195.9	89.4	285.3	P50 Model - Base Case
"P50" Model Cases with Alternate Reservoir Management														
120	P50	P50	Base	Max ACQ	Feb-13	n.a	Jan-17	194.9	62.4	257.3	194.9	88.9	283.8	P50 Produce Waarre alone for 1st 3 years
121	P50	P50	Base	Max ACQ	Jan-11	n.a	Sep-14	211.0	46.4	257.4	211.0	87.0	298.0	P50 Produce Waarre C alone to depletion

Table 4.4.5-c: Base Case Development with Waarre C Acceleration

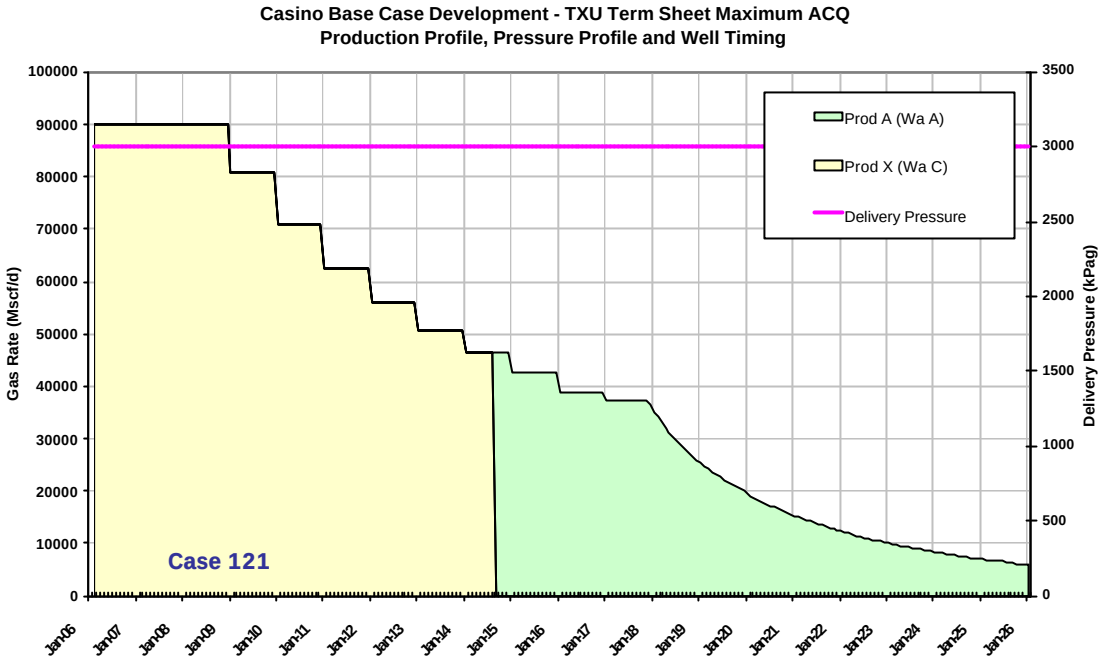

Figure 4.4.5-h: Base Case Development, P50, Accelerate Waarre C Production

Waarre C Standalone Case

As a sensitivity, the ability of the Waarre C reservoir by itself to deliver against the Term Sheet gas demand profile has been investigated. This is a test of the development in the highly unlikely event that the Waarre A reservoir is found to be subcommercial. In this case, the Waarre C is developed with the Prod X and Prod Y wells as per the Phased Development scenario but there is no second phase of development. Cases have been run with the P90 model and P50 model.

Results are summarised in Table 4.4.5-d. The P90 model has been tested against a modified production profile with initial offtake from the field at maximum ACQ for the first two years and a step down to minimum ACQ from this point forward (Figure 4.4.5-h, Case 110). On this basis, the Waarre C reservoir can maintain delivery against the Term Sheet minimum ACQ until July 2014 when Prod X waters out, or for all but the last 3 ½ years of the contract period.

The same profile was tested against the P50 model (Figure 4.4.5-i, Case 122) and shows the Waarre C reservoir alone can comfortably meet minimum ACQ obligations over the life of the contract period. An alternative case was investigated where the Waarre C formation was allowed to produce at Maximum ACQ rates for as long as possible (Figure 4.4.5-j, Case 123).

Case ID No	Base Model	Waarre A Perm Model	Dev Scenario	Market	Comp Required	Prod Y Waters Out	Prod X Waters Out	Recovery to 2017 (Bcf) Wa C	Wa A	Total	Field Life Recovery (Bcf) Wa C	Wa A	Total	Notes
P90 Reserves - June 17											**168.0**	**57.0**	**230.0**	
P50 Reserves - June 17											**200.0**	**86.0**	**280.0**	
"P90" Model Cases														
101	P90	P50	Base	Max ACQ	Aug-10	n.a	Aug-14	161.0	66.7	227.7	161.0	70.0	231.0	P90 Model - Base Case
104	P90	P50	Phased	Max ACQ	May-09	Feb-10	Nov-13	165.6	60.7	226.3	165.6	69.7	235.3	P90 Model - Phased
"P90" Model Case with No Waarre A														
110	P90	excluded	Phased	Max/Min ACQ	Jul-09	Jul-10	Jul-14	163.5	0.0	163.5	163.5	0.0	163.5	P90 No Waarre A, Step down to Min ACQ
"P50" Model Cases														
112	P50	P50	Base	Max ACQ	Sep-14	n.a	Jan-18	195.9	61.9	257.8	195.9	89.4	285.3	P50 Model - Base Case
115	P50	P50	Phased	Max ACQ	Mar-12	May-12	Jan-17	210.8	47.2	258.0	210.8	87.5	298.3	P50 Model - Phased
"P50" Model Case with No Waarre A														
122	P50	excluded	Phased	Max/Min ACQ	Jan-14	Jul-13	May-19	192.8	0.0	192.8	202.7	0.0	202.7	P50 No Waarre A, Step down to Min ACQ
123	P50	excluded	Phased	Max ACQ	Jan-11	Apr-12	Aug-15	224.2	0.0	224.2	224.2	0.0	224.2	P50 No Waarre A, Maintain Max ACQ

Table 4.4.5-d: Waarre C Standalone Cases

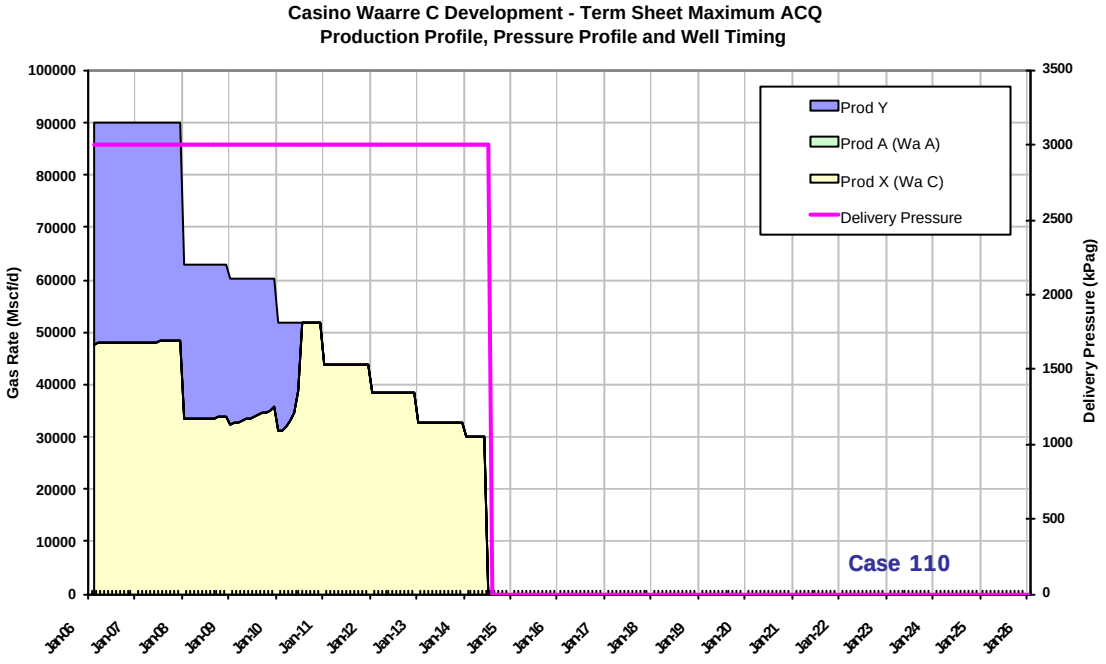

Figure 4.4.5-i: Waarre C P90 Standalone Case, Constrain Production at Min ACQ from Year 3

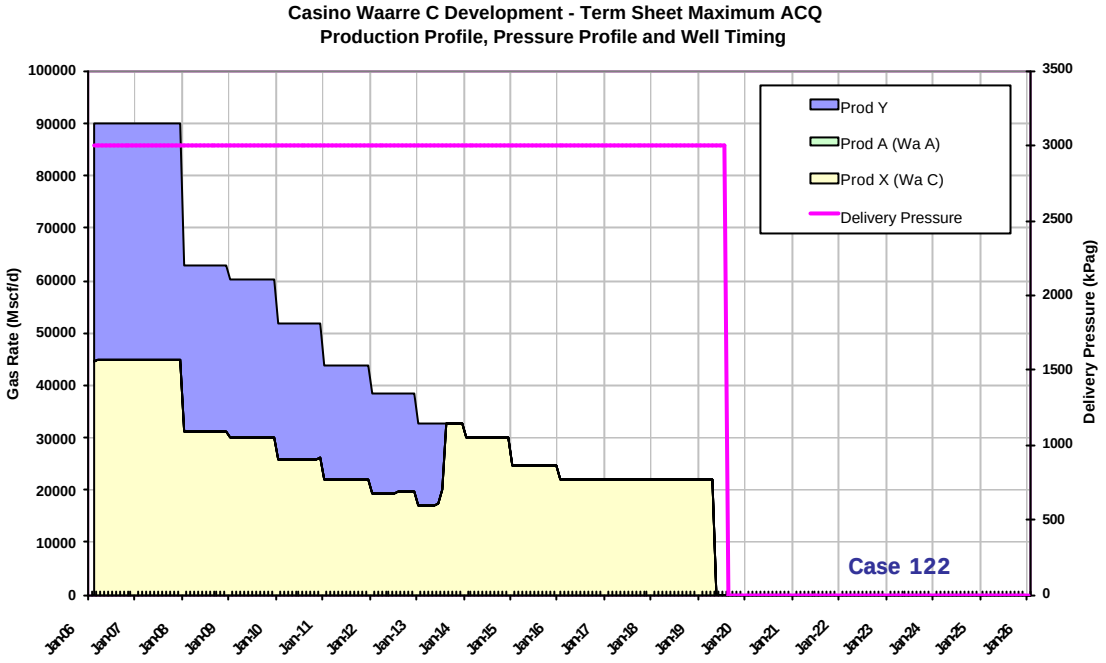

Figure 4.4.5-j: Waarre C P50 Standalone Case, Constrain Production at Min ACQ from Year 3

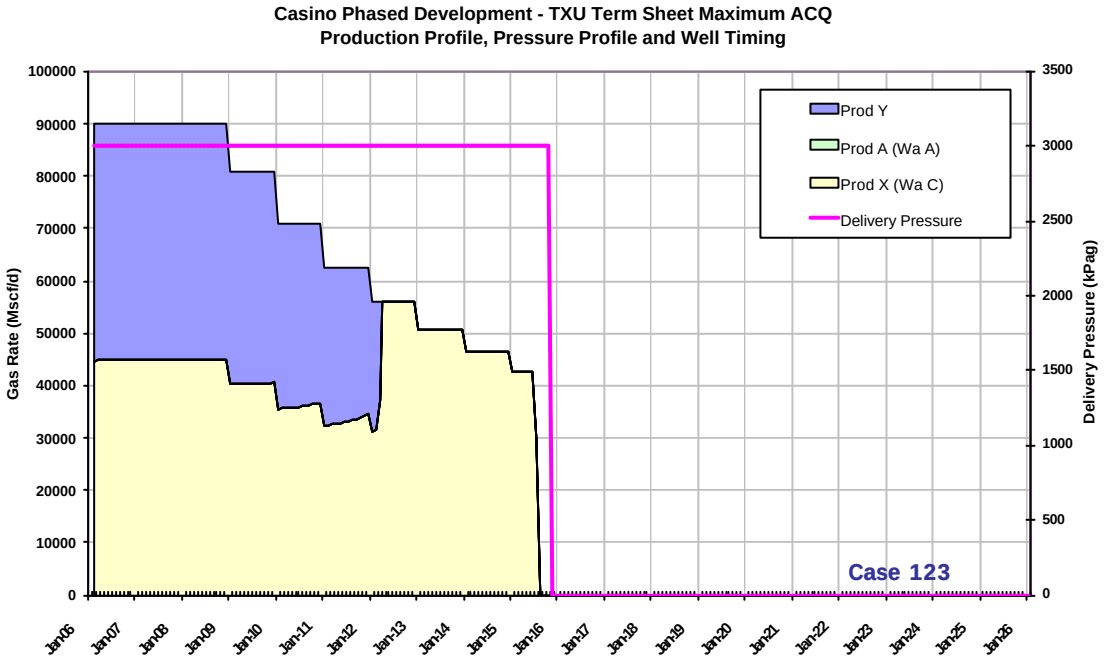

Figure 4.4.5-k: Waarre C P50 Standalone Case, Produce at Max ACQ

Term Sheet Maximum ACQ : Production Summary

The major conclusions drawn from this evaluation are as follows;

- Based on the current reservoir model, the Phased Development and the second Waarre C well (Prod Y) increase reserves only slightly over the Base Case.
- Accelerating Waarre C production relative to the Waarre A results in increased recovery.
- The requirement for compression timing is similar in both cases and compression may be required as early as 2009.
- With the Base Case development scenario and a mid to poor Waarre A well productivity outcome there is significant exposure to production shortfall in the event of failure of the Waarre C well Prod X. This exposure is substantially reduced and with appropriate reservoir management practices can be eliminated in a highside Waarre A well productivity outcome.
- For the Phased Development, there is no production shortfall exposure.

A summary of production profiles and expected compression timing is shown in Figure 4.4.5-l

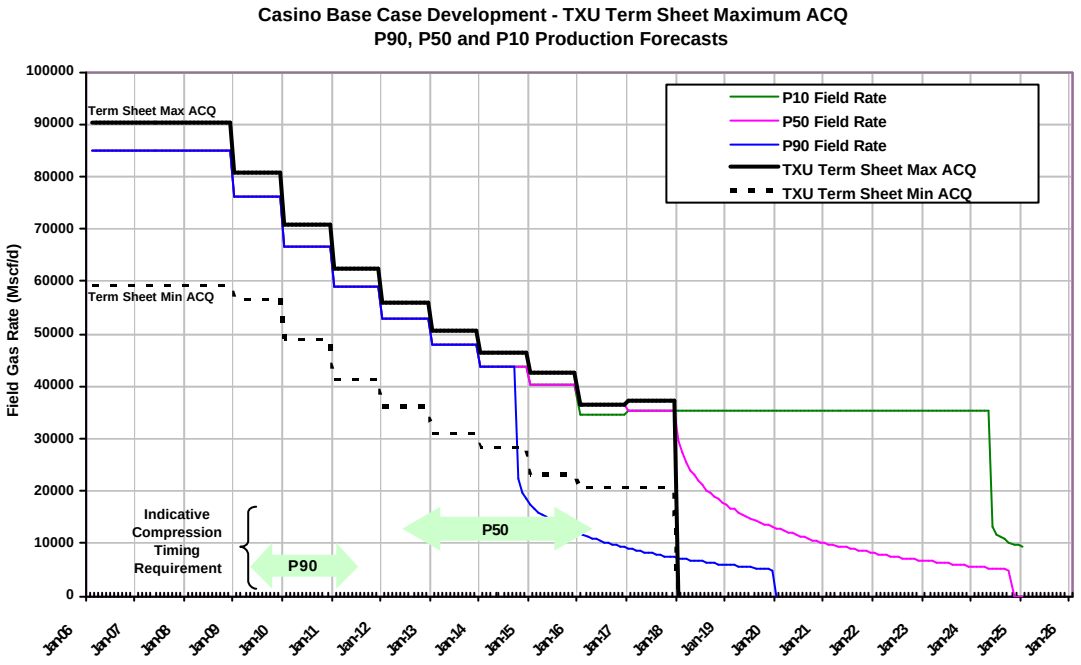

Figure 4.4.5-l: Term Sheet Maximum ACQ Production Profiles and Compression Timing

4.4.6 Extended Plateau Production: Base Case and Phased Development

Results

As part of the development planning work, the two alternate Casino development scenarios have also been examined against a production profile where the initial 35 PJ/a plateau is extended for as long as possible. The results of sets of cases examining the impact of individual parameters are discussed below. Examples of production and pressure plots for Case 116 and Case 119 (the respective P50 Base Case and Phased Development simulation runs) can be found in Figure 4.4.6-a-d.

Recovery – Base Case vs Phased Development

Results showing cases run to evaluate the impact of production at an extended plateau rate on total recovery can be found in Table 4.4.6-a.

These cases show the rate dependency of recovery from the Waarre C. Compared to the results at the Term Sheet Max ACQ Waarre C recovery is increased by approximately 20 Bcf at the P50 level (Case 116 vs Case 112). Waarre A recovery is not affected by the offtake rate.

The Phased Development with the associated second firm Waarre C well (Prod Y) again results in a small increase in Waarre C reserves compared to the Base Case as shown by a comparison of like for like cases. At the P50 level (cases 119 vs 116) this increase is approximately 13 Bcf, the same increase observed for production at Term Sheet Maximum ACQ rates. At the P90 level the reserve increase associated with the second Waarre C well at 35 PJ/a is negligible.

Case ID No	Base Model	Waarre A Perm Model	Dev Scenario	Market	Comp Required	Prod Y Waters Out	Prod X Waters Out	Recovery to 2017 (Bcf) Wa C	Wa A	Total	Field Life Recovery (Bcf) Wa C	Wa A	Total	Notes
"P90" Model Cases - Base Case														
101	P90	P50	Base	Max ACQ	Aug-10	n.a	Aug-14	161.0	66.7	227.7	161.0	70.0	231.0	P90 Model - Base Case
105	P90	P50	Base	35 PJ/a ext	Dec-09	n.a	Dec-13	175.0	67.8	242.8	175.0	70.0	245.0	P90 Model 35 PJ/a - Base Case
"P90" Model Cases - Phased Development														
104	P90	P50	Phased	Max ACQ	May-09	Feb-10	Nov-13	165.6	60.7	226.3	165.6	69.7	235.3	P90 Model - Phased
108	P90	P50	Phased	35 PJ/a ext	Mar-09	Jan-10	Apr-13	176.1	63.8	239.9	176.1	69.6	245.7	P90 Model 35 PJ/a - Phased
"P50" Model Cases - Base Case														
112	P50	P50	Base	Max ACQ	Sep-14	n.a	Jan-18	195.9	61.9	257.8	195.9	89.4	285.3	P50 Model - Base Case
116	P50	P50	Base	35 PJ/a ext	May-11	n.a	Jul-15	215.6	79.1	294.7	215.6	88.9	304.5	P50 Model 35 PJ/a - Base Case
"P50" Model Cases - Phased Development														
115	P50	P50	Phased	Max ACQ	Mar-12	May-12	Jan-17	210.8	47.2	258.0	210.8	87.5	298.3	P50 Model - Phased
119	P50	P50	Phased	35 PJ/a ext	Oct-10	Nov-11	Feb-15	228.1	70.0	298.1	228.1	88.4	316.5	P50 Model 35 PJ/a - Phased

Table 4.4.6-a: Production at 35 PJ/a Plateau, P90 and P50, Base Case and Phased Development

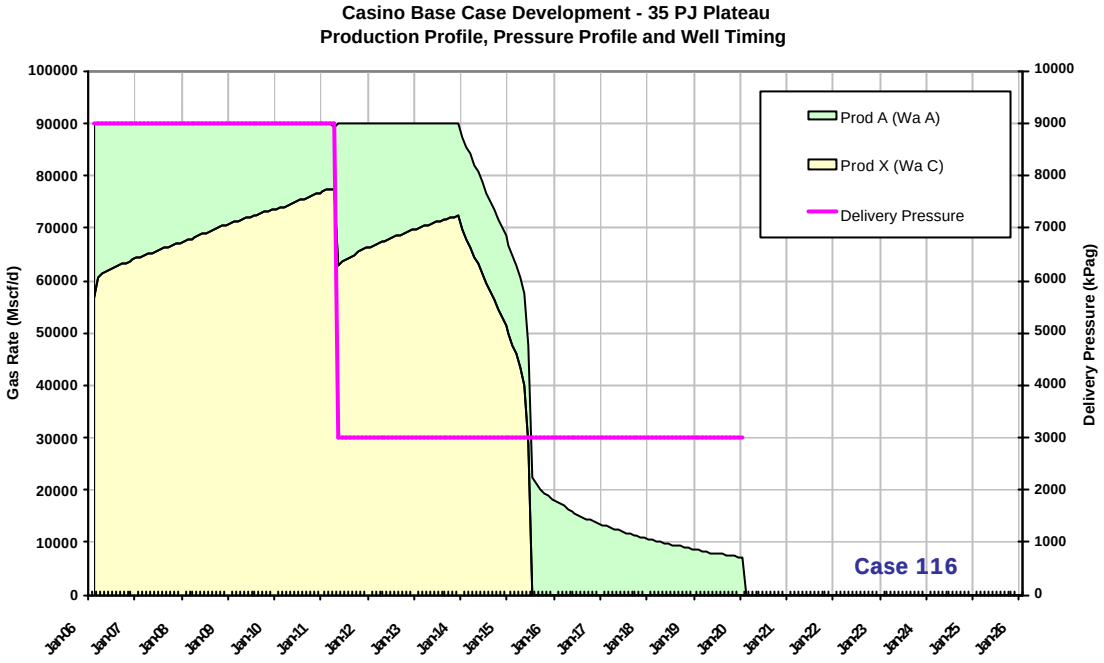

Figure 4.4.6-a: Casino Base Case Development at 35 PJ/a – P50 Production Profile (Case 116)

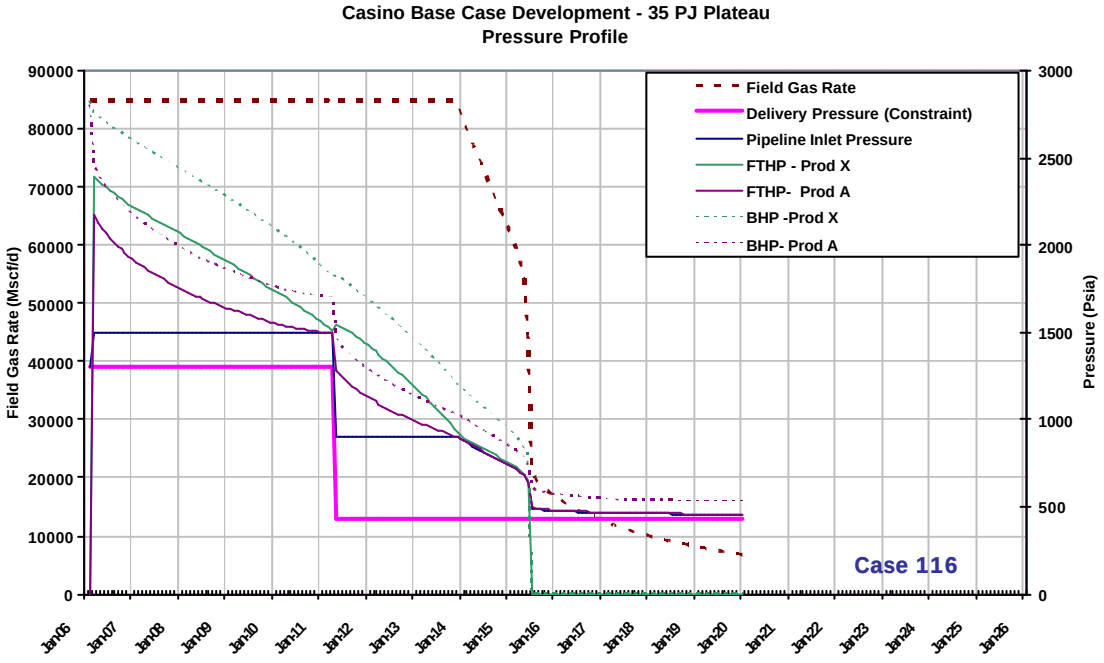

Figure 4.4.6-b: Casino Base Case Development at 35 PJ/a – P50 Production and Pressure Profile (Case 116)

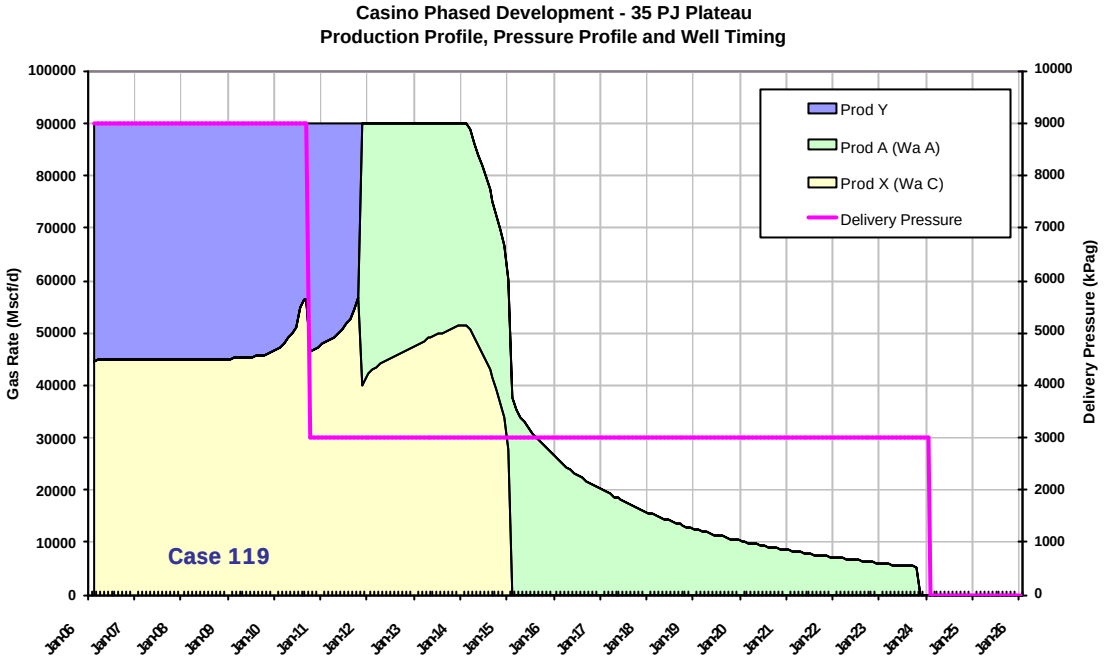

Figure 4.4.6-c: Casino Phased Case Development at 35 PJ/a – P50 Production Profile (Case 119)

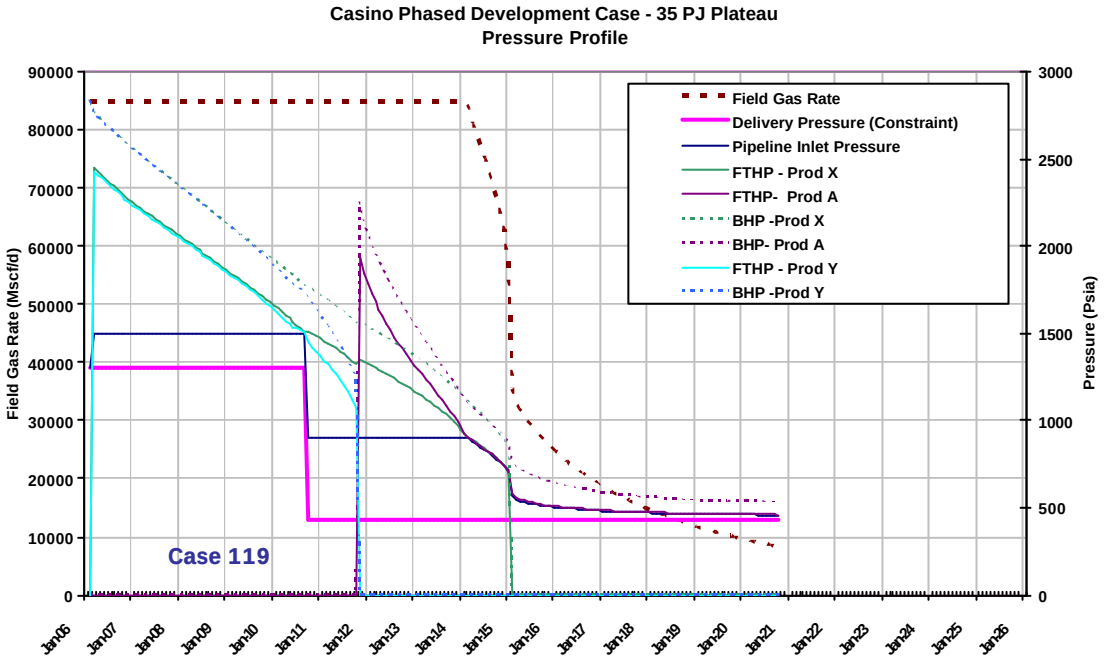

Figure 4.4.6-d: Casino Phased Development at 35 PJ/a – P50 Production and Pressure Profile (Case 119)

Compression Timing

The results of a set of cases run to evaluate the expected timing requirement for compression at an extended 35 PJ/a plateau can be found in Table 4.4.5-b below;

For production at an extended 35 PJ/a plateau the earliest requirement for compression is only slightly accelerated to March 2009 (case 108, P90 Model, Phased) however the window for requiring compression is narrowed considerably to the range 2009 – 2011.

Case ID No	Base Model	Waarre A Perm Model	Dev Scenario	Market	Comp Required	Prod Y Waters Out	Prod X Waters Out	Recovery to 2017 (Bcf) Wa C	Wa A	Total	Field Life Recovery (Bcf) Wa C	Wa A	Total	Notes
"P90" Model Cases														
105	P90	P50	Base	35 PJ/a ext	Dec-09	n.a	Dec-13	175.0	67.8	242.8	175.0	70.0	245.0	P90 Model 35 PJ/a - Base Case
106	P90	P90	Base	35 PJ/a ext	May-09	n.a	May-13	177.0	42.5	219.5	177.0	46.5	223.5	P90 Model 35 PJ/a with low Wa Perm
107	P90	P10	Base	35 PJ/a ext	Mar-10	n.a	Jul-14	174.0	83.0	257.0	174.0	83.0	257.0	P90 Model 35 PJ/a with high Wa Perm
108	P90	P50	Phased	35 PJ/a ext	Mar-09	Jan-10	Apr-13	176.1	63.8	239.9	176.1	69.6	245.7	P90 Model 35 PJ/a - Phased
"P50" Model Cases														
116	P50	P50	Base	35 PJ/a ext	May-11	n.a	Jul-15	215.6	79.1	294.7	215.6	88.9	304.5	P50 Model 35 PJ/a - Base Case
117	P50	P90	Base	35 PJ/a ext	Aug-10	n.a	Oct-14	217.7	48.8	266.5	217.7	62.8	280.5	P50 Model 35 PJ/a with low Wa Perm
118	P50	P10	Base	35 PJ/a ext	Apr-11	n.a	Apr-16	214.5	100.5	315.0	214.5	102.6	317.1	P50 Model 35 PJ/a with high Wa Perm
119	P50	P50	Phased	35 PJ/a ext	Oct-10	Nov-11	Feb-15	228.1	70.0	298.1	228.1	88.4	316.5	P50 Model 35 PJ/a - Phased

Table 4.4.6-b: Production at 35 PJ/a Plateau, Compression Timing

Plateau Length

The duration at which the 35 PJ/a plateau can be maintained was examined for both the Base Case and Phased Development scenarios. Despite the extra Waarre C well in the Phased Development scenario the plateau lengths are very similar (Figure 4.4.6-e). Using the P90 model, the Base Case development (Case 105) maintains plateau production for 72 months from production start-up while the Phased Development (Case 108) plateau ends 1 month earlier.

Using the P50 model, the Base Case development (Case 116) maintains plateau production for 95 months from production start-up while the Phased Development (Case 119) plateau ends only 3 months later.

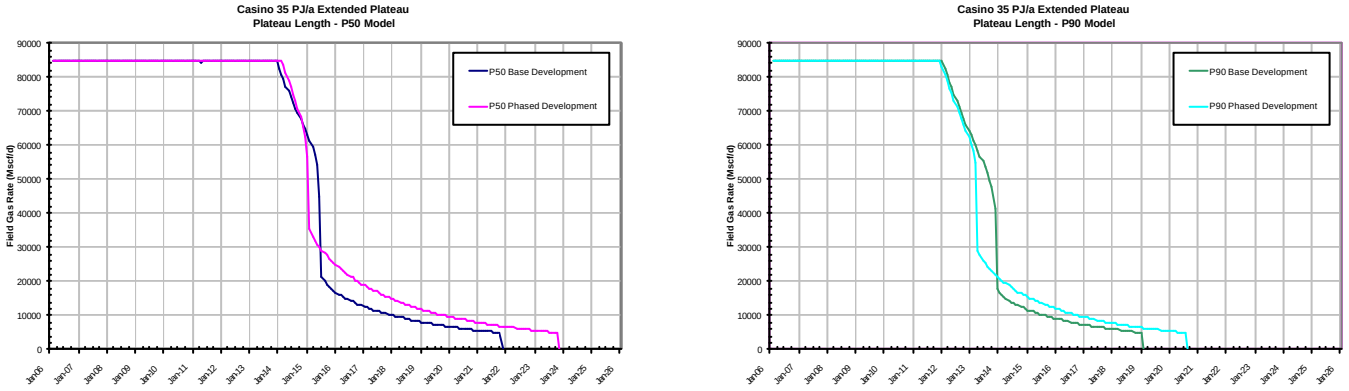

Figure 4.4.6-e: 35 PJ/a Extended Plateau Production : P50, P90 Plateau Length Comparison

Waarre C Water Breakthrough

With production at a 35 PJ/a extended plateau, the crestal Waarre C producer, Prod X is forecast to water out as early as May, 2013 (Case 106, P90 model, P90 Waarre A permeability). This is only 4 months earlier than the equivalent case run at Term Sheet Maximum ACQ.

35 PJ/a Extended Plateau : Production Summary

The major conclusions drawn from this evaluation are as follows;

- Increasing offtake rate from the field results in a significant increase to Waarre C recovery with no incremental capex requirement.
- The window for requiring for compression is significantly reduce compared to Production as per the Term Sheet Maximum ACQ and expected in the range 2009 – 2011. Significantly the actual compression power requirement will be significantly increased as this service will be required for an extended period at offtake rates above 90 MMscf/d

A summary of production profiles and expected compression timing for the 35 PJ/a extended plateau case is shown in Figure 4.4.6-e

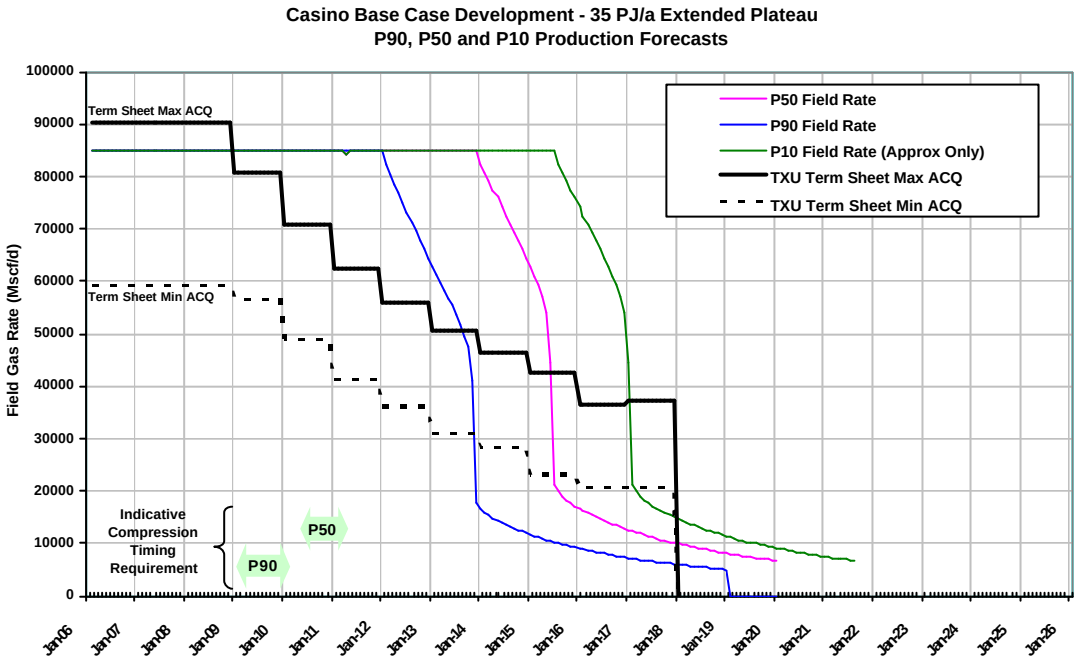

Figure 4.4.6-f: 35 PJ/a Extended Plateau Production Profiles and Compression Timing

4.4.7 Proposed Development Plan

Summary

The Development Plan proposed for the Casino field is the 2 well Base Case development scenario described in Section 4.4.3 and examined in Section 4.4.5 and Section 4.4.6. This scenario will include an initial development of the both the Waarre A and Waarre C reservoirs with separate wells at the Prod X and Prod A locations. The precise location of these wells is set out in Section 4.1.3.

This development scenario is preferred over the 3 well "Phased Development" for the following reasons;

- Development capex is minimised with a 2 well development.
- Ultimate gas recoveries for both scenarios are essentially the same. The small incremental Waarre C gas recovery associated with the 2nd Waarre C well in the "Phased Development" (4 – 13 Bcf) do not justify the additional capex associated with this 3rd well.
- Both scenarios offer the ability to accelerate production by extending the 35 PJ/a plateau with similar plateau lengths.
- The main benefit associated with the 3 well Phased Development is additional security of supply in the early years of production with the flank Prod Y well having sufficient capacity to produce at the daily contract quantity should the crestal Waarre C producer fail for any reason. Depending on the final outcome of the Waarre A producer, this well may also provide for a significant level of redundancy.

The Casino development will also include a vertical pilot hole to be drilled to further evaluate the Waarre A reservoir as the first operation in the Casino field development programme. The Waarre A reservoir will be cored, logged and extensively evaluated with formation pressure tests prior to the pilot hole being plugged back sidetracked to drill the subhorizontal development well. Acquisition of this core and log data will provide valuable data to better understand the performance of this reservoir while on production and reduce the current uncertainties regarding water saturation and intrinsic formation permeability. This data will also provide valuable information to assess the regional prospectivity of the Waarre A reservoir.

In summary, the Casino Development Plan is as follows (Figure 4.4.7-a);

1. Mobilise the Mobile Offshore Drilling Unit (MODU) to the Casino field.
2. Drill, core and log the Waarre A pilot hole, Prod A-p
3. Plug back the pilot hole to the 13 3/8" casing shoe, and sidetrack to drill a subhorizontal Waarre A development well, Prod A-h.
4. Complete the Waarre A development well, including the subsea tree, production test the well and suspend for future connection to the Casino production system.
5. Move to MODU to the location of the Waarre C development well, Prod X.
6. Drill and complete the Waarre C development well, Prod X, including the subsea tree.
7. Production test this well and suspend for future connection to the Casino production system.
8. Demobilise the MODU

Contingencies

The proposed Casino production facilities provide significant flexibility with regard to additional well connections. Pre-investment will be made in tie-in capability for up to 4 additional wells which may be utilised at any stage of the Casino field life. This may include a requirement to connect an additional Waarre C development well such as a well at the Prod Y location or development wells resulting from near field exploration success in the Casino area. The requirements for these additional well connections either within the Casino field or near field will be considered following an assessment of Waarre A well performance.

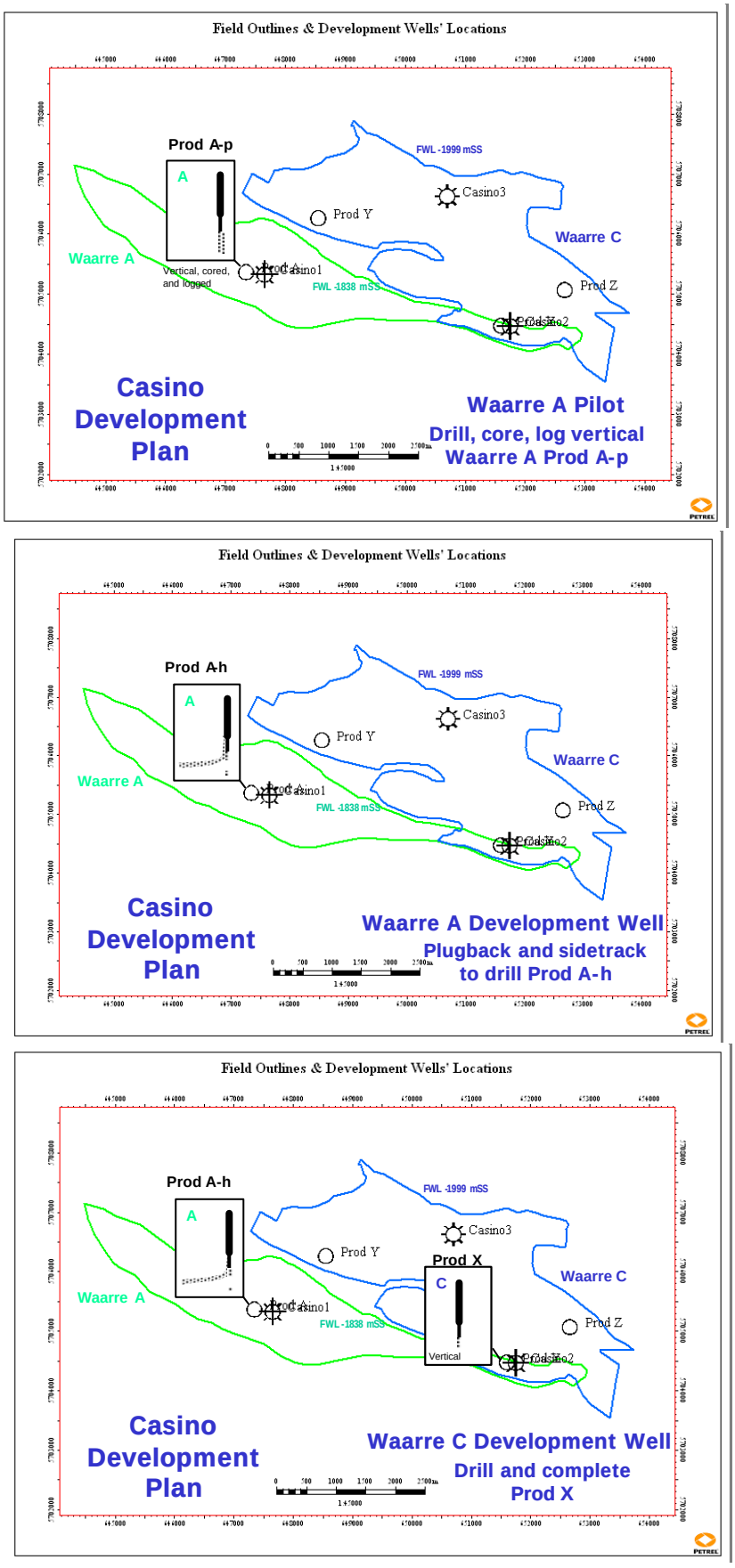

Figure 4.4.7-a: Proposed Casino Development Plan

4.4.8 Reservoir Management Plan

Background

A detailed reservoir management plan, will be prepared prior to commencing production from the Casino facilities.

The principal reservoir management objective will be to maximise recovery of the Casino gas resource. As indicated in Section 4.4.7 additional reservoir data will be obtained from the Waarre A reservoir when the development wells are drilled (via a pilot hole) and the production performance of each zone of each well will be closely monitored. As more data is obtained, the geological model and reservoir simulation model will be periodically updated to reflect the new information collected and ultimately will be history matched to actual production data.

This section sets out the evaluation programme for the planned development wells and reservoir management principles, which will be followed during production from the Casino field.

Well Evaluation

Waarre A Pilot Hole

As discussed in Chapter 3, there is only a small amount of core material from the Waarre A and no production test. Consequently there is a fair degree uncertainty not only with permeability (and hence deliverability) but also equivalent hydrocarbon (EHC) thickness (i.e. h*Sg*Phit) for the Waarre A. To address these uncertainties a comprehensive evaluation programme will be performed in a vertical, Waarre A pilot hole.

Upon penetration of the Waarre A, in the vertical pilot hole, a full core will be cut over a majority of the reservoir interval. A routine core analysis programme will be performed on core plugs cut from the full core. This programme will be designed to address the above objectives. This programme will comprise;

- Helium Injection Porosity at ambient and initial net overburden conditions (NOB).
- Air Permeability at ambient and initial NOB
- Grain density
- Formation Resistivity Factor (FRF) at multiple salinities (at NOB) to determine porosity exponent, “m”.

At the conclusion of the routine core analysis study a subset of core plugs will be selected for Special Core Analysis. The results of the programme will be used to update to the dynamic simulation model for the Waarre A, in particular initial gas saturation and gas-water relative permeability. The Special Core Analysis Program may comprise;

- Centrifuge, Drainage Capillary Pressure measurements (at NOB) to determine Swirr
- Centrifuge, Imbibition Capillary Pressure measurements (at NOB) to determine true Sgr.
- End-Point Water Relative Permeability (Krw’) at the termination of the Imbibition tests.
- Steady-State, Relative Permeability tests (air-brine).
- Cation Exchange Capacity (Wet Chemistry method) for shaly-sand Swt modelling.
- Rock mechanics for sand failure prediction work.
- Mercury Injection tests for pore throat size distribution.

The majority of core plug samples will be cleaned with a solvent followed by oven drying. A subset of core plugs will be humidity dried to assess the impact of drying procedures on porosity and permeability measurements.

Core plugs will be cut horizontal and perpendicular to the bedding planes to determine the kv/kh ratio of the reservoir. Plugs will also be cut perpendicular to significant siltstone/shale interbeds which are likely to have a significant impact on vertical permeability.

Open-hole wireline logging will be performed in the pilot hole once the core has been cut and recovered. This programme will comprise a standard logging suite i.e. GR, laterolog, Rxo, compressional transit-time, density and neutron. In addition to this standard suite of logs the following data will also be acquired;

- Wireline pressure survey eg. Schlumberger's MDT.
- Full bore micro resistivity imaging tool e.g. Schlumberger's FMI.
- Nuclear Magnetic Resonance Image tool e.g. Schlumberger's CMR Plus.

A wireline pressure survey will be run to acquire mobility measurements. In situ permeability will be calculated from these measurements which will be used to support routine core analysis measurements of permeability.

Nuclear Magnetic Resonance Image tool will be run. While the measurement of absolute porosity is unreliable in a gas reservoir the relative percentage of bound fluid (including clay bound water) does provide insight into the water saturation within the gas reservoir.

Full bore micro resistivity imaging tool will be run. An interpretation of the results will provide important information over the non-cored intervals such as the presence or absence of thin beds and natural fractures.

Development Wells (PRODX and PRODA)

The principal objective of the open-hole evaluation programmes in PRODX and PRODY is confirming the EHC thickness for the respective reservoirs.

The Waarre C development well, PRODX, will be a vertical well. Given the proximity of the PRODX to Casino-2 only a standard logging suite will be acquired. The suite will comprise GR, laterolog, Rxo, compressional transit-time, density and neutron logs. The Waarre C reservoir was extensively cored in Casino-2, as such it is not deemed necessary to acquire a full core in the PRODX well.

The Waarre A development well, PRODA, will be sub-horizontal through the reservoir section (approx 80 to 85 deg). It will not be possible to run logs on wireline at this well deviation. The preferred means to acquire log data is Measurement While Drilling (MWD) conveyed on drill pipe. The MWD suite will comprise; gamma-ray, compressional transit time, phase/attenuation resistivity and density-neutron. A comprehensive evaluation programme will be acquired from the Waarre A pilot hole as such the basic information from the MWD will suffice for the production hole.

In both development wells a cement bond evaluation log will be run down to the 9 5/8" casing shoe, in order to assess the quality of the cement bond.

Production Testing

Both development wells will be tested with the MODU after the sandface completions have been run and prior to MODU release. The objectives of the test are as follows;

- Flow back completion brine and 'clean up' flow
- Determine initial well deliverability
- Determine effective reservoir permeability-thickness (kh)
- Determine well skin i.e. Darcy Skin and Non-Darcy Skin (D-Factor)
- Calibrate VFP correlation to nodal pressure data.

The preliminary test design is shown in Table 4.4.8-a;

Duration (hrs)	Task
9	Clean up Flow (inc. BS&W)
6	Shut-In. Rig up e-line & RIH with PLT
4	1st Flow Period
4	2nd Flow Period
4	3rd Flow Period
2	Shut-In for Build Up
6	POOH with e-line PLT
35	**Total Test Duration**

Table 4.4.8-a: Preliminary test design for the development wells, PRODX and PRODA.

The duration of the clean up flow will be dependent on achieving a stable tubing head pressure, tubing head temperature and bulk solids & water (BS&W).

After the clean up period is complete, the well will be shutin (at surface) for an initial buildup period. As the production test will be performed with the completion installed no downhole shut-in will be possible.

The proposed completion for the development wells is not suitable for hanging down-hole gauges as there is not a perforated joint above the nipple profile. A modified PLT string with surface read-out (similar to Minerva-4) will be run to acquire downhole pressure and temperature. Additionally, a noise log will be included in the PLT string to assist in identifying inflow behind the sandscreens.

The principal objective of the "Flow-After-Flow" period is to determine non-Darcy Skin (or D-Factor). In high rate gas wells a significant portion of the wells' Total Skin (S) may be attributable to non-Darcy skin, as such quantifying the D-Factor is important in determining the productivity of the development wells. Flow will be diverted to a test separator during this period via a fixed choke. The first flow period will be at a low rate approximately one third of the maximum rate. The second flow period will be at a moderate rate, approximately two-thirds of the maximum rate and the third period will be at the maximum rate. The maximum rate will be determined by the clean-up period and is the maximum rate the well can deliver against the THP or the critical rate, whichever is lower.

During each of the "Flow-After-Flow" periods separator samples of gas and condensate will be collected for recombination and laboratory analysis to confirm the HC composition of each reservoir. Trace element analysis has yet to be performed on hydrocarbons from the Waarre A reservoir. During the "Flow-After-Flow" period of the PRODA test onsite analysis for Hg, H_2S, Total Sulphur and Mercaptans will be performed.

Production Measurement and Allocation

The subsea trees will comprise production measurement for production allocation and management purposes. Each subsea tree will comprise the following features;

- Be controlled by electro hydraulic subsea control modules (SCMs),
- Include chokes (remotely controlled from onshore with position indication),
- Provide connection and valves to facilitate corrosion and hydrate inhibitor injection into each well stream,
- Have flow-metering and sand monitoring capability,
- Have pressure and temperature instrumentation to allow monitoring of the annulus and tubing.

Each reservoir will have a dedicated production well, consequently it will be possible to allocate production and acquire data for reservoir management purposes for the Waarre C and Waarre A from PRODX and PRODA respectively. Flow-metering will not be of fiscal quality but will suffice for production allocation purposes. Fiscal production metering will be via new facilities to be installed at the Iona Gas Plant as described in Section 6.4.3.

Bottom-hole pressure and temperature measurements were not deemed necessary. The Casino reservoirs comprise a dry gas and no formation water production will be tolerated. As such calculation of shut-in and

flowing bottom hole pressure is relatively simple, particularly given that the VLP correlations will be calibrated to the well test data.

Reservoir Management Principles

The strategy for the initial commercial production from the Casino field is to preferentially produce the Waarre C reservoir at the highest offtake rate possible i.e. DCQ of approximately 90mmscf/d (of raw gas) while only producing the Waarre A reservoir periodically. Production from the development wells will be controlled by wellhead chokes operated onshore via electro-hydraulic umbilicals.

Initial delivery pressure at the Iona Gas Facility is 9000 kPa. Once the PRODX well cannot meet MDQ at this delivery pressure, the PRODA well will be beaned up to meet the shortfall. Once the deliverability from both the development wells is no longer sufficient to meet MDQ, compression will be commissioned at the Iona Gas Facility to lower flowing tubing head pressure and maintain deliverability at the contracted rates.

The justification to initially preferentially produce the PRODX well is threefold;

1. Maximise Waarre C ultimate recovery.
2. Reduce production shortfall in the case of PRODX failure.
3. Determine OGIP for Waarre A.

Dynamic simulation work has indicated that the recovery efficiency for the Waarre C will benefit from a high offtake rate. A relatively higher rate results in a lowering of the trapped gas pressure which manifests in a higher recovery efficiency in a water drive gas reservoir.

In the event of a mechanical failure of PRODX it is possible that the PRODA well will not be able to meet DCQ, certainty for a sustained period. If PRODA is only intermittently produced well delivery potential will be maintained for a longer period than if the well was producing on a continual basis. Consequently in the unlikely event of mechanical failure of PRODX the impact of a possible production shortfall will be reduced.

The dominate drive mechanism for the Waarre A gas reservoir is expected to be volumetric depletion. Periodic production followed by a shut-in will provide static reservoir pressures. This information can be used in analytical material balance calculations to determine the gas-in-place for the Waarre A reservoir. This estimate will be valuable for reserve assessment.

Water Production

The Iona Gas Facility, which will process the raw gas from Casino, is only designed to handle water of condensation. Once free water production occurs the offending development well will be shut-in.

Sand Production

A down-hole sand exclusion screen system will be installed in the wells across the reservoir sections to prevent formation sand passing into the production system. In addition, sand detection and erosion monitoring equipment will be installed in case of sand breakthrough. If sand is detected then flowrates will be adjusted to minimise the sand production.

4.5 References & Enclosures

4.5.1 References

4.2 Dynamic Reservoir Modelling

Barker, G and Vincent, P. 1988. Geological and Reservoir Engineering Consideration for the North Rankin Gas Recycling Project. APEA Journal.

Behrenbruch, P and Kozma, G. 1984. Interpretation of Results from Well Testing Gas-Condensate Reservoirs: Comparison of Theory and Field Cases. SPE Paper 13185, 59th Annual Technical Conference and Exhibition of the SPE of AIME, Houston.

Corelab. 2003. A Special Core Analyses Study Of the Selected Samples From the Well: Casino -2. Corelab Laboratories Australia Pty. Ltd. Santos unpublished report.

Corelab. 2004. A Special Core Analyses Study Of Selected Samples From Well: Casino -3. Corelab Laboratories Australia Pty. Ltd. Santos unpublished report.

Dake, L.P. 1978. Fundamentals of Reservoir Engineering. Elsevier Scientific Publishing Company.

Steyn, A.S. 2004. Casino Gas Field Development. Casino-3 Drill Stem Test Analysis Report. Santos unpublished report.

Stiles, J. 1999. Using Special Core Analysis in Reservoir Engineering. Short Course Notes. Imperial College of Science, Technology and Medicine.

4.5.2 Enclosures

Enclosure 3.3.3 b	Top Waarre C Main Pay Map Showing Waarre C Well Locations
Enclosure 3.3.3 d	Top Lower Waarre A Map Showing Waarre A Well Locations
Enclosure 4.2.7 a	Dynamic Simulation Sensitivity Scenarios
Enclosure 4.3.2 a	Ultimate Recovery Scenario Tree - P50
Enclosure 4.3.2 b	Ultimate Recovery Scenario Tree - P90
Enclosure 4.3.2 c	Ultimate Recovery Scenario Tree - P10

5 Drilling & Completions

5.1 Development Concept Overview

5.1.1 Summary

The proposed initial field development is to drill and complete two wells:

- one vertical sub-sea Waarre “C” well (Prod X) and
- one sub-horizontal sub-sea Waarre “A” well (Prod A)

Prod A will be drilled with a vertical pilot hole to obtain core in the Waarre A sand. The pilot hole will then be plugged back and sidetracked to drill the sub-horizontal well.

Details of the drilling and completions programs are provided below.

5.1.2 Drilling History

Three vertical exploration wells have been drilled in VIC/P44. A summary of well information is given in Table 5.1.2-a.

Well	Summary Information		Results / Status
Casino-1	Spud Date: TD: Spud to TD: Spud to TD (ex-WOW): Spud to Release: Spud to Release (ex-WOW):	26 Aug 2002 2118 m 20 days 13 days 29 days 18 days	Plugged & Abandoned Log #1 PEX-DSI-HALS Log #2 MDT Log #3 CST No cores No drill stem tests
Casino-2	Spud Date: TD: Spud to TD: Spud to Release:	24 Sept 2002 2112 m 10 days 18 days	Plugged & Abandoned Log #1 PEX-HALS-DSI-HNGS Log #2 MDT Log #3 CST 21m of core cut No drill stem tests
Casino-3	Spud Date: TD: Spud to TD: Spud to TD (ex-WOW): Spud to Release: Spud to Release (ex-WOW):	14 Oct 2003 2135 m 16 days 14 days 31 days 29 days	Plugged & Abandoned Log #1 DSI-GR-CAL-HALS Log #2 MDT Log #3 PEX-CMR-HGNS Log #4 MSCT Log #5 CST 27m of core cut Flow Tested Well

Table 5.1.2-a: Summary of Casino Well Information

No significant drilling problems were encountered in any of the above wells. Significant weather delays were encountered during Casino-1 and minor delays during Casino-3.

5.2 Drilling Completions Program

5.2.1 Drilling Program

The drilling and completion plan is based on information gained from the wells drilled to date.

The Ocean Patriot has been contracted to drill and complete the Casino development wells. The Ocean Patriot is a semi-submersible rig, rated for the Casino water depth and the planned well depths. Diamond Offshore, a reputable rig operator with proven Quality and HSE systems, operates the Ocean Patriot and has experience in operating in Australian and Victorian offshore environments.

The base plan is to drill a vertical pilot hole (Prod-A) into the Waarre "A" Sand, cut two 18 metre cores through the sand and complete the well. The pilot hole is to be located updip of Casino-1. A crestal vertical well (Prod-X) is to be drilled into the Waarre "C" Sand, adjacent to Casino-2, with expandable sand screens run across the reservoir section during well completion. Wire-wrapped sand screens will be run across the Waarre A reservoir.

All construction materials used in the exposed well casing(s), production tubing strings, all other completion materials and the sub-sea production trees will be made of selected corrosion resistant alloy steel materials which have been designed to last the life of the field without intervention.

A summary of borehole and casing sizes with approximate depths is given in Tables 5.2.1-a, -b & -c.

Hole Size	Purpose	Casing Size	Formations	mSS TVD	mSS MD
36" x 26"	Conductor	30" x 20"	Undifferentiated Tertiary	130	130
17 ½"	Surface Casing	20" x 13 3/8"	Nirranda Group	700	700
12 ¼"	Production Hole	n/a	Skull Creek Mudstone	1722	1722
TBA	Core	n/a	Waarre "A" Sand	1755	1755

Table 5.2.1-a: Pilot Vertical Well Hole Sizes with Depth (Prod-A)

Hole Size	Purpose	Casing Size	Formations	mSS TVD	mSS MD
36" x 26"	Conductor	30" x 20"	as above	as above	as above
17 ½"	Surface Casing	20" x 13 3/8"	as above	as above	as above
12 ¼"	Production Casing	10 ¾" x 9 5/8"	Skull Creek Mudstone	170/1698	170/1720
8 ½"	Production Hole	6 5/8" screens	Waarre "A" Sand	1712	1755

Table 5.2.1-b: Horizontal Well ex-Pilot Hole Sizes with Depth (Prod –A)

Hole Size	Purpose	Casing Size	Formations	mSS TVD	mSS MD
36" x 26"	Conductor	30" x 20"	Undifferentiated Tertiary	130	130
17 ½"	Surface Casing	20" x 13 3/8"	Nirranda Group	635	635
12 ¼"	Production Casing	10 ¾" x 9 5/8"	Skull Creek Mudstone	170/1722	170/1722
8 ½"	Production Hole	5 ½" ESS	Waarre "C" Sand	1755	1755

Table 5.2.1-c: Vertical Well Hole Sizes with Depth (Prod-X)

5.2.2 Casino Program

A 30" (762mm) conductor string, swaged down to a 20" (508mm) shoe will be utilised for both wells. The conductor string will be cemented back to the seabed.

The intermediate casing string will consist of 13 3/8" (340mm) casing set at approximately 50m above the Mepunga Formation. This string will have buttress connections and will be cemented in place.

The production casing string will consist of a 10 ¾" (273mm) string swaged down to a 9 5/8" (244mm) string at approx. 170 mSS to accommodate the TRSSSV. This string will have premium connections and be cemented in place. The 9-5/8" casing below the production packer will be corrosion resistant alloy as it will be exposed to the reservoir fluids.

An expandable sand screen will be run over the reservoir section in the vertical well and wire-wrapped sand screen run over the reservoir section in the deviated well.

5.2.3 Drilling Fluid Program

The drilling fluid program is being designed to enable the development wells to be drilled as efficiently as possible with a minimum amount of risk. It will be very similar to that used in the Casino exploration and appraisal wells. No significant hole problems were encountered on these wells.

The conductor and surface sections will be drilled using seawater with high viscosity sweeps to effect hole cleaning.

The 12-1/4" hole section will be drilled using a potassium chloride/polymer drilling fluid with glycol additions to provide inhibition over the Skull Creek Mudstone.

The use of oil based mud is not planned.

A drill-in fluid has not yet been selected for the reservoir section. It will be a low solids water based fluid.

5.2.4 Well Modelling

Waarre 'C" sand well.

The drilling and completion plan for the Waarre "C" sand development well is based on information gained from the wells drilled to date. This information includes wireline logs, well testing and full core analysis.

Waarre "C" development well will be drilled as sub sea vertical wells and completed open hole with expandable sand screens and with 7" corrosion resistant production tubing.

Waarre "A" sand well.

The drilling and completion plan for the Waarre "A" sand development well is based on information gained from wells drilled to date. The information includes wireline logs and a limited set of sidewall cores.

It is proposed to drill a pilot hole, targeting the Waarre "A" sand and obtain two 18 meter full hole cores of the interval. Analysis of these cores will enable optimisation of the well design. The most likely outcome will confirm that the Waarre "A" sand will be drilled and completed as high angle sub-sea well with the production hole drilled 400 - 600 meters across the entire productive interval.

This well will be completed open hole with sand exclusion screens and 7" corrosion resistant production tubing.

5.2.5 Sand Control

With the use of sub-sea completions, sand exclusion from the sub-sea tree is seen as having critical importance in order to ensure reliability of wellhead and subsurface equipment.

Sand prediction studies conducted by the CSIRO, including rock mechanical properties testing, suggest that sand production is likely from a horizontal well. For a vertical well, the study defines a safe operating window based on drawdown. However, the analysis requires some assumptions of the values of the regional stress which cannot be accurately known.

It is therefore proposed to install sand exclusion screens in all wells. It is proposed to use expandable sand screens for vertical wells and premium wire wrapped screens for horizontal wells.

5.2.6 Tubing Sizing and Completion Components

Detailed modelling work has been undertaken to select production tubing size with regard to required field production rate and ultimate recovery.

Due to the presence of CO_2 in the produced gas, all completion components and tubulars exposed to well fluids have been selected as corrosion resistant alloy steel.

A mechanical load and stress analysis of tubing, packer and completion components will be conducted during detailed completion design.

The following tubing specification is currently specified:

Tubing size	Tubing weight (lb/ft)	Metallurgy/Grade	Connection
7”	29	13Cr80	KS - Bear

5.2.7 Well Performance and Testing

The wells will be flowed to clean-up with the MODU prior to well suspension. This is to confirm well productivity and to ensure that the sand face and well screens are clean of drilling mud, filtrate and well solids. It is planned to record bottom hole pressure and temperature. The flow will include multiple rates and a short build up period. The wells will then be ready for commissioning.

5.2.8 Completion Program

It is proposed that each well will have an upper and a lower completion.

The upper completion will include a 7” TRSSSV and control line set at between 30 to 80 meters below the seafloor. The sub surface safety valve will be have a non equalizing flapper valve reducing a potential leak path. A hydraulic or hydrostatic pressure set production packer will be installed. Flow control equipment and a chemical cut sub will be installed.

The lower completion will include a sand screen hanger, a flow control nipple and either wire wrapped or expandable sand screen.

The casing between the upper and lower completions will be 13 Chrome metallurgy as it will be exposed to well fluids.

All completion equipment is specified as CO_2 corrosion resistant alloy steel.

Production casing will be set above the formation. 8-1/2” production hole will be drilled using a specially designed low solids, non damaging “drill-in” fluid. The lower completion will be run and set after conditioning the “drill-in” fluid. After the upper completion is run a clean up flow will be conducted to ensure the expected well productivity is achieved. The well will be left ready for commissioning.

A horizontal sub-sea tree will be installed on each of the wells. The horizontal tree allows the drilling of 12-1/4” and 8-1/2” hole through the tree. This option allows operational flexibility in original construction and if

well intervention is required in the life of the well. Tree metallurgy and valve trim is selected for expected wellhead pressures, temperatures and corrosive gas environment.

The proposed completion schematic is shown in Figure 5.2.8-a.

5.2.9 Workovers and Well Intervention

No routine well intervention is planned through the production life of the wells. The wells will be designed with premium equipment.

If the wells do suffer a downhole failure a MODU will likely be required for intervention. Completion design will allow MODU assisted production logging with coil tubing or electric/slick line deployed tools. Remediation of sand face problems such as screen failure or water breakthrough will require abandonment of the completed zone and re-drill of a side track. Horizontal sub sea trees will facilitate this activity if it is required.

5.2.10 Drilling and Completion

The drilling, completion and clean-up flow of the Casino development wells is expected to take 33 days for each well.

The timing of the drilling and completion programme will be driven by rig availability. It is expected that the first well will spud in the first quarter of 2005.

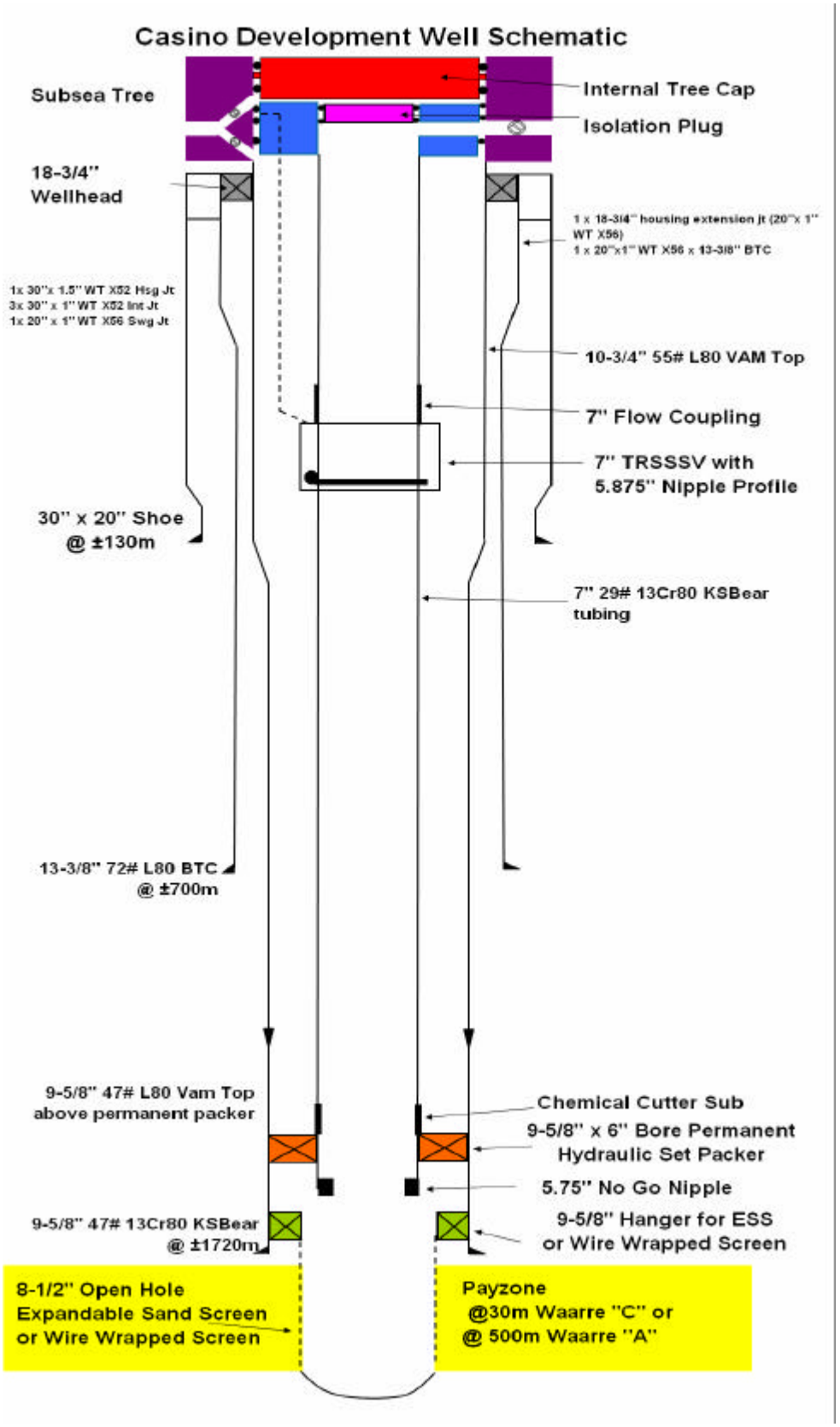

Figure 5.2.8-a: Summary of Casino Well Information

6 Process Facilities & Pipeline Construction

6.1 Facilities Description

6.1.1 Summary

The Casino gas field is being developed to supply gas to the Victorian and South Australian gas systems via the TXU Iona gas plant. Two subsea wells, an offshore pipeline, a horizontally directional drilled (HDD) shore crossing and onshore pipeline will be installed to deliver gas to the TXU Iona gas plant. This is depicted in Figure 6.1.1-a below.

Production from the Casino Gas Field of up to 100 MMscfd is planned. The relatively dry gas, low gas/liquids ratio and the expected reservoir pressure characteristics of the Casino reservoir, and well completion design, permits gas transmission to shore without any offshore processing. The control of hydrates during start-up and normal production requires the injection of mono-ethylene glycol at the wellheads as a hydrate inhibitor. In addition, corrosion inhibitor will be injected continuously at the wellheads to mitigate corrosion through the production life of the wells.

The development plan will comprise the following major components:

- Two subsea development wells complete with subsea trees (SSTs), subsea control modules, (SCMs) and chokes,
- An electro-hydraulic control umbilical to provide safe and effective well operations control from the shore and to transport hydrate and corrosion inhibitors to each wellhead,
- An offshore pipeline to transport the produced well fluids to the shore line,
- An HDD shore crossing,
- Main Line Valve site containing the end of line facilities for the onshore and offshore lines including a Hydraulic Power Unit (HPU) for supply of hydraulic control fluid for wellhead valve and tubing retrievable surface-controlled subsurface safety valve (TRSSSV) operation, a master control station (MCS) and electrical power unit (EPU), which together combine to provide well control functionality, power and signal inputs/outputs; and an onshore umbilical termination assembly (OUTA) which is the marshalling unit / interface between the onshore and offshore power, signal, hydraulic and chemical injection lines.
- An onshore well stream fluids pipeline, mono ethylene glycol lines and fibre optics cable from the MLV site to the TXU Iona gas plant,
- Additions and upgrades to the TXU Iona gas plant (undertaken by TXU).

Provision will be made for future tie-ins approximately 15 km from the shore crossing and at the end of the pipeline.

The facilities have a design life of 20 years.

The development will comply with applicable Commonwealth and State legislation and regulations and the requisite regulatory approvals.

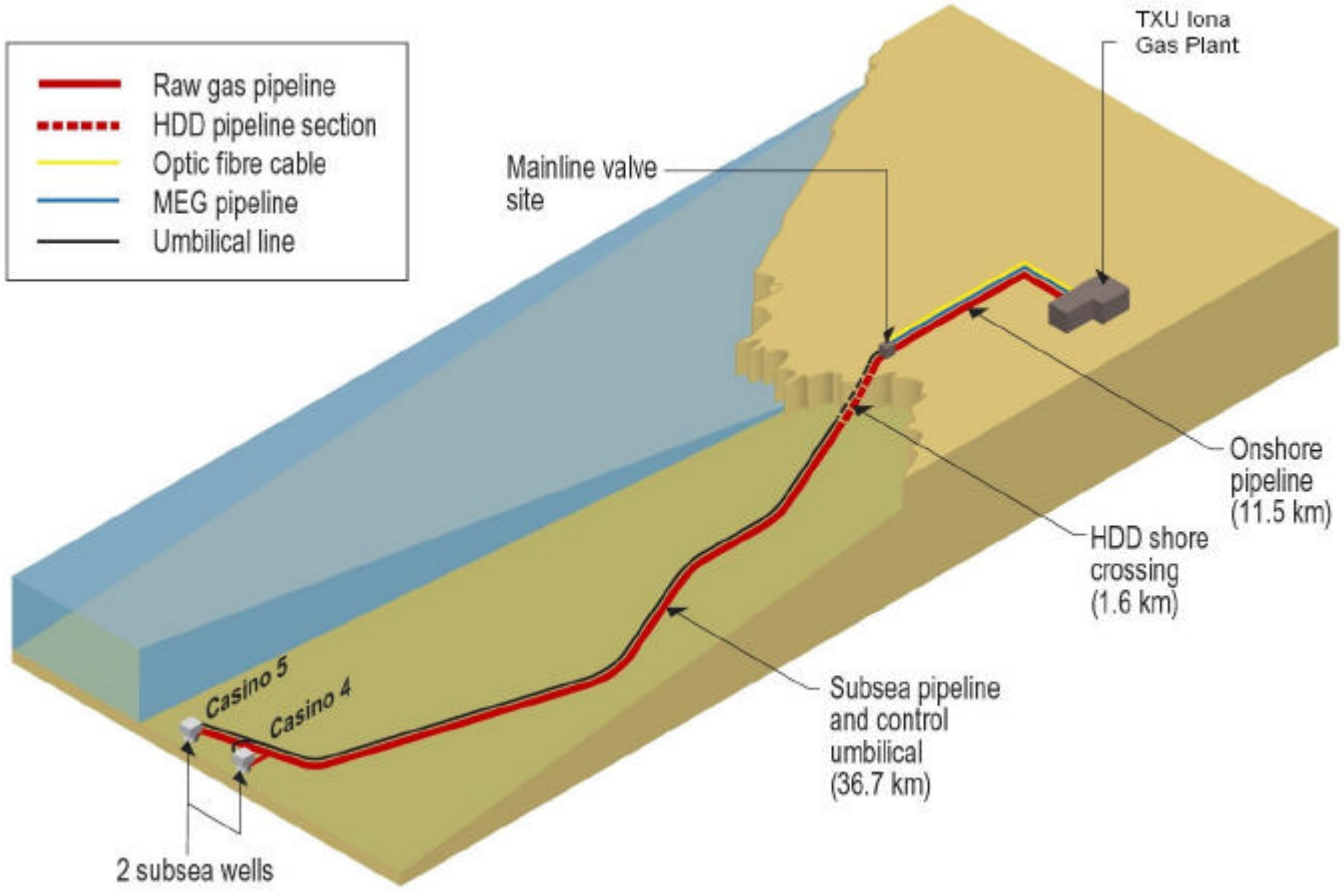

Figure 6.1.1-a: Casino Field Development Layout

6.2 Offshore Facilities

6.2.1 Wells and Wellheads

The offshore development is a subsea configuration comprising of two subsea wells tied into a subsea pipeline to permit free flowing of the well stream fluids to shore. Use of an offshore platform will not be necessary with this design strategy resulting in there being no visual or physical impact from such a structure and its operation.

The subsea christmas trees will be supported by wellheads and a permanent guide base in the conventional manner, and will be drill-through type. The trees will house the valves required to isolate and regulate flow, being master, wing and choke valves. Annulus and crossover valves will also be installed.

The trees will have the following features:

- Be horizontal drill-through type,
- Be controlled by electro hydraulic subsea control modules (SCMs),
- Include chokes (remotely controlled from onshore with position indication),
- Have a diver connectable interface to allow flexible spools to be connected from each well to the offshore pipeline,
- Provide connection and valves to facilitate corrosion and hydrate inhibitor injection into each well stream,
- Have flow-metering and sand monitoring capability,
- Have pressure and temperature instrumentation to allow monitoring at the annulus and production bores.

A down-hole sand screen system is being installed in the wells across the reservoir sections to prevent formation sand passing into the production system. In addition, sand detection and erosion monitoring equipment will be installed in case of sand breakthrough. If sand is detected then flowrates will be adjusted to minimise the sand production.

6.2.2 Control Systems

A multiplexed electro-hydraulic well control system is planned. The control system will initially provide for up to three wells producing simultaneously. The control system will operate and control two production wells with single subsea christmas trees (SST) installed. Each well contains a single string completion with tubing retrievable surface controlled sub-surface safety valve (TRSSSV), with wellhead controls and hydraulic systems for opening and closing wellhead valves and sub surface safety valves, with expandability to six wells.

The control system on each SST will consist of an subsea control modules (SCM) mounted on the SST and connected via flying leads to an umbilical termination assembly (UTA) located along the main electro-hydraulic umbilical leading to the onshore control system. The choke valve, SCM and jumper connections will be suitable for intervention by remotely operated vehicle (ROV). SST valves will also be suitable for operation by ROV.

The main features / components of the control system include:-

- Electro Hydraulic multiplex SCMs that are installable and retrievable by ROV,
- Retrievable subsea accumulator modules (SAMs) providing high pressure and low pressure hydraulic accumulation to the system for enhanced response times,
- Instrumentation and data gathering for collecting process data and status indication,
- Umbilical / interconnecting jumper system from the main line valve site to the wellheads. The system will contain duplicated hydraulic control systems cores, power and signal cables and the chemical injection lines.
- Umbilical termination assemblies (UTAs) that provide the connection points between the umbilical and the flying leads. The umbilical is laid at a nominal distance of 20-40 metres from the pipeline,
- A hydraulic power unit at the main line valve site,
- A master control station (MCS) and electrical power unit (EPU), both of which are located at the main line valve site. They together combine to provide well control functionality, power and signal inputs/outputs,

- An OUTA, which is the marshalling unit / interface between the onshore and offshore power, signal, hydraulic and chemical injection lines.

The control system will be designed to provide full redundancy so that there is no loss of control of production following the failure of any single component within the control system, including the onshore hydraulic power unit. The control system will be configured such that in event of complete loss of signal, well production can be stopped by the tripping of an ESD sequence command from the HPU to start venting of hydraulic pressure from the entire subsea system thereby initiating a total shutdown of the subsea valves. The subsea valves will close within some 15 to 20 minutes of ESD. It should be noted that ESD with control system operating normally will close subsea valves within 5 minutes.

6.2.3 Offshore Pipeline

The offshore pipeline will run from the most distant offshore well in an easterly direction past the second well and then will curve north to the shore crossing location. This route has been selected from 3 initially envisaged routes after a detailed route survey. The selected route was the only route shown to be free of major sea bed obstructions.

The Casino subsea production facilities have been configured to allow for the tie-in of an additional Casino well at the reservoir location. Also there is the ability to tie in a 12" pipeline from another field into the Casino pipeline termination assembly (PTA) located at the extreme end of the pipeline. Provisions have been made for tie in of a 6" pipeline about 15km from the shore crossing using an inline tee (ILT) tie in point.

The provisions for tie-ins are made with a double block and bleed valve arrangement and blind flange at each tie-in point.

The main specifications features of the offshore pipeline are:

- 12" nominal diameter,
- wall thickness 17.5mm and 22.2mm (for 6km at the near shore end),
- approximately 37 km in length,
- pipe steel grade DNV SML 450 IU,
- design pressure 17,600 kPa,
- water depth range 0 to 70 metres,
- corrosion coating 3 Layer Poly Propylene (3LPP),
- weight coating N/A (pipeline steel weight provides stability),
- external cathodic protection braclet anodes,
- operating temperature range 60-10 degrees Celsius,
- Design life of 20 years,
- Provision for future intelligent pigging of pipeline.

All flowline and manifold piping will be designed in accordance with AS 2885 – DNV-OS-F101, Submarine Pipeline Systems.

Critical pipeline design and operating parameters and means of control will be as follows:

Internal corrosion

The pipeline has been designed with an internal corrosion allowance of 3mm. Corrosion inhibitor and mono-ethylene glycol will be continuously injected at the wellheads. The iron content of the mono-ethylene glycol returning to the plant for regeneration will be monitored to confirm the effectiveness of the corrosion inhibitor.

On-bottom stability

The offshore pipeline will be designed to maintain on-bottom stability throughout its design life. It is anticipated that stability can be achieved over the pipeline length by adequate pipeline weight. This has been modelled to ensure that in particular the shallow interval of the pipeline (near-shore) remains stable. A thicker-walled section (22.2 mm) will be laid at the near-shore end for stability.

Free Spanning

Spans will be measured and evaluated according to DNV – 1981- Rules for Submarine Pipeline Systems. Post installation spans will be corrected prior to production start-up. Freespan analysis will be finalised once the final pipeline laying details are known. The planned (most likely) path to free span rectification is:

- Fatigue analysis
- Grout bag rectification

External Loadings

Apart from hydrodynamic forces, possible accidental loadings on the pipeline may in general be caused by anchor dragging, trawler fishing gear, dropped objects. While it is not possible to protect pipelines from dragging of large anchors, the vessel activity in the areas is limited. Large vessels requiring large anchors will not operate in this area. Trawler fishing does not normally take place in the Casino area. Pipelines and wellheads will be marked on fishing maps for the area to avoid anchoring. Drilling and construction vessels for the project will operate under procedures that will minimise the risk of dropped objects on the pipeline.

Well and Pipeline Control

The pipeline design pressure will be higher than the maximum well shut-in pressure, making the system fail-safe for the event that the system control or shut-down function for the SST valves is not operating as intended.

The pipeline system will be designed to include the provision for future intelligent pigging.

Field Layout

A field layout drawing showing the pipeline route and configuration is attached. (see Figure 6.2.1-a Casino Field Development offshore pipeline layout.)

Pipeline installation will generally be as follows:

Pipe Lay

The pipelay vessel will mobilize from Europe and take on board the full length of umbilical on a carousel below deck. Upon arrival of the vessel in Portland, pipe is loaded in port. Pipe is re-supplied on board at 4 more occasions when the vessel abandons the pipeline, sails to Portland, restocks pipe, returns to the field and recovers the pipeline to continue laying. This approach is preferred over supplying pipe to the vessel by Support Vessels due to the reduced weather sensitivity. In the event that weather forces a cessation of pipe lay operations, the vessel will sail to Portland to make an opportunity restock, thereby mitigating the weather impact.

Umbilical

The umbilical and the pipeline will be laid separately. This enables the pipeline to be abandoned if necessary in adverse weather without having to cut the umbilical. A suitable four-day window for the umbilical lay can be selected at any time during the installation period.

The tie-ins and the free span corrections will be conducted by divers from a DP2 class support vessel which is mobilized from Singapore. This support vessel will have ample space to store the saturation dive system, the grout equipment and cement.

Flexible spool pieces are used to avoid the need to perform metrology and fabricate spool pieces prior to installation.

The pipelay contractor has developed a detailed weather standby analysis. Limiting wave heights were assigned to all activities in the offshore pipelay/umbilical program, taking into account the weather sensitivity of all the individual activities. A total installation period of some 70 days (46% weather standby) for a 1 November 2005 start and 77 days (60% weather standby) for a 1 October 2005 start has been estimated. The net installation schedule duration without weather is 48 days.

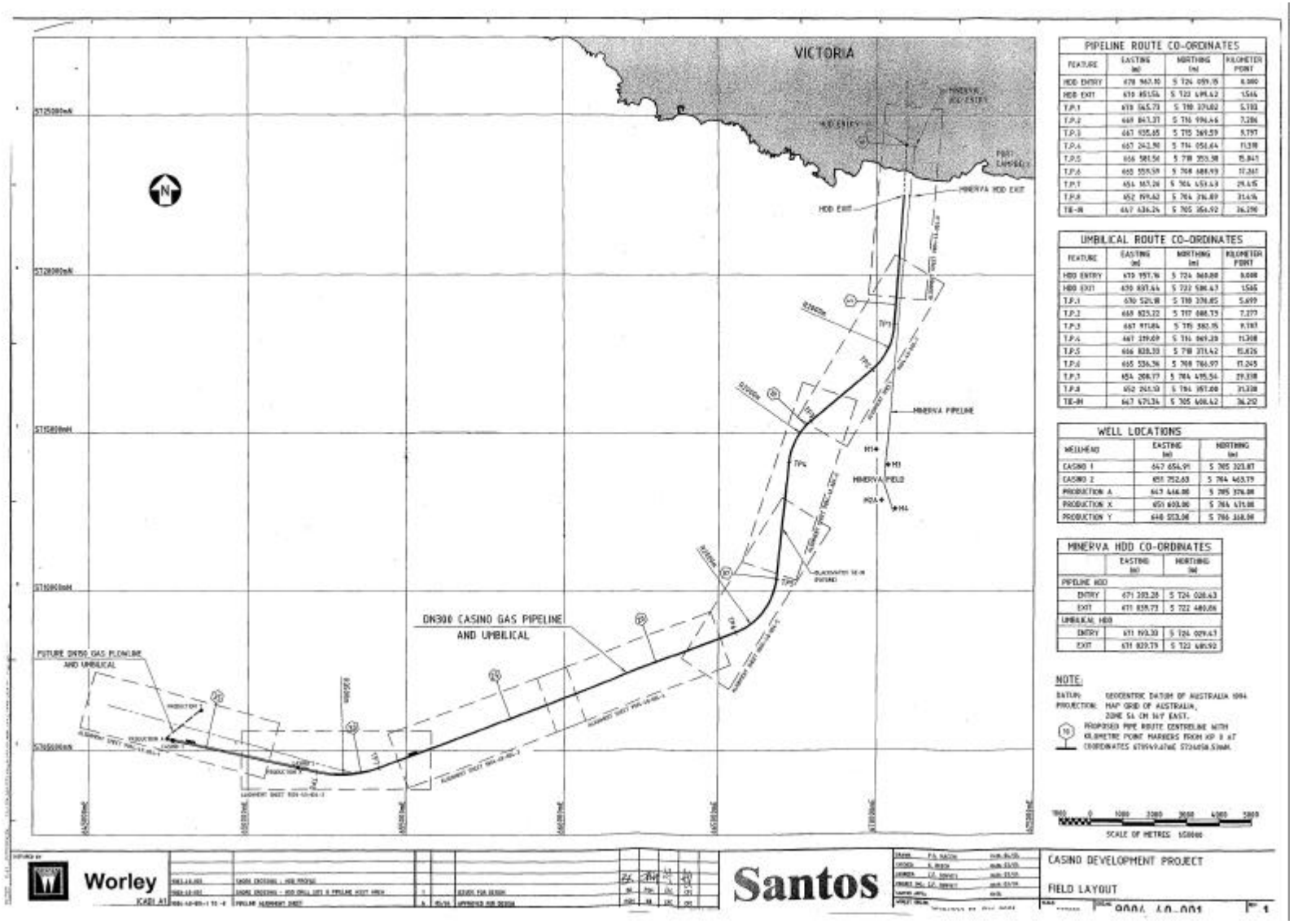

Figure 6.2.3-a: Casino Field Development Offshore Pipeline Layout

6.3 Pipeline Shore Crossing

6.3.1 General and Completion Schedule

The shore crossing will be horizontally directionally drilled (HDD) in order to avoid impacting the coastal zone, in particular the surface of the Port Campbell National Park, shoreline habitat and nearshore reef habitat. The HDD profile is shown in Figure 6.3.1-a. Drilling operations will use existing and proven technology and equipment, with experienced contractors selected to conduct the work. Continuous drilling operations will be required to minimise the likelihood of hole collapse while drilling and installing the pipe (approximately three months), with the site lit for operations at night.

At completion of the HDD operations, the site will be restored with the exception of a small (approx 20 x 35 m) fenced site which will contain the Main Line Valve (MLV).

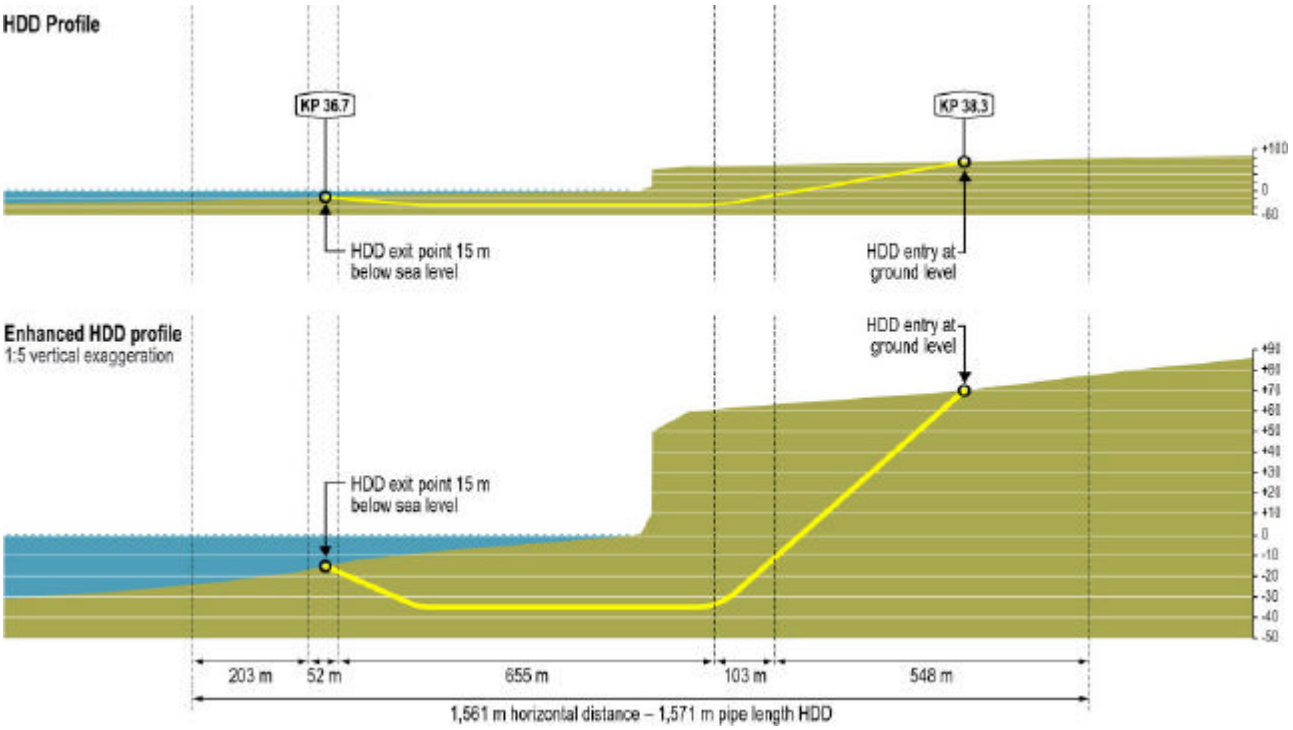

Figure 6.3.1-a: HDD Shore Crossing Profile

6.3.2 Installation

Horizontal directional drilling (HDD) of the shore crossing will take place from a site constructed in already-cleared farmland on the northern side of the Great Ocean Road at Two Mile Bay, approximately 2 km west of Port Campbell. The dimensions of the HDD site will be 100 m by 100 m, with a temporary hardstand area (crushed rock or similar) required at the site to provide all weather access for heavy vehicles and the drilling rig equipment.

Two drill holes, each approximately 1,600m in length, will be required, one for the gas pipeline and the other for the control umbilical. A horizontal distance of approximately 10 metres will separate these holes. The holes will be able to be cased if borehole stability requires using High Density PolyEthylene liner. While the HDD holes are being drilled, approximately 2 km of gas pipeline will be laid out along the onshore pipeline easement extending north from the HDD site, then welded and hydrotested. The pipeline will then be pushed through the HDD hole for tie-in to the offshore section by the pipelay vessel.

The pipeline will be cathodically protected either by an impressed current system or by anodes.

The main specifications features of the HDD pipeline are:

- 12" nominal diameter,
- wall thickness 12.0mm and 22.2mm (for 450m seabed end),
- approximately 2 km in length,
- length of HDD hole – 1.6km
- pipe steel grade DNV SML 450 I,
- design pressure 17,600 kPa,
- HDD entry point elevation +68m,
- HDD seabed exit point water depth 15m,
- water depth range 0 to 26 metres,
- corrosion coating 2 Layer Fusion Bonded Epoxy (FBE),
- weight coating N/A (pipeline steel weight provides stability),
- external cathodic protection ribbon anodes,
- operating temperature range 60-10 degrees Celsius,
- Design life of 20 years,
- Suitable for future intelligent pigging of pipeline.

The HDD Section of the pipeline will be designed in accordance with AS 2885.4 and DNV-OS-F101, Submarine Pipeline Systems.

The control umbilical will be pulled through its HDD sleeve from offshore by winch and hooked up on the onshore MLV site.

6.4 Onshore Facilities

The purpose of the onshore facilities is to receive the Casino field raw gas from the offshore pipeline, and transfer it to the TXU Iona gas plant for processing into sales gas and stabilised condensate.

6.4.1 Main Line Valve Site

The Main Line Valve Site will remain after the HDD site is restored, and is situated at the entry to the shore crossing. It is a fenced and gate secured compound 20 m x 35 m containing the following:

- End of line facilities for the offshore pipeline – including provision for the future installation of pig receivers/ launchers as required,
- Main Line Valve,
- Hydraulic power unit,
- A temperature controlled container housing the MCS, EPU, the ESD system, the UPS,
- The OUTA for terminating and routing the umbilical function lines,
- Pipe racks and conduits distributing the hydraulic, electrical, signal, chemical injection lines within the MLV site,
- Security lighting,
- All weather access track.

6.4.2 Onshore Pipeline

The onshore pipeline will run from the Main Line Valve site to the TXU-UGS Facility, Figure 6.4.2-a shows the pipeline route.

Figure 6.4.2-a: Pipeline Route

The pipeline runs along fence lines and existing easements where possible. It crosses under two bitumen surfaced roads that will have crossings directionally drilled to minimise traffic disturbance, and Campbells creek which will be crossed open cut.

The main specifications of the onshore pipeline works are:

- 12" nominal diameter,
- pipe general API 5L 323.9 mm OD, 9.7 mm WT X70 - heavy wall API 5L 323.9 mm OD, 11.1 mm WT, X70
- pipeline and service lines are approximately 11.5 km in length
- corrosion allowance of 2.5 mm
- 12" pipe coating – fusion bonded epoxy (FBE), 2" pipe coating – high density poly ethylene (HDPE)
- 3 x 2" carbon steel lines installed for transporting MEG/CI to the Main Line Valve site
- impressed current cathodic protection system,
- operating temperature 10 – 50 C,
- design life of 20 years,
- designed in accordance with AS 2885.

The 12" gas line, 3 x 2" MEG/Chemical Injection lines and the fibre optic cable will be located in the same trench except for the drilled road crossings.

The wellhead shut-in pressure (17,600 kPa) is greater than the design pressure of the onshore pipeline (15,300 kPa). The onshore pipeline is protected by the main line valve which automatically closes if a high pressure is detected upstream of the valve (pressure sensor is located upstream of the main line valve). The set point of the shut-in controller will be no greater than 15,300 kPa (to be determined). The pressure break is located on the shore side of the main line valve. In addition if high pressure greater than 15,300 kPa is

detected downstream of the wellhead chokes, the well will be shut-in automatically. There is design redundancy by way of dual redundant instrumentation and ESD control on the subsea control system. The MCS is also dual redundant.

6.4.3 TXU Iona Gas Plant

The TXU Iona gas plant is an existing plant that processes raw gas into sales gas which is either sold into the Victorian or South Australian gas market or injected into the underground storage facility for later sale. The basic existing process consists of:

- inlet separation,
- gas processing – dehydration and hydrocarbon dewpoint (LTS),
- hydrocarbon stabilisation,
- lean and rich glycol storage, glycol regeneration,
- compression,
- withdrawal and injection into and from the underground storage facility.

The following modifications are required to the TXU Iona gas plant and accept raw gas from the Casino gas field:

- additional lean / rich glycol storage,
- additional condensate storage,
- lean glycol pumping system,
- methanol storage and pumping system,
- installation of a slug catcher,
- metering.

Currently if the Casino field's gas is delivered at a pressure greater than 9000 kPa, the existing plant compression configuration is adequate to support the production. Once the gas is delivered below this pressure a low pressure agreement is invoked and further modifications to the existing compression system at TXU-UGS will be required. The extent of these modifications will vary depending on the other requirements of the plant.

Figure 6.4.3-a shows the proposed TXU Iona gas plant facility process to handle Casino gas field production.

Metering

Custody transfer metering will be installed on the gas outlet of the slug catcher using a metering skid mounted with ultrasonic flowmeter, flow computer and gas chromatograph. A redundant meter will not be incorporated into the design, and in the event of meter failure, flow values will be estimated using other plant flow meters and wellhead choke sizes. Allocation systems will be agreed to determine the stabilised condensate and off-gas attributed to the Casino production.

Flow metering will be installed on each subsea tree.

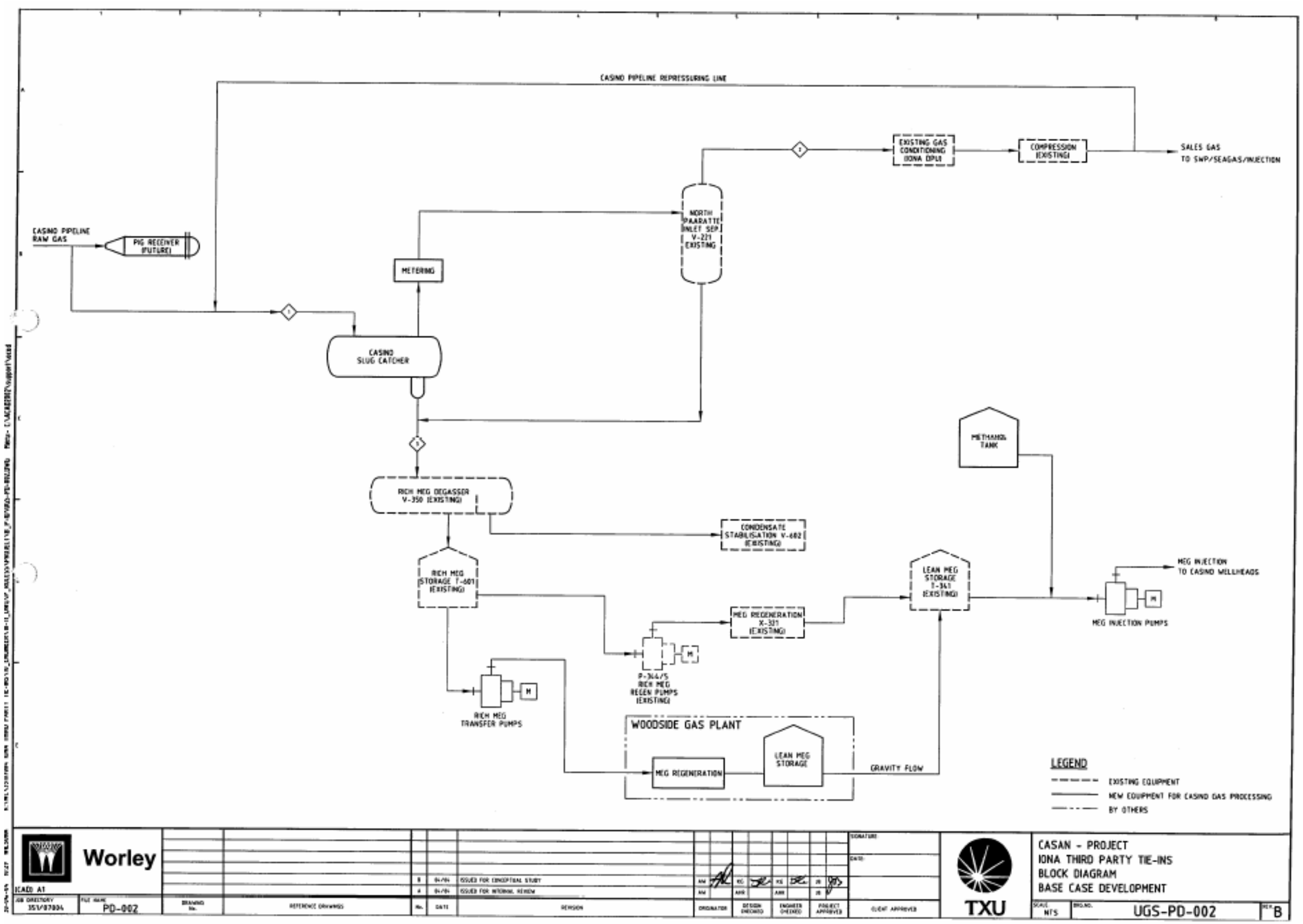

Figure 6.4.3-a: Proposed TXU Iona Facilities for processing Casino Gas.

6.5 Development Options

6.5.1 Subsea Wellheads or Wellhead Platform

A review was completed comparing the design options of subsea wellheads or a wellhead platform. The latter presented a higher cost solution, with the disadvantage of its visible presence above the sea, and additional project time required which would result in a significant schedule risk and delay to first gas.

Wellhead platform option

A wellhead platform would need to be located above the field, approximately 30km offshore. A small wellhead platform could be designed with minimum facilities including:

- Wellheads and manifolds,
- Helideck,
- Shelter,
- Pig launcher, minimal power generation (wind/solar),
- Communications,
- Davit crane,
- Vent boom.

The wellhead platform would be a steel structure piled to the seabed. Wells would be drilled by a jack-up following platform installation. Telemetry between the platform and onshore control room would require installation of an onshore control tower. The advantages of this option are primarily:

- Dry wellheads,
- No communications umbilical required,
- Simpler well intervention (wireline) – although a jackup would likely be required for major well workovers or redrills.

Subsea wellhead option

Subsea wellheads would be connected directly to shore by pipeline. Wells would be drilled by a floating drilling rig. The advantages of this option are primarily:

- Significantly less project fabrication and installation, with no concerns caused by seabed conditions for platform foundations, and less risk of project delays leading to first gas delay,
- no maintenance of platform facilities,
- considerably simpler well drilling as subsea wellheads can be located to maximise well “verticality”,
- no visibility above sealevel,
- better offshore facilities security.

6.5.2 Onshore Facilities

Limited options are realistically available. Design and construction of a dedicated plant was ruled out given that the considerably cheaper and simpler option of producing into a modified TXU Iona gas plant was available. High Pressure Delivery and Low Pressure Delivery options have been considered for defining the requirements for plant modifications and compression. Initially the plant will be configured for High Pressure Delivery.

7 Environment, Health & Safety

7.1 Introduction

7.1.1 Philosophy

Santos conducts its activities under the systematic requirements of The Santos "Environment, Health and Safety Management System" (EHSMS) which outlines the structured approach necessary to ensure its worldwide operations are conducted in a consistent and systematic manner. Santos is also committed to conducting its business so that it lightens the environmental footprint from its activities, and that all employees and contractors go home from work without injury or illness.

The Santos EHSMS also directs company activities to meet the requirements of Regulations; Federal, State and Local. These requirements have been incorporated into the Project Plan.

7.2 EHS Management for the Casino Project

7.2.1 Overview

Figure 7.2.1-a represents the EHSMS for the Project. The hierarchy and structure of the Project EHSMS is as follows:

- The Santos EHSMS is the overarching EHSMS for the Project. The Santos EHS policies and management standards contained therein shall apply to all Santos and Contractors' activities.
- The Project EHS Management Plan (EHSMP) represents the translation of Santos EHSMS requirements into project specific requirements for managing EHS. It describes the Project EHS policies and goals, and the practices and systems to be used to achieve them. The activities of the Santos Project Team are directed by this Project EHSMP.
- Each Contractor is required to carry out their scope of work in accordance with an EHSMP that is fully aligned with the Project EHSMP. Their activity scope is described in each of the respective contracts together with any specific EHS requirements and general guidelines.
- The main Contractors are required to have a Bridging Document that links to the EHSMP and their own EHS plans and systems. Suppliers of equipment, materials and services have their requirements described in their contracts.
- The processes and procedures by which each Contractor carries out their scope of work follows from the Contractor's EHSMP which must address any project-specific risks that differ from or have not been previously catered for by their systems and procedures. There are specific requirements that the main Contractors must meet to ensure that their Emergency Response Plan and Oil Spill Contingency Plan appropriately link to the main Santos Plans. Contractors must ensure that the project risks are understood, with appropriate controls, that these are communicated to those involved in the project and appropriate training conducted.
- Each supplier must meet the requirements of the Santos EHSMS. This is achieved by an assessment of each supplier's capabilities prior to contract award.

The Project Team aims to execute the Project with no accidents or injuries and no harm to the environment.

The Project EHS objectives to achieve this aim under the Santos EHS policies are:

- Provide resources and safe working practices designed to prevent harm to people.
- Manage, control and eliminate or reduce to ALARP the EHS hazards during the execution of the Project.

- Plan and implement activities such that adverse effects on the environment are either eliminated, where possible, or kept to an acceptable level while meeting all statutory requirements.
- Develop and foster a positive EHS culture amongst the Project Team and Contractors.
- Share all EHS lessons learnt, both positive and negative experiences, amongst the Project Team and Contractors.
- Set measurable targets for performance towards EHSMP implementation and,
- Provide training as required.

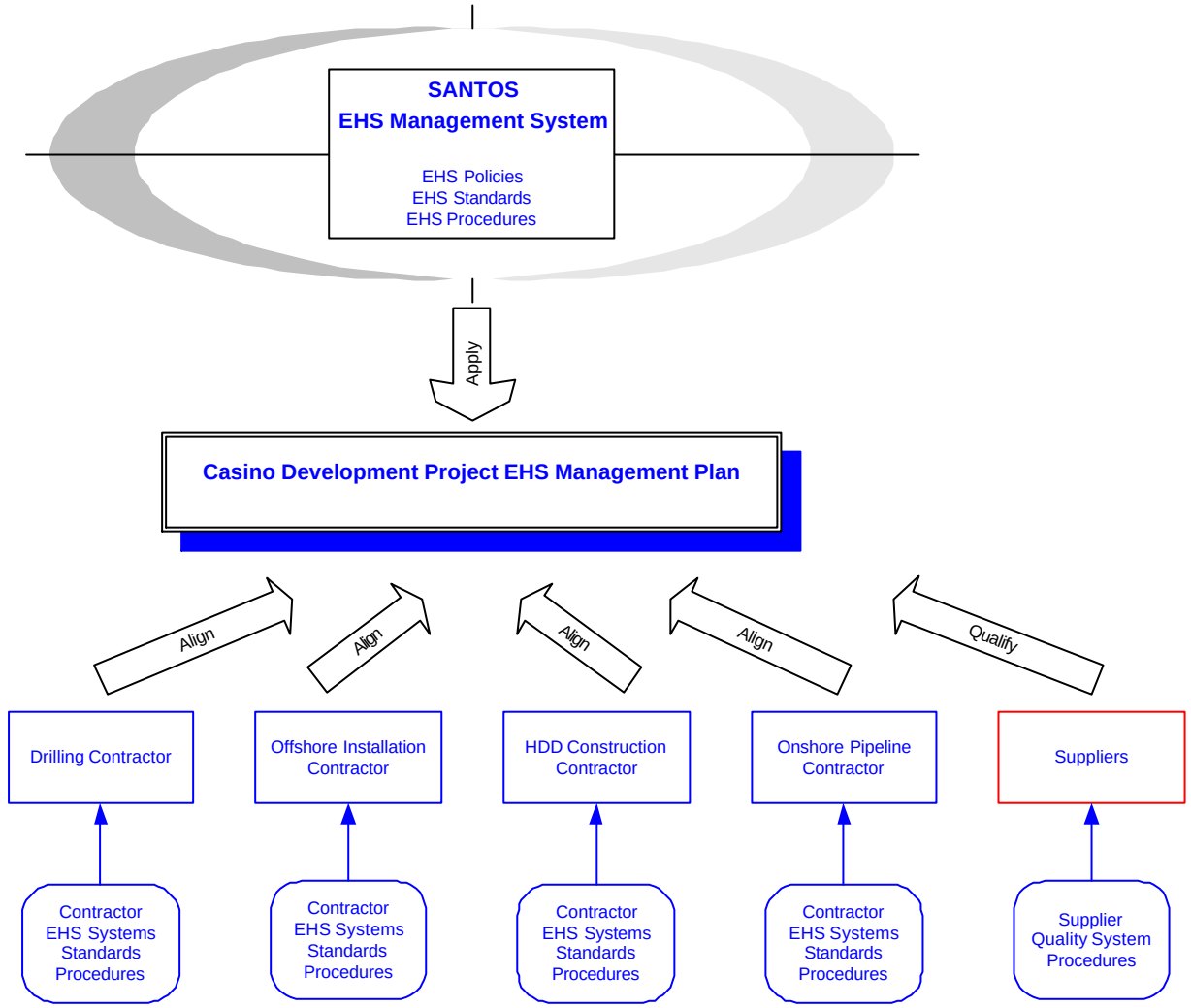

Figure 7.2.1-a: Casino Project EHSMS Structure.

7.2.2 Regulatory Framework

The proposed Casino Gas Field Development falls within three jurisdictions including Commonwealth and Victorian waters and onshore Victoria. Consequently, permits and licences are required respectively under the Commonwealth *Petroleum (Submerged Lands) Act 1967*, the Victorian *Petroleum (Submerged Lands) Act 1982* and the Victorian *Pipelines Act 1967*.

The Victorian Minister for Planning has determined that the magnitude and significance of potential impacts would not necessitate the preparation of an Environment Effects Statement.

In December 2003, the project was determined to be a controlled action under the *Environment Protection and Biodiversity Conservation Act 1999* (EPBC Act) based on the lack of certainty in construction timing and pipeline alignments and therefore potential impacts upon blue whales, and to a lesser degree, listed

terrestrial flora and fauna. The subsequent Commonwealth environmental assessment under the EPBC Act has been undertaken through separate Preliminary Documentation.

The details of ensuring Regulatory compliance will be managed by a regulatory plan specific to this project.

7.2.3 Environmental Risk Management

A project-specific environment plan (EP), for offshore components, and environmental management plan (EMP), for onshore components, will be prepared for the Casino Gas Field Development within the framework of the EHSMS.

Pipeline alignment is the most effective mitigation measure for minimising impacts. Residual impacts are then mitigated and managed through the implementation of appropriate measures and procedures.

7.2.4 Health & Safety Risk Management

Health and Safety risk management are incorporated into the Casino Project EHS Management Plan.

The objectives of this plan are to:

- define and communicate the Environment, Health and Safety (EHS) objectives, principles, expectations and requirements for the Project as derived from the Santos Corporate EHS Policies;
- define the criteria against which EHS performance will be judged;
- describe areas of EHS responsibilities for the Casino Project Team and Contractors;
- describe the Project EHS management practices that ensure EHS activities are organised, managed and reported in a systematic and consistent manner;
- describe the application of Safety Cases, the EHSMP and the Environment Plan;
- ensure the Project provides inherently safe and environmentally acceptable facilities;
- ensure that the project Contractors are adequately controlled to achieve that same objectives as Santos, and
- ensure that performance feedback is delivered through audit and inspection.

The scope of this plan covers the Casino development in permit VIC/P44 during the Implementation Phase and includes:

- detailed design and procurement;
- onshore facilities conversion and pipeline construction;
- horizontal directional drilled (HDD) shore crossing construction;
- production well drilling/completion and sub-sea tree installation; and
- offshore pipeline/umbilical installation and commissioning.

7.2.5 Safety Case

The Drilling Contractor and Offshore Installation Contractor are each obliged to prepare a Safety Case as required by legislation and as part of their contractual requirements with Santos. Each Contractor is directly responsible for EHS performance on their vessels as the vessels will be operated under each Contractor's EHSMS.

8 Project Plan and Management

8.1 Overview

8.1.1 Project Objectives

The project objective is to deliver a gas production system which optimises the economic recovery and maximises value from the Casino field for the VIC/P44 Joint Venture, without compromising Santos's EHS and Quality values.

The project goals are:

- Achieve all the conditions precedent milestones,
- Achieve earliest gas production,
- Meet performance criteria for gas deliverability and operating costs,
- Maximise project Net Present Value,
- Plan and execute activities such that project delivery and operation activities cause no health and safety harm,
- Plan and execute activities such that adverse effects on the environment are eliminated where possible, or kept to an acceptable level while meeting all statutory requirements,
- Enhance Santos's reputation in the Port Campbell area,
- Incur no substantial industrial relations disputes or legacies,
- Meet the agreed project budget and schedule, and
- Provide opportunities for Santos personnel to participate in project delivery.

8.1.2 Planning and Management Strategy

The project scope covers Concept Development, Definition and Implementation phases of the Santos Quality Asset Development (SQAD) process. An overview of the SQAD process in shown in Enclosure 8.1.2-a.

The key activities that relate to the Casino field development are summarised below.

Concept Development Phase

The Concept Development Phase is complete. The objective of the Concept Development Phase was to select a development concept and improve project scope, cost and schedule definition to allow the Joint Venture to make a decision to proceed to the next phase of project development, the Definition Phase.

In particular the aims of the Concept Development Phase are to:

- Review alternate development concepts and confirm or otherwise the Project Initiation Phase Reference Case Development as the development concept to take forward to the Definition Phase,
- Prepare conceptual process flow diagrams, process control diagrams, utility flow diagrams and preliminary layout drawings for the facilities,
- Identify and document all key project risks and mitigation strategies,
- Prepare a contracting and procurement strategy for the Project Definition and Implementation Phases,
- Prepare capital and operating cost estimates, and update the project schedule estimates,
- Document study outcomes in a Concept Development Study report, and
- Prepare the Project Definition Memorandum.

In parallel with the Concept Development Study, Santos has undertaken reservoir modelling and conceptual well and completion design studies using a combination of Santos personnel and external consultants. This is described in Sections 3 and 4 of this document.

Also in parallel with the Concept Development Study, Santos has commenced environmental studies leading to project environmental approval using a combination of Santos personnel and external environmental contractors.

Definition Phase

The Definition Phase is complete. The objective of the Definition Phase was to complete engineering and procurement activities adequate to allow Joint Ventures to make a decision to proceed to the next phase of project development, the Implementation Phase, conditional on obtaining environmental approval.

In particular the aims of the Definition Phase are to:

- Conduct further reservoir and analysis to improve reserve forecasts and optimise production,
- Perform production well and completion design studies,
- Perform engineering and the development of functional and technical specifications to enable issuing of tenders for the Implementation Phase contracts,
- Procure schedule-critical long lead equipment,
- Tender and evaluate tenders for the Implementation Phase contracts,
- Based upon tenders received, improve project cost and schedule definition,
- Commence planning for field operations and support,
- Prepare gas sales and associated agreements, ready for execution, and
- Progress environmental approvals and permits and licences-to-operate.

Implementation Phase

Following the completion of the Definition Phase, and subject to receiving Joint Venture approval to proceed, the project will immediately proceed to the Implementation Phase. The Implementation Phase is expected to run from August 2004 to early 2006. The objective of the Implementation Phase is to complete engineering, procurement, construction, installation, and commissioning activities, and to start-up and commence operations.

In particular the aims of the Implementation Phase are to:

- Finalise production well and completion design,
- Execute Implementation Phase contracts, conditional on obtaining environmental approval,
- Perform detailed engineering, procurement, construction, installation, and commissioning activities,
- Obtaining environmental approvals and permits and licences-to-operate,
- Execute gas sales and associated agreements, and
- Start-up and commence operations.

8.1.3 Risk Management Plan

Project risk assessments will be formally carried out at the completion of the various project phases. An early risk assessment was performed during the Concept Development Phase. The risk assessment was updated at the end of the Definition Phase.

The project risks considered will cover EHS, subsurface, drilling, facilities, project cost and schedule, commercial, operational, external etc. The project risk management plan includes a summary of any identified “high” risks, and measures proposed to address these.

The project risk reduction measures shall be incorporated into the Project Risk Management Plan. In particular, EHS risks shall be managed under the project EHS Management Plan.

8.1.4 Project Schedule

A project schedule is shown in Enclosure 8.1.4-a.

A detailed analysis has recently been completed (June 2004) to investigate and identify risks to the project schedule. Key items are:

- Award of Offshore Installation contract,
- Award of the Umbilical Supply contract,
- Awarding the contract for procurement of schedule-critical subsea trees and controls to ensure that drilling operations can commence as scheduled,
- Placing of orders for schedule-critical well tubulars, casing, line pipe and engineering,
- Obtaining environmental approvals, the Pipeline Licence,

- Scheduling construction activities around favourable seasonal weather conditions, and
- Building schedule space between offshore drilling and pipelay activities, and HDD shore crossing construction and offshore pipelay activities.

8.1.5 Key milestones

The enclosed project schedule contains this information. Of note are:

- All regulatory and licenses to be obtained by year-end 2004,
- All orders and contracts in place by end third quarter 2004,

8.1.6 Contracting Strategy

The contract packages are shown diagrammatically in Figure 8.1.6-a. The contracting strategy for this development is summarised below:

- Package 1: Procurement of Sub-sea Trees and Controls,
- Package 2: Procurement of Umbilical,
- Package 3: Well Construction and Sub-sea Tree Installation,
- Package 4: Offshore Pipeline & Umbilical Installation and Commissioning,
- Package 5: HDD Shore Crossing Construction,
- Package 6: Onshore Pipeline and MLV Site Construction and Commissioning,
- Package 7: Iona plant Tie-ins and Commissioning.

In addition Santos will procure and free issue to the relevant contractors schedule critical materials under the following contract packages:

- Package 3a: Procurement of Well Tubulars and Casing,
- Package 5a: Procurement of HDD Line Pipe,
- Package 6a: Procurement of Onshore Line Pipe.

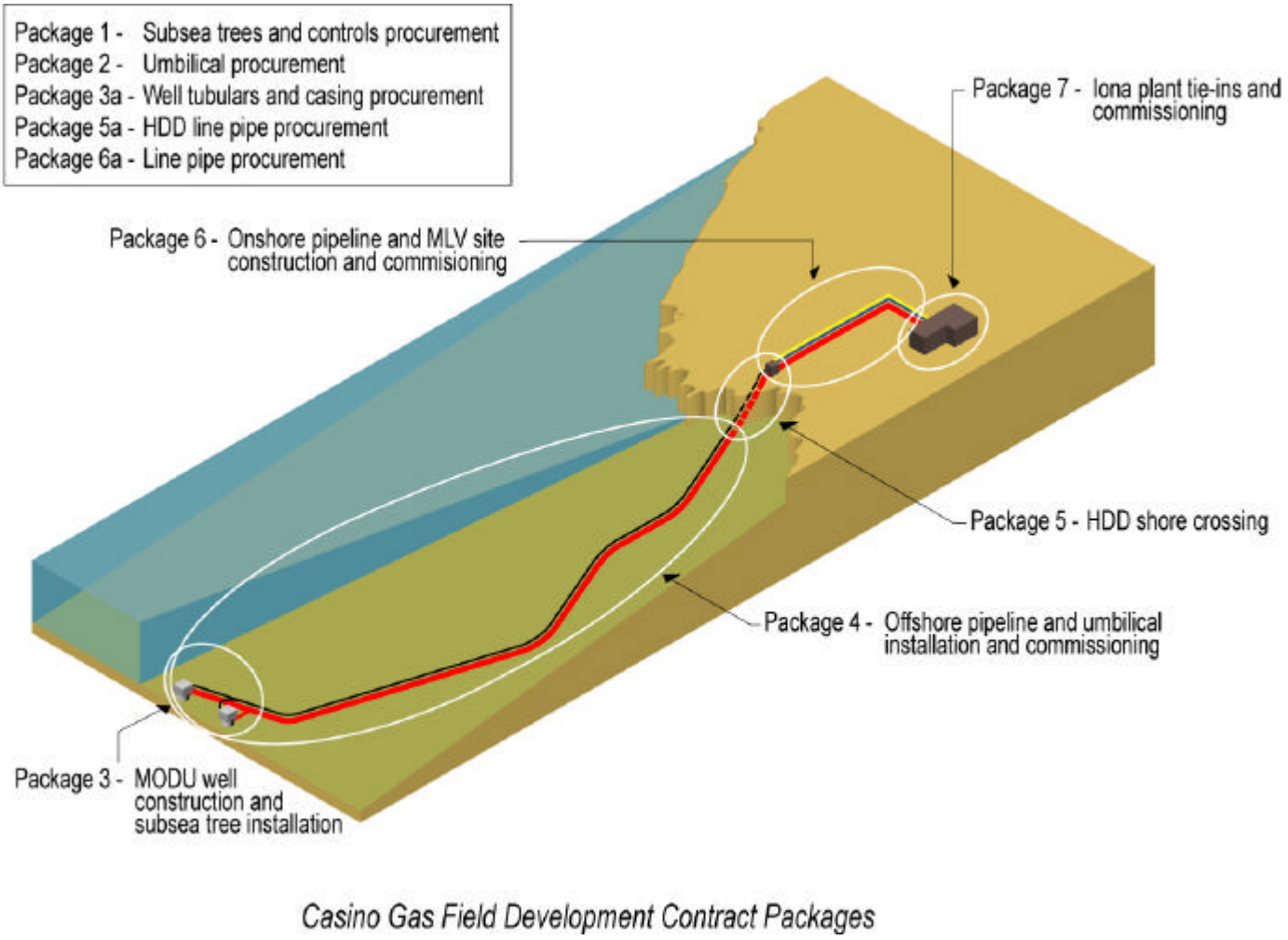

Figure 8.1.6-a: Casino Gas Field Contract Packages

8.2 Resources Plan

8.2.1 Overview

The Project Resources Plan is based upon the following:

- Resources required to implement the execution strategy and contracting strategy.
- A core project delivery team, consisting of Santos staff and contractor personnel.
- Field construction and commissioning personnel, engaged as Santos Site Representatives for planning and field construction and commissioning activities, supported by Third Party Services (TPS) companies for specialist inspection services.
- Santos and TPS contractors for project environment, environment, health and safety (EHS), technical, contract, legal, commercial, and industrial relations (IR) support to the project, as required.

The Implementation Phase will be managed by a core project delivery team, consisting of Santos staff and contractor personnel. The core team leadership will consist of a Project Manager, supported by a Sub-surface Manager, and Drilling and Completions Manager. An organisation outline is shown in Figure 8.2.1-a.

The Casino Project Manager will be responsible for overall project delivery meeting key project performance objectives covering EHS, quality, cost, schedule and regulatory compliance, and will be supported by the project delivery team consisting of area project mangers and project support personnel.

The Sub-surface Manager will be responsible for optimisation of the field development plan, and will be supported by a Senior Reservoir Engineer and Senior Staff Geologist. The Drilling and Completions

Manager will be responsible for detailed well and completions engineering, and will be supported by a Senior Completions Engineer, Completions Engineer and Drilling Manager.

Procurement and construction of facilities will be managed by an Offshore Construction Manager, an HDD Construction Manager, an Onshore Project Engineer, a Lead Sub-sea Trees Engineer, and a Lead Sub-sea Controls Engineer.

Supporting these personnel will be shared project resources for Administration, Financial Control, Project Controls, Permits and Licences, Contract Administration, Document Control and EHS Coordination. Operations support will also be provided.

In addition Santos Corporate support will be sourced on an as needed basis for EHS, technical (including quality), contracts, legal, and commercial (GSA support). TPS contractors will be used for IR support.

8.2.2 System Commissioning

System commissioning will be managed jointly by Santos and TXU. The commissioning team will consist of a Commissioning Supervisor, Mechanical Supervisor, Electrical/Instrumentation Supervisor, Operations Supervisor, Operations Technicians, Mechanical Technicians and Electrical/Instrumentation Technicians, sourced from Santos, TXU and TPS providers, supported by equipment Supplier personnel.

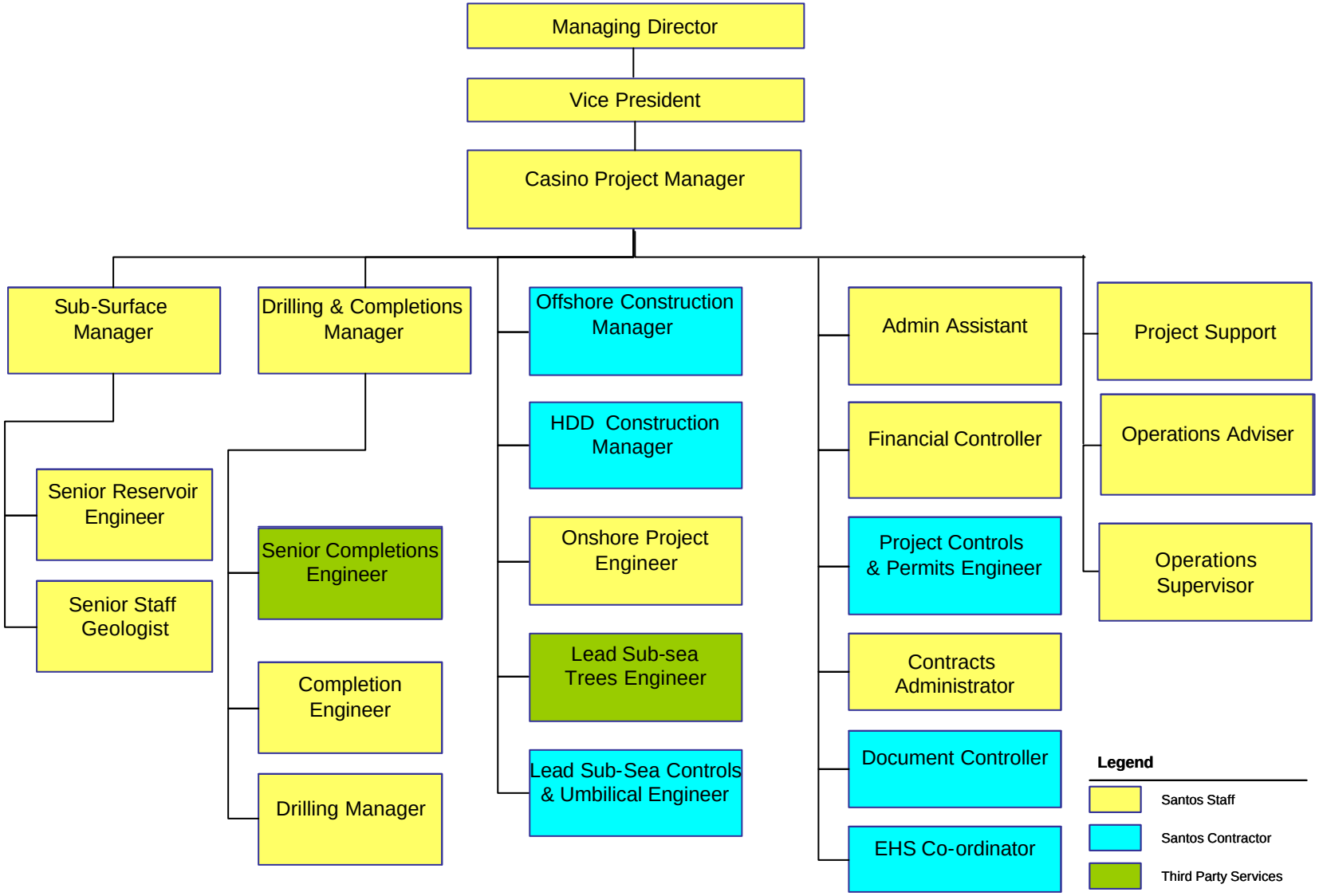

Figure 8.2.2-a: Santos Casino Project Organisation Chart

8.3 Quality Management

8.3.1 Scope

This Quality Plan describes the Quality Management activities which will be implemented during the Casino Development Project. This Quality Plan applies to all activities undertaken as a part of the Casino Development, including drilling and completion of the wells, pipeline construction and installation, and facilities at the Iona gas plant.

8.3.2 Objectives

The objective of the Quality Plan is to assure compliance with specified technical requirements and regulatory requirements and meet cost and schedule parameters.

In particular, the Quality Plan is intended to:

- Develop pro-active quality initiatives that support and effectively monitor project technical objectives and regulatory requirements set out for the Casino Development,
- Minimise the occurrence of non-conforming work, by ensuring that items of work are executed correctly the first time,
- Ensure that the Project Quality System provides confidence to stakeholders that the facilities that are produced meet specified requirements,
- Ensure facilities are designed, constructed, installed and commissioned in such a manner that risks to personnel and to the environment are reduced to as low as reasonably practicable,
- the construction team for the project develops the field in the most economical manner,
- Ensure that a technical record is provided to the facility operators to help maximise the output of the field.

The Project Quality approach is founded upon the principle of Product-Process-Organisation-Leadership-Commitment, as follows:

- Product is the primary focus for the organisation's purpose and achievement,
- Quality results require quality in the processes,
- Quality in the processes requires the right organisation,
- The right organisation requires the right motivation and competent leadership,
- Strong commitment by the individual supports achievement of the product.

8.3.3 Application of Santos QA/QC Arrangements

The application of Santos QA/QC arrangements will be as follows:

- where items are purchased directly by Santos - e.g. long lead items, SSTs, line pipe – Santos will directly apply its QA/QC arrangements; and
- where services are performed under contract to Santos – e.g. pipeline installation, drilling of the wells - Santos will indirectly apply its QA/QC arrangements.

The split between direct and indirect QA/QC arrangements recognises that substantial aspects of the work shall be contracted out, with primary responsibility for quality passing to the Contractor. In these cases, assessments of Contractors' quality management systems shall be undertaken to verify that their activities and products comply with requirements specified by the project.

In both direct and indirect QA/QC arrangements, the criticality analyses that shall be conducted as part of the risk assessments shall guide the Project Team in determining the appropriate level of QA/QC for each major item of equipment.

8.3.4 Standards

All Casino Development facilities shall be designed and built to the Basis of Design and Contractor Specifications. In the event of any conflict between documents referenced within the Basis of Design and Contract specifications, such documents shall be applied in the following order of precedence:

- Regulatory requirements
- Certification Body / Validation Body requirements
- Australian Standards
- International Standards
- Industry Standards

As a general philosophy, the Casino Development will adopt external standards, for example AS, ISO, ASTM, API, BS, etc. rather than generate internal standards, applying standards also as required under Regulations.

8.3.5 Project Verification Procedure

A detailed Project Verification Procedure will be developed which defines verification activities in relation to significant project milestone events and ongoing work. The Project Verification Procedure objectives aim to ensure that:

- Project activities are identified and performed in accordance with the Project Management System,
- Project performance meets identified performance indicators,
- Items/activities requiring improvement are identified for action,
- That project verification is planned in a structured manner with objective evidence being available to demonstrate compliance to specified requirements.

The Project Verification Procedure shall incorporate the regulatory requirement to conduct an independent "validation" of the pipelay vessel safety case, the Mobile Offshore Drilling Unit safety case and overall pipeline activities.

8.3.6 Decision Log Procedure

Key design or philosophy decisions that contributed to the development of the Basis of Design are recorded in the Decision Log. The Project Team will continue this practice, particularly where design decisions have an impact on EHS during construction and operations.

The Decision Log captures the objectives, assumptions, constraints, alternatives and reasoning behind each key design decision. It specifically addresses those decisions which require approval and/or agreement by several different groups within the Project Team, and/or by groups outside the Project Team (e.g. Contractors and other Santos Departments).

8.3.7 Design Control

Functional specifications should be developed to describe the deliverables of each individual major contract in the project. The engineering portion of the individual Contractor's scope of work shall be specified to be subject to design control as per the Contactor's quality procedures, complaint with ISO 9001. The standard Contractor's design control procedures shall be subject to audit by Santos.

8.3.8 Document Control

Project specific Document Control Procedure and Document Register systems have been developed and implemented by Worley and the same procedures shall be adopted during the implementation phase. A Document Management Plan will be developed as part of the Project Implementation phase.

8.4 Industrial Relations

8.4.1 Strategy

This is the first offshore project operated by Santos in Southeast Australia. There are many aspects of the Victorian industrial relations environment that differ from the other Australian states with which Santos is well familiar. Under the chosen contracting strategy of lump sums, there will be specified requirement for Contractors to produce high quality Human Relations Management Plans and involve Industrial Relations consultants for advice. The attendant discipline involved in the processes, that we will require to be included, will clearly demonstrate to Contractors and Unions that Santos will hold the Contractors accountable for their employee and industrial relations management.

A project Industrial Relations Plan has been developed with the objectives:

- To provide a framework for the management of employee and industrial relations across the Project, consistent with the employee and industrial relations strategies of Santos;
- To support the successful execution of the Project within defined safety, cost, time and quality parameters;
- To provide the necessary management processes which reduce, and where possible eliminate, risks associated with employee and industrial relations;
- To optimise the opportunities and benefits to the Project that are contained in the applicable forms of industrial regulation; and
- To assist in creating an environment that achieves effective working relationships between all people involved in the Project.

9 Operations and Maintenance

9.1 Overview

9.1.1 Strategy

The operations and maintenance of the Casino field facilities will be based on the philosophy of third party operated by TXU, the owner of the Iona gas plant and contracted buyer of the Casino field gas. The Gas Sales Agreement (GSA) and subsequent "process services" agreement binds Santos to the TXU Iona plant to provide services such as well operation and control, product measurement and condensate separation and storage. Specific operational and maintenance strategies will be developed by Santos in conjunction with TXU to effectively operate the field. The inspection and maintenance of the sub-sea equipment and sub-sea pipeline will fall outside the process services agreement, therefore; several other specialist contractors will be required to conduct these services.

9.1.2 Operating Goals and Objectives

Santos operating goals are as follows:

- meeting the contracted gas production profile,
- ensuring reliable gas supply to the Iona gas facility,
- minimising costs, while
- meeting all environmental, health and safety requirements,
- observing all laws and regulations, and
- working in a constructive manner with the local community.

Strategies to achieve these goals are to:

- Have a competent contract facility operator with the capability and knowledge to remotely operate the Casino wells from the Iona gas plant.
- Establish relationships with the Iona gas plant operator continually fostering their capacity to operate the Casino wells with knowledge and understanding of individual well operating parameters.
- Have a competent contractor group to maintain the subsurface facilities, offshore pipeline and onshore pipeline up to the Iona gas facility.
- Establish operating and maintenance procedures for wells and facilities to maximise well up time, pipeline and facility availability.
- Establish relationships with other operators in the area to promote synergies for third party contractor sharing of maintenance operations to reduce operating costs.

9.1.3 Third party services

Core sections of the operations have been identified and categorised according to areas of expertise. It is anticipated that prior to and during the life of the Casino field several key contracts will be necessary for services provided by third parties. Execution of the contracts will be subject to the project schedule and will be in accordance with the provisions for contract award by Santos.

The key services identified include:

- Processing and operating services,
- Separation, storage and loading of condensate,
- Routine pipeline and equipment surveillance,
- Main Line Valve (MLV) maintenance and testing,
- Well control surface equipment maintenance and testing,
- Shore pipeline CP and right of way monitoring and maintenance,
- Sub-surface pipeline inspection services,
- Sub-surface wellhead and manifold intervention and maintenance and
- Oil spill response.

9.2 Processing and Operating Services

9.2.1 General

Casino gas will be sold to TXU under the terms and conditions set out in the Casino GSA. A schedule of operating services will be prepared to detail the particular requirements of TXU in relation to chemical injection, well control, operations, surveillance and emergency response. Additionally, operating procedures and gas well operating parameters will be issued to the operator. Gas well parameters will change over time as the field depletes. Regular updates to TXU will be necessary to ensure optimum deliverability over the life of the field.

9.2.2 Condensate Handling

Under the terms and conditions of the Casino GSA, TXU will separate, store and load-out condensate for Santos. Santos will be responsible for the transport and sale of condensate to market. Specific procedures for the storage, handling and load-out of condensate will need to be reviewed and approved by Santos operations.

9.2.3 Surface Equipment Surveillance

The Main Line Valve (MLV) site will be located 11.5 kilometres from the Iona gas plant. At the MLV site there will be the main line valve, HPU, MCS and umbilical termination. Routine inspections and minor intervention will be necessary to ensure the security, operation and integrity of the equipment is maintained.

9.2.4 MLV Maintenance

Regular testing of the MLV will be required to ensure its integrity. Intermittent maintenance will also be necessary to rectify actuator or ancillary equipment faults as they occur. Services would also include maintenance and repair of gauges and small bore valves at the mainline station and attention to weeps and leaks if they occur.

9.2.5 Well Control Equipment

Specialist maintenance and servicing will be required during the production life of wells, specifically on the well control equipment. A services contract with the equipment's Australian service provider will be necessary.

9.2.6 Onshore Pipeline

Right of way inspection and management will be required as a component of the pipeline integrity management plan complying with pipeline licence regulations. Key requirements will be:

- Periodic right of way inspections,
- Cathodic protection monitoring and recording,
- Coating defect surveys and repairs,
- Repairs and maintenance to Cathodic protection systems,
- Clearing and removal of grass and weeds from the mainline valve station,
- Preparation of annual pipeline maintenance and activity reports.

9.2.7 Offshore Pipeline Inspections

Offshore pipeline inspections at determined intervals will be required to assess the condition of the pipeline, the occurrence of spanning and any other irregularities. Specific details and inspection requirements will be detailed in the sub-surface pipeline integrity management plan.

9.2.8 Sub-surface Intervention

Specialist sub-surface intervention may be necessary during the field life of the project. A services contract with the equipment's Australian service provider will be necessary. Systems will be designed for maintenance free operation during the life of the field. Should the need arise for maintenance and/or repair, ROV remote intervention methods will be planned unless they are shown to be less cost effective than diver intervention.

9.2.9 Real Time Data

Real time data will be provided within the Casino project. A Data Management Plan will be developed that incorporates the necessary data.

9.2.10 Interface Management

To establish and foster relations between Santos and TXU and to achieve the goals of this Operations and Maintenance Philosophy, the formation of an interface Process Services agreement is proposed. The interface agreement combined with regular meetings will form the basis of discussions and record philosophies and agreements between the parties.

9.3 Asset Management

9.3.1 Santos Asset Manager

The Casino field asset will be managed by a Santos Asset Manager who will be assigned to the field and will be responsible for all aspects of the operation. The following list, although not exhaustive, will form the nucleus of the position's responsibilities.

- Safety, health and environmental performance of the asset,
- Infield emergency response planning,
- Continuity of sales gas delivery to TXU and interface management,
- Condensate lifting's and custody transfer,
- Meeting production and cost budgets,
- Local community affairs and consultation,
- Monitoring and reporting of all environment, health and, safety production and maintenance activities,
- Management of business and production planning (budgets, cost control, approvals, monitoring, reporting),
- Management of external interfaces such as local, state and federal government agencies, local landholders, service agreements and contracts,
- Reservoir management, production forecasting well maintenance and workovers,
- Long term maintenance planning and integrity management,
- Witness, review and approval of gas meter calibrations,
- Technical advice to the contractors on production, maintenance and subsurface operations,
- Auditing of environment, health and safety and technical integrity,
- First contact for emergency response in support of the operations,
- Provision of well workover services,
- Development planning (if required after the Initial Phase),
- Minor facilities modifications (including design, verification, construction and installation) (if required),
- Accounting and reporting to government and JV parties,
- Overview of the Project Data Management Plan.

If a third party is contracted to operate and manage the facility including all interfaces on behalf of Santos the majority of these responsibilities move to the contracted third party. Functions such as pipeline integrity management and sub-surface reserves management will be retained by Santos.

9.4 Pipeline Management

9.4.1 Integrity

Pipeline management plans will be prepared for both the onshore and offshore sections as part of the pipeline licence applications. Integrity management plans will detail the responsibilities and functions required to maintain the pipelines over the life of the field. The Asset Manager will be responsible for updating and execution of the integrity management plans.

9.5 Operating Procedures

9.5.1 Procedure Development

Development of operating procedures will occur during the Implementation Phase of the project. It is the responsibility of the Casino project team to ensure procedures are prepared for all Santos installed equipment prior to commissioning and are vetted during the commissioning of facilities. Operations assistance should be seconded to assist with procedure development. Procedures will be developed into the categories of normal operating, critical operating and safety procedures.

Specific operating procedures pertaining to the equipment installed by TXU for the handling and processing of the Casino gas following sale from Santos will be the responsibility of TXU.

9.5.2 Training Requirements

During the pre-commissioning and commissioning phases of the project, operations and maintenance personnel from the Iona Gas Plant will require training and competency testing on all equipment associated with the Casino sub-sea completions. Additionally, training will be required for operations personnel on the various well control operating parameters advised by Santos. These parameters will include normal well flowing conditions, abnormal flowing conditions such as hydrate formation and sand production, safety critical conditions and emergency response.

9.6 Environment, Health & Safety

9.6.1 EHSMS

The Santos Environmental Health and Safety Management System (EHSMS) will provide the framework for Casino environment, health & safety management. The system's flexibility is designed to enable Asset Managers to develop strategic plans, detailed operating plans and procedures based on the level of risk associated with specific operations. A project EHS Plan has been developed and will be executed as part of the project plan.

9.7 Emergency Response

9.7.1 Emergency Response

An Emergency Response Plan and supporting procedures will be prepared in accordance with the guidance provided by the Victorian regulations and directives and the Santos EHSMS. Emergency response will also be a key feature of the Santos TXU interface document for the operation of the Casino field. The emphasis of the Santos incident management plan is on TXU support and response.

Within the framework of the Santos Incident Management Plan and related corporate procedures, arrangements will be put in place to ensure sufficient emergency response capability, in terms of off-site support, to cover all reasonably credible accident scenarios for the facilities. As needs change, additions will be made to these procedures to cover, for example:

- Drilling & well intervention,
- Installation,
- Commissioning,

- Production and
- Post start up combined operations.

More detailed procedures and practices will be prepared to cover facility emergency responses to ensure that adequate equipment and properly trained personnel are available at all times to cover all reasonably credible accidents.

9.7.2 Oil Spill Response

An oil spill contingency plan will be developed for operations as part of the Environment Plan to be approved under the Petroleum (*Submerged Lands*) Act (*Commonwealth*) and State Consent to install and use subsurface wells, offshore facilities and an offshore pipeline. The contingency plan will be developed in consultation with regulatory agencies and relevant stakeholders. No operational activity will be undertaken without an approved oil spill contingency plan in place.

Opportunities will be explored with local authorities e.g. Australian Marine Oil Spill Centre (AMOSC) and other operators in the area to undertake oil spill response co-operatively utilising shared services.

9.8 Community Relations

9.8.1 Philosophy

Santos's community management strategy and commitments will be in line with the overall Santos goal to apply the principles of sustainable development to our activities. Santos's goal is to be recognised by stakeholders and peers as being within the top quartile of the world's oil and gas companies. Santos intends to meet a range of community and social requirements as part of our project and operating approvals. These requirements will be integrated into operations plans.

9.9 Operations Design Input

9.9.1 Project Support

Experience shows that high levels of operability and maintainability are best achieved by an early interaction of the operations team with the project team. This has already occurred during the Definition Phase and will continue through the Implementation and Operations phases.

9.9.2 Implementation

The Casino development project team are responsible for onshore and offshore mechanical completion and pre-commissioning of the production facilities. The TXU operations team will provide support during this phase of work.

There will be a close involvement of operations personnel from TXU in the development of operating and commissioning procedures, onshore pre-commissioning of the pipelines, well chemical injection and sub-sea control equipment.

All onshore / offshore first gas commissioning will be undertaken jointly by the TXU operations team and the Casino project team

A formalised pre-commissioning and commissioning system will be established. The system will monitor and allow the efficient and safe hand over and receipt of systems from the Implementation phase to the Start-up Phase and then into the Operations Phase proper.

9.10 Simultaneous Operations

9.10.1 Strategy

During the operational life of the field there will be a requirement to undertake, manage and control simultaneous production, drilling, construction and or well intervention operations (SIMOPS). The authority to allow SIMOPS will reside with the Asset Manager whereas control of the SIMOPS will be the responsibility of the designated Santos site representative and managed via SIMOPS procedures and work instructions which will form a key part of the work program management plan.

10 Units

10.1 Units

NON SI UNITS		
Unit	**Description**	**Conversion from SI**
^{o}API	liquid specific gravity (API)	141.5/(kg/m^3/1000)-131.5
^{o}F	degrees Fahrenheit	1.8 * (K-273)+32
“	Inches	39.37 * m
bbl	barrels (general fluid)	6.293 * m^3
bbl/d	barrels per day (general fluid)	5.437e05 * m^3/s
bbl/hr	barrels per hour (general fluid)	2.265e04 * m^3/s
bfpd	barrels of fluid per day	5.437e05 * m^3/s
bopd	barrels of oil per day	5.437e05 * m^3/s
bwpd	barrels of water per day	5.437e05 * m^3/s
cp	centipoise	10 * kg/(ms)
dynes/cm	dynes per cm	1e05 * J
ft	feet	3.281 * m
g/cc	grammes per cubic centimetre	0.001 * kg/m^3
kph	kilometres per hour	3.6 * m/s
lb	pound	2.2 * kg
mD	milli-Darcy	1e15 * m^2
ppm	parts per million	1e06 * kg/m^3 or 1e06 * m^3/m^3
psi	pounds per square inch	1.45e-04 * Pa
psia	pounds per square inch (absolute)	1.45e-04 * Pa
psig	pounds per square inch (gauge)	1.45e-04 * Pa
pu	porosity units	100 * m^3/m^3
rb	reservoir barrels	6.293 * m^3
scf	standard cubic feet	35.317 * m^3
scf/d	standard cubic feet per day	3.051e06 * m^3/s
stb	stock tank barrels	6.293 * m^3
stb/d	stock tank barrels per day	5.437e05 * m^3/s
Prefix	**Description**	
B	1e09 * unit	
M	1e03 * unit	
MM	1e06 * unit	